BIOMECHANICS OF THE AGEING HUMAN KNEE

Thesis submitted in accordance with the requirements of the University of Liverpool for the degree of Doctor of Philosophy

by

Abby E. Peters

September 2017

Contents Page

Co-Author Contributions

Chapters Two - Five of this thesis have been submitted for publication in peer-reviewed scientific journals and have been produced in collaboration with other researchers. This thesis consists of a general introduction, followed by one review chapter (Chapter Two) and three results chapters (Chapters Three – Five). Results chapters are presented in published form as they appear in respective journals, although supplementary material has been included within the main text where appropriate. A summary discussion and conclusion follows these chapters and references relevant to these chapters are listed at the end of the thesis.

Authors contributing to specific chapters in this thesis include: Ms Abby Emma Peters (AEP), Dr Karl T Bates (KTB), Dr Riaz Akhtar (RA), Prof Eithne J Comerford (EJC), Miss Sophie Macaulay (SM), Dr Brendan Geraghty (BG) and Mrs Rosti Hama Rashid (RHR).

The nature of each co-author's contribution to published work will now be discussed explicitly in more detail. Chapter Two was published in PeerJ in January 2017 [Peters et al., 2018]. AEP and KTB conceived and planned the study. AEP carried out the systematic review and compiled and analysed the data. AEP wrote the manuscript. KTB, RA and EJC edited and approved the manuscript.

Chapter Three was published online in March 2017 in the Journal of the Mechanical Behaviour of Biomedical Materials [Peters et al., 2017] in collaboration with four co-authors. AEP and RA conceived and planned the study. AEP, EJC and SM dissected the specimen. AEP acquired the data. AEP analysed and interpreted the data. AEP wrote the manuscript. KTB, RA, EJC and SM edited and approved the manuscript.

Chapter Four has been published Scientific Reports in April 2018 [Peters et al., 2018]. This was produced in collaboration with four authors. AEP, RA, EJC and KTB conceived and planned the study. AEP, EC and KTB dissected the specimens. AEP acquired the data. AEP analysed and interpreted the data. AEP wrote the manuscript. KTB, RA and EJC edited and approved the manuscript.

Chapter Five will be submitted for consideration to the Journal of Biomechanics in 2018. This was produced in collaboration with five authors. AEP, RA, EJC, KTB and BG conceived and planned the study. AEP, EJC and KTB dissected the specimens. RHR and BG provided technical and logistical support for testing preparation. AEP acquired the data. AEP analysed and interpreted the data. AEP wrote the manuscript. BG provided Figure 2. KTB, RA, EJC, BG, RHR edited and approved the manuscript.

List of Tables

SECTION ONE

Chapter Two

SECTION TWO

Chapter Three

Chapter Four

Chapter Five

SECTION THREE

Chapter Nine

List of Figures

SECTION ONE

Chapter Two

SECTION TWO

Chapter Three

Chapter Four

Chapter Five

List of Abbreviations

1D	One Dimension
2D	Two Dimension
3D	Three Dimension
A	Contact Area
ACL	Anterior Cruciate Ligament
AFM	Atomic Force Microscopy
BMI	Body Mass Index
Ciw	Instrument Damping
CSM	Continued Stiffness Measurement
Csw	Total Measured Damping
CT	Computed Tomography
Cw	Contact Damping
D	Tip Diameter
DMCL	Deep Medial Collateral Ligament
E	Elastic Modulus
ECM	Extracellular Matrix
E_i	Indenter Elastic Modulus
E_r	Reduced Indentation Modulus
F	Female
FCLI	Femoral Condyle Lateral Inferior
FCLS	Femoral Condyle Lateral Superior
FCMI	Femoral Condyle Medial Inferior
FCMS	Femoral Condyle Medial Superior
FE	Finite Element
*G**	Complex Shear Modulus
G'	Shear Storage Modulus

G″	Shear Loss Modulus
GNS	Gender Not Specified
H	Hardness
ICRS	International Cartilage Repair Society
Ki	Instrument Stiffness
Ks	Total measured stiffness
LAT	Lateral
LCL	Lateral Collateral Ligament
M	Male
MCL	Medial Collateral Ligament
MED	Medial
MRI	Magnetic Resonance Image
NS	Not Specified
OA	Osteoarthritis
P	Maximum Load
PBS	Phosphate Buffered Saline
PCL	Posterior Cruciate Ligament
PCM	Peri-Cellular Matrix
PMC	Posteromedial Capsule
PMMA	Polymethyl-Methacrylate
S	Contact Stiffness
SD	Standard Deviation
SEM	Standard Error Mean
SMCL	Superficial Medial Collateral Ligament
Tan δ	Loss Factor
TPLA	Tibial Plateau Lateral Anterior
TPLP	Tibial Plateau Lateral Posterior
TPMA	Tibial Plateau Medial Anterior

TPMP	Tibial Plateau Medial Posterior
v	Poisson's Ratio
v_i	Indenter Poisson Ratio

Abstract

The knee joint is an integral component of the musculoskeletal system, aiding the absorption and transition of weight bearing forces. It is often subjected to injury or disease, with osteoarthritis (OA) being the most prevalent disease, particularly amongst the elderly population. It is now understood that OA is a whole-joint disease affecting the entire osteochondral unit at a molecular and cellular level; however to what extent this effects material properties is mostly unexplored. This thesis firstly aimed to comprehensively review the current knowledge of whole human knee joint material properties in young versus old and healthy versus OA samples, and their subsequent macro-scale application into existing finite element (FE) models. Results indicated unambiguous gaps in the literature for material properties, particularly evident in the aged and OA samples. Consequently, existing human knee FE models apply material properties from a variety of animal and human cohorts, obtained from differing anatomical localities and diverse cadaver demographics, reducing the biological accuracy of resultant mechanical behaviour predicted from such models. Secondly, this thesis aimed to determine the effects of multiple freeze-thaw cycles on cartilage material properties in an attempt to justify a reliable storage and perseveration technique for future work. Results showed that cartilage can undergo up to three freeze-thaw cycles without statistically compromising the integrity of samples. Although data should be interpreted and subsequently applied to future research with consideration in relation to its particular application due to high biological variability across samples. Finally, this thesis aimed to collect and analyse new primary material property data of spatially distributed cartilage, subchondral bone and trabecular bone by nanoindentation techniques, and the four primary knee joint ligaments by tensile testing. Samples were obtained from cadaveric specimens with a wide age range (31 – 88 years) and OA grade (International Cartilage Repair Society grades 0 – 4) to provide varying demographics that were evidently missing from the literature. Cartilage shear storage and loss modulus and subchondral bone elastic modulus significantly decreased with increasing age and grade of OA. Furthermore, a change in cartilage shear storage and loss modulus was correlated with a change in subchondral bone elastic modulus in site-matched samples. Trabecular bone elastic modulus was not correlated with age or OA. Results also showed preferential regional development of OA in the medial knee compartment and a decrease in cartilage shear storage modulus at site-specific locations. Additionally, the anterior cruciate ligament (ACL) and posterior cruciate ligament (PCL) material properties had correlations with age, and linear and failure mechanics showed some correlations with increasing OA grade. The medical collateral ligament (MCL) and lateral collateral ligament [LCL) failure mechanics also showed some correlated with an increase in age and OA grade. This thesis has provided, for the first time, whole-joint multiple tissue material properties from the same cadavers during ageing and disease, concluding that both age and OA affect the material properties of the entire osteochondral unit. Such valuable data can be applied to future FE modelling of the human knee to produce more accurate predication of mechanical behaviour. Current data can also be applied therapeutically, including the use of biomimetic materials, joint replacement and pharmacological interventions.

Declaration

No portion of the work referred to in this thesis has been submitted in support of an application for another degree or qualification of this or any other university or other institute of learning.

Copyright

I. The author of this thesis (including any appendices and/or schedules to this thesis) owns certain copyright or related rights in it (the "Copyright") and s/he has given The University of Liverpool certain rights to use such Copyright, including for administrative purposes.

II. Copies of this thesis, either in full or in extracts and whether in hard or electronic copy, may be made only in accordance with the Copyright, Designs and Patents Act 1988 (as amended) and regulations issued under it or, where appropriate, in accordance with licensing agreements which the University has from time to time. This page must form part of any such copies made.

III. The ownership of certain Copyright, patents, designs, trademarks and other intellectual property (the "Intellectual Property") and any reproductions of copyright works in the thesis, for example graphs and tables ("Reproductions"), which may be described in this thesis, may not be owned by the author and may be owned by third parties. Such Intellectual Property and Reproductions cannot and must not be made available for use without the prior written permission of the owner(s) of the relevant Intellectual Property and/or Reproductions.

The Author

The author graduated from Bournemouth University in July 2012 with a first class BSc (Hons) Exercise Science (Health and Rehabilitation) degree. Following this, in July 2013 she graduated from The University of Roehampton with an MSc in Biomechanics. With a passion for health care and musculoskeletal biology she then started a career as a Bone Health and Exercise Specialist within the NHS, providing health care for patients with joint and bone disease and implementing new care pathways within community settings. The author then joined the Institute of Ageing and Chronic Disease and the School of Engineering at the University of Liverpool to undertake this PhD in biomechanics of the human knee joint.

Acknowledgments

First and foremost I thank my wonderful parents, Mary and Bob. Your love and support has seen me through seven years at university where you have supported me emotionally and financially through it all. Without your continued support I wouldn't have achieved half as much as I have and indeed this thesis would not exist.

For the work presented in this thesis, my greatest thanks are owed to my primary supervisor Dr Karl Bates. You have supported and encouraged me through the last three years and I couldn't have asked for a more suitable supervisor. I have the upmost respect for you and I will be forever grateful for all you have done. I also thank my supervisors Professor Eithne Comerford and Dr Riaz Akhtar. Eithne, I am so appreciative of your help and guidance through all my practical work. You have trusted and had confidence in my ideas and plans and helped me grow as a researcher, aiding the changes I have seen in myself over the last three years. Riaz, I thank you mostly for the help and guidance with nanoindentation testing. It made up the majority of my lab work and the many hours spent in the basement have finally paid off with the completion of my thesis.

Next I thank Sam. You have supported me through the ups and downs of this PhD and I can't even begin to show my appreciation for you. Time spent with you reminds me that being happy is what really matters and your encouragement has motivated me to keep going at the hardest of times.

I also thank Sophie and Ali. Our friendship has meant so much to me and I couldn't imagine sharing the PhD experience with anyone else. I also thank the rest of my colleagues in the Evolutionary Morphology and Biomechanics research group and my colleagues in the

School of Engineering, in particular Brendan and Rosti for their help and support through ligament testing.

I also thank Phil Jackson from Newcastle Surgical Training Centre who provided support in obtaining cadaveric specimens; Val Adams from the Magnetic Resonance and Image Analysis Research Centre, University of Liverpool, who aided magnetic resonance imaging of cadaveric specimens; Lee Moore and the staff the Veterinary Teaching Suite, University of Liverpool who provided animal cadavers and surgical tools; Dave Atkinson from the School of Engineering, University of Liverpool, who provided training and equipment for testing.

Finally I thank those much more external to my PhD, my sisters and my friends from home and those closer by. The distractions have kept me happy and sane.

This work was jointly funded by the Biotechnology and Biological Sciences Research Council and the School of Engineering, University of Liverpool.

Section One – Introduction and Background

Chapter One: Introduction

Background

With an increasingly ageing population, diseases such as osteoarthritis (OA) have become more commonly diagnosed than ever before [Zhang & Jordan, 2008]. OA is a degenerative joint disease typically associated with cartilage wear, although more recently has been linked to changes across the entire osteochondral unit, and specifically with changes in subchondral and trabecular bone cellular activity [Nigg & Herzog, 2006; Lories & Luyten, 2011; Mahjoub et al., 2012]. Understanding the nature and magnitude of these changes can aid knowledge of how to prevent and treat those currently diagnosed with OA [Kuroki et al., 2011]. Clinical research into OA is multidisciplinary and involves analyses of varying tissues at the nano- [e.g. Stolz et al., 2009; Zuo et al., 2016], micro- [e.g. Desrochers et al., 2010] and macro-level [e.g. Setton et al., 1999]. Wen et al., [2014] suggests that research outcomes may influence clinical and therapeutic interventions used to treat OA including rehabilitation, pharmacology and arthroplasty operations, amongst others. However as with most diseases, understanding is continually improving as technology and research expands.

OA is most commonly found in the knee joint which is made up of a sophisticated network of soft and hard tissues stabilising and supporting movement [Zhang & Jordan, 2008]. Movement at the knee joint is primarily in the sagittal plane allowing mechanical flexion and extension between the diarthrosis articulation of the femur and tibia [Nigg & Herzog, 2006]. When biomechanical function of the knee joint reduces due to OA, daily activities such as sitting down, ascending and descending stairs and walking become challenging and full range of motion is less achievable [Zeni & Higginson, 2009].

OA is inherently associated with other injuries and diseases such as ligament degeneration [Mullaji et al., 2008; Hill et al., 2005], meniscal tears [Lange et al., 2007] and muscle weakness [Alnahdi et al., 2012]. It can lead to decreased stability during locomotion increasing the risk of falls [Hollman et al., 2007]. Locomotive patterns are altered and adapted, in turn effecting mobility and function and ultimately reducing quality of life [Kiss, 2011]. OA also has a high economic burden with reported values of up to 40% of the United States of America elderly population being diagnosed with the disease at the knee joint [Punzi et al., 2010], leading to direct medical costs in the region of $12,400 per individual over a lifetime [Losina et al., 2015].

The kinetics and kinematics of OA have been well researched aiding the understanding of disease mechanisms *in vivo*, most commonly showing that there is a decrease in knee flexion moment during gait and increase in knee adduction moment during stance [Zeni & Higginson, 2009; Deluzio & Astephen, 2007]. These kinematic alterations also appear to increase with increasing grade of OA [Astephen et al., 2008]. Furthermore, the contralateral knee is also affected [Zeni & Higginson, 2009; Metcalfe et al., 2013] which may influence the progression of the disease [Shakoor et al., 2002]. Whilst this type of *in vivo* research is useful for therapeutic applications such as physical rehabilitation, our understanding is limited to the external mechanical function of whole-joints. However, knowledge of internal structural adaptations that may occur at the nano- or micro-level, thus leading to such changes in macro mechanical functioning and joint behaviour, can be more accurately assessed *in vitro* [Nigg & Herzog, 2006], although this is practically and ethically more challenging to research particularly within human tissue.

A common *in vitro* measurement of soft and hard tissues is the obtainment of material properties. Material properties characterise the behaviour of a tissue, usually denoted in

terms of their stress-strain relationship. This valuable data can be used in a variety of applications including diagnostics and correlation with disease pathology, failure mechanics, synthetic tissue development and finite element (FE) modeling. Previous research has focused on collating material properties values to understand the effect of OA pathology on mechanical response of tissues. In relation to the knee joint, the literature shows that cartilage material properties exist for both healthy and OA samples, which consistently show a decline in the values in the presence of disease that progresses with increasing grade of OA [Kleemann et al., 2005; Wilusz et al., 2013]. However importantly, as ageing is a primary risk factor for OA, currently there is no study exploring the changes seen in cartilage during ageing or more specifically through a continuous increase in age. This makes it challenging to know how variations of material properties are attributed to biological variability or are distinct changes due to ageing and/or disease status.

Increased knowledge of such values can aid understanding of disease initiation and progression. Mechanical, biochemical and architectural properties of the articular cartilage extracellular matrix are known to change during the progression of OA, particularly within the highly aqueous superficial zone, which plays a vital role in the mechanical response of cartilage during loading [Marticke et al., 2010, Temple-Wong et al., 2009]. However it can be challenging to distinguish initial surface degeneration [Desrochers et al., 2012] despite this being a prerequisite to the progression of OA where a change in mechanical properties correlates with initial disease status. The diagnosis of OA during the early stages of the disease is difficult [Matyas et al., 2004]; however advances in nanotechnology are gradually allowing the detection of nano-scale structural changes that occur prior to initial detectable diagnosis [Stolz et al., 2009]. If such techniques are applied to a wide variation of healthy and diseased tissue, particularly those with early stage OA, material property changes may

be more accurately associated with progressive grades of OA and even allow knowledge of material property changes prior to any observed surface degradation.

Previous studies have also shown that histological staining highlights biochemical and morphological adaptations in both cartilage and bone when OA is induced, confirming a synergistic relationship between the two tissues [McDevitt et al., 1977]. Additionally, increased bone remodeling is site specific and associated with high or abnormal loads on a joint [Moss-Salentijn & Moss, 1991; Lanyon, 1993; Klein-Nulend et al., 2003]. This is consistent with degeneration of cartilage through increased mechanical loading. However while material property values for both healthy human knee joint cortical and trabecular bone [Rho et al., 1997; Behrens et al., 1974; Ducheyne et al., 1977; Burgers et al., 2008] exist within the literature, there lacks any analysis of the effect of ageing or OA.

Finally, ligament material properties are well known to adapt and decline with ageing in the literature spanning across young and old samples [Trent et al., 1976; Noyes & Grood, 1976; Woo et al., 1991; Chandrashekar et al., 2006]; however material properties are yet to be explored in OA samples. Although, histological analysis has shown impaired integrity of both the anterior cruciate ligament (ACL) and posterior cruciate ligament (PCL) in the presence of OA [Mullaji et al., 2008]. Evidently, ageing, as well as the initiation and progression of OA have been correlated with a change in either structure or function of multiple tissues of the knee joint. However gaps in the literature, as well as factors such as non-standardisation of testing methods and ranging donor demographics have led to a wide variation in reported material property values and difficulty in inter-study comparison.

Due to the lack of accurate material properties within multiple tissues of the human knee joint, it currently makes it challenging to use these values in further research applications including the knowledge of healthy mechanics, diagnostics of OA, prediction of failure mechanics, synthetic tissue development and FE modeling.

The diagnosis of OA is most commonly through medical imaging techniques, including radiographic, that can determine a change in cartilage thickness and detect indicative signs of OA such as joint space narrowing or osteophyte formation [Kiviranta et al., 2008]. However such signs are often associated with late stage OA, whereas the need for early detection is apparent. OA initiation begins with a reduction in proteoglycan content, which is thought to be reversible [Palmoski et al., 1981; Kiviranta et al., 1994]. However the subsequent reduction in swelling pressure in turn causes compressive stiffness to also reduce, meaning the cartilage structure may fail to resist normal physiological joint loading, causing a disruption to the collagen network which is not reversible [Buckwalter & Mankin, 1997; Helminen et al., 2000].

The need for early detection is evident and currently there are some exploratory ways for this. Indentation techniques performed on cartilage during arthroscopy is an *in vivo* method for determining material properties [Lyyra et al., 1998; Kiviranta et al., 2008]. If patients undergo these procedures for example during meniscus or ligament repair, it is currently possible to also determine cartilage material properties. Cartilage material properties are thought to decrease prior to any detectable surface degeneration caused by OA [Stolz et al., 2009]. This procedure therefore presents an opportunity to detect early stage OA if a decrease in material property values is identified. However there is currently a wide range of material properties reported in the literature for both healthy and mild stage

OA cartilage, obtained from a variety of human and animal specimens. This currently makes it challenging to understand how mild OA would manifest in varying individuals.

As well as *in vivo* indentation, imaging techniques can now also be used in the prediction of material properties, particularly within cartilage and bone when combined with numerical modelling [Neu, 2014; Loeser et al., 2013]. If *in vitro* material properties can be accurately collated for a range of young healthy and aged and/or diseased tissue, such knowledge can be inputted into and compared to other material property predictive models. This may then help indicate early signs of OA through a decrease in material property values which can be evident prior to macroscopic or radiographic detection of cartilage degradation.

In instances where early detection has not been possible, the need for replacement of damaged tissue may increase. In recent years synthetic tissue development has advanced where bio-realistic material properties can help design and create bio-material scaffolds, which are used in the repair and replacement of damaged tissue. Sophisticated scaffolding of cartilage tissue structure which has consistent material properties with the anatomical site in which it is being implanted, can increase accuracy and successful integration [Li et al., 2016; Wang et al., 2012]. Advances in material testing, specifically the ability to test for visco- and poro-elasticity, also mean the cartilage scaffolds can take on a more accurate architecture to allow for cell infiltration and vascularisation by incorporating a porous structure [O'brien, 2011]. Biological compatibility is also important for bone tissue, developing newer materials that are low in modulus and resilience compared to more conventional materials such as stainless steel [Long & Rack, 1998]. Material testing of human bone allows more accurate correlation of these materials to biological reality as well as an increase in knowledge of effects of factors such as cyclic loading, fatigue and

wear, which are vital in the implementation of artificial and synthetic materials [Long & Rack, 1998].

As well as cartilage and bone biomimetics, re-construction of human knee ligaments, most commonly the ACL, are often produced using either synthetic or biological tissue [Dhammi et al., 2015]. ACL grafts using synthetic material have shown evidence of failure at mid-term leading to the need for improved materials that would behave more accurately to the biological structure. Grafts constructed using the hamstring have a failure load of 2422N, while grafts using patella tendon only 1785N [Dheerendra et al., 2012], which when related to the failure mechanics of ligaments may indicate what other biological structures are best placed to reconstruct ligaments. More accurate material properties of ligaments in healthy and diseased samples, and in particular failure mechanics, can help direct research into graft materials and the behaviour they should exhibit for successful replacement in the knee joint. Failure mechanics are not only important for ligaments as trauma and repetitive stresses are associated with the pathogeneses of OA in the cartilage, therefore knowing where failure occurs, and areas for high stress concentrations can also help disease prognosis and intervention strategies [Donzelli et al., 1999].

Computational approaches such as FE modeling, which can be used in the prediction of *in vivo* joint behaviour, also utilise material property values and allows the user the gain an understanding of how a complex structure and each of its component parts behaves under stress [Strait et al., 2005]. It provides non-invasive predictions of stress-strain magnitudes and shows the behavioural response of the modelled structures, including sites of excessive strain and even failure. It has been extensively applied to the knee joint [e.g. Shirazi et al., 2008; Guess et al., 2010; Kazemi et al., 2011] including studies of knee joint OA [Pena et al., 2007; Dong et al., 2011; Mononen et al., 2012]. FE models can vary enormously in their

nature and complexity but all require some representation of three basic components; the anatomy or geometry of the structure, its material properties and the mechanical loads it experiences. True representation of anatomical geometry is essential for FE modelling to produce accurate predictions of mechanical behaviour, such as stress and strain [Richmond et al., 2005].

Many FE studies incorporate existing material properties sourced from the literature, although these often lack biological similarity to the tissue being presented and include data from animals [e.g. Pena et al., 2006; Wang et al., 2014] and human studies [e.g. Wang et al., 2014; Bendjaballah et al., 1995] with varying donor demographics. This can compromise the validity of a model [Gardiner & Weiss, 2003] as precise input of material property data is essential to accurately determine mechanical behaviour of the joint [Bonner et al., 2015]. Additionally, models often assume homogeneity across different ligaments [e.g. Wang et al., 2014; Li et al., 2001; Kazemi et al., 2014] despite it being well known that ligaments usually experience loading in multiple directions and material properties are correlated with specific orientation, structure and loading axis [Woo et al., 2006]. Furthermore, models often globally represent cartilage [e.g. Kazemi et al., 2014; Bendjaballah et al., 1995] and bone [e.g. Guo et al., 2009; Mootanah et al., 2014] with one representative value, despite material property data showing heterogeneity in such samples.

Despite advances in the field of tissue engineering, there remain considerable gaps in the literature regarding material properties, particularly the lack of a wide span of age for cartilage or bone material properties, and without a comparison of healthy and OA samples in bone and ligament samples. Additionally, no such data exists exploring more than one tissue from the same donor, and there is only minimal data on multiple samples across of

the same tissue from the same donor. These gaps in the literature may inhibit the advancement of the applications listed above, and can be explained by several logical factors. Firstly, it is ethically challenging to obtain human cadaveric material and more so acquiring demographically diverse samples, for example from a range of ages and / or disease states. If human cadaveric knee joints are able to be obtained, extracting multiple samples from the same donor can be geometrically difficult without compromising the integrity of adjacent tissues, hence the absence of multiple samples or multiple tissue type research from the same donor. Harvesting multiple location dependent samples poses its own challenges with regards to time and resources of testing equipment. In this circumstance storing and preserving samples would allow for a larger quantity of samples to be tested. To date, research suggests that bone can be stored and preserved in a solution of 70% ethanol maintaining its physiological state [Bembey et al., 2006], whilst ligaments can undergo at least two freezing cycles before any changes to mechanical properties are evident [Huang et al., 2011; Moon et al., 2006]. However the effect of storage of cartilage beyond one freezing cycle [Szarko et al., 2010] is yet unknown, potentially limiting the quantity or type of tissue tested.

A comprehensive review is therefore needed to fully understand what material property data exists for both healthy and OA tissues obtained from the human knee joint. To further our understanding, a review of one of the above applications is also needed to highlight how current applications involving the knee joint use these material property values. Whilst research to date has made significant advances in the knowledge of the mechanical alterations with OA in the human knee joint, applications using higher-level analysis of joint function are currently inhibited by the gaps in knowledge. This review will direct the experimental approach then needed to fill the gaps in the literature where in order to fully understand how OA affects the knee joint, it is essential to characterise the behaviour of all

the tissues involved, in both healthy and OA representations, using a standardized method of testing.

Such valuable data can be used in a variety of research, clinical and therapeutic interventions. Knowledge of how material properties of the human knee joint change with healthy ageing can aid the understanding of how OA initiates and progresses, potentially linking to diagnostic techniques and failure mechanics. This may also aid artificial joint or tissue replacement as well as computational representations to become more biologically accurate to subject- or cohort specific knee joint properties.

Aims and Objectives

The overall aim of this thesis is to obtain material properties of soft and hard tissues of the human knee from cadavers with varying demographics to aid the understanding of ageing and OA across the entire knee joint. This will be achieved by the following objectives:

1. Complete a comprehensive review of the current knowledge of human knee joint tissue material properties and its application into existing FE models;
2. Study the effect of storage and preservation on cartilage material properties to accompany existing storage techniques known for bone and ligaments;
3. Obtain human cadaver knee joints of varying demographics including age and OA grade to:
    a. Collate spatially distributed material properties of cartilage, cortical bone and trabecular bone by nanoindentation techniques;
    b. Harvest the four primary knee joint ligaments and collate their material properties by tensile testing.

Thesis Layout

This thesis contains nine chapters divided into three distinct sections. Following this introductory chapter in Section One, Chapter Two is a comprehensive literature review, which has been previously submitted for peer-review publication. It details existing human knee joint tissue material properties in the peer reviewed literature and their application in computational modelling in an attempt to highlight gaps in current knowledge. Section Two contains three experimental chapters investigating knee joint tissue material properties, presented as individual studies published or submitted for peer-reviewed publication. The aims and objectives of the thesis, as stated above, will be addressed in Chapters' Two to Five.

Section Three contains Chapter Six which discusses chapter by chapter the implications of this research presented with a comparison to similar research in the literature, and goes on to detail a critical evaluation of the current research with suggestions for future research. Chapters Seven and Eight conclude the main findings of this research and references cited in the introductory and discussion chapters of the thesis. In Section Four, Supplementary Material can be found in Chapter Nine, and publications from this thesis can be found in Chapter Ten.

Chapter Two: Tissue material properties and computational modelling of the human knee: A critical review

Abstract

Understanding how structural and functional alterations of individual tissues impact on whole-joint function is challenging, particularly in humans where direct invasive experimentation is difficult. Finite element computational models produce quantitative predictions of the mechanical and physiological behaviour of multiple tissues simultaneously, thereby providing a means to study changes that occur through healthy ageing and disease such as osteoarthritis. As a result, significant research investment has been placed in developing such models of the human knee. Previous work has highlighted that model predictions are highly sensitive to the various inputs used to build them, particularly the mathematical definition of material properties of biological tissues. The goal of this systematic review is two-fold. First, a comprehensive summation and evaluation of existing material property data for human knee joint tissues is provided, tabulating numerical values as a reference resource for future studies. Second, this thesis reviews efforts to model whole-knee joint mechanical behaviour through finite element modelling with particular focus on how studies have sourced tissue material properties. The last decade has seen a renaissance in material testing fueled by development of a variety of new engineering techniques that allow the mechanical behaviour of both soft and hard tissues to be characterised at a spectrum of scales from nano- to bulk tissue level. As a result, there now exists an extremely broad range of published values for human knee tissues. However, this systematic review highlights gaps and ambiguities that mean quantitative understanding of how tissue material properties alter with age and osteoarthritis is limited. It is therefore currently challenging to construct finite element

models of the knee that are truly representative of a specific age or disease-state. Consequently, recent whole-joint finite element models have been highly generic in terms of material properties even relying on non-human data from multiple species. This review highlights this by critically evaluating current ability to quantitatively compare and model 1) young and old and 2) healthy and osteoarthritis human knee joints. This review suggests that future research into both healthy and diseased knee function will benefit greatly from a subject- or cohort-specific approach in which finite element models are constructed using material properties, medical imaging and loading data from cohorts with consistent demographics and/or disease states.

Introduction

The knee joint is a primary component of the musculoskeletal system that aids the absorption and transition of weight bearing forces. As an integral part of biomechanical movement the knee joint is often subjected to injury or disease such as ligament rupture [Mullaji et al., 2008; Hill et al., 2005], meniscal tears [Lange et al., 2007] and osteoarthritis (OA) [Zhang & Jordan, 2008]. OA is one of the most common musculoskeletal conditions in the elderly population causing structural degeneration of tissues and ultimately leading to a decline in function [Rousseau & Garnero, 2012]. The most common type of OA exists in the knee joint which is the leading cause of locomotor disability [Zhang & Jordan, 2008]. The disease is encouraged by heredity influence, ageing, gender, obesity and trauma or injury to the affected joint [Manninen et al., 1996], known as secondary OA, and can often lead to joint replacement [Nigg & Herzog, 2006]. Where the cause of the disease is unknown this is referred to as primary OA. It is approximated that 40 % of adults over the age of 70 will be affected by OA of the knee in the United States of America [Punzi et al., 2010], with direct lifetime medical costs of $12,400 per person [Losina et al., 2015]. OA does not just present

with direct joint degeneration but is intrinsically linked to other diseases and neuromuscular complications which can further exacerbate age-related issues such as sarcopenia and a loss of movement control. Individuals with OA have increased variability of gait spatial-temporal parameters [Kiss, 2011] which in turn can decrease locomotor stability and increase the risk of falls [Lord et al., 1996; Hausdorff et al., 2001; Owings & Grabiner, 2004; Brach et al., 2005; Hollman et al., 2007].

Typically, research surrounding OA focuses on the deterioration of articular cartilage; however recent research has highlighted the need to consider structural changes of subchondral bone in the progression of OA [Nigg & Herzog, 2006]. Significant relationships have been identified between changes occurring in different tissues specifically observing molecular crosstalk [Lories & Luyten, 2011; Mahjoub et al., 2012]. OA is therefore more recently seen as a disease of the entire joint with biochemical and biomechanical factors influencing the progression and status of the disease. Each tissue has a specific role and functionality within the knee joint in order to aid movement and stability. Individual tissues have a distinct structure and material properties that define its adaptive and responsive behaviour in accordance with the biomechanics of movement [Punzi et al., 2010]. Biochemical and mechanical changes naturally occur during ageing even in the absence of clinically defined injury or disease and these changes have been shown to modify form-function relationships at the knee joint [Hansen et al., 2006a]; however data is limited.

In order to fully understand the onset and progression of OA it is essential to comprehend the basic relationships between structure and function within a healthy human knee and how tissues age in the absence of disease. Understanding biomechanics of anatomically complex structures like the knee joint is challenging particularly in humans where experimental approaches must largely be non-invasive. The difficulty of achieving direct

quantitative measures of tissue behaviour together with more widespread availability of imaging technology (i.e. magnetic resonance imaging (MRI), X-ray computed tomography (CT)) has led to an increasing use of computational approaches, notably finite element (FE) analysis, to study knee joint form and function [e.g. Pena et al., 2005; Pena et al., 2006; Wang et al., 2014]. Once suitably validated such FE models may potentially circumvent the issues surrounding direct invasive measurement of tissue mechanics by producing quantitative predictions of the mechanical and physiological behaviour of multiple tissues simultaneously, thereby inherently calculating tissue interaction. This could be particularly useful in identifying tissue interaction that may occur during ageing and in the presence of disease.

Through use of parameterization, models can also be used in a predictive capacity to address questions that cannot ethically or even practically be asked by experimentation on humans or animals. Specifically, iterations of the same model can be generated where aspects of structure including gross anatomy and material properties, and loading behaviour are non-invasively manipulated to quantify the impact on function. In this way parameterization enables cause-effect relationships between anatomy and mechanics to be identified, whilst allowing the impact of individual and combinations of morphological characteristics to be isolated [Li et al., 2001]. Model manipulations can also be used for testing surgical interventions, treatment strategies and prosthetics [e.g. Baldwin et al., 2012; Tuncer et al., 2013].

Models are by definition abstractions of reality and their constituent parts or input parameters are typically tailored to address a specific research question or hypothesis. Consequently models of the same anatomical structure, such as the knee joint, may vary considerably between studies according to the research objective. One way to summarise

this variation across studies is that models can either be conceptual or highly analytical. Conceptual models are therefore simplified, or generic inputs are chosen to give a more qualitative answer to a specific question (i.e. a yes or no answer; or “X is always higher than Y”). Conceptual models on the other hand are highly analytical where more comprehensive or complex inputs are used to derive a highly quantitative answer (i.e. “during X the stress/strain = Y”; or “because of X the stress/strain increases by Y %”). In the context of the human knee, for example, it is common for researchers to use models to answer questions on one specific tissue (e.g. ligament injuries under specific stress and strain) and as such effort and complexity is invested in these specific tissues while it is deemed sufficient to invest less towards input values for other tissues (i.e. therefore simplifying cartilage representation to a linear elastic material, or bone treated as a rigid-body). However, tissues within a joint inherently interact and behaviour of one is influenced by others, although to what extent to which tissues interact has not extensively been studied.

Subject specific FE modelling is useful in the application of OA as it can investigate the true interaction between multiple tissues and how changes in one can lead to implications in an adjacent tissue, which may lead to disease initiation or progression. For example, ligament ruptures are histologically known to occur in the presence of OA [Mullaji et al., 2008], yet the impact or causative link to cartilage degeneration is unknown. Whilst efforts have been made to investigate this disease through computational approaches, it is indeed clear that there is a lack of baseline healthy measurements providing a foundation for comparative analyses. Research into the material properties of young healthy tissues surrounding the human knee is needed to compare to other cohort-specific groups. In the context of joint biomechanics this is crucial to understanding how, for example, component parts of the joint function so that corrective therapeutics can restore joint function to the normal baseline as per the healthy sample measurements. Baseline healthy measurements are also

crucial for basic science contexts such as sports biomechanics, where increasing biomechanical function is directly linked to performance. The accuracy of computational modelling approaches in general has been shown repeatedly to rely on good input data [Guo et al., 2013; Kazemi et al., 2013; Freutel et al., 2014]. Direction of future research towards understanding the influence of donor age and 'healthy' versus pathological conditions on material properties with these new techniques has been cited as a key goal [Lewis & Nyman, 2008], but it is presently unclear of extent to which this has been achieved in the context of the human knee joint.

Evidently the human knee joint is crucial in biomechanical movement and function and has therefore the relevant literature has been reviewed extensively in recent years. Specifically, several reviews have discussed computational modelling of individual tissues of the knee joint. For example, Wilson et al., [2005] reviewed articular cartilage representations of behavioural and injury mechanisms, whilst Taylor & Miller, [2006] reviewed both micro- and macro-level representation of cartilage tissue. Computational modelling of ligaments has also been reviewed by Woo et al., [1993] and Weiss & Gardiner, [2001] focusing on viscoelasticity and one-dimension to three-dimension representations respectively. Whole knee joint modelling has also been reviewed in recent years by Pena et al., [2007], Elias & Cosgarea, [2007] and Kazemi et al., [2013]. Whilst these reviews focused on advances in modelling, to date no review paper has critically evaluated the nature of material property available for human knee joint tissues and subsequently how this data has been transferred to FE models, with particular reference to ageing and OA.

The aim of this review paper is two-fold. Firstly, to conduct a review of scientific literature to understand what material property data currently exists for cartilage, bone and ligament samples from the human knee joint in an attempt to understand alterations during healthy

ageing and disease status. Secondly, this paper aims to determine how this data has been subsequently applied within biomedical engineering in the form of existing FE models of the whole human knee joint. In doing so this review collates a comprehensive database of material properties of human knee joint cartilage, bone and ligaments to substantiate this critical review of recent advances and current limitations, whilst also serving as a resource for future research in this important area. The critical aspect of this review focuses on the question "how systematic or holistic is the material property data that exists for the human knee in terms of its ability to represent a specific human cohort or demographic"? To evaluate this question this review focuses on young healthy representation of material properties to understand the current baseline for accurate comparison to old OA representation.

Survey Methodology

Firstly, published scientific papers were sourced for review that contained material property data of soft and hard tissue from the human knee joint only. The selection criteria are outlined below. Literature search engines were used, including ScienceDirect, PubMed (NCBI), MedLine, SpringerLink and Wiley Online Library. Terminology including *cartilage, bone, ligament, human, knee, joint, femoral, femur, tibia, tibial, anterior, posterior, cruciate, medial, lateral, collateral, material properties, elastic modulus, Young's modulus, compression, tensile, indentation, FE, model, modelling, three dimensional,* and *computational* were used. All relevant studies meeting search criteria were included in this review.

For cartilage and bone material properties the research must have been on distal femoral and proximal tibia only (excluding patella samples). Studies must have also incorporated

the use of compression or indentation techniques for ease of comparison of testing techniques and data obtained (as opposed to tensile elongation, 3-point bending, 4-point bending or buckling techniques) to collate the elastic modulus, shear modulus or comparable parameters. For ligament material properties studies must have incorporated at least one of the following: anterior cruciate ligament (ACL), posterior cruciate ligament (PCL), medial collateral ligament (MCL), and lateral collateral ligament (LCL) from the human knee tested using tensile techniques. Compression and tensile testing techniques were specifically chosen to mimic primary biological *in vivo* mechanics.

Secondly, published scientific papers were sourced for review if they incorporated a three dimensional (3D) FE model of a whole human knee joint. This included any study modelling the femoral and tibial bone and cartilage structures and the four main ligaments of the knee joint – ACL, PCL, MCL and LCL. Studies not including all these structures were excluded. Additionally models may or may not have included the menisci or meniscal tissue, meniscectomies and studies of insoles or footwear, joint replacement or arthroplasty mechanics, and ligament reconstructions were also excluded. In addition, this review included models representing OA.

Structure, composition and material property data obtained from human knee joints were to initially be reviewed separately for cartilage, bone and ligament tissue (*Section A*), followed by a review of use of data within currently published human whole-knee joint FE models (*Section B*).

Section A - Material Properties

Articular Cartilage Structure and Composition

Articular cartilage is a type of fibrous connective tissue composed of cells forming between 2-15 % of the total weight and an extracellular matrix (ECM) forming the remaining 85-98 %, of which 65-80 % is water [Martini, 2007]. The extracellular matrix is heterogeneous in nature, where variations exist in biocomposition, structure and vascularity at a micro level. It is composed of proteoglycans, collagens and glycoproteins, which are all macromolecular components [Silver et al., 2002]. Proteoglycans are responsible for the compressive strength of cartilage have the ability to bear water that is fifty times their own weight [Hansen et al., 2006a]. Cartilage also contains chondrocytes that become embedded within the matrix and mature and divide to deposit new cartilage; however cartilage lacks the ability to remodel itself when damage and degeneration occurs, particularly due to osteoarthritis [Newman, 1998; Guilak et al., 2004].

Its primary function is to maintain a smooth surface allowing lubricated, near-frictionless movement and to help transmit articular forces, thereby minimising stress concentrations across the joint. It is most commonly found within synovial and diarthrodial joints forming a 1-6 mm thickness and covering the epiphysis of bone. The knee joint is composed of both hyaline and fibrocartilage in the form of articular cartilage covering the end of bones articulating within the joint and fibrocartilage forming the menisci [Martini, 2007].

Cartilage has four primary layers, consisting of the superficial, middle, deep and calcified cartilage zones. The superficial zone is further divided into a superficial and deep layer. The superficial compartment of the superficial zone contains randomly aligned crimped collagen fibres forming a thin (2µm) layer, creating a smooth layer to aid joint movement [Sophia Fox et al., 2009; Cohen et al., 1998; Nigg & Herzog, 2006]. The deep layer of the superficial zone contains flat chondrocyte cells and collagen fibres that sit parallel to the direction of movement of the joint and to the surface of the cartilage. The layer also has

decreased proteoglycan content when compared to other cartilage zones [Nigg & Herzog, 2006]. The superficial zone plays a vital role in the mechanical response of cartilage and degeneration i.e. through osteoarthritis, will leave the middle and deep zone susceptible to increased stresses via compression, tension and shear forces; however the middle and deep zone are not as well suited to absorb and transmit tensile and shear forces [Guo et al., 2015]. The water content of the superficial zone is highest of all the zones, hence its capability to resist tensile forces [Sophia Fox et al., 2009; Cohen et al., 1998; Nigg & Herzog, 2006].

The middle zone allows for a transition between the vast differences between the superficial and deep zones, with collagen fibres that are randomly organised. The orientation of the collagen fibres within the articular cartilage zones, dictates to some extent, its ability to resist tensile forces. It has a higher composition of proteoglycans and cells are typically spherical. The deep zone consists of collagen fibres that are perpendicular to the direction of joint, meaning the tensile modulus of the articular cartilage deep zone is decreased compared to the superficial zone [Krishnan et al., 2003]. This zone contains chondrocytes that are situated in columns of a radial nature. Proteoglycan content is the highest within this zone, whilst water content is the lowest [Cohen et al., 1998; Nigg & Herzog, 2006].

Articular cartilage also contains a calcified zone separating the subchondral bone from the soft cartilage tissue, and is distinguished by its hydroxyapatite composition, which is also found within bone. The calcified zone is distinguished and separated from the deep cartilage zone via the tidemark line [Nigg & Herzog, 2006]; however collagen fibres from the deep zone cross this tidemark and attach themselves onto the calcified zone in order to adhere bone to cartilage. The bone cartilage interface, including calcified cartilage and

subchondral bone, plays host to greater collagen and proteoglycan content, when compared to the superficial zones of articular cartilage [Mow et al., 2002, Saarakkala et al., 2010].

Material properties of articular cartilage have been widely reported giving compressive, tensile and shear forces at the macro- [Armstrong & Mow, 1982; Setton et al., 1999; Kleemann et al., 2005], micro- [Stolz et al., 2009; Desrochers et al., 2010] and nano-scale [Stolz et al., 2009] within the ECM of multiple species. Various techniques have been utilised including confined and unconfined compression [Kleemann et al., 2005; Hori & Mockros, 1976; Franz et al., 2001] and more recently atomic force microscopy (AFM) [Wen et al., 2012; Wilusz et al., 2013; Wang et al., 2013] and nanoindentation [Taffetani et al., 2014]. Custom made indentation instruments have also previously been used to measure articular cartilage stiffness during compression [Hori & Mockros, 1976; Kempson et al., 1971; Lyyra et al., 1995; Kiviranta et al., 2008] as well as being used to calculate dynamic modulus [Kiviranta et al., 2008], creep modulus [Kempson et al., 1971], shear, bulk and elastic modulus and Poisson's ratio [Hori & Mockros, 1976]. Varying formulations of elasticity are also used to measure and represent material properties, including linear elastic, viscoelastic and poroelastic [Mansour, 2003; Nigg & Herzog, 2006].

The development of increasingly sophisticated testing techniques has further advanced the understanding of cartilage material properties by allowing measurements to be made at the nano-scale. With the use of nano-scale indentation stiffening of cartilage due to age-related influences alongside stiffness differences in healthy and OA cartilage can be detected more accurately in comparison to microindentation [Stolz et al., 2009]. It has been shown that microindentation is either unable to detect such changes or produces a lower stiffness measurement when compared to nanoindentation [Stolz et al., 2009; Stolz

et al., 2004]. Additionally, stiffness is higher in articular cartilage collagen fibrils than in proteoglycans; however when measured at micro-scale, this differentiation may not be detected [Loparic et al., 2010]. A change in the structure and content of proteoglycans often accompanies the process of OA along with reduced stiffness through loosening of the collagen network causing alteration to the material properties, further enhancing the need for testing at the nano-scale [Wang et al., 2013].

Indenter tip radius and geometry can alter the material properties obtained during data collection. Some studies at the nano-scale have used sharp pyramidal tips with shallow indentations to obtain the mechanical behaviour of individual structural elements, such as collagen fibres or cellular matrix [e.g. Stolz et al., 2004]. According to Stolz et al., [2009], such measurements at the nano-scale are able to detect subtle changes in the ECM that occur during ageing and disease, which are undetectable at the micro-scale. However when a sharp pyramidal tips are used this can cause plastic deformation or damage to the sample [Ebenstein et al., 2004], and flat punch indenters may be more suitable to soft biological tissues [Akhtar et al., 2011]. In these instances a larger tip will measure average moduli of the entire sample it comes into contact with, whereas a smaller tip will have a more precise measurement to the exact location under investigation [Ebenstein et al., 2006] and producing higher modulus values. Therefore varying tip geometries applied at different length scales can alter the material property values obtained and contribute to variability seen in reported data.

The formulation of elasticity in which cartilage is measured with can also effect material property values. Whilst both micro- and macro-scale measurements provide similar results for modulus, values for permeability are not consistent, potentially due to length scale dependency of poroelastic behaviour [Miller & Morgan, 2010]. Biological tissues were

traditionally tested and modelled as linearly elastic materials, in that they deform in a linearly fashion proportionate to the stress applied, often interpreted as single phasic. However it is now widely accepted that these tissues in fact have viscoelastic properties where the stress strain relationship has time-dependent factors and/or fluid flow properties making the tissue viscoelastic or poroelastic and often interpreted as biphasic or triphasic [Mansour, 2003; Nigg & Herzog, 2006]. Such important properties are now being more widely represented for both healthy and diseased cartilage, such to the porous nature of cartilage structure allowing for movement of fluid [e.g. Taffetani et al., 2014; Nia et al., 2011].

This movement of fluid will subsequently affect the stress-strain relationship and ability for the tissue to bear load. The biphasic nature of the articular cartilage allows 85-95% of the applied load to be carried by the fluid within the joint [Stolz & Ateshian, 1998]. However the fluid pressure can be disrupted if the superficial layer of the articular cartilage is damage or degenerated, i.e. due to OA, therefore exposing the more permeable middle and deeper zones to the same level of stress [Hansen et al., 2006a]. The tensile strength of articular cartilage is attributed to the collagen fibre network, which helps maintain the integrity of the ECM. Meanwhile ECM hydration under high mechanical stress is maintained by proteoglycans due to their high osmotic pressure [Wen et al., 2012]. Proteoglycans are responsible for the compression stiffness which have been shown to decline in OA and ageing. The superficial zone of the articular cartilage is essential for the effective mechanical transition of forces across a joint; however alterations in the mechanical properties of the superficial zone of articular cartilage can occur whilst a patient is asymptomatic of OA [Lu & Mow, 2008]. A change in the structure of proteoglycans, including a decline in density, often accompanies the process of OA, along with higher aqueous composition or permeability, and reduced stiffness through loosening of the

collagen network, and therefore the capability to absorb and transmit mechanical loading [Wang et al., 2013]. Therefore, research is now focusing on obtaining the viscous and/or porous response of cartilage as well as the elastic response, to enable detection of these subtle changes. According to Miller & Morgan, [2010], measuring cartilage material properties at the micro-scale allows the testing of a higher volume of tissue which enables the poroelastic behaviour to be characterised; however measurements at this length scale may result in ECM changes going undetected due to reduced sensitivity when compared to nano-scale.

Articular Cartilage Literature Review

One of the first studies to explore human knee joint cartilage material properties utilised uniaxial confined compression on 20 proximal tibia samples. Age and gender of donors were not specified; however each sample was classified with a grade of OA using the Bollet system [Bollet et al., 1963 cited in Hori & Mockros, 1976]. Progressive compression loads were manually applied giving an elastic modulus between 1.3-10.2 MPa. When categorising elastic modulus to grade of OA averages were 6.82 MPa, 6.74 MPa, 4.76 MPa and 2.99 MPa for grades 0, 1, 2 and 3 respectively, although this correlation was not significant [Hori & Mockros, 1976]. Testing specifications and resultant data can be seen in Table 1 alongside information from all reviewed human knee joint cartilage material property research.

Table 1. Summary of current literature for human knee cartilage material property compression or indentation testing including age, gender, health status of specimens, number and location of samples tested and technique (including tip indenter size where given) used to obtain elastic modulus values. Abbreviations: NS (not specified); F (female); M (male); OA (osteoarthritis); AFM (atomic force microscopy); ECM (extra cellular matrix); PCM (peri-cellular matrix). *Samples were dehydrated prior to testing.

Author	Quantity & Locality	Age, Gender & Health Status	Testing Technique	Results per Cohort: Elastic Modulus (MPa)	
Hori & Mockros, 1976	20 x Donors Proximal Tibia	Age: NS; Gender: NS; Health: Healthy & OA Grade 1	Uniaxial Confined Compression 10-30.4mm indenter	*Healthy & OA Grade 1*	1.3-10.2
Shepherd & Seedhom, 1997	5 x Donors Femoral Condyle & Tibial Plateau	Age: NS; Gender: NS; Health: Healthy	Spring Loaded Indentation 1.59mm indenter	*Healthy*	2.6-18.6
Shepherd & Seedhom, 1999a	11 x Donors Femoral Condyle & Tibial Plateau	Age: 33-80; Gender: 8F/3M; Health: Healthy	Spring Loaded Indentation 1.59 indenter	*Healthy*	6.0-11.8
Franz et al., 2001	24 x Femoral Condyle	Age: 32-89; Gender: NS; Health: Healthy & OA Grade 1	Handheld Indentation 1.0mm indenter	*Healthy & OA Grade 1*	4.3-4.9
Kleemann et al., 2005	21 x Donors Tibial Plateau	Age: 70±13; Gender: 15F/6M; Health: OA Grades 1-3	Uniaxial Unconfined Compression	*OA Grade 1* *OA Grade 2* *OA Grade 3*	0.5 0.4 0.3
Thambyah et al., 2006	7 x Donors Tibia	Age: 62-70; Gender: M; Health: Healthy	Uniaxial Unconfined Compression 1.0mm indenter	*Healthy*	2.1-5.1
Wen et al., 2012	3 x Donors Knee Samples	Age: 35-59; Gender: F; Health: Healthy & OA Grade 1	AFM 10nm indenter	*Healthy* *OA Grade 1*	2650.0-3700.0* 2370.0-5640.0*
Wilusz et al., 2013	8 X Donors Femoral Condyle	Age: 53-83; Gender: NS; Health: Healthy & OA Grades 2-3	AFM 5µm indenter	*Healthy PCM & ECM* *OA Grade 2-3 PCM & ECM*	0.1 & 0.3 0.1 & 0.5
Wang et al., 2013	5 x Donors Femoral Condyle	Age: NS; Gender: NS; Health: Healthy & OA Grade 1-3	AFM 40nm indenter	*Healthy* *OA Grade 1* *OA Grade 2-3*	0.2 0.6 0.2

In more recent decades there has been considerable focus on micro-scale unconfined compression testing. In consecutive studies by Shepherd and Seedhom, [1997; 1999a], human femoral condyle and tibial plateau cartilage were tested. Earlier research utilised a total of five donors although no age or gender was specified. Results indicated an elastic modulus of between 2.6-18.6 MPa depending on physiological loading rate [Shepherd & Seedhom, 1997]. In the latter study 11 humans cadavers (three males and 8 females, aged 33 - 80 years old) were tested giving an elastic modulus of 6.0-11.8 MPa (Table 1) across all cadavers with no correlation with age [Shepherd & Seedhom, 1999a].

Thambyah et al., [2006] tested cartilage from seven fresh frozen healthy human male tibias (62 – 70 years old) using uniaxial tensile testing at a rate of 300 kPa/s to compare articular cartilage from beneath the menisci to that independent from the menisci. Results showed an individual mean elastic modulus from all seven cadavers between 2.13 and 5.13 MPa (Table 1) across varying testing locations. Hydration maintenance was not specified within the methodology.

Kleemann et al., [2005] explored the macroscopic composition of articular cartilage within 15 female and six male OA tibial plateau samples (70 ± 13 years old). Research obtained architectural data from histology using haematoxylin and eosin staining and elastic modulus of cartilage was determined by unconfined uniaxial compression. An inverse correlation was observed between the elastic modulus of the articular cartilage against the International Cartilage Repair Society (ICRS) grade [Brittberg & Peterson, 1998] seen in Figure 1 (Grade 1 0.50 MPa, Grade 2 0.37 MPa, and Grade 3 0.28 MPa (Table 1)). The research also suggested a relationship between changes in histology, structure and mechanics of the articular cartilage during all stages of OA degeneration although this was not compared with age of donor. Moreover Bae et al., [2003] found decreased indentation

stiffness and an increased ICRS score was associated with degeneration of cartilage rather than with age or cartilage thickness. This suggests that it is possible to reliably distinguish degeneration of cartilage by microscopic histological analysis and macroscopic observations.

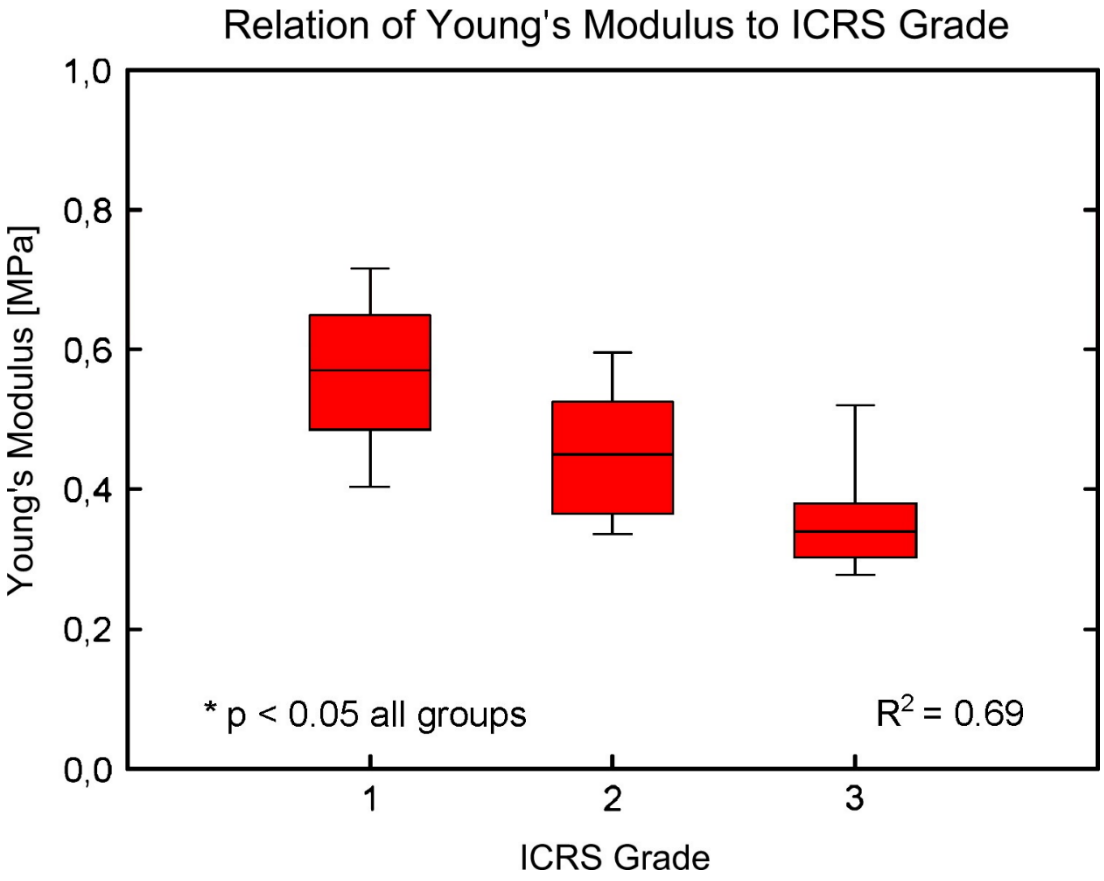

Figure 1. Stiffness reduction of degenerated cartilage with increasing International Cartilage Repair Society (ICRS) Grade related to boxplots displaying median values and interquartile range. (Adopted from Kleemann et al., [2005]: Elsevier License Permission: 4095850046133).

Franz et al., [2001] used a handheld indenter with a constant load of 300 µm to collate the shear modulus of 24 human cartilage samples (32 – 89 years old) obtained from the medial

and lateral femoral condyles. Shear modulus was converted to elastic modulus (using the Poisson's ratio expressed in the original research) for the purpose of this paper, which were 4.32 MPa and 4.88 MPa (Table 1) in the lateral and medial femoral condyles respectively; however this was not correlated with the age of cadaver. Cartilage samples were graded for OA using the Mankin system [Mankin et al., 1971] and results indicated a positive correlation between a slightly roughened cartilage surface and stiffness at the medial femoral condyle. However it should be noted that no samples presented with gross fibrillation or surface irregularities. Sample shear modulus was however presented in age categories with corresponding proteoglycan and collagen content which are known to adapt during ageing and disease (Fig. 2).

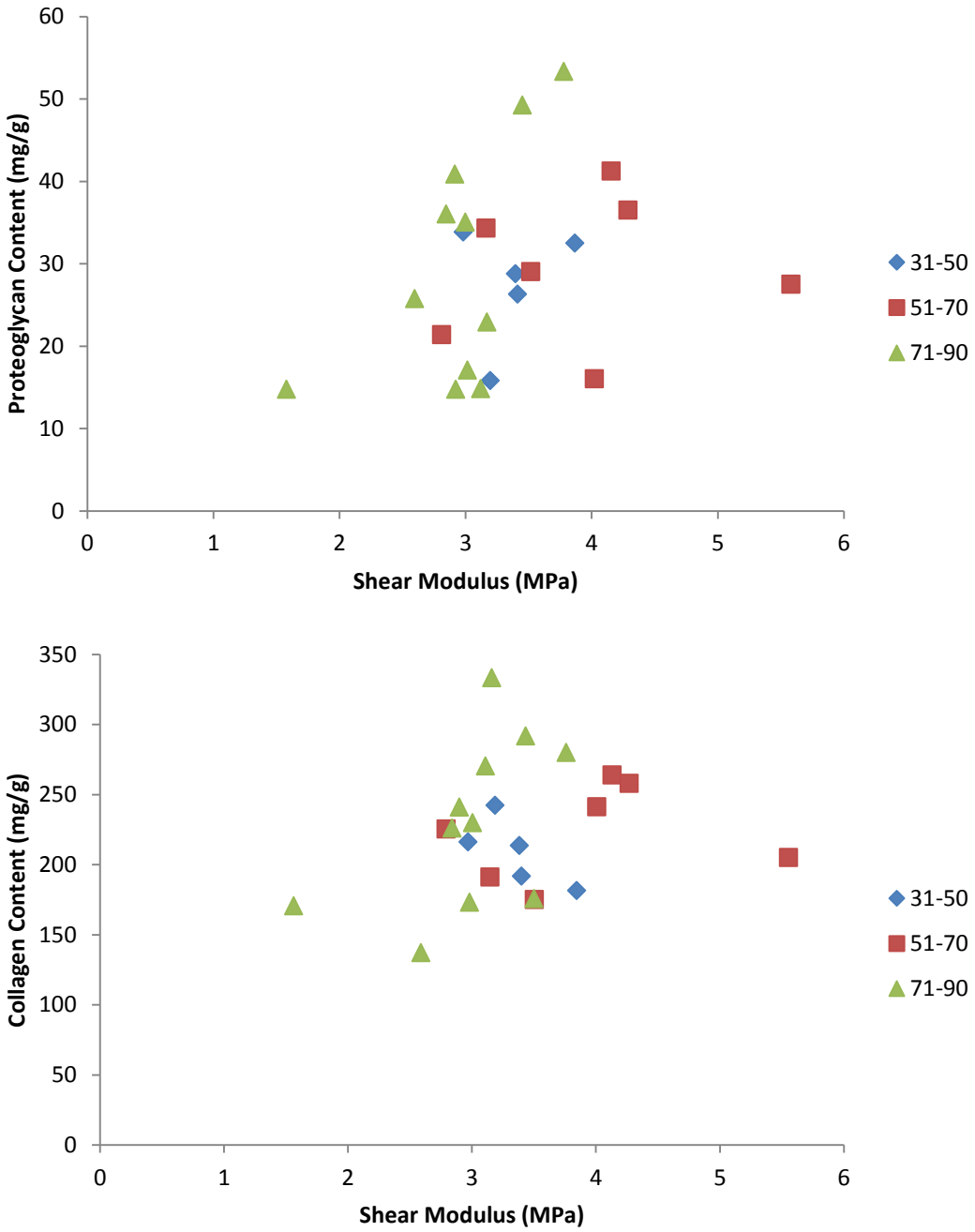

Figure 2. Total proteoglycan content (mg/g tissue wet weight) versus cartilage compressive stiffness (shear modulus in MPa) for the lateral femoral condyle, and total collagen content (mg/g tissue wet weight) versus cartilage compressive stiffness (shear modulus in MPa) for the lateral femoral condyle. All subjects are divided into three age groups (31 – 50 years, 51 – 70 years, and 71 – 90 years) to demonstrate that the variation of total proteoglycan and collagen content is not due to the large age range. (Recreated from Franz et al., [2001]: Elsevier License Permission: 4095850249345).

Incorporating nanotechnology, Wen et al., [2012] utilised AFM at a loading rate of 2.11 nm/s to test elastic modulus of tibial plateau articular cartilage fragments obtained from three female patients undergoing arthroplasty surgery. Samples from the surface, superficial middle, deep middle and bone-cartilage interface regions were graded for OA with the Outerbridge scoring system [Outerbridge, 1961]. Collagen fibres were obtained from the overlap zone from each layer which can be mechanically stiffer than collagen fibres in the gap region [Minary-Jolandan & Yu, 2009]. Results show there is a significant mechanical stiffening of individual human collagen fibrils between healthy (aged 35 years old) and mild OA (aged 52 and 59 years old), at the surface of articular cartilage (2650 – 3110 MPa respectively) through to the bone-cartilage interface (3700 – 5640 MPa respectively) (Table 1). It must be noted that tissue samples were dehydrated with ethanol prior to testing which will alter the true mechanical properties of cartilage; however the aim of this research was to identify the differences in elastic modulus of healthy and OA tissues where mechanical alterations would change simultaneously in both healthy and OA samples.

Wilusz et al., [2013] also used AFM at a rate of 15 μm/s on eight human femoral condyles (six female and two male) aged 53 – 83 years old. Cadavers were graded for OA using the Collins System [Collins, 1939 & Collins, 1949 cited in Wilusz et al., 2013] giving four healthy and four OA samples grades 2 – 3. Results indicate that elastic modulus of the pericellular matrix (PCM) decreased in OA samples (0.096 ± 0.016 MPa) when compared to healthy controls (0.137 ± 0.022 MPa). Also the ECM elastic modulus was decreased in OA samples (0.270 ± 0.076 MPa) when compared to healthy controls (0.491 ± 0.112 MPa) (Table 1); although this was only significant on the medial femoral condyle. In agreement, Wang & Peng, [2015] used AFM to quantify elastic modulus of 12 knee articular cartilage samples (age and gender not specified) in various grades of OA and found an increase in elastic

modulus in the presence of mild and moderate OA but a decrease with severe OA, although actual values are not stated.

AFM has also been used to identify nanoscale adaptations at varying indentation depths in five human (age and gender not specified) femoral condyles obtained from healthy, mild and severe OA cartilage [Wang & Peng, 2015]. Cartilage samples were graded using the Outerbridge scoring system [Outerbridge, 1961] and exposed to PBS during testing to maintain hydration. Stiffness was higher at a lower indentation depth for all cohorts; however stiffness was highest with mild OA (0.61 MPa) and lowest with healthy controls (0.16 MPa) when comparing to severe OA (0.19 MPa) (Table 1) [Wang & Peng, 2015].

Bone Structure and Composition

The skeletal system is a sophisticated network of cells, including osteoblasts and osteoclasts, which work in coordination to repair and remodel the structure of bone, in order to maintain is resilience against internal and external mechanical forces. These cells are considered bone mass regulators, and recognise the bone loading potential, in order to preserve bone homeostasis. Bone remodeling is a regular process which is related to consistent high or abnormal loads on a joint [Cowin et al., 1991; Lanyon, 1993; Klein-Nulend et al., 2003]. There are two different types of bone including cortical and trabecular material. The cortical material is found on the outside of bone and is highly dense in nature and the trabecular material is located inside of the bone and has a greater porosity. The low and high densities work in coordination to absorb stresses through the rigid outer surface and strains through the spongy inner material in order to resist breaking or deformation [Nigg & Herzog, 2006; Martini, 2007].

Cortical bone is composed of osteon units that are derived from concentric layers of lamellae. These contain randomly situated mature bone cells, which lie within small pockets called lacunae. Within the osteon is a haversian canal, which contains blood vessels and nerves that allow for the transportation of blood to and from the osteon [Weiner & Wagner, 1998; Martini, 2007]. Each lamella contains collagen fibres that add strength and resiliency to the structure of bone, through a spiraled morphology that must uncoil during loading [Nigg & Herzog, 2006]. Canaliculi are narrow pathways that spread throughout the lamellae, to allow for the exchange of nutrients, toxins and gases interconnecting between each lacuna [Martini, 2007]. Trabecular bone, however, is not structured into osteons, but rather more the matrix forms a porous interlaced network of bone, with the absence of a haversian canal. Nutrients therefore must diffuse the matrix along the canaliculi to reach the osteocytes, via the blood vessels of the red bone marrow found between the matrix [Martini, 2007].

Bone is composed of organic and inorganic substances, with the organic material providing a foundation where inorganic material can form on. The organic material of bone is composed of mostly collagen fibres, making up approximately one third of the total weight of a bone [Weiner & Wagner, 1998; Martini, 2007]. These fibres allow for flexibility and strength in resisting tension during bending and torsion motions; however collagen is ineffective during compression forces (Nigg & Herzog, 2006). The inorganic material of bone, which makes up the remaining two thirds of the weight of bone, is primarily composed of calcium and phosphorous. Crystalline salts are also deposited within the bone matrix, and combine with the calcium and phosphorus to form hydroxyapatite crystals [Olszta et al., 2007; Martini, 2007]. These crystals are tough with limited flexibility, and can withstand excessive mechanical compression; however they are at risk of shattering if exposed to rapid impact, or disproportionate torsion and bending [Nigg & Herzog, 2006].

The primary cells within bone make up just two percent of its organic material, and include osteoclasts, osteoblasts and osteocytes [Weiner & Wagner, 1998; Olszta et al., 2007]. Osteoclasts are found within the bone marrow, and function to resorb bone. They work by anchoring themselves to the surface of the bone, and releasing an acidic material containing lysosomal enzymes, to disintegrate the collagen fibres and fibrous overlay, through a process called osteolysis [Olszta et al., 2007]. This results in the release of calcium into the interstitial fluid [Nigg & Herzog, 2006].

Osteoblasts synthesize new bone matrix through a process of osteogenesis, and follow the osteoclasts with the aim of laying down new organic material within the cavities created. The newly laid bone matrix is primarily composed of collagen, and is known as an osteoid [Martini, 2006]. This forms a foundation by which minerals including calcium and phosphate can crystallise to form hydroxyapatite, and transform the osteoid into bone [Nigg & Herzog, 2006]. Some osteoblasts may become embedded within the bone matrix and mature into osteocytes. These cells inhabit a lacuna, where a small gap junction between each cell allows for the exchange of nutrients and hormones, either between single cells or into the surrounding interstitial fluid [Nigg & Herzog, 2006].

Osteocytes also serve as mechanoreceptors, in order to distinguish any changes in mechanical loading through the bone. They detect changes in the hydrostatic pressure of the interstitial fluid as a result of the impact loading, and receive and convert this mechanical stimulus and reaction to fluid motion, into a chemical response. This response is then communicated to the osteoblasts and osteoclasts in order for them to undertake remodeling [Nigg & Herzog, 2006]. The greater the load and deformation on bone, the greater the flow of fluid through the bone matrix, and increased need for bone cell activity [Nigg & Herzog, 2006; Martini, 2007].

Bone is a viscoelastic, heterogeneous and anisotropic material, due to various geometries of cancellous and trabecular bone, along with variations of density and material properties in different anatomical sites [Rho et al., 1998]. Its anisotropic nature arises from its significant variation in different directions (i.e. transverse versus sagittal). Elasticity of bone refers to its ability to return to its original shape following applied stresses, whilst viscosity of bone refers to its stress relaxation and creep behaviour, regarding its ability to transmit energy and stiffness properties [Rho et al., 1998; Pal, 2014; Nigg & Herzog, 2006]. Despite bone being recognised as a viscoelastic heterogeneous anisotropic material, most commonly it is analysed as a homogeneous isotropic material as normal physiological loading will not exceed the elastic linear region; however this is somewhat dictated by the aims of the research in question [Pal, 2014; Nigg & Herzog, 2006] i.e. the investigation of failure mechanics may necessitate the addition of viscous analysis as stress applied will exceed normal physiological loading.

Wolff's Law states that a bone will adapt and remodel according to the stresses consistently placed upon it, therefore the shape of a bone is highly dependent on the force, specifically the direction and magnitude encountered [Currey, 2012; Nigg & Herzog, 2006; Ruff et al., 2006]. Bone also shows properties of fatigue where repetitive loads will cause it to reach its failure point at a lower magnitude [Rho et al., 1998; Nigg & Herzog, 2006]. This is due to an accumulation of micro-trauma that threatens its structural integrity. It is in response to high frequencies of stress below its failure point that the adaptive remodeling process takes place. Bone's response to loading is location specific to the area in which the stress is applied [Nigg & Herzog, 2006; Ruff et al., 2006].

The material properties of bone will not just vary according to orientation and location, but also due to the length scale the sample is tested at. Indenter tip radius and geometry can

alter the mechanical properties obtained during data collection. For example a larger tip will measure the average moduli of the entire sample it comes into contact with, whereas a smaller tip will have a more precise measurement to the individual structure tested [Ebenstein et al., 2006]. The effect of indenter tip radius on material properties of bone has previously been investigated, resulting in a smaller indenter (5µm) increasing the elastic properties when compared to a larger indenter (25µm, 65µm and 200µm). Sensitivity to variations in mechanical properties is more easily achieved with a smaller indenter tip, as there are heterogeneous discrepancies existing between lamellar and inter-lamellar regions, creating a 2 GPa difference in modulus [Paietta et al., 2011]. In addition material properties of cortical osteons have been shown to be significantly higher than interstitial bone tissue [Hoffler et al., 2005]. When testing bone samples haversian canals and porous localities should be avoided as this can present a site specific softening of the material, which can alter the hardness and elastic modulus [Zhang et al., 2008]. Differences in orientation (i.e. longitudinal or transverse), location (i.e. osteons or interstitial bone tissue) and length scale (i.e. nano- or micro- indentation) can contribute to the variability seen within results reported in the literature, discussed below.

Bone Literature Review

Recent research has started to direct focus onto the relationship between cartilage and bone in the progression of OA. Research has observed abnormal remodeling of subchondral bone in OA showing the trabecular structure alters in density, quantity and separation, with the greatest proliferation in volume evident at the bone-cartilage interface [Kamibayashi et al., 1995; Bobinac et al., 2003]. This suggests a synergistic relationship between bone and cartilage during the progression of OA. The role of subchondral bone in OA appears to be an essential component in the initiation and advancement of the disease

[Burr, 1998; Lajeunesse & Reboul, 2003; Madry et al., 2010]. However research is unclear as to whether disruption of subchondral bone remodeling occurs pre- or post- initiation of OA [Intema et al., 2010; Kuroki et al., 2011]. Kuroki et al., [2011] suggested that a more comprehensive understanding of the disease mechanisms of OA including material properties of all tissues involved could yield considerable progression in clinical practice and treatment methods.

In previous decades uniaxial compression testing of human femoral and tibial trabecular bone was carried out by several researchers in order to obtain macro-scale material properties. Behrens et al., [1974] tested both femoral condyle and tibial plateau trabecular bone samples from six females and four males (40 – 92 years old) resulting in an elastic modulus of 158.9 - 277.5 MPa for femoral bone and 139.3 - 231.4MPa for tibial samples (Table 2). Testing only femoral condyle trabecular bone, Ducheyne et al., [1977] found a slightly lower elastic modulus of 1.9 - 166.1 MPa (Table 2) based on donors aged 43 - 77 years old (four males, two females).

Table 2. Summary of current literature for human knee bone material property compression or indentation testing including age, gender, health status of specimens, number and location of samples tested and technique (including tip indenter size where given) used to obtain elastic modulus values. Abbreviations: GNS (gender not specified); F (female); M (male); OA (osteoarthritis). *Elastic modulus value for individual OA grade not specified – value taken as approximation from graph.

Author	Quantity & Locality	Age, Gender & Health Status	Testing Technique	Results per Cohort: Elastic Modulus (MPa)	
Behrens et al., 1974	10 x Donors Femoral Condyle & Tibial Plateau Trabecular Bone	Age: 40-92; Gender: 6F/4M; Health: Healthy	Uniaxial compression	*Femoral Condyle* *Tibial Plateau*	158.9-277.5 139.3-231.4
Lindahl, 1976	8 x Donors Tibial Plateau Trabecular Bone	Age: 14-89; Gender: 4F/4M; Health: Healthy	Uniaxial compression	*Males* *Females*	34.6 23.1
Carter & Hayes, 1977	100 x Samples Tibial Plateau Trabecular Bone	Age: NS; Gender: NS; Health: Healthy	Uniaxial compression		56.6-83.7
Ducheyne et al., 1977	6 x Donors Femoral Condyle Trabecular Bone	Age: 43-77; Gender: 2F/2M; Health: Healthy	Uniaxial compression		1.9-166.1
Goldstein et al., 1983	5 x Donors Tibial Plateau Trabecular Bone	Age: 50-70; Gender: 2F/3M; Health: Healthy	Uniaxial compression		4.2-430
Hvid & Hansen, 1985	12 x Donors Tibial Plateau Trabecular Bone	Age: 26-83; Gender: 3F/9M; Health: Healthy	Uniaxial compression 2.5mm indenter	*Medial* *Lateral*	13.8-116.4 9.1-47.5
Zysset et al., 1994	6 x Donors Tibial Trabecular Bone	Age: 61-91; Gender: NS; Health: OA Grades 1-3	Uniaxial Compression	*Subchondral* *Epiphyseal/ Metaphyseal*	31.0-1116.0* 8.0-1726.0*
Rho et al., 1997	2 x Donors Tibial Cortical Bone	Age: 57 & 61; Gender: M; Health: Healthy	Nanoindentation 20nm indenter		22500.0-25800.0
Burgers et al., 2008	10 X Donors Femoral Condyle Trabecular Bone	Age: 45-92; Gender: NS; Health: Healthy	Uniaxial Compression		131.0-664.0

Carter & Hayes, [1977] tested 100 human trabecular bone samples (age and gender unspecified) from tibial plateaus by uniaxial compression and found an elastic modulus between 56.6 - 83.7 MPa (Table 2). Also using uniaxial compression, Lindahl, [1976] tested four female and four male human cadavers (14 – 89 years old) showing a higher elastic modulus in males (average 34.6 MPa) compared to females (average 23.1 MPa) (Table 2).

Interestingly, as well as differences between male and female cadavers, material properties also vary according to anatomical location. Goldstein et al., [1983] utilised uniaxial compression testing to determine the elastic modulus of trabecular bone from the tibial plateau from 5 cadavers (50 – 70 years old) across varying depths of the joint. Results showed high variation across cadavers and testing location (4.2 - 430 MPa (Table 2)) with the highest values at load bearing sites. Utilising an alternative method, Hvid & Hansen, [1985], used an osteopenetrometer on the tibial plateau of 12 healthy human donors aged 26 - 83 years old (three female and nine male). Medial tibial plateau samples had an elastic modulus of 13.8 - 116.4 MPa and lateral tibial plateau samples had a lower elastic modulus of 9.1 - 47.5 MPa (Table 2) further evidencing high variability in material properties across the joint.

Burgers et al., [2008] obtained four male and four female human cadavers (totaling ten femurs aged 45 - 92 years old). Cylindrical trabecular specimens (n = 28) were tested using unconfined compression. Results were separated into superior or inferior and medial or lateral samples giving a pooled elastic modulus of 376 MPa ± 347 MPa (Table 2) with the greatest variation apparent between superior and inferior femoral condyle samples.

Previous studies researching human knee bone material properties, specifically in OA, are abundantly missing; however one study by Zysset et al., [1994] explored human tibial

material properties from six cadavers (61 - 91 years old) with grades 1 - 3 OA, scored using the Ahlback system [Ahlback, 1968]. Compression tests were conducted on cuboidal specimens giving an axial elastic modulus of the subchondral trabecular bone between 31 and 1116 MPa which decreased with increasing grades of OA. Although epiphyseal and metaphyseal trabecular bone samples showed that elastic modulus increased with OA grade in the axial (range 102 – 1726 MPa) and coronal (8 – 287 MPa) planes (Table 2). Corresponding OA grade and elastic modulus values can be seen in Figure 3.

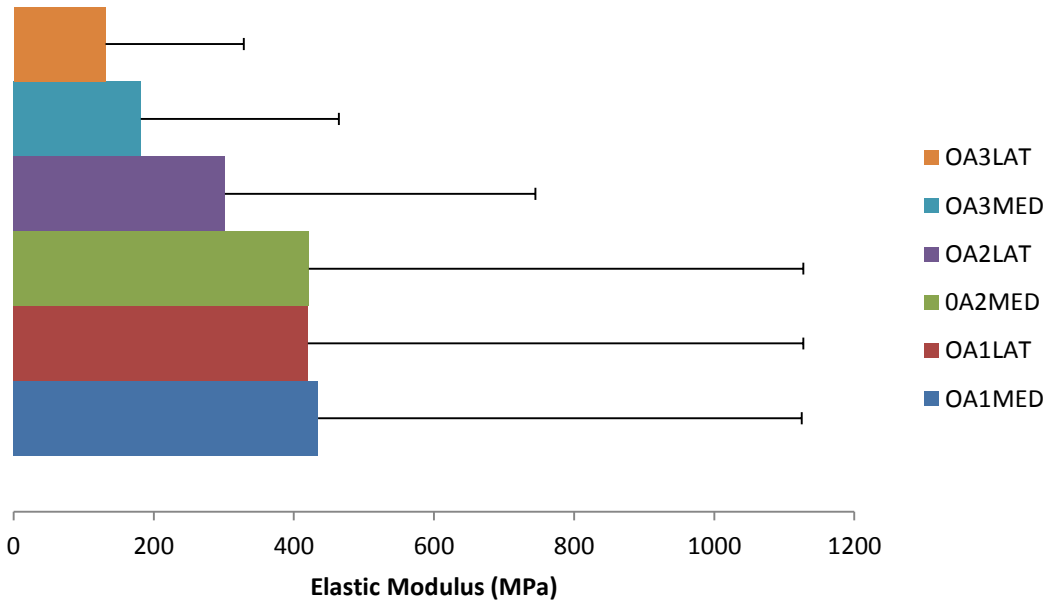

Figure 3. Compressive axial elastic modulus of subchondral bone for a range of osteoarthritis (OA) grades (1-3). Average elastic modulus decreases with degenerative grade in the medial (MED) and especially lateral (LAT) compartments. (Recreated from Zysset et al., [1994]: Elsevier License Permission: 4095850483612).

In more recent years, testing bone at the tissue level has proven to be more accurate [Nigg & Herzog, 2006] particularly for the inclusion of FE models; however this has rarely been applied to femoral or tibial human bone. Using nanoindentation Rho et al., [1997] explored

the tissue level material properties of a single osteon and interstitial lamellae of two longitudinal human (57 and 61 years old) tibial cortical bone. Results presented an elastic modulus of 22500 MPa and 25800 MPa for osteon and interstitial lamellae samples respectively (Table 2).

Ligament Structure and Composition

Ligaments are soft tissues that are fibrous in nature and composed primarily of collagen. They have a hierarchal structure of fibres, fibrils, sub fibrils, micro fibrils and tropocollagen but also contain water, proteoglycans and several glycoproteins. They function to guide and resist motion at a joint by connecting bone to bone. It has also been suggested that they act as a strain sensor to restrict degrees of freedom in order to stabilise the joint and prevent excessive movement [Harner et al., 1995; Woo et al., 2006]. Ligaments have direct and indirect insertions into the bone and periosteum respectively allowing variation in fibre bundles to respond to different movements and resist loading during ranges of rotation at the joint. The entheses portion of the ligament is stiffer compared to the medial portion allowing decreased concentrations of stress and therefore reducing the opportunity for damage or tears at the bone-ligament interface [Woo et al., 2006].

Ligaments as a complete structure are considered non-linear, anisotropic and homogeneous; however fibroblasts within the ligament are heterogeneous. Fibroblasts are situated parallel to the direction of the ligament, and play a role in the repair of damage on a micro-scale [Woo et al., 2006]. Collagen fibres within ligaments are crimped, in order to allow an easy transition of movement in low stress circumstances. As the crimp straightens the ligament exhibits non-linear behaviour. Only under higher stress circumstances will the ligament become stiffer and resist these forces in order to protect the joint from excessive

displacement (Nigg & Herzog, 2006). The viscoelastic behaviour of ligaments can be attributed to various structures such as collagen fibres, extracellular matrix or fluid content [Rubin & Bodner, 2002; Chimich et al., 1992]. Their anisotropy dictates directional dependence during loading meaning viscoelastic response will be determined by the direction of applied load [Bonifasi-Lista et al., 2005]. Knowledge of ligament viscoelastic behaviour can improve understanding of individual tissue material behaviour in relation to structure and function during injury and disease [Bonifasi-Lista et al., 2005]. Following injury, viscoelastic properties improve with healing; however do not return to normal [Thornton et al., 2000]. Additionally during ageing, important structural components will diminish, including collagen content which play an important role in the viscoelastic response [Woo et al., 1991].

Ligaments usually experience loading in multiple directions, where material properties are correlated with its specific orientation, structure and loading axis [Woo et al., 2006]. Variations seen within the literature can be partly attributed to the orientation that is used. A comparison of both longitudinal and transverse behaviour of human MCL's showed marked differences between the two, where longitudinal modulus was significantly higher [Quapp et al., 1998]. Further orientation in relation to loading axis showed ligaments tested along their native axis compared to the tibial axis were also significantly higher in material property values [Woo et al., 1991].

Ligament Literature Review

When measuring material properties of knee ligaments (ACL, PCL, MCL and LCL) typical analyses includes tensile stress and strain at ultimate failure, tangent modulus and strain energy density, primarily obtained using a tensile testing machine. These parameters are

tested *in vitro* by taking either a cross-section of the involved ligament [Quapp & Weiss, 1998] or more commonly a bone-ligament-bone sample (e.g. Fig. 4). During this process bone blocks are ordinarily embedded within polymethyl-methacrylate (PMMA) and the ligaments are wrapped in saline soaked gauze for protection [Harner et al., 1995; Butler et al., 1992; Momersteeg et al., 1995; Hewitt et al., 2001; Robinson et al., 2005; Bonner et al., 2015]. Additionally samples may be tested as a whole structure or divided into anatomical fibre bundles. Woo et al., [2006] suggests that the ACL has an anteromedial and posterolateral bundle and the PCL has an anterolateral and posteromedial bundle which are loaded differently. Ligaments therefore may need to be separated during tensile testing, in order to gain a true understanding of their unique material properties. A summary of the reviewed ligament material property research papers is provided in Table 3.

Table 3. Summary of current literature for human knee ligament material properties including location and number of samples, age, gender, health status of donors, testing technique and resultant data. N.B. for comparison purposes only those papers testing ligaments to failure will be included in this table. Abbreviations: GNS (gender not specified); F (female); M (male); ACL (anterior cruciate ligament); PCL (posterior cruciate ligament); MCL (medial collateral ligament); LCL (lateral collateral ligament). *Values are approximated from graph data.

Author	Quantity & Locality	Age, Gender & Health Status	Testing Technique	**Results**					
				Tissue Type	**Stiffness N/mm**	**Failure Load N**	**Elastic Modulus MPa**	**Max Stress MPa**	**Max Strain %**
Trent et al., 1976	7 x ACL, PLC, MCL & LCL	Age: 29-55; Gender: NS; Health: Healthy	Bone-Ligament-Bone	*ACL* *PCL* *MCL* *LCL*	138.3 179.5 70.6 59.8	620.8 658.0 515.8 376.6			
Noyes & Grood, 1976	26 x ACL	Age: 16-86; Gender: NS; Health: Healthy	Bone-Ligament-Bone	*Young* *Old*	182.0 129.0	1730.0 734.0	*111.0* *65.3*	*37.8* *13.3*	*44.3* *30.0*
Butler et al., 1986	3 x ACL, PLC & LCL	Age: 21-30; Gender: 2F/1M; Health: Healthy	Bone-Ligament-Bone	*ACL* *PCL* *LCL*			*278.0-310.0** *280.0-447.0** *375.0-25.0**	*30.0-40.0** *34.0-44.0** *31.0-43.0**	*14.0-16.0** *14.0-19.0** *11.0-17.0**
Woo et al., 1991	27 x ACL Bilateral	Age: 22-97; Gender: NS; Health: Healthy	Bone-Ligament-Bone	*Young 22-35* *Middle 40-50* *Old 60-97*	218.0-242.0 192.0-220.0 124.0-180.0	1602.0-2160.0 1160.0-1503.0 495.0-658.0			
Butler et al., 1992	7 x ACL	Age: 26±4; Gender: NS; Health: Healthy	Bone-Ligament-Bone	*Anteromedial Fibres* *Anterolateral Fibres* *Posterior Fibres*			238.1 285.9 154.9	54.7 30.6 15.4	19.1 16.1 15.2
Race & Amis, 1994	10 x PCL	Age: 53-98; Gender: NS; Health: Healthy	Bone-Ligament-Bone	*Anterolateral Fibres* *Posteromedial Fibres*	*347.0* *77.0*	1620.0 258.0	248.0 145.0	35.9 24.4	18.0 19.5
Harner et al., 1995	5 x PCL	Age: 48-77; Gender: NS; Health: Healthy	Bone-Ligament-Bone	*Anterolateral Fibres* *Posteromedial Fibres*	120.0 57.0	1120.0 419.0			
Quapp & Weiss, 1998	10 X MCL	Age: 62±18; Gender: NS; Health: Healthy	Ligament Sample Only	*Longitudinal* *Transverse*			38.6 1.7		17.1 1.7

Robinson et al., 2005	8 x MCL	Age: 77±5.3; Gender: NS; Health: Healthy	Bone-Ligament-Bone	*Superficial MCL* *Deep MCL* *Posteromedial capsule*		534.0 194.0 425.0			
Chandrashekar et al., 2006	17 x ACL	Age: 17-50; Gender: 9F/8M; Health: Healthy	Bone-Ligament-Bone	*ACL Total* *Male* *Female*	250.0 308.0 199.0	1526.0 1818.0 1266.0	113.0 128.0 99.0	24.4 26.4 22.8	

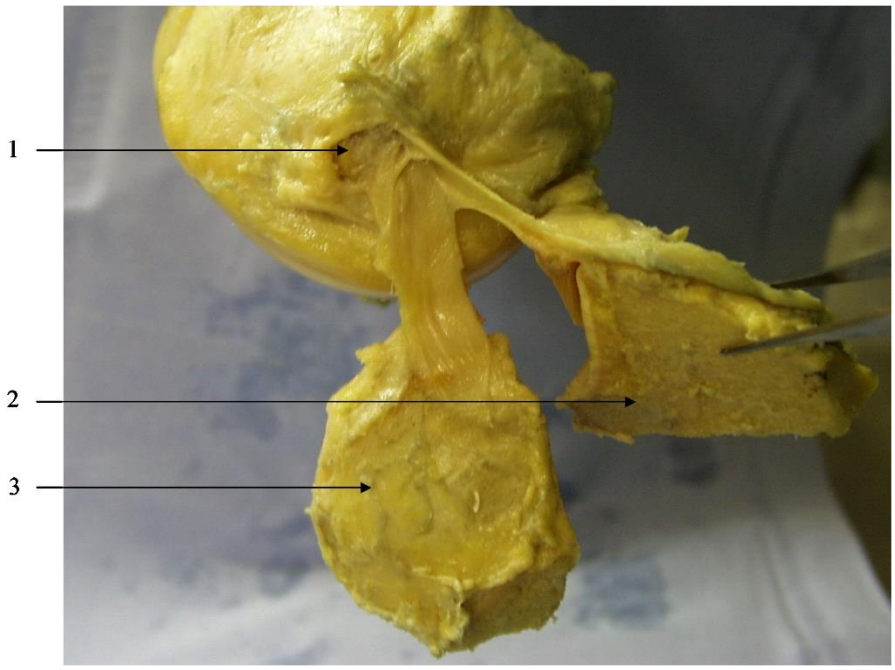

Figure 4. Medial collateral bone–ligament–bone tensile testing specimen which is divided into the 1) sMCL (superficial medial collateral ligament) (image is post-failure of this fibre attachment at the medial epicondyle of femur), 2) PMC (posteromedial capsule) fibres and bone block, 3) dMCL (deep medial collateral ligament) fibres and bone block. (Adopted from Robinson et al., [2005]: Elsevier License Permission: 4095850605057).

Harvesting a cross-sectional area of a ligament, Quapp & Weiss, [1998] explored the longitudinal and transverse mechanical behaviour of the MCL from ten human cadavers (62 ± 18 years old). Specimens were preconditioned and loaded to failure. Results included average tensile strength (38.6 MPa and 1.7 MPa), average ultimate strain (17.1 % and 1.7 %) and average tangent modulus (332.2 MPa and 11.0 MPa) for longitudinal and transverse specimens respectively (Table 3).

Further research on the tensile properties of ligaments utilised the bone-ligament-bone method. One of the first studies to explore ligament material properties harvested the ACL, PCL, MCL and LCL from seven healthy human cadavers aged 29 - 55 years old (gender not specified). Ligaments were preconditioned over five cycles and loaded to failure at 100 % strain rate, which is a change in strain equivalent to the initial length of the ligament. Stiffness was measured at 138.3 N/mm, 179.5 N/mm, 70.3 N/mm and 59.8 N/mm for the ACL, PCL, MCL and LCL respectively, whilst failure load resided at 620.8 N, 658.0 N, 515.8 N and 376.6 N (Table 3) [Trent et al., 1976].

Noyes & Grood, [1976] tested young (16 - 26 years old) and old (48 - 86 years old) anterior cruciate bone-ligament-bone material properties, also at a 100 % strain rate, although excluded any preconditioning. The research found a reduction in stiffness (129 and 182 N/mm), failure load (734.0 and 1730.0 N), elastic modulus (65.3 and 111.0 MPa), maximum stress (13.3 and 37.8 MPa) and strain (30.0 and 44.3 %) when comparing older samples to younger samples respectively (Table 3).

Butler et al., [1986] also tested young (21 - 30 years old) ACL, PCL and LCL elastic modulus (278 – 447 MPa), maximum stress (30 – 44 MPa) and maximum strain (11 - 19 %) where ranges were inclusive of all ligaments. Approximate values are given in Table 3 estimated from presented graphs [Butler et al., 1986]. The ligaments were divided into their fibre bundles and tested to failure at a 100 %/s strain rate (Table 3). Further research by Butler et al., [1992] looked at the differences in seven human ACL (26 ± 4 years old) divided into anteromedial, anterolateral and posterior fibre bundles. Specimens were not exposed to preconditioning but were loaded to failure at a 100 %/s strain rate. This resulted in anterior fibres having a higher maximum modulus (284 MPa), stress (38 MPa) and strain rate (17.6 %) when compared to posterior fibres (155 MPa, 15 MPa, 15.2 %) at failure (Table 3).

Race & Amis, [1994] and Harner et al., [1995] loaded to failure the anterolateral and posteromedial fibres bundles of the human PCL. Race & Amis, [1994] obtained ten samples from donors aged 53 – 98 years old which resulted in higher stiffness (347.0 N/mm and 770 N/mm), failure load (1620.0 N and 258.0 N), elastic modulus (248.0 MPa and 145.0 MPa) and maximum stress (35.9 MPa and 24.4 MPa) for the anterolateral fibres in comparison to the posteromedial fibres respectively (Table 3). Interestingly maximum strain was lower for the anterolateral fibres (18.0 %) when compared to the posteromedial fibres (19.0 %). Harner et al., [1995] tested five samples (48 – 77 years old) and also found a higher failure load in the anterolateral fibres (1120.0 N) in comparison to the posteromedial fibres (419.0 N) (Table 3) showing in both studies wide variation depending on the location of the tissue.

A more recent study by Robinson et al., [2005] harvested three sections of the femur-MCL-tibia complex from eight humans (77 ± 5.3 years old), namely the superficial MCL (SMCL), deep MCL (DMCL) and posteromedial capsule (PMC) based on fibre orientation and tested samples using the bone-ligament-bone approach. The SMCL is often used to define the overall MCL length; however it is thought that each section tenses and fully elongates under different loading axis or directions and functions to stabilise the knee joint in various ways. Samples were preconditioned and loaded to failure resulting in failure loads of 534 N, 194 N and 425 N for the SMCL, DMCL and PMC respectively (Table 3). The results indicated a bony avulsion in 75 % of tested samples after which the bone was removed and the end of the ligament was attached directly in the clamps and re-loaded to failure. Additionally mid-substance failure of the ligament as opposed to bony avulsion equated to 74 % higher maximum load.

Further variations in tensile properties can exist due to the angle of the femur in correlation with the tibia and the loading axis in correlation with ligament fibre loading

direction. Woo et al., [1991] preconditioned and tested the ACL to failure along both the tibial and ligament axis and found higher stiffness values on the ligament axis with increasing extension angle when testing young and old cadavers. Significant variations in anatomical orientation failure load were apparent between age groups: 2160 N for 22 – 35 years old (N = 9), 1503 N for 40 - 50 years old (N = 9) and 658 N for 60 – 97 years old (N = 9) (Table 3) as seen in Figure 5. However there was no correlation between age and orientation.

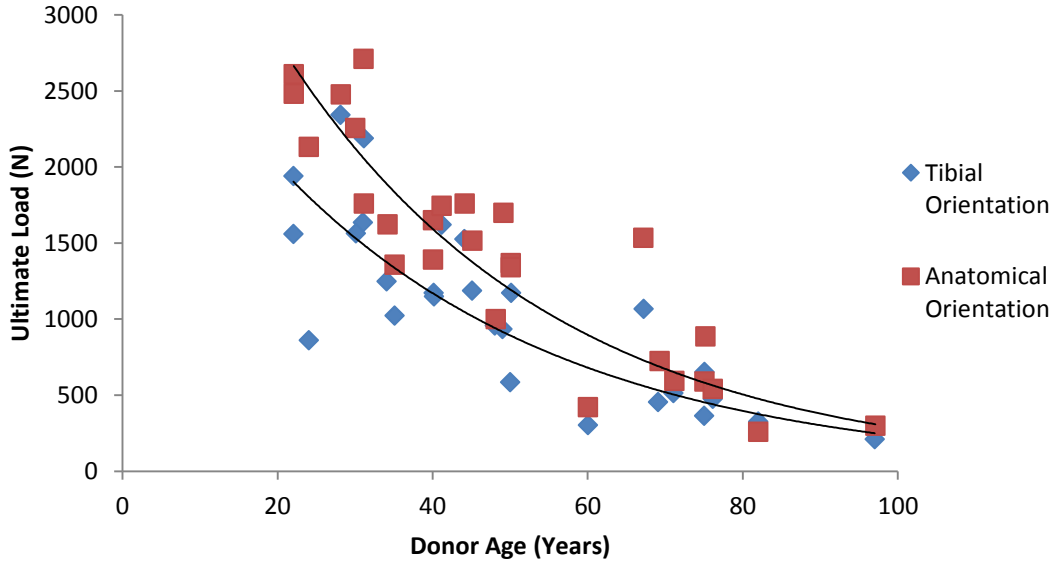

Figure 5. Effect of specimen age on anterior cruciate ligament (ACL) ultimate load. Data on ultimate load as a function of specimen age and orientation demonstrated that the strength of the ACL decreases in an exponential manner. (Recreated from Woo et al., [1991]: Sage Publishing Gratis Reuse Granted).

Interestingly, Chandrashekar et al., [2006] found gender-based differences in tensile properties showing human female ACL (N = 9) (17 – 50 years old) had 22.49 % lower elastic modulus and 8.3 % and 14.3 % lower maximum strain and stress respectively when

compared to human male ACL (N = 8) (26 – 50 years old) (Table 3). These differences can be partially accounted for due to the physically smaller size of the female ACL [Anderson et al., 2001; Chandrashekar et al., 2005]; however when adjusted for covariates the tensile properties of the ACL are still lower. This may in turn explain the higher rates of ACL injuries in female athletes [Chandrashekar et al., 2006].

Finally an analysis by Momersteeg et al., [1995] chose not to separate the fibre bundles but instead tilted the orientation of the loading axis at 5° increments (up to 25°) to recruit different fibres at varying angles to explore the changes in tensile properties during sub-ultimate testing. Bone-ligament-bone samples were harvested for the ACL, PCL, MCL and LCL of five human cadavers (63 - 81 years old) and subjected to preconditioning before applying up to 7 % and 10 % strain rates for the collateral and cruciate ligaments respectively. Results indicate that strain levels were higher for cruciate ligaments than collateral ligaments and for every 5˚ of tilt there was a decrease in tensile stiffness (averages: -11.6 Nmm^{-1} ACL, -20.96 Nmm^{-1} PCL, -2.66 Nmm^{-1} MCL, -3.76 Nmm^{-1} LCL) (Table 3). The research suggests there is a greater decrease in stiffness for the cruciate ligaments as they have a shorter and wider morphology when compared to the long thin nature of collateral ligaments. These authors go on to conclude that ligaments are highly sensitive to a small change in orientation and therefore unidirectional tensile testing is not effective at defining ligament stiffness properties [Momersteeg et al., 1995].

Section B: Finite Element (FE) Modelling

Freutel et al., [2014] presented a non-systematic review on the current research on FE modelling within soft tissues with a specific focus on the human knee joint and intervertebral disc. They reviewed strategies for modelling various material properties,

considering the interaction between soft tissues during contact and their sensitivity to changes in properties and environment (i.e. loading and boundary conditions). Their review concluded that inaccuracy or abstraction in each of these areas could manifest into important limitations in structurally complex models such as those of the human knee joint. Material property definition was cited by Freutel et al., [2014] and indeed by others [Gardiner & Weiss, 2003], as a research area with potential for significant improvement either through improved modelling approaches or *in vivo* inclusion of material properties particularly given the advances in techniques for characterising biological tissue behaviour in recent decades.

Following on from this review of available material property data for human knee joint tissues in *Section A* (above) the focus is subsequently on the material property data that has actually been utilised in published whole-joint FE models of the human knee. It is expected that clarifying the FE models that currently exist in the literature and their accuracy according to how they have obtained their material property data (i.e. primary data collection or from various data sets and donors) will help identify gaps within the knowledge and aid future directions for research.

Advances in FE modelling have allowed researchers to represent cartilage as a non-linear anisotropic material with varying material properties as opposed to the traditional representation of a linear elastic isotropic material. This advance means cartilage can now be presented more closely to biological reality and therefore computational predictions of behaviour are more accurate. Several authors have adopted this advanced approach in recent years [Tanska et al., 2015; Halonen et al., 2013]; however due to the complexity of such models and computational expensive approach, individual tissues are often modelled in isolation, meaning other structures not relevant to the research hypothesis are excluded.

Although useful in particular applications, if representing OA of the knee joint, modelling tissues in isolation has its limitations. It is now well established that this is a disease of the entire joint with molecular crosstalk and changes in subchondral bone structure [Lories & Luyten, 2011; Mahjoub et al., 2012], and histological evidence of ligament structural changes [e.g. Mullaji et al., 2008]. Therefore if investigating such diseases it is now inherently clear that whole-joint representation is needed to fully understand the implications of tissue interaction and disease progression on the knee joint.

When cartilage is modelled with linear elasticity it assumes an instantaneous response to stress and strain; however nonlinear representation allows for viscoelastic or time dependent factors such as those represented in Mononen et al., [2011] and Mononen et al., [2012]. It is now well established that cartilage and ligaments are nonlinear and viscoelastic and material property testing is starting to incorporate time-dependent testing by including a hold period. This review is intended to analyse whole-joint representations only. Studies presenting only singular tissues of the human knee joint with advanced modelling approaches are outside the scope of this review, although the recent efforts in modelling hyperelastic formulations of cartilage and efforts towards representing tissue anisotropy and viscoelasticity are summarised below.

Modelling cartilage as a fibril reinforced poroviscoelastic tissue with multiple material properties, Tanska et al., [2015] explored chondrocyte compression during walking, whilst research by Halonen et al., [2013] explored cartilage deformation under large compression. Further, work by Dabiri & Li [2013] also modelled cartilage with depth-dependent properties, making it possible to use a fibril-reinforced model to explore inhomogeneity within the tissue and analyses into fluid pressurization within the tissue. Meng et al., [2014] considered cartilage as a fibril reinforced biphasic material to explore knee joint contact

behaviour under body weight. Other examples of research representing cartilage as a poroelastic or poroviscoelastic material include the work of Kazemi et al., [2011], Mononen et al., [2011] and Mononen et al., [2012]. These studies represented whole-joints and are therefore discussed in more detail below.

For the purpose of this review, research papers that have presented a FE model of a healthy human knee joint incorporating the femur, tibia, cartilage and four major ligaments each within a 3D form will be presented, addressing how and where these models have sourced material property data for their models. Following this, models that have included all these structures but most commonly represented them in a simplified form of one, two and 3D forms will also be reviewed. Finally the existing attempts to simulate the effects of OA within the knee joint using FE models will be discussed.

3D FE Models of Healthy Human Knee Joints

This review reveals that FE models most commonly use previously published data for material properties; however there is usually a lengthy referencing chain when tracing these material properties to their original and primary data research article. Material properties are likely to vary with age, gender and disease status [e.g. Kleemann et al., 2005; Lindahl, 1976; Woo et al., 1991; Chandrashekar et al., 2006] and therefore donor demographics in previously published material property studies will undoubtedly impact upon the quantitative results obtained in FE analyses. This review highlights a wide spectrum of matches in this respect to the extent that the absence of appropriate data has in some cases led to the use of non-human material properties in FE models of the knee. Material property sources from reviewed FE models are summarised in Table 4.

Table 4. Summary of recent FE models of whole human knee joints, the purpose of the investigation with relevant loading and/or motion, and the type of sample each original primary data collection was based on including location of sample, and age if human samples were used. *Age not specified in original research article. **Multiple references are available in cited reference – unclear as to which study the FE model is using. ***Material properties are not represented – papers are referenced with use of geometry and orientation of structure. Abbreviations: ACL (anterior cruciate ligament); PCL (posterior cruciate ligament); MCL (medial collateral ligament); LCL (lateral collateral ligament)

	Purpose	Bone	Cartilage	Menisci	Ligaments
Blankevoort et al., 1991	Rigid and deformable articular contact during axial and varus/valgus rotations	N/a	Information untraceable**	N/a	Human (ACL, PCL, LCL) 43-74 years; Some information untraceable [Butler et al., 1986; Blankevoort et al., 1988***]
Blankevoort & Huiskes, 1991	Ligament-bone interaction during axial and varus/valgus rotations	N/a	Information untraceable**	N/a	Human (ACL, PCL, LCL) 43-74 years; Some information untraceable [Butler et al., 1986; Blankevoort et al., 1988***]
Bendjabellah et al., 1995	Articular cartilage deformation under compression up to 1000N	N/a	Human (tibial plateau) 48-70 years [Hayes & Mockros, 1971]	Human (menisci) 29-45 years; Some information untraceable [Tissakht & Ahmed, 1995]	Human (ACL, PCL, LCL) 53-98 year* [Butler et al., 1986; Race & Amis, 1994]
Bendjabellah et al., 1997	Role of collateral ligaments in varus-valgus motion	N/a	Human (tibial plateau) 48-70 years [Hayes & Mockros, 1971]	Human (menisci) 29-45 years; Some information untraceable [Tissakht & Ahmed, 1995]	Human (ACL, PCL, LCL) 53-98 year* [Butler et al., 1986; Race & Amis, 1994]
Jilani et al., 1997	Non-linear elastostatic response of ligaments during axial rotation with 10N torque	N/a	Human (tibial plateau) 48-70 years [Hayes & Mockros, 1971]	Human (menisci) 29-45 years; Some information untraceable [Tissakht & Ahmed, 1995]	Human (ACL, PCL, LCL) 53-98 year* [Butler et al., 1986; Race & Amis, 1994]
Bendjabellah et al., 1998	Anterior-posterior drawer forces on cartilage under compression up to 400N loads	N/a	Human (tibial plateau) 48-70 years [Hayes & Mockros, 1971]	Human (menisci) 29-45 years; Some information untraceable [Tissakht & Ahmed, 1995]	Human (ACL, PCL, LCL) 53-98 year* [Butler et al., 1986; Race & Amis, 1994]
Li et al., 1999	Ligament forces in response to internal-external moments up to 10Nm	N/a	Information untraceable**	N/a	Human (ACL, PCL, LCL) 43-74 years; Some information untraceable [Butler et al., 1986; Blankevoort et al., 1988***

Li et al., 2001	Cartilage contact stress sensitivity analysis with compression up to 1400N	N/a	Information untraceable	N/a	Human (ACL, PCL, LCL) 43-74 years; Some information untraceable [Butler et al., 1986; Blankevoort et al., 1988***]
Moglo & Shirazi-Adl, 2003	Cruciate ligament behavior under 100N femoral load in flexion	N/a	Human (tibial plateau) 48-70 years [Hayes & Mockros, 1971]	Human (menisci) 29-45 years; Some information untraceable [Tissakht & Ahmed, 1995]	Human (ACL, PCL, LCL) 53-98 year* [Butler et al., 1988; Race & Amis, 1994]
Beillas et al., 2004	*In vivo* kinematics and ground reaction forces during one leg hop with compression up to 1790N	Human (proximal femur and mid femur) 28-91 years* Bovine (distal femur and patella) Some information untraceable [Lotz et al., 1991; Reilly & Burstein, 1975; Mente & Lewis, 1994]	Human (tibial plateau) age not specified* Some information untraceable [Repo & Finlay, 1977]	Human (menisci) age not specified* [Fithian et al., 1990]	Human (ACL, PCL, MCL, LCL) 16-97 years*; Some information untraceable [Trent et al., 1976; Noyes & Grood, 1976; Woo et al., 1991]
Pena et al., 2005	Compare stresses on menisci and cartilage healthy joints to meniscal tears and meniscectomies under compression up to 1150N	N/a	Information untraceable	Canine (menisci) [LeRoux & Setton, 2002]	Theoretical Data [Weiss & Gardiner, 2001]
Pena et al., 2006	Ligament and Menisci behaviour in healthy during compressive load transmission up to 1150N	N/a	Information untraceable	Canine (menisci) [LeRoux & Setton, 2002]	Human (ACL, PCL, MCL, LCL) 37-74 years* [Butler et al., 1986; Gardiner & Weiss, 2003; Blankevoort et al., 1988***; Brantigan & Voshell, 1941***; Butler et al., 1990]
Donlagic et al., 2008	Simulated knee joint kinematics during flexion	Human (proximal femur and mid femur) years* Bovine (distal femur and patella) Some information untraceable [Lotz et al., 1991; Reilly & Burstein, 1975; Mente & Lewis, 1994]	Human (tibial plateau) age not specified*; Bovine (femoral condyle and tibial plateau); Porcine (femoral condyle and tibial plateau); Some information untraceable [Repo & Finlay, 1977; Laasanen, 2003]	Human (menisci) age not specified* [Fithian et al., 1990]	Human (ACL, PCL, MCL, LCL) 16-97 years*; Some information untraceable [Trent et al., 1976; Noyes & Grood, 1976; Woo et al., 1991]
Shirazi et al., 2008	Role of collagen fibrils under compression up to 2000N	N/a	Human (tibial plateau) 48-70 years [Hayes & Mockros, 1971]	Human (menisci) 29-45 years; Some information untraceable [Tissakht & Ahmed, 1995]	Human (ACL, PCL, LCL) 53-98 year* [Butler et al., 1986; Race & Amis, 1994]
Guo et al., 2009	Cartilage contact pressures during the gait cycle	Information untraceable	Information untraceable	Canine (menisci) [LeRoux & Settton, 2002]	Information untraceable

Yang et al., 2010	Tibiofemoral angle effect on cartilage pressure during stance phase of gait	N/a	Information untraceable**	Information untraceable	Human (ACL, PCL, LCL) 43-74 years; Some information untraceable [Butler et al., 1986; Blankevoort et al., 1988***]
Kazemi et al., 2011	Creep behaviour of cartilage and menisci under 300N compression in healthy	N/a	Bovine (humeral head) [Langelier & Buschmann, 1999; Woo et al., 1976]	Human (menisci) 29-45 years [Tissakht & Ahmed, 1995]	Human (Patella Tendon, Achilles Tendon) 29-93 years; Rat (Tail Tendon) [Hansen et al., 2006b; Johnson et al., 1994; Louis-Ugbo et al., 2004; Ault & Hoffman, 1992a]
Wang et al., 2014	Cartilage stress during kneeling and standing with up to 1000N compression	Human (tibial plateau and femoral neck) 53-93 years* [Rho et al., 1993; Zysset et al., 1999]	Human (femoral condyle and tibial plateau) 33-80 years [Shepherd & Seedhom, 1999a]	Human (menisci) 29-45 years*; Bovine (menisci); Some information untraceable [Tissakht & Ahmed, 1995; Skaggs et al., 1994]	Human (ACL, PCL, LCL, Quadriceps Tendon, Patella Ligament) 24-98 years*; Some information untraceable [Butler et al., 1986; Race & Amis, 1994; Staubli et al., 1999; Blankevoort et al., 1988***; Brantigan & Voshell, 1941***]
Mootanah et al., 2014	Joint forces/pressures due to malalignment with axial loads of 374N	Human (femoral condyle and tibial plateau) 45-68 years [Hobatho et al., 1991]	Human (femoral condyle and tibial plateau) 33-80 years [Shepherd & Seedhom, 1997; Blankevoort et al., 1988***]	Information untraceable	Human (ACL, PCL, MCL, LCL) 50 years Primary Data
Kazemi et al., 2014	Viscoelastic poromechanical response of cartilage and menisci with compression up to 700N	N/a	Human (tibial plateau) 48-70 years; Bovine (humeral head) [Langelier & Buschmann, 1999; Woo et al., 1976; Hayes & Mockros, 1971]	Human (menisci) 29-45 years [Tissakht & Ahmed, 1995]	Human (ACL, PCL, LCL, Patella Tendon, Achilles Tendon) 29-98 years*; Rat (Tail Tendon) [Butler et al., 1986; Race & Amis, 1994; Blankevoort et al., 1988***; Brantigan & Voshell, 1941***; Hansen et al., 2006b; Johnson et al., 1994; Louis-Ugbo et al., 2004; Ault & Hoffman, 1992a]

Wang et al., [2014] attempted to estimate cartilage stress under forces incurred during kneeling in a young healthy male (26 year-old), using primary MRI data to create their FE model (Fig. 6). The referencing chain starting from Wang et al., [2014] follows up to five secondary references until the original research article is cited. Original demographics include human tibial plateau and femoral neck samples for bone [Rho et al., 1993; Zysset et al., 1999], human femoral condyle and tibial plateau samples for cartilage [Shepherd & Seedhom, 1999a], human [Tissakht & Ahmed et al., 1995] and bovine menisci [Skaggs et al., 1994] and human ACL, PCL, LCL, quadriceps tendon and patella ligament samples for ligament material properties [Race & Amis, 1994; Woo et al., 1991; Staubli et al., 1999; Blankevoort et al., 1988; Brantigan & Voshell, 1941]. Where human samples were used for bone material properties the original research articles either do not state donor age [Rho et al., 1993] or donor age was 53-93 years old [Zysset et al., 1999]. Human cartilage ranged from 33 - 80 years old [Shepherd & Seedhom, 1999a] whilst menisci was either 29 - 45 years old [Skaggs et al., 1994] or information was not available. Human ligament samples had an average age of 24.9 years old [Staubli et al., 1999], an age range of 53 - 98 years old [Race & Amis, 1994], 43 - 74 years old [Blankevoort et al., 1988], or it stated that donors were 'young' [Butler et al., 1986] or it was unspecified [Brantigan & Voshell, 1941] (Table 4). The specific material properties used within Wang et al., [2014], can be found in the Table 5 alongside the material properties from other FE modelling studies reviewed.

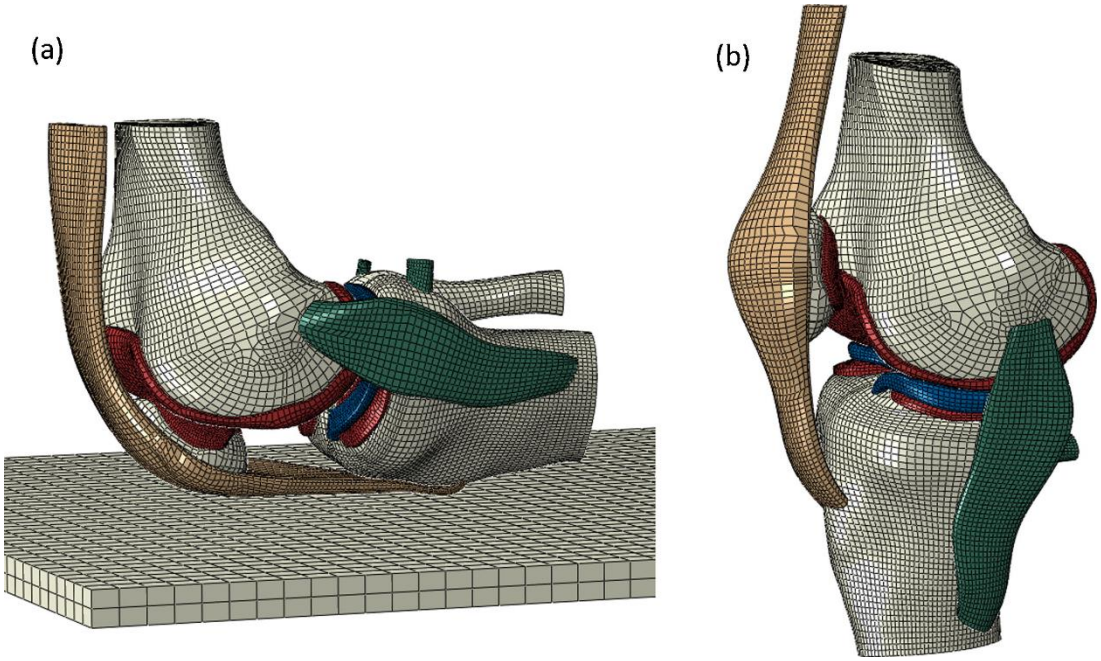

Figure 6. A FE model of the knee joint in (a) Kneeling position and (b) standing position. All structures are modelled in three dimension including the distal femur, proximal tibia and patella bones, femoral and tibial cartilage, medial and lateral menisci, ACL (anterior cruciate ligament), PCL (posterior cruciate ligament), MCL (medial collateral ligament), LCL (lateral collateral ligament) and patella tendon (Reproduced from Wang et al., [2014]: Elsevier License Permission: 4095850783229).

Table 5. Material property values included in each of the finite element modelling studies. Abbreviations: *E* (elastic modulus), *v* (Poisson's ratio), NM (not modelled), NS (not specified); ACL (anterior cruciate ligament); PCL (posterior cruciate ligament); MCL (medial collateral ligament); LCL (lateral collateral ligament).

	Bone		Cartilage		Menisci		ACL		PCL		MCL		LCL	
	E (MPa)	v	E (MPa)	v	E (MPa)	v	E (MPa) OR Stiffness (N)	Initial Strain (%/mm)	E (MPa) OR Stiffness (N)	Initial Strain (%/mm)	E (MPa) OR Stiffness (N)	Initial Strain (%/mm)	E (MPa) OR Stiffness (N)	Initial Strain (%/mm)
Wang et al., 2014	20,000	0.3	10	0.05-0.45	20-140	0.2	NS	0.0-0.1%	NS	0.0-0.1%	NS	0.0-0.1%	NS	0.0-0.1%
Pena et al., 2006	Rigid	Rigid	5	0.46	59	0.49	1.95 MPa	0.0-0.1%	3.25 MPa	0.0-0.1%	1.44 MPa	0.0-0.1%	1.44 MPa	0.0-0.1%
Pena et al., 2005	Rigid	Rigid	5	0.46	59	0.49	5.83 MPa	NS	6.06 MPa	NS	6.43 MPa	NS	6.06 MPa	NS
Guo et al., 2009	11,000	0.3	5	0.45	59	0.46	NS	NS	NS	NS	NS	NS	NS	NS
Mootanah et al., 2014	1,000	0.3	25	0.45	20-120	0.2-0.3	154 MPa	NS	40 MPa	NS	43 MPa	NS	56 MPa	NS
Kazemi et al., 2011	Rigid	Rigid	0.26-1600	0.36	0.5-28	0.36	10-14,000 MPa	NS	10-14,000 MPa	NS	10-14,000 MPa	NS	10-14,000 MPa	NS
Kazemi & Li, 2014	Rigid	Rigid	0.413-367.14	NS	0.0- 12.84	NS	46.47 - 1118.6 MPa	2.5%	46.47-1118.6 MPa	0%	46.47-1118.6 MPa	2%	46.5-1118.6 MPa	2%
Donlagic et al., 2008	1,000	0.3	67.6	0.3	130	0.3	200-260 MPa	NS	200-260 MPa	NS	114-134 MPa	NS	114-134 MPa	NS
Li et al., 2001	Rigid	Rigid	3.5-10	0.45	NM	NM	5000N	0.3-0.8mm	9000N	2.3-3mm	2750N	0.2-0.4mm	2000N	-0.4mm
Li et al., 1999	Rigid	Rigid	5	0.45	NM	NM	5000N	0.3-0.8mm	9000N	2.3-3mm	2750N	0.2-0.4mm	2000N	-0.4mm
Blankevoort et al., 1991;	Rigid	Rigid	5	0.45	NM	NM	5000N	0.06-0.1%	9000N	-0.03- -0.24%	2750N	0.03-0.04%	2000N	-0.05 – -0.25%
Blankevoort & Huiskes, 1991;	Rigid	Rigid	5	0.45	NM	NM	5000N	0.06-0.1%	9000N	-0.03- -0.24%	2750N	0.03-0.04%	2000N	-0.05 – -0.25%

Bendjabellah et al., 1995;	Rigid	Rigid	12	0.45	8-15	0.45	NS	1.2-4%	NS	-1 – -16.9%	NS	1.8-3.4%	NS	2.6-5%
Bendjabellah et al., 1997;	Rigid	Rigid	12	0.45	8-15	0.45	NS	1.2-4%	NS	-1 – -16.9%	NS	1.8-3.4%	NS	2.6-5%
Bendjabellah et al., 1998;	Rigid	Rigid	12	0.45	8-15	0.45	NS	1.2-4%	NS	-1 – -16.9%	NS	1.8-3.4%	NS	2.6-5%
Jilani et al., 1997;	Rigid	Rigid	12	0.45	8-15	0.45	NS	1.2-4%	NS	-1 – -16.9%	NS	1.8-3.4%	NS	2.6-5%
Moglo & Shirazi-Adl, 2003;	Rigid	Rigid	12	0.45	8-15	0.45	NS	1.2-4%	NS	-1 – -16.9%	NS	1.8-3.4%	NS	2.6-5%
Shirazi et al., 2008	Rigid	Rigid	12	0.45	8-15	0.45	NS	1.2-4%	NS	-1 – -16.9%	NS	1.8-3.4%	NS	2.6-5%
Yang et al., 2010	Rigid	Rigid	15	0.45	20-140	0.2-0.3	5000N	0.06-0.1%	9000N	-0.03- -0.24%	2750N	0.03-0.04%	2000N	-0.05 – -0.25%
Beillas et al., 2004	75-17500	0.3	20	0.45	250	0.45	150 MPa	NS	150 MPa	NS	60 MPa	NS	60 MPa	NS

Consecutive studies by Pena et al., [2005; 2006] carried out FE modelling of a healthy knee joint using CT and MRI data of a healthy male volunteer (age not specified) to generate a model that included bone, ligaments, tendons and articular and meniscal cartilages using previously published material property data. The aim of these studies were to compare healthy human knee biomechanics to meniscal tears and meniscectomies [Pena et al., 2005] and to analyse the non-uniform stress-strain fields that the menisci and ligaments encounter during the loading of the human knee joint [Pena et al., 2006]. The referencing chain starting from Pena et al., [2006] also follows up to four secondary references until the original research article is cited. As bones were modelled as rigid this requires no material property input; cartilage material properties could not be traced; menisci material properties were based on canine meniscal material properties [LeRoux & Setton, 2002] and ligaments on human ACL, PCL, MCL and LCL material properties with ages specified as 38 years old [Butler et al., 1990], 37 - 61 years old [91], 43 - 74 years old [Blankevoort et al., 1988] or simply denoted as 'young' [Butler et al., 1986] or unspecified [Brantigan & Voshell, 1941]. Pena et al., [2005] used the same original sources for cartilage and menisci material properties and adopted ligament material property data from a review article [Weiss & Gardiner, 2001], summarised in Table 4.

Guo et al., [2009] created a 3D human knee joint model from a CT scan on a 45 year old healthy female to understand the contact pressures on the femoral and tibial cartilages during different phases of the gait cycle. Material properties were referenced from previous FE modelling papers; however the referencing chain provides information that menisci data was originally presented by LeRoux & Setton, [2002] based on canine meniscal properties. Unfortunately, bone, cartilage and ligament material property sources cannot be traced back to a primary data collection reference (Table 4).

A recent FE study explored misalignment differentiation of the knee joint to understand how this influences contact pressure [Mootanah et al., 2014]. An MRI of a 50 year old cadaveric male was used for geometry and validation of the model through mounting the knee joint and matching loading and boundary conditions. Mootanah et al., [2014] obtained material properties from the literature with a referencing chain going back through three other research papers to the original primary research article. Bone material properties were based on human femoral condyle and tibial plateau samples aged 45 - 68 years old [Hobatho et al., 1991] whilst cartilage was based on ages stated as 33 - 80 years old [Shepherd & Seedhom, 99997; Shepherd & Seedhom, 1999b]. It is unclear how the meniscal material properties were obtained. Ligament material property data was obtained through primary data collection of the ACL, PCL, MCL and LCL giving validated values for the geometry of the FE model (Table 4).

Kazemi et al., [2011] used a MRI scan of a healthy 26 year old male to construct an FE model to understand the differences in creep behaviour of intact knee joints that have undergone meniscectomies. Subsequent research by Kazemi & Li, [2014] similarly used an MRI of a healthy 27 year old male, and modelled structures with the same modelling theories as Kazemi et al., [2011], although marginally adapted these material property inputs in order to understand the poroelastic response of soft tissues in the knee joint under large compression forces. Original data collection for material properties used within both studies was derived from bovine humeral head cartilage [Langelier & Buschmann, 1999; Woo et al., 1976] and human tibial plateau (29 - 45 years old) along with human menisci [Tissakht & Ahmed, 1995]. However ligament material properties, specifically toe region fibril data, were based on previous studies of the human patella tendon aged 29 - 93 years old [Hansen et al., 2006b; Johnson et al., 1994] and human calcaneal (Achilles) tendon aged 57 - 93 years old [Louis-Ugbo et al., 2004]. The non-fibril ligament material

properties can be traced back to a theoretical modelling paper [Ault & Hoffman, 1992a], whose results are represented in a companion paper with experimental work carried out on a rat tail tendon [Ault & Hoffman, 1992b]. Ligament initial strains used within Kazemi et al., [2014] can be traced back to Pena et al., [2006] which as discussed previously are originally sourced from human specimens aged 43 - 74 years old [Blankevoort et al., 1998], 53 - 98 years old [Race & Amis, 1994], or ages are described as 'young' [Butler et al., 1986] or unspecified [Brantigan & Voshell, 1941] (Table 4).

Simplified FE Models of the Healthy Human Knee Joint

For computational simplicity FE models of a human knee joint often make adjustments to their model including representing ligaments as non-linear one dimensional springs [e.g. Li et al., 2001; Blankevoort & Huiskes, 1991; Blankevoort et al., 1991; Li et al., 1999; Donlagic et al., 2008], bones as rigid bodies lacking material properties [e.g. Li et al., 2001; Li et al., 1999; Bendjaballah et al., 1995; Jilani et al., 1997; Shirazi et al., 2008] or exclusion of particular structures such as the menisci [e.g. Blankevoort & Huiskes, 1991; Blankevoort et al., 1991] or ligaments [Guess et al., 2010; Donahue et al., 2002; Donahue et al., 2003].

Models that have been highly simplified but still integrate all the main structures of the knee joint include studies by Blankevoort et al., [1991] and Blankevoort & Huiskes, [1991] who created mathematical models of the knee joint, developed originally by Wismans et al., [1980], specifically focusing on the articular contact and interaction between ligaments and bones. Utilising the previously developed modelling theories [Blankevoort & Huiskes, 1991; Blankevoort et al., 1991]. Li et al., [1999; 2001] used a MRI of a 65 year old male cadaver to create a 3D model of the knee joint and conducted a sensitivity analysis varying input parameters to assess the effect on joint contact stresses. In continuation, Yang et al.,

[2010] also utilised the work proposed by Blankevoort et al., [1991] and Blankevoort & Huiskes, [1991] to define MRI scans from three young volunteers (21 - 23 years old) to determine cartilage contact stress during gait; however noticeable differences between studies include the representation of the menisci within Yang et al., [2010].

Within these corresponding studies ligaments were modelled as 'bars', which are one-dimension (1D) non-linear tension-only elements with just two nodes, although material properties are still assigned. It should also be noted that Li et al., [2001] stated that ligament stiffness was optimised for the model to ensure numerical stability and model convergence. Blankevoort et al., [1991], Blankevoort & Huiskes, [191], Yang et al., [2010], Li et al., [1999] and Li et al., [2001] sourced ligament material properties from human ACL, PCL and LCL samples aged 'young' [Butler et al., 1986] or aged 43 - 74 years old [Blankevoort et al., 1988]. Unfortunately, cartilage material properties were ambiguous due to multiple references available in the cited sources [Kempson, 1980; Mow et al., 1982] making the origin of the input data unclear. Additionally, the menisci were modelled within Yang et al., [2010]; however the original data collection reference could not be traced. Referencing information from these FE studies are summarised in Table 4.

Except for simplifying anatomical geometry it is also common for investigators to reuse medical image data sets to create different models. In sequential studies CT data of a 27 year-old female was used to construct a FE model of the human knee joint to explore contact pressures [Bendjaballah et al., 1995], varus and valgus alignment [Bendjaballah et al., 1997], axial rotation [Jilani et al., 1997], anterior-posterior forces [Bendjaballah et al., 1998], ACL and PCL coupling [Moglo & Shirazi-Adl, 2003] and cartilage collagen fibril response to compression [Shirazi et al., 2008]. Figure 7 illustrates the model created within these studies and highlights the differences in comparison to Figure 6 in mesh generation

and inclusion of all structures in 3D form. When tracing the material properties assigned to structures within these corresponding FE models cartilage primary data was ascertained from human tibial plateau samples aged 48 - 70 years old [Hayes & Mockros, 1971], ligaments from human ACL, PLC, and LCL samples, referenced with ages of 53 - 98 years old [Race & Amis, 1994], or from samples described as 'young' [Butler et al., 1986]. Menisci material properties were based on human meniscal samples aged 29 - 45 years old [Tissakht & Ahmed, 1995] alongside additional data which could not be traced (Table 4).

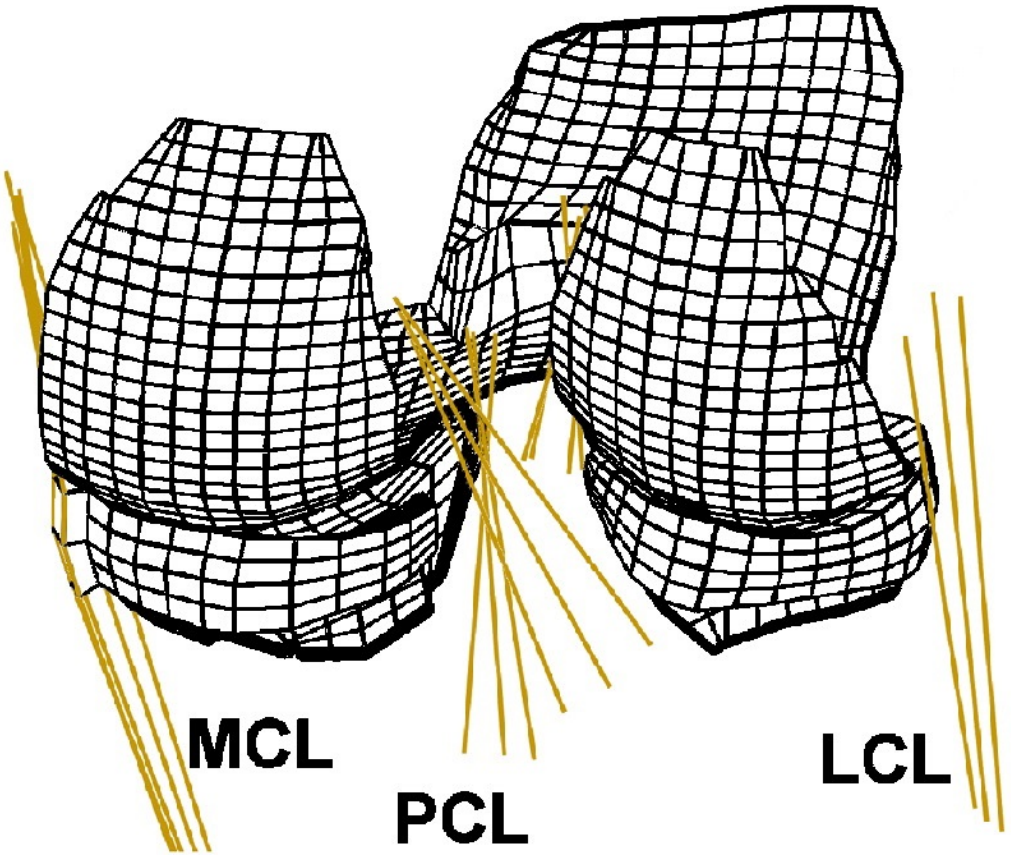

Figure 7. Posterior view of a finite element mesh showing soft tissues (menisci and articular cartilage layers). Ligaments are modelled as one dimensional line elements. Rigid bodies representing the femur and the tibia are not shown. (Reproduced from Shirazi et al., [2008]: Elsevier License Number: 4095851087452).

Another simplified FE model was developed by Beillas et al., [2004] who modelled the whole lower limb of a 30 year old male and coordinated this with *in vivo* kinematics of a one-leg hop. However, this model was simplified with a 1D representation of the ligaments. Bone material properties were originally obtained from proximal femur and mid femur human samples aged either 28 - 91 years old [Lotz et al., 1991], or age was unspecified [Reilly & Burstein, 1975], or bovine samples were used [Mente & Lewis, 1994]. Cartilage material properties can be traced to human tibial plateau samples although age was not specified [Repo & Finlay, 1977] and some further cartilage information was untraceable. Menisci data also came from human samples although again age was not specified [Fithian et al., 1990]. Finally, ligament material properties were based on human ACL, PCL, MCL, and LCL data obtained from donors aged 16 - 86 years old [Noyes & Grood, 1976], 29 - 55 years old [Trent et al., 1976], and 22 - 97 years old [Woo et al., 1991] (Table 4).

Incorporating some of the material properties presented by Beillas et al., [2004], Donlagic et al., [2008] utilised a patient specific approach to derive geometry and loads for their FE model using an MRI of a 22 and 52 year old male alongside primary kinematic data of flexion and extension locomotion. However additional material property sources were also used for the representation of the cartilage including bovine and porcine femoral condyle and tibial plateau samples [Laasanen, 2003] (Table 4).

FE Models of OA Human Knee Joints

It was discussed previously (*Section A*, above) that changes in tissues structure during OA progression can result in changes in material properties. This in turn would correlate with a change in the response to loads and biomechanics of the whole knee joint. With this in mind, FE modelling has the potential to analyse such alterations in the presence of OA,

assuming that tissue material properties representative of diseased tissues are incorporated into models. Although some FE studies have attempted to investigate contact stresses to understand how OA can initiate and progress [Pena et al., 2007; Dong et al., 2011; Mononen et al., 2011; Mononen et al., 2012] or how arthroplasty procedures can affect the knee joint [e.g. Baldwin et al., 2012; Tuncer et al., 2013] there is only a handful of research papers that utilise a whole knee joint FE model based specifically on healthy versus OA material properties.

One of the first studies to attempt this examined how osteochondral defects influence the ongoing degeneration and stress concentrations of cartilage in the knee joint during compression based on the geometry and anatomical location of the defect as seen in Figure 8 [Pena et al., 2007]. Healthy material properties were identical to Pena et al., [2006] described in detail above and therefore included human and canine tissue. However, when modelling cartilage with defects the elastic modulus of the cartilage was adjusted to 1.5 MPa with data originally sourced from Athanasiou et al., [1995] who explored the elastic modulus of rabbit cartilage with artificially induced OA. A similar study by Dong et al., [2011] also explored the cartilage defects but kept the elastic modulus consistent for both healthy and OA simulations.

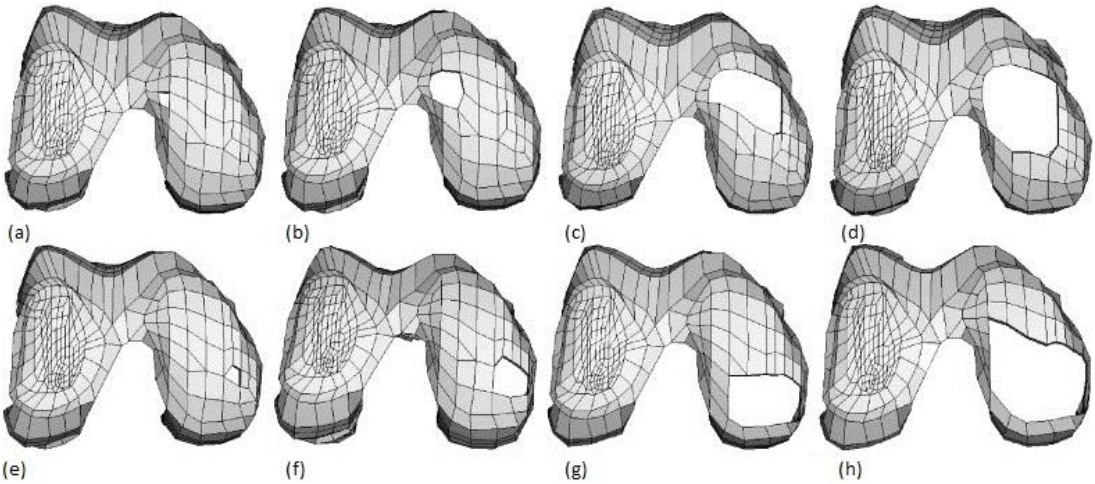

Figure 8. A FE model of cartilage defects in a high-weight-bearing area in the medial condyle: (a) 0.19 cm^2 area defect; (b) 0.78 cm^2 area defect; (c) 1.76 cm^2 area defect; and (d) 3.14 cm^2 area defect and a low-weight-bearing area in the medial condyle: (e) 0.19 cm^2 area defect; (f) 0.78 cm^2 area defect; (g) 1.76 cm^2 area defect; and (h) 3.14 cm^2 area defect. (Adopted from Pena et al., [2007]: Elsevier License Number: 4095850931678).

Although not modelling a whole knee, consecutive studies by Mononen et al., [2011; 2012] segmented the femoral and tibial cartilage from 29 and 61 year old healthy males for FE analysis modelling the cartilage with fibril-reinforced poroviscoelastic properties. Mononen et al., [2011] compared normal, OA and repaired cartilage giving a strain dependent fibril network modulus of 673 MPa, 168 MPa and 7 - 505 MPa respectively; an initial fibril network modulus of 0.47 MPa, 0.47 MPa and 0.005 - 0.35 MPa respectively; an elastic modulus of 0.31 MPa, 0.08 MPa and 0.31 MPa respectively; and finally a Poisson's ratio of 0.42 for all samples. Mononen et al., [2012] compared only normal and OA samples with the same material properties. When following the referencing chain and tracing cartilage material properties back to their original research they used input data from bovine articular cartilage [DiSilvestro & Suh, 2001; Korhonen et al., 2003] where OA was artificially induced [Korhonen et al., 2003].

Discussion

Material Properties

There is considerable variation in the elastic modulus of articular cartilage obtained from the human knee joint within the literature. This can be at least attributed to differences in testing parameters and structure and quality of the tissue sample, in addition to known and ambiguous variation in donor characteristics. To summarise, samples within the literature include hydrated [Wilusz et al., 2013; Kleemann et al., 2005; Hori & Mockros, 1976; Franz et al., 2001; Wang et al., 2013; Shepherd & Seedhom, 1997; Shepherd & Seedhom, 1999a] and dehydrated [Wen et al., 2012] femoral and tibial localities and ages between 32 and 89 years old. Furthermore OA samples have been graded using the Collins [Collins, 1939 and Collins, 1949 cited in Wilusz et al., 2013], Bollet [Bollet et al., 1963 cited in Hori & Mockros, 1976] and Outerbridge [Outerbridge, 1961] scoring systems, creating inconsistencies in categorisation. Both confined and unconfined compression testing has been employed [Kleemann et al., 2005; Hori & Mockros, 1976; Thambyah et al., 2006] alongside indentation techniques [Franz et al., 2001; Shepherd & Seedhom, 1997; Shepherd & Seedhom, 1999a] and AFM [Wen et al., 2012; Wilusz et al., 2013; Wang et al., 2013]. Research also incorporates extensive ranges in testing specifications including indentation tip radius (10 nm – 30.4 mm) [Hori & Mockros, 1976; Wen et al., 2012; Franz et al., 2001; Shepherd & Seedhom, 1997; Shepherd & Seedhom, 1999a; Thambyah et al., 2006; Wilusz et al., 2013; Wang et al., 2013], loading force (0.019 - 11.8 N) [Kleemann et al., 2005; Hori & Mockros, 1976] and recovery phases if included (5 mins) [Thambyah et al., 2006].

As discussed in Section A, length scale dependency can affect testing where heterogeneity can be more easily identified in cartilage using nanoindentation when compared to

microindentation [Stolz et al., 2009; Stolz et al., 2004], which is particularly important when changes due to OA can be subtle. When reviewing current efforts at measuring elastic modulus of human knee joint cartilage, variation will indeed exist due to differing length scales between 10 nm [Wen et al., 2012] and 30.4 mm [Hori & Mockros, 1976] subsequently having an effect on obtained modulus. Moreover, studies also present varying elastic modulus, namely instantaneous [Franz et al., 2001; Hori & Mockros, 1976; Shepherd & Seedhom, 1997; Shepherd & Seedhom, 1999; Thambyah et al., 2006; Wilusz et al., 2013] and equilibrium modulus with some citing a 30 second [Wen et al., 2012] to 10 minute [Kleemann et al., 2005] hold period. Under what circumstances these are measured will influence the results, and therefore the ability to compare across studies and accuracy apply such data in FE modelling. It has previously been shown that there are vast differences in instantaneous and equilibrium modulus, where instantaneous produces a much higher value [Julkunen et al., 2009], highlighting the need for a more standardised method of testing to determine any subtle change in material properties during healthy ageing and OA that may not be comparable across multiple data sources.

With these variations in mind elastic modulus for hydrated healthy cartilage samples varies between 0.1 – 18.6 MPa [Wilusz et al., 2013; Thambyah et al., 2006; Brittberg & Peterson, 1998; Bae et al., 2003; Shepherd & Seedhom, 1997; Shepherd & Seedhom, 1999a], hydrated OA grade 1 samples range between 0.5 - 10.2 MPa [Kleemann et al., 2005; Hori & Mockros, 1976; Franz et al., 2001; Wang et al., 2013] and hydrated OA grade 2 and 3 between 0.1 - 0.5 MPa [Wilusz et al., 2013; Kleemann et al., 2005; Wang et al., 2013], noting that different OA grading systems are used across these studies. Furthermore, age ranges stated within the literature have a wide variation, the broadest being 33 - 80 years old within one study [Shepherd & Seedhom, 1999a]. Some values cannot be explicitly linked to age ranges. Future work is required to more definitely define changes in cartilage

material properties associated to explicitly with age and therefore help understand how alterations through disease can be separated from alterations during healthy ageing.

In comparison to the available data on human knee joint cartilage, there is significantly less data for femoral or tibial bone samples. Indeed, this research found only one study that quantitatively measured material properties of cortical bone from the human knee joint [Rho et al., 1997]. Data on trabecular properties is present but it is difficult to compare data from different anatomical locations collected with different techniques, specifically traditional compression approaches [e.g. Lindahl, 1976; Goldstein et al., 1983; Burgers et al., 2008] and more recent nanoindentation methods [Rho et al., 1997], which is yet to be applied to the human femoral condyle. Similar ambiguity in the relationship between age and material properties also exists. Age ranges vary between 14 - 92 years old across studies with the smallest age cohort (with the exception of individual donors) spanning 20 years in one study [Goldstein et al., 1983]. Some studies also used donors under the age of 30 where donors may not have reached skeletal maturity and material properties may not reflect peak bone mass [Matkovic et al., 1994]. Overall, trabecular bone elastic modulus ranges from 1.9 - 664.0 MPa across reviewed studies [Behrens et al., 1974; Ducheyne et al., 1977; Carter & Hayes, 1977; Lindahl, 1976; Goldstein et al., 1983; Hvid & Hansen, 1985; Burgers et al., 2008; Zysset et al., 1994] and cortical bone from 22,500 - 25,800 MPa [Rho et al., 1997].

Studies reviewed in *Section A* mostly involve experimental work on trabecular bone which is less commonly used within FE models. Compression techniques utilised to obtain macro-scale measurements of trabecular bone as a whole structure as opposed to measuring individual trabeculae, will inevitably produce lower elastic modulus values due to the nature of testing; however more sophisticated techniques incorporating tissue level

material properties can more accurately represent a structure such as trabecular bone at the level in which it is typically modelled in FE research [Nigg & Herzog, 2006]. This variability in techniques inevitably makes a comparison between studies challenging as well as the lack of distinct age cohorts to ultimately define young and old parameters in order to definitively link this to a change in properties due to injury or disease, such as OA. Despite some research incorporating material properties of varying OA grades there are no healthy controls included to explicitly link significant findings to OA status [Zysset et al., 1994]. Evidently there is also no material property data for human trabecular bone obtained from the distal femur or proximal tibia at the tissue level, comparing healthy and OA samples.

It should be noted that the studies present varying indenter sizes ranging from 20 nm [Rho et al., 1997] to 2.5 mm [Hvid & Hansen, 1985]. A length scale under 200 nm is able to determine more heterogeneity in bone structure than those applied above 200 nm. When comparing studies discussed it should be considered that comparisons are challenging, and indeed reiterates the importance of site and subject-specific material properties, preferably obtained at the nano-scale to accuracy present the human knee joint using FE modelling [Yao et al., 2011].

Likewise, there is also significant variation in ligament tensile properties reported in the literature and this could be attributed to a number of factors including the variation in cadaver cohorts, equipment, testing protocol and technique, and structure and orientation of the sample. As discussed previously material properties of ligaments are correlated with orientation, structure and loading axis [Woo et al., 2006]. Experimental procedures for ligament material properties vary between cross-sectional samples [Momersteeg et al., 1995] or bone-ligament-bone samples spanning a variety of age ranges with current data in the literature ranging from 16 - 97 years old [Harner et al., 1995; Quapp & Weiss, 1998;

Butler et al., 1992; Robinson et al., 2005; Trent et al., 1976; Noyes & Grood, 1976; Butler et al., 1986; Race & Amis, 1994; Woo et al., 1991; Chandrashekar et al., 2006].These wide variations will in part dictate the material property outcomes. Preconditioning, which is often included as a 'warm up' for the ligament to achieve load-displacement parameters that are repeatable [Momersteeg et al., 1995] is absent from some research studies [Momersteeg et al., 1995; Noyes & Grood, 1976]. Furthermore data varies across individual studies where elastic modulus of the knee ligaments ranges between 1.7 - 447.0 MPa [Quapp & Weiss, 1998; Butler et al., 1992; Noyes & Grood, 1976; Butler et al., 1986; Race & Amis, 1994; Chandrashekar et al., 2006] and failure load between 194.0 - 2160.0 N [Harner et al., 1995; Robinson et al., 2005; Trent et al., 1976; Noyes & Grood, 1976; Race & Amis, 1994; Woo et al., 1991; Chandrashekar et al., 2006]. Comparisons between young and old have been correlated for the ACL in two studies [Noyes & Grood, 1976; Woo et al., 1991] both concluding that young donors have a higher stiffness and failure load. However, this is yet to be explored in the PCL, MCL and LCL along with research into how ligament tensile properties are correlated with pathological existence in the form of OA.

Variability exists across each tissue type reported in the literature potentially due to testing techniques, location, orientation of samples, length scale of testing and donor demographics. These differences between investigations makes inter study comparisons challenging and is related to the level of biorealism each study presents. However in the field of biomechanics the level of realism needed is in some instances is driven by the aims of the investigation. For example, work presented by Wen et al., [2012] aimed to understand individual cartilage collagen fibril changes during ageing and disease at the nano-scale. To achieve data at this length scale, samples were measured with a 10 nm indenter tip using AFM; however samples were dehydrated (as maintaining hydration during this technique is challenging), which would affect absolute material property values

obtained. As all samples were treated consistently a change in material properties to healthy controls were relative, and the absolute values were less important than the change seen. Although this was reflected in the realism of the values which were much higher than those studies that hydrated samples. Also measuring individual components, Rho et al, [1997] measured singular trabecular bone struts between two donors and therefore also required a nano-length scale with ability for spatial resolution to map indentations. Measuring material properties at smaller scales can help increase the level of biorealism by measuring individual structures; however being able to translate such measurements into a macro-scale representation may be challenging.

Other work presented by Thambyah et al., [2006] aimed to understand topographical variation of cartilage for the purposes of using localised values in FE modelling. An average moduli of structure was obtained as opposed to individual components, therefore samples were measured with a 1.0 mm indenter tip and a smaller scale was not needed. At a larger scale, cuboidal bone specimens were compressed in order to correlate modulus to bone mineral density [Burgers et al., 2008] making measurements at the macro-scale necessary for the aims of this investigation.

Other work by Shepherd and Seedhom, [1999a] looked to measure compressive stiffness from the proximal femur, tibia, and talus to understand site-specific properties. In this research instantaneous elastic modulus was used to make this comparison, and any viscous properties were not presented. Whilst simplicity can increase biological accuracy, non-linear behaviour is needed for biologically accurate representations of soft tissue [Dastjerdi et al., 2008]. However the aims of the investigation were for varying site comparisons and not extended formulations of elasticity despite this being more biologically representative of cartilage.

Biological accuracy can also be compromised by using animal samples and varying locations of samples. It is now well researched that animal material properties are not representative of human tissue [e.g. Demarteau et al., 2006; Jeffrey & Aspden, 2006], and also that varying anatomical locations have different material property values [e.g. Shepherd & Seedhom, 1999a]. Additionally, depending on the application intended may also dictate how material properties are utilised. For example some modelling studies aim to determine the behaviour of one isolated tissue, and therefore the realism needed for other surrounding tissues is of less importance [e.g. Tanska et al., 2015; Halonen et al., 2013]. Most often during FE analysis the bone is modelled as a rigid body [e.g. Pena et al., 2006; Li et al., 2001], which has been suggested to only make a difference of 2% to the resultant outputs from the model when compared to assigning *in vivo* material properties [Donahue et al., 2002]. If for example, researchers are obtaining material properties for use of cartilage 3D cell printing [e.g. Campos et al., 2012], the level of biorealism will naturally need to be higher. An interesting study by Zhang, [2001] discussed the need for biomechanical realism versus computational efficiency and weighed up whether realism or efficiency takes priority depending on the specific aim of the study in question.

FE Modelling

FE Models have been used for various applications involving the whole knee joint including healthy representation [e.g. Pena et al., 2006; Wang et al., 2014], joint replacement mechanics [e.g. Baldwin et al., 2012; Tuncer et al., 2013], meniscectomy research [Tanska et al., 2015], cartilage contact stresses [e.g. Li et al., 2001; Guo et al., 2009] and ligament-bone interaction [e.g. Blankevoort et al., 1991] to name a few. Material properties used within the reviewed FE models are often sourced from the literature including previous modelling studies or primary experimental research. This typically results in highly variable

data sets based on multiple structures and species. The material properties of human tissue vary according to its mineral and protein composition and the orientation of its micro-architecture [Wilusz et al., 2013; Marticke et al., 2010; Temple-Wong et al., 2009]. These factors in turn vary with anatomical location (e.g. femur vs humerus; knee vs ankle), age and health of the tissue. Therefore, donor characteristics will significantly impact results. It is clear that current whole joint FE models use material properties with highly variable, or non-specific material properties, with variation in the age, species, location and disease state of the tissue from which material properties were obtained

When the values used for material properties within published FE models are traced to their original research citation it becomes clear that there is considerable variation in terms of age range. FE models produced by Beillas et al., [2004] and Donlagic et al., [2008] have a total age range across all structures of 16 - 97 years old. The smallest age range used for material properties within a single study is 43 - 74 years old [Li et al., 2001; Blankevoort & Huiskes, 1991; Blankevoort et al., 1991; Li et al., 1999; Yang et al., 2010], with other ages ranging between 37 - 74 years old [Pena et al., 2005], 33 - 80 years old [Mootanah et al., 2014], 29 - 93 years old [Kazemi et al., 2014], 29 - 98 years old [Kazemi & Li, 2014; Bendjaballah et al., 1995; Jilani et al., 1997; Shirazi et al., 2008; Bendjaballah et al., 1997; Bendjaballah et al., 1998, Moglo & Shirazi-Adl, 2003] and 25 - 98 years old [Wang et al., 2014]. In many FE modelling studies, some information including age of donors from the original sources of material properties could not be traced [Pena et al., 2005; Pena et al., 2006; Wang et al., 2014; Li et al., 2001; Guo et al., 2009; Mootanah et al., 2014; Kazemi & Li, 2014; Blankevoort & Huiskes, 1991; Blankevoort et al., 1991; Li et al., 1999; Donlagic et al., 2008; Bendjaballah et al., 1995; Jilani et al., 1997; Shirazi et al., 2008; Yang et al., 2010; Bendjaballah et al., 1997; Bendjaballah et al., 1998, Moglo & Shirazi-Adl, 2003; Beillas et al., 2004]. Where material properties are categorised by age there are considerable differences

between cohorts, most noticeably in ligament data [Noyes & Grood, 1976; Woo et al., 1991]. In particular Woo et al., [1991] recorded the site of failure in ligaments when loaded in the anatomical location and concluded that in younger donors the ACL will predominantly fail by avulsion and in older donors the ACL will predominantly fail at the mid-substance, due to a change in material properties. This is especially important to factor into FE models if safety factors in the joint are being researched. The effect of using material properties from broad, and in some cases unknown age ranges, impacts on the conclusions of FE modelling is currently unclear because at present no study has compared these models to one constructed using anatomical geometry and material properties for all tissues from the same individual, or a homogeneous age and gender cohort of individuals. Such a model would clearly represent the 'gold-standard' with respect to geometry and material property definition in a FE knee model.

As well as wide variation in age, some FE models use material property data based just on tibial plateau cartilage [Kazemi & Li, 2014; Donlagic et al., 2008; Bendjaballah et al., 1995; Jilani et al., 1997; Shirazi et al., 2008; Bendjaballah et al., 1997; Bendjaballah et al., 1998; Moglo & Shirazi-Adl, 2003; Beillas et al., 2004] or bone samples lacking any femoral condyle measurements [Wang et al., 2014]. Furthermore, they may be based on non-knee joint anatomical locations including femoral neck and mid femur bone material properties [Donlagic et al., 2008; Beillas et al., 2004] and humeral head for cartilage material properties [Kazemi et al., 2011; Kazemi & Li, 2014]. As an example of the magnitude of disparity in material properties between different anatomical locations, Shepherd & Seedhom, [1999a] tested the elastic modulus of ankle, knee and hip joint cartilage finding differences of up to 6.8 MPa (36.6 %) between ankle and knee cartilage samples from the same donor and 3.6 MPa (30.54 %) between knee and hip cartilage samples from the same donor. Indeed, it has been shown that variations in material properties from the same

tissue exists within and across the knee joint suggesting that a location dependent modulus for various tissues would be most appropriate for FE models [Behrens et al., 1974; Deneweth et al., 2015; Akizuki et al., 1986]. Thus, while better than using values from outside the knee joint itself, representing structures with homogeneous (i.e. only one value) properties, or for example, assuming tibial and femoral material properties are identical, may be sub-optimal and functionally important. Ligament material properties are also often replicated where original data is only based on selective ligaments of the knee joint [Wang et al., 2014; Li et al., 2001; Kazemi & Li, 2014; Blankevoort & Huiskes, 1991; Blankevoort et al., 1991; Li et al., 1999; Bendjaballah et al., 1995; Jilani et al., 1997; Shirazi et al., 2008; Yang et al., 2010; Bendjaballah et al., 1997; Bedenjaballah et al., 1998; Moglo & Shirazi-Adl, 2003]. In some instances tendon data is used for the representation of ligament material properties including the quadriceps tendon [Wang et al., 2014], patella tendon [Wang et al., 2014; Kazemi et al., 2011; Kazemi & Li, 2014], Achilles tendon [Kazemi et al., 2011; Kazemi & Li, 2014] and rodent tail tendon [Kazemi et al., 2011; Kazemi & Li, 2014].

Animal material property data is also commonly used in the representation of human knee FE models including bovine [Wang et al., 2014; Mootanah et al., 2014; Shepherd & Seedhom, 1999b; Kazemi & Li, 2014; Donlagic et al., 2008; Beillas et al., 2004; Mononen et al., 2011; Mononen et al., 2012], canine [Pena et al., 2005; Pena et al., 2006; Guo et al., 2009], porcine [Donlagic et al., 2008], rat [Kazemi et al., 2011; Kazemi & Li, 2014] and rabbit [Pena et al., 2007] data. A number of recent studies have highlighted the structural, mechanical and physiological differences between bovine and human soft tissue and questioned the suitability of bovine material property data for functional studies of humans [Demarteau et al., 2006; Jeffrey & Aspden, 2006; Nissi et al., 2007; Pedersen et al., 2013; Plumb & Aspden, 2005]. Athanasiou et al., [1991] explored the differences between

material properties of cartilage from the femoral condyle of different species and found variation between the Poisson's ratio of human (0.074 - 0.098), canine (0.3 - 0.372), bovine (0.383 - 0.396), and rabbit (0.197 - 0.337) along with aggregate modulus of human (0.588 - 0.701 MPa), canine (0.603 - 0.904 MPa), bovine (0.894 - 0.899 MPa) and rabbit (0.537 - 0.741 MPa). Although differences were not statistically significant, potentially due to low samples numbers (n = 4 – 10) there was evidently a difference between species all of which have been used in some of the reviewed FE models.

As discussed earlier, it is very common for FE modeling studies to source and reference their material property data from previous modelling studies rather than the original experimental studies in which practical measurements were obtained. However, when the referencing chain is followed through sequentially cited modeling papers it is often the case that the primary experimental source of material property data is untraceable [e.g. Yang et al., 2010; Pena et al., 2006]. In other instances it eventually becomes clear that material property values are not source for direct experimental measures, but have been derived directly or indirectly from theoretical research in which mathematical solutions for modelling a specific structure have been derived [e.g. Mak et al., 1987 cited in Pena et al., 2005; Pena et al., 2006; Li et al., 2001; Guo et al., 2009].

Use of varying ages, species and anatomical locations for material property information undoubtedly represent important limitations in current FE models, but the magnitude of error is presently difficult to quantify and probably varies widely across studies due to the highly 'mixed' nature of input data used. At present, the best indication of error comes from studies that have conducted sensitivity analyses on material properties. Li et al., [2001] conducted a sensitivity analysis varying cartilage elastic modulus from 3.5 – 10 MPa and showed that peak contact stresses linearly increased by up to 10%, whilst an increase

in Poisson's ratio significantly varied peak von Mises stress by 100% in the knee joint cartilage. Additionally, a more sophisticated sensitivity analysis was carried out by Dhaher et al., [2010] who adjusted the intrinsic material properties of knee joint ligaments to aid understanding of the functional consequences of different activity levels, age, gender and even species. The research measured simulation outcomes by incorporating a multi-factorial global assessment, which indicated a change in tibial-femoral internal and external rotation, patella tilt and patella peak contact stresses, associated with modified ligament material properties [Dhaher et al., 2010].

This review of published material property (*Section A*) and FE modelling (*Section B*, above) studies of the human knee raises the question of how well specific cohorts or even human demographics can currently be accurately represented in a FE model. For example, does sufficient material property data exist to construct a whole-knee joint FE model representative of a young, healthy human or to represent a knee of any age with a specific category of OA? Attempting to build an FE model of a healthy knee joint from the literature data tabulated in *Section A* (Tables 1-3) yields data for healthy femoral and tibial cartilage, although without the breakdown of age specific material properties; healthy tibial cortical bone from older donors; healthy ACL, PCL, MCL and LCL from young donors, and ACL, PCL and MCL from healthy older donors. Thus, 'healthy' material properties can be pieced together from different studies for most tissues but mixing gender and a considerable age range (16 - 97 years old) is necessary. In terms of a model for studying OA, data exists for cartilage material properties based on OA grades 1 - 3 although this is not broken down into age categories, whilst trabecular bone material properties do exist for OA grades 1 - 3 for older donors although challenges occur as no healthy control was used within this particular study as a baseline measurement. Further, no study has yet explored the effect of OA on cortical bone material properties in the human knee. There is currently no data

incorporating the effect of OA on ligament material properties despite it being well known that there is a relationship between OA and ligament injury [Mullaji et al., 2008; Cushner et al., 2003]. However, there are currently no research papers to the authors' knowledge that have collected primary data on bone and cartilage material properties and used these measurements to build a subject specific FE model. Hence, material properties are still collated from various sources within the literature. A key goal for future research should be adoption of a more subject specific approach in which material properties from all tissues are derived from homogenous donor cohorts to improve accuracy and precision of knee FE models.

Conclusions and Future Directions

Integrating tissues-specific material property data into FE models has the potential to provide considerable insight into both healthy and diseased knee joint mechanics, circumventing the difficulty of direct invasive measures of human functionality. Herein, this review has provided a comprehensive summation and evaluation of existing material property data for human knee joint tissues with all numerical values tabulated as a reference resource for future studies. A renaissance in material testing and engineering approaches in the last decade has yielded an abundance of data on the mechanical properties of both hard and soft tissues from the human knee joint. However, comparison of material properties between studies can be challenging due to the differences in cadaver age, data collection techniques, including orientation of the tissue and loading specifics [Chandrashekar et al., 2006]. It is well documented that material properties alter during ageing [Hansen et al., 2006a], therefore the demographics of cadavers will highly influence material property data. This review highlights that material properties from multiple (>1) tissue types have rarely been collected from cadavers with homogeneous age, gender and

health status characteristics. More consistent data collection with particular emphasis on extracting data on multiple tissues from the same donors will enable a much more robust examination of the structural and mechanical changes occurring during ageing, injury and disease, notably during OA progression which currently represents a significant socio-economic burden that is likely to increase further within ageing populations.

The benefits of a more exhaustive subject- or cohort-specific approach to materials testing will inherently feed directly into improved FE models of whole-knee function. Efforts have been made to produce an openly available finite element model for clinical and scientific explorations to be made [Erdemir, 2016]. With more accurate material property data from cohort specific sources data could be applied into this freely available model without the need to obtain medical imagery to create a new FE model which is costly in time and resources. More demographically homogenous material property data sets will eliminate the current widespread use of material properties sourced from distinctively diverse human cadavers and/or animal specimens. Embracing this more systematic subject- or cohort-specific approach to FE modelling can only improve comparisons between injured and diseased tissue within the knee joint, and enhance understanding of behavioural response to mechanical loads observed during ageing or disease progression. It is notable at present that no FE modelling study has compared healthy and OA whole-knee joints. Increasing ageing populations within western societies provide particular incentive for this research with a clear need to direct research efforts into better integration of mechanical engineering approaches and biomechanical simulation, particularly in the presence of disease status.

References

1. Ahlback, S. 1968, "Osteoarthrosis of the knee. A radiographic investigation", *Acta Radiologica: Diagnosis,* pp. Suppl 277:7-72.
2. Akhtar, R., Sherratt, M.J., Cruickshank, J.K. & Derby, B. 2011, "Characterizing the elastic properties of tissues", *Materials Today,* vol. 14, no. 3, pp. 96-105.
3. Akizuki, S., Mow, V.C., Müller, F., Pita, J.C., Howell, D.S. & Manicourt, D.H. 1986, "Tensile properties of human knee joint cartilage: I. Influence of ionic conditions, weight bearing, and fibrillation on the tensile modulus", *Journal of Orthopaedic Research,* vol. 4, no. 4, pp. 379-392.
4. Anderson, A.F., Dome, D.C., Gautam, S., Awh, M.H. & Rennirt, G.W. 2001, "Correlation of anthropometric measurements, strength, anterior cruciate ligament size, and intercondylar notch characteristics to sex differences in anterior cruciate ligament tear rates", *The American Journal of Sports Medicine,* vol. 29, no. 1, pp. 58-66.
5. Armstrong, C.G. & Mow, V.C. 1982, "Variations in the intrinsic mechanical properties of human articular cartilage with age, degeneration, and water content", *The Journal of Bone and Joint Surgery. American Volume,* vol. 64, no. 1, pp. 88-94.
6. Athanasiou, K., Fischer, R., Niederauer, G. & Puhl, W. 1995, "Effects of excimer laser on healing of articular cartilage in rabbits", *Journal of Orthopaedic Research,* vol. 13, no. 4, pp. 483-494.
7. Athanasiou, K., Rosenwasser, M., Buckwalter, J., Malinin, T. & Mow, V. 1991, "Interspecies comparisons of in situ intrinsic mechanical properties of distal femoral cartilage", *Journal of Orthopaedic Research,* vol. 9, no. 3, pp. 330-340.

8. Ault, H. & Hoffman, A. 1992, "A composite micromechanical model for connective tissues: Part II—Application to rat tail tendon and joint capsule", *Journal of Biomechanical Engineering,* vol. 114, no. 1, pp. 142-146.
9. Ault, H. & Hoffman, A. 1992, "A composite micromechanical model for connective tissues: Part I—theory", *Journal of Biomechanical Engineering,* vol. 114, no. 1, pp. 137-141.
10. Bae, W.C., Temple, M.M., Amiel, D., Coutts, R.D., Niederauer, G.G. & Sah, R.L. 2003, "Indentation testing of human cartilage: sensitivity to articular surface degeneration", *Arthritis & Rheumatism,* vol. 48, no. 12, pp. 3382-3394.
11. Baldwin, M.A., Clary, C.W., Fitzpatrick, C.K., Deacy, J.S., Maletsky, L.P. & Rullkoetter, P.J. 2012, "Dynamic finite element knee simulation for evaluation of knee replacement mechanics", *Journal of Biomechanics,* vol. 45, no. 3, pp. 474-483.
12. Behrens, J., Walker, P. & Shoji, H. 1974, "Variations in strength and structure of cancellous bone at the knee", *Journal of Biomechanics,* vol. 7, no. 3, pp. 201-207.
13. Beillas, P., Papaioannou, G., Tashman, S. & Yang, K. 2004, "A new method to investigate *in vivo* knee behavior using a finite element model of the lower limb", *Journal of Biomechanics,* vol. 37, no. 7, pp. 1019-1030.
14. Bendjaballah, M., Shirazi-Adl, A. & Zukor, D. 1997, "Finite element analysis of human knee joint in varus-valgus", *Clinical Biomechanics,* vol. 12, no. 3, pp. 139-148.
15. Bendjaballah, M., Shirazi-Adl, A. & Zukor, D. 1998, "Biomechanical response of the passive human knee joint under anterior-posterior forces", *Clinical Biomechanics,* vol. 13, no. 8, pp. 625-633.
16. Bendjaballah, M.Z., Shirazi-Adl, A. & Zukor, D. 1995, "Biomechanics of the human knee joint in compression: reconstruction, mesh generation and finite element analysis", *The knee,* vol. 2, no. 2, pp. 69-79.

17. Blankevoort, L. & Huiskes, R. 1991, "Ligament-bone interaction in a three-dimensional model of the knee", *Journal of Biomechanical Engineering,* vol. 113, no. 3, pp. 263-269.
18. Blankevoort, L., Huiskes, R. & De Lange, A. 1988, "The envelope of passive knee joint motion", *Journal of Biomechanics,* vol. 21, no. 9, pp. 705711-709720.
19. Blankevoort, L., Kuiper, J., Huiskes, R. & Grootenboer, H. 1991, "Articular contact in a three-dimensional model of the knee", *Journal of Biomechanics,* vol. 24, no. 11, pp. 1019-1031.
20. Bobinac, D., Spanjol, J., Zoricic, S. & Maric, I. 2003, "Changes in articular cartilage and subchondral bone histomorphometry in osteoarthritic knee joints in humans", *Bone,* vol. 32, no. 3, pp. 284-290.
21. Bollet, A.J., Handy, J.R. & Sturgill, B.C. 1963, "Chondroitin sulfate concentration and protein-polysaccharide composition of articular cartilage in osteoarthritis", *The Journal of Clinical Investigation,* vol. 42, pp. 853-859.
22. Bonifasi-Lista, C., Lake, S.P., Small, M.S. & Weiss, J.A. 2005, "Viscoelastic properties of the human medial collateral ligament under longitudinal, transverse and shear loading", *Journal of Orthopaedic Research,* vol. 23, no. 1, pp. 67-76.
23. Bonner, T.J., Newell, N., Karunaratne, A., Pullen, A.D., Amis, A.A., Bull, A.M. & Masouros, S.D. 2015, "Strain-rate sensitivity of the lateral collateral ligament of the knee", *Journal of the Mechanical Behavior of Biomedical Materials,* vol. 41, pp. 261-270.
24. Brach, J.S., Berlin, J.E., VanSwearingen, J.M., Newman, A.B. & Studenski, S.A. 2005, "Too much or too little step width variability is associated with a fall history in older persons who walk at or near normal gait speed", *Journal of Neuroengineering and Rehabilitation,* vol. 2, no. 1, pp. 1.

25. Brantigan, O.C. & Voshell, A.F. 1941, "The mechanics of the ligaments and menisci of the knee joint", *The Journal of Bone and Joint Surgery. American Volume,* vol. 23, no. 1, pp. 44-66.
26. Brittberg, M. & Peterson, L. 1998, "Introduction of an articular cartilage classification", *ICRS Newsletter,* vol. 1, no. 1, pp. 5-8.
27. Burgers, T.A., Mason, J., Niebur, G. & Ploeg, H.L. 2008, "Compressive properties of trabecular bone in the distal femur", *Journal of Biomechanics,* vol. 41, no. 5, pp. 1077-1085.
28. Burr, D.B. 1998, "The importance of subchondral bone in osteoarthrosis", *Current Opinion in Rheumatology,* vol. 10, no. 3, pp. 256-262.
29. Butler, D., Sheh, M., Stouffer, D., Samaranayake, V. & Levy, M.S. 1990, "Surface strain variation in human patellar tendon and knee cruciate ligaments", *Journal of Biomechanical Engineering,* vol. 112, no. 1, pp. 38-45.
30. Butler, D.L., Guan, Y., Kay, M.D., Cummings, J.F., Feder, S.M. & Levy, M.S. 1992, "Location-dependent variations in the material properties of the anterior cruciate ligament", *Journal of Biomechanics,* vol. 25, no. 5, pp. 511-518.
31. Butler, D.L., Kay, M.D. & Stouffer, D.C. 1986, "Comparison of material properties in fascicle-bone units from human patellar tendon and knee ligaments", *Journal of Biomechanics,* vol. 19, no. 6, pp. 425-432.
32. Carter, D.R. & Hayes, W.C. 1977, "The compressive behavior of bone as a two-phase porous structure", *The Journal of Bone and Joint Surgery. American Volume,* vol. 59, no. 7, pp. 954-962.
33. Chandrashekar, N., Mansouri, H., Slauterbeck, J. & Hashemi, J. 2006, "Sex-based differences in the tensile properties of the human anterior cruciate ligament", *Journal of Biomechanics,* vol. 39, no. 16, pp. 2943-2950.

34. Chandrashekar, N., Slauterbeck, J. & Hashemi, J. 2005, "Sex-based differences in the anthropometric characteristics of the anterior cruciate ligament and its relation to intercondylar notch geometry: a cadaveric study", *The American Journal of Sports Medicine,* vol. 33, no. 10, pp. 1492-1498.
35. Chimich, D., Shrive, N., Frank, C., Marchuk, L. & Bray, R. 1992, "Water content alters viscoelastic behaviour of the normal adolescent rabbit medial collateral ligament", *Journal of Biomechanics,* vol. 25, no. 8, pp. 831-837.
36. Cohen, N.P., Foster, R.J. & Mow, V.C. 1998, "Composition and dynamics of articular cartilage: structure, function, and maintaining healthy state", *Journal of Orthopaedic & Sports Physical Therapy,* vol. 28, no. 4, pp. 203-215.
37. Collins, D. 1939, "The pathology of osteoarthritis", *British Journal of Rheumatology,* vol. 1, no. 248, pp. e62.
38. Collins, D.H. 1949, *The pathology of articular and spinal diseases,* Edward Arnold.
39. Cowin, S.C., Moss-Salentijn, L. & Moss, M.L. 1991, "Candidates for the mechanosensory system in bone", *Journal of Biomechanical Engineering,* vol. 113, no. 2, pp. 191-197.
40. Currey, J.D. 2012, "The structure and mechanics of bone", *Journal of Materials Science,* vol. 47, no. 1, pp. 41-54.
41. Cushner, F.D., La Rosa, D.F., Vigorita, V.J., Scuderi, G.R., Scott, W.N. & Insall, J.N. 2003, "A quantitative histologic comparison: ACL degeneration in the osteoarthritic knee", *The Journal of Arthroplasty,* vol. 18, no. 6, pp. 687-692.
42. Dabiri, Y. & Li, L. 2013, "Influences of the depth-dependent material inhomogeneity of articular cartilage on the fluid pressurization in the human knee", *Medical Engineering & Physics,* vol. 35, no. 11, pp. 1591-1598.
43. Dastjerdi, M.M. & Mahloojifar, A. 2008, "Towards realistic modeling of breast elasticity modulus alterations in medical simulation", *Knowledge Acquisition and*

Modeling Workshop, 2008. KAM Workshop 2008. IEEE International Symposium, pp. 1148.

44. Demarteau, O., Pillet, L., Inaebnit, A., Borens, O. & Quinn, T. 2006, "Biomechanical characterization and *in vitro* mechanical injury of elderly human femoral head cartilage: comparison to adult bovine humeral head cartilage", *Osteoarthritis and Cartilage,* vol. 14, no. 6, pp. 589-596.
45. Deneweth, J.M., Arruda, E.M. & McLean, S.G. 2015, "Hyperelastic modeling of location-dependent human distal femoral cartilage mechanics", *International Journal of Non-Linear Mechanics,* vol. 68, pp. 146-156.
46. Desrochers, J., Amrein, M.A. & Matyas, J.R. 2010, "Structural and functional changes of the articular surface in a post-traumatic model of early osteoarthritis measured by atomic force microscopy", *Journal of Biomechanics,* vol. 43, no. 16, pp. 3091-3098.
47. Dhaher, Y.Y., Kwon, T. & Barry, M. 2010, "The effect of connective tissue material uncertainties on knee joint mechanics under isolated loading conditions", *Journal of Biomechanics,* vol. 43, no. 16, pp. 3118-3125.
48. DiSilvestro, M.R. & Suh, J.F. 2001, "A cross-validation of the biphasic poroviscoelastic model of articular cartilage in unconfined compression, indentation, and confined compression", *Journal of Biomechanics,* vol. 34, no. 4, pp. 519-525.
49. Donahue, T.L.H., Hull, M., Rashid, M.M. & Jacobs, C.R. 2002, "A finite element model of the human knee joint for the study of tibio-femoral contact", *Journal of Biomechanical Engineering,* vol. 124, no. 3, pp. 273-280.
50. Donahue, T.L.H., Hull, M., Rashid, M.M. & Jacobs, C.R. 2003, "How the stiffness of meniscal attachments and meniscal material properties affect tibio-femoral contact

pressure computed using a validated finite element model of the human knee joint", *Journal of Biomechanics,* vol. 36, no. 1, pp. 19-34.

51. Dong, Y., Hu, G., Zhang, L., Hu, Y., Dong, Y. & Xu, Q. 2011, "Accurate 3D reconstruction of subject-specific knee finite element model to simulate the articular cartilage defects", *Journal of Shanghai Jiaotong University (Science),* vol. 16, pp. 620-627.
52. Donlagic, D., Cigale, B., Heric, D., Cibula, E., Zazula, D. & Potocnik, B. 2008, "A Patient-specific Knee Joint Computer Model Using MRI Data and '*in vivo*' Compressive Load from the Optical Force Measuring System", *CIT.Journal of Computing and Information Technology,* vol. 16, no. 3, pp. 209-222.
53. Ducheyne, P., Heymans, L., Martens, M., Aernoudt, E., de Meester, P. & Mulier, J.C. 1977, "The mechanical behaviour of intracondylar cancellous bone of the femur at different loading rates", *Journal of Biomechanics,* vol. 10, no. 11, pp. 747-762.
54. Ebenstein, D. & Pruitt, L. 2004, "Nanoindentation of soft hydrated materials for application to vascular tissues", *Journal of Biomedical Materials Research Part A,* vol. 69, no. 2, pp. 222-232.
55. Ebenstein, D.M. & Pruitt, L.A. 2006, "Nanoindentation of biological materials", *Nano Today,* vol. 1, no. 3, pp. 26-33.
56. Elias, J.J. & Cosgarea, A.J. 2007, "Computational modeling: an alternative approach for investigating patellofemoral mechanics", *Sports Medicine and Arthroscopy Review,* vol. 15, no. 2, pp. 89-94.
57. Erdemir, A. 2016, "Open Knee: Open Source Modeling and Simulation in Knee Biomechanics", *Journal of Knee Surgery,* vol. 29, no. 02, pp. 107-116.
58. Fithian, D.C., Kelly, M.A. & Mow, V.C. 1990, "Material properties and structure-function relationships in the menisci", *Clinical Orthopaedics and Related Research,* vol. 252, pp. 19-31.

59. Franz, T., Hasler, E., Hagg, R., Weiler, C., Jakob, R. & Mainil-Varlet, P. 2001, "In situ compressive stiffness, biochemical composition, and structural integrity of articular cartilage of the human knee joint", *Osteoarthritis and Cartilage,* vol. 9, no. 6, pp. 582-592.
60. Freutel, M., Schmidt, H., Dürselen, L., Ignatius, A. & Galbusera, F. 2014, "Finite element modeling of soft tissues: Material models, tissue interaction and challenges", *Clinical Biomechanics,* vol. 29, no. 4, pp. 363-372.
61. Gardiner, J.C. & Weiss, J.A. 2003, "Subject-specific finite element analysis of the human medial collateral ligament during valgus knee loading", *Journal of Orthopaedic Research,* vol. 21, no. 6, pp. 1098-1106.
62. Goldstein, S.A., Wilson, D.L., Sonstegard, D.A. & Matthews, L.S. 1983, "The mechanical properties of human tibial trabecular bone as a function of metaphyseal location", *Journal of Biomechanics,* vol. 16, no. 12, pp. 965-969.
63. Guess, T.M., Thiagarajan, G., Kia, M. & Mishra, M. 2010, "A subject specific multibody model of the knee with menisci", *Medical Engineering & Physics,* vol. 32, no. 5, pp. 505-515.
64. Guilak, F., Fermor, B., Keefe, F.J., Kraus, V.B., Olson, S.A., Pisetsky, D.S., Setton, L.A. & Weinberg, J.B. 2004, "The role of biomechanics and inflammation in cartilage injury and repair", *Clinical Orthopaedics and Related Research®,* vol. 423, pp. 17-26.
65. Guo, H., Maher, S.A. & Spilker, R.L. 2013, "Biphasic finite element contact analysis of the knee joint using an augmented Lagrangian method", *Medical Engineering & Physics,* vol. 35, no. 9, pp. 1313-1320.
66. Guo, H., Maher, S.A. & Torzilli, P.A. 2015, "A biphasic finite element study on the role of the articular cartilage superficial zone in confined compression", *Journal of Biomechanics,* vol. 48, no. 1, pp. 166-170.

67. Guo, Y., Zhang, X. & Chen, W. 2009, "Three-Dimensional Finite Element Simulation of Total Knee Joint in Gait Cycle", *Acta Mechanica Solida Sinica,* vol. 22, no. 4, pp. 347-351.

68. Halonen, K.S., Mononen, M.E., Jurvelin, J.S., Töyräs, J. & Korhonen, R.K. 2013, "Importance of depth-wise distribution of collagen and proteoglycans in articular cartilage—A 3D finite element study of stresses and strains in human knee joint", *Journal of Biomechanics,* vol. 46, no. 6, pp. 1184-1192.

69. Hansen, P., Bojsen-Moller, J., Aagaard, P., Kjaer, M. & Magnusson, S.P. 2006b, "Mechanical properties of the human patellar tendon, *in vivo*", *Clinical Biomechanics,* vol. 21, no. 1, pp. 54-58.

70. Hansen, U., Masouros, S. & Amis, A.A. 2006a, "(iii) Material properties of biological tissues related to joint surgery", *Current Orthopaedics,* vol. 20, no. 1, pp. 16-22.

71. Harner, C.D., Xerogeanes, J.W., Livesay, G.A., Carlin, G.J., Smith, B.A., Kusayama, T., Kashiwaguchi, S. & Woo, S.L. 1995, "The human posterior cruciate ligament complex: an interdisciplinary study. Ligament morphology and biomechanical evaluation", *The American Journal of Sports Medicine,* vol. 23, no. 6, pp. 736-745.

72. Hausdorff, J.M., Rios, D.A. & Edelberg, H.K. 2001, "Gait variability and fall risk in community-living older adults: a 1-year prospective study", *Archives of Physical Medicine and Rehabilitation,* vol. 82, no. 8, pp. 1050-1056.

73. Hayes, W.C. & Mockros, L.F. 1971, "Viscoelastic properties of human articular cartilage", *Journal of Applied Physiology,* vol. 31, no. 4, pp. 562-568.

74. Hewitt, J., Guilak, F., Glisson, R. & Vail, T.P. 2001, "Regional material properties of the human hip joint capsule ligaments", *Journal of Orthopaedic Research,* vol. 19, no. 3, pp. 359-364.

75. Hill, C.L., Seo, G.S., Gale, D., Totterman, S., Gale, M.E. & Felson, D.T. 2005, "Cruciate ligament integrity in osteoarthritis of the knee", *Arthritis & Rheumatism,* vol. 52, no. 3, pp. 794-799.

76. Hobatho, M., Rho, J., Ashman, R., Van Der Perre, G., Lowet, G. & Borgwardt, A. 1991, "*In vivo* assessment of bone quality by vibration and wave propagation techniques", *Part II.Leuven: ACCO Publishing,* , pp. 7-32.

77. Hoffler, C.E., Guo, X.E., Zysset, P.K. & Goldstein, S.A. 2005, "An application of nanoindentation technique to measure bone tissue lamellae properties", *Journal of Biomechanical Engineering,* vol. 127, no. 7, pp. 1046-1053.

78. Hollman, J.H., Kovash, F.M., Kubik, J.J. & Linbo, R.A. 2007, "Age-related differences in spatiotemporal markers of gait stability during dual task walking", *Gait & Posture,* vol. 26, no. 1, pp. 113-119.

79. Hori, R.Y. & Mockros, L. 1976, "Indentation tests of human articular cartilage", *Journal of Biomechanics,* vol. 9, no. 4, pp. 259-268.

80. Hvid, I. & Hansen, S.L. 1985, "Trabecular bone strength patterns at the proximal tibial epiphysis", *Journal of Orthopaedic Research,* vol. 3, no. 4, pp. 464-472.

81. Intema, F., Hazewinkel, H., Gouwens, D., Bijlsma, J., Weinans, H., Lafeber, F. & Mastbergen, S. 2010, "In early OA, thinning of the subchondral plate is directly related to cartilage damage: results from a canine ACLT-meniscectomy model", *Osteoarthritis and Cartilage,* vol. 18, no. 5, pp. 691-698.

82. Jeffrey, J.E. & Aspden, R.M. 2006, "The biophysical effects of a single impact load on human and bovine articular cartilage", *Proceedings of the Institution of Mechanical Engineers.Part H, Journal of Engineering in Medicine,* vol. 220, no. 6, pp. 677-686.

83. Jilani, A., Shirazi-Adl, A. & Bendjaballah, M. 1997, "Biomechanics of human tibio-femoral joint in axial rotation", *The Knee,* vol. 4, no. 4, pp. 203-213.

84. Johnson, G.A., Tramaglini, D.M., Levine, R.E., Ohno, K., Choi, N. & L-Y Woo, S. 1994, "Tensile and viscoelastic properties of human patellar tendon", *Journal of Orthopaedic Research,* vol. 12, no. 6, pp. 796-803.

85. Julkunen, P., Harjula, T., Iivarinen, J., Marjanen, J., Seppänen, K., Närhi, T., Arokoski, J., Lammi, M.J., Brama, P.A., Jurvelin, J.S. and Helminen, H.J., 2009, "Biomechanical, biochemical and structural correlations in immature and mature rabbit articular cartilage", *Osteoarthritis and Cartilage*, vol 17, no. 12, pp. 1628-1638.

86. Kamibayashi, L., Wyss, U., Cooke, T. & Zee, B. 1995, "Trabecular microstructure in the medial condyle of the proximal tibia of patients with knee osteoarthritis", *Bone,* vol. 17, no. 1, pp. 27-35.

87. Kazemi, M. & Li, L. 2014, "A viscoelastic poromechanical model of the knee joint in large compression", *Medical Engineering & Physics,* vol. 36, no. 8, pp. 998-1006.

88. Kazemi, M., Dabiri, Y. & Li, L.P. 2013, "Recent advances in computational mechanics of the human knee joint", *Computational and Mathematical Methods in Medicine,* vol. 2013, pp. 718423.

89. Kazemi, M., Li, L., Savard, P. & Buschmann, M. 2011, "Creep behavior of the intact and meniscectomy knee joints", *Journal of the Mechanical Behavior of Biomedical Materials,* vol. 4, no. 7, pp. 1351-1358.

90. Kempson, G., Freeman, M. & Swanson, S. 1971, "The determination of a creep modulus for articular cartilage from indentation tests on the human femoral head", *Journal of Biomechanics,* vol. 4, no. 4, pp. 239-250.

91. Kempson, G.E. 1980, "The mechanical properties of articular cartilage", *The Joints and Synovial Fluid,* vol. 2, pp. 177-238.

92. Kiss, R.M. 2011, "Effect of severity of knee osteoarthritis on the variability of gait parameters", *Journal of Electromyography and Kinesiology,* vol. 21, no. 5, pp. 695-703.

93. Kiviranta, P., Lammentausta, E., Töyräs, J., Kiviranta, I. & Jurvelin, J. 2008, "Indentation diagnostics of cartilage degeneration", *Osteoarthritis and Cartilage,* vol. 16, no. 7, pp. 796-804.

94. Kleemann, R., Krocker, D., Cedraro, A., Tuischer, J. & Duda, G. 2005, "Altered cartilage mechanics and histology in knee osteoarthritis: relation to clinical assessment (ICRS Grade)", *Osteoarthritis and Cartilage,* vol. 13, no. 11, pp. 958-963.

95. Klein-Nulend, J., Nijweide, P.J. & Burger, E.H. 2003, "Osteocyte and bone structure", *Current Osteoporosis Reports,* vol. 1, no. 1, pp. 5-10.

96. Korhonen, R.K., Laasanen, M.S., Töyräs, J., Lappalainen, R., Helminen, H.J. & Jurvelin, J.S. 2003, "Fibril reinforced poroelastic model predicts specifically mechanical behavior of normal, proteoglycan depleted and collagen degraded articular cartilage", *Journal of Biomechanics,* vol. 36, no. 9, pp. 1373-1379.

97. Krishnan, R., Park, S., Eckstein, F. & Ateshian, G.A. 2003, "Inhomogeneous cartilage properties enhance superficial interstitial fluid support and frictional properties, but do not provide a homogeneous state of stress", *Journal of Biomechanical Engineering,* vol. 125, no. 5, pp. 569-577.

98. Kuroki, K., Cook, C. & Cook, J. 2011, "Subchondral bone changes in three different canine models of osteoarthritis", *Osteoarthritis and Cartilage,* vol. 19, no. 9, pp. 1142-1149.

99. Laasanen, M. 2003, *Development and Validation of Mechano-acoustic Techniques and Instrument for Evalution of Articular Cartilage,* Kuopion yliopisto.

100. Lajeunesse, D. & Reboul, P. 2003, "Subchondral bone in osteoarthritis: a biologic link with articular cartilage leading to abnormal remodeling", *Current Opinion in Rheumatology,* vol. 15, no. 5, pp. 628-633.

101. Lange, A., Singh, M.F., Smith, R., Foroughi, N., Baker, M., Shnier, R. & Vanwanseele, B. 2007, "Degenerative meniscus tears and mobility impairment in

women with knee osteoarthritis", *Osteoarthritis and Cartilage,* vol. 15, no. 6, pp. 701-708.

102. Langelier, E. & Buschmann, M. 1999, "'Amplitude Dependent Mechanical Alteration and Nonlinearity of Articular Cartilage Material Behavior in Unconfined Compression", *ORS Transactions,* vol. 24, pp. 647.

103. Lanyon, L. 1993, "Osteocytes, strain detection, bone modeling and remodeling", *Calcified Tissue International,* vol. 53, no. 1, pp. S102-S107.

104. LeRoux, M.A. & Setton, L.A. 2002, "Experimental and biphasic FEM determinations of the material properties and hydraulic permeability of the meniscus in tension", *Journal of Biomechanical Engineering,* vol. 124, no. 3, pp. 315-321.

105. Lewis, G. & Nyman, J.S. 2008, "The use of nanoindentation for characterizing the properties of mineralized hard tissues: State-of-the art review", *Journal of Biomedical Materials Research Part B: Applied Biomaterials,* vol. 87, no. 1, pp. 286-301.

106. Li, G., Gil, J., Kanamori, A. & Woo, S. 1999, "A validated three-dimensional computational model of a human knee joint", *Journal of Biomechanical Engineering,* vol. 121, no. 6, pp. 657-662.

107. Li, G., Lopez, O. & Rubash, H. 2001, "Variability of a three-dimensional finite element model constructed using magnetic resonance images of a knee for joint contact stress analysis", *Journal of Biomechanical Engineering,* vol. 123, no. 4, pp. 341-346.

108. Lindahl, O. 1976, "Mechanical properties of dried defatted spongy bone", *Acta Orthopaedica Scandinavica,* vol. 47, no. 1, pp. 11-19.

109. Loparic, M., Wirz, D., Daniels, A., Raiteri, R., VanLandingham, M.R., Guex, G., Martin, I., Aebi, U. & Stolz, M. 2010, "Micro-and nanomechanical analysis of

articular cartilage by indentation-type atomic force microscopy: validation with a gel-microfiber composite", *Biophysical Journal,* vol. 98, no. 11, pp. 2731-2740.

110. Lord, S.R., Lloyd, D.G. & Li, S.K. 1996, "Sensori-motor function, gait patterns and falls in community-dwelling women", *Age and Ageing,* vol. 25, no. 4, pp. 292-299.

111. Lories, R.J. & Luyten, F.P. 2011, "The bone–cartilage unit in osteoarthritis", *Nature Reviews Rheumatology,* vol. 7, no. 1, pp. 43-49.

112. Losina, E., Paltiel, A.D., Weinstein, A.M., Yelin, E., Hunter, D.J., Chen, S.P., Klara, K., Suter, L.G., Solomon, D.H. & Burbine, S.A. 2015, "Lifetime medical costs of knee osteoarthritis management in the United States: impact of extending indications for total knee arthroplasty", *Arthritis Care & Research,* vol. 67, no. 2, pp. 203-215.

113. Lotz, J.C., Gerhart, T.N. & Hayes, W.C. 1991, "Mechanical properties of metaphyseal bone in the proximal femur", *Journal of Biomechanics,* vol. 24, no. 5, pp. 317327-325329.

114. Louis-Ugbo, J., Leeson, B. & Hutton, W.C. 2004, "Tensile properties of fresh human calcaneal (Achilles) tendons", *Clinical Anatomy,* vol. 17, no. 1, pp. 30-35.

115. Lu, X.L. & Mow, V.C. 2008, "Biomechanics of articular cartilage and determination of material properties", *Medicine and Science in Sports and Exercise,* vol. 40, no. 2, pp. 193-199.

116. Lyyra, T., Jurvelin, J., Pitkänen, P., Väätäinen, U. & Kiviranta, I. 1995, "Indentation instrument for the measurement of cartilage stiffness under arthroscopic control", *Medical Engineering & Physics,* vol. 17, no. 5, pp. 395-399.

117. Madry, H., van Dijk, C.N. & Mueller-Gerbl, M. 2010, "The basic science of the subchondral bone", *Knee Surgery, Sports Traumatology, Arthroscopy,* vol. 18, no. 4, pp. 419-433.

118. Mahjoub, M., Berenbaum, F. & Houard, X. 2012, "Why subchondral bone in osteoarthritis? The importance of the cartilage bone interface in osteoarthritis", *Osteoporosis International,* vol. 23, no. 8, pp. 841-846.

119. Mak, A., Lai, W. & Mow, V. 1987, "Biphasic indentation of articular cartilage—I. Theoretical analysis", *Journal of Biomechanics,* vol. 20, no. 7, pp. 703-714.

120. Mankin, H.J., Dorfman, H., Lippiello, L. & Zarins, A. 1971, "Biochemical and metabolic abnormalities in articular cartilage from osteo-arthritic human hips. II. Correlation of morphology with biochemical and metabolic data", *The Journal of bone and joint surgery.American volume,* vol. 53, no. 3, pp. 523-537.

121. Manninen, P., Riihimaki, H., Heliovaara, M. & Makela, P. 1996, "Overweight, gender and knee osteoarthritis", *International Journal of Obesity and Related Metabolic Disorders : Journal of the International Association for the Study of Obesity,* vol. 20, no. 6, pp. 595-597.

122. Mansour, J.M. 2003, "Biomechanics of cartilage", *Kinesiology: the mechanics and pathomechanics of Human Movement,* Lippincott Williams and Wilkins, Philadelphia, pp. 66-79.

123. Marticke, J.K., Hösselbarth, A., Hoffmeier, K.L., Marintschev, I., Otto, S., Lange, M., Plettenberg, H.K., Spahn, G. & Hofmann, G.O. 2010, "How do visual, spectroscopic and biomechanical changes of cartilage correlate in osteoarthritic knee joints?", *Clinical Biomechanics,* vol. 25, no. 4, pp. 332-340.

124. Martini, F. 1998, *'Anatomy and Physiology' 2007 Ed,* Rex Bookstore, Inc.

125. Matkovic, V., Jelic, T., Wardlaw, G.M., Ilich, J.Z., Goel, P.K., Wright, J.K., Andon, M.B., Smith, K.T. & Heaney, R.P. 1994, "Timing of peak bone mass in Caucasian females and its implication for the prevention of osteoporosis. Inference

from a cross-sectional model", *The Journal of Clinical Investigation,* vol. 93, no. 2, pp. 799-808.

126. Meng, Q., Jin, Z., Wilcox, R. & Fisher, J. 2014, "Computational investigation of the time-dependent contact behaviour of the human tibiofemoral joint under body weight", *Proceedings of the Institution of Mechanical Engineers, Part H: Journal of Engineering in Medicine,* vol. 228, no. 11, pp. 1193-1207.

127. Mente, P. & Lewis, J. 1994, "Elastic modulus of calcified cartilage is an order of magnitude less than that of subchondral bone", *Journal of Orthopaedic Research,* vol. 12, no. 5, pp. 637-647.

128. Miller, G.J. & Morgan, E.F. 2010, "Use of microindentation to characterize the mechanical properties of articular cartilage: comparison of biphasic material properties across length scales", *Osteoarthritis and Cartilage,* vol. 18, no. 8, pp. 1051-1057.

129. Minary-Jolandan, M. & Yu, M. 2009, "Nanomechanical heterogeneity in the gap and overlap regions of type I collagen fibrils with implications for bone heterogeneity", *Biomacromolecules,* vol. 10, no. 9, pp. 2565-2570.

130. Moglo, K. & Shirazi-Adl, A. 2003, "On the coupling between anterior and posterior cruciate ligaments, and knee joint response under anterior femoral drawer in flexion: a finite element study", *Clinical Biomechanics,* vol. 18, no. 8, pp. 751-759.

131. Momersteeg, T., Blankevoort, L., Huiskes, R., Kooloos, J., Kauer, J. & Hendriks, J. 1995, "The effect of variable relative insertion orientation of human knee bone-ligament-bone complexes on the tensile stiffness", *Journal of Biomechanics,* vol. 28, no. 6, pp. 745-752.

132. Mononen, M., Julkunen, P., Töyräs, J., Jurvelin, J., Kiviranta, I. & Korhonen, R. 2011, "Alterations in structure and properties of collagen network of

osteoarthritic and repaired cartilage modify knee joint stresses", *Biomechanics and Modeling in Mechanobiology,* vol. 10, no. 3, pp. 357-369.

133. Mononen, M.E., Mikkola, M.T., Julkunen, P., Ojala, R., Nieminen, M.T., Jurvelin, J.S. & Korhonen, R.K. 2012, "Effect of superficial collagen patterns and fibrillation of femoral articular cartilage on knee joint mechanics—A 3D finite element analysis", *Journal of Biomechanics,* vol. 45, no. 3, pp. 579-587.

134. Mootanah, R., Imhauser, C.W., Reisse, F., Carpanen, D., Walker, R.W., Koff, M.F., Lenhoff, M.W., Rozbruch, S.R., Fragomen, A.T., Dewan, Z., Kirane, Y.M., Cheah, K., Dowell, J.K. & Hillstrom, H.J. 2014, "Development and validation of a computational model of the knee joint for the evaluation of surgical treatments for osteoarthritis.", *Computer Methods in Biomechanics and Biomedical Engineering,* vol. 17, no. 13, pp. 1502-1517.

135. Mow, V., Lai, W. & Holmes, M. 1982, "Advanced theoretical and experimental techniques in cartilage research" in *Biomechanics: Principles and applications,* Springer, pp. 47-74.

136. Mow, V.C. & Guo, X.E. 2002, "Mechano-electrochemical properties of articular cartilage: their inhomogeneities and anisotropies", *Annual Review of Biomedical Engineering,* vol. 4, no. 1, pp. 175-209.

137. Mullaji, A.B., Marawar, S.V., Simha, M. & Jindal, G. 2008, "Cruciate ligaments in arthritic knees: a histologic study with radiologic correlation", *The Journal of Arthroplasty,* vol. 23, no. 4, pp. 567-572.

138. Newman, A.P. 1998, "Articular cartilage repair", *The American Journal of Sports Medicine,* vol. 26, no. 2, pp. 309-324.

139. Nigg, B. & Herzog, W. (eds) 2006, *Biomechanics of the Musculoskeletal System*, 3rd edn, Wiley, West Sussex.

140. Nissi, M., Rieppo, J., Töyräs, J., Laasanen, M., Kiviranta, I., Nieminen, M. & Jurvelin, J. 2007, "Estimation of mechanical properties of articular cartilage with MRI–dGEMRIC, T 2 and T 1 imaging in different species with variable stages of maturation", *Osteoarthritis and Cartilage,* vol. 15, no. 10, pp. 1141-1148.

141. Noyes, F.R. & Grood, E.S. 1976, "The strength of the anterior cruciate ligament in humans and Rhesus monkeys", *The Journal of bone and joint surgery. American volume,* vol. 58, no. 8, pp. 1074-1082.

142. Olszta, M.J., Cheng, X., Jee, S.S., Kumar, R., Kim, Y., Kaufman, M.J., Douglas, E.P. & Gower, L.B. 2007, "Bone structure and formation: a new perspective", *Materials Science and Engineering: R: Reports,* vol. 58, no. 3-5, pp. 77-116.

143. Outerbridge, R. 1961, "The etiology of chondromalacia patellae", *Journal of Bone & Joint Surgery. British Volume,* vol. 43.

144. Owings, T.M. & Grabiner, M.D. 2004, "Step width variability, but not step length variability or step time variability, discriminates gait of healthy young and older adults during treadmill locomotion", *Journal of Biomechanics,* vol. 37, no. 6, pp. 935-938.

145. Paietta, R.C., Campbell, S.E. & Ferguson, V.L. 2011, "Influences of spherical tip radius, contact depth, and contact area on nanoindentation properties of bone", *Journal of Biomechanics,* vol. 44, no. 2, pp. 285-290.

146. Pal, S. 2014, "Mechanical properties of biological materials" in *Design of Artificial Human Joints & Organs* Springer, pp. 23-40.

147. Pedersen, D.R., Goetz, J.E., Kurriger, G.L. & Martin, J.A. 2013, "Comparative digital cartilage histology for human and common osteoarthritis models", *Orthopedic Research and Reviews,* vol. 2013, no. 5, pp. 13-20.

148. Pena, E., Calvo, B., Martinez, M. & Doblare, M. 2006, "A three-dimensional finite element analysis of the combined behavior of ligaments and menisci in the healthy human knee joint", *Journal of Biomechanics,* vol. 39, no. 9, pp. 1686-1701.

149. Pena, E., Calvo, B., Martinez, M., Palanca, D. & Doblaré, M. 2005, "Finite element analysis of the effect of meniscal tears and meniscectomies on human knee biomechanics", *Clinical Biomechanics,* vol. 20, no. 5, pp. 498-507.

150. Peña, E., Calvo, B., Martínez, M.A. & Doblaré, M. 2007, "Effect of the size and location of osteochondral defects in degenerative arthritis. A finite element simulation", *Computers in Biology and Medicine,* vol. 37, no. 3, pp. 376-387.

151. Peña, E., Del Palomar, A.P., Calvo, B., Martínez, M. & Doblaré, M. 2007, "Computational modelling of diarthrodial joints. Physiological, pathological and pos-surgery simulations", *Archives of Computational Methods in Engineering,* vol. 14, no. 1, pp. 47-91.

152. Plumb, M. & Aspden, R. 2005, "The response of elderly human articular cartilage to mechanical stimuli *in vitro*", *Osteoarthritis and Cartilage,* vol. 13, no. 12, pp. 1084-1091.

153. Punzi, L., Oliviero, F. & Ramonda, R. 2010, "New horizons in osteoarthritis", *Swiss Medical Weekly,* vol. 140, pp. 16.

154. Quapp, K. & Weiss, J.A. 1998, "Material characterization of human medial collateral ligament", *Journal of Biomechanical Engineering,* vol. 120, no. 6, pp. 757-763.

155. Race, A. & Amis, A.A. 1994, "The mechanical properties of the two bundles of the human posterior cruciate ligament", *Journal of Biomechanics,* vol. 27, no. 1, pp. 13-24.

156. Reilly, D.T. & Burstein, A.H. 1975, "The elastic and ultimate properties of compact bone tissue", *Journal of Biomechanics,* vol. 8, no. 6, pp. 393IN9397-396IN11405.

157. Repo, R.U. & Finlay, J.B. 1977, "Survival of articular cartilage after controlled impact", *The Journal of Bone and Joint Surgery. American volume,* vol. 59, no. 8, pp. 1068-1076.

158. Rho, J., Tsui, T.Y. & Pharr, G.M. 1997, "Elastic properties of human cortical and trabecular lamellar bone measured by nanoindentation", *Biomaterials,* vol. 18, no. 20, pp. 1325-1330.

159. Rho, J.Y., Ashman, R.B. & Turner, C.H. 1993, "Young's modulus of trabecular and cortical bone material: ultrasonic and microtensile measurements", *Journal of Biomechanics,* vol. 26, no. 2, pp. 111-119.

160. Rho, J.Y., Kuhn-Spearing, L. & Zioupos, P. 1998, "Mechanical properties and the hierarchical structure of bone", *Medical Engineering & Physics,* vol. 20, no. 2, pp. 92-102.

161. Robinson, J.R., Bull, A.M. & Amis, A.A. 2005, "Structural properties of the medial collateral ligament complex of the human knee", *Journal of Biomechanics,* vol. 38, no. 5, pp. 1067-1074.

162. Rousseau, J.C. & Garnero, P. 2012, "Biological markers in osteoarthritis", *Bone,* vol. 51, no. 2, pp. 265-277.

163. Rubin, M. & Bodner, S. 2002, "A three-dimensional nonlinear model for dissipative response of soft tissue", *International Journal of Solids and Structures,* vol. 39, no. 19, pp. 5081-5099.

164. Ruff, C., Holt, B. & Trinkaus, E. 2006, "Who's afraid of the big bad Wolff?:“Wolff's law” and bone functional adaptation", *American Journal of Physical Anthropology,* vol. 129, no. 4, pp. 484-498.

165. Saarakkala, S., Julkunen, P., Kiviranta, P., Makitalo, J., Jurvelin, J.S. & Korhonen, R.K. 2010, "Depth-wise progression of osteoarthritis in human articular cartilage: investigation of composition, structure and biomechanics", *Osteoarthritis and Cartilage,* vol. 18, no. 1, pp. 73-81.

166. Setton, L.A., Elliott, D.M. & Mow, V.C. 1999, "Altered mechanics of cartilage with osteoarthritis: human osteoarthritis and an experimental model of joint degeneration", *Osteoarthritis and Cartilage,* vol. 7, no. 1, pp. 2-14.

167. Shepherd, D.E. & Seedhom, B.B. 1997, "A technique for measuring the compressive modulus of articular cartilage under physiological loading rates with preliminary results", *Proceedings of the Institution of Mechanical Engineers. Part H, Journal of Engineering in Medicine,* vol. 211, no. 2, pp. 155-165.

168. Shepherd, D.E. & Seedhom, B.B. 1999a, "The 'instantaneous' compressive modulus of human articular cartilage in joints of the lower limb", *Rheumatology (Oxford, England),* vol. 38, no. 2, pp. 124-132.

169. Shepherd, D.E. & Seedhom, B.B. 1999b, "Thickness of human articular cartilage in joints of the lower limb", *Annals of the Rheumatic Diseases,* vol. 58, no. 1, pp. 27-34.

170. Shirazi, R., Shirazi-Adl, A. & Hurtig, M. 2008, "Role of cartilage collagen fibrils networks in knee joint biomechanics under compression", *Journal of Biomechanics,* vol. 41, no. 16, pp. 3340-3348.

171. Silver, F.H., Bradica, G. & Tria, A. 2002, "Elastic energy storage in human articular cartilage: estimation of the elastic modulus for type II collagen and changes associated with osteoarthritis", *Matrix Biology,* vol. 21, no. 2, pp. 129-137.

172. Skaggs, D., Warden, W. & Mow, V. 1994, "Radial tie fibers influence the tensile properties of the bovine medial meniscus", *Journal of Orthopaedic Research,* vol. 12, no. 2, pp. 176-185.

173. Soltz, M.A. & Ateshian, G.A. 1998, "Experimental verification and theoretical prediction of cartilage interstitial fluid pressurization at an impermeable contact interface in confined compression", *Journal of Biomechanics,* vol. 31, no. 10, pp. 927-934.

174. Sophia Fox, A.J., Bedi, A. & Rodeo, S.A. 2009, "The basic science of articular cartilage: structure, composition, and function", *Sports Health,* vol. 1, no. 6, pp. 461-468.

175. Staubli, H.U., Schatzmann, L., Brunner, P., Rincon, L. & Nolte, L.P. 1999, "Mechanical tensile properties of the quadriceps tendon and patellar ligament in young adults", *The American Journal of Sports Medicine,* vol. 27, no. 1, pp. 27-34.

176. Stolz, M., Gottardi, R., Raiteri, R., Miot, S., Martin, I., Imer, R., Staufer, U., Raducanu, A., Düggelin, M. & Baschong, W. 2009, "Early detection of aging cartilage and osteoarthritis in mice and patient samples using atomic force microscopy", *Nature Nanotechnology,* vol. 4, no. 3, pp. 186-192.

177. Stolz, M., Raiteri, R., Daniels, A., VanLandingham, M.R., Baschong, W. & Aebi, U. 2004, "Dynamic elastic modulus of porcine articular cartilage determined at two different levels of tissue organization by indentation-type atomic force microscopy", *Biophysical Journal,* vol. 86, no. 5, pp. 3269-3283.

178. Taffetani, M., Gottardi, R., Gastaldi, D., Raiteri, R. & Vena, P. 2014, "Poroelastic response of articular cartilage by nanoindentation creep tests at different characteristic lengths", *Medical Engineering & Physics,* vol. 36, no. 7, pp. 850-858.

179. Tanska, P., Mononen, M.E. & Korhonen, R.K. 2015, "A multi-scale finite element model for investigation of chondrocyte mechanics in normal and medial meniscectomy human knee joint during walking", *Journal of Biomechanics,* vol. 48, no. 8, pp. 1397-1406.

180. Taylor, Z.A. & Miller, K. 2006, "Constitutive modeling of cartilaginous tissues: a review", *Journal of Applied Biomechanics,* vol. 22, no. 3, pp. 212-229.

181. Temple-Wong, M.M., Bae, W.C., Chen, M.Q., Bugbee, W.D., Amiel, D., Coutts, R.D., Lotz, M. & Sah, R.L. 2009, "Biomechanical, structural, and biochemical indices of degenerative and osteoarthritic deterioration of adult human articular cartilage of the femoral condyle", *Osteoarthritis and Cartilage,* vol. 17, no. 11, pp. 1469-1476.

182. Thambyah, A., Nather, A. & Goh, J. 2006, "Mechanical properties of articular cartilage covered by the meniscus", *Osteoarthritis and Cartilage,* vol. 14, no. 6, pp. 580-588.

183. Thornton, G., Leask, G., Shrive, N. & Frank, C. 2000, "Early medial collateral ligament scars have inferior creep behaviour", *Journal of Orthopaedic Research,* vol. 18, no. 2, pp. 238-246.

184. Tissakht, M. & Ahmed, A. 1995, "Tensile stress-strain characteristics of the human meniscal material", *Journal of Biomechanics,* vol. 28, no. 4, pp. 411-422.

185. Trent, P.S., Walker, P.S. & Wolf, B. 1976, "Ligament length patterns, strength, and rotational axes of the knee joint", *Clinical Orthopaedics and Related Research,* vol. 117, pp. 263-270.

186. Tuncer, M., Cobb, J.P., Hansen, U.N. & Amis, A.A. 2013, "Validation of multiple subject-specific finite element models of unicompartmental knee replacement", *Medical Engineering & Physics,* vol. 35, no. 10, pp. 1457-1464.

187. Wang, M. & Peng, Z. 2015, "Investigation of the nano-mechanical properties and surface topographies of wear particles and human knee cartilages", *Wear,* vol. 324, pp. 74-79.

188. Wang, M., Peng, Z., Price, J. & Ketheesan, N. 2013, "Study of the nano-mechanical properties of human knee cartilage in different wear conditions", *Wear,* vol. 301, no. 1, pp. 188-191.

189. Wang, Y., Fan, Y. & Zhang, M. 2014, "Comparison of stress on knee cartilage during kneeling and standing using finite element models", *Medical Engineering & Physics,* vol. 36, no. 4, pp. 439-447.

190. Weiner, S. & Wagner, H.D. 1998, "The material bone: structure-mechanical function relations", *Annual Review of Materials Science,* vol. 28, no. 1, pp. 271-298.

191. Weiss, J.A. & Gardiner, J.C. 2001, "Computational modeling of ligament mechanics", *Critical Reviews™ in Biomedical Engineering,* vol. 29, no. 3.

192. Wen, C., Wu, C., Tang, B., Wang, T., Yan, C., Lu, W., Pan, H., Hu, Y. & Chiu, K. 2012, "Collagen fibril stiffening in osteoarthritic cartilage of human beings revealed by atomic force microscopy", *Osteoarthritis and Cartilage,* vol. 20, no. 8, pp. 916-922.

193. Wilson, W., Van Donkelaar, C., Van Rietbergen, R. & Huiskes, R. 2005, "The role of computational models in the search for the mechanical behavior and damage mechanisms of articular cartilage", *Medical Engineering & Physics,* vol. 27, no. 10, pp. 810-826.

194. Wilusz, R.E., Zauscher, S. & Guilak, F. 2013, "Micromechanical mapping of early osteoarthritic changes in the pericellular matrix of human articular cartilage", *Osteoarthritis and Cartilage,* vol. 21, no. 12, pp. 1895-1903.

195. Wismans, J., Veldpaus, F., Janssen, J., Huson, A. & Struben, P. 1980, "A three-dimensional mathematical model of the knee-joint", *Journal of Biomechanics,* vol. 13, no. 8, pp. 677-685.

196. Woo, S., Akeson, W. & Jemmott, G. 1976, "Measurements of nonhomogeneous, directional mechanical properties of articular cartilage in tension", *Journal of Biomechanics,* vol. 9, no. 12, pp. 785-791.

197. Woo, S., Johnson, G. & Smith, B. 1993, "Mathematical modeling of ligaments and tendons", *Transactions – American Society of Mechanical Engineers Journal of Biomechanical Engineering,* vol. 115, pp. 468-468.

198. Woo, S.L., Abramowitch, S.D., Kilger, R. & Liang, R. 2006, "Biomechanics of knee ligaments: injury, healing, and repair", *Journal of Biomechanics,* vol. 39, no. 1, pp. 1-20.

199. Woo, S.L., Hollis, J.M., Adams, D.J., Lyon, R.M. & Takai, S. 1991, "Tensile properties of the human femur-anterior cruciate ligament-tibia complex. The effects of specimen age and orientation", *The American Journal of Sports Medicine,* vol. 19, no. 3, pp. 217-225.

200. Yang, N.H., Nayeb-Hashemi, H., Canavan, P.K. & Vaziri, A. 2010, "Effect of frontal plane tibiofemoral angle on the stress and strain at the knee cartilage during the stance phase of gait", *Journal of Orthopaedic Research,* vol. 28, no. 12, pp. 1539-1547.

201. Yao, H., Dao, M., Carnelli, D., Tai, K. and Ortiz, C., 2011, "Size-dependent heterogeneity benefits the mechanical performance of bone", *Journal of the Mechanics and Physics of Solids*, vol. 59, no. 1, pp. 64-74.

202. Zhang, J., Niebur, G.L. & Ovaert, T.C. 2008, "Mechanical property determination of bone through nano- and micro-indentation testing and finite element simulation", *Journal of Biomechanics,* vol. 41, no. 2, pp. 267-275.

203. Zhang, X. 2001, *Biomechanical realism versus algorithmic efficiency: A trade-off in human motion simulation modeling,* SAE Technical Paper.

204. Zhang, Y. & Jordan, J.M. 2008, "Epidemiology of Osteoarthritis", *Rheumatic Disease Clinics of North America,* vol. 34, no. 3, pp. 515-529.

205. Zysset, P., Sonny, M. & Hayes, W. 1994, "Morphology-mechanical property relations in trabecular bone of the osteoarthritic proximal tibia", *The Journal of Arthroplasty,* vol. 9, no. 2, pp. 203-216.

206. Zysset, P.K., Guo, X.E., Hoffler, C.E., Moore, K.E. & Goldstein, S.A. 1999, "Elastic modulus and hardness of cortical and trabecular bone lamellae measured by nanoindentation in the human femur", *Journal of Biomechanics,* vol. 32, no. 10, pp. 1005-1012.

Section Two – Material Properties

Chapter Three: Micromechanical properties of canine femoral articular cartilage following multiple freeze-thaw cycles

Abstract

Tissue material properties are crucial to understanding their mechanical function, both in healthy and diseased states. However, in certain circumstances logistical limitations can prevent testing on fresh samples necessitating one or more freeze-thaw cycles. To date, the nature and extent to which the material properties of articular cartilage are altered by repetitive freezing have not been explored. Therefore, the aim of this study is to quantify how articular cartilage mechanical properties, measured by nanoindentation, are affected by multiple freeze-thaw cycles. Canine cartilage plugs (n = 11) from medial and lateral femoral condyles were submerged in phosphate buffered saline, stored at 3 - 5˚C and tested using nanoindentation within 12 hours. Samples were then frozen at -20°C and later thawed at 3 - 5°C for 3 hours before material properties were re-tested and samples re-frozen under the same conditions. This process was repeated for all 11 samples over three freeze-thaw cycles. Overall mean and standard deviation of shear storage modulus decreased from 1.76 ± 0.78 to 1.21 ± 0.77 MPa (p = 0.91), shear loss modulus from 0.42 ± 0.19 to 0.39 ± 0.17 MPa (p = 0.70) and elastic modulus from 5.13 ± 2.28 to 3.52 ± 2.24 MPa (p = 0.20) between fresh and three freeze-thaw cycles respectively. The loss factor increased from 0.31 ± 0.38 to 0.71 ± 1.40 (p = 0.18) between fresh and three freeze-thaw cycles. Inter-sample variability spanned as much as 10.47 MPa across freezing cycles and this high-level of biological variability across samples likely explains why overall mean "whole-joint" trends do not reach statistical significance across the storage conditions tested. As a result multiple freeze-thaw cycles cannot be explicitly or statistically linked to

mechanical changes within the cartilage. However, the changes in material properties observed herein may be sufficient in magnitude to impact on a variety of clinical and scientific studies of cartilage, and should be considered when planning experimental protocols.

Introduction

Articular cartilage is a viscoelastic heterogeneous material divided into layered zones with varying material properties and functionalities [Silver et al., 2002]. The extracellular matrix (ECM) is heterogeneous in nature where variations exist in composition, structure and vascularity at a micro-level. It is composed of proteoglycans, collagens and glycoproteins, which are all macromolecular components [Silver et al., 2002]. Cartilage also contains chondrocytes that become embedded within the matrix, maturing and dividing to deposit new cartilage. Its primary function is to maintain a smooth surface allowing lubricated frictionless movement and to help transmit articular forces, therefore minimising stress concentrations across the joint [Nigg & Herzog, 2006].

Knowledge of material properties of cartilage is crucial to understanding its mechanical function and morpho-functional alterations that occur during ageing, disease and injury [Wen et al., 2012; Kleemann et al., 2005]. Whilst valuable data in isolation, material property information is also crucial to other mechanical analyses, including computational models that attempt to predict *in vivo* joint behaviour [e.g. Wang et al., 2014; Guo et al., 2009; Pena et al., 2006]. Material properties of articular cartilage ECM have been widely reported utilising varying testing, storage and preservation techniques [e.g. Shepherd & Seedhom, 1997; Kleemann et al., 2005; Wen et al., 2012]. Specific testing techniques have changed over time and varied according to investigator preference and overall

experimental goals. In general, however, all studies seeking to quantify the mechanical behaviour of biological tissues strive to maintain biological fidelity of the testing conditions in the experiment; for example testing fresh tissue samples under hydrated conditions that are representative of the internal environment of the studied organism [Brandt et al., 2010]. However, accomplishing this may be challenging for numerous reasons including the need for transportation between dissection and testing locations, availability or failure of testing equipment and the desire to test large sample numbers from individual specimens thereby minimising tissue waste. In such circumstances it is standard practice to store and preserve samples, often requiring tissue to undergo one or more freeze-thaw cycles before mechanical tests can be carried out [e.g. Wilusz et al., 2013; Lau et al., 2008; Li et al., 2006].

Therefore in situations where logistical limitations prevent testing of fresh samples, it is beneficial to explore if preservation of tissues samples through freezing can be utilised without compromising mechanical properties. In recent years there have been a number of systematic investigations into the effects of multiple freeze-thaw cycles on the mechanical properties of ligaments and tendon [Huang et al., 2011; Moon et al., 2006; Woo et al., 1986]. Although some variation between individual studies exists, these analyses suggest that ligament and tendon tissue can undergo a minimum of two freeze-thaw cycles before significant changes to their material properties occur, thereby providing important constraints on experimental designs involving these tissues. However, despite its fundamental importance to joint biomechanics, to the best of the authors' knowledge, no such data exists exploring the effect of more than one freeze-thaw cycle on material properties of articular cartilage. The aim of this paper is therefore to quantify how articular cartilage mechanical properties are affected by multiple freeze-thaw cycles directly addressing this important gap in knowledge. Dynamic nanoindentation is used to determine the shear storage modulus (G'), shear loss modulus (G''), elastic modulus (E) and

the loss factor (*tan δ*) of canine femoral condyle articular cartilage across three freeze-thaw cycles.

Materials and Methods

Specimen Preparation

One disease free canine cadaveric knee joint from a skeletally mature Staffordshire Bull cross mix was dissected 36 hours after being euthanized. Ethical permission for use of this cadaveric material was granted by the Veterinary Research Ethics Committee, University of Liverpool (VREC327). Healthy articular cartilage samples (n = 11) measuring < 1cm², were harvested from the medial and lateral bilateral femoral condyles (Fig. 1) using a low speed band saw (deSoutter Medical, Bucks, UK). Gross examination of the samples showed no sign of fibrillation or wear.

Figure 1. Photograph of the medial and lateral femoral condyle of the canine specimen to scale (cm), from which samples were harvested.

Following dissection, each of the 11 samples were submerged in phosphate buffered saline (PBS) and stored in cooled temperatures (3 - 5°C) for up to 12 hours until they were tested when still fresh using nanoindentation techniques, as detailed below. Following testing, all 11 samples were then frozen at -20°C for up to 48 hours. Samples were then individually thawed for three hours at 3 - 5°C and re-tested using the same nanoindentation protocol after having undergone one freeze-thaw cycle. This was completed within one hour and hydration of cartilage was maintained through constant exposure to PBS prior to and during testing [Brandt et al., 2010]. This freeze-thaw procedure was repeated for three cycles and material properties of all 11 samples were measured after each freeze-thaw cycle. Samples were specifically thawed in cooled conditions (3 - 5˚C), as room temperatures have been shown to thaw cartilage samples too quickly and cause damage to the ECM [Szarko et al., 2010].

Nanoindentation Testing

Cartilage samples underwent dynamic nanoindentation (G200 Nanoindenter, Keysight Technologies, Chandler, AZ, USA) equipped with an ultra-low load DCM-II actuator utilising a Continuous Stiffness Measurement (CSM) module to determine the micromechanical complex shear modulus.

Samples were mounted into a custom made liquid cell holder, with a 1 cm radius and 2 mm deep well, which could allow partial submersion of the samples in PBS during testing (Fig. 2). Samples were then examined under the built-in optical microscope to randomly select ten indent locations per sample (> 100 µm spacing between each indentation to avoid immediate overlap) totaling 110 measurements per cycle of freezing. Given that it was not possible to differentiate between microstructural features in the cartilage with the optical

microscope, indentation sites were based on topographical homogeneity for accurate surface detection. Repetition or overlapping indentations in subsequent cycles of freezing was possible although it has previously been reported that there is no visible deformation of cartilage following low loads such as those experienced during nanoindentation when a recovery time is incorporated [Franke et al., 2011]. Similarly to previous research investigating viscoelastic materials [e.g. Cheng et al., 1999; Jurvelin et al., 2000], a flat-ended cylindrical 100 µm punch tip (Synton-MDP Ltd, Nidau, Switzerland) was utilised as opposed to a sharp Berkovich tip which has been used in other studies testing cartilage [Hargrave-Thomas et al., 2015; Campbell et al., 2012; Franke et al., 2007; Gupta et al., 2005].

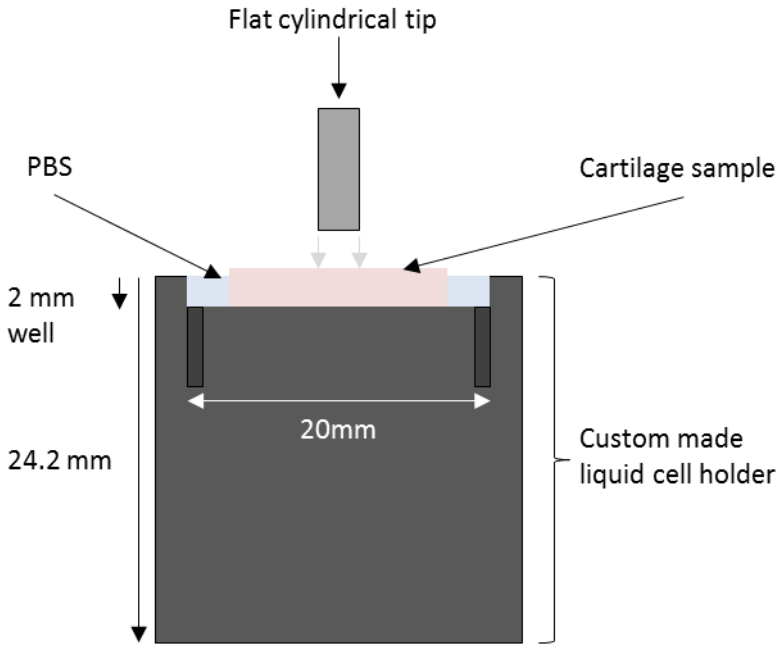

Figure 2. A schematic of the custom made liquid cell holder holding the cartilage sample and phosphate buffered saline (PBS).

A Poisson's ratio of 0.46 [Jin & Lewis, 2004] was assumed for cartilage allowing the calculation of *G'*, *G''* and the loss factor (i.e. ratio of *G''* / *G'*) after each indentation. The

theoretical basis is outlined in brief below and has been described in more detail previously [Herbert et al., 2008; Herbert et al., 2009]. Complex shear modulus (*G**) is calculated by adding the shear storage modulus *G'* (real intrinsic elastic component) to the shear loss modulus *G"* (imaginary viscous component):

$$G^* = G' + iG'' \quad (1)$$

Sneddon's analysis [Sneddon, 1965] is used to calculate the shear storage modulus using the Poisson's ratio (*v*), contact stiffness (*S*) and tip diameter (*D*), based on using a flat cylindrical punch:

$$G' = \frac{S\,(1-v)}{(2D)} \quad (2)$$

The above components along with contact damping (*Cw*) can be used to calculate the shear loss modulus:

$$G'' = \frac{Cw\,(1-v)}{(2D)} \quad (3)$$

Contact stiffness (*S*) is calculated by subtracting the instrument stiffness (*Ki*) from the total measured stiffness (*Ks*):

$$S = Ks - Ki \quad (4)$$

Contact damping (*Cw*) is calculated by subtracting the instrument damping (*Ciw*) from the total measured damping (*Csw*):

$$\mathrm{C}w = \mathrm{C}sw - \mathrm{C}iw \quad (5)$$

The elastic modulus (*E*) was then calculated using the shear storage modulus (*G'*) and Poisson's Ratio (*v*) [Landau & Lifshitz, 1986]:

$$E = 2G'(1 + v) \quad (6)$$

After the indenter head detected the surface of the sample, a pre-compression of 8 µm was applied until the indenter was fully in contact with the sample. The surface detection was determined by a phase shift of the displacement measurement. In order to accurately detect the surface, the phase shift was monitored over a number of data points which has previously been shown to be effective [Akhtar et al., 2016]. Once the surface detection requirement was fulfilled over the predefined number of data points, the initial contact was determined from the first data point in the sequence. Once the indenter was fully in contact with the sample surface it vibrated at a fixed frequency of 110 Hz (the resonant frequency of the indenter) with 500 nm oscillation amplitude. Contact stiffness and damping were obtained through electromagnetic oscillation sequences. The initial oscillation measured instrument stiffness and damping and these were subtracted from the total measurement to obtain the contact response. Material properties were then obtained during the second oscillation.

After each indentation, the tip was cleaned to prevent any transfer of biological material to the subsequent indentation site which may affect measurements. This was achieved by indenting an adjacent sample holder which was mounted with 3M double-sided Scotch tape. This method was found to be effective at cleaning the tip without picking up any residue from the Scotch tape. Following testing of each sample, further indents were made

on fused silica with the test sites remaining free of any residue, hence confirming that the tip was clean before further cartilage testing.

Statistical Analysis

An a-priori power analysis was performed using G*Power software [Faul et al., 2007] which specified a total of eight samples would be required to distinguish an effect size of 0.8 with α error probability of 0.05 and power of 0.95 across four groups of testing parameters. Statistical analysis of *G'*, *G"* and *E*, as well as the loss factor, were conducted using a repeated measures ANOVA in SPSS (SPSS software, Version 22.0, SPSS, Inc., Chicago, IL), specifically Mauchly's Test of Sphericity, after which a Bonferroni post-hoc test was performed if results were significant, producing pairwise comparisons. Individual sample means were analysed after each cycle of freezing, as well as the means of all samples combined, to give a whole specimen analysis.

Results

Overall Trends

The overall mean *G'*, *G"*, *E* and loss factor for all 11 samples combined for the different cycles are presented in Figure 3. Shear modulus (*G'*) decreased from 1.76 ± 0.78, 1.41 ± 0.77, 1.25 ± 0.54 to 1.21 ± 0.77 MPa (mean ± standard deviation (SD)) between fresh samples and samples tested after one, two and three freeze-thaw cycles respectively (Fig. 3a). Shear loss modulus (*G"*) increased from 0.42 ± 0.19 to 0.46 ± 0.18 MPa (mean ± SD) between fresh and one freeze-thaw cycle, but then decreased to 0.43 ± 0.15 and 0.39 ± 0.17 MPa following two and three freeze-thaw cycles respectively (Fig. 3b). Elastic Modulus (*E)* were 5.13 ± 2.28, 4.11 ± 2.25, 3.64 ± 1.57 and 3.52 ± 2.24 MPa (mean ± SD) during fresh,

one, two and three freeze-thaw cycles respectively (Fig. 3c). The mean and SD of the loss factor changed throughout each cycle from 0.31 ± 0.38, 0.58 ± 1.66, 0.41 ± 0.26 and 0.71 ± 1.40 when using a mean of all 11 samples during fresh, one, two and three freeze-thaw cycles respectively (Fig. 3d). Changes in the values for *G'*, *G"*, *E* and the loss factor, across freeze-thaw cycles were not found to be statistically significant (Mauchley's Test of Sphericity, $p = 0.91$, $p = 0.70$, $p = 0.20$, $p = 0.18$ respectively).

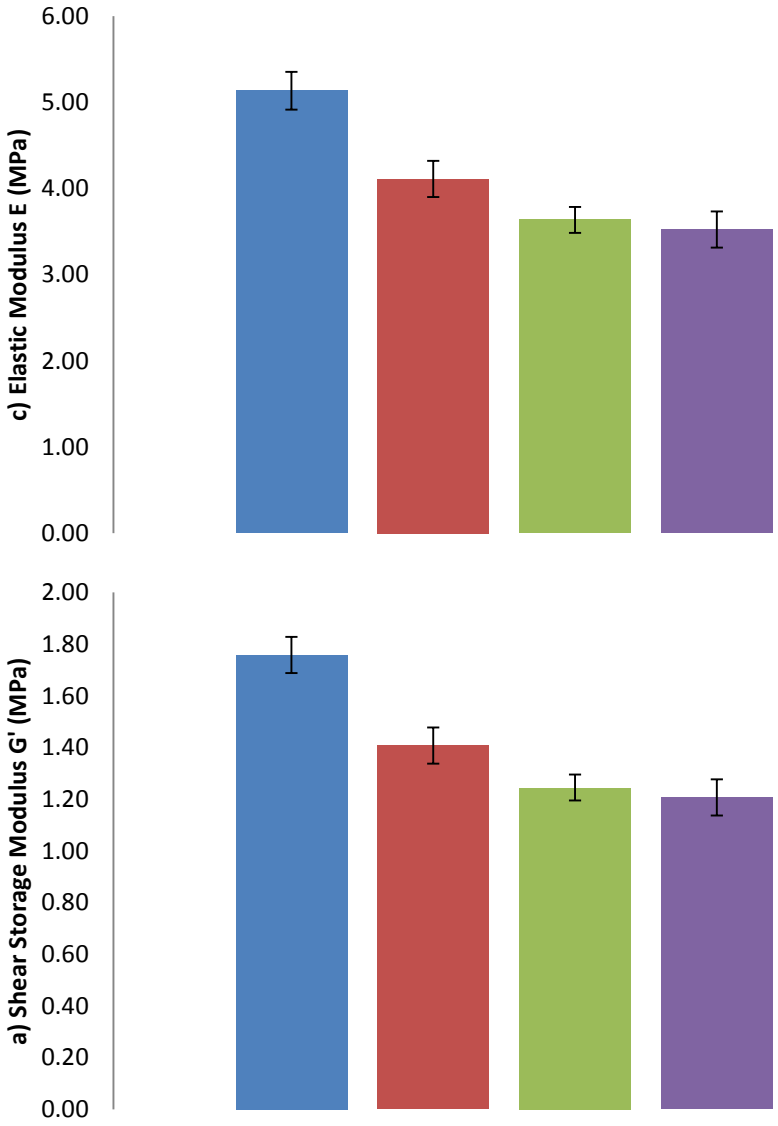

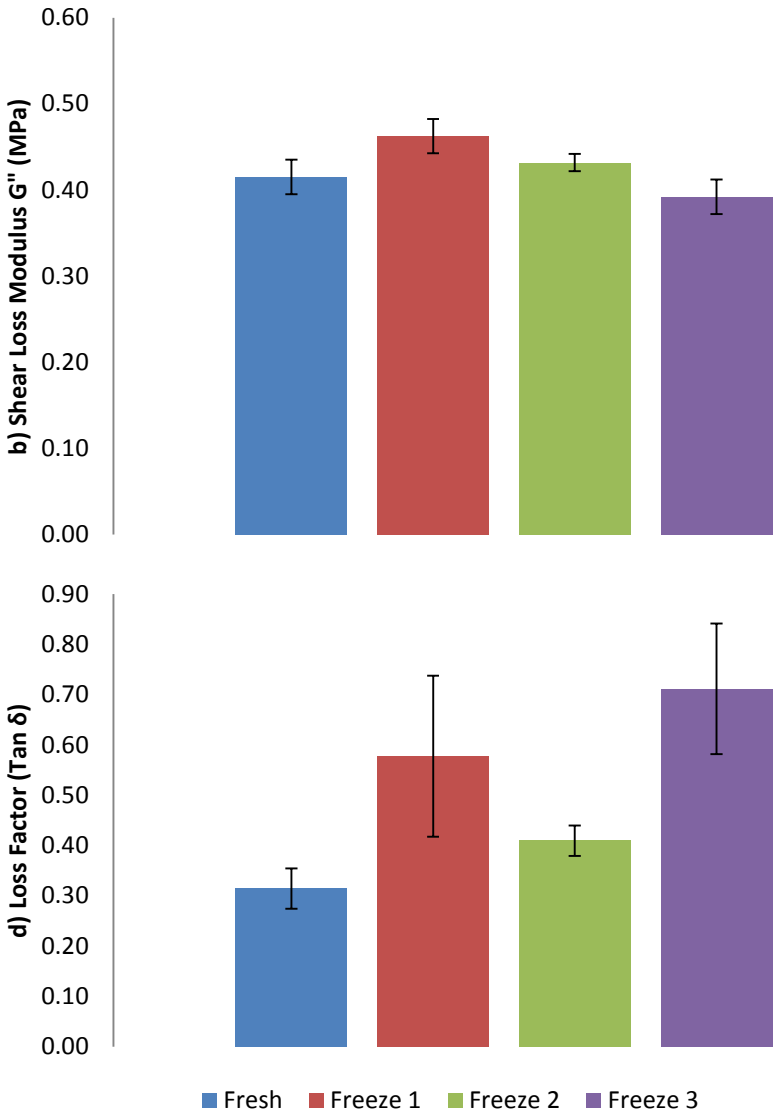

Figure 3. a) Mean shear storage modulus (*G'*), b) Shear loss modulus (*G"*), c) Elastic modulus (*E*) and the d) Loss factor for all samples combined during different storage and freezing conditions. Error bars represent the standard error of mean (SEM).

Inter-Sample Variability

Numerical results for individual samples are tabulated in Tables 1 - 4. Repeated freeze-thaw cycles led to some significant differences in *G'* (p = 0.016) and *E* (p = 0.019) across

individual samples but no differences in *G″* (p = 0.122) or the loss factor (p = 0.178). Bonferroni post-hoc pairwise comparisons showed between freeze-thaw cycle effects on the individual sample mean *G′* and *E* were not statistically significant between fresh and one freeze-thaw cycle (p = 0.45), one freeze-thaw and two freeze-thaw cycles (p = 1.00), and two freeze-thaw and three freeze-thaw cycles (p = 1.00). Further post-hoc pairwise comparison was not necessary for *G″* or the loss factor, as these were not statistically significant.

A high degree of variability in each mechanical property was observed both within and between the 11 discrete samples analysed at each freeze-thaw cycle, as indicated by high standard deviations about the overall mean values (as listed above) and the substantial absolute ranges of individual sample means and coefficient of variation (CoV) (Tables 1 - 4). For example, the *E* value in an individual sample in the same cycle of fresh testing varied by as much as 10.47 MPa equivalent to a change of up to 96.29 % of the overall mean value on one occasion (Table 3). Across the 11 samples tested, *E* varied by as much as 14.73 MPa or equivalent to a 188.89 % change to the overall mean within the same cycle of freezing (mean / SD) seen in Table 3. Inter-sample variation was such that in some instances individual samples exhibited changes in mechanical properties across freeze-thaw cycles that differed qualitatively from the overall mean trends (Fig. 4).

Table 1. Mean ± standard deviation (SD), standard error mean (SEM) and coefficient of variation (CoV) for Shear storage modulus (MPa) for each tested sample during each cycle of freezing.

Shear Storage Modulus *G'* (MPa)												
	Fresh			Freeze 1			Freeze 2			Freeze 3		
Sample	Mean±SD	SEM	CoV%	Mean±SD	SEM	CoV%	Mean±SD	SEM	CoV%	Mean±SD	SEM	CoV%
1	2.57±0.39	0.12	15.17	2.61±0.28	0.09	10.73	1.24±0.42	0.13	33.87	1.65±0.45	0.14	27.27
2	1.11±0.13	0.04	11.71	1.16±0.12	0.04	10.34	1.04±0.43	0.14	41.35	1.29±0.13	0.04	10.08
3	2.58±1.05	0.33	40.70	0.77±0.58	0.18	75.32	0.76±0.50	0.16	65.79	0.54±0.52	0.16	96.30
4	2.22±0.26	0.08	11.71	2.20±0.35	0.11	15.91	1.64±0.24	0.08	14.63	2.32±0.65	0.21	28.02
5	1.05±0.47	0.15	44.76	1.04±0.53	0.17	50.96	1.06±0.22	0.07	20.75	0.19±0.15	0.05	78.95
6	1.72±0.37	0.12	21.51	0.70±0.21	0.07	30.00	1.36±0.22	0.07	16.18	1.38±0.19	0.06	13.77
7	2.07±0.21	0.07	10.14	2.12±0.12	0.04	5.66	1.25±0.12	0.04	9.60	1.84±0.10	0.03	5.43
8	2.41±0.28	0.09	11.62	1.85±0.24	0.08	12.97	1.85±0.22	0.07	11.89	1.40±0.79	0.25	56.43
9	1.31±0.17	0.05	12.98	1.12±0.12	0.04	10.71	0.79±0.15	0.05	18.99	0.22±0.02	0.01	9.09
10	1.70±0.55	0.17	32.35	1.63±0.58	0.18	35.58	2.10±0.45	0.14	21.43	1.64±0.50	0.16	30.49
11	0.60±0.39	0.12	65.00	0.29±0.17	0.05	58.62	0.61±0.07	0.02	11.48	0.79±0.12	0.04	15.19

Table 2. Mean ± standard deviation (SD), standard error mean (SEM) and coefficient of variation (CoV) for Shear loss modulus (MPa) for each tested sample during each cycle of freezing.

Shear Loss Modulus *G″* (MPa)												
	Fresh			Freeze 1			Freeze 2			Freeze 3		
Sample	Mean±SD	SEM	CoV%	Mean±SD	SEM	CoV%	Mean±SD	SEM	CoV%	Mean±SD	SEM	CoV%
1	0.54±0.06	0.02	11.11	0.62±0.08	0.03	12.90	0.44±0.13	0.04	29.55	0.53±0.08	0.02	15.09
2	0.24±0.02	0.01	8.33	0.31±0.02	0.01	6.45	0.25±0.09	0.03	36.00	0.28±0.02	0.01	7.14
3	0.42±0.48	0.15	114.29	0.48±0.18	0.06	37.50	0.49±0.12	0.04	24.49	0.49±0.17	0.05	34.69
4	0.60±0.07	0.02	11.67	0.74±0.09	0.03	12.16	0.53±0.05	0.02	9.43	0.60±0.10	0.03	16.67
5	0.37±0.14	0.04	37.84	0.42±0.14	0.04	33.33	0.45±0.07	0.02	15.56	0.06±0.05	0.01	83.33
6	0.40±0.07	0.02	17.50	0.38±0.03	0.01	7.89	0.37±0.03	0.01	8.11	0.33±0.03	0.01	9.09
7	0.49±0.02	0.01	4.08	0.58±0.01	0.00	1.72	0.37±0.03	0.01	8.11	0.43±0.02	0.01	4.65
8	0.45±0.03	0.01	6.67	0.38±0.04	0.01	10.53	0.39±0.03	0.01	7.69	0.50±0.18	0.06	36.00
9	0.40±0.03	0.01	7.50	0.57±0.06	0.02	10.53	0.68±0.03	0.01	4.41	0.39±0.02	0.01	5.13
10	0.46±0.11	0.03	23.91	0.47±0.11	0.04	23.40	0.58±0.07	0.02	12.07	0.48±0.10	0.03	20.83
11	0.19±0.06	0.02	31.58	0.13±0.03	0.01	23.08	0.21±0.02	0.01	9.52	0.22±0.01	0.00	4.55

Table 3. Mean ± standard deviation (SD), standard error mean (SEM) and coefficient of variation (CoV) for Elastic modulus (MPa) for each tested sample during each cycle of freezing.

Elastic Modulus *E* (MPa)												
	Fresh			Freeze 1			Freeze 2			Freeze 3		
Sample	Mean±SD	SEM	CoV%	Mean±SD	SEM	CoV%	Mean±SD	SEM	CoV%	Mean±SD	SEM	CoV%
1	7.52±1.14	0.36	15.16	7.62±0.83	0.26	10.89	3.61±1.22	0.38	33.80	4.83±1.32	0.42	27.33
2	3.24±0.39	0.12	12.04	3.39±0.35	0.11	10.32	3.04±1.27	0.40	41.78	3.76±0.39	0.12	10.37
3	7.55±3.07	0.97	40.66	2.24±1.68	0.53	75.00	2.22±1.46	0.46	65.77	1.57±1.51	0.48	96.18
4	6.48±0.75	0.24	11.57	6.42±1.02	0.32	15.89	4.80±0.71	0.22	14.79	3.79±1.89	0.60	49.87
5	3.08±1.38	0.44	44.81	3.04±1.55	0.49	50.99	3.10±0.65	0.21	20.97	0.56±0.44	0.14	78.57
6	5.01±1.09	0.34	21.76	2.05±0.63	0.20	30.73	3.97±0.65	0.21	16.37	4.04±0.56	0.18	13.86
7	6.04±0.61	0.19	10.10	6.19±0.36	0.11	5.82	3.65±0.35	0.11	9.59	5.37±0.31	0.10	5.77
8	7.03±0.80	0.25	11.38	5.39±0.70	0.22	12.99	5.39±0.63	0.20	11.69	4.09±2.31	0.73	56.48
9	3.83±0.49	0.15	12.79	3.28±0.34	0.11	10.37	2.31±0.43	0.14	18.61	0.66±0.07	0.02	10.61
10	4.97±1.60	0.51	32.19	4.75±1.70	0.54	35.79	6.13±1.30	0.41	21.21	4.79±1.46	0.46	30.48
11	1.75±1.15	0.36	65.71	0.84±0.49	0.16	58.33	1.77±0.21	0.07	11.86	2.29±0.34	0.11	14.85

Table 4. Mean ± standard deviation (SD), standard error mean (SEM) and coefficient of variation (CoV) for Loss factor for each tested sample during each cycle of freezing.

Loss Factor												
	Fresh			Freeze 1			Freeze 2			Freeze 3		
Sample	Mean±SD	SEM	CoV%	Mean±SD	SEM	CoV%	Mean±SD	SEM	CoV%	Mean±SD	SEM	CoV%
1	0.21±0.03	0.01	14.29	0.24±0.01	0.00	4.17	0.36±0.04	0.01	11.11	0.34±0.11	0.04	32.35
2	0.22±0.01	0.00	4.55	0.27±0.01	0.00	3.70	0.25±0.03	0.01	12.00	0.22±0.01	0.00	4.55
3	0.21±0.14	0.04	66.67	2.46±5.33	1.69	216.67	0.85±0.46	0.14	54.12	2.02±2.41	0.76	119.31
4	0.27±0.01	0.00	3.70	0.34±0.03	0.01	8.82	0.33±0.03	0.01	9.09	0.27±0.04	0.01	14.81
5	0.36±0.05	0.02	13.89	0.45±0.13	0.04	28.89	0.43±0.06	0.02	13.95	0.31±0.01	0.00	3.23
6	0.24±0.02	0.01	8.33	0.61±0.24	0.07	39.34	0.28±0.04	0.01	14.29	0.24±0.02	0.00	8.33
7	0.24±0.02	0.01	8.33	0.27±0.01	0.00	3.70	0.30±0.01	0.00	3.33	0.24±0.00	0.00	0.00
8	0.19±0.01	0.00	5.26	0.21±0.01	0.00	4.76	0.21±0.01	0.00	4.76	1.83±3.42	1.08	186.89
9	0.31±0.04	0.01	12.90	0.51±0.07	0.02	13.73	0.88±0.12	0.04	13.64	1.76±0.11	0.04	6.25
10	0.28±0.05	0.02	17.86	0.31±0.06	0.02	19.35	0.29±0.04	0.01	13.79	0.30±0.04	0.01	13.33
11	0.93±1.12	0.35	120.43	0.68±0.62	0.20	91.18	0.34±0.02	0.01	5.88	0.29±0.04	0.01	13.79

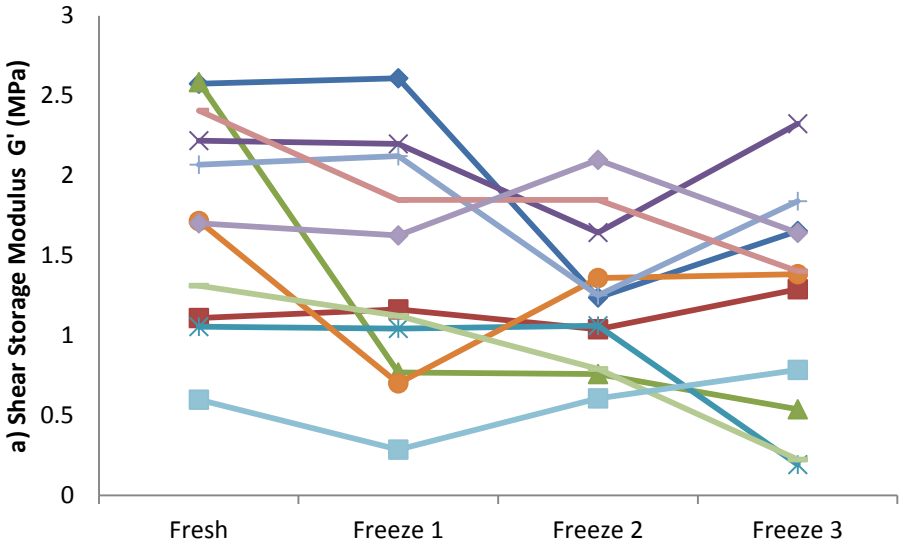
a) Shear Storage Modulus G' (MPa)
3
2.5
2
1.5
1
0.5
0
Fresh
Freeze 1
Freeze 2
Freeze 3

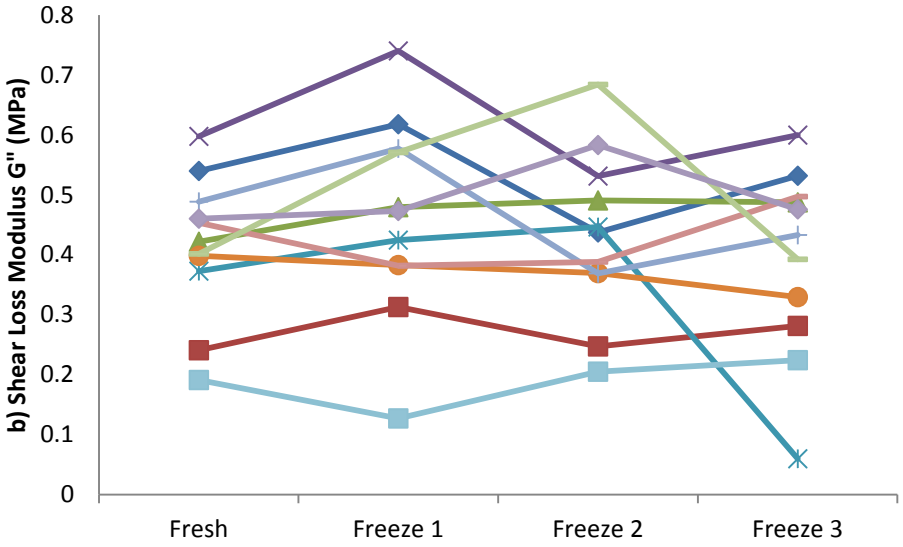
b) Shear Loss Modulus G'' (MPa)
0.8
0.7
0.6
0.5
0.4
0.3
0.2
0.1
0
Fresh
Freeze 1
Freeze 2
Freeze 3

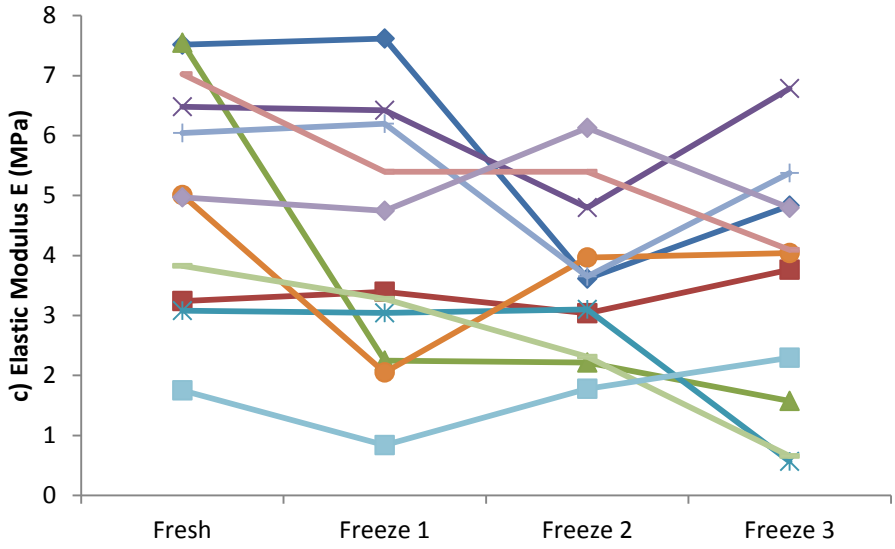
c) Elastic Modulus E (MPa)
8
7
6
5
4
3
2
1
0
Fresh
Freeze 1
Freeze 2
Freeze 3

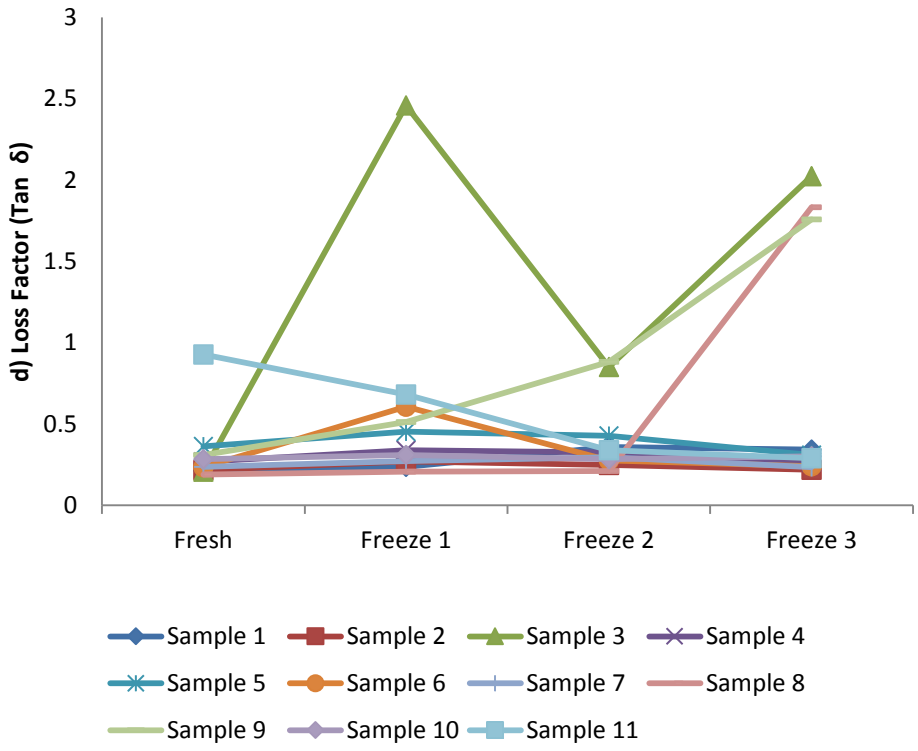

Figure 4. a) Mean shear storage modulus (*G'*), b) Shear loss modulus (*G"*), c) Elastic modulus (*E*) and the d) Loss factor for individual samples (n = 11) across multiple freeze-thaw cycles. Note not only the high level of variability across individual samples, but also the changes in mechanical properties across multiple freeze-thaw cycles sometimes differ qualitatively from the overall mean trends shown in Figure 2 (e.g. samples 4 and 11).

Discussion

This study provides the first systematic investigation of the effects of multiple freeze-thaw cycles on the mechanical properties of articular cartilage. Szarko et al., [2010] compared the mechanical properties of canine femoral articular cartilage stored at -20˚C, -80˚C and snap frozen in liquid nitrogen using indentation techniques. They found that with rapid thawing (37.5°C) and exposure to PBS, both -20˚C and -80˚C can be used as reliable

preservation methods for one freeze-thaw cycle as this produced results consistent with those from fresh samples. However, snap freezing tissue can cause ice crystallisation to form on the sample and therefore compromises the integrity of the tissue. Further research [Moore & Burris, 2015] also considered the effects of one freeze-thaw cycle at -80°C on the mechanical properties of bovine femoral and tibial articular cartilage in comparison to fresh samples. Using a custom made indenter samples were exposed to PBS to maintain hydration and thawed at room temperature. No significant change in material properties was found with a tensile modulus of 4.1 ± 2.2 MPa for fresh samples and 4.5 ± 2.4 MPa for frozen samples [Moore & Burris, 2015]. However, individual samples were randomly assigned to a fresh or frozen cohort and testing was not repeated on the same sample. Therefore results did not account for biological variability that may exist spatially within one specimen or cadaver. Wilusz et al., [2013] used two freeze thaw cycles at -20°C of human femoral articular cartilage prior to atomic force microscopy (AFM)-based indentation. Justification for using two freeze-thaw cycles was recommended by Athanasiou et al., [1991] who established this aspect of the protocol on anecdotal unpublished data. Samples were exposed to PBS to maintain hydration and results from healthy cartilage ECM presented an *E* of 491 kPa. However in this study, a comparison to fresh samples was not made therefore what effect two freeze-cycles had on the material properties is unknown [Wilusz et al., 2013].

This research study demonstrated that mean cartilage *G'* and *E* for the joint overall showed a sharp decreasing trend after one cycle of freezing, although this reduction appeared to lessen following two and three freeze-thaw cycles, despite not reaching statistical significance (Fig. 3). Interestingly *G"* and the loss factor showed no such trends and both increased and decreased during various cycles of freezing (Fig. 3). The loss factor in particular showed high standard error mean (SEM) (Fig. 3) in comparison to other

parameters. When analysing the SD it appears that there is no consistent trend or change in *G'* and *E* where values both increase and decrease in various cycles of freezing (Tables 1 & 3). With the exception of two outliers, *G"* and the loss factor SD remains unchanged during all cycles of freezing (Tables 2 & 4).

Systematic testing of articular cartilage across multiple freeze-thaw cycles in this study shows that samples can undergo three freezing cycles without statistically significant changes to material properties when handled and stored correctly (Fig. 3). These results therefore provide some support for the use of freezing as a method of preservation of cartilage where material properties are required to remain unchanged for mechanical testing. However the authors note that a number of changes in individual mean material properties for the joint were observed here (Fig. 1), and although these fell below thresholds of statistical significance in this study they may represent meaningful magnitudes in the context of other studies. For example, the overall mean *E* showed relatively large decreases with increasing number of freeze thaw cycles such that the values decreased by 1.02 MPa (one freeze-thaw), 0.47 MPa (two freeze-thaw) and 0.12 MPa (three freeze-thaw) of the mean value compared to fresh samples. Such relative changes in magnitude may well be extremely important in the context of comparative studies such as comparison of material properties between cohorts of different age and/or disease status [Wen et al., 2012; Kleeman et al., 2005; Franz et al., 2001] and computational modelling studies of joint biomechanics [Mononen et al., 2012; Pena et al., 2007; Blankevoort et al., 1991]. Kleemann et al., [2005] researched the differences in cartilage material properties obtained from human tibial plateau samples and found that changes of as little as 0.1 MPa or 20 % can be found between grade one and grade two osteoarthritic samples (graded by the International Cartilage Repair Society). Furthermore, in a human knee finite element model sensitivity analysis by Li et al., [2001] the material properties of cartilage were varied

between 3.5 – 10 MPa, to understand the effect on joint contact stresses. Results showed that magnitude changes had substantial effects on the functional predictions of the model, specifically that *E* linearly increased with peak contact stresses and a Poisson's ratio increase significantly increased peak von Mises stress and hydrostatic pressure in the knee joint cartilage.

Given the absolute and relative changes in overall material properties measured across freeze-thaw cycles (Fig. 3), it may be preferable for experiments seeking to test multiple tissue types from the same cadaver to prioritise cartilage for fresh testing (or minimal freeze-thaw cycles), particularly given that previous research has suggested that other joint tissues are relatively insensitive to freezing [Jung et al., 2011; Huang et al., 2011; Moon et al., 2006; Woo et al., 1986]. For example, Jung et al., [2011] concluded that the human patella-tendon can be exposed to eight freeze-thaw cycles without compromising mechanical properties; provided testing conditions and tissue handling are approached with great care. This protocol involved allowing samples to re-freeze for a minimum of 6 hours and thaw at room temperature for 6 hours with exposure to saline. Furthermore, a study has shown the human flexor digitorum superficialis and flexor pollicis longus can undergo three freeze-thaw cycles before the integrity of their material properties is compromised. In addition, freeze-thawing over five times also results in decreased mechanical and structural behaviour [Huang et al., 2011]. Other studies focusing on ligaments include Woo et al., [1986] who explored the mechanical properties of the rabbit medial collateral ligament (MCL) following one prolonged freezing cycle and concluded that this has no effect when compared to fresh samples. Moon et al., [2006] also used the rabbit MCL to determine the effect when two freeze-thaw cycles and likewise concluded that no apparent changes to material properties occurred when compared to fresh samples. Therefore most published studies are in agreement that at least two freeze-

cycles, under the correct handling and storage conditions, allow ligament and tendon samples to remain mechanically unchanged [Jung et al., 2011; Huang et al., 2011; Moon et al., 2006; Woo et al., 1986].

The modulus values obtained within this study fall within the range of those reported in the literature for other mammalian femoral condylar articular cartilage. Shepherd & Seedhom, [1999] and Wilusz et al., [2013] reported a range of *E* from 0.1 - 18.6 MPa for human femoral condyle articular cartilage, although Moore & Burris [2015] reported lower values of 0.62 ± 0.10 MPa for bovine stifle cartilage. In the current study mean values for *E* lie between 0.56 - 7.62 MPa, falling within this range already reported; however in both the literature and the current study there is a high variability of modulus. More specifically, previous canine research has found an *E* of 0.12 ± 0.10 MPa [Leroux et al., 2001], and 0.385 - 0.964 MPa [Jurvelin et al., 2000] when samples have undergone indentation testing following one freeze cycle. These values are generally lower than those reported in the current study and have smaller absolute variability. Previous canine cartilage studies have reported CoV's of up to 23.61 % [Jurvelin et al., 2000], which although being quite considerable are much lower than the CoV's reported here up to 96.3 % for *G'* and 114.29 % for *G"* (Tables 1-4). Although the current data is more variable than previous canine research, it should be noted that it is less variable than the human studies discussed above.

Cartilage is a highly heterogeneous material and therefore some variability of modulus is widely expected and accepted [e.g. Jurvelin et al., 2000]; however differences seen in the current study as compared to other studies in the literature may be as a result of the frequency-dependent properties of cartilage. Higher frequencies have been shown to increase *G'* [Pearson & Espino, 2013] and *E* [Taffetani et al., 2015]; however *G"* remains unaffected [Pearson & Espino, 2013]. In the current study, 110 Hz was selected for the

testing because it is the resonant frequency of the indenter and thus most sensitive frequency for the surface detection. In other studies in the literature, a range of frequencies have been used including 0.5 Hz [Taffetani et al., 2015], 10 Hz [Franke et al., 2011] and much higher frequencies up to 200 Hz [Taffetani et al., 2015] and 250 Hz [Franke et al., 2011] where dynamic nanoindentation [Franke et al., 2011] and mechanical analysis methods were also utilised [Taffetani et al., 2015]. Although high frequencies may account for increases in *G'* when compared to other canine studies [Leroux et al., 2001; Jurvelin et al., 2000], the most important comparison is that seen between each freeze cycle, where frequency used remained standardised throughout testing cycles.

Additional limitations to the current study which may also affect variability include indenting sites affected by preceding measurements; however it has been suggested that low load indentation has been shown to cause no visible deformation of samples [Franke et al., 2011]. It is also estimated that during each cycle of testing on a ~1cm² sample, 10 measurements using a 100µm tip would cover 0.1% of the surface area, meaning the chance of overlapping measurements in subsequent test cycles is unlikely. Further, although some variability may be expected from the nanoindentation technique used in the current study, other researchers have found that it yields highly repeatable data on other compliant materials which have a more homogenous structure than cartilage e.g. on a type of ballistic gelatin (Perma-Gel) the CoV for the elastic modulus was 3.3 % following ten indentation tests [Moronkeji et al., 2016].

As the nanoindenter was unable to differentiate between cellular and non-cellular substance, the current study is subject to high variability in results depending on the exact material tested, limiting interpretation of changes to modulus. Other studies have attempted to differentiate the material properties of cartilage sub-components using AFM

and found variation between *E* of the peri- (0.1 MPa) and extra cellular matrix (0.3 MPa) [Wilusz et al., 2013]. However soft tissues are often dehydrated during AFM testing and maintaining hydration can be challenging [Wen et al., 2012].

With these considerations in mind, future research could aim to accurately assess the effect of freezing on articular cartilage by first repeatedly indenting the same site of a fresh sample to fully understand the effect and variability of material properties seen in an identical position. Then secondly, indenting an identical position following multiple freeze-thaw cycles, aided by marking an area of the cartilage and noting at which exact position the sample was tested to understand the effect of freezing.

Conclusion

In summary, the results of this study suggest that three freeze-thaw cycles do not have a statistically significant effect on the overall 'whole-joint' material properties of canine femoral condyle cartilage samples provided the correct handling, storage and hydration of the tissue are maintained throughout preparation and testing. However, relative changes in mean material properties are observed and the failure to reach thresholds for statistical significance is likely the product of high biological variability across the joint. Therefore the changes in material properties observed over multiple freeze-thaw cycles may be sufficient to significantly impact on certain comparative or functional studies, such as finite element modelling, where subtle changes in material properties can indeed modify the true behaviour of articular cartilage under mechanical stress. Changes in material properties reported here should be considered when planning experimental protocols, as they may be sufficient in magnitude to impact on clinical or scientific cartilage studies.

References

1. Akhtar, R., Draper, E.R., Adams, D.J. & Pfaff, H. 2016, "Complex shear modulus of hydrogels using dynamic nanoindentation method", *Mechanics of Biological Systems and Materials, Proceedings of the 2015 Annual Conference on Experimental and Applied Mechanics,* vol. 6, pp. 141-145.
2. Athanasiou, K., Rosenwasser, M., Buckwalter, J., Malinin, T. & Mow, V. 1991, "Interspecies comparisons of in situ intrinsic mechanical properties of distal femoral cartilage", *Journal of Orthopaedic Research,* vol. 9, no. 3, pp. 330-340.
3. Blankevoort, L., Kuiper, J., Huiskes, R. & Grootenboer, H. 1991, "Articular contact in a three-dimensional model of the knee", *Journal of Biomechanics,* vol. 24, no. 11, pp. 1019-1031.
4. Brandt, J., Briere, L., Marr, J., MacDonald, S., Bourne, R. & Medley, J. 2010, "Biochemical comparisons of osteoarthritic human synovial fluid with calf sera used in knee simulator wear testing", *Journal of Biomedical Materials Research Part A,* vol. 94, no. 3, pp. 961-971.
5. Campbell, S.E., Ferguson, V.L. & Hurley, D.C. 2012, "Nanomechanical mapping of the osteochondral interface with contact resonance force microscopy and nanoindentation", *Acta Biomaterialia,* vol. 8, no. 12, pp. 4389-4396.
6. Cheng, L., Xia, X., Yu, W., Scriven, L. & Gerberich, W. 2000, "Flat-punch indentation of viscoelastic material", *Journal of Polymer Science Part B: Polymer Physics,* vol. 38, no. 1, pp. 10-22.
7. Faul, F., Erdfelder, E., Lang, A. & Buchner, A. 2007, "G* Power 3: A flexible statistical power analysis program for the social, behavioral, and biomedical sciences", *Behavior Research Methods,* vol. 39, no. 2, pp. 175-191.

8. Franke, O., Durst, K., Maier, V., Göken, M., Birkholz, T., Schneider, H., Hennig, F. & Gelse, K. 2007, "Mechanical properties of hyaline and repair cartilage studied by nanoindentation", *Acta Biomaterialia,* vol. 3, no. 6, pp. 873-881.
9. Franke, O., Göken, M., Meyers, M., Durst, K. & Hodge, A. 2011, "Dynamic nanoindentation of articular porcine cartilage", *Materials Science and Engineering: C,* vol. 31, no. 4, pp. 789-795.
10. Franz, T., Hasler, E., Hagg, R., Weiler, C., Jakob, R. & Mainil-Varlet, P. 2001, "In situ compressive stiffness, biochemical composition, and structural integrity of articular cartilage of the human knee joint", *Osteoarthritis and Cartilage,* vol. 9, no. 6, pp. 582-592.
11. Guo, Y., Zhang, X. & Chen, W. 2009, "Three-dimensional finite element simulation of total knee joint in gait cycle", *Acta Mechanica Solida Sinica,* vol. 22, no. 4, pp. 347-351.
12. Gupta, H., Schratter, S., Tesch, W., Roschger, P., Berzlanovich, A., Schoeberl, T., Klaushofer, K. & Fratzl, P. 2005, "Two different correlations between nanoindentation modulus and mineral content in the bone–cartilage interface", *Journal of Structural Biology,* vol. 149, no. 2, pp. 138-148.
13. Hargrave-Thomas, E., van Sloun, F., Dickinson, M., Broom, N. & Thambyah, A. 2015, "Multi-scalar mechanical testing of the calcified cartilage and subchondral bone comparing healthy vs early degenerative states", *Osteoarthritis and Cartilage,* vol. 23, no. 10, pp. 1755-1762.
14. Herbert, E., Oliver, W., Lumsdaine, A. & Pharr, G.M. 2009, "Measuring the constitutive behavior of viscoelastic solids in the time and frequency domain using flat punch nanoindentation", *Journal of Materials Research,* vol. 24, no. 03, pp. 626-637.

15. Herbert, E., Oliver, W. & Pharr, G. 2008, "Nanoindentation and the dynamic characterization of viscoelastic solids", *Journal of Physics D: Applied Physics,* vol. 41, no. 7, pp. 074021.
16. Huang, H., Zhang, J., Sun, K., Zhang, X. & Tian, S. 2011, "Effects of repetitive multiple freeze–thaw cycles on the biomechanical properties of human flexor digitorum superficialis and flexor pollicis longus tendons", *Clinical Biomechanics,* vol. 26, no. 4, pp. 419-423.
17. Jin, H. & Lewis, J.L. 2004, "Determination of Poisson's ratio of articular cartilage by indentation using different-sized indenters", *Journal of Biomechanical Engineering,* vol. 126, no. 2, pp. 138-145.
18. Jung, H., Vangipuram, G., Fisher, M.B., Yang, G., Hsu, S., Bianchi, J., Ronholdt, C. & Woo, S.L. 2011, "The effects of multiple freeze–thaw cycles on the biomechanical properties of the human bone-patellar tendon-bone allograft", *Journal of Orthopaedic Research,* vol. 29, no. 8, pp. 1193-1198.
19. Jurvelin, J.S., Arokoski, J.P., Hunziker, E.B. & Helminen, H.J. 2000, "Topographical variation of the elastic properties of articular cartilage in the canine knee", *Journal of Biomechanics,* vol. 33, no. 6, pp. 669-675.
20. Kleemann, R., Krocker, D., Cedraro, A., Tuischer, J. & Duda, G. 2005, "Altered cartilage mechanics and histology in knee osteoarthritis: relation to clinical assessment (ICRS Grade)", *Osteoarthritis and Cartilage,* vol. 13, no. 11, pp. 958-963.
21. Landau, L.D. & Lifshitz, E. 1986, "Theory of Elasticity, vol. 7", *Course of Theoretical Physics,* vol. 3, pp. 109.
22. Lau, A., Oyen, M.L., Kent, R.W., Murakami, D. & Torigaki, T. 2008, "Indentation stiffness of aging human costal cartilage", *Acta Biomaterialia,* vol. 4, no. 1, pp. 97-103.

23. Leroux, M., Cheung, H.S., Bau, J., Wang, J., Howell, D. & Setton, L. 2001, "Altered mechanics and histomorphometry of canine tibial cartilage following joint immobilization", *Osteoarthritis and Cartilage,* vol. 9, no. 7, pp. 633-640.
24. Li, C., Pruitt, L.A. & King, K.B. 2006, "Nanoindentation differentiates tissue-scale functional properties of native articular cartilage", *Journal of Biomedical Materials Research Part A,* vol. 78, no. 4, pp. 729-738.
25. Li, G., Lopez, O. & Rubash, H. 2001, "Variability of a three-dimensional finite element model constructed using magnetic resonance images of a knee for joint contact stress analysis", *Journal of Biomechanical Engineering,* vol. 123, no. 4, pp. 341-346.
26. Martins, P.A., Ferreira, F., Natal Jorge, R., Parente, M. & Santos, A. 2015, "Necromechanics: Death-induced changes in the mechanical properties of human tissues", *Proceedings of the Institution of Mechanical Engineers, Part H: Journal of Engineering in Medicine,* vol. 229, no. 5, pp. 343-349.
27. Mononen, M., Mikkola, M., Julkunen, P., Ojala, R., Nieminen, M., Jurvelin, J. & Korhonen, R. 2012, "Effect of superficial collagen patterns and fibrillation of femoral articular cartilage on knee joint mechanics—A 3D finite element analysis", *Journal of Biomechanics,* vol. 45, no. 3, pp. 579-587.
28. Moon, D.K., Woo, S.L., Takakura, Y., Gabriel, M.T. & Abramowitch, S.D. 2006, "The effects of refreezing on the viscoelastic and tensile properties of ligaments", *Journal of Biomechanics,* vol. 39, no. 6, pp. 1153-1157.
29. Moore, A. & Burris, D. 2015, "Tribological and material properties for cartilage of and throughout the bovine stifle: support for the altered joint kinematics hypothesis of osteoarthritis", *Osteoarthritis and Cartilage,* vol. 23, no. 1, pp. 161-169.

30. Moronkeji, K., Todd, S., Dawidowska, I., Barrett, S. & Akhtar, R. 2016, "The role of subcutaneous tissue stiffness on microneedle performance in a representative *in vitro* model of skin", *Journal of Controlled Release,* In Press, Corrected Proof.
31. Nigg, B. & Herzog, W. (eds) 2006, *Biomechanics of the Musculoskeletal System*, 3rd edn, Wiley, West Sussex.
32. Oliver, W.C. & Pharr, G.M. 2004, "Measurement of hardness and elastic modulus by instrumented indentation: Advances in understanding and refinements to methodology", *Journal of Materials Research,* vol. 19, no. 01, pp. 3-20.
33. Pearson, B. & Espino, D.M. 2013, "Effect of hydration on the frequency-dependent viscoelastic properties of articular cartilage", *Proceedings of the Institution of Mechanical Engineers, Part H: Journal of Engineering in Medicine,* vol. 227, no. 11, pp. 1246-1252.
34. Pena, E., Calvo, B., Martinez, M. & Doblare, M. 2006, "A three-dimensional finite element analysis of the combined behavior of ligaments and menisci in the healthy human knee joint", *Journal of Biomechanics,* vol. 39, no. 9, pp. 1686-1701.
35. Pena, E., Calvo, B., Martinez, M., Palanca, D. & Doblaré, M. 2005, "Finite element analysis of the effect of meniscal tears and meniscectomies on human knee biomechanics", *Clinical Biomechanics,* vol. 20, no. 5, pp. 498-507.
36. Shepherd, D.E. & Seedhom, B.B. 1999, "The 'instantaneous' compressive modulus of human articular cartilage in joints of the lower limb", *Rheumatology (Oxford, England),* vol. 38, no. 2, pp. 124-132.
37. Shepherd, D.E. & Seedhom, B.B. 1997, "A technique for measuring the compressive modulus of articular cartilage under physiological loading rates with preliminary results", *Proceedings of the Institution of Mechanical Engineers. Part H, Journal of engineering in medicine,* vol. 211, no. 2, pp. 155-165.

38. Silver, F.H., Bradica, G. & Tria, A. 2002, "Elastic energy storage in human articular cartilage: estimation of the elastic modulus for type II collagen and changes associated with osteoarthritis", *Matrix Biology,* vol. 21, no. 2, pp. 129-137.
39. Sneddon, I.N. 1965, "The relation between load and penetration in the axisymmetric Boussinesq problem for a punch of arbitrary profile", *International Journal of Engineering Science,* vol. 3, no. 1, pp. 47-57.
40. Szarko, M., Muldrew, K. & Bertram, J.E. 2010, "Freeze-thaw treatment effects on the dynamic mechanical properties of articular cartilage", *BMC Musculoskeletal Disorders,* vol. 11, no. 1, pp. 231.
41. Taffetani, M., Raiteri, R., Gottardi, R., Gastaldi, D. & Vena, P. 2015, "A quantitative interpretation of the response of articular cartilage to atomic force microscopy-based dynamic nanoindentation tests", *Journal of Biomechanical Engineering,* vol. 137, no. 7, pp. 071005.
42. Wang, Y., Fan, Y. & Zhang, M. 2014, "Comparison of stress on knee cartilage during kneeling and standing using finite element models", *Medical Engineering & Physics,* vol. 36, no. 4, pp. 439-447.
43. Wen, C., Wu, C., Tang, B., Wang, T., Yan, C., Lu, W., Pan, H., Hu, Y. & Chiu, K. 2012, "Collagen fibril stiffening in osteoarthritic cartilage of human beings revealed by atomic force microscopy", *Osteoarthritis and Cartilage,* vol. 20, no. 8, pp. 916-922.
44. Wilusz, R.E., Zauscher, S. & Guilak, F. 2013, "Micromechanical mapping of early osteoarthritic changes in the pericellular matrix of human articular cartilage", *Osteoarthritis and Cartilage,* vol. 21, no. 12, pp. 1895-1903.
45. Woo, S.L., Orlando, C.A., Camp, J.F. & Akeson, W.H. 1986, "Effects of postmortem storage by freezing on ligament tensile behavior", *Journal of Biomechanics,* vol. 19, no. 5, pp. 399-404.

Chapter Four: The effect of ageing and osteoarthritis on the mechanical properties of cartilage and bone in the human knee joint

Abstract

Osteoarthritis is traditionally associated with cartilage degeneration although is now widely accepted as a whole-joint disease affecting the entire osteochondral unit; however site-specific cartilage and bone material properties during healthy ageing and disease are absent limiting our understanding. Cadaveric specimens (n = 12; 31 - 88 years) with grades 0 - 4 osteoarthritis, were dissected and spatially correlated cartilage, subchondral and trabecular bone samples (n = 8 per cadaver) were harvested from femoral and tibial localities. Nanoindentation was utilised to obtain cartilage shear storage modulus (*G'*) and shear loss modulus (*G"*), and bone elastic modulus (*E*). Cartilage *G'* and *G"* are strongly correlated with age ($p = 0.003$, $p = 0.011$ respectively) and osteoarthritis grade ($p = 0.007$, $p = 0.002$ respectively). A correlation analysis was also performed between subchondral bone *E* and age ($p = 0.072$), and subchondral bone *E* and osteoarthritis grade which was strongly correlated ($p = 0.013$). Trabecular bone *E* showed no correlation with age ($p = 0.372$) or osteoarthritis grade ($p = 0.778$). Results indicated preferential medial osteoarthritis development and a non-significant relationship between a change in cartilage *G'* with sample location ($p = 0.083$). Changes to cartilage *G'* and *G"* were significantly correlated with changes in subchondral bone *E* ($p = 0.007$, $p = 0.002$ respectively). This demonstrated for the first time significant correlations between site-matched cartilage and subchondral bone material property changes during progressive ageing and osteoarthritis, supporting the role of bone in disease initiation and progression. This clinically relevant data indicates a causative link with osteoarthritis and medial habitual loading.

Introduction

Osteoarthritis (OA) is one of the most prevalent musculoskeletal conditions amongst the adult population with the most common diagnosis at the knee joint [Zhang & Jordan, 2008]. Individuals with OA have increased variability in gait spatial-temporal parameters [Kiss, 2011], which in turn can lead to a decline in locomotor stability and increase the risk of falls through reduced functionality [Hollman et al., 2007]. Ageing is a high risk factor for the development and progression of knee OA and is known to influence mechanical and biochemical changes within tissue structure, even in the absence of OA and other disease or injury status [Hansen et al., 2006; Manninen et al., 1996].

OA is traditionally associated with degeneration of the articular cartilage; however it is now more widely accepted that OA is a whole-joint disease that alters the integrity of multiple tissues of the osteochondral unit [Mahjoub et al., 2012]. A recent review suggests tissue-level adaptations of the subchondral bone are thought to occur in OA prior to degeneration of the overlying articular cartilage [Burr & Gallant et al, 2012]; however this has been rarely explored in the human knee joint. Abnormal remodeling of the subchondral bone has been identified, including high proliferation of volume at the bone-cartilage interface, with observations of changes to density, separation and quantity of the trabecular bone [Kamibayashi et al., 1995, Bobinac et al., 2003]. These structural modifications of bone and cartilage occur in synergy further suggesting subchondral bone plays an important but mostly unexplored role in the initiation and progression of the disease [Madry et al., 2010].

These structural adaptations may logically influence the mechanical strength of such tissues. Research shows that cartilage elastic modulus (*E*) declines with progressive grades of OA [Kleemann et al., 2005, Wilusz et al., 2013]. However, there is minimal research on

the effect of OA on subchondral bone material properties. Indeed there has been no comparison of the material properties of site matched cartilage and bone from the same donor in the presence of OA when compared to healthy controls. Knowledge of material properties of all tissues involved would enhance the development of treatment and clinical outcomes by advancing our understanding of disease mechanisms [Kuroki et al., 2011].

Subsequently the aim of this research is to systematically quantify age and OA related trends in the material properties of multiple tissues from the human knee joint. Articular cartilage, subchondral bone and trabecular bone samples from a cohort of donors spanning a large age range were tested using nanoindentation techniques. This study included samples with varying grades of OA in order to understand how ageing and disease status affects multiple tissues of the knee joint simultaneously. Extraction of multiple, spatially distributed samples of all tissues from the same donors allowed the explicit test for localised changes within tissues and furthermore for correlated changes between tissues during ageing and OA progression for the first time.

Materials and Methods

Specimens

Fresh-frozen human knee joints (n = 12) were sourced aged 31 – 88 years (4 female, 8 male). Specific cadaver demographics can be seen in Table 1, including height, weight, body mass index (BMI) and cause of death. All cadaveric specimens were initially frozen post rigor mortis, which has been shown to decrease deformation in muscle tissue, although this has not been explored in cartilage or bone [Martins et al., 2015] Cadavers underwent one freeze-thaw cycle prior to dissection, which has been shown to cause no significant change

to integrity of tissues [e.g. Peters et al., 2017; Moon et al., 2006]. Ethical permission for use of this human cadaveric material was granted by the NRES (15/NS/0053).

Table 1. Cadaver demographics.

	Age	Gender	Race	Height (cm)	Weight (kg)	BMI	Cause of Death
Cadaver 1	31	Female	Not known	172.7	47.2	15.81	Cardiac arrest
Cadaver 2	37	Female	White	160.0	79.4	31.00	Intracerebral hemorrhage; Severe hypertension
Cadaver 3	43	Female	White	170.2	64.4	22.24	Metastatic cervical carcinoma
Cadaver 4	49	Male	White	175.3	58.5	19.05	Unknown
Cadaver 5	51	Male	White	182.9	104.3	31.19	Cardiac arrhythmia; Coronary artery disease
Cadaver 6	58	Male	White	188.0	84.8	24.01	Gunshot wound of head and neck
Cadaver 7	72	Male	Puerto Rican	162.6	70.3	26.60	Atherosclerotic heart disease of native coronary
Cadaver 8	72	Male	White	167.6	72.6	25.82	Debility; Alzheimer's disease
Cadaver 9	79	Male	White	172.7	72.1	24.17	Acute myocardial infarction; Coronary artery disease
Cadaver 10	80	Male	White	182.9	83.9	25.09	Myocardial infarction; Cardiac arrest; Hypertension
Cadaver 11	86	Female	White	165.1	63.5	23.29	Respiratory failure; Pneumonia
Cadaver 12	88	Male	White	177.8	68.0	21.52	Natural causes; Unspecified

Individual samples dissected from each cadaver (n = 8 samples per tissue type from each cadaver) were graded for OA using the International Repair Cartilage Society (ICRS) grading system, which is defined in Table 2. The cadaveric knee joints were photographed and blind graded by two individuals at a later date three times, one week apart, with the mean score used. Photographs from each cadaver can be seen in Figures 1 – 12.

Table 2. International Cartilage Repair Society (ICRS) Grading.

ICRS Grade	Description
0 **Normal**	No lesions fissures or cracks.
1 **Nearly Normal**	Superficial lesions. Soft indentation and/or superficial fissures and cracks.
2 **Abnormal**	Lesions extending down to <50% of cartilage depth.
3 **Severely Abnormal**	Cartilage defects extending down >50% of cartilage depth as well as down to calcified layer and down to but not through the subchondral bone. Blisters are included in this Grade.
4 **Severely Abnormal**	Cartilage defects extending down >75% of cartilage depth as well as down to calcified layer and through the subchondral bone. Blisters are included in this Grade.

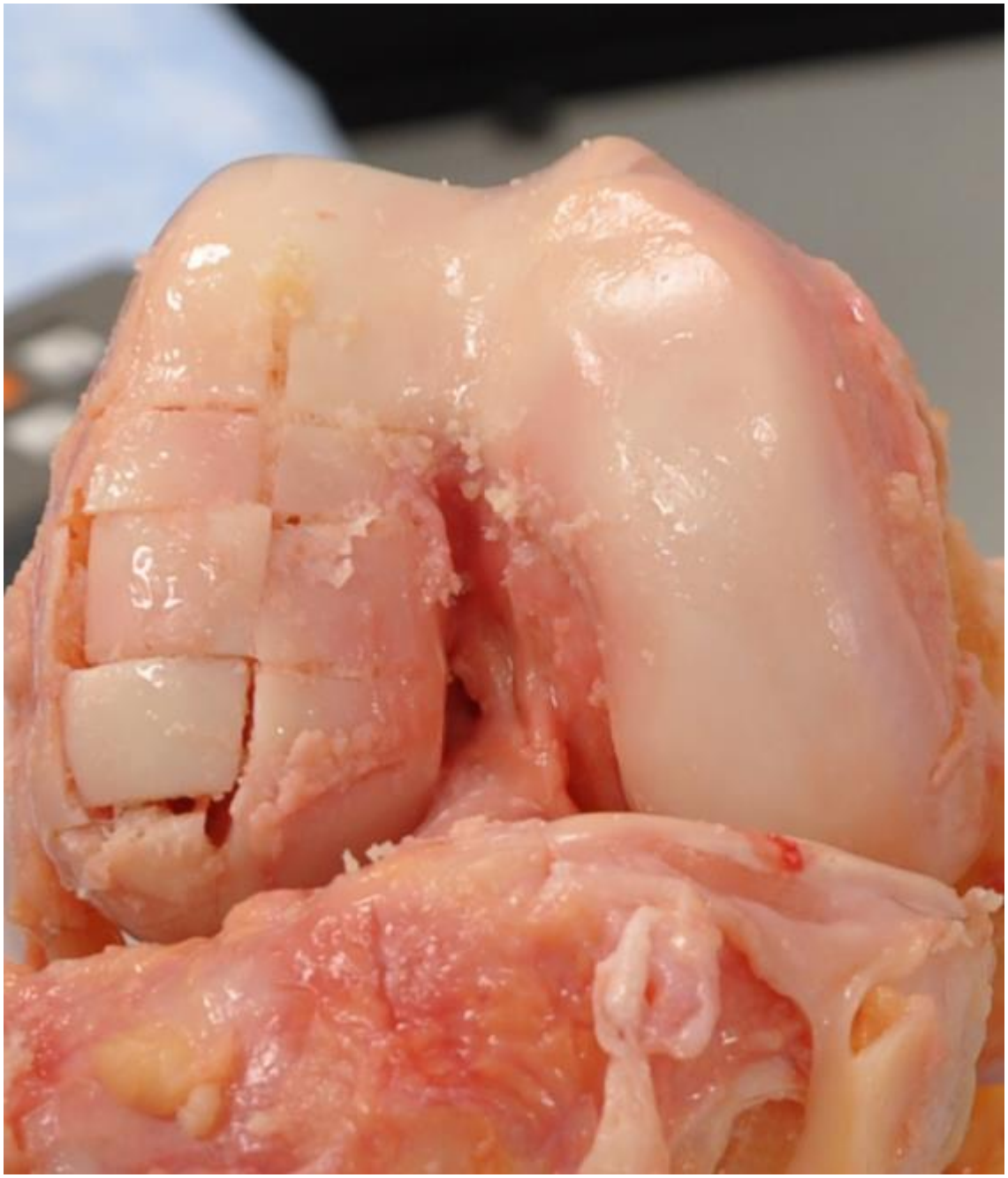

Figure 1. Cadaver 1, 31 years.

Figure 2. Cadaver 2, 37 years.

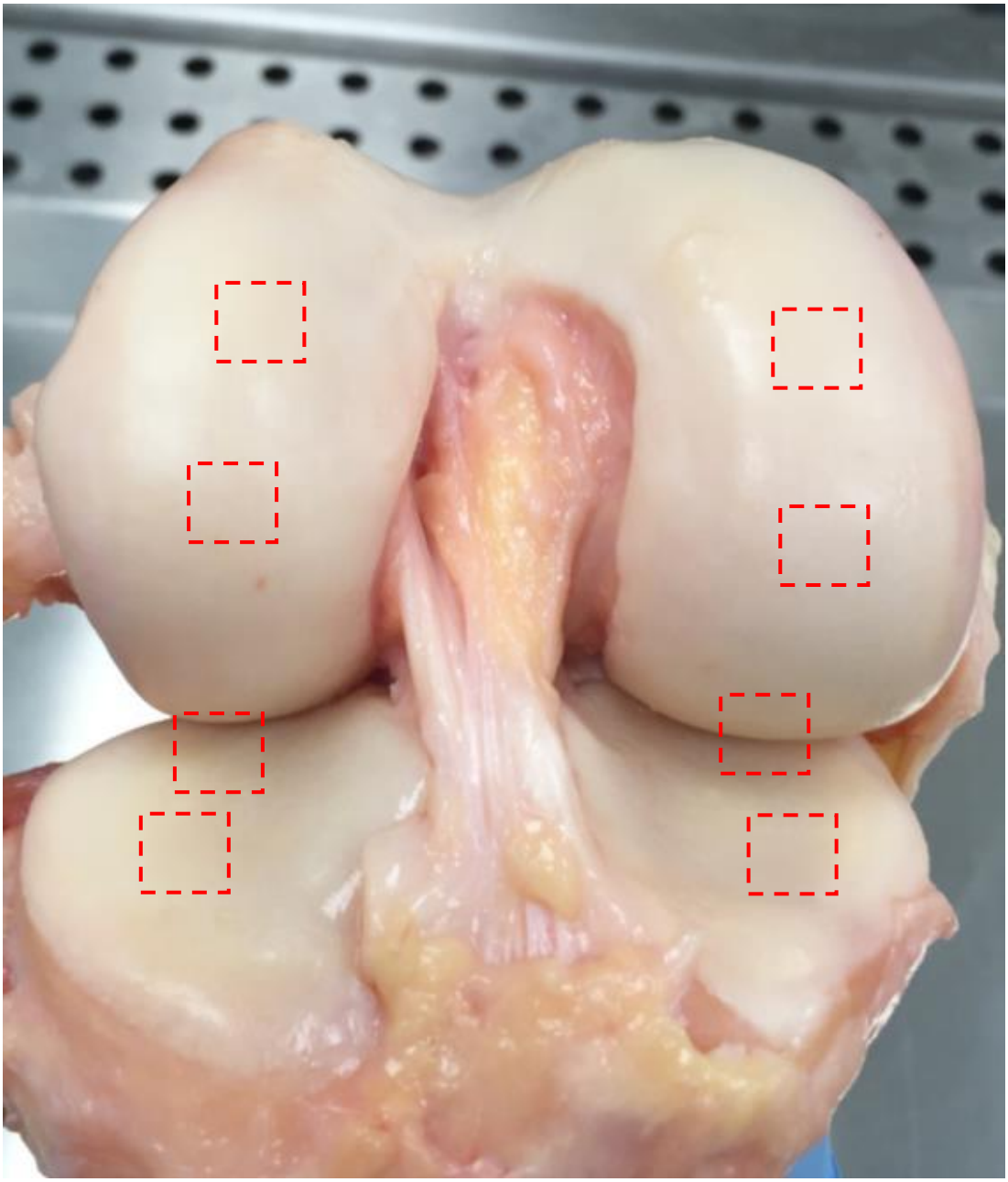

Figure 3. Cadaver 3, 43 years. Red boxes indicate test locations: femoral condyle lateral superior, femoral condyle lateral inferior, femoral condyle medial superior, femoral condyle medial inferior, tibial plateau lateral posterior, tibial plateau lateral anterior, tibial plateau medial posterior, tibial plateau medial anterior.

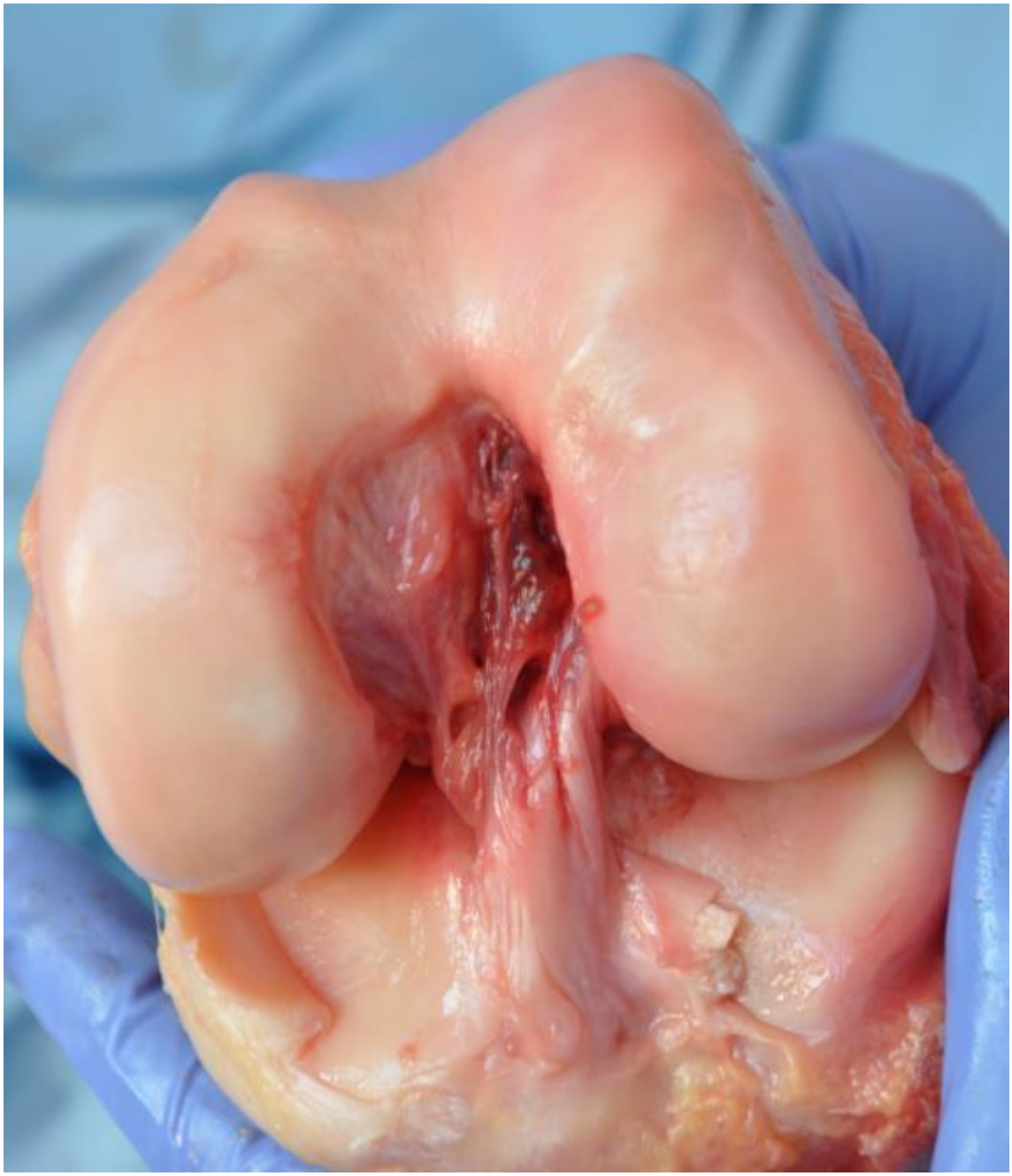

Figure 4. Cadaver 4, 49 years.

Figure 5. Cadaver 5, 51 years.

Figure 6. Cadaver 6, 58 years.

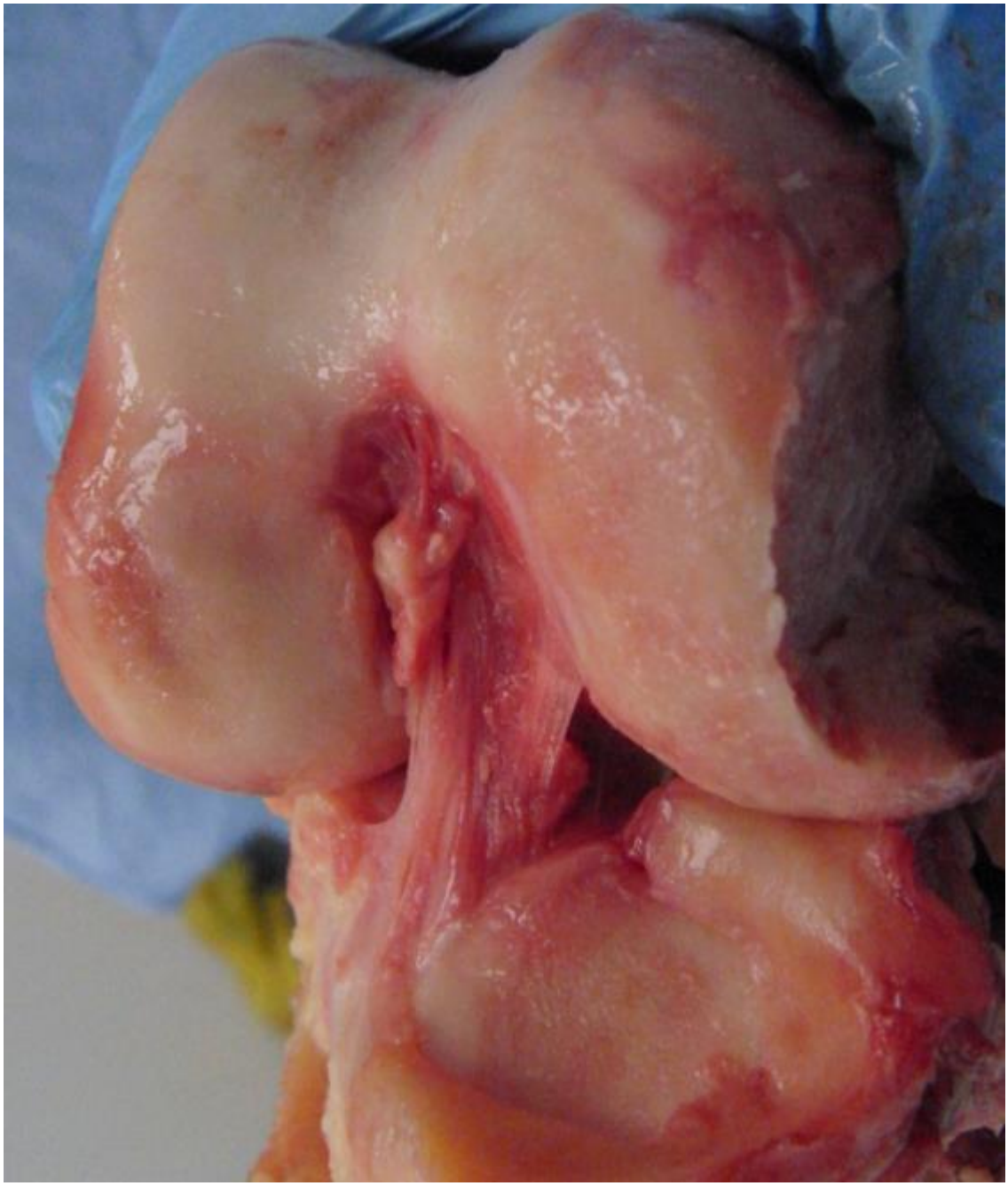

Figure 7. Cadaver 7, 72 years.

Figure 8. Cadaver 8, 72 years.

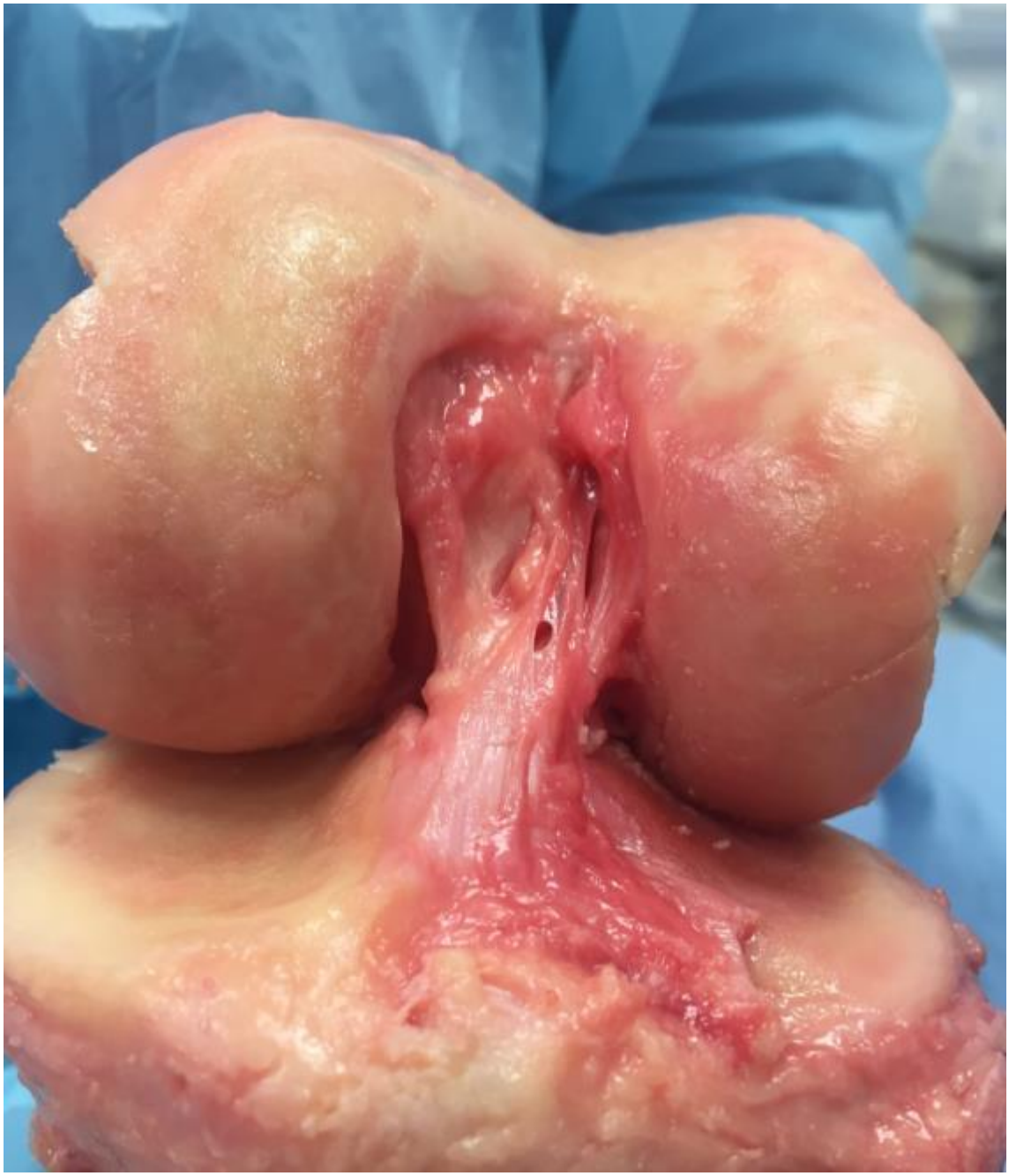

Figure 9. Cadaver 9, 79 years.

Figure 10. Cadaver 10, 80 years.

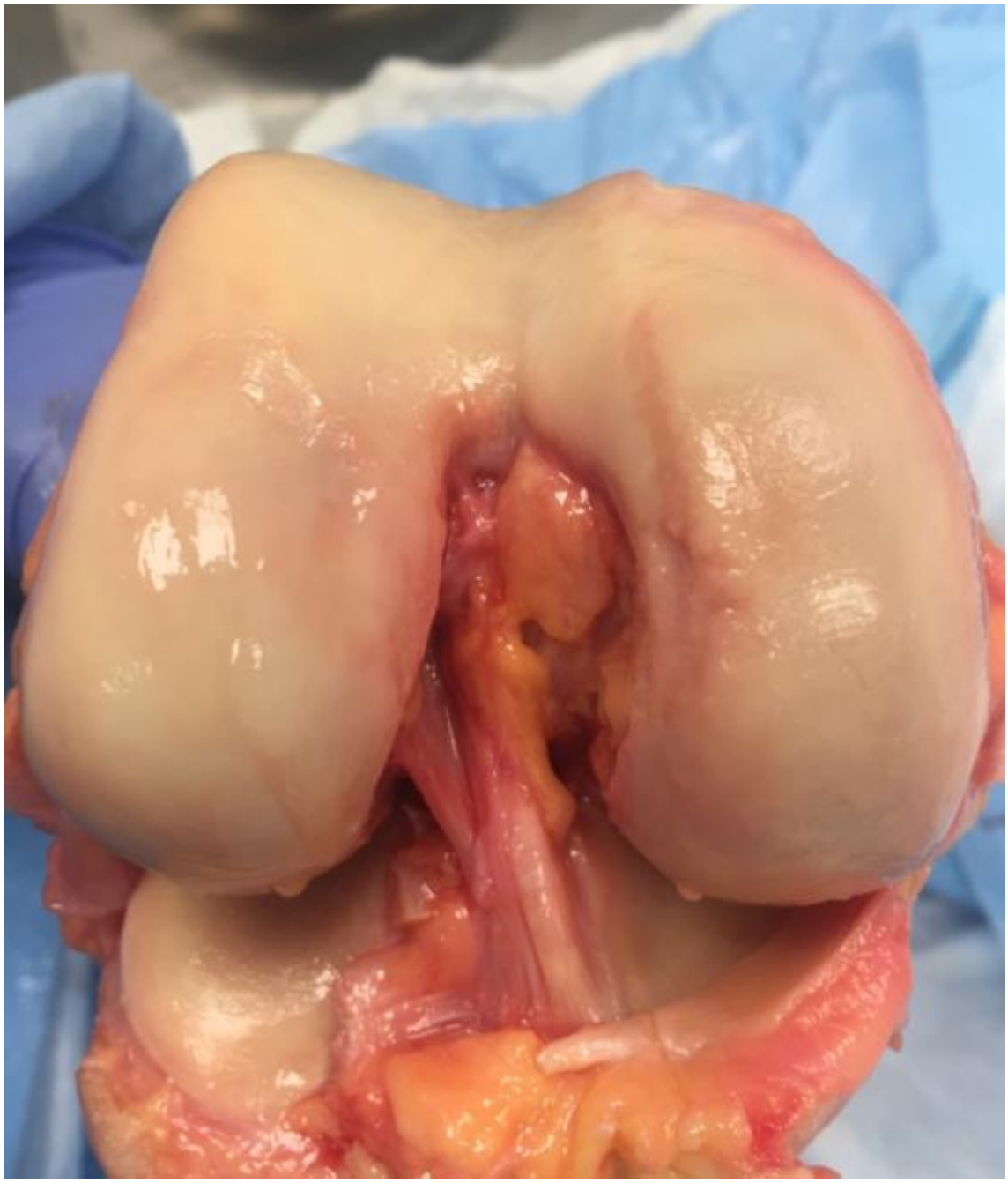

Figure 11. Cadaver 11, 86 years.

Figure 12. Cadaver 12, 88 years.

Eight articular cartilage, eight subchondral bone and eight trabecular bone samples from each of the 12 cadavers were extracted using a low speed oscillating saw (deSoutter Medical, Bucks, UK). Samples were extracted from the following localities: femoral condyle medial inferior (FCMI), femoral condyle medial superior (FCMS), femoral condyle lateral inferior (FCLI), femoral condyle lateral superior (FCLS), tibial plateau medial anterior (TPMA), tibial plateau medial posterior (TPMP), tibial plateau lateral anterior (TPLA) and tibial plateau lateral posterior (TPLP).

Cartilage

The overlying cartilage (n = 96 samples (n = 8 per cadaver)) was separated from the subchondral bone using a scalpel blade. Cartilage samples were fully submerged in phosphate buffered saline (PBS), transferred on ice and stored at 3 - 5˚C until testing. All cartilage samples were tested within 72 hours post dissection to avoid any change to material properties [Changoor et al., 2010].

Dynamic Nanoindentation Testing

Dynamic nanoindentation (G200 Nanoindenter, Keysight Technologies, Chandler, AZ, USA) was used to obtain the complex shear modulus (G^*) of articular cartilage at the micro level. The indenter was equipped with an ultra-low load DCM-II actuator utilising a Continuous Stiffness Measurement (CSM) module and a flat-ended cylindrical 100 µm punch tip (Synton-MDP Ltd, Nidau, Switzerland). Samples were partially submerged in PBS during testing through mounting in a custom-made liquid cell holder measuring a 1 cm radius and 2 mm deep well. Spatially correlated indentation locations (>100 µm spacing between each

indentation) were randomly chosen under the optical microscope to achieve 10 measurements per individual sample.

The calculation of shear storage modulus (*G'*), shear loss modulus (*G''*) and the loss factor (tan delta (δ)) (i.e. ratio of *G''*/*G'*) were applied following each indentation by assuming a Poisson's ratio of 0.46 [Jin & Lewis, 2004]. The theoretical basis is detailed elsewhere [Herbert et al., 2009; Herbert et al., 2008; Sneddon, 1965; Landau & Lifshitz, 1986] and has been applied using this method previously [Peters et al., 2017], and is briefly outlined here.

Complex shear modulus (*G**) is calculated by adding *G'* (real intrinsic elastic component) to *G''* (imaginary viscous component):

$$G^* = G' + iG'' \quad (1)$$

Sneddon's analysis is used to calculate the shear storage modulus using the Poisson's ratio (*v*), contact stiffness (*S*) and tip diameter (*D*), based on using a flat cylindrical punch:

$$G' = \frac{S\,(1-v)}{(2D)} \quad (2)$$

The above components along with contact damping (C*w*) can be used to calculate the shear loss modulus:

$$G'' = \frac{Cw\,(1-v)}{(2D)} \quad (3)$$

Contact stiffness (*S*) is calculated by subtracting the instrument stiffness (*Ki*) from the total measured stiffness (*Ks*):

$$S = Ks - Ki \quad (4)$$

Contact damping (C*w*) is calculated by subtracting the instrument damping (C*iw*) from the total measured damping (C*sw*):

$$\mathrm{C}w = \mathrm{C}sw - \mathrm{C}iw \quad (5)$$

The elastic modulus (*E*) was then calculated using the shear storage modulus (*G'*) and Poisson's Ratio (*v*):

$$E = 2G'(1 + v) \quad (6)$$

After the indenter head detected the surface of the sample, a pre-compression of 8µm was applied until the indenter was fully in contact with the sample. The surface detection was determined by a phase shift of the displacement measurement. In order to accurately detect the surface, the phase shift was monitored over a number of data points. Once the surface detection requirement was fulfilled over the predefined number of data points, the initial contact was determined from the first data point in the sequence. Once the indenter was fully in contact with the sample surface it vibrated at a fixed frequency of 110 Hz (the resonant frequency of the indenter) with 500 nm oscillation amplitude. Contact stiffness and damping were obtained through electromagnetic oscillation sequences. The initial oscillation measured instrument stiffness and damping and these were subtracted from the total measurement to obtain the contact response. Material properties were then obtained during the second oscillation.

After each indentation an adjacent sample holder mounted with 3M double-sided Scotch tape was indented, in order to clean the tip and prevent the transfer of biological material to subsequent test sites, as this may affect measurements. Following testing of each sample fused silica was indented to ensure the tip remained free from residue. Accuracy of the technique and measurements has previously been evidenced on other compliant homogenous structures [Moronkeji et al., 2016].

Bone

Bone samples (n = 80 subchondral bone, n = 96 trabecular bone (n = 8 per cadaver)) were temporarily stored in 70 % ethanol to preserve their physiological state [Linde & Sorensen, 1993]. Note: Subchondral bone samples were unable to be tested for cadaver 1 and 4 due to difficulties in polishing preparation caused by a technical error. Samples were then washed in a piezoelectric ultrasonic bath using distilled water and pure ethanol to remove any debris, before being embedded in a low viscosity epoxy resin at a transverse angle as to expose both subchondral and trabecular surfaces. Samples were then grinded with progressive silicon carbide paper (300, 600, 1200, 2400, 4000 grit) whilst under constant water irrigation to remove any debris, and polished with alumni paste to a surface finish on 1 µm and colloidal silica to 40 nm.

Quasi Static Nanoindentation Testing

Bone samples underwent quasi-static nanoindentation (G200 Nanoindenter, Keysight Technologies, Chandler, AZ, USA) to determine the nano-mechanical hardness (*H*) and *E*. Samples were examined under the optical microscope to randomly choose ten spatially correlated indents per sample (>100 µm spacing between each indentation). A Berkovich

sharp pyramidal tip was utilised (20 nm radius) and a Poisson's ratio of 0.3 [Reilly & Burstein, 1975] was assumed for bone. A penetration depth of 2000 nm was used for subchondral bone and 1200 nm for trabecular bone with a peak hold time of 30 seconds to factor in any viscoelastic response of tissues [Chudoba & Ritcher, 2001]. Due to the porous nature of trabecular bone the surface approach distance was set at 2000 nm to address any topographic variation in sample height. For subchondral bone this was set to 1000 nm. Surface stiffness detection was limited to 125 Nm^{-1} and samples were unloaded to 90 % and held before final unloading to establish thermal drift, which was set to an acceptance level of 0.15 Nm/s [Oyen, 2013]. The nanoindenter was calibrated using fused silica prior and after testing, which has known material property values [Oliver & Pharr, 1992].

This protocol thus achieves continuous loading and partial unloading of samples with an indenter of known geometry and material properties, with loading and penetration depth precisely measured. This approach allows the calculation of *H* and *E* using an established theory [Oliver & Pharr, 1992], which is briefly outlined here.

Hardness (*H*) is calculated by dividing the maximum load (*P*) reached at peak penetration depth, by the contact area (*A*):

$$H = \frac{P\max}{A} \tag{7}$$

The initial unloading stiffness is calculated as below where *P* is the load and h is the depth and *dP*/*dh* is the slope of the line in tangent to the initial unloading curve in the load-displacement plot.

$$S = \frac{dP}{dh} = \frac{2}{\sqrt{\pi}} E_{\mathrm{r}} \sqrt{A} \tag{8}$$

The reduced indentation modulus (E_r) is then calculated as below where v and v_i represent the sample and indenter Poisson's ratio respectively, and E and E_i are the sample and the indenter modulus respectively.

$$\frac{1}{E_r} = \frac{(1-v^2)}{E} + \frac{(1-v_i^2)}{E_i} \quad (9)$$

Statistical Analysis

An a-priori power analysis was performed using G*Power software [Faul et al., 2007]. A total of 42 samples per tissue type was required to distinguish either an effect size of 0.8 with α error probability of 0.05 and power of 0.95 when determining the relationship between multiple tissue means; or an effect size of 0.5 with α error probability of 0.05 and power of 0.95 for correlations of tissue interaction. Normal distribution of all measured individual sample material properties was analysed using a Kolmogorov-Smirnov test accounting for skewness and kurtosis of results. Where data was not significant and therefore normally distributed, homogeneity of variance was analysed using the Levene's test. Homoscedastic data was then tested for linearity using a two-tailed Pearson's correlation. Data violating the assumptions of Pearson's correlation testing were analysed using a two-tailed Spearman's Rank (SPSS software, Version 22.0, SPSS, Inc., Chicago, IL). Bivariate correlation coefficients with significance to age, OA, spatial distribution and BMI of samples was determined. Individual sample and combined sample mean and standard deviation (SD), and 95 % confidence interval (CI) were analysed for each tissue from each cadaver. The overall joint mean material properties were also correlated with age and overall joint OA grade (n = 12), and to sample site (n = 8 locations) using a Kendall's Tau-b test. Joint means were used to account for within-subject dependence of samples. The

effect of within and between-subject variables were analysed using a mixed linear model, combing the effects of both age and OA.

The results primarily focus on the intrinsic elastic *G'* of cartilage and imaginary viscous *G"*, and *E* of subchondral and trabecular bone, as these are the most commonly reported and therefore comparable results. Shear and elastic properties are also most closely linked to tissue function *in vivo*. However to aid a full interpretation of data collected, additional data is also reported within Chapter Nine Supplementary Material.

Results

Overall cartilage *G'* (0.14 – 1.30 MPa), cartilage *G"* (0.01 – 2.58 MPa) subchondral bone *E* (11.12 – 15.33 GPa) and trabecular bone *E* (10.75 – 13.66 GPa) varied considerably across cadavers. The average mean and SD from individual indents from samples across the whole joint for all tissues can be seen in Table 3, along with age and grade of OA of the cadaver. Note that results herein present cartilage *G'*, cartilage *G"*, and subchondral and trabecular bone *E*. Values of all parameters including the addition of bone hardness (*H*) and cartilage *E* and loss factor can be found in Chapter Nine Supplementary Material.

Table 3. Mean and standard deviation (SD) of cartilage shear storage modulus (*G'*) (MPa), cartilage shear loss modulus (*G"*) (MPa), subchondral bone elastic modulus (*E*) (GPa) and trabecular bone elastic modulus (*E*) (GPa) for from individual indents from samples across the whole joint. Age, osteoarthritis (OA) International Cartilage Repair Society (ICRS) grade (0 - 4) and limb side is also shown. *Note. OA grade is based on all 8 samples extracted, hence multiple grades per cadaver due to regional spatial variation in OA across the joint.

	Age (Years)	Gender	Limb	OA ICRS Grade*	Cartilage *G'* (MPa)	Cartilage *G"* (MPa)	Subchondral Bone *E* (GPa)	Trabecular Bone *E* (GPa)
					Mean ± SD	Mean ± SD	Mean ± SD	Mean ± SD
Cadaver 1	31	Female	Left	Grade 0	1.30 ± 0.65	1.07±0.74	-	13.13 ± 3.34
Cadaver 2	37	Female	Left	Grade 0	1.0 ± 0.74	0.42±0.31	11.96 ± 1.90	12.29 ± 2.87
Cadaver 3	43	Female	Right	Grade 0	0.90 ± 0.55	0.63±0.56	11.89 ± 1.64	11.67 ± 2.88
Cadaver 4	49	Male	Left	Grade 0-1	0.65 ± 0.51	0.33±0.26	-	13.37 ± 2.16
Cadaver 5	51	Male	Right	Grade 0-1	0.96 ± 0.50	0.40±0.27	12.83 ± 1.64	13.09 ± 2.75
Cadaver 6	58	Male	Right	Grade 1-2	0.41 ± 0.54	0.17±0.29	11.12 ± 2.18	10.75 ± 2.90
Cadaver 7	72	Male	Right	Grade 2-3	0.14 ± 0.31	0.05±0.11	14.18 ± 1.99	12.13 ± 3.78
Cadaver 8	72	Male	Left	Grade 1-3	0.55 ± 0.45	0.20±0.17	14.34 ± 2.03	13.66 ± 3.13
Cadaver 9	79	Male	Left	Grade 1-2	0.15 ± 0.09	0.04±0.03	14.31 ± 1.57	12.29 ± 3.89
Cadaver 10	80	Male	Left	Grade 1-4	0.31 ± 0.48	0.10±0.17	15.33 ± 1.70	12.08 ± 2.68
Cadaver 11	86	Female	Right	Grade 0-1	0.40 ± 0.34	0.37±0.52	13.76 ± 1.93	11.64 ± 3.21
Cadaver 12	88	Male	Right	Grade 1-3	0.27 ± 0.36	0.10±0.14	14.30 ± 1.68	12.43 ± 2.63

Effect of Ageing

Increasing age is strongly correlated with a decrease in cartilage *G'* (τb = -0.657, p = 0.003) and cartilage *G"* (τb = -0.565, p = 0.011) and showed an increasing trend with subchondral bone *E* (τb = 0.449, p = 0.072) using overall joint means. However there is no significant correlation between increasing age and trabecular *E* (τb = -0.198; p = 0.372). These trends are shown in Figure 13 by combined sample mean and SD plotted against age, along with the mean of each of the eight individual spatially correlated samples.

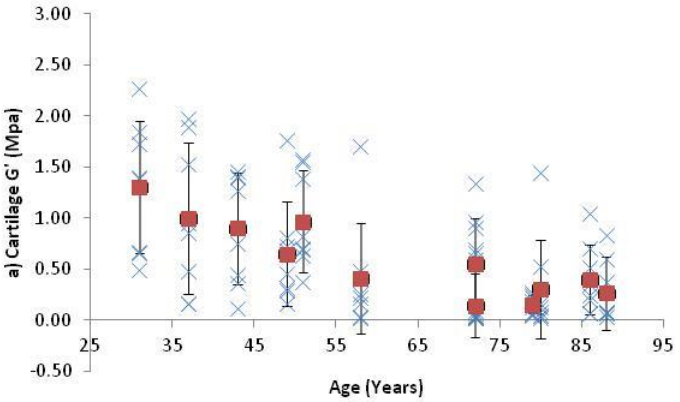
a) Cartilage G' (Mpa)
3.00
2.50
2.00
1.50
1.00
0.50
0.00
-0.50
25
35
45
55
65
75
85
95
Age (Years)

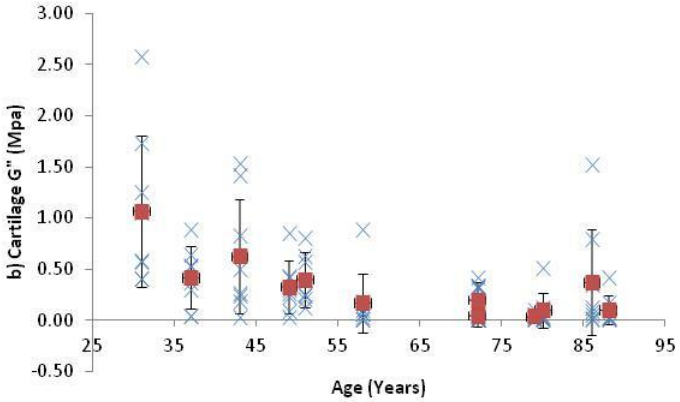
b) Cartilage G'' (Mpa)
3.00
2.50
2.00
1.50
1.00
0.50
0.00
-0.50
25
35
45
55
65
75
85
95
Age (Years)

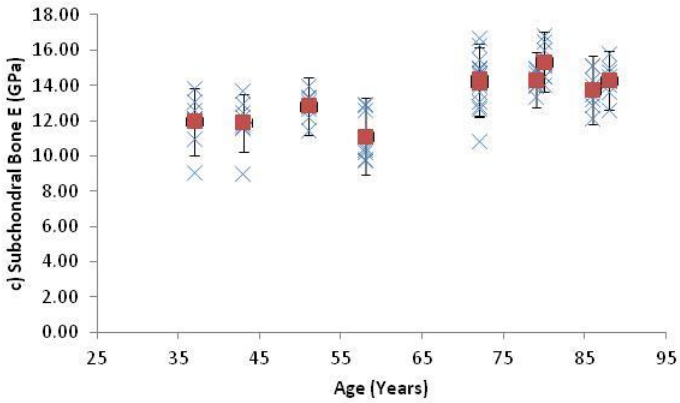
c) Subchondral Bone E (GPa)
18.00
16.00
14.00
12.00
10.00
8.00
6.00
4.00
2.00
0.00
25
35
45
55
65
75
85
95
Age (Years)

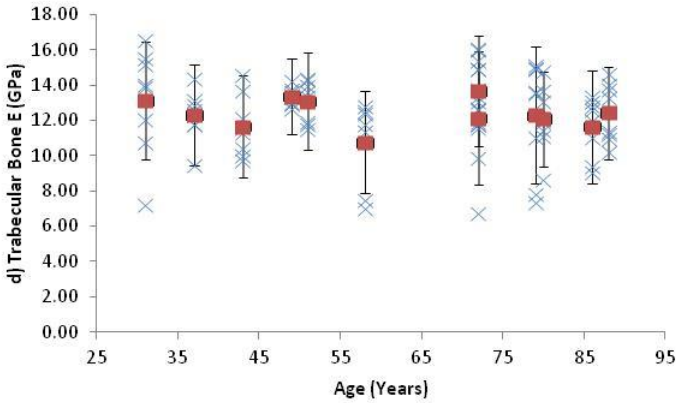
d) Trabecular Bone E (GPa)
18.00
16.00
14.00
12.00
10.00
8.00
6.00
4.00
2.00
0.00
25
35
45
55
65
75
85
95
Age (Years)

Figure 13. Mean of whole joint a) Cartilage shear storage modulus (*G'*) (MPa), b) Cartilage shear loss modulus (*G"*) (MPa), c) Subchondral bone elastic modulus (*E*) (GPa) and c) Trabecular bone elastic modulus (*E*) (GPa) correlated with age (squares). Error bars represent standard deviation (SD) from individual indents. The mean of each eight individual spatially correlated samples from cadavers correlated against age is also presented (crosses).

Increasing age was also strongly correlated with cartilage *E* (τb = -0.657; *p* = 0.003) and moderately correlated with cartilage loss factor (τb = -0.462; *p* = 0.039). A correlation analysis was also performed between age and subchondral bone *H* (τb = 0.276; *p* = 0.277) and trabecular bone *H* (τb = 0.394; *p* = 0.083) (calculated using Kendall's Tau-b for overall joint means) (see values in Chapter Nine Supplementary Material).

Effect of Osteoarthritis

Increasing grade of OA is strongly correlated with a decrease in cartilage *G'* (τb = -0.625; *p* = 0.007) and cartilage *G"* (τb = -0.724, *p* = 0.002), and an increase in subchondral bone *E* (τb = 0.645; *p* = 0.013) using overall joint grading (Fig. 14). Trabecular bone *E* showed no significant correlation between overall joint OA grade (τb = -0.066; *p* = 0.778) (Fig. 14).

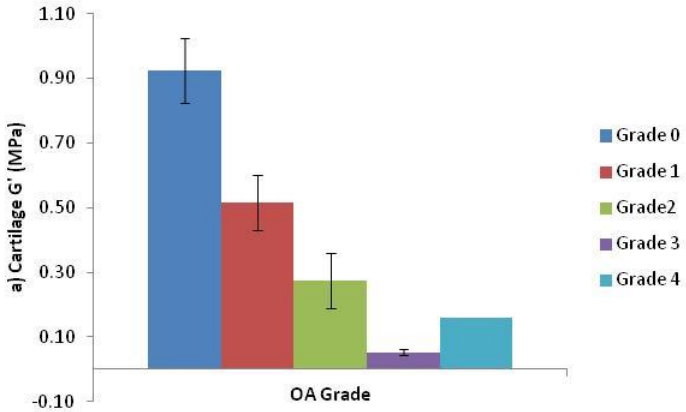
1.10
0.90
0.70
0.50
0.30
0.10
-0.10
a) Cartilage G' (MPa)
OA Grade
Grade 0
Grade 1
Grade2
Grade 3
Grade 4

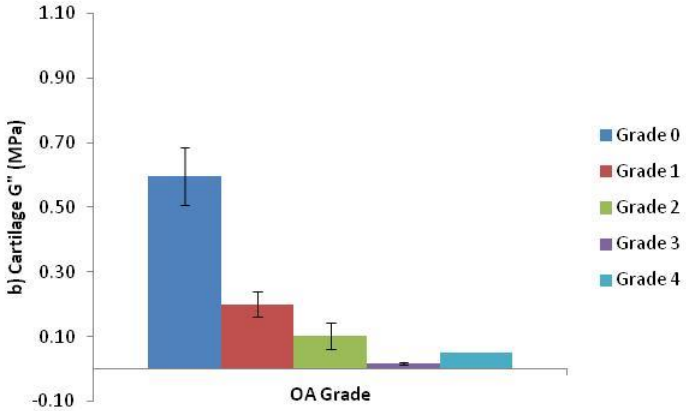
1.10
0.90
0.70
0.50
0.30
0.10
-0.10
b) Cartilage G'' (MPa)
OA Grade
Grade 0
Grade 1
Grade 2
Grade 3
Grade 4

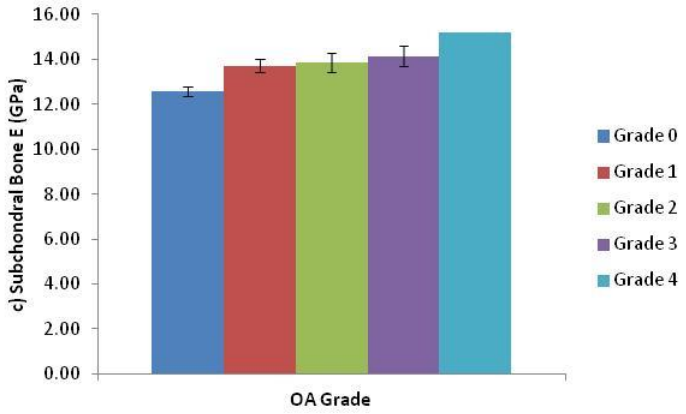
16.00
14.00
12.00
10.00
8.00
6.00
4.00
2.00
0.00
c) Subchondral Bone E (GPa)
OA Grade
Grade 0
Grade 1
Grade 2
Grade 3
Grade 4

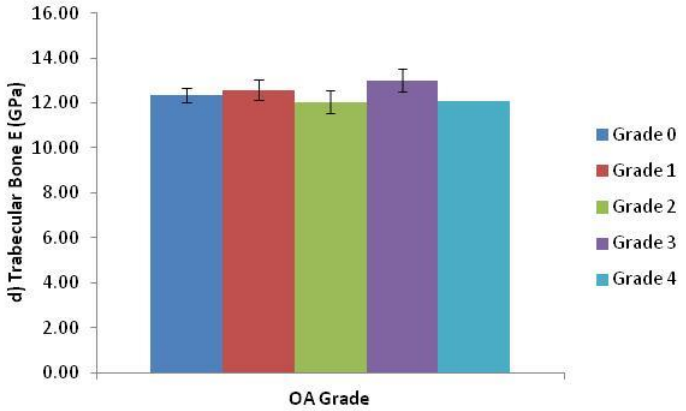
16.00
14.00
12.00
10.00
8.00
6.00
4.00
2.00
0.00
d) Trabecular Bone E (GPa)
OA Grade
Grade 0
Grade 1
Grade 2
Grade 3
Grade 4

Figure 14. The relationship between a) Cartilage shear storage modulus (*G'*) (MPa), b) Cartilage shear loss modulus (*G"*) (MPa), c) Subchondral bone elastic modulus (*E*) (GPa), and c) Trabecular bone elastic modulus (*E*) (GPa) to osteoarthritis International Cartilage Repair Society (ICRS) grade (0 - 4). Error bars represent standard error of the mean.

Overall joint grade of OA was strongly correlated with cartilage loss factor (p = 0.006), cartilage E (p = 0.007) and subchondral bone H (p = 0.033). A correlation analysis was also performed between overall joint grade of OA and trabecular bone H (p = 0.087) (calculated using Kendall's Tau-b) (see values in Chapter Nine Supplementary Material).

There is also a significant positive correlation between age and overall joint grade of OA (τb = 0.663; p = 0.005) (Fig. 15).

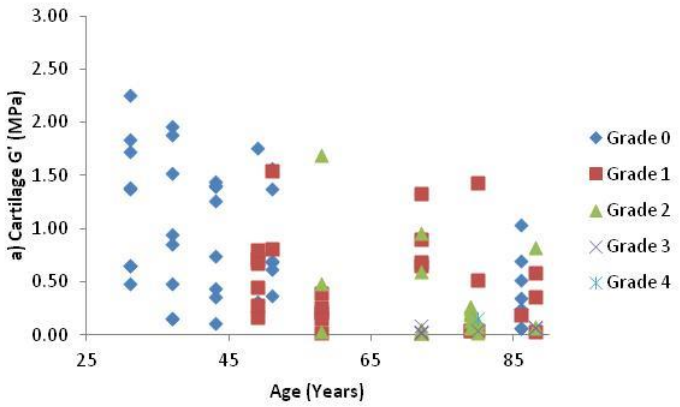
a) Cartilage G' (MPa)
3.00
2.50
2.00
1.50
1.00
0.50
0.00
25
45
65
85
Age (Years)
Grade 0
Grade 1
Grade 2
Grade 3
Grade 4

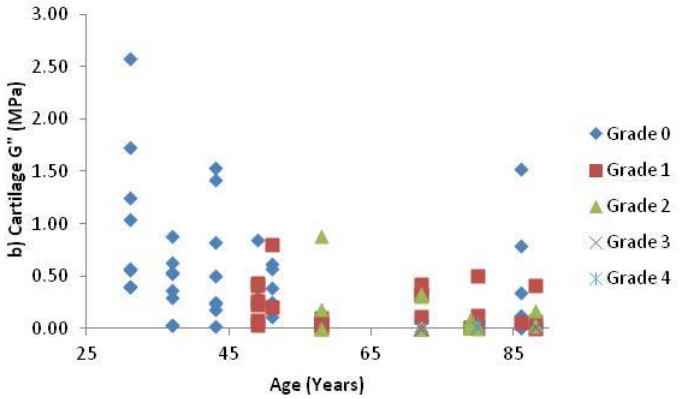
b) Cartilage G'' (MPa)
3.00
2.50
2.00
1.50
1.00
0.50
0.00
25
45
65
85
Age (Years)
Grade 0
Grade 1
Grade 2
Grade 3
Grade 4

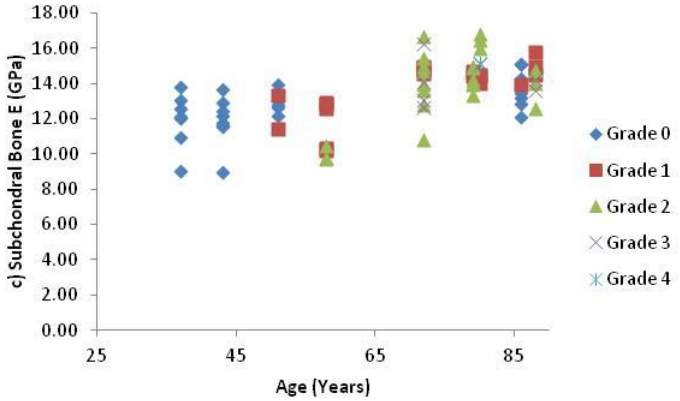
c) Subchondral Bone E (GPa)
18.00
16.00
14.00
12.00
10.00
8.00
6.00
4.00
2.00
0.00
25
45
65
85
Age (Years)
Grade 0
Grade 1
Grade 2
Grade 3
Grade 4

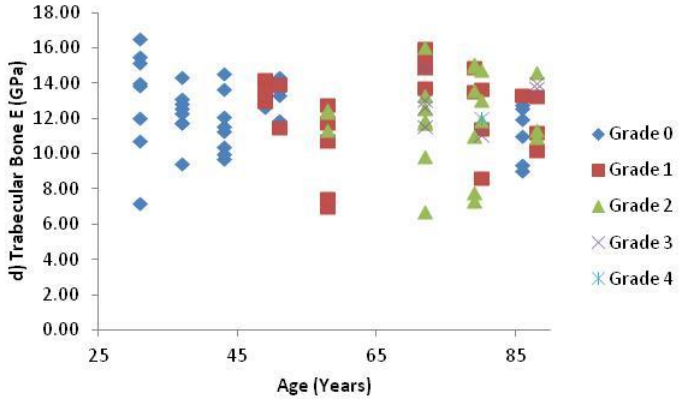
d) Trabecular Bone E (GPa)
18.00
16.00
14.00
12.00
10.00
8.00
6.00
4.00
2.00
0.00
25
45
65
85
Age (Years)
Grade 0
Grade 1
Grade 2
Grade 3
Grade 4

Figure 15. a) Cartilage shear storage modulus (*G'*) (MPa), b) Cartilage shear loss modulus (*G"*) (MPa), Subchondral bone elastic modulus (*E*) (GPa) and c) Trabecular bone elastic modulus (*E*) (GPa) correlated with age (years) representing n = 8 samples from each cadaver, grouped according to osteoarthritis (OA) International Cartilage Repair Society (ICRS) grade (0 - 4).

Cartilage and Bone Tissue Interaction

Correlations between the multiple tested tissues can be seen in Figure 16. There is a significant positive correlation between cartilage *G'* and cartilage *G"* (ρ = 0.924; *p* = 0.000). There is also a significant negative correlation between site-matched cartilage *G'* and subchondral bone *E* (ρ = -0.299; *p* = 0.007) and site-matched cartilage *G"* and subchondral bone *E* (ρ = -0.339; *p* = 0.002). However there is no significant correlation between site-matched cartilage *G'* and trabecular bone *E* (ρ = 0.105; *p* = 0.309), site-matched *G"* and trabecular bone *E* (ρ = 0.072; *p* = 0.484) or site-matched subchondral versus trabecular bone *E* (ρ = 0.210; *p* = 0.061).

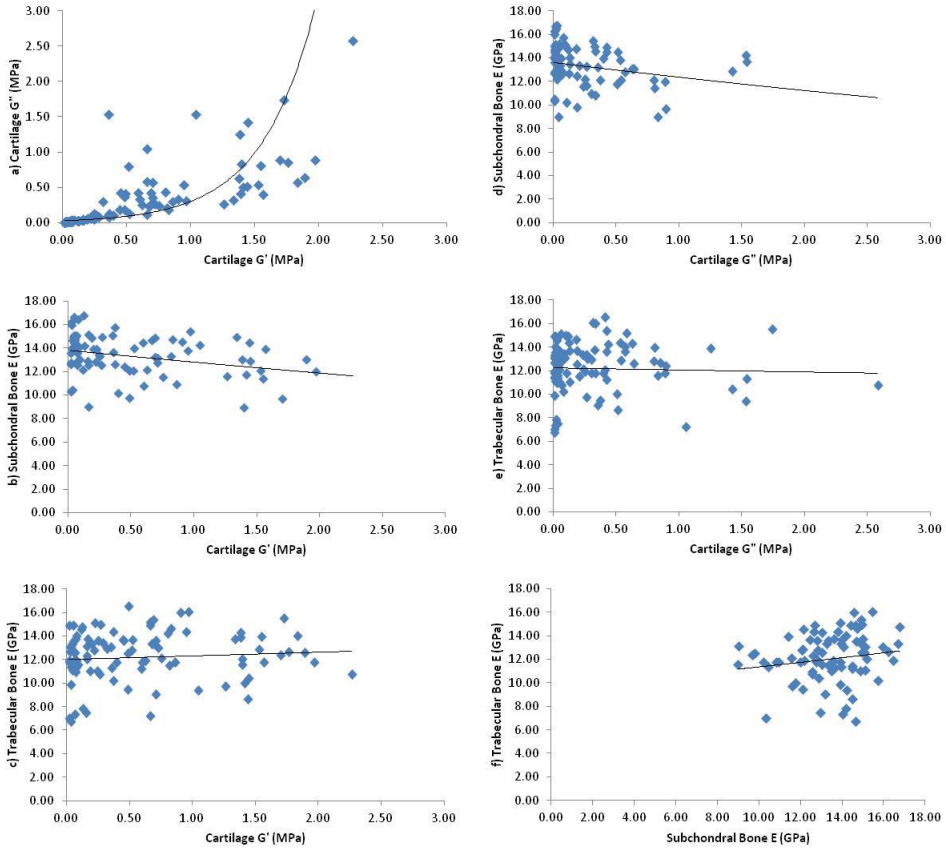

Figure 16. Tissue interaction between a) Cartilage shear storage modulus (*G'*) (MPa) and cartilage shear loss modulus (*G"*) (MPa), b) Cartilage shear storage modulus (*G'*) (MPa) and subchondral bone elastic modulus (*E*) (GPa), c) Cartilage shear storage modulus (*G'*) (MPa) and trabecular bone elastic modulus (*E*) (GPa), d) Cartilage shear loss modulus (*G"*) (MPa) and subchondral bone elastic modulus (*E*) (GPa), e) Cartilage shear loss modulus (*G"*) (MPa) and trabecular bone elastic modulus (*E*) (GPa), f) Subchondral bone elastic modulus (*E*) (GPa) and trabecular bone elastic modulus (*E*) (GPa).

Spatial Distribution of Cartilage and Bone

A correlation analysis was performed between combined site G' and spatial location (τb = -0.500; p = 0.083) and G" and spatial location (τb = -0.327, p = 0.262) across the 12 cadavers

(Fig. 17). Differences were most common between the mean of femoral and tibial sites, with the lowest *G'* and *G"* found at the TPMA and highest *G'* at the FCLS and highest *G"* at the FCMS. Lower values of *G'* were more marked at medial sites, but *G"* tended to be lower at lateral sites. Mean and SD femoral and tibial cartilage *G'* was 0.77 ± 0.62 and 0.40 ± 0.47 MPa respectively, whilst medial versus lateral *G'* were 0.53 ± 0.63 and 0.64 ± 0.53 MPa respectively. Mean and SD femoral and tibial cartilage *G"* was 0.43 ± 0.50 and 0.21 ± 0.36 MPa respectively, whilst medial versus lateral *G"* was 0.29 ± 0.29 and 0.35 ± 0.56 MPa respectively.

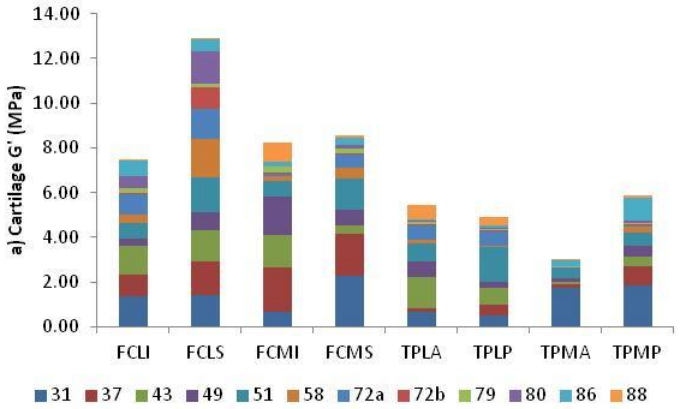
a) Cartilage G' (MPa)
14.00
12.00
10.00
8.00
6.00
4.00
2.00
0.00
FCLI FCLS FCMI FCMS TPLA TPLP TPMA TPMP
31 37 43 49 51 58 72a 72b 79 80 86 88

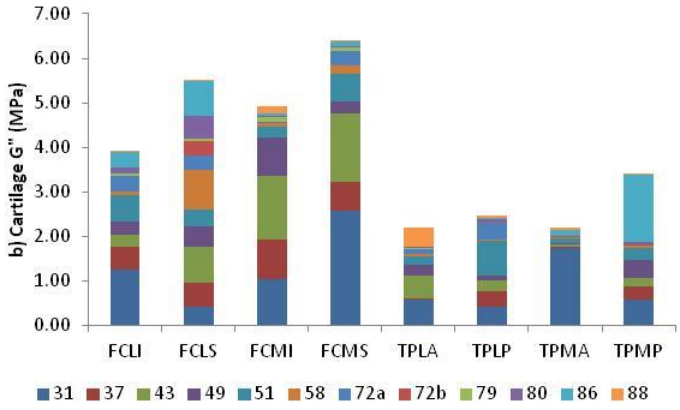
b) Cartilage G'' (MPa)
7.00
6.00
5.00
4.00
3.00
2.00
1.00
0.00
FCLI FCLS FCMI FCMS TPLA TPLP TPMA TPMP
31 37 43 49 51 58 72a 72b 79 80 86 88

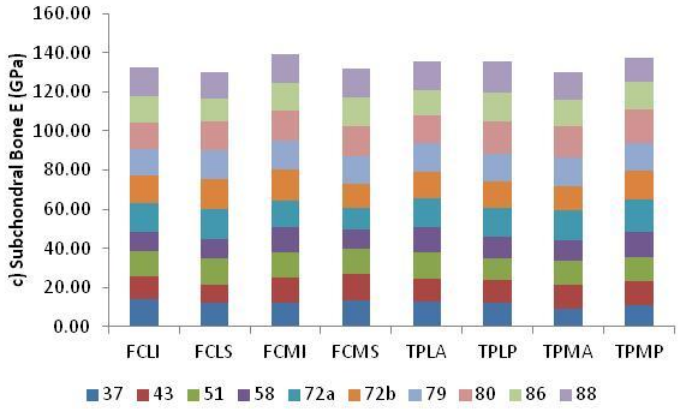
c) Subchondral Bone E (GPa)
160.00
140.00
120.00
100.00
80.00
60.00
40.00
20.00
0.00
FCLI FCLS FCMI FCMS TPLA TPLP TPMA TPMP
37 43 51 58 72a 72b 79 80 86 88

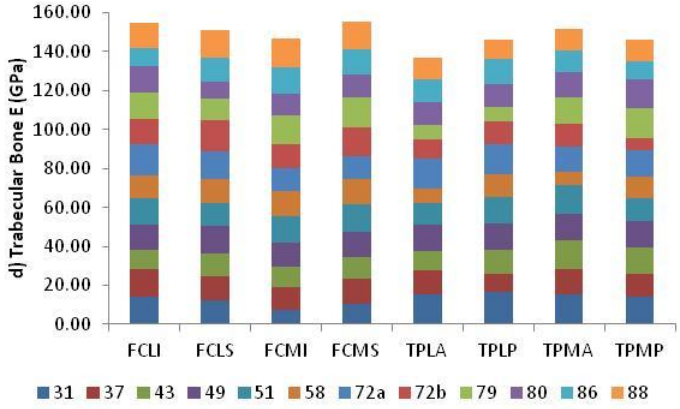
d) Trabecular Bone E (GPa)
160.00
140.00
120.00
100.00
80.00
60.00
40.00
20.00
0.00
FCLI FCLS FCMI FCMS TPLA TPLP TPMA TPMP
31 37 43 49 51 58 72a 72b 79 80 86 88

Figure 17. Collated values for a) Cartilage shear storage modulus (*G'*) (MPa), b) Cartilage shear loss modulus (*G"*) (MPa), c) Subchondral bone elastic modulus (*E*) (GPa) and d) Trabecular bone elastic modulus (*E*) (GPa) from all cadavers at site specific locations. Femoral condyle medial inferior (FCMI), femoral condyle medial superior (FCMS), femoral condyle lateral inferior (FCLI), femoral condyle lateral superior (FCLS), tibial plateau medial anterior (TPMA), tibial plateau medial posterior (TPMP), tibial plateau lateral anterior (TPLA), tibial plateau lateral posterior (TPLP).

Subchondral bone and trabecular bone *E* also varied across site-specific locations but no consistent patterns or differences were seen at any one particular site. Mean and SD femoral and tibial subchondral bone *E* was 13.34 ± 1.69 and 13.46 ± 1.78 GPa respectively and medial versus lateral samples were 13.46 ± 1.77 and 13.34 ± 1.70 GPa respectively. Mean and SD femoral and tibial trabecular bone *E* was 12.65 ± 1.79 and 12.10 ± 2.36 GPa respectively and medial versus lateral *E* was 12.48 ± 2.02 and 12.27 ± 2.19 GPa respectively.

Combined Effect of Variables

To consider individual sample material properties both within and between subjects, while adjusting for both age and OA grade as variables, a compound symmetry mixed linear model was used, showing the random effects on individual sample cartilage *G'* and *G"* were significantly different between subjects (both $p = <0.001$), but not within subjects ($p = 0.429$, $p = 0.465$ respectively). This suggests there was no significant difference of within-subject cartilage *G'* and *G"*. Using these model assumptions, cartilage *G'* was significantly correlated with age ($p = 0.003$) but not OA grade ($p = 0.052$), and cartilage *G"* was not correlated with age ($p = 0.055$) or OA grade ($p = 0.142$) when adjusted for one another and within-subject effects. The random effects of subchondral and trabecular bone *E* were also

significantly different between subjects (both p = <0.001), but not within subjects (p = 0.132 and p = 0.547 respectively). Subchondral bone E was significantly correlated with age (p = 0.010), but not OA grade (p = 0.892) when adjusted for one another and within-subject effects. Trabecular bone E was not correlated with either age (p = 0.432) or OA grade (p = 0.809).

Discussion

This study presents the first systematic quantification of changes in the material properties of multiple human knee tissues by applying a single method to a cohort of cadaveric specimens spanning a wide range in age (31 - 88 years) and disease state (OA ICRS grade 0 - 4). These results allows the determinacy of how properties of all tissues change in the absence of confounding factors of variation of donor demographics and testing methods between studies for the first time (Figs. 13 – 17). Spatial sampling of multiple tissues also allows assesses these correlations at the sub-joint level, which is crucial given suggestions of preferential regional development and progression of OA [Pelletier et al., 2007] as well as local changes to tissue morphology and structure thought to be associated with medial compartment mechanical loading of the human knee during habitual locomotion [Kumar et al., 2013].

A number of previous studies have reported the material properties of healthy human knee joint articular cartilage [e.g. Shepherd & Seedhom, 1999; Thambyah et al., 2006] and compared data from healthy samples to those with OA [e.g. Kleemann et al., 2005; Wilusz et al., 2013; Hori & Mockros, 1976; Franz et al., 2001; Wang et al., 2013]. These studies consistently report a decline in modulus in the presence of disease as an independent variable, which correlates with the statistically significant and highly correlated [Cohen,

1988] negative relationship found here (Fig. 14). Healthy and OA grade 1 human knee joint cartilage *G'* has been reported between 0.07 – 6.7 MPa assuming a Poisson's ratio of 0.46 [Jin & Lewis, 2004], whilst OA grade 2-3 samples fall between 0.07 – 0.17 MPa [e.g. Kleemann et al., 2005; Wilusz et al., 2013; Shepherd & Seedhom, 1999; Thambyah et al., 2006; Hori & Mockros, 1976; Franz et al., 2001; Wang et al., 2013]. Most recently Robinson et al., [2016] found that cartilage *G'* at tibial and femoral sites in old (69.7 ± 9.3 years) healthy controls was 6.0 ± 1.6 MPa compared to OA samples (4.6 ± 1.8 MPa). However these earlier studies have not categorised samples according to age, or tested a wide span of age and therefore our ability to understand age-related trends and their influence on OA was limited.

The new data generated herein demonstrates clear changes in the material properties of knee joint tissues with ageing as well as in the presence of disease (Figs. 13 - 15). The absolute *G'* values reported for healthy and grade 1 OA samples tend to fall towards the lower end of previously reported results (Fig. 14a) whilst values of OA grades 2 - 4 tend to fall towards the higher end of previously reported results (Fig. 14a). Variation across previous studies may be due to different testing techniques, donor demographics and preservation and storage methods, which make it challenging to accurately compare data. Importantly, some previous studies and the data generated herein focus primarily on the intrinsic viscoelastic response of cartilage which has been shown to functionally identify surface changes in the presence of early OA [Desrochers et al., 2012]. Whilst there is a body of literature also exploring the poroelastic response of cartilage considering the fluid-flow mechanics [e.g. Taffetani et al., 2014; Nia et al., 2011], such measurements are outside the scope of the current research.

Interestingly, when determining the changes in cartilage *G'* in a multi-variable analysis, this was correlated with age but not OA (p = 0.052) when adjusted for one another and the dependence effect of multiple samples per donor. This suggests that ageing has a more prominent effect on cartilage *G'* than OA grade. As ageing is a primary risk factor for OA, a concurrent relationship is often expected, which makes its challenging to determine the effects of each variable separately. By using a mixed linear model the ability to account for multiple variables allows to see how each contributes to any correlation seen independently, which suggests ageing has a significant effect on cartilage G', but the effect of OA falls just outside the acceptance level.

Previous studies have often neglected to report the cartilage G" making comparison to other studies difficult. However a select number have reported this parameter, although not in human cartilage samples [Simon et al., 1989; Fulcher et al., 2009; Peters et al., 2017]. Simon et al., [1989] reported healthy mature bovine cartilage G" at 0.13 ± 0.03 MPa, while immature bovine cartilage tissue has been reported higher at 4.8 ± 1.0 MPa [Fulcher et al., 2009]. Healthy canine cartilage G" has also been reported at 0.19 – 0.60 MPa. Whilst providing valuable data for healthy animal samples, current literature does not explore the effect of either ageing or OA on the G" in human knee cartilage.

The new data presented herein allows for comparison between a variety of donor demographics where values for G" range between 0.04 – 1.07MPa which is in the range of previously reported values for G" in animals [Simon et al., 1989; Fulcher et al., 2009; Peters et al., 2017]. Higher values for G" are seen within young healthy donors and lower values in older donor with more advanced OA (Fig.13 – 15, Table 3). The mixed linear models presented allows the analysis to account for age and OA grade as separate contributing

variables within the same donor, and showed that age had a more prominent effect, although this fell outside the significant acceptance level.

Our study also found evidence for a linear increase in subchondral bone *E* with increasing age (Fig. 13) and OA (Fig. 14). Therefore this data demonstrates, for the first time, a significantly correlated relationship [Cohen, 1988] between a change in site-matched cartilage and subchondral bone material properties (Fig. 16). These findings provide direct support for conceptual representations of cartilage and subchondral bone as a single functional unit [Mahjoub et al., 2012]. Values between 22.0 – 25.8 GPa have previously been reported for healthy cortical bone *E* from the human knee joint [Rho et al., 1997], which are relatively higher than the average samples means across the whole joint with values reported in this study of 11.12 – 15.33 GPa. However more recently Zuo et al., [2016] characterised tissue level mechanical strength of the subchondral bone in OA samples and found higher stiffness values in lamellae of grade 4 samples (17.33 ± 3.13 GPa) when compared to grade 1 samples (13.90 ± 2.75 GPa); however there were no healthy controls included in this study. Thus prior to this research (Figs. 14c and 15c) it has not been possible to systematically assess OA material property trends in subchondral bone. Specifically, in the current study older cadavers with OA had higher subchondral bone *E* when compared to healthy aged-matched controls (Fig. 15), further supporting the involvement of subchondral bone in the presence of disease. Endochondral ossification is observed with advancing OA and may cause mechanical stiffening of the subchondral bone [Cox et al., 2013], which could account for the increase in *E* with increasing grade of OA (Fig.14). The multi-variable analysis presented also correlated a change in subchondral bone *E* to age, but not OA grade when adjusting for one another, indicating, as with cartilage *G'*, that age relates more strongly to subchondral bone *E* than increasing OA grade, but it is difficult to isolate these variables as they usually happen concurrently.

Previous research has also suggested that a change in the density and separation of trabecular bone occurs in the presence of OA [Kamibayashi et al., 1995; Bobinac et al., 2003]; however due to inconsistencies in cadaver demographics and variation in testing methods it was previously impossible to gauge how trabecular *E* changes with age or disease. Human knee joint trabecular bone *E* has previously been reported with values between 0.002 – 1.15 GPa [e.g. Behrens et al., 1974; Ducheyne et al., 1977; Burgers et al., 2008; Zysset et al., 1994] spanning three orders of magnitude. It should be noted that these studies represent varying testing methods and tip geometries which can account for some variation in results; however this concurrently makes inter-study comparison between cohorts challenging. Data generated herein shows no systematic change in material properties (ICRS 0: 12.33 ± 3.04 GPa; ICRS 4: 12.07 ± 1.83 GPa) (Figs. 13 - 14), suggesting that changes seen in the presence of OA [Kamibayashi et al., 1995; Bobinac et al., 2003] may be limited to structural adaptations. Further supporting this, our multi-variable analysis showed no correlation of trabecular bone *E* to age or OA when adjusted for one another.

An additional notable finding here which may contribute to varying results from within and between subject analysis, is the relative high level of variability in material properties in all tissue types and in particular cartilage, within cadavers of all genders, ages and disease status (Figs. 13 - 14). No obvious or systematic trends in the magnitude of variability with increasing age or OA were identified in the data. The heterogeneous nature of the extracellular matrix of articular cartilage is influenced by variations in composition, structure and vascularity at the micro-level where cartilage material property variability within one specimen at different localities has previously been identified [Moore & Burris, 2015]. This strengthens the need to represent such structures locally with interchangeable material properties.

Furthermore the geometry, density and spatial locality plays a role in the variability of bone material properties [Zysset et al., 1999]. The functional importance of spatial heterogeneity in material properties has been conceptually demonstrated in computer simulations of joint mechanics. For example, Mononen et al., [2012] represented cartilage as a heterogeneous tissue, varying *E* accordingly to healthy and OA spatial material properties. Regions with OA, and therefore a reduced *E*, had increased tissue deformation and strain and significantly altered contact and pore pressures, where stresses increased at the interface between healthy and OA tissue [Mononen et al., 2012]. Herein site specific cartilage material property differences exist in individual cadavers (Fig. 17) with absolute differences of up to 1.77 MPa equivalent to a relative difference of 461.2 %. Therefore with the current data in mind this suggests a more local approach should be considered in attempts to understand the mechanical function of knee joint tissues, particularly in the presence of OA (Fig. 14).

The data presented in this study demonstrates that OA affects medially located samples more than laterally located ones. The individual ICRS grading of cartilage samples along with shear modulus also suggests preferential development of OA medially, which is consistent with current diagnostic literature [Pelletier et al., 2007]. Additionally, motion analysis of healthy individuals also shows increased loading during gait on the medial femoral-tibial joint compared to lateral [Kumar et al., 2013] as well as increased cartilage strains [Adouni et al., 2012]. This is highly suggestive of a causative link between habitual joint loading and the suggested increase in medial OA seen within the current study. Medial femoral condyle cartilage *G'* declines with ageing; however such differences are not seen between medial and lateral samples in young healthy cadavers (Fig. 17a and Supplementary Material Chapter Nine). Interestingly, regional development of OA has previously been applied in finite element (FE) models showing medial femoral condyle OA

may create potential failure regions in the lateral condyle [Mononen et al., 2012]. With the current data in consideration this would suggest that a decline in material properties seen in this study in ageing and with the presence of OA may be related to regional joint loading. Of note, cadaver BMI, which may affect magnitude of joint loading, was analysed in the current study against cartilage *G'* and *G"*, subchondral bone *E* and trabecular bone *E*, although no correlations were found, likely due to low sample numbers.

Spatially correlated material properties (Fig. 17) are practically important for the assessment of OA and resultant interventions. Developing targeted OA therapies relies on understanding alterations of multiple tissues involved in whole-joint function [Goldring & Goldring, 2016]. As suggested by Wen et al., [2014] alterations in OA therapies will come from a more in-depth knowledge of the role subchondral bone plays in disease progression, which may include physical therapy, pharmaceuticals, or the development of biomimetic materials. Bisphosphonates such as alendronate inhibit bone remodeling and as a consequence reduce cartilage degeneration in animal experimental models [Hayami et al., 2004]. With the current study supporting the role of an increase in bone to a decrease in cartilage mechanical stiffness (Fig. 16), such therapeutic interventions may be introduced in the presence of OA in an attempt to inhibit disease progression. Applications that rely on material property data such as polymer hydrogels are also increasingly being used to mimic viscoelastic properties of articular cartilage due to their structural similarities [Li et al., 2016; Wang et al., 2012]. Tissue engineering including repair, replacement and regeneration of cellular scaffolding using these biomimetic materials should be based on accurate material properties sourced from healthy spatially distributed cartilage.

This study is however limited in that whilst the analysis focuses on the effect of ageing and OA, it is currently difficult to separate the two parameters as they often happen

concurrently. As ageing is a primary risk factor for the development of OA, even with the current data advancing the knowledge of material properties, it is difficult to determine how much both ageing and presence of disease separately contribute to the change in material properties. The linear model presented here suggests that while ageing has the greatest effect on material properties, low sample numbers and the inability to absolutely separate the parameters makes this unclear.

This study is also limited in that multiple samples taken from the same donor will lack independence during correlation analysis, despite being derived from varying geographical locations of the joint. Combining sample material properties from the same donor accounted for the lack of independence; however this in turn lowered the sample number for comparison. To overcome this, the mixed linear model used allowed the analysis of individual samples whilst accounting that there were multiple samples per donor. In this instance it showed that there were significant differences between donors but not within donors.

Conclusion

Our study has, for the first time, provided novel material property data across a wide span of age and OA grade for site matched cartilage and bone from varying localities in the human knee joint. This data demonstrates that cartilage and bone material properties alter in a synergistic relationship during ageing and disease, where a decrease in cartilage *G'* and *G"* is accompanied by an increase in subchondral bone *E*. However this relationship appears to be isolated to the subchondral bone and not the trabecular structure despite morphological changes known to occur during disease [Kamibayashi et al., 1995; Bobinac et al., 2003]. Furthermore cartilage and subchondral bone material properties are also

strongly correlated with age and OA grade independently, whilst changes in cartilage are also site dependent. Medial preferential development of OA was also noted where cartilage modulus was correlated with site dependency. This may suggest higher mechanical loading previously observed is a causative link to disease progression. This clinically relevant data can now be applied therapeutically via physical therapy, pharmaceuticals or the development of biomimetic materials where a subject- or cohort-specific approach would be more biologically representative.

References

1. Adouni, M., Shirazi-Adl, A. & Shirazi, R. 2012, "Computational biodynamics of human knee joint in gait: from muscle forces to cartilage stresses", *Journal of Biomechanics,* vol. 45, no. 12, pp. 2149-2156.
2. Behrens, J., Walker, P. & Shoji, H. 1974, "Variations in strength and structure of cancellous bone at the knee", *Journal of Biomechanics,* vol. 7, no. 3, pp. 201-207.
3. Bobinac, D., Spanjol, J., Zoricic, S. & Maric, I. 2003, "Changes in articular cartilage and subchondral bone histomorphometry in osteoarthritic knee joints in humans", *Bone,* vol. 32, no. 3, pp. 284-290.
4. Burgers, T.A., Mason, J., Niebur, G. & Ploeg, H.L. 2008, "Compressive properties of trabecular bone in the distal femur", *Journal of Biomechanics,* vol. 41, no. 5, pp. 1077-1085.
5. Burr, D.B. & Gallant, M.A. 2012, "Bone remodelling in osteoarthritis", *Nature Reviews Rheumatology,* vol. 8, no. 11, pp. 665-673.
6. Changoor, A., Fereydoonzad, L., Yaroshinsky, A. & Buschmann, M.D. 2010, "Effects of refrigeration and freezing on the electromechanical and biomechanical properties of articular cartilage", *Journal of Biomechanical Engineering,* vol. 132, no. 6, pp. 064502.
7. Chudoba, T. & Richter, F. 2001, "Investigation of creep behaviour under load during indentation experiments and its influence on hardness and modulus results", *Surface and Coatings Technology,* vol. 148, no. 2, pp. 191-198.
8. Cohen, J. 1988, "Statistical power analysis for the behavioural sciences". Hilsdale, *NJ: Lawrence Earlbaum Associates,* vol. 2.
9. Cox, L., van Donkelaar, C., van Rietbergen, B., Emans, P. & Ito, K. 2013, "Alterations to the subchondral bone architecture during osteoarthritis: bone adaptation vs

endochondral bone formation", *Osteoarthritis and Cartilage,* vol. 21, no. 2, pp. 331-338.

10. Desrochers, J., Amrein, M. & Matyas, J. 2012, "Viscoelasticity of the articular cartilage surface in early osteoarthritis", *Osteoarthritis and Cartilage,* vol. 20, no. 5, pp. 413-421.
11. Ducheyne, P., Heymans, L., Martens, M., Aernoudt, E., de Meester, P. & Mulier, J.C. 1977, "The mechanical behaviour of intracondylar cancellous bone of the femur at different loading rates", *Journal of Biomechanics,* vol. 10, no. 11, pp. 747-762.
12. Faul, F., Erdfelder, E., Lang, A. & Buchner, A. 2007, "G* Power 3: A flexible statistical power analysis program for the social, behavioral, and biomedical sciences", *Behavior Research Methods,* vol. 39, no. 2, pp. 175-191.
13. Franz, T., Hasler, E., Hagg, R., Weiler, C., Jakob, R. & Mainil-Varlet, P. 2001, "In situ compressive stiffness, biochemical composition, and structural integrity of articular cartilage of the human knee joint", *Osteoarthritis and Cartilage,* vol. 9, no. 6, pp. 582-592.
14. Fulcher, G.R., Hukins, D.W. & Shepherd, D.E. 2009, "Viscoelastic properties of bovine articular cartilage attached to subchondral bone at high frequencies", *BMC Musculoskeletal Disorders,* vol. 10, no. 1, pp. 61.
15. Goldring, S.R. & Goldring, M.B. 2016, "Changes in the osteochondral unit during osteoarthritis: structure, function and cartilage-bone crosstalk", *Nature Reviews Rheumatology,* vol. 12, no. 11, pp. 632-644.
16. Hansen, U., Masouros, S. & Amis, A.A. 2006, "(iii) Material properties of biological tissues related to joint surgery", *Current Orthopaedics,* vol. 20, no. 1, pp. 16-22.
17. Hayami, T., Pickarski, M., Wesolowski, G.A., Mclane, J., Bone, A., Destefano, J., Rodan, G.A. & Duong, L.T. 2004, "The role of subchondral bone remodeling in osteoarthritis: reduction of cartilage degeneration and prevention of osteophyte

formation by alendronate in the rat anterior cruciate ligament transection model", *Arthritis & Rheumatism,* vol. 50, no. 4, pp. 1193-1206.

18. Herbert, E., Oliver, W., Lumsdaine, A. & Pharr, G.M. 2009, "Measuring the constitutive behavior of viscoelastic solids in the time and frequency domain using flat punch nanoindentation", *Journal of Materials Research,* vol. 24, no. 03, pp. 626-637.
19. Herbert, E., Oliver, W. & Pharr, G. 2008, "Nanoindentation and the dynamic characterization of viscoelastic solids", *Journal of Physics D: Applied Physics,* vol. 41, no. 7, pp. 074021.
20. Hollman, J.H., Kovash, F.M., Kubik, J.J. & Linbo, R.A. 2007, "Age-related differences in spatiotemporal markers of gait stability during dual task walking", *Gait & Posture,* vol. 26, no. 1, pp. 113-119.
21. Hori, R.Y. & Mockros, L. 1976, "Indentation tests of human articular cartilage", *Journal of Biomechanics,* vol. 9, no. 4, pp. 259-268.
22. Jin, H. & Lewis, J.L. 2004, "Determination of Poisson's ratio of articular cartilage by indentation using different-sized indenters", *Journal of Biomechanical Engineering,* vol. 126, no. 2, pp. 138-145.
23. Kamibayashi, L., Wyss, U., Cooke, T. & Zee, B. 1995, "Trabecular microstructure in the medial condyle of the proximal tibia of patients with knee osteoarthritis", *Bone,* vol. 17, no. 1, pp. 27-35.
24. Kiss, R.M. 2011, "Effect of severity of knee osteoarthritis on the variability of gait parameters", *Journal of Electromyography and Kinesiology,* vol. 21, no. 5, pp. 695-703.
25. Kleemann, R., Krocker, D., Cedraro, A., Tuischer, J. & Duda, G. 2005, "Altered cartilage mechanics and histology in knee osteoarthritis: relation to clinical assessment (ICRS Grade)", *Osteoarthritis and Cartilage,* vol. 13, no. 11, pp. 958-963.

26. Kumar, D., Manal, K.T. & Rudolph, K.S. 2013, "Knee joint loading during gait in healthy controls and individuals with knee osteoarthritis", *Osteoarthritis and Cartilage,* vol. 21, no. 2, pp. 298-305.
27. Kuroki, K., Cook, C. & Cook, J. 2011, "Subchondral bone changes in three different canine models of osteoarthritis", *Osteoarthritis and Cartilage,* vol. 19, no. 9, pp. 1142-1149.
28. Landau, L.D. & Lifshitz, E. 1986, "Theory of Elasticity, vol. 7", *Course of Theoretical Physics,* vol. 3, pp. 109.
29. Li, W., Wang, D., Yang, W. & Song, Y. 2016, "Compressive mechanical properties and microstructure of PVA–HA hydrogels for cartilage repair", *RSC Advances,* vol. 6, no. 24, pp. 20166-20172.
30. Linde, F. & Sørensen, H.C.F. 1993, "The effect of different storage methods on the mechanical properties of trabecular bone", *Journal of Biomechanics,* vol. 26, no. 10, pp. 1249-1252.
31. Madry, H., van Dijk, C.N. & Mueller-Gerbl, M. 2010, "The basic science of the subchondral bone", *Knee Surgery, Sports Traumatology, Arthroscopy,* vol. 18, no. 4, pp. 419-433.
32. Mahjoub, M., Berenbaum, F. & Houard, X. 2012, "Why subchondral bone in osteoarthritis? The importance of the cartilage bone interface in osteoarthritis", *Osteoporosis International,* vol. 23, no. 8, pp. 841-846.
33. Manninen, P., Riihimaki, H., Heliovaara, M. & Makela, P. 1996, "Overweight, gender and knee osteoarthritis", *International Journal of Obesity and Related Metabolic Disorders : journal of the International Association for the Study of Obesity,* vol. 20, no. 6, pp. 595-597.
34. Mononen, M., Mikkola, M., Julkunen, P., Ojala, R., Nieminen, M., Jurvelin, J. & Korhonen, R. 2012, "Effect of superficial collagen patterns and fibrillation of

femoral articular cartilage on knee joint mechanics—A 3D finite element analysis", *Journal of Biomechanics,* vol. 45, no. 3, pp. 579-587.

35. Moon, D.K., Woo, S.L., Takakura, Y., Gabriel, M.T. & Abramowitch, S.D. 2006, "The effects of refreezing on the viscoelastic and tensile properties of ligaments", *Journal of Biomechanics,* vol. 39, no. 6, pp. 1153-1157.
36. Moore, A. & Burris, D. 2015, "Tribological and material properties for cartilage of and throughout the bovine stifle: support for the altered joint kinematics hypothesis of osteoarthritis", *Osteoarthritis and Cartilage,* vol. 23, no. 1, pp. 161-169.
37. Moronkeji, K., Todd, S., Dawidowska, I., Barrett, S. & Akhtar, R. 2016, "The role of subcutaneous tissue stiffness on microneedle performance in a representative *in vitro* model of skin", *Journal of Controlled Release,* In Press, Corrected Proof.
38. Nia, H.T., Han, L., Li, Y., Ortiz, C. & Grodzinsky, A. 2011, "Poroelasticity of cartilage at the nanoscale", *Biophysical Journal,* vol. 101, no. 9, pp. 2304-2313.
39. Oliver, W.C. & Pharr, G.M. 1992, "An improved technique for determining hardness and elastic modulus using load and displacement sensing indentation experiments", *Journal of Materials Research,* vol. 7, no. 06, pp. 1564-1583.
40. Oyen, M. 2013, "Nanoindentation of biological and biomimetic materials", *Experimental Techniques,* vol. 37, no. 1, pp. 73-87.
41. Pelletier, J., Raynauld, J., Berthiaume, M., Abram, F., Choquette, D., Haraoui, B., Beary, J.F., Cline, G.A., Meyer, J.M. & Martel-Pelletier, J. 2007, "Risk factors associated with the loss of cartilage volume on weight-bearing areas in knee osteoarthritis patients assessed by quantitative magnetic resonance imaging: a longitudinal study", *Arthritis Research & Therapy,* vol. 9, no. 4, pp. R74.
42. Peters, A.E., Comerford, E.J., Macaulay, S., Bates, K.T. & Akhtar, R. 2017, "Micromechanical properties of canine femoral articular cartilage following

multiple freeze-thaw cycles", *Journal of the Mechanical Behavior of Biomedical Materials,* vol. 71, pp. 114-121.

43. Reilly, D.T. & Burstein, A.H. 1975, "The elastic and ultimate properties of compact bone tissue", *Journal of Biomechanics,* vol. 8, no. 6, pp. 393IN9397-396IN11405.
44. Rho, J., Tsui, T.Y. & Pharr, G.M. 1997, "Elastic properties of human cortical and trabecular lamellar bone measured by nanoindentation", *Biomaterials,* vol. 18, no. 20, pp. 1325-1330.
45. Robinson, D.L., Kersh, M.E., Walsh, N.C., Ackland, D.C., de Steiger, R.N. & Pandy, M.G. 2016, "Mechanical properties of normal and osteoarthritic human articular cartilage", *Journal of the Mechanical Behavior of Biomedical Materials,* vol. 61, pp. 96-109.
46. Shepherd, D.E. & Seedhom, B.B. 1999, "The 'instantaneous' compressive modulus of human articular cartilage in joints of the lower limb", *Rheumatology (Oxford, England),* vol. 38, no. 2, pp. 124-132.
47. Simon, W.H., Mak, A. & Spirt, A. 1990, "The effect of shear fatigue on bovine articular cartilage", *Journal of Orthopaedic Research,* vol. 8, no. 1, pp. 86-93.
48. Sneddon, I.N. 1965, "The relation between load and penetration in the axisymmetric Boussinesq problem for a punch of arbitrary profile", *International Journal of Engineering Science,* vol. 3, no. 1, pp. 47-57.
49. Taffetani, M., Gottardi, R., Gastaldi, D., Raiteri, R. & Vena, P. 2014, "Poroelastic response of articular cartilage by nanoindentation creep tests at different characteristic lengths", *Medical Engineering & Physics,* vol. 36, no. 7, pp. 850-858.
50. Thambyah, A., Nather, A. & Goh, J. 2006, "Mechanical properties of articular cartilage covered by the meniscus", *Osteoarthritis and Cartilage,* vol. 14, no. 6, pp. 580-588.

51. Wang, M., Peng, Z., Price, J. & Ketheesan, N. 2013, "Study of the nano-mechanical properties of human knee cartilage in different wear conditions", *Wear,* vol. 301, no. 1, pp. 188-191.
52. Wang, Q., Hou, R., Cheng, Y. & Fu, J. 2012, "Super-tough double-network hydrogels reinforced by covalently compositing with silica-nanoparticles", *Soft Matter,* vol. 8, no. 22, pp. 6048-6056.
53. Wen, C., Lu, W.W. & Chiu, K.Y. 2014, "Importance of subchondral bone in the pathogenesis and management of osteoarthritis from bench to bed", *Journal of Orthopaedic Translation,* vol. 2, no. 1, pp. 16-25.
54. Wilusz, R.E., Zauscher, S. & Guilak, F. 2013, "Micromechanical mapping of early osteoarthritic changes in the pericellular matrix of human articular cartilage", *Osteoarthritis and Cartilage,* vol. 21, no. 12, pp. 1895-1903.
55. Zhang, Y. & Jordan, J.M. 2008, "Epidemiology of Osteoarthritis", *Rheumatic Disease Clinics of North America,* vol. 34, no. 3, pp. 515-529.
56. Zuo, Q., Lu, S., Du, Z., Friis, T., Yao, J., Crawford, R., Prasadam, I. & Xiao, Y. 2016, "Characterization of nano-structural and nano-mechanical properties of osteoarthritic subchondral bone", *BMC Musculoskeletal Disorders,* vol. 17, no. 1, pp. 367.
57. Zysset, P.K., Guo, X.E., Hoffler, C.E., Moore, K.E. & Goldstein, S.A. 1999, "Elastic modulus and hardness of cortical and trabecular bone lamellae measured by nanoindentation in the human femur", *Journal of Biomechanics,* vol. 32, no. 10, pp. 1005-1012.
58. Zysset, P., Sonny, M. & Hayes, W. 1994, "Morphology-mechanical property relations in trabecular bone of the osteoarthritic proximal tibia", *The Journal of Arthroplasty,* vol. 9, no. 2, pp. 203-216.

Chapter Five: Effect of ageing and osteoarthritis on ligament material properties of the human knee

Abstract

Human knee ligaments work to stabilise the joint and prevent excessive movement. Whilst ligaments are known to decline in structure and function with ageing, effects of osteoarthritis (OA) on material properties is currently unexplored. This study aims to collate anterior cruciate ligament (ACL), posterior cruciate ligament (PCL), medial collateral ligament (MCL), and lateral collateral ligament (LCL) material properties from demographically diverse cadavers (31 – 88 years, OA grade 0 - 4). Human knee joints (n = 12) were dissected and bone-ligament-bone samples loaded to failure. Results indicated trends between increasing age and a decrease in linear failure, linear stress, Young's modulus, tangent modulus, failure load, failure stress and stiffness in the ACL and PCL. Decreasing trends were also evident in failure stress of the MCL and tangent modulus and failure load of the LCL when correlated with increasing age. Increasing OA grade was correlated with linear mechanics in the ACL and PCL, and failure mechanics in the ACL, PCL, MCL and LCL. Ligaments were also categorised into young healthy (31 – 43 years, ICRS grade 0), young OA (49 – 58 years, ICRS grades 1 – 2) and old OA (72 – 88 years, ICRS grades 1 – 4) cohorts, although no significant trends could be seen between the means of material properties from each group. In conclusion both advancing age and disease status relate to multiple material properties on a linear scale of all four primary knee joint ligaments. Knowledge of healthy whole-joint mechanics can aid reconstruction and graft replacements and advance finite element models, whilst knowledge of aged/diseased mechanics can help direct therapeutics.

Introduction

The knee joint is composed of both soft and hard tissues, forming a diarthrosis articulation between the femur and tibia, allowing flexion and extension in the sagittal plane [Nigg & Herzog, 2006]. Primary human knee joint ligaments act as strain sensors, restricting degrees of freedom to provide stabilisation and prevent excessive movement [Harner et al., 1995; Woo et al., 2006]. Structurally, ligaments have direct and indirect insertions into the bone and periosteum [Woo et al., 2006] allowing fibre bundle variations to respond to different movements and resist loading during tension or rotation at the joint [Hansen et al., 2006].

Tensile properties of the anterior cruciate ligament (ACL), posterior cruciate ligament (PCL), medial collateral ligament (MCL) and lateral collateral ligament (LCL) have been explored by numerous researchers [e.g. Noyes & Grood, 1976; Woo et al., 1991; Robinson et al., 2005; Bonner et al., 2015; Race & Amis, 1994], providing important information on the health and mechanical strength of such structures. Data for all four ligaments exists across various sources in the literature; however, these are most often harvested and tested in isolation, obtaining just one ligament type from donors. To date, only one study has explored all four ligaments from the same donor (n = 4 young healthy donors), showing increased stiffness and failure load in the cruciate ligaments when compared to the collaterals [Trent et al., 1976]. Despite data existing for all four ligaments, there is marked variability in reported values, likely due to variations in testing techniques and donor demographics, which currently makes it challenging to understand whole-joint functioning.

The lack of a consistent baseline of healthy measurements means that our understanding of how tensile properties of all four ligaments within the same knee joint change with

ageing or disease is presently unclear. These structural and functional capabilities are known to decline with ageing in the ACL with specific observations of decreased ultimate failure load from older donors (67- 90 years), when compared to middle-aged (40 – 50 years) and young donors (22 – 35 years) [Woo et al., 1991]. This is also reflected at a ligament cellular level with increasing ACL histologic scores associated with increasing age [Hasegawa et al., 2012]. However, any differences in material properties in the PCL, MCL and LCL are yet to be correlated with different age categories. Changes to integrity and tensile properties not only leave ligaments vulnerable to further injury but also affect the peri-articular tissues leading to muscle weakening through immobility, and whole-joint disruption including the development of osteoarthritis (OA) [Rousseau & Garnero, 2012; Manninen et al., 1996]. To what extent the effect of OA has on the tensile properties of the knee joint ligaments is also relatively unknown, with current explorations focusing primarily on histological analyses. Such examinations show impaired integrity of the ACL and PCL during total knee replacements in the presence of OA [e.g. Hasegawa et al., 2012; Mullaji et al., 2008].

Further understanding of the effect of ageing and OA on the functioning of the human knee joint can help link previously observed micro-scale morphological changes to overall mechanical function of the joint, where it is widely known that gait adaptations occur during habitual locomotion with the presence of OA [Kumar et al., 2013; Adouni et al., 2012]. Such knowledge can also aid our understanding of injury patterns and therefore help predict under what circumstances they may occur. In this context, computational modelling is often used as a predictive tool, but requires reliable input data including material properties of the tissues being modelled [Freutel et al., 2014; Guo et al., 2013]. These properties can indicate behavioural responses of ligaments and therefore whole joints under varying stresses and strains [e.g. Wang et al., 2014], which would be expected

to change during ageing and disease across different cohorts. Therefore, the aim of this paper is to obtain such material properties of the four primary ligaments of the knee joint from human cadavers with wide demographics including range of age and grade of OA to provide a pool of data for use in therapeutics, biomaterial development or finite element (FE) modeling.

Materials and Methods

Specimens

Fresh-frozen human cadaveric knee joints were sourced aged 31 – 88 years (n = 12; 4 female, 8 male). Specific cadaver demographics can be found in Table 1, Chapter Four of this thesis, including height, weight, body mass index and cause of death. Ethical permission for use of this human cadaveric material was granted by the NRES (15/NS/0053).

Cadaver limbs were initially frozen at -20°C and thawed at 3 – 5°C for 5 days prior to dissection. Four bone-ligament-bone samples (e.g. Fig. 1a) were harvested from each cadaver using a low speed oscillating saw (deSoutter Medical, Bucks, UK). Extracted samples were then stored at -20°C before individual samples were thawed for 24 hours at 3 – 5°C with exposure to phosphate buffered saline (PBS). Overall the samples underwent two freeze-thaw cycles, which has previously been shown to have no effect on ligament and tendon material properties [Jung et al., 2011; Huang et al., 2011; Moon et al., 2006; Woo et al., 1986]. Cadavers were photographed at the time of dissection and graded for OA using the International Cartilage Repair Society (ICRS) (see Table 2, Chapter Four of this thesis for grading).

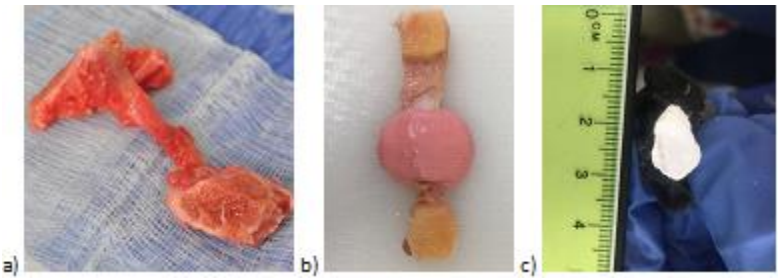

Figure 1. a) Bone-ligament-bone samples b) Ligament encased in impression material c) Polymethyl-methacrylate cast of ligament photographed for cross-sectional area measurement.

Cross-Sectional Measurements

The cross-sections of all ligament samples were obtained using the methods as described previously by Goodship and Birch, [2005]. However in brief, using a fast setting alginate impression paste (UnoDent, Essex, England) ligaments were encased in the material and left to set for two minutes (Fig. 1b). Once the impression material was set a scalpel blade was used to slice the mould which was then filled with polymethyl-methacrylate (PMMA) (Teknovit 6091, Heraeus Kulzer GmbH, Wehrheim, Germany) to create a replica of the ligament structure. Once the PMMA was set, the mould was sliced transversely and the resulting ends coloured with permanent white marker pen (Fig. 1c). The cement mould ends were then photographed and digitally measured using ImageJ [Schneider et al., 2012*]* to obtain the cross-sectional area of the ligament.

Sample Preparation

The bony insertion and origin sites of each ligament sample were cut into a suitable shape for testing using a hand saw (Fig. 1a). The bone ends of the samples were potted into steel

holders and screwed in place. PMMA was then poured into the holder and left to cure for 4 – 5 minutes. Samples were then attached to the load cell and encased into a water tight chamber. The chamber was filled with PBS to ensure hydration during testing (Fig. 2 and Fig. 3).

Tensile Testing Protocol

Using a uniaxial tensile tester (Instron 3366, Buckinghamshire, UK) with a 5 kN load cell, a 1 N preload was applied and all ligaments underwent ten preconditioning cycles at 10 mm/min with a load of 1 – 40 N, which provides a stable and repeatable viscoelastic response [Momersteeg et al., 1995]. Loading was then set to zero and ligaments were loaded to failure at 500 mm/min. A fast strain rate was chosen over slow stain rates because this been shown to mimic physiological loading [Noyes & Grood, 1976] and replicate a realistic injury environment [Robinson et al., 2005]. Additionally, faster strain rates improve the chances of the ligament rupturing mid-substance as opposed to a bony avulsion [Noyes & Grood, 1976].

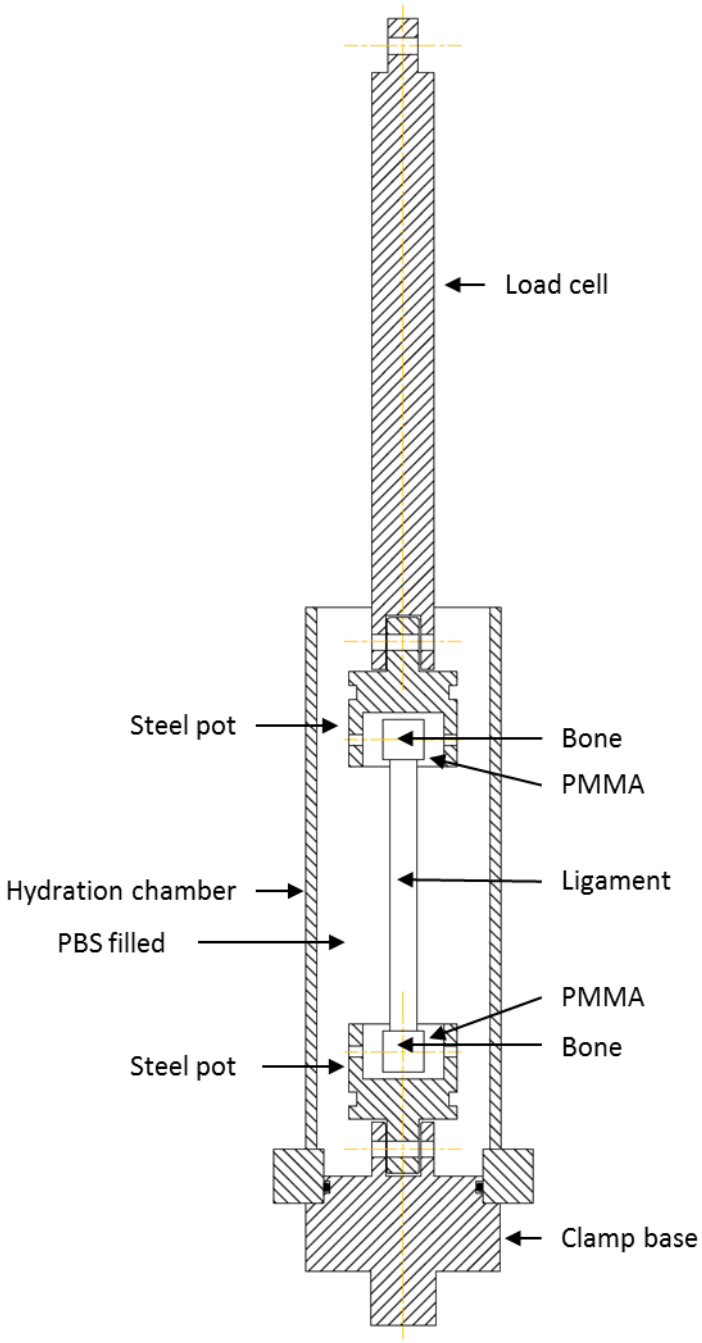

Figure 2. Schematic illustration of the custom-made rig for tensile testing of ligaments.

Figure 3. Photograph of the custom-made rig for tensile testing of ligaments.

Material Properties

The bone-ligament-bone samples were tested and analysed to collate multiple material property data. In summary the following parameters were used:

Linear force (N) and linear strain (mm and %) were calculated from the last data point on the linear slope of the curve (Fig. 4).

$$Linear\ Stress\ (MPa) = \frac{Linear\ Force\ (N)}{Cross\ Sectional\ Area\ (mm^2)} \quad (1)$$

Failure load (N) and failure strain (mm and %) were calculated from the maximum load reached (Fig. 4).

$$Failure\ Stress\ (MPa) = \frac{Failure\ Load\ (N)}{Cross\ Sectional\ Area\ (mm^2)} \quad (2)$$

$$Young's\ Modulus\ (MPa) = \frac{Linear\ Force\ (N)}{Linear\ Strain\ (\%)/Ligament\ Length\ (mm)} \quad (3)$$

$$Tangent\ Modulus\ (MPa) = \frac{Max\ Linear\ Force\ (N) - Submax\ Linear\ Force\ (N)}{Max\ Linear\ Strain\ (mm) - Submax\ Linear\ Strain\ (mm)} \quad (4)$$

$$Stiffness\ Nmm = \frac{Cross\ Sectional\ Area * Youmgs\ Modulus}{Ligament\ Length} \quad (5)$$

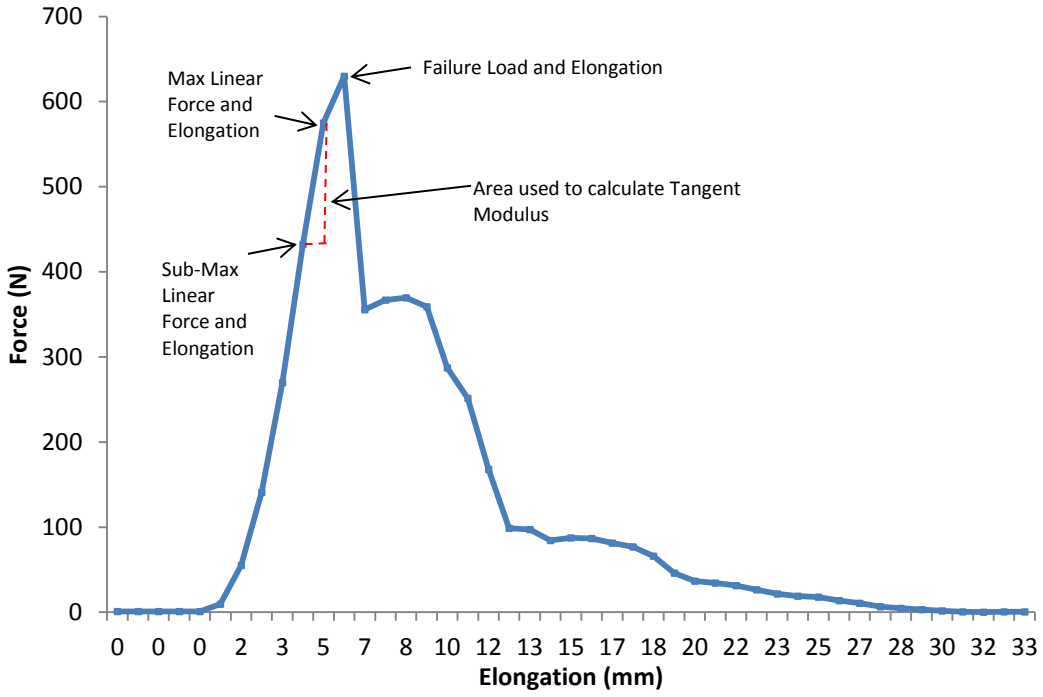

Figure 4. Example force (N) elongation (mm) curve, giving submaximal linear force and elongation, maximal linear force and elongation, failure load and elongation, and highlights the slope used to calculate tangent modulus.

Statistical Analysis

Ligament material properties were correlated with increasing age and increasing grade of OA using a Kendall's Tau-b correlation coefficient. Ligaments were then categorised into young healthy (31 – 43 years, ICRS grade 0), young with OA (49-58 years, ICRS grades 1-2) and old with OA (72-88 years, ICRS grades 1-4), with the mean and standard deviation (SD) for each cohort presented. Statistical analysis of ligament material properties was conducted using a Kruskal-Wallis one-way ANOVA (SPSS software, Version 22.0, SPSS, Inc., Chicago, IL) to see if there are differences between the means of young healthy, young OA and old OA cohorts. To summarise, the following morphological measurements including length and cross-sectional as well as the following material properties were included in analyses: linear force, linear stress, linear strain, failure load, failure stress, failure strain, Young's (secant) modulus, tangent modulus, stiffness and failure site. A Kendall's Tau-b correlation was also used to see if a material properties in one ligament was correlated with a change in another ligament from the same donor.

Results

ACL (n = 12), PCL (n = 12), MCL (n = 12), and LCL (n = 12) samples were obtained from twelve cadavers. One MCL sample from a young healthy donor was severely abnormal (see Fig. 5), and data from one MCL sample from an older ICRS grade 1 donor was unable to be retained. Both were excluded from statistical analysis. The mean and SD for all parameters measured for young healthy, young OA and old OA cohorts can be found in Tables 1 and 2. Values for individual ligament samples from each donor can be found in Table 13 (Chapter Nine, Supplementary Material).

Figure 5. Abnormal MCL excluded from analysis.

Correlation with Age

Increasing age was significantly correlated with ACL linear force (τb = -0.657, p = 0.003), linear stress (τb = -0.504, p = 0.023), Young's modulus (τb = -0.443, p = 0.046), failure load (τb = -0.443, p = 0.046), failure stress (τb = -0.657, p = 0.003) and stiffness (τb = -0.534, p = 0.016). A correlation analysis was also performed between age and ACL tangent modulus, although this was not significant (τb = -0.351, p = 0.114).

Increasing age was significantly correlated with PCL linear force (τb = -0.473, p = 0.033), linear stress (τb = -0.443, p = 0.046), Young's modulus (τb = -0.443, p = 0.046) and failure stress (τb = -0.534, p = 0.016). A correlation analysis was also performed between age and PCL tangent modulus (τb = -0.412, p = 0.063), failure load (τb = -0.382, p = 0.086) and stiffness (τb = -0.382, p = 0.086), although these were not significant.

A correlation analysis was also performed between age and MCL length (τb = 0.432, p = 0.087), cross sectional area (τb = 0.315, p = 0.209) and failure stress (τb = -0.449, p = 0.072), and LCL tangent modulus (τb = -0.412, p = 0.063) and failure load (τb = -0.412, p = 0.063), although these were not significant.

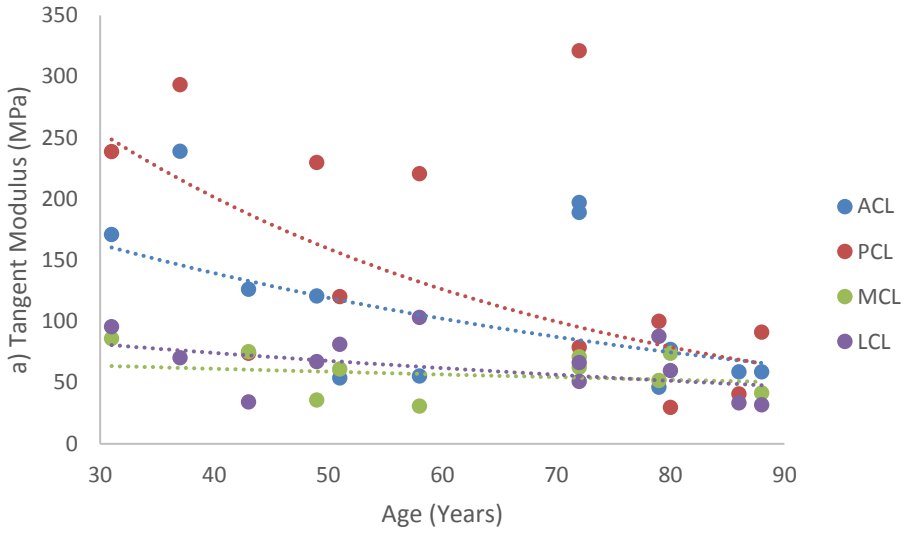
a) Tangent Modulus (MPa)
350
300
250
200
150
100
50
0
30
40
50
60
70
80
90
Age (Years)
ACL
PCL
MCL
LCL

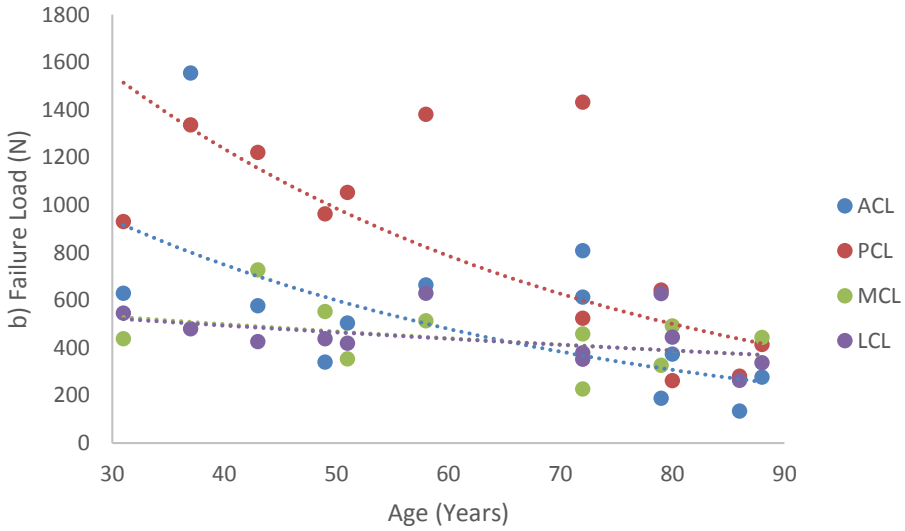
b) Failure Load (N)
1800
1600
1400
1200
1000
800
600
400
200
0
30
40
50
60
70
80
90
Age (Years)
ACL
PCL
MCL
LCL

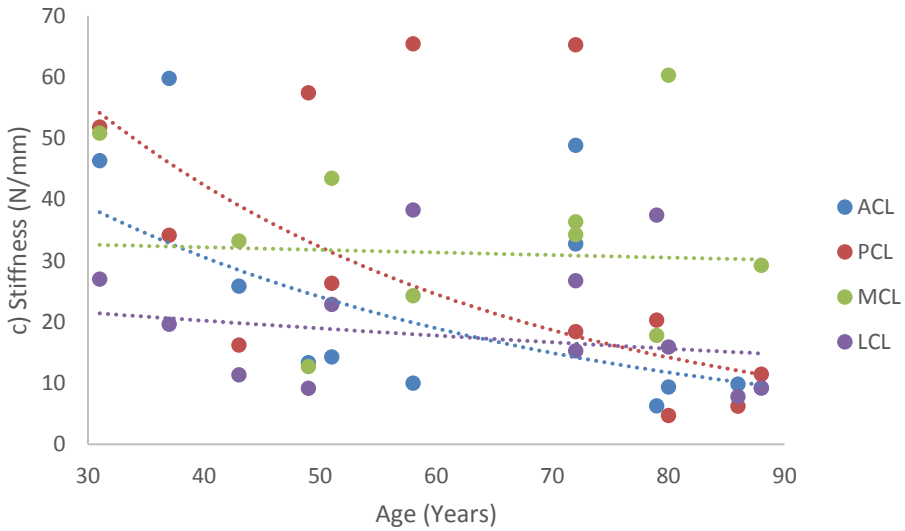
c) Stiffness (N/mm)
70
60
50
40
30
20
10
0
30
40
50
60
70
80
90
Age (Years)
ACL
PCL
MCL
LCL

Figure 6. a) Tangent modulus (MPa) b) Failure load (N), and c) Stiffness (N/mm) of anterior cruciate ligament (ACL), posterior cruciate ligament (PCL), medial collateral ligament (MCL), lateral collateral ligament (LCL) against age of cadaver.

Correlation with Osteoarthritis

Increasing OA grade was significantly correlated with ACL linear stress (τb = -0.526, p = 0.024) and failure stress (τb = -0.461, p = 0.048). A correlation analysis was also performed between age and linear force (τb = -0.428, p = 0.066), linear strain (τb = -0.362, p = 0.120), Young modulus (τb = -0.428, p = 0.066) and stiffness (τb = -0.362, p = 0.120) although these were not significant.

Increasing OA grade was significantly correlated with PCL failure stress (τb = -0.461, p = 0.048). A correlation analysis was also performed between OA grade and PCL cross sectional area (τb = 0395, p = 0.090) and linear force (τb = -0.329, p = 0.158), although these were not significant.

Further analsyis was performed between increasing OA grade and MCL length (τb = 0.386, p = 0.140), and failure stress (τb = -0.406, p = 0.118), and LCL failure stress (τb = -0.329, p = 0.158), and failure strain (τb = -0.329, p = 0.158), although again these were not significant.

Multi-Variable Analysis

Due to low sample numbers and multiple categories of OA, multi-variable analysis considering both age and OA was not possible. Therefore data was categorised into ‘young healthy’, ‘young OA’ and ‘old OA’ cohorts to determine difference in the mean of each

group using a non-parametric one-way ANOVA (Kruskal-Willis) to attempt to account for both age and OA status. There was a significant relationship in the MCL tangent modulus (p = 0.047); however there were no observed significant differences between cohorts in any other measured material property variable. Despite no significant relationships between cohorts, trends can be found in Tables 1 and 2 and Figure 7, identifying differences in the means of each group and these are discussed below.

Mean ACL linear force, linear stress, Young's modulus, tangent modulus, failure load, failure stress and stiffness showed decreasing trends between the young health cohort and the young OA cohort (Table 1). Mean ACL failure load also showed decreasing trends between the young OA and old OA cohort. Exemplar failure load to failure deformation and failure stress to failure strain graphs from one young healthy cadaver, one young OA cadaver and one old OA cadaver can be seen in Figures 8 and 9.

A greater number of decreasing trends were seen between the young OA cohort and old OA cohort for PCL material properties, including linear force, Young's modulus, tangent modulus, failure load, failure stress and stiffness (Table 1).

A decrease in linear force between young healthy and young OA cohorts was also observed with increasing age, as well as linear stress, Young's modulus, tangent modulus, failure load and stiffness in the MCL. A further decrease was seen in linear force and failure load between young OA and old OA cohorts (Table 2).

No obvious increasing or decreasing trends were observed in all parameters measured in the LCL between young healthy, young OA and old OA cohorts. Whilst some values changed slightly (Table 2), high overlapping SD's meant that trends were not clear.

It should be noted that SDs were high and overlapped between cohorts (Tables 1 & 2). To aid full interpretation of the results, all resultant data from individual cadavers is summarised in Table 13, Chapter Nine Supplementary Material.

Failure site in the ACL was mixed with failures at the mid substance, insertion and by bony avulsion across all three cohorts. The PCL failed more by mid substance in the young healthy category and more by insertion in the young OA and old OA cohorts. Failure occurred more frequently in the mid-substance of the younger MCL and LCL cohorts, and more failed by insertion or bony avulsion in the older OA cohort (Fig. 10).

Table 1. Mean and standard deviation (SD) of material properties of the anterior cruciate ligament (ACL) and posterior cruciate ligament (PCL) for young healthy (31-43 years, ICRS grade 0), young OA (49-58 years, ICRS grades 1-2) and old OA cadavers (72-88 years, ICRS grades 1-4).

	ACL			**PCL**		
	Young Healthy (n=3)	Young OA (n=3)	Old OA (n=6)	Young Healthy (n=3)	Young OA (n=3)	Old OA (n=6)
	Mean ± SD	**Mean ± SD**	**Mean ± SD**	**Mean ± SD**	**Mean ± SD**	**Mean ± SD**
Length mm	34.0±5.3	36.3±7.2	32.7±3.2	32.0±3.5	41.3±6.4	36.0±4.9
CS Area mm²	61.2±11.6	61.4±31.3	58.9±27.6	70.6±19.5	80.9±20.0	90.0±34.2
Linear Force N	795.9±478.9	216.3±41.5	224.6±179.0	700.5±375.0	712.1±306.3	351.2±369.4
Linear Stress MPa	14.4±11.6	4.4±2.4	4.2±3.6	11.6±9.7	8.5±1.9	4.3±4.1
Linear Strain mm	5.8±0.9	6.2±1.2	4.5±2.0	7.0±2.7	5.9±1.0	5.7±1.1
Linear Strain %	17.7±5.1	17.2±0.3	13.7±5.6	22.4±10.2	14.3±0.7	16.0±3.1
Young's Mod. MPa	25.9±13.0	9.1±5.7	11.5±11.1	16.31±8.63	25.1±8.7	8.78±7.67
Tangent Mod. MPa	178.9±56.7	76.7±38.2	104.6±69.3	202.0±114.2	190.3±60.9	110.4±107.0
Failure Load N	920.4±549.5	503.4±161.8	399.3±262.2	1162.6±209.3	1132.2±219.9	592.8±436.2
Failure Stress MPa	16.7±13.4	8.7±1.6	7.0±4.6	18.0±8.5	14.4±3.2	7.3±5.0
Failure Strain mm	8.1±2.1	12.1±2.6	7.6±2.4	11.4±3.4	11.8±3.5	11.7±3.2
Failure Strain %	24.5±8.9	34.3±10.5	23.1±6.8	36.5±13.5	29.9±14.2	32.4±8.2
Stiffness N/mm	44.0±17.1	12.5±2.3	19.4±17.4	34.1±17.8	49.7±20.7	21.1±22.6

Table 2. Mean and standard deviation (SD) of material properties of the medial collateral ligament (MCL) and lateral collateral ligament (LCL) for young healthy (31-43 years, ICRS grade 0), young OA (49-58 years, ICRS grades 1-2) and old OA cadavers (72-88 years, ICRS grades 1-4).

	MCL			**LCL**		
	Young Healthy (n=3)	Young OA (n=3)	Old OA (n=6)	Young Healthy (n=3)	Young OA (n=3)	Old OA (n=6)
	Mean ± SD	**Mean ± SD**	**Mean ± SD**	**Mean ± SD**	**Mean ± SD**	**Mean ± SD**
Length mm	105.5±3.5	114.0±13.0	117.4±4.6	59.3±3.8	52.3±5.5	63.7±6.1
CS Area mm²	26.4±2.7	30.8±9.6	39.0±11.8	33.9±32.9	40.4±4.6	36.4±20.3
Linear Force N	337.8±7.6	189.0±78.5	250.6±99.6	280.0±198.1	336.4±54.5	251.3±160.2
Linear Stress MPa	12.8±1.0	6.0±0.8	7.4±4.5	12.7±13.2	8.4±2.0	8.9±9.4
Linear Strain mm	8.9±3.1	8.7±1.9	9.4±5.2	7.7±3.3	9.6±5.5	8.5±2.0
Linear Strain %	8.4±2.7	7.8±2.6	7.9±4.3	13.1±5.4	18.6±10.7	13.3±2.5
Young's Mod. MPa	170.2±61.4	94.9±33.2	119.6±79.5	55.6±41.4	32.4±25.9	42.5±40.2
Tangent Mod. MPa	80.7±7.5	42.6±16.4	60.2±13.6	66.8±30.9	84.0±18.1	55.1±21.2
Failure Load N	583.0±204.4	473.5±104.9	389.8±110.3	484.0±59.8	495.7±116.2	401.1±125.9
Failure Stress MPa	21.8±5.5	17.0±8.1	11.2±5.3	24.0±15.0	12.6±4.3	14.6±10.1
Failure Strain mm	14.0±7.8	15.4±1.9	15.1±3.1	11.4±0.4	15.4±6.3	14.7±3.7
Failure Strain %	13.1±7.0	13.7±3.2	12.8±2.4	19.2±1.1	30.1±13.1	23.1±4.5
Stiffness N/mm	42.0±12.5	26.8±15.5	35.6±15.6	19.3±7.8	23.4±14.6	18.7±11.4

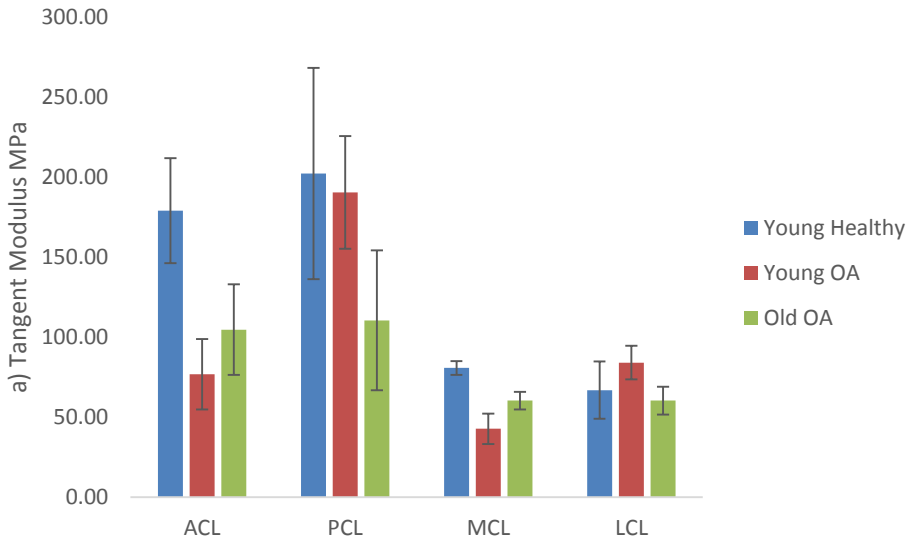
a) Tangent Modulus MPa
300.00
250.00
200.00
150.00
100.00
50.00
0.00
ACL
PCL
MCL
LCL
Young Healthy
Young OA
Old OA

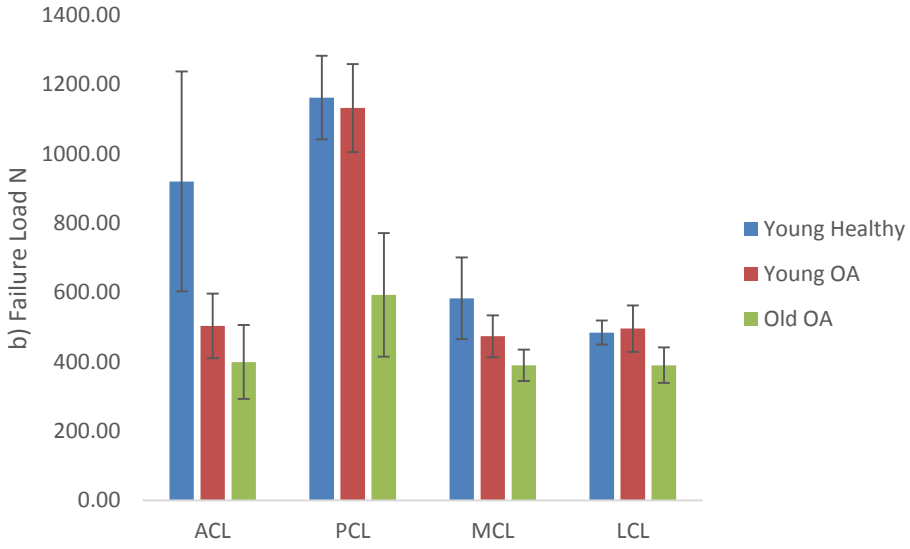
b) Failure Load N
1400.00
1200.00
1000.00
800.00
600.00
400.00
200.00
0.00
ACL
PCL
MCL
LCL
Young Healthy
Young OA
Old OA

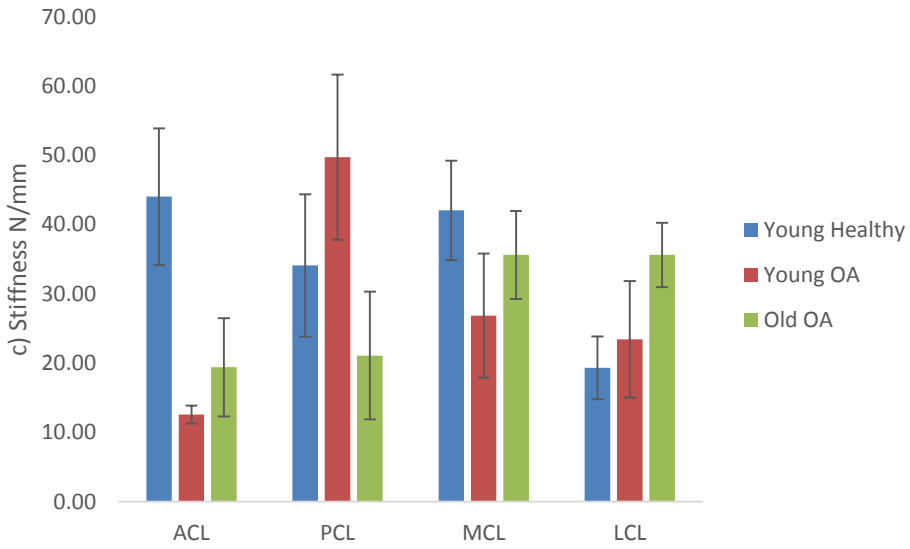
c) Stiffness N/mm
70.00
60.00
50.00
40.00
30.00
20.00
10.00
0.00
ACL
PCL
MCL
LCL
Young Healthy
Young OA
Old OA

Figure 7. Mean of a) Tangent modulus (MPa) b) Failure load (N), and c) Stiffness (N/mm) of anterior cruciate ligament (ACL), posterior cruciate ligament (PCL), medial collateral ligament (MCL), lateral collateral ligament (LCL) for young healthy (31-43 years, ICRS grade 0), young OA (49-58 years, ICRS grades 1-2) and old OA cadavers (72-88 years, ICRS grades 1-4). Error bars represent standard error of mean (SEM).

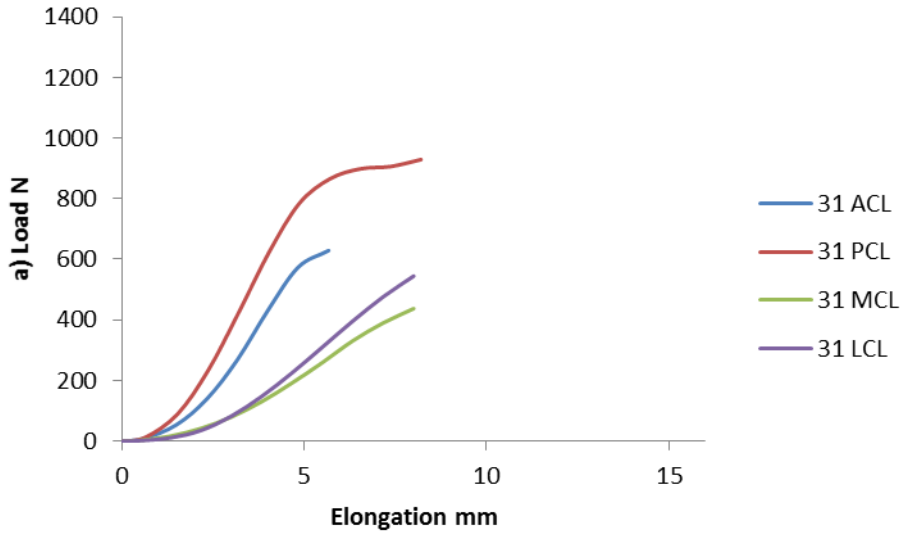
1400
1200
1000
800
600
400
200
0
a) Load N
0
5
10
15
Elongation mm
31 ACL
31 PCL
31 MCL
31 LCL

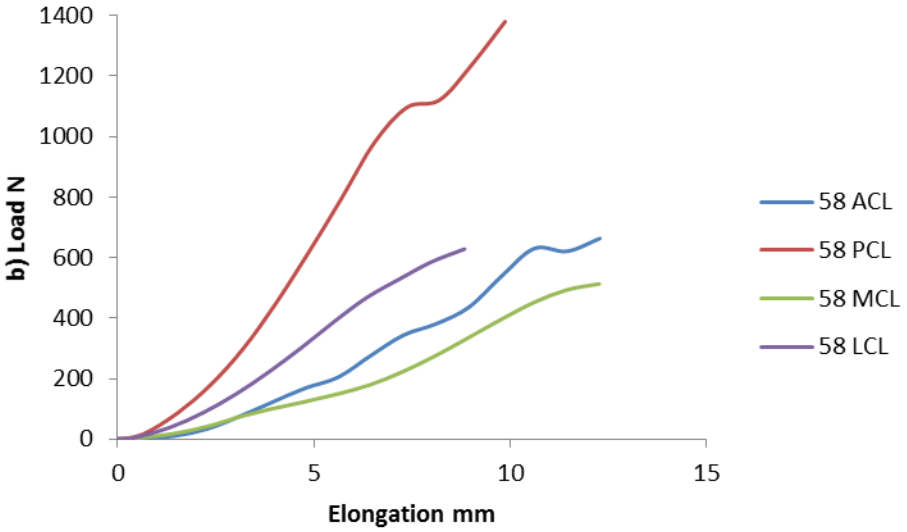
1400
1200
1000
800
600
400
200
0
b) Load N
0
5
10
15
Elongation mm
58 ACL
58 PCL
58 MCL
58 LCL

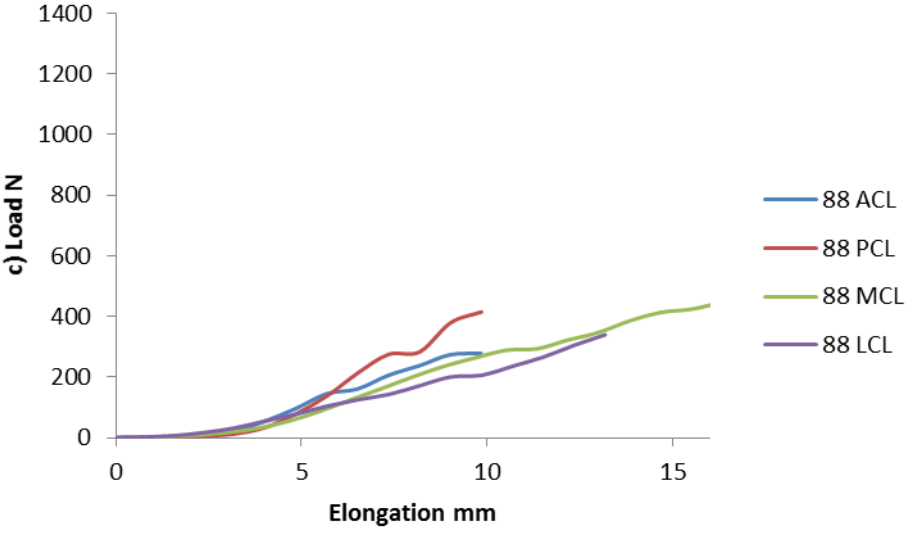
1400
1200
1000
800
600
400
200
0
c) Load N
0
5
10
15
Elongation mm
88 ACL
88 PCL
88 MCL
88 LCL

Figure 8. Example of load (N) against elongation (mm) in the anterior cruciate ligament (ACL), posterior cruciate ligament (PCL), medial collateral ligament (MCL) and lateral collateral ligament (LCL) in a) young healthy cadaver (31 years, grade 0) b) young osteoarthritis cadaver (58 years, grade 2) and c) old osteoarthritis cadaver (88 years, grade 3).

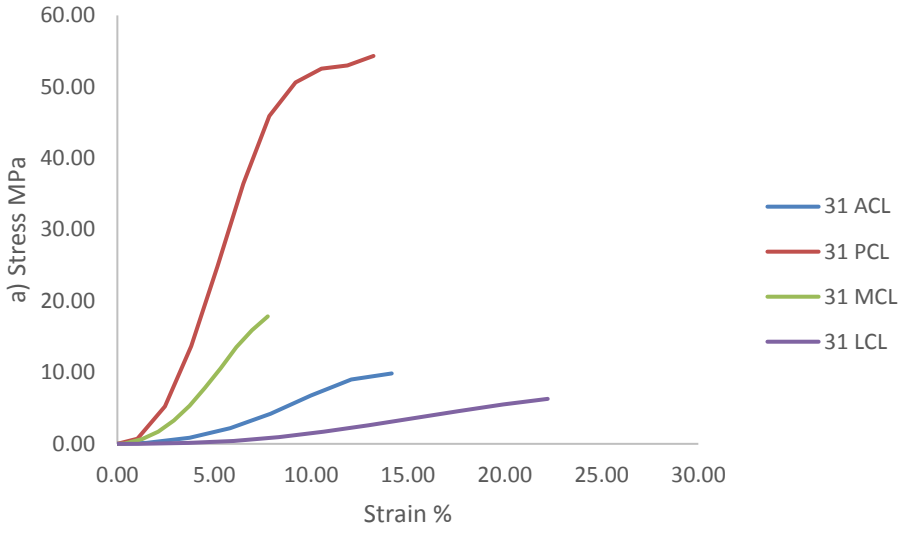
60.00
50.00
40.00
30.00
20.00
10.00
0.00
a) Stress MPa
0.00
5.00
10.00
15.00
20.00
25.00
30.00
Strain %
31 ACL
31 PCL
31 MCL
31 LCL

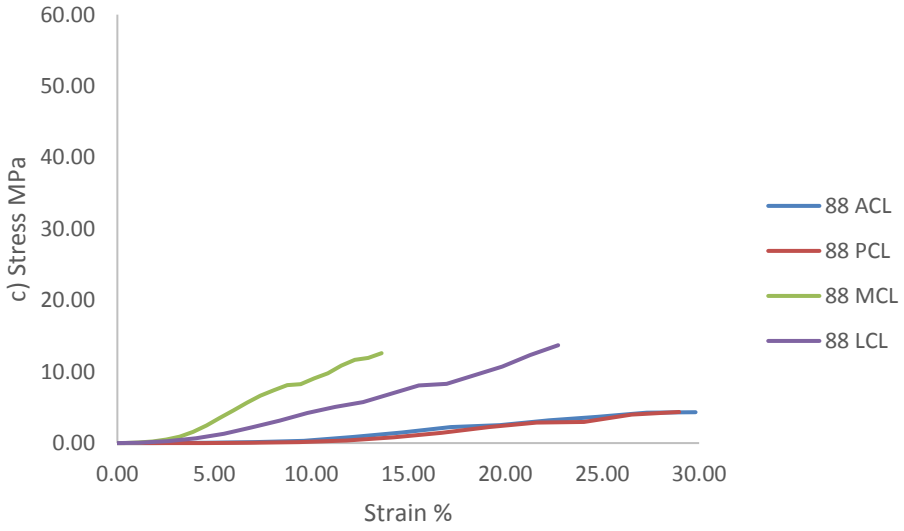
60.00
50.00
40.00
30.00
20.00
10.00
0.00
c) Stress MPa
0.00
5.00
10.00
15.00
20.00
25.00
30.00
Strain %
88 ACL
88 PCL
88 MCL
88 LCL

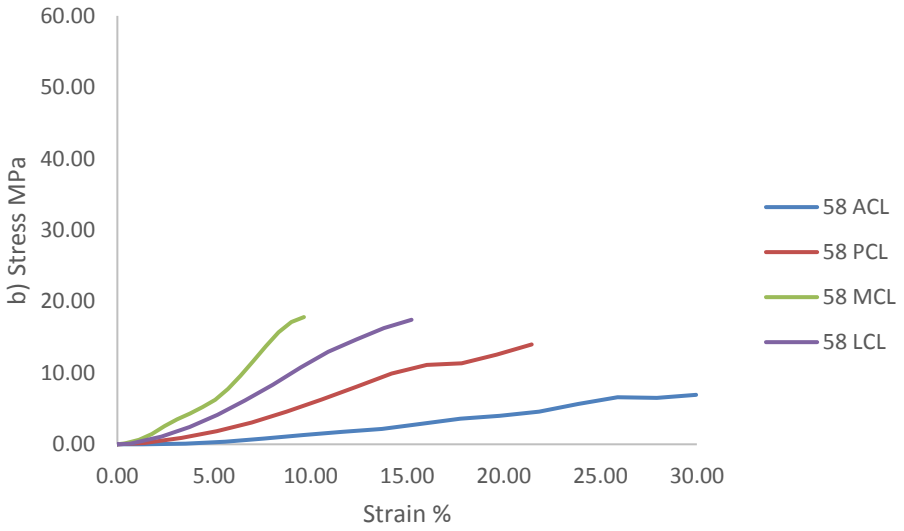
60.00
50.00
40.00
30.00
20.00
10.00
0.00
b) Stress MPa
0.00
5.00
10.00
15.00
20.00
25.00
30.00
Strain %
58 ACL
58 PCL
58 MCL
58 LCL

Figure 9. Example of stress (MPa) against strain (%) in the anterior cruciate ligament (ACL), posterior cruciate ligament (PCL), medial collateral ligament (MCL) and lateral collateral ligament (LCL) in a) young healthy cadaver (31 years, grade 0) b) young osteoarthritis cadaver (58 years, grade 2) and c) old osteoarthritis cadaver (88 years, grade 3).

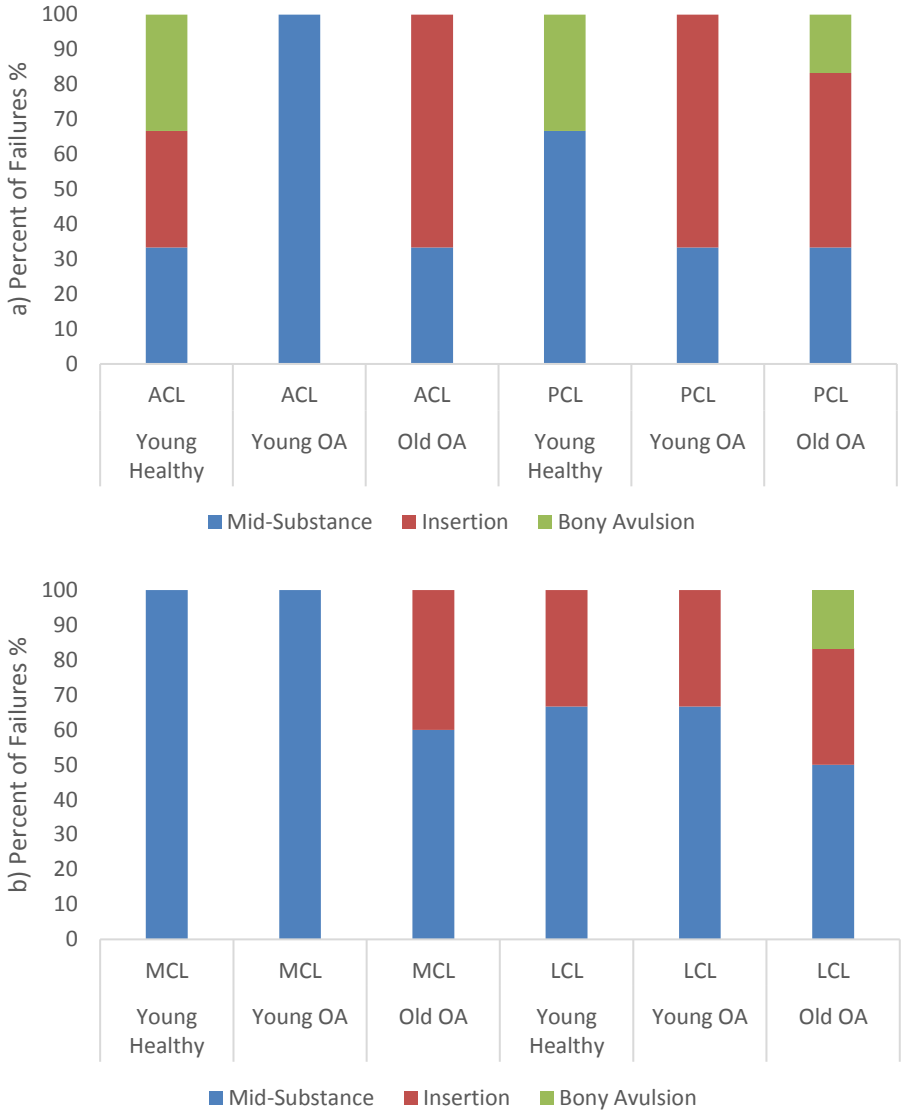

Figure 10. Failure site in percentage of young healthy (31-43 years, ICRS grade 0), young OA (49-58 years, ICRS grades 1-2) and old OA cadavers (72-88 years, ICRS grades 1-4) for a) anterior cruciate ligament (ACL), posterior cruciate ligament (PCL) and b) medial collateral ligament (MCL) and lateral collateral ligament LCL).

Within and Between Subject Correlations

Correlations between different ligaments within the same cadavers were analysed to determine if a change in material properties in one ligament could predict a change in material properties in another ligament from the same donor. A change in the PCL stiffness was significantly correlated with a change in the LCL stiffness (τb = 0.455, p = 0.04) and LCL tangent modulus (τb = 0.485, p = 0.028). All other parameters were not significant. Correlation with a change in material properties from the same ligament are presented in Table 3.

Table 3.Correlation of material property changes within the same ligament.

Ligament	Material Property	Kendall's τb	Significance (*p*)*
ACL	Tangent modulus : Failure Load	0.545	0.014*
	Tangent modulus : Stiffness	0.697	0.002*
	Failure load : Stiffness	0.727	0.001*
PCL	Tangent modulus : Failure Load	0.606	0.006*
	Tangent modulus : Stiffness	0.727	0.001*
	Failure load : Stiffness	0.697	0.002*
MCL	Tangent modulus : Failure Load	-0.022	0.929
	Tangent modulus : Stiffness	0.511	0.040*
	Failure load : Stiffness	-0.156	0.531
LCL	Tangent modulus : Failure Load	0.667	0.003*
	Tangent modulus : Stiffness	0.727	0.001*
	Failure load : Stiffness	0.576	0.009*

*significant at *p* = <0.005

Discussion

This study presents the first systematic quantification of the effects of ageing and OA on the material properties of the four primary knee ligaments from the same cadaveric joints within a wide span of age (31 – 88 years old) and OA grade (ICRS 0 – 4). This is crucial for

understanding joint mechanics and provides an insight into the initiation and progression of OA as a whole-joint disease as well as the effects of ageing.

Despite the small sample number, correlations and trends were seen between increasing age and numerous ACL and PCL material properties including linear force, linear stress, Young's modulus, tangent modulus, failure load, failure stress and stiffness. Fewer correlations were made between increasing age and MCL and LCL material properties. Failure loads previously reported across any age category span two orders of magnitude between 495 – 2160 N in the ACL [Noyes & Grood, 1976; Woo et al., 1991; Trent et al., 1976; Chandrashekar et al., 2006], 258 – 1620 N in the PCL [Harner et al., 1995; Race & Amis, 1994; Trent et al., 1976], 194 – 534 N in the MCL [Race & Amis, 1994; Trent et al., 1976] and 376 N in the LCL [Trent et al., 1976]. Furthermore, stiffness values range between 124 – 308 N/mm in the ACL [Noyes & Grood, 1976; Woo et al., 1991; Trent et al., 1976; Chandrashekar et al., 2006], 57 – 347 N/mm in the PCL [Harner et al., 1995; Race & Amis, 1994; Trent et al., 1976], 70 N/mm in the MCL [Trent et al., 1976] and 59 N/mm in the LCL [Trent et al., 1976], where values reported for failure load and stiffness in the current study fall within the previously reported range (Figs. 6 & 7, Tables 1 & 2).

Previous research has also indicated a decrease in the ACL failure load with increasing age, which is consistent with the current study (Fig. 6). Age based differences presented by Woo et al., [1991] show failure loads of up to 2160 N amongst younger donors (22 – 35 years), 1503 N in middle-aged donors (40 – 50 years) and 658 N amongst older donors (60 – 97 years), although any indication of degeneration of joint integrity was not stated or explored.

To the authors' knowledge this is the first study to correlate OA status to ligament material properties in humans (Fig. 7). The current research showed a decrease in the failure stress of all four ligaments with increasing grade of OA. Further, linear force showed a decreasing relationship with increasing grade of OA in the ACL and PCL. The ACL also showed decreasing trends with increasing grade of OA to linear stress and strain, Young's modulus and stiffness.

Currently, it is challenging to separate the effects OA and ageing as they often happen concurrently. In an attempt to separate the two variables and understand more their individual effects of ligament material properties, the cadavers were assigned to one of three cohorts; young healthy (31 – 43 years, ICRS grade 0), young OA (49 – 58 years, ICRS grade 1 – 2) or old OA (72 – 88 years, ICRS grade 1 – 4). Whilst material property analysis failed to reach statistical significance when comparing the means of the three cohorts (young healthy, young OA, and old OA) (Tables 1 & 2), which likely due to low samples numbers, population means show for the first time how ligaments interact and change across the entire joint in varying age and OA categories.

Although high overlapping standard deviations existed between groups, the results did suggest that ACL material properties most commonly decreased between the young healthy and young OA cohort. Interestingly failure load also decreased between young OA and old OA cohorts. These trends suggest that even mild OA in younger donors has an effect on material properties which is further exacerbated with ageing and advanced OA. It is currently controversial whether ligament injury initiates the onset of OA, or whether OA is indeed a whole-joint disease impairing the integrity of associated tissues including ligaments [Poole, 2012]; however the current research may suggest that the ligament injury or degeneration occurs in the primary instance.

Interestingly, the current results also show that the MCL material properties decline most between the young healthy and young OA cohorts similarly to the ACL, and that the failure load also decreased between young OA and old OA cohorts. The ACL and MCL are the most commonly injured ligaments, further supporting the argument that a ligament injury may subsequently lead to the initiation and progression of OA. PCL material properties most commonly decreased between the young OA and old OA cohorts, suggesting that changes to this ligament are more evident with advanced ageing and grade of OA. LCL material properties showed no clear trends between any cohort, suggesting they are largely unaffected by either ageing or OA.

The influence of OA has previously been investigated in animal models and suggested a reduction in tensile properties of the rat ACL 10 weeks after collagen induced arthritis. Ultimate failure load reduced by 25.1% and stiffness by 38.0% when compared to controls [Nawata et al., 2001]. Despite a lack of material properties in the literature associated to OA in humans, previous research has found that between 39 – 78% of patients with OA have a degenerated ACL [Mullaji et al., 2008; Allain et al,. 2001; Cushner et al., 2003; Lee et al., 2005; Watanabe et al., 2011], and between 7 – 80% have a degenerated PCL [Mullaji et al., 2008; Stubbs et al., 2005; Nelissen & Hogendoorn, 2001]. Such degeneration is consistent with the decline in material properties observed in the current study, particularly evident in the load-elongation and stress strain curves (Figs. 8 & 9). However, one study suggested 100% of PCLs were histologically normal in OA patients [Cushner et al., 2003], which is not consistent with the current results where PCL material properties largely change concurrently with those of the ACL, albeit with the older cohort with more advanced OA. (Figs. 6, 7, 8 & 9).

The reduction in numerous measured material properties of the ACL between the young healthy and young OA cohorts and some between the old OA cohorts (Figs. 6, 7, 8 & 9) may be attributed to the relatively high loading forces experienced during walking. Studies show a consensus that peak force experienced by the ACL occurs at contralateral toe off during the stance phase of the gait cycle, although high variation exists with values reported between 156 – 2350 N or the equivalent of 3.5 times body weight [Shelburne et al., 2004; Morrison, 1970; Collins & O'Connor, 1991]. In particular, these high ACL kinematic forces may be consistent with the widely reported histological degeneration of the ACL in the presence of disease [e.g. Mullaji et al., 2008], suggesting high habitual forces could influence subsequent degeneration observed. Peak force of the PCL has also been reported as 329 N or 0.2 – 0.6 times body weight during walking [Morrison, 1970; Collins & O'Connor, 1991], whilst the MCL and LCL are only 128N and 262N respectively [Morrison, 1970]. Decreased capacity of the ACL to resist motion due to reduced mechanical strength may alter mechanical forces of the knee joint, potentially causing increased loading on the medial femoral condyle and contributing to the preferential medial development of OA that is recognised in the literature [Pelletier et al., 2007; Lohmander et al., 2007].

Interestingly, in the current study, failure site appeared to occur in a mixed fashion in the ACL of all three cohorts, occurring at the mid substance, insertional portion and by bony avulsion, with no obvious trends. However in the PCL the young healthy cohorts failed more by the mid-substance, while the young OA and old OA cohorts failed more by the insertional portion. The MCL and LCL failed most by mid-substance in the younger cohorts and by either insertional portion or bony avulsion in the old OA cohort (Fig. 10). When ligaments fail by bony avulsion results may indicate the material properties of the insertional attachment or bone structure as opposed to the ligament mid-substance [Robinson et al., 2005]. Failure of the ligament at the mid-substance has been shown to

produce maximum loads of up to 74% higher than when failure occurs by bony avulsion [Robinson et al., 2005]. It must be noted that difficulties then arise in separating the mechanical behaviour of the bone from the ligament, and specifically understanding the true material properties of the insertional portion of the ligament compared to the mid-substance [Nigg & Herzog, 2006].

As expected the current analysis showed that there is a correlation between tangent modulus, failure load and stiffness from the same ligament, meaning as one material property changes, there is an expected change in other measured material properties. However, interestingly, this research showed that there was no correlation between changes in material properties from one ligament to a change in an articulating ligament from the same knee joint, meaning ligaments mechanical properties from the same donor are unrelated.

With only 12 cadavers and five groups of ICRS grades (0 – 4), it was challenging to statistically attribute changes in ligament material properties to specific cadaver cohorts. Whilst there were many moderate to significantly strong correlations of material property values to increasing age or increasing grade of OA as separate parameters, determining if these changes are due to age or OA where the donor is advanced in both is difficult as they often happen concurrently; however this research could at least separate younger donors by those that were healthy and those that had mild OA. This showed clear trends using the population mean over several material properties measured for the ACL and MCL between the young healthy and young OA cohorts, and for the PCL between young OA and old OA cohorts.

Further limitations of the current study aside from sample number included varying donor demographics such as gender, which is known to affect tensile properties and likelihood of knee ligament injury. Chandrashekar et al., [2006], found that young human female ACL had 22.49% lower Young's modulus, and 8.3% and 14.3% lower failure strain and stress respectively, when compared to young human male ACL. These differences can be partially attributed to the physically smaller size of the female ACL, which can in turn be linked to higher rates of ACL injuries in female athletes [Chandrashekar et al., 2005; Anderson et al., 2001]. Females are also known to be at a greater risk of knee OA than males [Hame & Alexander, 2013]. Again due to low sample numbers, this study was unable to separate ligaments by gender for statistical analyses, although high standard deviations may be apparent due to differences in cadaver demographics.

Finally, the current study may be limited by testing ligaments as whole bone-ligament-bone specimens along their loading axis. It has previously been acknowledged that ligaments may be best divided into their fibre bundles in order to recruit fibres to their maximal potential and eliminate any slack due to orientation [Woo et al., 1991; Race & Amis, 1994]. Significant differences have been reported between the anterior and posterior fibres of the ACL [Butler et al., 1992] and PCL [Harner et al., 1995; Race & Amis, 1994] suggesting that fibres play different roles in the stabilisation of the knee joint [Race & Amis, 1994]; although ligaments naturally work as one functional unit.

Such global approaches have previously been used in the representation of ligaments in FE models as one functional unit. However, due to the lack of data on all four ligaments from the same donor (and in certain cases the same demographic or disease conditions of donor) in the literature, material properties have often been applied globally in FE models, where values for one ligament are replicated for all others [Wang et al., 2014; Kazemi & Li,

2014; Li et al., 2001; Blankevoort & Huiskes, 1991]. In some instances tendon material properties have been used [Wang et al., 2014; Kazemi & Li, 2014; Kazemi et al., 2011]. A sensitivity analysis was carried out by Dhaher et al., [2010] to understand how changes in intrinsic ligament material properties that may be apparent due to age, gender, species and activity levels, affect the functional capabilities of the knee joint. Results showed varying material properties caused changes to internal and external rotation of the tibia-femoral joint, patella tilt and patella peak contact stress. Such analysis explicitly shows that modelling ligaments with a biologically inaccurate representation can cause wide spread erroneousness in the prediction of mechanical behaviour. As such, the data in this study allows future research to apply a more subject- or cohort-specific approach to computational modelling of the human knee joint to improve accuracy and predictive behaviour patterns of ligaments.

Further, the knowledge of baseline material properties of all four ligaments from healthy donors can be used to replicate ligaments by developing more biologically accurate synthetic materials for the repair and replacement following injury or degeneration [Ratcliffe et al., 2015; Yang et al., 2013]. Both tensile and failure mechanics are used during the development of such materials where the synthetic material should have strength properties that exceed the peak loads experienced *in vivo*, and stretch properties that do not allow the strain to go above the *in vivo* toe region [Ratcliffe et al., 2015]. The data collected herein allows an insight into not only the healthy range for these parameters but also how they change concurrently with surrounding ligaments during ageing and disease.

Conclusion

This research is the first to correlate material property alterations in the human knee joint across all four primary ligaments during ageing and disease presence. This research has confirmed the findings of previous research that the ACL tensile and failure properties decline with age, and also provided new evidence that the PCL tensile and failure properties decline with increasing age. Further, population means differed most apparently between young healthy and young OA ACL material properties and young OA and old OA PCL material properties, suggesting that ageing and arthritic changes occur in the ACL first. These changes in the ACL in the presence of disease are also consistent with kinematic data of gait loading. Interestingly the MCL and LCL showed some changes with increasing age and OA grade, which has not previously been demonstrated. This also supports current research stating that OA is a whole joint disease affecting many peri-articular tissues within the knee. Such valuable data may now be applied in future applications including the development of biomaterials, FE analysis and OA diagnostics.

References

1. Adouni, M., Shirazi-Adl, A. & Shirazi, R. 2012, "Computational biodynamics of human knee joint in gait: from muscle forces to cartilage stresses", *Journal of Biomechanics,* vol. 45, no. 12, pp. 2149-2156.
2. Allain, J., Goutallier, D. & Voisin, M.C. 2001, "Macroscopic and histological assessments of the cruciate ligaments in arthrosis of the knee", *Acta Orthopaedica Scandinavica,* vol. 72, no. 3, pp. 266-269.
3. Anderson, A.F., Dome, D.C., Gautam, S., Awh, M.H. & Rennirt, G.W. 2001, "Correlation of anthropometric measurements, strength, anterior cruciate ligament size, and intercondylar notch characteristics to sex differences in anterior cruciate ligament tear rates", *The American Journal of Sports Medicine,* vol. 29, no. 1, pp. 58-66.
4. Blankevoort, L. & Huiskes, R. 1991, "Ligament-bone interaction in a three-dimensional model of the knee", *Journal of Biomechanical Engineering,* vol. 113, no. 3, pp. 263-269.
5. Bonner, T.J., Newell, N., Karunaratne, A., Pullen, A.D., Amis, A.A., Bull, A.M. & Masouros, S.D. 2015, "Strain-rate sensitivity of the lateral collateral ligament of the knee", *Journal of the Mechanical Behavior of Biomedical Materials,* vol. 41, pp. 261-270.
6. Butler, D.L., Guan, Y., Kay, M.D., Cummings, J.F., Feder, S.M. & Levy, M.S. 1992, "Location-dependent variations in the material properties of the anterior cruciate ligament", *Journal of Biomechanics,* vol. 25, no. 5, pp. 511-518.
7. Chandrashekar, N., Mansouri, H., Slauterbeck, J. & Hashemi, J. 2006, "Sex-based differences in the tensile properties of the human anterior cruciate ligament", *Journal of Biomechanics,* vol. 39, no. 16, pp. 2943-2950.

8. Chandrashekar, N., Slauterbeck, J. & Hashemi, J. 2005, "Sex-based differences in the anthropometric characteristics of the anterior cruciate ligament and its relation to intercondylar notch geometry: a cadaveric study", *The American Journal of Sports Medicine,* vol. 33, no. 10, pp. 1492-1498.
9. Collins, J.J. & O'Connor, J.J. 1991, "Muscle-ligament interactions at the knee during walking", *Proceedings of the Institution of Mechanical Engineers. Part H, Journal of engineering in medicine,* vol. 205, no. 1, pp. 11-18.
10. Cushner, F.D., La Rosa, D.F., Vigorita, V.J., Scuderi, G.R., Scott, W.N. & Insall, J.N. 2003, "A quantitative histologic comparison: ACL degeneration in the osteoarthritic knee", *The Journal of Arthroplasty,* vol. 18, no. 6, pp. 687-692.
11. Dhaher, Y.Y., Kwon, T. & Barry, M. 2010, "The effect of connective tissue material uncertainties on knee joint mechanics under isolated loading conditions", *Journal of Biomechanics,* vol. 43, no. 16, pp. 3118-3125.
12. Freutel, M., Schmidt, H., Dürselen, L., Ignatius, A. & Galbusera, F. 2014, "Finite element modeling of soft tissues: Material models, tissue interaction and challenges", *Clinical Biomechanics,* vol. 29, no. 4, pp. 363-372.
13. Goodship, A.E. & Birch, H.L. 2005, "Cross sectional area measurement of tendon and ligament *in vitro*: a simple, rapid, non-destructive technique", *Journal of Biomechanics,* vol. 38, no. 3, pp. 605-608.
14. Guo, H., Maher, S.A. & Spilker, R.L. 2013, "Biphasic finite element contact analysis of the knee joint using an augmented Lagrangian method", *Medical Engineering & Physics,* vol. 35, no. 9, pp. 1313-1320.
15. Hame, S.L. & Alexander, R.A. 2013, "Knee osteoarthritis in women", *Current Reviews in Musculoskeletal Medicine,* vol. 6, no. 2, pp. 182-187.
16. Hansen, U., Masouros, S. & Amis, A.A. 2006, "(iii) Material properties of biological tissues related to joint surgery", *Current Orthopaedics,* vol. 20, no. 1, pp. 16-22.

17. Harner, C.D., Xerogeanes, J.W., Livesay, G.A., Carlin, G.J., Smith, B.A., Kusayama, T., Kashiwaguchi, S. & Woo, S.L. 1995, "The human posterior cruciate ligament complex: an interdisciplinary study. Ligament morphology and biomechanical evaluation", *The American Journal of Sports Medicine,* vol. 23, no. 6, pp. 736-745.
18. Hasegawa, A., Otsuki, S., Pauli, C., Miyaki, S., Patil, S., Steklov, N., Kinoshita, M., Koziol, J., D'Lima, D.D. & Lotz, M.K. 2012, "Anterior cruciate ligament changes in the human knee joint in aging and osteoarthritis", *Arthritis & Rheumatism,* vol. 64, no. 3, pp. 696-704.
19. Huang, H., Zhang, J., Sun, K., Zhang, X. & Tian, S. 2011, "Effects of repetitive multiple freeze–thaw cycles on the biomechanical properties of human flexor digitorum superficialis and flexor pollicis longus tendons", *Clinical Biomechanics,* vol. 26, no. 4, pp. 419-423.
20. Jung, H., Vangipuram, G., Fisher, M.B., Yang, G., Hsu, S., Bianchi, J., Ronholdt, C. & Woo, S.L. 2011, "The effects of multiple freeze–thaw cycles on the biomechanical properties of the human bone-patellar tendon-bone allograft", *Journal of Orthopaedic Research,* vol. 29, no. 8, pp. 1193-1198.
21. Kazemi, M. & Li, L. 2014, "A viscoelastic poromechanical model of the knee joint in large compression", *Medical Engineering & Physics,* vol. 36, no. 8, pp. 998-1006.
22. Kazemi, M., Li, L., Savard, P. & Buschmann, M. 2011, "Creep behavior of the intact and meniscectomy knee joints", *Journal of the Mechanical Behavior of Biomedical Materials,* vol. 4, no. 7, pp. 1351-1358.
23. Kumar, D., Manal, K.T. & Rudolph, K.S. 2013, "Knee joint loading during gait in healthy controls and individuals with knee osteoarthritis", *Osteoarthritis and Cartilage,* vol. 21, no. 2, pp. 298-305.
24. Lee, G., Cushner, F.D., Vigoritta, V., Scuderi, G.R., Insall, J.N. & Scott, W.N. 2005, "Evaluation of the anterior cruciate ligament integrity and degenerative arthritic

patterns in patients undergoing total knee arthroplasty", *The Journal of Arthroplasty,* vol. 20, no. 1, pp. 59-65.

25. Li, G., Lopez, O. & Rubash, H. 2001, "Variability of a three-dimensional finite element model constructed using magnetic resonance images of a knee for joint contact stress analysis", *Journal of Biomechanical Engineering,* vol. 123, no. 4, pp. 341-346.
26. Lohmander, L.S., Englund, P.M., Dahl, L.L. & Roos, E.M. 2007, "The long-term consequence of anterior cruciate ligament and meniscus injuries: osteoarthritis", *The American Journal of Sports Medicine,* vol. 35, no. 10, pp. 1756-1769.
27. Manninen, P., Riihimaki, H., Heliovaara, M. & Makela, P. 1996, "Overweight, gender and knee osteoarthritis", *International Journal of Obesity and Related Metabolic Disorders : Journal of the International Association for the Study of Obesity,* vol. 20, no. 6, pp. 595-597.
28. Momersteeg, T., Blankevoort, L., Huiskes, R., Kooloos, J., Kauer, J. & Hendriks, J. 1995, "The effect of variable relative insertion orientation of human knee bone-ligament-bone complexes on the tensile stiffness", *Journal of Biomechanics,* vol. 28, no. 6, pp. 745-752.
29. Moon, D.K., Woo, S.L., Takakura, Y., Gabriel, M.T. & Abramowitch, S.D. 2006, "The effects of refreezing on the viscoelastic and tensile properties of ligaments", *Journal of Biomechanics,* vol. 39, no. 6, pp. 1153-1157.
30. Morrison, J. 1970, "The mechanics of the knee joint in relation to normal walking", *Journal of Biomechanics,* vol. 3, no. 1, pp. 51-61.
31. Mullaji, A.B., Marawar, S.V., Simha, M. & Jindal, G. 2008, "Cruciate ligaments in arthritic knees: a histologic study with radiologic correlation", *The Journal of Arthroplasty,* vol. 23, no. 4, pp. 567-572.

32. Nawata, K., Enokida, M., Yamasaki, D., Minamizaki, T., Hagino, H., Morio, Y. & Teshima, R. 2001, "Tensile properties of rat anterior cruciate ligament in collagen induced arthritis", *Annals of the Rheumatic Diseases,* vol. 60, no. 4, pp. 395-398.
33. Nelissen, R.G. & Hogendoorn, P.C. 2001, "Retain or sacrifice the posterior cruciate ligament in total knee arthroplasty? A histopathological study of the cruciate ligament in osteoarthritic and rheumatoid disease", *Journal of Clinical Pathology,* vol. 54, no. 5, pp. 381-384.
34. Nigg, B. & Herzog, W. (eds) 2006, *Biomechanics of the Musculoskeletal System*, 3rd edn, Wiley, West Sussex.
35. Noyes, F.R. & Grood, E.S. 1976, "The strength of the anterior cruciate ligament in humans and Rhesus monkeys", *The Journal of Bone and Joint Surgery. American Volume,* vol. 58, no. 8, pp. 1074-1082.
36. Pelletier, J., Raynauld, J., Berthiaume, M., Abram, F., Choquette, D., Haraoui, B., Beary, J.F., Cline, G.A., Meyer, J.M. & Martel-Pelletier, J. 2007, "Risk factors associated with the loss of cartilage volume on weight-bearing areas in knee osteoarthritis patients assessed by quantitative magnetic resonance imaging: a longitudinal study", *Arthritis Research & Therapy,* vol. 9, no. 4, pp. R74.
37. Poole, A.R. 2012, "Osteoarthritis as a whole joint disease", *HSS Journal,* vol. 8, no. 1, pp. 4-6.
38. Race, A. & Amis, A.A. 1994, "The mechanical properties of the two bundles of the human posterior cruciate ligament", *Journal of Biomechanics,* vol. 27, no. 1, pp. 13-24.
39. Ratcliffe, A., Butler, D.L., Dyment, N.A., Cagle, P.J., Proctor, C.S., Ratcliffe, S.S. & Flatow, E.L. 2015, "Scaffolds for tendon and ligament repair and regeneration", *Annals of Biomedical Engineering,* vol. 43, no. 3, pp. 819-831.

40. Robinson, J.R., Bull, A.M. & Amis, A.A. 2005, "Structural properties of the medial collateral ligament complex of the human knee", *Journal of Biomechanics,* vol. 38, no. 5, pp. 1067-1074.
41. Rousseau, J.C. & Garnero, P. 2012, "Biological markers in osteoarthritis", *Bone,* vol. 51, no. 2, pp. 265-277.
42. Schneider, C.A., Rasband, W.S. & Eliceiri, K.W. 2012, "NIH Image to ImageJ: 25 years of image analysis", *Nature Methods,* vol. 9, no. 7, pp. 671.
43. Shelburne, K.B., Pandy, M.G., Anderson, F.C. & Torry, M.R. 2004, "Pattern of anterior cruciate ligament force in normal walking", *Journal of Biomechanics,* vol. 37, no. 6, pp. 797-805.
44. Stubbs, G., Dahlstrom, J., Papantoniou, P. & Cherian, M. 2005, "Correlation between macroscopic changes of arthrosis and the posterior cruciate ligament histology in the osteoarthritic knee", *ANZ Journal of Surgery,* vol. 75, no. 12, pp. 1036-1040.
45. Trent, P.S., Walker, P.S. & Wolf, B. 1976, "Ligament length patterns, strength, and rotational axes of the knee joint", *Clinical Orthopaedics and Related Research,* vol. 117, pp. 263-270.
46. Wang, Y., Fan, Y. & Zhang, M. 2014, "Comparison of stress on knee cartilage during kneeling and standing using finite element models", *Medical Engineering & Physics,* vol. 36, no. 4, pp. 439-447.
47. Watanabe, A., Kanamori, A., Ikeda, K. & Ochiai, N. 2011, "Histological evaluation and comparison of the anteromedial and posterolateral bundle of the human anterior cruciate ligament of the osteoarthritic knee joint", *The Knee,* vol. 18, no. 1, pp. 47-50.

48. Woo, S.L., Abramowitch, S.D., Kilger, R. & Liang, R. 2006, "Biomechanics of knee ligaments: injury, healing, and repair", *Journal of Biomechanics,* vol. 39, no. 1, pp. 1-20.
49. Woo, S.L., Hollis, J.M., Adams, D.J., Lyon, R.M. & Takai, S. 1991, "Tensile properties of the human femur-anterior cruciate ligament-tibia complex. The effects of specimen age and orientation", *The American Journal of Sports Medicine,* vol. 19, no. 3, pp. 217-225.
50. Woo, S.L., Orlando, C.A., Camp, J.F. & Akeson, W.H. 1986, "Effects of postmortem storage by freezing on ligament tensile behavior", *Journal of Biomechanics,* vol. 19, no. 5, pp. 399-404.
51. Yang, G., Rothrauff, B.B. & Tuan, R.S. 2013, "Tendon and ligament regeneration and repair: clinical relevance and developmental paradigm", *Birth Defects Research Part C: Embryo Today: Reviews,* vol. 99, no. 3, pp. 203-222.

Section Three – Synthesis and Conclusions

Chapter Six: Discussion

Overview and Evaluation of Chapters Two to Five

This thesis first presents a systematic review of current research efforts in obtaining human knee joint tissue material properties and subsequent representation via finite element (FE) modelling. Following this, the effect of multiple freeze-thaw cycles on canine articular cartilage material properties is researched. Finally, over two chapters, material properties of human knee joint cartilage, subchondral bone, trabecular bone and the four primary knee joint ligaments are researched from twelve cadavers with varying donor demographics including age and osteoarthritis (OA) status.

Chapter Two of this thesis firstly comprehensively reviews the current state of affairs in the literature with regard to explorations into existing material property data for soft and hard tissues of the human knee joint, with an aim to present resultant data in tabulated form. Secondly, this chapter reviews current efforts to model the whole human knee joint using FE analyses, with a specific focus on original sourcing and representation of material property data. This review highlighted the wide variation in reported material property values across cartilage, bone and ligaments of the human knee with a lack of any cohort- or subject- specific representation. Consistency across studies is mostly non-existent with variations in tissue locality, donor demographics, storage and preservation techniques and testing methods. Subsequently, this has led to highly variable and in some cases questionable representation of material properties in whole joint FE models of the human knee. Notably, FE models have often relied on both non-human and human data from varying anatomical localities to gain input values for knee tissue material properties. However, it has now been established that animal material properties may not be

representative of human material properties [Demarteau et al., 2006; Jeffrey & Aspden, 2006; Nissi et al., 2007; Pedersen et al., 2013; Plumb & Aspden, 2005]. Further, upon critical evaluation, this review goes on to highlight the gap in the knowledge to be able to present specific cohorts with accurate human material property data, and in particular young healthy, or aged and/or diseased human knee joints.

This review highlighted not only the need for a subject- or cohort-specific approach but also a consideration for spatial heterogeneity in samples. Heterogeneity was found in previous research, showing higher medial femoral condyle cartilage elastic modulus when compared to lateral [Hvid & Hansen, 1985], as well as differences in superiorly and inferiorly located femoral condyle trabecular bone elastic modulus [Burgers et al., 2008]. Evidently, representing such structures requires a more heterogeneous local approach where interchangeable material properties can be site-specific.

To the authors' knowledge, no such tabulation of data exists to be able to compare multiple material properties and FE studies and present the gaps in the literature in one place. However, Chapter Two is indeed limited by only reviewing whole knee joint models. Justification for this is based around OA now being inherently known as a whole-joint disease [Mahjoub et al., 2012], therefore the review focused on current efforts to present whole-joints only. Evidently, some FE research studies present just one tissue and focus computational efforts into presenting the complexity and biological reality of the primary concerned tissue [e.g. Tanska et al., 2015; Dabiri & Li, 2013]. For example, material properties of soft tissues would traditionally be modelled with linear isotropy, assuming elastic behaviour [e.g. Blankevoort et al., 1991]; however in more recent years it has become well established that cartilage and ligaments have non-linear anisotropic viscoelastic properties that should be tested and subsequently presented in FE models in a

more complex manner. This review is limited in that it focuses only on whole-joint FE models regardless of the computational approach they have used to present such soft tissues. Whilst this included the representation of cartilage and ligaments as both elastic and viscoelastic structures, several advances in representation were not discussed at length as they did not present whole-joints, but rather focused the computational effort and time on the primary tissue surrounding the research hypothesis [e.g. Tanska et al., 2015; Dabiri & Li, 2013]. However it should be noted that these studies did not address the primary question comparing healthy young cohorts to for example old OA cohorts.

Inaccurate or sub-optimal biological predictions should be expected in FE models when abstract or non-representative material properties are used; however with more accurate subject-specific material properties the error margin can be reduced whilst enhancing knowledge of the mechanical behaviour of such structures. Hence forth, and on conclusion of this review, a model with subject- or cohort-specific material properties would be highly advantageous in order to eliminate widespread inaccuracy, potentially arising from distinctively diverse animal or human cadavers, or different testing techniques or equipment as presented in Chapter Two.

Chapter Three of this thesis aimed to explore the effect of multiple freeze-thaw cycles on the material properties of canine articular cartilage in an attempt to understand how experimental studies (particularly those that aim to test multiple tissues from the same donor(s)) are logistically limited with regards to storage and preservation of samples. This study demonstrated that articular cartilage can undergo up to three freeze-thaw cycles without statistically compromising the integrity of the tissue with altered material properties at the whole-joint level. To the authors' knowledge this is the first study to examine such changes beyond one freezing cycle. The literature does present research that

explored freezing effects of cartilage in both -20 and -80 °C compared to fresh samples [Szarko et al., 2010], which although presented no change in material properties, research was limited to the application of one freeze-thaw cycle only. Additional research in the literature also supports the use of up to one freeze-thaw cycle as a storage and preservation technique for cartilage [Moore & Burris, 2015].

Interestingly, results of this study were expected to show more consistency between samples across the different freezing cycles; however the results subsequently produced wide variability in the mean shear storage modulus, shear loss modulus, elastic modulus and the loss factor values across samples in the same cycle of freezing, and moreover across different cycles of freezing. A definite increasing or decreasing trend in material properties was not apparent and therefore contributed towards the results failing to reach statistical significance, which would indicate a systematic change in material properties across freezing cycles. The likely explanation of this is due to natural variability which is recognised in biological samples across the literature [e.g. Jurvelin et al., 2010], in addition to some of the limitations acknowledged below. Although it should also be recognised that the reported values in Chapter Three fall within previously reported modulus values for other mammalian femoral condyle articular cartilage [e.g. Shepherd & Seedhom, 1999; Wilusz et al., 2013; Moore & Burris, 2015].

This study has a number of possible limitations as discussed in Chapter Three. Firstly, a relatively low number of samples were tested (n = 11). Logistically, testing an increased sample number is challenging particularly when samples are obtained from the same cadaver; however in future studies this could help eliminate any inconsistencies in material properties across freezing cycles. Secondly, as discussed in detail in Chapter Three, indentation measurements may overlap in subsequent cycle of freezing, although this has

been addressed previously showing that nanoindentation causes no visible deformation to samples [Franke et al., 2011]. Finally, results do not enable the understanding of changes to cartilage structure that could be determined through different testing and analyses techniques such as histological staining. Although outside the logistical scope of the current research, such analyses accompanied by material property data could help determine reasons for high biological variability (i.e. differentiation between extracellular matrix and cellular material).

This variability seen also makes it challenging to generalize the results in relation to other research, and as discussed previously, results of this study and subsequent application in the future should be undertaken with caution. Practically, the results mean that cartilage can undergo three freeze-thaw cycles without a statistical change to material properties when averaged across the whole-joint; however such changes in magnitude may need to be interpreted with caution when applying to, for example, computational modeling of such structures where it has previously been shown that subtle changes can alter joint behavior in response to mechanical stresses and strains [Li et al., 2001]. Further, it is recommended that if multiple tissues types are to be tested, that cartilage samples be prioritized to eliminate the need for multiple freezing cycles where possible. Proven storage techniques currently exist for both bone and ligament samples, concluding that bone can be stored in a 70% ethanol solution to preserve its physiological state [Linde & Sorensen, 1993] and ligaments can undergo a minimum of two freeze-thaw cycles before tissue integrity is compromised [Moon et al., 2006], further supporting the recommendation to test cartilage as a priority if obtaining multiple tissue types together. This qualitative result guided the experimental protocol used in Chapters Four and Five, in which testing of cartilage samples was priortised over bone and ligament samples from the same donors. As a result, all cartilage samples underwent only one freeze-thaw cycle, while

all ligament samples underwent two freeze-thaw cycles, as indicated to be appropriate previously in the literature [e.g. Moon et al., 2006].

Chapter Four of this thesis aimed to collate spatially distributed material properties of articular cartilage, subchondral bone and trabecular bone from human cadaver knee joints of varying demographics including age and disease status. Material property analyses focused on shear storage and loss modulus for articular cartilage and elastic modulus for subchondral and trabecular bone, obtained using dynamic and quasi-static nanoindentation techniques respectively.

Results of the study showed for the first time a statistically significant decrease in articular cartilage shear storage and loss modulus and an increase in subchondral bone elastic modulus with both increasing age and increasing grade of OA. Interestingly, the results showed no statistically significant trend or change in trabecular bone elastic modulus associated with age or OA grade. Further, the results show that a change in articular cartilage shear storage and loss modulus was significantly correlated with a change in subchondral bone elastic modulus in site-matched samples. The development of OA also showed preferential regional development in the medial knee compartment, which is correlated with a decrease in articular cartilage shear storage modulus.

The current study is consistent with previous research reporting a decline in cartilage shear storage modulus with increasing grade of OA with similar reported values [e.g. Kleemann et al., 2005; Wilusz et al., 2013]; however to the authors' knowledge no study exists specifically outlining age related changes in articular cartilage modulus. Therefore the current research is the first to present age-related trends alongside influential changes indicative of OA status for both cartilage shear storage and loss modulus. Subchondral and

trabecular bone elastic modulus values reported within the current research are lower than those reported in the literature, potentially evident due to variations in donor demographics and testing techniques. Despite this, prior to the data presented here, no studies have presented material properties of subchondral or trabecular bone in both a wide span of age or OA grades with comparison to healthy controls. Further, no studies have tested both the cartilage, subchondral and trabecular bone from the same donor, or from multiple sites from the same donor. The gap in the knowledge prior to the current research is extremely vast, thereby providing ample evidence of the importance of such advances in knowledge. Unexpectedly, trabecular bone elastic modulus was not significantly correlated with any parameters measured and specifically to age and OA. Previous research has been consistent in reporting a synergistic relationship between cartilage and bone in the presence of OA, and in particular found changes in quantity, separation and density of trabecular bone [Kamibayashi et al., 1995; Bobinac et al., 2003]. The current results indicate that trabecular bone material properties remain unchanged despite structural changes previously observed with OA.

Knowledge of such data has correlated well with previous research showing that OA has preferential regional development in the medial knee compartment [Pelletier et al., 2007]. Whilst this is well established through magnetic resonance imaging diagnosis and through altered kinematics during habitual locomotion [Kumar et al., 2013], this study is the first to explore differences in material properties from medial versus lateral samples, both from tibial and femoral localities, and additionally across ageing and varying OA grades. Spatial heterogeneity of material properties causes functional differences in tissue behaviour which has previously been presented in FE modelling [Mononen et al., 2011].

It should be noted that there were high levels of variability within and between donor cartilage and bone material properties, even within those that were young and healthy. In donors with advancing age and OA grade the variations can be attributed to these factors as well as prolonged high repetitive mechanical loading during advancing age, particularly on weight bearing sites in the knee joint, i.e. the medial femoral condyle, which was seen to have lower cartilage modulus values and higher bone modulus values. However in young healthy donors with no sign of fibrillation or wear, but where high variation still existed, it is challenging to understand whether changes in values may indicate early onset of disease or whether simply topographical variation exists within normal biological tissue.

Cartilage is heterogeneous in nature, and in particular the extracellular matrix will have varying material properties determined by its composition, structure and vascularity which has previously been evidenced in the same specimen at different localities [Moore & Burris, 2015]. Lyyra et al., [1999] conducted *in vivo* indentation on 20 healthy knee joints during arthroplasty procedures at 8 different sites, as per the current thesis. The research found up to 29% variation in values reported from the same subject; however this is significantly less than the relative difference of up to 461.2% found between measurements in the current thesis in young healthy donors, or an absolute difference of 1.77 MPa (range 0.49 – 2.26 MPa) (see Supplementary Material, Chapter Nine). Interestingly, variation in an older donor with up to ICRS grade 4 OA also had high variability with a relative difference of 4,800.0% and absolute difference of 1.41 MPa (range 0.03 – 1.44 MPa) (see Supplementary Material, Chapter Nine), suggesting that such variation is evident independent of age or disease status. Within subject variability is not uncommon and variations in cartilage material properties reflect functional requirements in the local region [Lyyra et al., 1999] having been shown to have high topographical variability. As cartilage tissue begins to age and potentially be at risk of OA, greater variability in material properties would be

expected. The current data suggests that topographical variation may be site specific and local approaches to future applications using material properties are more bio-realistic.

High variability also existed across both subchondral and trabecular bone samples. Relative variations of up to 153.2% and absolute differences of 4.8 GPa (range 9.02 – 13.82 GPa) existed for subchondral bone samples in younger donors and up to 1540% or 5.85 GPa (range 10.84 – 16.69 GPa) in older donors with up to ICRS grade 3 OA. For trabecular bone relative differences of up to 228.5% and absolute differences of 9.29 GPa (range 7.23 – 16.52 GPa) existed for young healthy donors and up to 239.3% or 9.35 GPa (range 6.71 – 16.06 GPa) in older donors with up to ICRS grade 3 OA (see Supplementary Material, Chapter Nine). As with cartilage these variations can be attributed to spatial locality, as well as the geometry and density of the bone [Zysset et al., 1999]. Additionally, increased heterogeneity in bone structure is more evident in a length scale under 200nm [Yao et al., 2011], therefore this may contribute to some of the variation seen in the current thesis for both subchondral and trabecular bone.

This study has a number of possible limitations. The current research utilises twelve human cadaver knee joints. Whilst it is possible to define inclusion and exclusion criteria, such as age range, gender and body mass index (BMI), it was not possible to request further medical history of the cadaver such as, for example, musculoskeletal health status of the knee. Nine cadavers had a healthy BMI according to the World Health Organisation categories (18 – 25), whilst one young cadaver with OA ICRS grade 0 had a low BMI (15.81), one young cadaver with OA ICRS grade 0 had a high BMI (31.00), and one young cadaver with OA ICRS grade 1 had a high BMI (31.19). Obesity is a known indicator for OA [Manninen et al., 1996]; however weight and obesity were not considered throughout this research. Additionally, no musculoskeletal medical history or physical activity levels were

available for the cadavers, which could have influenced resultant material properties if, for example, one cadaver had a previous ligament injury, or experienced high levels of continuous impact loading through a sport such as running.

Another limitation included not being able to obtain cortical bone material properties for two cadavers (aged 31 and 49 years), as a technical error occurred due to over polishing sample, meaning the surface area could not be tested. This error meant that data for cortical bone material properties was only available for ten cadavers, and it is uncertain to what extent the additional data may have influenced resultant data and statistics. However there is no reason to doubt that these measurements would be different from the rest of the cohort i.e. no visual differences or deformities.

Despite the limitations listed above these results are of direct practical relevance to a variety of clinical and research applications. It has previously been suggested that therapies used to treat OA, for example physical therapy, pharmaceutical interventions, or surgery involving biomimetic materials may be advanced and altered upon a more conclusive understanding of the role of the subchondral bone in the initiation and progression of OA [Wen et al., 2014]. With the current data in mind, physical therapy may alter regional loading mechanics in an attempt to reduce bone turnover as stiffened subchondral bone is statistically correlated with a decrease in cartilage stiffness. Pharmaceutical interventions have previously been applied to experimental models in animals, introducing the bisphosphonate alendronate to reduce cartilage degeneration [Hayami et al., 2004]. Such early explorations may be used in coordination with the current research to target regional areas for therapeutics and further the understanding of the role of subchondral bone in cartilage degeneration. Additionally, the current data may be applied in future research involving the application of biomimetic materials. These are used to replace and repair

tissue structures and would benefit from mimicking cohort- or subject-specific material properties that will more accurately present biological reality [Li et al., 2016; Wang et al., 2012].

Future research should aim to use the presented material property data for subject- or cohort-specific computational representation of joint behavior predictions. As presented in Chapter Two of this thesis, there are vast gaps in the knowledge with regard to human tissue material properties in healthy samples before even considering those from aged or diseased samples. The data presented in Chapter Four and Five (discussed below) can now be utilised to improve source references for future FE representation of the human knee joint, providing data to accurately represent cohort- or subject-specific models. Mechanical behavioural can now be applied therapeutically in the knowledge that predictions are more biologically accurate.

Chapter Five of this thesis aimed to collate material property data for the four primary human knee joint ligaments from the previously obtained human cadaver knee joints of varying demographics including age and disease status. Material properties focused on the linear stress and strain, Young's modulus, tangent modulus, failure stress and strain, linear and failure load, stiffness and failure region of the anterior cruciate ligament (ACL), posterior cruciate ligament (PCL), medial collateral ligament (MCL) and lateral collateral ligament (LCL), obtained via tensile testing.

Initially material properties were correlated with both age and OA on a linear scale and showed relationships between increasing age and a decrease in linear failure, linear stress, Young's modulus, tangent modulus, failure load, failure stress and stiffness in the ACL and PCL. Negative trends were also seen in the MCL failure stress and LCL failure load and

tangent modulus. Increasing OA grade was correlated with ACL and PCL linear mechanics, and ACL, PCL, MCL and LCL failure mechanics.

Correlations to a change in material properties with age was closely aligned to what the literature indicated would be expected [e.g. Noyes & Grood, 1976; Trent et al., 1976; Woo et al., 1991]. Previous research has directed its focus on histological analyses of the gross structure primarily of the ACL [e.g. Mullaji et al., 2008] and in some instances the PCL [e.g. Allain et al., 2001]. This has consistently shown impaired integrity of ligament fibres and structure in the presence of disease. With this in mind, material property data would be expected to show a decline in parameters such as tangent modulus and failure load. Previous research exploring the material properties of the human ACL have found similar values to those reported here, and consistently shown a decline in material property values with increasing age categories [Woo et al., 1991]. However this is the first study of its kind to explore the effect of age on the material properties of the PCL, MCL and LCL as well, and the effect of OA grades on material properties in all primary knee joint ligaments.

For the first time, this research has presented data from all four primary knee joint ligaments from the same donor, across a wide span of age and OA grade. To the authors' knowledge only one previous study has compared all four ligaments. Results from Trent et al., [1976] showed that increased stiffness and failure load was evident in the cruciate ligaments (ACL and PCL) when compared to the collaterals (MCL and LCL), although there was no comparison to aged or diseased samples. Evidently, the current research presented in Chapter Five significantly advancing the understanding of how ligament material properties change across the same cadaver, with the added analyses of effect of age and OA.

There are several limiting factors within Chapter Five. Firstly, only 10 – 12 ligament samples were obtained per group (n = 12 ACL, n = 12 PCL, n = 10 MCL, n = 12 LCL). Each ligament is known to have differing material properties based on its anatomical location, orientation and loading axis. Within each ligament type cadavers varied by age, OA grade and gender further separating cohorts. During analyses it was evidently challenging to make statistically significant conclusions between cohorts due to these low population numbers. Therefore it is more useful to discuss consistent cohort trends irrespective of statistical analyses, which may or may not be reached due to low numbers.

Tensile testing in the current research was limited by the rate of the machine (maximum 500mm/min). The strain rate has been shown to affect the resultant material properties and resultant failure mechanics of the ligament [Bonner et al., 2015], where slower strain rates produce a higher failure load and tangent modulus. However, faster strain rates (500mm/min and upwards) replicate physiological reality of ligament injury and failure load, therefore is more likely to provide accurate and representative mechanics [Noyes & Grood, 1976; Robinson et al., 2005]. Further, four ligaments failed by bony avulsion and it has been suggested previously that when this occurs, results actually present the bone mechanics as opposed to the ligament mechanics [Noyes & Grood, 1976; Nigg & Herzog, 2006]. Ideally, ligaments should fail at the mid-substance to provide true material properties of the ligament fibre bundles.

Practical applications of Chapter Five are similar to those discussed regarding Chapter Four with regards to more accurate representation of subject- or cohort-specific FE modelling and biomaterial development. These results provide strong justification to use individual material properties for ligament in FE models, as opposed to replicating data for all four ligaments modelled, as previously presented in several studies [e.g. Wang et al., 2014;

Kazemi & Li, 2014]. With more accurate material property data inputted into FE models, behavioural predictions will again be more biologically realistic and help alter physical therapy prescriptions for aged and OA patients where rehabilitation may focus on stabilising the ACL and PCL more. Movement and sport biomechanics can also be advanced, by combining current data on healthy cadavers with that already present in the literature to provide a spectrum of material properties and failure mechanics at baseline. Further, as indicated by Woo et al., [1991] knowledge of baseline healthy measurements including peak force and toe region mechanics [Ratcliffe et al., 2015] can aid design and structure of ligament grafts and replacements.

Biomechanics of the ageing human knee

This thesis has documented for the very first time how material properties alter across the entire knee joint during healthy ageing and disease. In Chapters Four and Five of this thesis, material properties of articular cartilage, subchondral and trabecular bone and ligaments are presented. They are divided into two chapters for this thesis due to publication; however data is collected from the same 12 cadavers, aiding whole-joint knowledge.

As noted extensively throughout chapters Two to Five, inconsistencies in donor demographics throughout previous studies made it challenging to develop a hypothesis for how the material properties of knee joint tissues change during ageing and OA development. Piecing together different evidence from the literature prior to the work carried out herein [e.g. Kleemann et al., 2005; Mullaji et al., 2008], one might have hypothesised a decrease in values used to describe the material properties of cartilage and ligaments in ageing and OA, whilst the magnitudes of these parameters for bone might have been hypothesised an increase. This thesis refines and expands upon these

hypotheses regarding changes in knee tissues properties during ageing and OA progression by demonstrating a decline in cartilage shear storage and loss modulus in age and OA, an increase in subchondral bone elastic modulus in age and OA and a decrease in material properties of ACL and PCL in age and presence of OA (Fig. 1). However, no trends were observed in trabecular bone, while the MCL and LCL had some decreasing trends with age and OA.

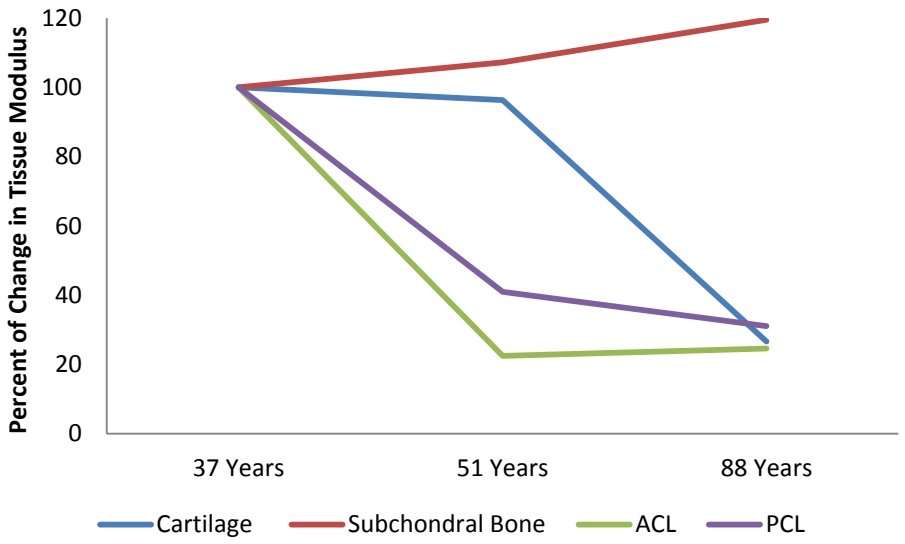

Figure 1. Percent of change to cartilage shear storage modulus (MPa), cortical bone elastic modulus (GPa), anterior cruciate ligament (ACL) and posterior cruciate ligament (PCL) tangent modulus (MPa) results using three examples: the 31 year old cadaver with osteoarthritis grade 0, 51 year old cadaver with grade 2 osteoarthritis, compared to the 88 year old cadaver with osteoarthritis grade 3.

The conceptual diagram (Fig. 1) shows changes in multiple tissues occurring concurrently (at the same time and at the same rate). Specifically it shows a young cadaver (37 years old) providing a baseline for measured material properties at 100% normal for cartilage shear storage modulus, subchondral bone elastic modulus and the ACL and PCL tangent

modulus. In comparison , there is a percentage change from the normal baseline in both the ACL (22.5%) and PCL (41.0%) tangent modulus which happened more rapidly that any percentage change from baseline normal to cartilage shear storage modulus (96.3%) or subchondral bone elastic modulus (107.2%) by middle age (51 years). Following this, a percent decline in cartilage shear storage modulus (26.6%), and a percent incline in subchondral bone elastic modulus (119.5%) is observed during older age (88 years), which is closely aligned to the percent decline in ACL (24.6%) and PCL (31.1%) tangent modulus at the same age. The data presented in Figure. 1 supports the hypothesis of a change in one tissue (the ACL and PCL), is correlated with a change in another tissue (cartilage and subchondral bone), and that degeneration of the ligaments may occur prior to any material property change of other tissues in the human knee joint.

However, the data set presented is comparatively small therefore relative changes cannot be conclusively linked to a specific cause-effect relationship during healthy ageing and the presence of OA in all specimens. To address this issue, widening the sample population would allow further testing for a more concrete conclusion to be drawn on such relationships. Indeed, due to low sample numbers it is challenging to distinctly separate the effects of ageing from the effects of OA. Evidently, the presence of OA accelerates changes seen during ageing but exactly how much, and if it is linear and consistent across ages cannot be completely stated from the data herein.

Recently published work by Kaplan et al., [2017] showed that high repetitive mechanical loading of cartilage samples causes softening of cartilage tissue, whilst low load magnitudes caused tissues to stiffen. This initial softening of cartilage tissue is suggested to be the first sign of degradation [Lyyra et al., 1995]. The authors hypothesise that cyclic loading causes mechanical fatigue through disruption of the collagen network. Further, cartilage thickness

was shown to decease with increased loading cycles, where each iteration produced double the recommended daily steps of a healthy adult [Tudor-Locke & Basset, 2004]. Without sufficient recovery in between each iteration permanent damage may be caused to the cartilage depending on the activity undertaken and force magnitude it causes. Practically, *in vivo*, this suggests that experiencing high mechanical loads on a regular basis can cause such degradation to the cartilage structure.

Previously published work [e.g. Lanyon, 1992] shows that the ability for bone to regenerate and adapt to responses placed upon may cause an increase in material properties such as elastic modulus; however continuous high loading may cause the cartilage to degrade, as it does not have the same ability to regenerate and lay down new matrix without the presence of a chondroblast cell. With the data presented in this thesis showing a decline in cartilage shear modulus is significantly correlated with an incline in subchondral bone elastic modulus, this may suggest that greater locomotive mechanical loading causes an increase in bone turnover and elastic modulus [e.g. Lanyon, 1992]. Further, such cyclic or repetitive loading has also been shown to have a detrimental effect on the ligaments of the knee joint [Thornton et al., 2007], where both the ACL and PCL experience varying ranges of mechanical loading during locomotion [Morrison, 1970; Collins & O'Connor, 1991]. Figure 1 could help hypothesise that if repetitive mechanical loading had led to a decline in ligament tangent modulus, this is prior to any significant changes to cartilage or subchondral bone material properties.

Conclusions drawn from this research can help hypothesise the causes of such material property changes. This thesis has linked changes in cartilage and bone material properties, preferentially on the medial side, which may be linked to increased mechanical loading suggested in the literature on the medial compartment of the knee joint. This research also

observed changes in ligament tensile properties and failure loads during ageing and disease which may be linked to higher mechanical loading during habitual locomotion, and in particular in the ACL. This research could help hypothesise that weakening of the ACL and PCL as seen in Figure 1 (51 years) may increase medial loading that contributes to the aforementioned changes to material properties in cartilage and bone (Fig. 1, 88 years). These conceptual ideas link to the subsequent medial development of OA discussed in Chapter Four of this thesis, along with the locomotive evidence of medial gait changes presented across the literature [e.g. Kumar et al., 2013].

In the future this hypothesis could be addressed by several ways. Firstly, increasing the sample population could help draw more statistically significant conclusions that it is currently challenging to reach due to a sample number of 12 cadavers. Further research may also include such cyclic mechanical loading such as those referenced above, to understand the effect of mechanical fatigue on multiple tissues obtained from the same human cadaver knee joint. This would give a greater insight into tissue interaction from a subject-specific perspective. Finally, such subject-specific findings can be applied into computational approaches that represent continual static or dynamic loading of a knee joint to understand behavioural responses on individual tissues and their subsequent effect of adjacent tissue structures.

Perspectives on Future Applications and Advances in the Field

In summary this thesis has firstly reviewed current efforts at modelling the human knee joint, and the source of input data used to create such models. Second, this thesis advances the knowledge on storage and preservation techniques for articular cartilage, allowing future researchers to adapt testing protocols. Lastly, this thesis has provided, for the first

time, human knee joint material property data from multiple tissues and regions within the same cadaver, and from cadavers with demographics spanning from 31 – 88 years old, and healthy through to OA ICRS grade 4 joints. Potential improvements to this work, notably increasing samples sizes, have been noted throughout, but additionally the data and results obtained herein suggest a number of avenues for important future work on the biomechanics of the ageing human knee.

Whilst it is currently not feasible to obtain both subject-specific *in vivo* and *in vitro* material property data, a cohort-specific approach would aid closing this gap in the knowledge considerably, whilst largely increasing the accuracy and bio realism of future applications such as diagnostics, failure mechanics, synthetic tissue development and FE modelling.

Diagnostics and Imaging

OA is a condition most commonly diagnosed through medical imaging techniques, and in particular radiographic images that can detect indicative signs of the disease such as joint space narrowing, cartilage thinning and osteophyte formation. However these signs often accompany late stage OA, where more invasive treatment may be necessary. A change in material properties, and in particular stiffness values, is known to occur during mild, moderate and severe OA, caused by a reduction in proteoglycan content and the subsequent inability to bear compressive forces [Kiviranta et al., 2008].

Increasing the level of bio realism is being researched in the form of measuring mechanical properties with poro or viscoelastic behaviour in cartilage in order to account for extracellular matrix deformation and fluid flow within soft hydrated biological tissue. The current research along with previous research has identified that the viscoelastic response

of cartilage can functionally identify surface changes in early OA which is vital in the early diagnosis of the disease [Desrochers et al., 2012]. The poroelastic response of cartilage is an area of advancing research in the field of tissue engineering which is often combined with numerical modeling to predict the various material property parameters most accurate to native tissue behaviour [e.g. Taffetani et al., 2014; Nia et al., 2011].

Indeed, it has been suggested that a decrease in material properties is evident prior to any detectable surface degeneration [Stolz et al., 2009]. Most often material property values are obtained *in vitro*; however some researchers have explored these *in vivo* [Lyyra et al., 1999; Kiviranta et al., 2008]. Indentation and probing techniques can be applied during arthroplasty procedures, which can be used to reveal early stage pathology [Lyyra et al., 1999; Kivranta et al., 2008; Ryd et al., 2015; Oakley et al., 2005], and to evaluate and follow up on effects of medical or operative treatment to the cartilage or surrounding tissue [Lyyra et al., 1999]; however is still in the developmental stage [Ryd et al., 2015]. Probing techniques can be used to determine prognosis of patients in the long term development of OA [Ryd et al., 2015]; however it has been noted that an effective treatment protocol for OA is yet to be accomplished [Ryd et al., 2015].

This level of personalised medicine is an increasing focus in healthcare in order to increase early detection of OA and improve the bio realism to each patient in such procedures. Knowledge of healthy human knee joint cartilage material properties is essential as a baseline for such procedures to be accurate in the detection of early OA. Whilst it is often challenging to obtain these on human subjects, other techniques are now being employed to obtain such material property data.

The level of sophistication for predicting material properties of soft and hard tissues is increasing through the use of medical imaging techniques in order to help diagnose early stage OA [Neu, 2014; Loeser et al., 2013; Ryd et al., 2015]. In particular MRI is an area of advancing research which can help quantify mechanical functioning at tissue level including stress, strain and material properties. MRI may be used as a screening method as it is non-invasive and non-destructive [Neu, 2014; Ryd et al., 2015]. It provides visualisation of multiple tissues known to be involved in OA and can monitor a change in shape or size over a period of time where mechanical loading takes place to measure stain [Neu, 2014]. Stress data which quantifies force exerted on the tissue, as well as material properties can be calculated through constitutive equations. This is often done through combining imaging data and numerical modelling [Neu, 2014].

Textural image analysis is another advancing technique also being explored in the prediction of bone material properties. As OA is now recognized as whole joint disease, early signs may manifest in other tissues surrounding the cartilage where macro-scale observations of the disease are most obvious. Such techniques can be used to asses bone mineral density and much like MRI imaging, it can also combined with numerical modelling to predict material properties [Neu, 2014].

Both probing and imaging techniques rely on accurate healthy baseline material properties from human samples, where those presented in the current thesis can help increase the understanding on how such values manifest and vary across individuals. Stevens, [2008] commented on the difficulty in transferring clinical data from *in vitro* to *in vivo*, and from animal to human applications. This highlights how valuable the current data is in moving from animals to human applications, which can help direct future *in vivo* such as those involved in arthroplasty indentations.

Earlier diagnosis of OA may enable intervention before arthroplasty procedures become necessary as these are expensive and invasive. However, where OA becomes too advanced the development of replacement materials may be contribute to improved disease prognostics and may defer the need for total knee replacement procedures [Ivirico et al., 2017].

Cartilage is an avascular structure meaning its healing capabilities are limited. When damage occurs the tissue will not regenerate, and normal biomechanical functioning will progress degeneration. For this reason development of synthetic materials is an area of research that has advanced in recent years and is continually improving in the level of bio realism [Duarte Campos et al., 2012]. Synthetics used to replace biological tissues should have biomechanical characteristics including material properties that are similar to the tissue it is replacing. In particular, the functional capabilities of cartilage should match those of the surrounding native tissue in order to support with applied loads. The replacement synthetic may deform excessively under these applied loads if the material properties are too soft, and in opposition if the replacement synthetic is too stiff it will absorb a greater proportion of the applied load and may contribute to further degeneration of the associated joint [Beddoes et al., 2016].

Hydrogels are often used as a synthetic material in the replacement of cartilage [Beddoes et al., 2016; Jeuken et al., 2016; Ivirico et al., 2017]. Hydrogels have a three dimensional polymer network with high water content, where depending on the polymer structure, the material properties are varied. By combining different polymer structures with different densities into one material, the mechanical properties can be manipulated to match other

materials such as cartilage thereby increasing the level of bio realism of the material. The elastic modulus, fracture energy and hysteresis can be tuned making them an ideal synthetic in the replacement of biological tissues [Beddoes et al., 2016]. In this instance, being able to adapt material properties to those found within varying demographics may increase the likelihood of successful implementation of the synthetic and long-lasting effects without further degradation of the surrounding native tissue. Even more so, the field is advancing by researching patient-specific resurfacing implants in the intervention of joint degradation which would rely on the knowledge of individual cartilage material properties [Jeuken et al., 2016].

Materials used in the replacement of bone have also been well researched, with advances in the field focusing on developing materials that are similar in nature biologically and mechanically to that of native bone in order to ensure sufficient vascularization [Stevens, 2008; Sheikh et al., 2015]. In particular bioactive materials that interact with existing cells and molecules are integral to successful tissue regeneration [Langer & Vacanti, 1993; Hench & Polak, 2002], meaning that materials such as ceramics, glasses and polymers are often utilised. Increasing the level of bio realism in these tissues is a particular focus, with research attempting to replicate the topographical scaffold of bone at the nanoscale [Stevens, 2008]. Although bone material properties have been well researched at the nano-scale, the results presented in this thesis are the first to collate data from the human knee joint from a variety of donor demographics, aiding the knowledge of biological variability in healthy, aged and diseased cortical and trabecular bone at the nano-scale.

CT imaging is being used for both bone and cartilage replacement. A concept by Duarte Campos et al., [2012] shows that using CT imaging, a cartilage like scaffold of cells can be individually designed and bio-printed. Three dimensional printing of biomimetic scaffolds

as well as cells and biologics is a new research interest that may enable the development of highly sophisticated and ever more bio realistic replacement materials and techniques [Hollister, 2005; Calvert, 2007].

Scaffolds are not only used in the repair and replacement of cartilage and bone, but also ligament structures [Ratcliffe et al., 2015; Yang et al., 2013]. Successful implementation of ligament scaffolds can result in faster rehabilitation of functional capabilities and reduced long term health costs [Ratcliffe et al., 2015]. They act as a structural foundation for cells and new tissue formation in ligaments and aim to mimic the biomechanical properties of the native tissue as well the structural organisation of the fibres. The strength of the scaffold should be higher than the ligament peak loads experienced *in vivo* to ensure it does not fail under normal loading conditions and it must also not stretch more than the *in vivo* toe region of the native ligament [Ratcliffe et al., 2015]. These specific requirements rely on accurate knowledge of native ligament biomechanical characteristics in order to ensure the scaffold lies within the appropriate mechanical region. The data provided in this thesis gives a wide range of biomechanical parameters whilst highlighting the differences seen between varying cohorts. In particular noting how a change in one ligament material properties may affect the surrounding ligaments.

Computational Modelling

Using subject- or cohort-specific data sets of multiple tissue material properties in the application of FE modelling can be used in the production of quantitative predictions of simultaneous mechanical and physiological behaviour, aiding the understanding of tissue interaction, which is inherently more apparent during ageing and in the presence of OA. Freutel et al., [2014] reviewed soft tissue sensitivity to changes in material properties and

environment, showing that inaccuracy of these parameters can limit the utilisation of FE applications. Moreover, defining material properties either through FE modelling or *in vivo* data collection has been identified as an area with potential significant improvements [Freutel et al., 2014; Gardiner & Weiss, 2003], where this thesis has subsequently provided such data which can be used in the application of such computational approaches.

It should be noted that CT and MRI data of eight of the cadavers were obtained. Due to time and resources of the current thesis/PhD project, the collated imaging data has not yet been made into an FE model and is beyond the time frame and scope this project. However such data could be used in the future, with subject-specific material properties obtained within the current research to produce the most accurate subject FE model to date.

Further research could also collate loading kinematic data *in vivo* and age/OA grade matched participants to the current cadaver demographics and make FE models even more specific. For example, work presented by Miranda et al., [2013] shows how biplanar videoradiography can be utilised to obtain skeletal motion without soft tissue artifact, i.e. movement of skin, which can reduce the accuracy of joint metrics of ligaments and other articulating surfaces. Efforts have also been made to produce an openly available finite element model for clinical and scientific explorations to be made [Erdemir, 2016] that allows the user to input varying material property data into an existing human knee joint FE model, to predict stress strain behaviour under varying conditions and input values. Data presented in this thesis could be utilised in coordination with Open Knee to predict behaviour of cohort specific groups such as young versus old, or healthy versus OA. A sensitivity analyses could be conducted to understand the effect of subject specific material properties on behaviour.

Increasing the level of bio realism is an ongoing aim in the field of tissue engineering, with the main focuses primarily on the early diagnosis of OA, developing more biologically accurate replacement materials, and creating more subject- or cohort- specific treatment approaches in the form of computational imaging and numerical predictive modelling. These overall applications will further increase in their accuracy as the field continues to understand the mechanical behaviour of such tissues involved. Importantly these applications are not only used for better disease prognosis, but in a variety of clinical and therapeutic areas, where in particular knowledge of healthy human knee tissue mechanics is also advantageous.

Chapter Seven: Conclusion

To conclude, Chapter Two of this thesis has provided a comprehensive review on the current state of affairs regarding tissue material properties of the human knee joint and the current representation in FE modelling, prior to the data collected herein. Chapter two found high variability in material properties across cartilage, bone and ligaments of the human knee joint in healthy and aged/diseased samples. Variations in testing methods and donor demographics have created varied interpretations and applications into FE models. Further, existing FE models of the whole human knee joint source material property data of such tissues from multiple animals and localities further exacerbating the inaccurate representation of the human knee joint and associated behaviour through FE analysis.

To increase knowledge on the effects of ageing and disease on tissue material properties explored in Chapter Two, it was first important to understand how these tissue types can be stored and preserved in preparation for material property testing, if not currently known within the literature. Chapter Three supported the use of freezing as a method to preserve cartilage tissue for up to three cycles of freeze-thawing without compromising the integrity of its material properties. Although statistically significant changes were not recovered at the whole-joint level, there was a high variability and often high magnitude of changes to cartilage material properties. The implications of this are for use in further material property testing where indeed the current research suggests that cartilage should be prioritised for immediate testing over other tissues where they are able to undergo additional freezing cycles.

With the knowledge of how to preserve cartilage tissue if necessary, this thesis then presented material property data of human knee joint cartilage, bone and ligament tissues

within demographically diverse cadavers. For the first time multiple tissues from the same donor were harvested and tested using standardized methods for the accurate determination of the change in material properties during ageing and disease.

Chapter Four of this thesis demonstrated a synergistic relationship between cartilage and bone, where a decrease in cartilage shear storage and loss modulus relates to an increase in subchondral cortical bone elastic modulus in site-matches samples. Such changes in cartilage and subchondral bone were statistically correlated with an increase in age and OA grade. Changes to cartilage shear storage modulus were also site dependent within the knee joint, demonstrating preferential medial development of OA associated with a decline in shear modulus. Clinically, this data can have implications on future therapeutic interventions including physical therapy, pharmacological aid and the development of more biologically accurate biomimetic materials.

Chapter Five of this thesis demonstrated the ACL and PCL show a decline in all material properties measured during ageing and disease and that both the LCL and MCL show some changes, although low sample numbers made it challenging to draw statistically significant conclusions. It is hypothesized that changes occurring in ligaments happens prior to any change evident in the cartilage or bone during the initiation and/or progression or OA. Such valuable data can be implemented into future FE analysis on a subject- or cohort-specific basis to increase the understanding of ligament and whole-joint behavior during mechanical loading. Other applications include the development of biomimetic scaffolds used in the repair and replacement of tissue.

This thesis provides evidence that both soft and hard tissue within or surrounding the osteochondral unit are significantly affected by age and OA, and that in particular OA

should be considered a whole-joint disease affecting multiple tissues. Such data should be applied in future research involving diagnostics and prognostics of OA, the development of synthetic biomaterials for the repair and replacement of soft and hard tissues and computational representation of the human knee joint.

Chapter Eight: References

1. Allain, J., Goutallier, D. & Voisin, M.C. 2001, "Macroscopic and histological assessments of the cruciate ligaments in arthrosis of the knee", *Acta Orthopaedica Scandinavica,* vol. 72, no. 3, pp. 266-269.
2. Alnahdi, A.H., Zeni, J.A. & Snyder-Mackler, L. 2012, "Muscle impairments in patients with knee osteoarthritis", *Sports Health,* vol. 4, no. 4, pp. 284-292.
3. Astephen, J.L., Deluzio, K.J., Caldwell, G.E. & Dunbar, M.J. 2008, "Biomechanical changes at the hip, knee, and ankle joints during gait are associated with knee osteoarthritis severity", *Journal of Orthopaedic Research,* vol. 26, no. 3, pp. 332-341.
4. Beddoes, C.M., Whitehouse, M.R., Briscoe, W.H. & Su, B. 2016, "Hydrogels as a replacement material for damaged articular hyaline cartilage", *Materials,* vol. 9, no. 6, pp. 443.
5. Behrens, J., Walker, P. & Shoji, H. 1974, "Variations in strength and structure of cancellous bone at the knee", *Journal of Biomechanics,* vol. 7, no. 3, pp. 201-207.
6. Bembey, A., Oyen, M., Bushby, A. & Boyde, A. 2006, "Viscoelastic properties of bone as a function of hydration state determined by nanoindentation", *Philosophical Magazine,* vol. 86, no. 33-35, pp. 5691-5703.
7. Bendjaballah, M.Z., Shirazi-Adl, A. & Zukor, D. 1995, "Biomechanics of the human knee joint in compression: reconstruction, mesh generation and finite element analysis", *The Knee,* vol. 2, no. 2, pp. 69-79.
8. Blankevoort, L., Kuiper, J., Huiskes, R. & Grootenboer, H. 1991, "Articular contact in a three-dimensional model of the knee", *Journal of Biomechanics,* vol. 24, no. 11, pp. 1019-1031.

9. Bobinac, D., Spanjol, J., Zoricic, S. & Maric, I. 2003, "Changes in articular cartilage and subchondral bone histomorphometry in osteoarthritic knee joints in humans", *Bone,* vol. 32, no. 3, pp. 284-290.
10. Bonner, T.J., Newell, N., Karunaratne, A., Pullen, A.D., Amis, A.A., Bull, A.M. & Masouros, S.D. 2015, "Strain-rate sensitivity of the lateral collateral ligament of the knee", *Journal of the Mechanical Behavior of Biomedical Materials,* vol. 41, pp. 261-270.
11. Buckwalter, J. & Mankin, H. 1997, "Articular cartilage: Part II Degeneration and osteoarthrosis, repair, regeneration, and transplantation", *JBJS,* vol. 79, no. 4, pp. 612-632.
12. Burgers, T.A., Mason, J., Niebur, G. & Ploeg, H.L. 2008, "Compressive properties of trabecular bone in the distal femur", *Journal of Biomechanics,* vol. 41, no. 5, pp. 1077-1085.
13. Calvert, P. 2007, "Materials science. Printing cells", *Science (New York, N.Y.),* vol. 318, no. 5848, pp. 208-209.
14. Chandrashekar, N., Mansouri, H., Slauterbeck, J. & Hashemi, J. 2006, "Sex-based differences in the tensile properties of the human anterior cruciate ligament", *Journal of Biomechanics,* vol. 39, no. 16, pp. 2943-2950.
15. Collins, J.J. & O'Connor, J.J. 1991, "Muscle-ligament interactions at the knee during walking", *Proceedings of the Institution of Mechanical Engineers. Part H, Journal of engineering in medicine,* vol. 205, no. 1, pp. 11-18.
16. Dabiri, Y. & Li, L. 2013, "Influences of the depth-dependent material inhomogeneity of articular cartilage on the fluid pressurization in the human knee", *Medical Engineering & Physics,* vol. 35, no. 11, pp. 1591-1598.

17. Deluzio, K. & Astephen, J. 2007, "Biomechanical features of gait waveform data associated with knee osteoarthritis: an application of principal component analysis", *Gait & Posture,* vol. 25, no. 1, pp. 86-93.
18. Demarteau, O., Pillet, L., Inaebnit, A., Borens, O. & Quinn, T. 2006, "Biomechanical characterization and *in vitro* mechanical injury of elderly human femoral head cartilage: comparison to adult bovine humeral head cartilage", *Osteoarthritis and Cartilage,* vol. 14, no. 6, pp. 589-596.
19. Desrochers, J., Amrein, M. & Matyas, J. 2012, "Viscoelasticity of the articular cartilage surface in early osteoarthritis", *Osteoarthritis and Cartilage,* vol. 20, no. 5, pp. 413-421.
20. Desrochers, J., Amrein, M.A. & Matyas, J.R. 2010, "Structural and functional changes of the articular surface in a post-traumatic model of early osteoarthritis measured by atomic force microscopy", *Journal of Biomechanics,* vol. 43, no. 16, pp. 3091-3098.
21. Dhammi, I.K., Rehan-Ul-Haq & Kumar, S. 2015, "Graft choices for anterior cruciate ligament reconstruction", *Indian Journal of Orthopaedics,* vol. 49, no. 2, pp. 127-128.
22. Dheerendra, S.K., Khan, W.S., Singhal, R., Shivarathre, D.G., Pydisetty, R. & Johnstone, D. 2012, "Anterior cruciate ligament graft choices: a review of current concepts", *The Open Orthopaedics Journal,* vol. 6, pp. 281-286.
23. Dong, Y., Hu, G., Zhang, L., Hu, Y., Dong, Y. & Xu, Q. 2011, "Accurate 3D reconstruction of subject-specific knee finite element model to simulate the articular cartilage defects", *Journal of Shanghai Jiaotong University (Science),* vol. 16, pp. 620-627.

24. Donzelli, P.S., Spilker, R.L., Ateshian, G.A. & Mow, V.C. 1999, "Contact analysis of biphasic transversely isotropic cartilage layers and correlations with tissue failure", *Journal of Biomechanics,* vol. 32, no. 10, pp. 1037-1047.
25. Duarte Campos, D.F., Drescher, W., Rath, B., Tingart, M. & Fischer, H. 2012, "Supporting biomaterials for articular cartilage repair", *Cartilage,* vol. 3, no. 3, pp. 205-221.
26. Ducheyne, P., Heymans, L., Martens, M., Aernoudt, E., de Meester, P. & Mulier, J.C. 1977, "The mechanical behaviour of intracondylar cancellous bone of the femur at different loading rates", *Journal of Biomechanics,* vol. 10, no. 11, pp. 747-762.
27. Erdemir, A. 2016, "Open Knee: Open Source Modeling and Simulation in Knee Biomechanics", *Journal of Knee Surgery,* vol. 29, no. 02, pp. 107-116.
28. Franke, O., Göken, M., Meyers, M., Durst, K. & Hodge, A. 2011, "Dynamic nanoindentation of articular porcine cartilage", *Materials Science and Engineering: C,* vol. 31, no. 4, pp. 789-795.
29. Freutel, M., Schmidt, H., Dürselen, L., Ignatius, A. & Galbusera, F. 2014, "Finite element modeling of soft tissues: Material models, tissue interaction and challenges", *Clinical Biomechanics,* vol. 29, no. 4, pp. 363-372.
30. Gardiner, J.C. & Weiss, J.A. 2003, "Subject-specific finite element analysis of the human medial collateral ligament during valgus knee loading", *Journal of Orthopaedic Research,* vol. 21, no. 6, pp. 1098-1106.
31. Guess, T.M., Thiagarajan, G., Kia, M. & Mishra, M. 2010, "A subject specific multibody model of the knee with menisci", *Medical Engineering & Physics,* vol. 32, no. 5, pp. 505-515.
32. Guo, Y., Zhang, X. & Chen, W. 2009, "Three-dimensional finite element simulation of total knee joint in gait cycle", *Acta Mechanica Solida Sinica,* vol. 22, no. 4, pp. 347-351.

33. Hayami, T., Pickarski, M., Wesolowski, G.A., Mclane, J., Bone, A., Destefano, J., Rodan, G.A. & Duong, L.T. 2004, "The role of subchondral bone remodeling in osteoarthritis: reduction of cartilage degeneration and prevention of osteophyte formation by alendronate in the rat anterior cruciate ligament transection model", *Arthritis & Rheumatism,* vol. 50, no. 4, pp. 1193-1206.
34. Helminen, H.J., Hyttinen, M.M., Lammi, M.J., Arokoski, J.P., Lapveteläinen, T., Jurvelin, J., Kiviranta, I. & Tammi, M.I. 2000, "Regular joint loading in youth assists in the establishment and strengthening of the collagen network of articular cartilage and contributes to the prevention of osteoarthrosis later in life: a hypothesis", *Journal of Bone and Mineral Metabolism,* vol. 18, no. 5, pp. 245-257.
35. Hench, L.L. & Polak, J.M. 2002, "Third-generation biomedical materials", *Science (New York, N.Y.),* vol. 295, no. 5557, pp. 1014-1017.
36. Hill, C.L., Seo, G.S., Gale, D., Totterman, S., Gale, M.E. & Felson, D.T. 2005, "Cruciate ligament integrity in osteoarthritis of the knee", *Arthritis & Rheumatism,* vol. 52, no. 3, pp. 794-799.
37. Hollister, S.J. 2005, "Porous scaffold design for tissue engineering", *Nature Materials,* vol. 4, no. 7, pp. 518.
38. Hollman, J.H., Kovash, F.M., Kubik, J.J. & Linbo, R.A. 2007, "Age-related differences in spatiotemporal markers of gait stability during dual task walking", *Gait & posture,* vol. 26, no. 1, pp. 113-119.
39. Huang, H., Zhang, J., Sun, K., Zhang, X. & Tian, S. 2011, "Effects of repetitive multiple freeze–thaw cycles on the biomechanical properties of human flexor digitorum superficialis and flexor pollicis longus tendons", *Clinical Biomechanics,* vol. 26, no. 4, pp. 419-423.
40. Hvid, I. & Hansen, S.L. 1985, "Trabecular bone strength patterns at the proximal tibial epiphysis", *Journal of Orthopaedic Research,* vol. 3, no. 4, pp. 464-472.

41. Ivirico, J.L.E., Bhattacharjee, M., Kuyinu, E., Nair, L.S. & Laurencin, C.T. 2017, "Regenerative engineering for knee osteoarthritis treatment: biomaterials and cell-based technologies", *Engineering,* vol. 3, no. 1, pp. 16-27.
42. Jeffrey, J.E. & Aspden, R.M. 2006, "The biophysical effects of a single impact load on human and bovine articular cartilage", *Proceedings of the Institution of Mechanical Engineers.Part H, Journal of Engineering in Medicine,* vol. 220, no. 6, pp. 677-686.
43. Jeuken, R.M., Roth, A.K., Peters, R.J., van Donkelaar, C.C., Thies, J.C., van Rhijn, L.W. & Emans, P.J. 2016, "Polymers in cartilage defect repair of the knee: current status and future prospects", *Polymers,* vol. 8, no. 6, pp. 219.
44. Jurvelin, J.S., Arokoski, J.P., Hunziker, E.B. & Helminen, H.J. 2000, "Topographical variation of the elastic properties of articular cartilage in the canine knee", *Journal of Biomechanics,* vol. 33, no. 6, pp. 669-675.
45. Kamibayashi, L., Wyss, U., Cooke, T. & Zee, B. 1995, "Trabecular microstructure in the medial condyle of the proximal tibia of patients with knee osteoarthritis", *Bone,* vol. 17, no. 1, pp. 27-35.
46. Kaplan, J.T., Neu, C.P., Drissi, H., Emery, N.C. & Pierce, D.M. 2017, "Cyclic loading of human articular cartilage: The transition from compaction to fatigue", *Journal of the Mechanical Behavior of Biomedical Materials,* vol. 65, pp. 734-742.
47. Kazemi, M. & Li, L. 2014, "A viscoelastic poromechanical model of the knee joint in large compression", *Medical Engineering & Physics,* vol. 36, no. 8, pp. 998-1006.
48. Kazemi, M., Li, L., Savard, P. & Buschmann, M. 2011, "Creep behavior of the intact and meniscectomy knee joints", *Journal of the Mechanical Behavior of Biomedical Materials,* vol. 4, no. 7, pp. 1351-1358.

49. Kiss, R.M. 2011, "Effect of severity of knee osteoarthritis on the variability of gait parameters", *Journal of Electromyography and Kinesiology,* vol. 21, no. 5, pp. 695-703.

50. Kiviranta, I., Tammi, M., Jurvelin, J., Arokoski, J., Säämänen, A. & Helminen, H.J. 1994, "Articular cartilage thickness and glycosaminoglycan distribution in the young canine knee joint after remobilization of the immobilized limb", *Journal of Orthopaedic Research,* vol. 12, no. 2, pp. 161-167.

51. Kiviranta, P., Lammentausta, E., Toyras, J., Kiviranta, I. & Jurvelin, J.S. 2008, "Indentation diagnostics of cartilage degeneration", *Osteoarthritis and Cartilage,* vol. 16, no. 7, pp. 796-804.

52. Kleemann, R., Krocker, D., Cedraro, A., Tuischer, J. & Duda, G. 2005, "Altered cartilage mechanics and histology in knee osteoarthritis: relation to clinical assessment (ICRS Grade)", *Osteoarthritis and Cartilage,* vol. 13, no. 11, pp. 958-963.

53. Klein-Nulend, J., Nijweide, P.J. & Burger, E.H. 2003, "Osteocyte and bone structure", *Current Osteoporosis Reports,* vol. 1, no. 1, pp. 5-10.

54. Kumar, D., Manal, K.T. & Rudolph, K.S. 2013, "Knee joint loading during gait in healthy controls and individuals with knee osteoarthritis", *Osteoarthritis and Cartilage,* vol. 21, no. 2, pp. 298-305.

55. Kuroki, K., Cook, C. & Cook, J. 2011, "Subchondral bone changes in three different canine models of osteoarthritis", *Osteoarthritis and Cartilage,* vol. 19, no. 9, pp. 1142-1149.

56. Lange, A., Singh, M.F., Smith, R., Foroughi, N., Baker, M., Shnier, R. & Vanwanseele, B. 2007, "Degenerative meniscus tears and mobility impairment in women with knee osteoarthritis", *Osteoarthritis and Cartilage,* vol. 15, no. 6, pp. 701-708.

57. Langer, R., Vacanti JP. 1993, “Tissue engineering”, *Science*, vol.14, no.260, pp.920-926.

58. Lanyon, L. 1993, "Osteocytes, strain detection, bone modeling and remodeling", *Calcified Tissue International,* vol. 53, pp. S102-S107.
59. Lanyon, L.E. 1992, "Control of bone architecture by functional load bearing", *Journal of Bone and Mineral Research,* vol. 7, no. S2.
60. Li, G., Lopez, O. & Rubash, H. 2001, "Variability of a three-dimensional finite element model constructed using magnetic resonance images of a knee for joint contact stress analysis", *Journal of Biomechanical Engineering,* vol. 123, no. 4, pp. 341-346.
61. Li, W., Wang, D., Yang, W. & Song, Y. 2016, "Compressive mechanical properties and microstructure of PVA–HA hydrogels for cartilage repair", *RSC Advances,* vol. 6, no. 24, pp. 20166-20172.
62. Linde, F. & Sørensen, H.C.F. 1993, "The effect of different storage methods on the mechanical properties of trabecular bone", *Journal of Biomechanics,* vol. 26, no. 10, pp. 1249-1252.
63. Loeser, R.F., Goldring, S.R., Scanzello, C.R. & Goldring, M.B. 2012, "Osteoarthritis: a disease of the joint as an organ", *Arthritis & Rheumatology,* vol. 64, no. 6, pp. 1697-1707.
64. Long, M. & Rack, H. 1998, "Titanium alloys in total joint replacement—a materials science perspective", *Biomaterials,* vol. 19, no. 18, pp. 1621-1639.
65. Lories, R.J. & Luyten, F.P. 2011, "The bone–cartilage unit in osteoarthritis", *Nature Reviews Rheumatology,* vol. 7, no. 1, pp. 43-49.
66. Losina, E., Paltiel, A.D., Weinstein, A.M., Yelin, E., Hunter, D.J., Chen, S.P., Klara, K., Suter, L.G., Solomon, D.H. & Burbine, S.A. 2015, "Lifetime medical costs of knee osteoarthritis management in the United States: impact of extending indications for total knee arthroplasty", *Arthritis Care & Research,* vol. 67, no. 2, pp. 203-215.

67. Lyyra, T., Jurvelin, J., Pitkänen, P., Väätäinen, U. & Kiviranta, I. 1995, "Indentation instrument for the measurement of cartilage stiffness under arthroscopic control", *Medical Engineering & Physics,* vol. 17, no. 5, pp. 395-399.
68. Lyyra, T., Kiviranta, I., Väätäinen, U., Helminen, H.J. & Jurvelin, J.S. 1999, "In vivo characterization of indentation stiffness of articular cartilage in the normal human knee", *Journal of Biomedical Materials Research Part A,* vol. 48, no. 4, pp. 482-487.
69. Mahjoub, M., Berenbaum, F. & Houard, X. 2012, "Why subchondral bone in osteoarthritis? The importance of the cartilage bone interface in osteoarthritis", *Osteoporosis International,* vol. 23, no. 8, pp. 841-846.
70. Manninen, P., Riihimaki, H., Heliovaara, M. & Makela, P. 1996, "Overweight, gender and knee osteoarthritis", *International Journal of Obesity and Related Metabolic Disorders: Journal of the International Association for the Study of Obesity,* vol. 20, no. 6, pp. 595-597.
71. Marticke, J.K., Hösselbarth, A., Hoffmeier, K.L., Marintschev, I., Otto, S., Lange, M., Plettenberg, H.K., Spahn, G. & Hofmann, G.O. 2010, "How do visual, spectroscopic and biomechanical changes of cartilage correlate in osteoarthritic knee joints?", *Clinical Biomechanics,* vol. 25, no. 4, pp. 332-340.
72. Matyas, J.R., Atley, L., Ionescu, M., Eyre, D.R. & Poole, A.R. 2004, "Analysis of cartilage biomarkers in the early phases of canine experimental osteoarthritis", *Arthritis & Rheumatology,* vol. 50, no. 2, pp. 543-552.
73. McDevitt, C., Gilbertson, E. & Muir, H. 1977, "An experimental model of osteoarthritis; early morphological and biochemical changes", *The Journal of Bone and Joint Surgery. British Volume,* vol. 59, no. 1, pp. 24-35.
74. Metcalfe, A., Stewart, C., Postans, N., Barlow, D., Dodds, A., Holt, C., Whatling, G. & Roberts, A. 2013, "Abnormal loading of the major joints in knee osteoarthritis and the response to knee replacement", *Gait & Posture,* vol. 37, no. 1, pp. 32-36.

75. Miranda, D.L., Rainbow, M.J., Crisco, J.J. & Fleming, B.C. 2013, "Kinematic differences between optical motion capture and biplanar videoradiography during a jump–cut maneuver", *Journal of Biomechanics,* vol. 46, no. 3, pp. 567-573.
76. Mononen, M., Julkunen, P., Töyräs, J., Jurvelin, J., Kiviranta, I. & Korhonen, R. 2011, "Alterations in structure and properties of collagen network of osteoarthritic and repaired cartilage modify knee joint stresses", *Biomechanics and Modeling in Mechanobiology,* vol. 10, no. 3, pp. 357-369.
77. Mononen, M., Mikkola, M., Julkunen, P., Ojala, R., Nieminen, M., Jurvelin, J. & Korhonen, R. 2012, "Effect of superficial collagen patterns and fibrillation of femoral articular cartilage on knee joint mechanics—A 3D finite element analysis", *Journal of Biomechanics,* vol. 45, no. 3, pp. 579-587.
78. Moon, D.K., Woo, S.L., Takakura, Y., Gabriel, M.T. & Abramowitch, S.D. 2006, "The effects of refreezing on the viscoelastic and tensile properties of ligaments", *Journal of Biomechanics,* vol. 39, no. 6, pp. 1153-1157.
79. Moore, A. & Burris, D. 2015, "Tribological and material properties for cartilage of and throughout the bovine stifle: support for the altered joint kinematics hypothesis of osteoarthritis", *Osteoarthritis and Cartilage,* vol. 23, no. 1, pp. 161-169.
80. Mootanah, R., Imhauser, C., Reisse, F., Carpanen, D., Walker, R., Koff, M., Lenhoff, M., Rozbruch, S., Fragomen, A. & Dewan, Z. 2014, "Development and validation of a computational model of the knee joint for the evaluation of surgical treatments for osteoarthritis", *Computer Methods in Biomechanics and Biomedical Engineering,* vol. 17, no. 13, pp. 1502-1517.
81. Morrison, J. 1970, "The mechanics of the knee joint in relation to normal walking", *Journal of Biomechanics,* vol. 3, no. 1, pp. 51-61.

82. Moss-Salentijn, L. & Moss, M. 1991, "Candidates for the mechanosensory system in bone", *Journal of Biomechanical Engineering,* vol. 113, pp. 191.
83. Mullaji, A.B., Marawar, S.V., Simha, M. & Jindal, G. 2008, "Cruciate ligaments in arthritic knees: a histologic study with radiologic correlation", *The Journal of Arthroplasty,* vol. 23, no. 4, pp. 567-572.
84. Neu, C.P. 2014, "Functional imaging in OA: role of imaging in the evaluation of tissue biomechanics", *Osteoarthritis and Cartilage,* vol. 22, no. 10, pp. 1349-1359.
85. Nia, H.T., Han, L., Li, Y., Ortiz, C. & Grodzinsky, A. 2011, "Poroelasticity of cartilage at the nanoscale", *Biophysical Journal,* vol. 101, no. 9, pp. 2304-2313.
86. Nigg, B. & Herzog, W. (eds) 2006, *Biomechanics of the Musculoskeletal System*, 3rd edn, Wiley, West Sussex.
87. Nissi, M., Rieppo, J., Töyräs, J., Laasanen, M., Kiviranta, I., Nieminen, M. & Jurvelin, J. 2007, "Estimation of mechanical properties of articular cartilage with MRI–dGEMRIC, T 2 and T 1 imaging in different species with variable stages of maturation", *Osteoarthritis and Cartilage,* vol. 15, no. 10, pp. 1141-1148.
88. Noyes, F.R. & Grood, E.S. 1976, "The strength of the anterior cruciate ligament in humans and Rhesus monkeys", *The Journal of Bone and Joint Surgery. American Volume,* vol. 58, no. 8, pp. 1074-1082.
89. Oakley, S.P., Portek, I., Szomor, Z., Appleyard, R.C., Ghosh, P., Kirkham, B.W., Murrell, G.A. & Lassere, M.N. 2005, "Arthroscopy -- a potential "gold standard" for the diagnosis of the chondropathy of early osteoarthritis", *Osteoarthritis and Cartilage,* vol. 13, no. 5, pp. 368-378.
90. O'brien, F.J. 2011, "Biomaterials & scaffolds for tissue engineering", *Materials Today,* vol. 14, no. 3, pp. 88-95.

91. Palmoski, M.J. & Brandt, K.D. 1981, "Running inhibits the reversal of atrophic changes in canine knee cartilage after removal of a leg cast", *Arthritis & Rheumatology,* vol. 24, no. 11, pp. 1329-1337.
92. Pedersen, D.R., Goetz, J.E., Kurriger, G.L. & Martin, J.A. 2013, "Comparative digital cartilage histology for human and common osteoarthritis models", *Orthopedic Research and Reviews,* vol. 2013, no. 5, pp. 13-20.
93. Pelletier, J., Raynauld, J., Berthiaume, M., Abram, F., Choquette, D., Haraoui, B., Beary, J.F., Cline, G.A., Meyer, J.M. & Martel-Pelletier, J. 2007, "Risk factors associated with the loss of cartilage volume on weight-bearing areas in knee osteoarthritis patients assessed by quantitative magnetic resonance imaging: a longitudinal study", *Arthritis Research & Therapy,* vol. 9, no. 4, pp. R74.
94. Pena, E., Calvo, B., Martinez, M. & Doblare, M. 2006, "A three-dimensional finite element analysis of the combined behavior of ligaments and menisci in the healthy human knee joint", *Journal of Biomechanics,* vol. 39, no. 9, pp. 1686-1701.
95. Peña, E., Calvo, B., Martínez, M.A. & Doblaré, M. 2007, "Effect of the size and location of osteochondral defects in degenerative arthritis. A finite element simulation", *Computers in Biology and Medicine,* vol. 37, no. 3, pp. 376-387.
96. Plumb, M. & Aspden, R. 2005, "The response of elderly human articular cartilage to mechanical stimuli *in vitro*", *Osteoarthritis and Cartilage,* vol. 13, no. 12, pp. 1084-1091.
97. Punzi, L., Oliviero, F. & Ramonda, R. 2010, "New horizons in osteoarthritis", *Swiss Medical Weekly,* vol. 140, pp. 16.
98. Ratcliffe, A., Butler, D.L., Dyment, N.A., Cagle, P.J., Proctor, C.S., Ratcliffe, S.S. & Flatow, E.L. 2015, "Scaffolds for tendon and ligament repair and regeneration", *Annals of Biomedical Engineering,* vol. 43, no. 3, pp. 819-831.

99. Rho, J., Tsui, T.Y. & Pharr, G.M. 1997, "Elastic properties of human cortical and trabecular lamellar bone measured by nanoindentation", *Biomaterials,* vol. 18, no. 20, pp. 1325-1330.

100. Richmond, B.G., Wright, B.W., Grosse, I., Dechow, P.C., Ross, C.F., Spencer, M.A. & Strait, D.S. 2005, "Finite element analysis in functional morphology", *The Anatomical Record Part A: Discoveries in Molecular, Cellular, and Evolutionary Biology,* vol. 283, no. 2, pp. 259-274.

101. Robinson, J.R., Bull, A.M. & Amis, A.A. 2005, "Structural properties of the medial collateral ligament complex of the human knee", *Journal of Biomechanics,* vol. 38, no. 5, pp. 1067-1074.

102. Ryd, L., Brittberg, M., Eriksson, K., Jurvelin, J.S., Lindahl, A., Marlovits, S., Möller, P., Richardson, J.B., Steinwachs, M. & Zenobi-Wong, M. 2015, "Pre-osteoarthritis: definition and diagnosis of an elusive clinical entity", *Cartilage,* vol. 6, no. 3, pp. 156-165.

103. Setton, L.A., Elliott, D.M. & Mow, V.C. 1999, "Altered mechanics of cartilage with osteoarthritis: human osteoarthritis and an experimental model of joint degeneration", *Osteoarthritis and Cartilage,* vol. 7, no. 1, pp. 2-14.

104. Shakoor, N., Block, J.A., Shott, S. & Case, J.P. 2002, "Nonrandom evolution of end-stage osteoarthritis of the lower limbs", *Arthritis & Rheumatism,* vol. 46, no. 12, pp. 3185-3189.

105. Sheikh, Z., Najeeb, S., Khurshid, Z., Verma, V., Rashid, H. & Glogauer, M. 2015, "Biodegradable materials for bone repair and tissue engineering applications", *Materials,* vol. 8, no. 9, pp. 5744-5794.

106. Shepherd, D.E. & Seedhom, B.B. 1999, "The 'instantaneous' compressive modulus of human articular cartilage in joints of the lower limb", *Rheumatology (Oxford, England),* vol. 38, no. 2, pp. 124-132.

107. Shirazi, R., Shirazi-Adl, A. & Hurtig, M. 2008, "Role of cartilage collagen fibrils networks in knee joint biomechanics under compression", *Journal of Biomechanics,* vol. 41, no. 16, pp. 3340-3348.

108. Stevens, M.M. 2008, "Biomaterials for bone tissue engineering", *Materials Today,* vol. 11, no. 5, pp. 18-25.

109. Stolz, M., Gottardi, R., Raiteri, R., Miot, S., Martin, I., Imer, R., Staufer, U., Raducanu, A., Düggelin, M. & Baschong, W. 2009, "Early detection of aging cartilage and osteoarthritis in mice and patient samples using atomic force microscopy", *Nature Nanotechnology,* vol. 4, no. 3, pp. 186-192.

110. Strait, D.S., Wang, Q., Dechow, P.C., Ross, C.F., Richmond, B.G., Spencer, M.A. & Patel, B.A. 2005, "Modeling elastic properties in finite-element analysis: How much precision is needed to produce an accurate model?", *The Anatomical Record Part A: Discoveries in Molecular, Cellular, and Evolutionary Biology,* vol. 283, no. 2, pp. 275-287.

111. Szarko, M., Muldrew, K. & Bertram, J.E. 2010, "Freeze-thaw treatment effects on the dynamic mechanical properties of articular cartilage", *BMC Musculoskeletal Disorders,* vol. 11, no. 1, pp. 231.

112. Taffetani, M., Gottardi, R., Gastaldi, D., Raiteri, R. & Vena, P. 2014, "Poroelastic response of articular cartilage by nanoindentation creep tests at different characteristic lengths", *Medical Engineering & Physics,* vol. 36, no. 7, pp. 850-858.

113. Tanska, P., Mononen, M.E. & Korhonen, R.K. 2015, "A multi-scale finite element model for investigation of chondrocyte mechanics in normal and medial meniscectomy human knee joint during walking", *Journal of Biomechanics,* vol. 48, no. 8, pp. 1397-1406.

114. Temple-Wong, M.M., Bae, W.C., Chen, M.Q., Bugbee, W.D., Amiel, D., Coutts, R.D., Lotz, M. & Sah, R.L. 2009, "Biomechanical, structural, and biochemical indices of degenerative and osteoarthritic deterioration of adult human articular cartilage of the femoral condyle", *Osteoarthritis and Cartilage,* vol. 17, no. 11, pp. 1469-1476.

115. Thornton, G.M., Schwab, T.D. & Oxland, T.R. 2007, "Cyclic loading causes faster rupture and strain rate than static loading in medial collateral ligament at high stress", *Clinical Biomechanics,* vol. 22, no. 8, pp. 932-940.

116. Trent, P.S., Walker, P.S. & Wolf, B. 1976, "Ligament length patterns, strength, and rotational axes of the knee joint", *Clinical Orthopaedics and Related Research,* vol. 117, pp. 263-270.

117. Tudor-Locke, C. & Bassett, D.R. 2004, "How many steps/day are enough?", *Sports Medicine,* vol. 34, no. 1, pp. 1-8.

118. Wang, Q., Hou, R., Cheng, Y. & Fu, J. 2012, "Super-tough double-network hydrogels reinforced by covalently compositing with silica-nanoparticles", *Soft Matter,* vol. 8, no. 22, pp. 6048-6056.

119. Wang, Y., Fan, Y. & Zhang, M. 2014, "Comparison of stress on knee cartilage during kneeling and standing using finite element models", *Medical Engineering & Physics,* vol. 36, no. 4, pp. 439-447.

120. Wen, C., Lu, W.W. & Chiu, K.Y. 2014, "Importance of subchondral bone in the pathogenesis and management of osteoarthritis from bench to bed", *Journal of Orthopaedic Translation,* vol. 2, no. 1, pp. 16-25.

121. Wilusz, R.E., Zauscher, S. & Guilak, F. 2013, "Micromechanical mapping of early osteoarthritic changes in the pericellular matrix of human articular cartilage", *Osteoarthritis and Cartilage,* vol. 21, no. 12, pp. 1895-1903.

122. Woo, S.L., Abramowitch, S.D., Kilger, R. & Liang, R. 2006, "Biomechanics of knee ligaments: injury, healing, and repair", *Journal of Biomechanics,* vol. 39, no. 1, pp. 1-20.

123. Woo, S.L., Hollis, J.M., Adams, D.J., Lyon, R.M. & Takai, S. 1991, "Tensile properties of the human femur-anterior cruciate ligament-tibia complex. The effects of specimen age and orientation", *The American Journal of Sports Medicine,* vol. 19, no. 3, pp. 217-225.

124. Yang, G., Rothrauff, B.B. & Tuan, R.S. 2013, "Tendon and ligament regeneration and repair: clinical relevance and developmental paradigm", *Birth Defects Research Part C: Embryo Today: Reviews,* vol. 99, no. 3, pp. 203-222.

125. Yao, H., Dao, M., Carnelli, D., Tai, K. and Ortiz, C., 2011, "Size-dependent heterogeneity benefits the mechanical performance of bone", *Journal of the Mechanics and Physics of Solids*, vol. 59, no. 1, pp. 64-74.

126. Zeni, J.A. & Higginson, J.S. 2009, "Differences in gait parameters between healthy subjects and persons with moderate and severe knee osteoarthritis: a result of altered walking speed?", *Clinical Biomechanics,* vol. 24, no. 4, pp. 372-378.

127. Zhang, Y. & Jordan, J.M. 2008, "Epidemiology of Osteoarthritis", *Rheumatic Disease Clinics of North America,* vol. 34, no. 3, pp. 515-529.

128. Zuo, Q., Lu, S., Du, Z., Friis, T., Yao, J., Crawford, R., Prasadam, I. & Xiao, Y. 2016, "Characterization of nano-structural and nano-mechanical properties of osteoarthritic subchondral bone", *BMC Musculoskeletal Disorders,* vol. 17, no. 1, pp. 367.

129. Zysset, P.K., Guo, X.E., Hoffler, C.E., Moore, K.E. & Goldstein, S.A. 1999, "Elastic modulus and hardness of cortical and trabecular bone lamellae measured by nanoindentation in the human femur", *Journal of Biomechanics,* vol. 32, no. 10, pp. 1005-1012.

Section Four – Appendices

Chapter Nine: Supplementary Material

Table 1. Cartilage, subchondral bone and trabecular bone raw data for cadaver 1, 31 years.

	31, Female									
	Cartilage						Trabecular Bone			
	G' kPa	G'' kPa	Tan Delta	G' MPa	G'' MPa	E MPa	E GPa	H GPa	D nm	Load mN
Femoral Condyle Medial Inferior	593.61	727.47	1.23	0.59	0.73	1.73	8.06	0.46	1398.70	15.73
	617.24	885.83	1.44	0.62	0.89	1.80	7.25	0.37	1384.05	13.00
	541.54	807.60	1.49	0.54	0.81	1.58	8.60	0.51	1395.33	17.19
	527.91	930.51	1.76	0.53	0.93	1.54	7.94	0.43	1387.34	14.75
	497.54	1076.16	2.16	0.50	1.08	1.45	7.12	0.36	1392.53	12.68
	552.09	900.30	1.63	0.55	0.90	1.61	6.13	0.39	1394.37	12.95
	626.42	1431.86	2.29	0.63	1.43	1.83	7.65	0.34	1374.99	12.15
	690.92	1252.14	1.81	0.69	1.25	2.02	7.53	0.43	1383.38	14.48
	736.99	1193.55	1.62	0.74	1.19	2.15	6.42	0.32	1362.62	10.87
	1224.09	1344.40	1.10	1.22	1.34	3.57	5.56	0.33	1383.62	10.90
Mean	660.83	1054.98	1.65	0.66	1.05	1.93	7.23	0.39	1385.69	13.47
SD	211.33	240.56	0.37	0.21	0.24	0.62	0.94	0.06	10.78	2.05
COV%	31.98	22.80	22.68	31.98	22.80	31.98	13.05	15.44	0.78	15.22
Femoral Condyle Medial Superior	2391.99	3230.15	1.35	2.39	3.23	6.98	12.56	0.55	1326.96	18.30
	1835.17	2510.12	1.37	1.84	2.51	5.36	11.96	0.49	1329.19	16.67
	1471.27	2607.83	1.77	1.47	2.61	4.30	12.36	0.53	1337.41	17.98
	1781.54	2438.70	1.37	1.78	2.44	5.20	10.93	0.39	1335.02	13.72
	2080.36	1924.29	0.93	2.08	1.92	6.07	12.35	0.55	1339.74	18.44
	2772.44	2748.04	0.99	2.77	2.75	8.10	10.51	0.50	1368.48	17.21

	2602.87	2468.52	0.95	2.60	2.47	7.60	9.11	0.41	1354.54	14.07
	2336.70	2465.09	1.06	2.34	2.47	6.82	8.83	0.37	1349.33	12.82
	2584.77	2699.28	1.04	2.58	2.70	7.55	10.53	0.44	1373.38	15.77
	2783.35	2660.17	0.96	2.78	2.66	8.13	8.03	0.34	1357.61	12.04
Mean	2264.05	2575.22	1.18	2.26	2.58	6.61	10.72	0.46	1347.17	15.70
SD	452.95	325.33	0.28	0.45	0.33	1.32	1.63	0.08	16.12	2.38
COV%	20.01	12.63	23.50	20.01	12.63	20.01	15.19	16.71	1.20	15.16
Femoral Condyle Lateral Inferior	1161.21	881.64	0.76	1.16	0.88	3.39	15.77	0.64	1316.29	21.17
	1283.40	1059.76	0.83	1.28	1.06	3.75	12.73	0.52	1318.76	17.20
	1436.30	1228.26	0.86	1.44	1.23	4.19	11.25	0.42	1328.66	14.60
	1601.69	1458.46	0.91	1.60	1.46	4.68	13.17	0.55	1324.79	18.49
	1708.69	1526.57	0.89	1.71	1.53	4.99	13.85	0.51	1338.96	17.81
	1587.62	1717.08	1.08	1.59	1.72	4.64	14.10	0.52	1330.68	17.99
	1482.86	1552.44	1.05	1.48	1.55	4.33	14.54	0.50	1331.21	17.59
	1086.68	884.16	0.81	1.09	0.88	3.17	12.46	0.46	1327.71	15.91
	1313.24	1220.48	0.93	1.31	1.22	3.83	15.01	0.58	1330.10	19.97
	1188.41	1003.56	0.84	1.19	1.00	3.47	16.05	0.70	1336.18	23.52
Mean	1385.01	1253.24	0.90	1.39	1.25	4.04	13.89	0.54	1328.33	18.43
SD	210.34	297.63	0.10	0.21	0.30	0.61	1.52	0.08	7.00	2.57
COV%	15.19	23.75	11.38	15.19	23.75	15.19	10.94	15.05	0.53	13.97
Femoral Condyle Lateral Superior	1788.10	725.20	0.41	1.79	0.73	5.22	9.57	0.47	1340.73	15.51
	1509.81	489.33	0.32	1.51	0.49	4.41	10.25	0.43	1330.41	14.51
	1485.38	400.18	0.27	1.49	0.40	4.34	10.58	0.50	1326.79	16.38
	1406.37	349.41	0.25	1.41	0.35	4.11	13.63	0.53	1309.04	17.67
	1427.49	318.91	0.22	1.43	0.32	4.17	12.27	0.66	1333.67	21.13
	1463.91	341.72	0.23	1.46	0.34	4.27	12.00	0.47	1316.60	15.72

	1438.65	358.12	0.25	1.44	0.36	4.20	13.90	0.52	1322.71	17.73
	1216.38	333.87	0.27	1.22	0.33	3.55	13.02	0.49	1319.75	16.59
	1101.29	344.58	0.31	1.10	0.34	3.22	13.01	0.46	1317.79	15.68
	1086.80	399.69	0.37	1.09	0.40	3.17	11.95	0.51	1316.44	16.79
Mean	1392.42	406.10	0.29	1.39	0.41	4.07	12.02	0.50	1323.39	16.77
SD	209.98	122.52	0.06	0.21	0.12	0.61	1.47	0.06	9.50	1.82
COV%	15.08	30.17	20.86	15.08	30.17	15.08	12.21	12.74	0.72	10.87
Tibial Plateau Medial Anterior	1683.82	1925.44	1.14	1.68	1.93	4.92	13.85	0.50	1304.65	16.84
	1741.93	1650.07	0.95	1.74	1.65	5.09	14.25	0.50	1314.49	17.08
	2005.47	1745.34	0.87	2.01	1.75	5.86	14.05	0.49	1310.38	16.55
	1794.91	1615.76	0.90	1.79	1.62	5.24	12.64	0.50	1315.09	16.60
	1665.57	1714.89	1.03	1.67	1.71	4.86	16.88	0.57	1306.23	19.40
	1472.68	1741.65	1.18	1.47	1.74	4.30	16.07	0.56	1304.94	18.86
	1576.42	1776.49	1.13	1.58	1.78	4.60	19.27	0.56	1302.55	19.51
	1693.89	1783.03	1.05	1.69	1.78	4.95	17.26	0.62	1318.47	21.06
	1807.48	1700.51	0.94	1.81	1.70	5.28	14.07	0.44	1296.19	14.83
	1842.22	1699.90	0.92	1.84	1.70	5.38	16.80	0.57	1311.20	19.55
Mean	1728.44	1735.31	1.01	1.73	1.74	5.05	15.51	0.53	1308.42	18.03
SD	147.65	84.79	0.11	0.15	0.08	0.43	2.05	0.05	6.74	1.92
COV%	8.54	4.89	11.00	8.54	4.89	8.54	13.21	10.18	0.52	10.64
Tibial Plateau Medial Posterior	1702.31	490.63	0.29	1.70	0.49	4.97	14.11	0.51	1301.14	16.90
	1984.32	575.69	0.29	1.98	0.58	5.79	11.41	0.46	1303.45	15.03
	1905.29	587.56	0.31	1.91	0.59	5.56	11.81	0.51	1302.34	16.37
	1346.62	414.72	0.31	1.35	0.41	3.93	17.55	0.65	1308.15	21.61
	1897.00	721.74	0.38	1.90	0.72	5.54	11.97	0.51	1308.74	16.72
	1863.92	679.32	0.36	1.86	0.68	5.44	15.77	0.64	1311.17	21.12

	1857.40	632.71	0.34	1.86	0.63	5.42	11.71	0.42	1318.95	14.42
	1852.07	540.93	0.29	1.85	0.54	5.41	15.53	0.47	1310.12	16.40
	2072.79	579.41	0.28	2.07	0.58	6.05	15.38	0.54	1303.50	18.02
	1889.08	511.44	0.27	1.89	0.51	5.52	14.62	0.52	1311.84	17.64
Mean	1837.08	573.41	0.31	1.84	0.57	5.36	13.98	0.52	1307.94	17.42
SD	196.71	90.62	0.04	0.20	0.09	0.57	2.14	0.07	5.47	2.34
COV%	10.71	15.80	11.87	10.71	15.80	10.71	15.31	13.74	0.42	13.43
Tibial Plateau Lateral Anterior	233.62	678.97	2.91	0.23	0.68	0.68	14.48	0.41	1304.29	14.44
	438.70	715.46	1.63	0.44	0.72	1.28	15.31	0.42	1323.14	15.16
	651.85	601.44	0.92	0.65	0.60	1.90	13.36	0.58	1321.90	19.28
	820.30	638.19	0.78	0.82	0.64	2.40	18.73	0.59	1297.97	20.13
	880.90	529.84	0.60	0.88	0.53	2.57	12.00	0.45	1314.35	15.14
	770.18	455.39	0.59	0.77	0.46	2.25	16.53	0.68	1311.35	22.29
	825.24	478.33	0.58	0.83	0.48	2.41	14.95	0.57	1310.57	19.09
	742.91	546.18	0.74	0.74	0.55	2.17	13.50	0.53	1313.55	17.79
	651.63	573.08	0.88	0.65	0.57	1.90	15.17	0.57	1311.46	19.08
	607.86	625.10	1.03	0.61	0.63	1.77	17.49	0.54	1314.73	18.83
Mean	662.32	584.20	1.07	0.66	0.58	1.93	15.15	0.53	1312.33	18.12
SD	198.43	83.94	0.72	0.20	0.08	0.58	2.02	0.08	7.42	2.50
COV%	29.96	14.37	67.35	29.96	14.37	29.96	13.31	15.71	0.57	13.82
Tibial Plateau Lateral Posterior	715.85	431.19	0.60	0.72	0.43	2.09	15.11	0.51	1295.81	16.97
	552.70	415.18	0.75	0.55	0.42	1.61	15.77	0.54	1304.55	18.28
	614.93	483.26	0.79	0.61	0.48	1.80	18.54	0.63	1304.61	21.32
	599.82	486.58	0.81	0.60	0.49	1.75	18.27	0.65	1291.53	21.42
	593.89	492.31	0.83	0.59	0.49	1.73	13.42	0.42	1311.38	14.67
	508.57	451.62	0.89	0.51	0.45	1.49	14.36	0.43	1311.12	15.00

	353.07	328.52	0.93	0.35	0.33	1.03	15.93	0.49	1318.46	17.35
	319.33	302.70	0.95	0.32	0.30	0.93	20.86	0.71	1292.52	23.47
	284.33	325.28	1.14	0.28	0.33	0.83	14.91	0.55	1298.75	18.06
	356.39	337.21	0.95	0.36	0.34	1.04	18.08	0.55	1311.59	19.03
Mean	489.89	405.39	0.86	0.49	0.41	1.43	16.52	0.55	1304.03	18.56
SD	149.73	75.00	0.14	0.15	0.08	0.44	2.31	0.09	9.16	2.83
COV%	30.56	18.50	16.77	30.56	18.50	30.56	14.00	16.89	0.70	15.27
Mean	1302.50	1073.48	0.91	1.30	1.07	3.80	13.13	0.50	1327.16	17.06
SD	646.60	744.00	0.52	0.65	0.74	1.89	3.34	0.09	27.50	2.76
COV%	49.64	69.31	56.78	49.64	69.31	49.64	25.44	17.21	2.07	16.16

Table 2. Cartilage, subchondral bone and trabecular bone raw data for cadaver 2, 37 years.

	37, Female													
	Cartilage						Subchondral Bone				Trabecular Bone			
	G' kPa	G'' kPa	Tan Delta	G' MPa	G'' MPa	E MPa	E GPa	H GPa	D nm	Load mN	E GPa	H GPa	D nm	Load mN
Femoral Condyle Medial Inferior	2047.01	696.32	0.34	2.05	0.70	5.98	13.53	0.43	2174.80	40.50	14.72	0.59	1291.25	18.99
	2290.73	931.16	0.41	2.29	0.93	6.69	12.43	0.42	2193.23	39.64	13.32	0.49	1276.93	15.78
	2172.43	1051.90	0.48	2.17	1.05	6.34	13.68	0.51	2205.67	48.05	11.84	0.40	1281.74	12.96
	1881.20	1088.35	0.58	1.88	1.09	5.49	9.98	0.32	2197.97	30.67	11.38	0.44	1278.45	13.92
	1659.05	1266.12	0.76	1.66	1.27	4.84	11.54	0.37	2192.70	34.91	12.31	0.41	1295.82	13.84
	1656.07	1203.68	0.73	1.66	1.20	4.84	10.68	0.30	2187.10	29.33	7.96	0.45	1295.17	13.46
	1385.68	708.18	0.51	1.39	0.71	4.05	12.43	0.47	2195.34	43.41	10.18	0.35	1288.03	11.53
	2031.41	768.56	0.38	2.03	0.77	5.93	12.40	0.44	2205.06	42.02	11.63	0.36	1301.82	12.41
	2321.26	675.94	0.29	2.32	0.68	6.78	11.38	0.41	2221.14	39.38	13.83	0.45	1295.02	15.05
	2259.60	500.28	0.22	2.26	0.50	6.60	12.09	0.38	2186.25	36.18	10.82	0.35	1316.68	12.25
Mean	1970.44	889.05	0.47	1.97	0.89	5.75	12.01	0.41	2195.93	38.41	11.80	0.43	1292.09	14.02
SD	317.17	256.06	0.18	0.32	0.26	0.93	1.16	0.06	12.71	5.75	1.94	0.07	11.89	2.17
COV%	16.10	28.80	38.14	16.10	28.80	16.10	9.66	15.99	0.58	14.96	16.41	17.33	0.92	15.46
Femoral Condyle Medial Superior	1967.84	761.73	0.39	1.97	0.76	5.75	12.68	0.42	2213.12	40.21	16.67	0.65	1286.98	20.78
	2292.14	732.69	0.32	2.29	0.73	6.69	12.42	0.38	2203.42	37.24	12.87	0.46	1295.97	15.22
	2534.46	653.25	0.26	2.53	0.65	7.40	13.22	0.45	2221.59	43.42	11.90	0.42	1283.37	13.78
	2481.57	517.98	0.21	2.48	0.52	7.25	15.01	0.46	2192.17	43.84	13.32	0.53	1281.45	16.88
	2425.53	582.62	0.24	2.43	0.58	7.08	14.36	0.46	2192.72	43.92	11.81	0.46	1284.90	14.70
	1839.57	531.58	0.29	1.84	0.53	5.37	11.34	0.45	2195.30	40.97	14.64	0.56	1293.43	18.24

	1658.44	558.03	0.34	1.66	0.56	4.84	10.12	0.32	2178.98	30.55	11.51	0.46	1295.13	14.89
	1400.47	560.26	0.40	1.40	0.56	4.09	13.64	0.48	2177.04	44.32	12.51	0.54	1304.41	17.41
	1187.10	633.70	0.53	1.19	0.63	3.47	15.07	0.55	2185.26	50.94	8.00	0.38	1297.16	11.85
	1118.06	832.92	0.75	1.12	0.83	3.26	12.66	0.48	2176.59	43.90	12.75	0.48	1290.10	15.63
Mean	1890.52	636.48	0.37	1.89	0.64	5.52	13.05	0.44	2193.62	41.93	12.60	0.49	1291.29	15.94
SD	538.07	107.36	0.16	0.54	0.11	1.57	1.57	0.06	15.32	5.33	2.23	0.08	7.21	2.50
COV%	28.46	16.87	43.39	28.46	16.87	28.46	12.04	13.66	0.70	12.72	17.72	15.54	0.56	15.70
Femoral Condyle Lateral Inferior	989.06	465.08	0.47	0.99	0.47	2.89	16.78	0.66	2210.68	61.71	13.06	0.47	1308.12	15.93
	1009.83	514.09	0.51	1.01	0.51	2.95	13.76	0.45	2186.87	42.63	12.71	0.49	1310.04	16.35
	1063.49	617.13	0.58	1.06	0.62	3.11	13.73	0.51	2214.49	48.03	11.46	0.60	1312.50	18.61
	903.24	527.07	0.58	0.90	0.53	2.64	13.13	0.41	2206.84	39.43	9.38	0.53	1301.36	15.78
	1019.52	680.87	0.67	1.02	0.68	2.98	13.97	0.56	2231.94	53.33	20.73	1.05	1290.46	31.87
	875.41	527.46	0.60	0.88	0.53	2.56	13.96	0.51	2215.33	48.54	13.18	0.51	1279.52	16.08
	833.15	459.36	0.55	0.83	0.46	2.43	13.32	0.43	2196.55	41.29	14.63	0.50	1296.98	16.75
	873.24	473.17	0.54	0.87	0.47	2.55	13.19	0.42	2221.86	41.28	12.67	0.35	1289.43	11.94
	994.66	560.94	0.56	0.99	0.56	2.90	13.13	0.45	2231.17	43.92	15.63	0.48	1316.65	16.84
	920.99	479.45	0.52	0.92	0.48	2.69	13.20	0.41	2166.58	38.24	20.04	0.42	1290.14	14.88
Mean	948.26	530.46	0.56	0.95	0.53	2.77	13.82	0.48	2208.23	45.84	14.35	0.54	1299.52	17.50
SD	76.68	71.93	0.05	0.08	0.07	0.22	1.09	0.08	20.27	7.26	3.60	0.19	12.15	5.32
COV%	8.09	13.56	9.82	8.09	13.56	8.09	7.92	17.00	0.92	15.84	25.07	35.54	0.93	30.42
Femoral Condyle Lateral Superior	1653.46	553.03	0.33	1.65	0.55	4.83	9.38	0.29	2142.14	26.69	12.40	0.57	1291.79	17.69
	1504.57	505.58	0.34	1.50	0.51	4.39	10.05	0.35	2159.34	32.09	9.59	0.33	1268.70	10.50
	1533.45	533.00	0.35	1.53	0.53	4.48	13.01	0.47	2133.80	41.56	9.88	0.40	1284.78	12.76
	1504.82	538.97	0.36	1.50	0.54	4.39	11.08	0.44	2134.43	37.98	10.94	0.50	1288.00	15.52
	1543.18	572.63	0.37	1.54	0.57	4.51	14.48	0.45	2116.56	40.50	13.50	0.60	1297.92	19.00
	1448.68	516.52	0.36	1.45	0.52	4.23	12.62	0.37	2123.09	33.93	14.51	0.58	1281.72	18.39

	1505.78	531.45	0.35	1.51	0.53	4.40	13.39	0.45	2122.66	39.94	12.13	0.39	1276.16	12.88
	1614.55	588.37	0.36	1.61	0.59	4.71	12.81	0.44	2131.72	38.95	15.02	0.47	1287.00	15.65
	1522.98	551.75	0.36	1.52	0.55	4.45	12.65	0.43	2135.44	38.54	16.39	0.45	1261.96	14.82
	1440.53	540.53	0.38	1.44	0.54	4.21	11.64	0.40	2151.39	36.36	14.03	0.42	1277.85	13.90
Mean	1527.20	543.18	0.36	1.53	0.54	4.46	12.11	0.41	2135.06	36.65	12.84	0.47	1281.59	15.11
SD	65.86	24.65	0.01	0.07	0.02	0.19	1.57	0.06	13.16	4.57	2.25	0.09	10.78	2.71
COV%	4.31	4.54	3.80	4.31	4.54	4.31	12.93	13.56	0.62	12.47	17.53	19.12	0.84	17.95
Tibial Plateau Medial Anterior	218.82	50.36	0.23	0.22	0.05	0.64	8.96	0.40	2186.36	35.33	14.48	0.56	1291.94	18.09
	138.09	30.69	0.22	0.14	0.03	0.40	8.97	0.37	2167.93	32.93	15.39	0.49	1313.24	17.07
	91.86	21.01	0.23	0.09	0.02	0.27	8.17	0.34	2202.60	31.16	11.88	0.32	1308.27	11.28
	178.15	43.41	0.24	0.18	0.04	0.52	8.45	0.38	2187.87	33.46	13.88	0.46	1311.91	15.71
	252.75	70.77	0.28	0.25	0.07	0.74	8.51	0.49	2190.45	41.10	11.76	0.42	1311.04	14.15
	255.74	70.48	0.28	0.26	0.07	0.75	8.56	0.44	2134.55	35.71	13.04	0.50	1327.01	17.23
	82.92	20.27	0.24	0.08	0.02	0.24	8.46	0.40	2182.27	34.94	15.50	0.65	1343.83	22.39
	142.87	31.42	0.22	0.14	0.03	0.42	9.82	0.53	2214.38	46.04	11.00	0.39	1311.69	13.19
	124.01	26.22	0.21	0.12	0.03	0.36	8.55	0.41	2197.66	35.99	13.03	0.44	1307.11	14.98
	157.11	34.48	0.22	0.16	0.03	0.46	11.72	0.35	2121.45	31.39	11.16	0.40	1288.93	13.19
Mean	164.23	39.91	0.24	0.16	0.04	0.48	9.02	0.41	2178.55	35.80	13.11	0.46	1311.50	15.73
SD	61.50	18.63	0.02	0.06	0.02	0.18	1.05	0.06	29.51	4.58	1.67	0.09	15.67	3.16
COV%	37.45	46.69	10.02	37.45	46.69	37.45	11.69	15.00	1.35	12.79	12.71	20.31	1.20	20.07
Tibial Plateau Medial Posterior	730.57	254.71	0.35	0.73	0.25	2.13	12.02	0.44	2191.97	41.12	13.83	0.44	1293.86	14.95
	678.83	244.76	0.36	0.68	0.24	1.98	12.23	0.42	2200.56	40.20	15.02	0.50	1302.55	17.02
	344.34	114.96	0.33	0.34	0.11	1.01	11.65	0.41	2163.58	37.25	12.47	0.42	1296.97	14.01
	369.97	129.87	0.35	0.37	0.13	1.08	9.87	0.22	2170.36	22.02	13.01	0.44	1296.81	14.85
	647.45	249.24	0.39	0.65	0.25	1.89	11.20	0.37	2211.16	35.71	9.44	0.27	1277.86	8.93
	1030.17	431.17	0.42	1.03	0.43	3.01	10.59	0.35	2181.58	33.18	5.59	0.30	1290.40	9.07

	992.34	369.45	0.37	0.99	0.37	2.90	9.98	0.26	2181.26	25.07	12.97	0.47	1297.59	15.56
	1046.82	345.22	0.33	1.05	0.35	3.06	11.38	0.37	2207.86	35.90	12.28	0.44	1301.76	14.64
	1370.37	449.93	0.33	1.37	0.45	4.00	9.26	0.27	2178.64	26.01	11.44	0.32	1273.44	10.74
	1384.19	455.46	0.33	1.38	0.46	4.04	11.40	0.42	2226.65	40.40	11.99	0.46	1303.68	15.17
Mean	859.50	304.48	0.36	0.86	0.30	2.51	10.96	0.35	2191.36	33.68	11.80	0.41	1293.49	13.49
SD	367.79	125.34	0.03	0.37	0.13	1.07	0.99	0.08	19.91	6.94	2.63	0.08	10.28	2.85
COV%	42.79	41.16	8.29	42.79	41.16	42.79	9.05	21.88	0.91	20.61	22.30	19.64	0.79	21.12
Tibial Plateau Lateral Anterior	91.79	20.40	0.22	0.09	0.02	0.27	13.29	0.49	2178.71	45.26	14.66	0.50	1297.85	16.83
	96.56	22.07	0.23	0.10	0.02	0.28	14.00	0.54	2187.98	49.65	14.39	0.47	1268.36	15.13
	99.06	21.85	0.22	0.10	0.02	0.29	10.97	0.33	2187.56	31.52	13.32	0.39	1268.53	12.90
	119.35	27.01	0.23	0.12	0.03	0.35	12.48	0.40	2175.96	37.22	12.82	0.38	1302.35	13.03
	153.52	33.96	0.22	0.15	0.03	0.45	13.22	0.48	2169.57	43.55	12.43	0.58	1297.24	18.11
	157.09	41.00	0.26	0.16	0.04	0.46	12.62	0.49	2204.47	45.63	12.50	0.35	1290.96	11.95
	219.77	57.23	0.26	0.22	0.06	0.64	11.71	0.40	2190.63	38.01	16.28	0.63	1304.62	20.67
	274.51	61.71	0.23	0.27	0.06	0.80	10.86	0.41	2185.90	37.82	8.01	0.20	1269.96	6.61
	191.34	45.01	0.24	0.19	0.05	0.56	15.47	0.61	2185.67	55.37	5.91	0.11	1275.67	3.97
	181.99	44.28	0.24	0.18	0.04	0.53	11.53	0.43	2195.68	40.08	12.92	0.47	1295.77	15.44
Mean	158.50	37.45	0.23	0.16	0.04	0.46	12.62	0.46	2186.21	42.41	12.32	0.41	1287.13	13.46
SD	59.84	14.86	0.02	0.06	0.01	0.17	1.44	0.08	9.92	6.93	3.11	0.16	14.79	5.07
COV%	37.75	39.69	6.58	37.75	39.69	37.75	11.42	17.61	0.45	16.33	25.20	39.24	1.15	37.67
Tibial Plateau Lateral Posterior	547.75	161.89	0.30	0.55	0.16	1.60	10.06	0.43	2160.12	37.54	12.31	0.44	1287.27	14.48
	550.38	201.72	0.37	0.55	0.20	1.61	13.28	0.47	2191.54	44.31	9.09	0.46	1314.18	14.55
	1153.58	761.88	0.66	1.15	0.76	3.37	13.89	0.48	2186.50	44.64	4.45	0.15	1273.38	4.83
	615.78	334.78	0.54	0.62	0.33	1.80	9.44	0.29	2174.62	27.76	5.01	0.36	1281.84	9.70
	490.46	526.36	1.07	0.49	0.53	1.43	9.08	0.30	2177.15	28.08	6.72	0.45	1292.48	12.66
	418.88	528.30	1.26	0.42	0.53	1.22	13.35	0.45	2135.33	40.34	8.59	0.34	1310.66	11.28

	397.84	547.76	1.38	0.40	0.55	1.16	12.35	0.43	2177.58	39.80	10.30	0.35	1308.05	11.90
	551.78	563.90	1.02	0.55	0.56	1.61	14.42	0.45	2193.25	43.22	13.88	0.60	1321.29	19.73
	61.58	24.37	0.40	0.06	0.02	0.18	12.72	0.44	2193.68	41.31	12.25	0.39	1298.60	13.36
	47.54	18.00	0.38	0.05	0.02	0.14	12.75	0.38	2160.23	35.77	12.21	0.51	1306.25	16.70
Mean	483.55	366.90	0.74	0.48	0.37	1.41	12.13	0.41	2175.00	38.28	9.48	0.41	1299.40	12.92
SD	309.02	255.69	0.41	0.31	0.26	0.90	1.91	0.07	18.60	6.13	3.28	0.12	15.37	4.02
COV%	63.90	69.69	55.31	63.90	69.69	63.90	15.71	16.08	0.86	16.03	34.63	29.66	1.18	31.13
Mean	1000.28	418.49	0.42	1.00	0.42	2.92	11.96	0.42	2182.99	39.13	12.29	0.45	1294.50	14.77
SD	736.32	307.97	0.23	0.74	0.31	2.15	1.90	0.08	27.10	6.87	2.87	0.12	14.73	3.79
COV%	73.61	73.59	54.68	73.61	73.59	73.61	15.88	17.91	1.24	17.55	23.32	26.91	1.14	25.62

Table 3. Cartilage, subchondral bone and trabecular bone raw data for cadaver 3, 43 years.

	43, Female													
	Cartilage						Subchondral Bone				Trabecular Bone			
	G' kPa	G'' kPa	Tan Delta	G' MPa	G'' MPa	E MPa	E GPa	H GPa	D nm	Load mN	E GPa	H GPa	D nm	Load mN
Femoral Condyle Medial Inferior	1554.52	1700.29	1.09	1.55	1.70	4.54	9.99	0.28	2215.61	27.78	11.60	0.53	1295.95	16.73
	1611.93	1712.88	1.06	1.61	1.71	4.71	11.94	0.40	2217.27	38.96	9.63	0.36	1292.18	11.87
	1572.22	1617.03	1.03	1.57	1.62	4.59	15.41	0.61	2214.75	57.03	11.43	0.38	1289.94	12.67
	1356.84	1165.31	0.86	1.36	1.17	3.96	13.07	0.45	2234.44	44.37	12.00	0.38	1292.77	12.77
	1270.92	1065.26	0.84	1.27	1.07	3.71	11.38	0.39	2197.70	36.58	9.50	0.34	1303.64	11.32
	1315.94	1224.50	0.93	1.32	1.22	3.84	15.72	0.57	2190.55	52.75	8.61	0.27	1292.88	9.24
	1331.02	1225.29	0.92	1.33	1.23	3.89	12.53	0.41	2216.91	39.59	4.17	0.38	1289.83	9.46
	1441.04	1510.31	1.05	1.44	1.51	4.21	12.87	0.40	2224.23	39.27	11.20	0.41	1297.66	13.59
	1509.94	1541.02	1.02	1.51	1.54	4.41	11.87	0.38	2222.96	37.18	13.15	0.50	1309.65	16.82
	1525.26	1441.91	0.95	1.53	1.44	4.45	14.20	0.49	2218.43	47.17	12.74	0.54	1322.18	17.96
Mean	1448.96	1420.38	0.97	1.45	1.42	4.23	12.90	0.44	2215.29	42.07	10.40	0.41	1298.67	13.24
SD	122.15	234.11	0.09	0.12	0.23	0.36	1.79	0.10	12.67	8.50	2.63	0.09	10.39	3.05
COV%	8.43	16.48	9.06	8.43	16.48	8.43	13.89	22.15	0.57	20.22	25.28	21.45	0.80	23.03
Femoral Condyle Medial Superior	368.70	1380.29	3.74	0.37	1.38	1.08	15.02	0.53	2180.04	49.24	9.28	0.42	1307.37	13.53
	118.93	1572.89	13.23	0.12	1.57	0.35	14.22	0.51	2194.18	47.92	9.13	0.42	1307.29	13.37
	254.95	1373.77	5.39	0.25	1.37	0.74	11.82	0.41	2205.88	38.66	10.49	0.54	1295.87	16.45
	185.80	1534.27	8.26	0.19	1.53	0.54	13.63	0.42	2182.94	39.91	5.33	0.22	1338.95	7.52
	291.14	1543.87	5.30	0.29	1.54	0.85	14.34	0.48	2225.56	47.13	11.87	0.44	1320.70	14.95
	119.07	1849.69	15.53	0.12	1.85	0.35	12.80	0.48	2223.37	45.86	12.58	0.46	1307.52	15.32

	401.45	1796.40	4.48	0.40	1.80	1.17	13.77	0.46	2217.89	44.61	15.92	0.63	1301.08	20.58
	678.76	1531.09	2.26	0.68	1.53	1.98	13.84	0.46	2215.49	44.61	14.55	0.56	1303.87	18.43
	803.59	1310.12	1.63	0.80	1.31	2.35	14.99	0.52	2202.69	49.30	12.56	0.51	1304.60	16.74
	362.46	1449.03	4.00	0.36	1.45	1.06	12.35	0.41	2222.77	39.54	11.03	0.41	1314.29	13.89
Mean	358.49	1534.14	6.38	0.36	1.53	1.05	13.68	0.47	2207.08	44.68	11.27	0.46	1310.15	15.08
SD	226.68	175.36	4.62	0.23	0.18	0.66	1.07	0.05	16.81	4.02	2.99	0.11	12.19	3.50
COV%	63.23	11.43	72.41	63.23	11.43	63.23	7.80	9.92	0.76	9.00	26.55	24.19	0.93	23.19
Femoral Condyle Lateral Inferior	1204.13	244.57	0.20	1.20	0.24	3.52	11.39	0.37	2203.45	35.80	14.04	0.46	1286.66	15.17
	1192.60	227.87	0.19	1.19	0.23	3.48	12.93	0.45	2220.34	43.24	11.73	0.39	1280.59	12.66
	1391.43	265.34	0.19	1.39	0.27	4.06	9.74	0.37	2208.66	34.73	10.17	0.33	1286.81	11.09
	1365.24	264.39	0.19	1.37	0.26	3.99	11.48	0.39	2181.72	36.48	7.49	0.32	1273.32	9.85
	1528.21	301.78	0.20	1.53	0.30	4.46	11.78	0.35	2215.87	34.34	8.31	0.27	1289.14	9.12
	1631.85	323.99	0.20	1.63	0.32	4.76	11.52	0.34	2215.62	33.92	6.92	0.42	1300.22	12.33
	1080.29	244.00	0.23	1.08	0.24	3.15	11.29	0.34	2206.06	32.84	4.33	0.29	1259.66	7.80
	1354.17	290.50	0.22	1.35	0.29	3.95	11.91	0.42	2215.77	40.15	10.10	0.60	1317.96	18.26
	1034.66	253.39	0.25	1.03	0.25	3.02	12.52	0.40	2217.99	39.29	12.67	0.42	1285.62	13.84
	854.09	207.05	0.24	0.85	0.21	2.49	11.69	0.37	2207.60	35.82	11.60	0.37	1291.02	12.51
Mean	1263.67	262.29	0.21	1.26	0.26	3.69	11.62	0.38	2209.31	36.66	9.74	0.39	1287.10	12.26
SD	236.36	35.18	0.02	0.24	0.04	0.69	0.84	0.04	11.21	3.25	2.97	0.10	15.39	3.06
COV%	18.70	13.41	9.83	18.70	13.41	18.70	7.22	9.39	0.51	8.86	30.46	24.85	1.20	24.93
Femoral Condyle Lateral Superior	1738.89	892.91	0.51	1.74	0.89	5.08	8.88	0.29	2174.92	27.51	11.62	0.57	1277.37	16.99
	1461.44	735.11	0.50	1.46	0.74	4.27	8.73	0.32	2169.97	28.84	12.40	0.46	1274.04	14.49
	1465.86	745.57	0.51	1.47	0.75	4.28	9.61	0.32	2177.07	30.19	14.93	0.54	1280.55	17.53
	1512.58	851.17	0.56	1.51	0.85	4.42	9.49	0.33	2173.72	30.19	16.50	0.59	1269.78	18.62
	1447.09	796.31	0.55	1.45	0.80	4.23	7.64	0.24	2191.84	23.06	11.14	0.40	1283.24	13.00
	1244.35	689.10	0.55	1.24	0.69	3.63	8.66	0.31	2229.65	29.69	6.46	0.41	1258.47	11.16

	1356.45	824.22	0.61	1.36	0.82	3.96	8.62	0.33	2216.53	30.76	10.67	0.44	1296.41	14.04
	1191.50	760.32	0.64	1.19	0.76	3.48	9.18	0.44	2225.45	39.80	10.73	0.34	1280.22	11.13
	1355.12	977.10	0.72	1.36	0.98	3.96	9.97	0.41	2221.52	38.48	9.20	0.51	1307.28	15.46
	1202.17	1019.62	0.85	1.20	1.02	3.51	9.24	0.36	2205.05	33.19	11.99	0.53	1284.58	16.54
Mean	1397.54	829.14	0.60	1.40	0.83	4.08	9.00	0.33	2198.57	31.17	11.56	0.48	1281.19	14.90
SD	166.18	107.50	0.11	0.17	0.11	0.49	0.65	0.06	23.76	4.95	2.79	0.08	13.51	2.60
COV%	11.89	12.96	18.31	11.89	12.96	11.89	7.25	17.19	1.08	15.89	24.11	17.10	1.05	17.46
Tibial Plateau Medial Anterior	156.81	42.86	0.27	0.16	0.04	0.46	11.34	0.37	2208.34	35.70	14.31	0.44	1311.42	15.27
	144.79	38.74	0.27	0.14	0.04	0.42	11.06	0.38	2252.65	37.50	13.24	0.46	1318.09	15.81
	106.37	28.57	0.27	0.11	0.03	0.31	12.15	0.41	2210.84	39.39	14.66	0.54	1312.66	18.13
	115.37	32.21	0.28	0.12	0.03	0.34	11.26	0.38	2195.03	36.14	14.94	0.50	1311.72	17.19
	98.98	25.72	0.26	0.10	0.03	0.29	13.56	0.44	2185.00	41.75	17.57	0.66	1338.61	22.96
	84.77	23.12	0.27	0.08	0.02	0.25	12.06	0.39	2189.32	37.09	14.01	0.47	1311.54	16.01
	76.34	18.28	0.24	0.08	0.02	0.22	13.48	0.51	2181.03	46.41	14.58	0.53	1313.74	17.82
	124.38	29.75	0.24	0.12	0.03	0.36	11.36	0.37	2168.28	34.79	13.16	0.39	1324.24	13.85
	149.49	34.86	0.23	0.15	0.03	0.44	12.24	0.37	2164.73	34.79	16.25	0.53	1329.05	18.74
	105.74	24.99	0.24	0.11	0.02	0.31	13.07	0.48	2183.80	44.21	13.05	0.45	1314.13	15.42
Mean	116.30	29.91	0.26	0.12	0.03	0.34	12.16	0.41	2193.90	38.78	14.58	0.50	1318.52	17.12
SD	27.33	7.46	0.02	0.03	0.01	0.08	0.94	0.05	25.44	4.08	1.43	0.07	9.24	2.54
COV%	23.50	24.93	7.03	23.50	24.93	23.50	7.70	12.00	1.16	10.52	9.82	14.90	0.70	14.85
Tibial Plateau Medial Posterior	832.49	461.08	0.55	0.83	0.46	2.43	12.33	0.37	2214.80	36.29	9.83	0.29	1314.61	10.33
	753.99	352.00	0.47	0.75	0.35	2.20	14.01	0.49	2217.74	46.94	12.16	0.46	1304.14	15.32
	725.63	305.78	0.42	0.73	0.31	2.12	14.50	0.50	2198.45	46.93	15.57	0.53	1301.72	17.96
	738.06	305.10	0.41	0.74	0.31	2.16	12.70	0.40	2178.42	37.92	12.58	0.50	1317.44	16.84
	512.93	196.71	0.38	0.51	0.20	1.50	11.29	0.35	2207.44	34.24	15.90	0.68	1315.18	22.31
	332.08	117.32	0.35	0.33	0.12	0.97	12.13	0.39	2190.52	37.38	13.00	0.46	1292.08	15.21

	165.51	47.36	0.29	0.17	0.05	0.48	12.11	0.39	2208.14	37.87	14.30	0.40	1307.09	13.96
	176.60	47.73	0.27	0.18	0.05	0.52	11.42	0.34	2240.44	33.87	14.39	0.53	1308.88	17.84
	119.02	30.57	0.26	0.12	0.03	0.35	12.06	0.40	2216.86	38.38	15.83	0.58	1302.13	19.31
	99.83	23.08	0.23	0.10	0.02	0.29	12.08	0.31	2159.63	30.08	13.14	0.48	1297.34	15.86
Mean	445.61	188.67	0.36	0.45	0.19	1.30	12.46	0.39	2203.24	37.99	13.67	0.49	1306.06	16.49
SD	298.73	158.31	0.10	0.30	0.16	0.87	1.04	0.06	22.75	5.35	1.92	0.10	8.19	3.23
COV%	67.04	83.91	28.54	67.04	83.91	67.04	8.31	15.02	1.03	14.07	14.03	21.08	0.63	19.56
Tibial Plateau Lateral Anterior	1469.22	593.41	0.40	1.47	0.59	4.29	12.37	0.38	2184.15	36.61	9.82	0.55	1300.38	16.54
	1446.28	608.26	0.42	1.45	0.61	4.22	13.61	0.49	2183.16	45.24	10.11	0.54	1299.00	16.35
	862.90	310.30	0.36	0.86	0.31	2.52	11.12	0.44	2229.75	41.50	12.59	0.55	1305.70	17.82
	1494.52	524.38	0.35	1.49	0.52	4.36	11.29	0.43	2217.81	40.80	5.97	0.39	1280.54	10.88
	1483.75	587.78	0.40	1.48	0.59	4.33	10.16	0.38	2232.34	36.36	7.83	0.45	1303.75	13.58
	1700.07	571.73	0.34	1.70	0.57	4.96	11.55	0.49	2249.51	46.84	8.03	0.51	1302.81	14.85
	1428.43	468.47	0.33	1.43	0.47	4.17	12.83	0.51	2207.38	47.53	7.11	0.37	1289.10	11.12
	1527.55	514.03	0.34	1.53	0.51	4.46	11.88	0.40	2194.13	37.83	10.94	0.49	1285.74	15.19
	1436.15	472.85	0.33	1.44	0.47	4.19	11.45	0.44	2192.06	40.43	13.71	0.55	1319.02	18.49
	1266.51	407.22	0.32	1.27	0.41	3.70	11.33	0.44	2218.33	41.15	14.16	0.59	1305.85	19.30
Mean	1411.54	505.84	0.36	1.41	0.51	4.12	11.76	0.44	2210.86	41.43	10.03	0.50	1299.19	15.41
SD	220.17	94.32	0.04	0.22	0.09	0.64	0.97	0.05	22.47	4.01	2.83	0.07	11.28	2.89
COV%	15.60	18.65	9.99	15.60	18.65	15.60	8.25	10.53	1.02	9.67	28.18	14.92	0.87	18.77
Tibial Plateau Lateral Posterior	976.83	357.71	0.37	0.98	0.36	2.85	11.53	0.38	2189.24	35.80	13.36	0.50	1297.42	16.55
	546.14	158.17	0.29	0.55	0.16	1.59	9.82	0.34	2254.49	33.85	10.70	0.39	1286.61	12.69
	390.24	113.26	0.29	0.39	0.11	1.14	11.03	0.40	2218.62	37.85	11.07	0.51	1298.55	16.07
	680.59	222.19	0.33	0.68	0.22	1.99	12.82	0.46	2217.05	43.78	10.65	0.40	1295.96	12.99
	945.28	331.53	0.35	0.95	0.33	2.76	12.10	0.43	2213.80	41.14	9.48	0.38	1288.09	12.23
	1079.46	372.80	0.35	1.08	0.37	3.15	10.84	0.29	2145.24	27.51	12.09	0.73	1318.59	21.99

	1078.35	352.93	0.33	1.08	0.35	3.15	11.58	0.42	2201.95	39.50	12.77	0.46	1307.70	15.42
	580.23	163.20	0.28	0.58	0.16	1.69	12.07	0.44	2207.62	41.24	16.01	0.74	1331.83	24.35
	703.52	193.30	0.28	0.70	0.19	2.05	12.54	0.49	2226.69	46.76	13.85	0.56	1320.80	18.83
	538.84	138.96	0.26	0.54	0.14	1.57	11.42	0.35	2204.80	33.68	11.03	0.37	1315.10	12.82
Mean	751.95	240.40	0.31	0.75	0.24	2.20	11.57	0.40	2207.95	38.11	12.10	0.50	1306.07	16.39
SD	248.84	102.19	0.04	0.25	0.10	0.73	0.88	0.06	28.04	5.61	1.93	0.14	15.12	4.18
COV%	33.09	42.51	11.82	33.09	42.51	33.09	7.60	15.28	1.27	14.72	15.94	27.02	1.16	25.47
Mean	899.26	626.35	1.18	0.90	0.63	2.63	11.89	0.41	2205.78	38.86	11.67	0.47	1300.87	15.11
SD	550.46	558.88	2.53	0.55	0.56	1.61	1.64	0.07	21.24	6.27	2.88	0.10	16.31	3.41
COV%	61.21	89.23	214.02	61.21	89.23	61.21	13.83	16.81	0.96	16.14	24.72	21.92	1.25	22.53

Table 4. Cartilage, subchondral bone and trabecular bone raw data for cadaver 4, 49 years.

	49, Male									
	Cartilage						Trabecular Bone			
	G' kPa	G'' kPa	Tan Delta	G' MPa	G'' MPa	E MPa	E GPa	H GPa	D nm	Load mN
Femoral Condyle Medial Inferior	2,619.97	1,266.88	0.48	2.62	1.27	7.65	14.58	0.52	1,310.14	17.70
	1,956.39	938.75	0.48	1.96	0.94	5.71	14.13	0.52	1,323.13	17.77
	1,528.28	799.02	0.52	1.53	0.80	4.46	10.58	0.51	1,326.51	16.53
	1,539.69	689.00	0.45	1.54	0.69	4.50	12.54	0.47	1,324.99	16.20
	1,591.22	847.77	0.53	1.59	0.85	4.65	10.91	0.52	1,328.39	16.98
	1,756.89	899.47	0.51	1.76	0.90	5.13	12.02	0.50	1,346.19	17.39
	1,667.40	902.01	0.54	1.67	0.90	4.87	14.54	0.53	1,327.80	18.35
	1,953.89	987.94	0.51	1.95	0.99	5.71	13.89	0.56	1,319.95	18.84
	2,005.51	856.98	0.43	2.01	0.86	5.86	14.52	0.59	1,342.19	20.34
	1,004.66	315.73	0.31	1.00	0.32	2.93	8.57	0.49	1,325.08	15.09
Mean	1,762.39	850.36	0.48	1.76	0.85	5.15	12.63	0.52	1,327.44	17.52
SD	419.76	240.34	0.07	0.42	0.24	1.23	2.08	0.03	10.31	1.47
COV%	23.82	28.26	14.23	23.82	28.26	23.82	16.47	6.52	0.78	8.38
Femoral Condyle Medial Superior	242.57	74.41	0.31	0.24	0.07	0.71	16.25	0.57	1,365.86	20.90
	426.01	140.06	0.33	0.43	0.14	1.24	15.31	0.68	1,332.76	22.63
	679.72	240.20	0.35	0.68	0.24	1.98	13.43	0.54	1,329.27	18.25
	565.71	224.85	0.40	0.57	0.22	1.65	15.13	0.62	1,332.81	21.16
	884.99	327.37	0.37	0.88	0.33	2.58	11.27	0.44	1,333.16	15.10
	980.40	370.92	0.38	0.98	0.37	2.86	14.81	0.54	1,323.23	18.63

	877.62	334.15	0.38	0.88	0.33	2.56	10.79	0.40	1,333.38	13.93
	818.54	304.11	0.37	0.82	0.30	2.39	8.96	0.59	1,327.86	17.54
	868.05	310.45	0.36	0.87	0.31	2.53	9.31	0.54	1,335.45	16.83
	905.50	340.83	0.38	0.91	0.34	2.64	14.99	0.50	1,319.76	17.36
Mean	724.91	266.73	0.36	0.72	0.27	2.12	13.03	0.54	1,333.35	18.23
SD	241.63	96.24	0.03	0.24	0.10	0.71	2.70	0.08	12.45	2.72
COV%	33.33	36.08	7.37	33.33	36.08	33.33	20.75	15.14	0.93	14.94
Femoral Condyle Lateral Inferior	218.08	188.25	0.86	0.22	0.19	0.64	11.79	0.52	1,338.90	17.65
	218.07	162.83	0.75	0.22	0.16	0.64	14.52	0.55	1,351.91	19.62
	216.86	141.26	0.65	0.22	0.14	0.63	12.69	0.57	1,367.68	19.96
	355.79	315.71	0.89	0.36	0.32	1.04	13.07	0.50	1,350.51	17.62
	394.23	333.29	0.85	0.39	0.33	1.15	12.78	0.55	1,363.94	19.27
	438.59	410.50	0.94	0.44	0.41	1.28	13.00	0.58	1,356.60	20.12
	384.28	367.23	0.96	0.38	0.37	1.12	14.06	0.55	1,375.38	20.06
	353.05	384.33	1.09	0.35	0.38	1.03	13.24	0.57	1,395.84	21.07
	320.19	368.62	1.15	0.32	0.37	0.93	13.51	0.52	1,374.13	18.97
	289.48	332.16	1.15	0.29	0.33	0.85	10.44	0.55	1,372.96	18.62
Mean	318.86	300.42	0.93	0.32	0.30	0.93	12.91	0.55	1,364.79	19.30
SD	80.56	98.57	0.17	0.08	0.10	0.24	1.15	0.03	16.15	1.11
COV%	25.27	32.81	17.86	25.27	32.81	25.27	8.88	4.88	1.18	5.73
Femoral Condyle Lateral Superior	1,075.78	754.29	0.70	1.08	0.75	3.14	16.75	0.68	1,314.99	22.64
	884.16	457.72	0.52	0.88	0.46	2.58	16.82	0.51	1,305.31	17.57
	642.40	282.99	0.44	0.64	0.28	1.88	10.97	0.31	1,305.24	10.81
	735.66	338.40	0.46	0.74	0.34	2.15	11.16	0.48	1,306.26	15.58
	657.77	297.71	0.45	0.66	0.30	1.92	15.90	0.47	1,310.99	16.33
	721.63	341.13	0.47	0.72	0.34	2.11	14.38	0.45	1,316.96	15.80

	904.03	486.65	0.54	0.90	0.49	2.64	15.17	0.55	1,299.09	18.29
	855.37	497.56	0.58	0.86	0.50	2.50	14.79	0.57	1,325.99	19.48
	791.93	456.84	0.58	0.79	0.46	2.31	11.97	0.48	1,318.14	16.10
	768.72	463.90	0.60	0.77	0.46	2.24	14.14	0.41	1,314.12	14.46
Mean	803.75	437.72	0.53	0.80	0.44	2.35	14.20	0.49	1,311.71	16.71
SD	130.50	137.59	0.08	0.13	0.14	0.38	2.16	0.10	7.90	3.14
COV%	16.24	31.43	15.46	16.24	31.43	16.24	15.24	20.27	0.60	18.78
Tibial Plateau Medial Anterior	139.89	32.60	0.23	0.14	0.03	0.41	14.24	0.56	1,318.72	18.94
	51.09	14.01	0.27	0.05	0.01	0.15	14.29	0.55	1,322.64	18.55
	58.99	16.01	0.27	0.06	0.02	0.17	17.13	0.63	1,322.33	21.63
	162.30	35.67	0.22	0.16	0.04	0.47	11.36	0.54	1,316.29	17.21
	231.97	50.98	0.22	0.23	0.05	0.68	7.30	0.49	1,313.99	14.12
	264.92	57.64	0.22	0.26	0.06	0.77	14.45	0.61	1,309.86	19.83
	236.06	46.36	0.20	0.24	0.05	0.69	16.11	0.63	1,323.09	21.26
	165.19	31.23	0.19	0.17	0.03	0.48	14.42	0.60	1,311.11	19.59
	288.59	58.16	0.20	0.29	0.06	0.84	15.13	0.56	1,318.66	18.91
	61.21	14.59	0.24	0.06	0.01	0.18	13.26	0.57	1,310.15	18.64
Mean	166.02	35.73	0.23	0.17	0.04	0.48	13.77	0.57	1,316.68	18.87
SD	88.45	17.21	0.03	0.09	0.02	0.26	2.75	0.05	5.21	2.11
COV%	53.27	48.18	12.77	53.27	48.18	53.27	19.94	7.90	0.40	11.20
Tibial Plateau Medial Posterior	254.66	330.14	1.30	0.25	0.33	0.74	13.19	0.49	1,311.79	16.44
	430.95	454.49	1.06	0.43	0.45	1.26	12.19	0.46	1,319.37	15.47
	623.11	662.09	1.06	0.62	0.66	1.82	18.30	0.68	1,312.34	22.87
	540.48	512.22	0.95	0.54	0.51	1.58	11.02	0.42	1,315.80	14.26
	487.70	423.00	0.87	0.49	0.42	1.42	8.13	0.45	1,322.85	14.06
	412.38	366.98	0.89	0.41	0.37	1.20	14.60	0.53	1,322.14	18.15

	467.27	393.18	0.84	0.47	0.39	1.36	14.43	0.60	1,324.24	20.09
	380.36	323.37	0.85	0.38	0.32	1.11	12.98	0.51	1,324.36	17.18
	495.39	393.25	0.79	0.50	0.39	1.45	17.67	0.66	1,334.80	23.02
	455.48	346.42	0.76	0.46	0.35	1.33	13.84	0.53	1,325.42	18.09
Mean	454.78	420.51	0.94	0.45	0.42	1.33	13.63	0.53	1,321.31	17.96
SD	98.05	102.95	0.16	0.10	0.10	0.29	2.97	0.09	6.87	3.20
COV%	21.56	24.48	17.22	21.56	24.48	21.56	21.80	16.56	0.52	17.83
Tibial Plateau Lateral Anterior	650.29	303.02	0.47	0.65	0.30	1.90	15.68	0.62	1,322.04	20.99
	687.93	271.56	0.40	0.69	0.27	2.01	13.68	0.55	1,340.84	19.07
	677.39	243.19	0.36	0.68	0.24	1.98	12.39	0.46	1,333.15	15.97
	671.61	241.38	0.36	0.67	0.24	1.96	13.63	0.57	1,324.59	19.18
	611.33	208.46	0.34	0.61	0.21	1.79	13.96	0.57	1,323.51	19.08
	509.59	156.06	0.31	0.51	0.16	1.49	12.28	0.50	1,326.58	16.81
	647.23	197.39	0.31	0.65	0.20	1.89	13.52	0.55	1,303.73	17.83
	687.22	190.28	0.28	0.69	0.19	2.01	12.79	0.55	1,335.05	18.68
	858.10	269.77	0.31	0.86	0.27	2.51	11.52	0.51	1,324.96	16.79
	766.72	217.67	0.28	0.77	0.22	2.24	14.18	0.63	1,324.04	20.73
Mean	676.74	229.88	0.34	0.68	0.23	1.98	13.36	0.55	1,325.85	18.51
SD	91.31	44.31	0.06	0.09	0.04	0.27	1.18	0.05	9.88	1.67
COV%	13.49	19.27	16.89	13.49	19.27	13.49	8.80	9.62	0.75	9.00
Tibial Plateau Lateral Posterior	303.97	85.13	0.28	0.30	0.09	0.89	11.97	0.50	1,297.80	16.03
	298.20	81.14	0.27	0.30	0.08	0.87	14.29	0.72	1,313.79	22.67
	333.90	86.92	0.26	0.33	0.09	0.97	12.98	0.55	1,350.20	18.97
	368.51	96.58	0.26	0.37	0.10	1.08	11.91	0.39	1,334.69	13.95
	395.04	110.94	0.28	0.40	0.11	1.15	14.55	0.53	1,314.98	18.03
	325.20	95.20	0.29	0.33	0.10	0.95	14.81	0.58	1,328.16	19.87

	156.13	35.82	0.23	0.16	0.04	0.46	9.86	0.42	1,337.94	14.30
	265.39	75.72	0.29	0.27	0.08	0.77	12.92	0.51	1,305.30	16.75
	160.69	38.44	0.24	0.16	0.04	0.47	14.94	0.58	1,311.87	19.38
	260.95	164.30	0.63	0.26	0.16	0.76	16.10	0.53	1,321.46	18.54
Mean	286.80	87.02	0.30	0.29	0.09	0.84	13.43	0.53	1,321.62	17.85
SD	79.31	36.28	0.12	0.08	0.04	0.23	1.85	0.09	16.09	2.66
COV%	27.65	41.70	38.48	27.65	41.70	27.65	13.80	17.16	1.22	14.91
Mean	649.28	328.55	0.51	0.65	0.33	1.90	13.37	0.54	1,327.84	18.12
SD	508.46	263.84	0.28	0.51	0.26	1.48	2.16	0.07	18.76	2.39
COV%	78.31	80.31	53.98	78.31	80.31	78.31	16.13	13.17	1.41	13.21

Table 5. Cartilage, subchondral bone and trabecular bone raw data for cadaver 5, 51 years.

	51, Male													
	Cartilage						Subchondral Bone				Trabecular Bone			
	G' kPa	G'' kPa	Tan Delta	G' MPa	G'' MPa	E MPa	E GPa	H GPa	D nm	Load mN	E GPa	H GPa	D nm	Load mN
Femoral Condyle Medial Inferior	338.46	106.68	0.32	0.34	0.11	0.99	16.12	0.49	2153.43	45.37	12.35	0.45	1305.79	14.93
	305.85	88.47	0.29	0.31	0.09	0.89	12.50	0.41	2169.26	38.41	13.23	0.39	1294.44	13.26
	327.30	104.29	0.32	0.33	0.10	0.96	17.63	0.53	2158.62	49.66	19.54	0.76	1309.24	25.10
	983.37	360.70	0.37	0.98	0.36	2.87	12.46	0.40	2181.57	37.51	11.90	0.33	1285.47	11.21
	1230.51	504.26	0.41	1.23	0.50	3.59	11.93	0.36	2189.80	34.77	17.62	0.55	1296.81	18.59
	1157.22	446.73	0.39	1.16	0.45	3.38	11.94	0.38	2182.50	35.97	12.59	0.47	1300.11	15.57
	1058.42	428.53	0.41	1.06	0.43	3.09	9.61	0.24	2168.71	23.54	11.88	0.49	1307.83	15.93
	540.17	188.41	0.35	0.54	0.19	1.58	13.82	0.40	2189.86	38.97	11.20	0.56	1308.86	17.52
	376.00	152.46	0.41	0.38	0.15	1.10	13.94	0.38	2194.17	37.36	9.43	0.34	1299.45	11.20
	604.26	231.57	0.38	0.60	0.23	1.76	12.66	0.38	2204.93	37.36	13.99	0.48	1296.45	16.10
Mean	692.15	261.21	0.36	0.69	0.26	2.02	13.26	0.40	2179.28	37.89	13.37	0.48	1300.44	15.94
SD	374.65	159.07	0.04	0.37	0.16	1.09	2.27	0.08	16.42	6.80	3.03	0.12	7.61	4.04
COV%	54.13	60.90	11.84	54.13	60.90	54.13	17.14	19.14	0.75	17.94	22.68	26.01	0.59	25.32
Femoral Condyle Medial Superior	1435.20	638.67	0.45	1.44	0.64	4.19	13.57	0.32	2139.06	30.55	15.29	0.52	1309.16	17.71
	1576.60	804.41	0.51	1.58	0.80	4.60	11.25	0.42	2167.49	38.23	14.28	0.39	1308.38	13.80
	1399.07	735.95	0.53	1.40	0.74	4.09	14.45	0.40	2170.68	38.26	16.60	0.61	1300.25	20.22
	1254.20	667.24	0.53	1.25	0.67	3.66	14.64	0.47	2182.77	44.04	16.50	0.46	1288.38	15.65
	1370.41	738.12	0.54	1.37	0.74	4.00	12.59	0.40	2183.14	38.10	12.01	0.37	1299.54	12.62
	1442.49	683.38	0.47	1.44	0.68	4.21	12.76	0.39	2183.61	36.89	14.86	0.63	1303.46	20.43

	1526.43	668.65	0.44	1.53	0.67	4.46	10.93	0.40	2190.63	37.51	11.47	0.45	1302.39	14.67
	1478.76	574.32	0.39	1.48	0.57	4.32	13.47	0.42	2198.07	40.16	13.05	0.44	1309.29	15.07
	1021.70	324.69	0.32	1.02	0.32	2.98	13.14	0.41	2189.62	39.14	14.78	0.45	1293.24	15.26
	1309.64	431.90	0.33	1.31	0.43	3.82	13.64	0.48	2199.94	44.98	13.74	0.47	1311.15	16.11
Mean	1381.45	626.73	0.45	1.38	0.63	4.03	13.04	0.41	2180.50	38.79	14.26	0.48	1302.52	16.16
SD	158.60	147.04	0.08	0.16	0.15	0.46	1.22	0.04	17.88	3.98	1.72	0.09	7.45	2.58
COV%	11.48	23.46	18.21	11.48	23.46	11.48	9.33	10.33	0.82	10.25	12.09	17.95	0.57	15.94
Femoral Condyle Lateral Inferior	771.77	883.40	1.15	0.77	0.88	2.25	12.84	0.46	2209.85	43.92	13.90	0.40	1292.51	13.67
	680.14	628.47	0.92	0.68	0.63	1.99	15.37	0.50	2191.44	47.82	13.56	0.45	1316.49	15.50
	637.03	708.25	1.11	0.64	0.71	1.86	12.36	0.37	2183.58	35.64	12.62	0.43	1314.55	14.72
	554.81	462.74	0.83	0.55	0.46	1.62	11.95	0.42	2199.97	39.37	11.22	0.48	1315.97	15.66
	660.74	620.20	0.94	0.66	0.62	1.93	12.44	0.41	2186.82	38.72	12.62	0.46	1315.88	15.57
	735.31	632.35	0.86	0.74	0.63	2.15	14.08	0.42	2195.02	40.63	15.44	0.47	1317.56	16.48
	703.72	483.45	0.69	0.70	0.48	2.05	13.24	0.44	2196.07	41.46	11.65	0.35	1279.37	11.65
	762.71	514.85	0.68	0.76	0.51	2.23	9.95	0.27	2215.89	27.13	14.46	0.48	1311.38	16.50
	755.37	422.29	0.56	0.76	0.42	2.21	12.56	0.42	2214.00	40.83	13.87	0.31	1276.67	10.61
	797.26	364.85	0.46	0.80	0.36	2.33	13.19	0.42	2177.56	39.90	16.44	0.52	1296.53	17.70
Mean	705.89	572.08	0.82	0.71	0.57	2.06	12.80	0.41	2197.02	39.54	13.58	0.43	1303.69	14.80
SD	74.17	153.86	0.22	0.07	0.15	0.22	1.41	0.06	12.98	5.42	1.63	0.07	16.09	2.23
COV%	10.51	26.89	27.46	10.51	26.89	10.51	11.00	14.72	0.59	13.71	11.97	15.03	1.23	15.06
Femoral Condyle Lateral Superior	2171.05	534.13	0.25	2.17	0.53	6.34	14.63	0.54	2181.76	49.35	9.64	0.42	1292.84	13.32
	1972.78	507.11	0.26	1.97	0.51	5.76	13.58	0.41	2176.21	39.02	10.64	0.43	1287.50	13.70
	1740.85	442.09	0.25	1.74	0.44	5.08	15.43	0.52	2175.93	48.15	10.29	0.45	1280.69	14.03
	1821.51	525.74	0.29	1.82	0.53	5.32	13.63	0.41	2184.52	39.55	4.22	0.26	1288.17	7.49
	1467.08	400.85	0.27	1.47	0.40	4.28	14.87	0.48	2216.24	46.38	14.06	0.52	1296.06	16.99
	1503.24	383.88	0.26	1.50	0.38	4.39	12.92	0.43	2210.91	41.04	14.59	0.49	1293.91	16.23

	1426.22	328.07	0.23	1.43	0.33	4.16	14.63	0.46	2183.36	43.51	12.76	0.49	1303.51	16.23
	1329.55	305.20	0.23	1.33	0.31	3.88	12.57	0.50	2220.74	46.59	11.76	0.39	1311.79	13.31
	1155.45	270.58	0.23	1.16	0.27	3.37	14.49	0.49	2182.26	45.59	15.85	0.52	1306.09	17.76
	1085.14	256.59	0.24	1.09	0.26	3.17	12.53	0.40	2189.46	37.97	14.05	0.44	1298.65	15.02
Mean	1567.29	395.42	0.25	1.57	0.40	4.58	13.93	0.46	2192.14	43.71	11.79	0.44	1295.92	14.41
SD	352.19	104.65	0.02	0.35	0.10	1.03	1.02	0.05	17.05	4.08	3.35	0.08	9.41	2.90
COV%	22.47	26.47	7.77	22.47	26.47	22.47	7.36	10.34	0.78	9.34	28.44	17.34	0.73	20.15
Tibial Plateau Medial Anterior	543.23	187.65	0.35	0.54	0.19	1.59	12.72	0.44	2195.48	41.47	12.10	0.39	1320.00	13.67
	600.85	254.41	0.42	0.60	0.25	1.75	12.88	0.42	2182.81	39.73	13.16	0.44	1319.82	15.40
	290.90	106.32	0.37	0.29	0.11	0.85	12.18	0.36	2200.48	34.94	16.92	0.64	1313.36	21.40
	110.02	28.66	0.26	0.11	0.03	0.32	10.60	0.37	2165.93	33.94	12.54	0.42	1327.89	14.67
	225.71	75.61	0.34	0.23	0.08	0.66	13.84	0.44	2180.95	41.54	17.72	0.60	1313.34	20.57
	151.38	43.05	0.28	0.15	0.04	0.44	14.00	0.41	2171.80	38.91	14.83	0.47	1319.03	16.45
	266.95	75.73	0.28	0.27	0.08	0.78	13.03	0.44	2204.50	42.04	15.27	0.52	1319.00	18.04
	478.38	139.40	0.29	0.48	0.14	1.40	13.29	0.44	2199.46	42.22	15.12	0.62	1316.21	20.47
	554.23	167.98	0.30	0.55	0.17	1.62	12.56	0.41	2228.91	40.32	12.25	0.37	1310.11	12.98
	482.08	136.47	0.28	0.48	0.14	1.41	11.36	0.34	2210.14	33.32	13.72	0.51	1314.19	17.21
Mean	370.37	121.53	0.32	0.37	0.12	1.08	12.64	0.41	2194.05	38.84	14.36	0.50	1317.29	17.09
SD	180.93	69.88	0.05	0.18	0.07	0.53	1.05	0.04	18.97	3.47	1.95	0.09	5.00	3.00
COV%	48.85	57.50	15.57	48.85	57.50	48.85	8.32	9.36	0.86	8.94	13.56	19.08	0.38	17.53
Tibial Plateau Medial Posterior	436.50	135.99	0.31	0.44	0.14	1.27	13.37	0.39	2183.71	37.12	9.42	0.43	1300.43	13.63
	398.44	142.17	0.36	0.40	0.14	1.16	12.53	0.44	2196.65	41.36	8.25	0.38	1290.77	11.92
	506.36	212.69	0.42	0.51	0.21	1.48	11.47	0.36	2207.99	35.31	13.10	0.46	1307.83	15.60
	525.09	239.92	0.46	0.53	0.24	1.53	14.28	0.41	2178.79	39.47	11.91	0.48	1309.21	15.74
	474.20	174.32	0.37	0.47	0.17	1.38	12.02	0.39	2189.95	36.91	15.17	0.55	1304.05	18.49
	644.29	250.84	0.39	0.64	0.25	1.88	11.19	0.36	2208.73	35.16	15.90	0.55	1299.27	18.32

	863.39	364.41	0.42	0.86	0.36	2.52	11.62	0.35	2220.42	34.30	15.03	0.47	1300.07	15.95
	778.76	261.52	0.34	0.78	0.26	2.27	10.58	0.32	2208.97	31.30	13.54	0.42	1305.12	14.56
	860.17	359.60	0.42	0.86	0.36	2.51	11.40	0.34	2191.19	33.07	9.96	0.43	1305.75	13.81
	776.32	342.78	0.44	0.78	0.34	2.27	13.54	0.40	2164.10	38.07	6.85	0.41	1311.64	12.26
Mean	626.35	248.42	0.39	0.63	0.25	1.83	12.20	0.38	2195.05	36.21	11.91	0.46	1303.41	15.03
SD	180.33	85.42	0.05	0.18	0.09	0.53	1.19	0.04	16.95	3.01	3.15	0.06	6.03	2.25
COV%	28.79	34.38	12.15	28.79	34.38	28.79	9.77	9.54	0.77	8.31	26.45	12.31	0.46	14.97
Tibial Plateau Lateral Anterior	820.98	169.08	0.21	0.82	0.17	2.40	13.70	0.45	2197.77	42.71	9.89	0.44	1296.59	13.81
	314.95	57.36	0.18	0.31	0.06	0.92	15.24	0.53	2174.16	49.15	10.99	0.55	1307.66	17.19
	394.41	76.55	0.19	0.39	0.08	1.15	12.03	0.28	2146.48	26.90	12.07	0.38	1307.55	13.20
	645.40	164.13	0.25	0.65	0.16	1.88	15.28	0.39	2112.98	35.44	12.13	0.33	1290.94	11.46
	879.78	249.87	0.28	0.88	0.25	2.57	11.09	0.31	2185.03	29.91	12.48	0.41	1303.80	13.94
	1315.51	469.19	0.36	1.32	0.47	3.84	11.71	0.31	2151.19	29.02	11.75	0.39	1302.49	13.29
	1024.27	273.94	0.27	1.02	0.27	2.99	10.46	0.47	2181.60	41.64	9.20	0.24	1285.67	8.29
	956.37	233.51	0.24	0.96	0.23	2.79	12.00	0.34	2186.34	33.23	11.84	0.44	1306.78	14.59
	969.09	211.22	0.22	0.97	0.21	2.83	13.83	0.45	2188.36	42.96	11.27	0.29	1296.53	10.12
	862.38	153.04	0.18	0.86	0.15	2.52	18.29	0.69	2204.71	64.37	13.64	0.53	1309.61	17.67
Mean	818.31	205.79	0.24	0.82	0.21	2.39	13.36	0.42	2172.86	39.53	11.52	0.40	1300.76	13.36
SD	298.16	116.12	0.06	0.30	0.12	0.87	2.40	0.13	27.96	11.33	1.27	0.10	8.03	2.89
COV%	36.44	56.43	23.25	36.44	56.43	36.44	17.96	29.70	1.29	28.65	11.05	24.24	0.62	21.63
Tibial Plateau Lateral Posterior	1680.39	1041.66	0.62	1.68	1.04	4.91	12.40	0.37	2182.31	35.31	9.46	0.47	1321.78	14.93
	1676.65	1106.69	0.66	1.68	1.11	4.90	11.09	0.38	2194.22	35.66	10.98	0.54	1304.46	16.78
	1681.31	1060.25	0.63	1.68	1.06	4.91	9.35	0.39	2189.65	34.93	9.98	0.50	1335.30	16.36
	1607.78	1046.21	0.65	1.61	1.05	4.69	12.15	0.43	2200.45	40.27	16.67	0.55	1302.24	18.75
	1764.21	1025.96	0.58	1.76	1.03	5.15	11.23	0.36	2195.96	34.10	18.48	0.69	1321.48	23.62
	1526.04	670.11	0.44	1.53	0.67	4.46	11.98	0.40	2180.28	37.18	19.89	0.65	1308.21	22.39

	970.41	331.88	0.34	0.97	0.33	2.83	10.98	0.38	2168.54	35.29	10.10	0.41	1319.40	13.73
	1356.07	549.25	0.41	1.36	0.55	3.96	11.94	0.45	2185.14	41.62	15.34	0.58	1328.01	19.99
	1754.09	799.78	0.46	1.75	0.80	5.12	12.84	0.42	2181.12	39.28	13.20	0.43	1320.02	14.95
	1435.61	436.90	0.30	1.44	0.44	4.19	10.21	0.43	2191.43	38.60	15.54	0.49	1318.48	17.01
Mean	1545.26	806.87	0.51	1.55	0.81	4.51	11.42	0.40	2186.91	37.22	13.96	0.53	1317.94	17.85
SD	242.24	291.00	0.13	0.24	0.29	0.71	1.06	0.03	9.34	2.57	3.77	0.09	10.32	3.29
COV%	15.68	36.06	26.52	15.68	36.06	15.68	9.32	7.68	0.43	6.91	26.98	17.44	0.78	18.42
Mean	963.38	404.76	0.42	0.96	0.40	2.81	12.83	0.41	2187.23	38.97	13.09	0.46	1305.25	15.58
SD	498.27	270.16	0.20	0.50	0.27	1.45	1.64	0.07	19.00	5.88	2.75	0.09	11.66	3.14
COV%	51.72	66.75	48.33	51.72	66.75	51.72	12.81	15.93	0.87	15.08	20.98	20.05	0.89	20.13

Table 6. Cartilage, subchondral bone and trabecular bone raw data for cadaver 6, 58 years.

	58, Male													
	Cartilage						Subchondral Bone				Trabecular Bone			
	G' kPa	G'' kPa	Tan Delta	G' MPa	G'' MPa	E MPa	E GPa	H GPa	D nm	Load mN	E GPa	H GPa	D nm	Load mN
Femoral Condyle Medial Inferior	119.70	29.92	0.25	0.12	0.03	0.35	10.62	0.32	2186.93	30.75	13.10	0.46	1312.01	15.60
	104.17	26.13	0.25	0.10	0.03	0.30	11.12	0.31	2209.75	30.71	12.87	0.49	1332.00	16.90
	203.70	58.35	0.29	0.20	0.06	0.59	11.94	0.41	2205.19	38.85	15.37	0.64	1318.55	21.17
	517.97	194.97	0.38	0.52	0.19	1.51	11.97	0.42	2201.34	39.34	11.27	0.33	1278.55	11.05
	224.07	63.94	0.29	0.22	0.06	0.65	15.45	0.48	2201.10	46.39	12.24	0.45	1324.50	15.52
	194.61	58.61	0.30	0.19	0.06	0.57	13.19	0.49	2209.54	46.00	12.33	0.48	1311.61	15.95
	250.43	77.24	0.31	0.25	0.08	0.73	12.82	0.45	2208.34	42.63	13.79	0.56	1331.94	19.18
	221.29	70.73	0.32	0.22	0.07	0.65	13.67	0.49	2215.81	46.40	12.79	0.50	1326.05	16.98
	232.05	74.68	0.32	0.23	0.07	0.68	14.54	0.51	2206.93	48.14	12.41	0.52	1319.01	17.16
	104.39	30.41	0.29	0.10	0.03	0.30	13.06	0.43	2224.28	41.91	11.78	0.45	1315.63	15.02
Mean	217.24	68.50	0.30	0.22	0.07	0.63	12.84	0.43	2206.92	41.11	12.79	0.49	1316.99	16.45
SD	119.05	48.38	0.04	0.12	0.05	0.35	1.49	0.07	9.80	6.29	1.14	0.08	15.37	2.66
COV%	54.80	70.63	12.27	54.80	70.63	54.80	11.62	15.93	0.44	15.30	8.93	16.44	1.17	16.18
Femoral Condyle Medial Superior	426.41	139.61	0.33	0.43	0.14	1.25	10.33	0.39	2189.54	35.88	14.85	0.60	1314.37	19.98
	380.88	124.38	0.33	0.38	0.12	1.11	8.24	0.33	2242.35	31.21	11.12	0.35	1301.28	11.98
	310.24	96.95	0.31	0.31	0.10	0.91	14.17	0.49	2203.79	46.61	12.97	0.55	1318.84	18.23
	652.61	274.23	0.42	0.65	0.27	1.91	11.67	0.45	2201.49	41.75	10.93	0.47	1332.74	15.77
	725.76	348.66	0.48	0.73	0.35	2.12	8.03	0.30	2241.38	29.18	11.51	0.47	1300.20	15.20
	633.56	251.08	0.40	0.63	0.25	1.85	7.08	0.27	2239.42	26.00	11.73	0.50	1323.94	16.58

	564.25	204.48	0.36	0.56	0.20	1.65	8.78	0.32	2218.58	30.31	15.95	0.65	1302.64	21.24
	236.39	72.15	0.31	0.24	0.07	0.69	6.95	0.25	2195.07	23.69	10.01	0.57	1312.87	17.29
	626.52	235.59	0.38	0.63	0.24	1.83	11.42	0.36	2214.68	35.09	12.11	0.48	1310.95	16.04
	289.98	103.27	0.36	0.29	0.10	0.85	11.39	0.38	2232.03	37.16	13.91	0.59	1329.30	19.79
Mean	484.66	185.04	0.37	0.48	0.19	1.42	9.81	0.35	2217.83	33.69	12.51	0.52	1314.71	17.21
SD	176.10	91.26	0.05	0.18	0.09	0.51	2.36	0.08	20.05	7.05	1.88	0.09	11.52	2.73
COV%	36.33	49.32	14.85	36.33	49.32	36.33	24.06	21.48	0.90	20.94	15.05	16.63	0.88	15.84
Femoral Condyle Lateral Inferior	221.89	54.66	0.25	0.22	0.05	0.65	8.18	0.27	2052.83	22.43	9.48	0.39	1297.03	12.64
	200.68	47.31	0.24	0.20	0.05	0.59	7.41	0.25	2046.35	20.78	10.53	0.37	1280.21	11.98
	897.06	249.44	0.28	0.90	0.25	2.62	10.09	0.36	2045.67	29.33	11.15	0.46	1297.27	14.71
	510.31	137.16	0.27	0.51	0.14	1.49	11.48	0.35	2047.28	29.49	9.52	0.41	1302.87	13.10
	410.73	102.45	0.25	0.41	0.10	1.20	12.19	0.46	2044.74	37.34	13.57	0.53	1294.48	17.30
	314.78	84.78	0.27	0.31	0.08	0.92	10.69	0.39	2099.34	33.40	12.06	0.41	1288.10	13.54
	387.49	102.81	0.27	0.39	0.10	1.13	9.68	0.31	2075.92	26.28	13.12	0.49	1289.22	15.91
	358.00	98.38	0.28	0.36	0.10	1.05	9.92	0.34	2101.07	29.31	12.08	0.62	1287.72	18.64
	382.94	100.18	0.26	0.38	0.10	1.12	11.37	0.45	2079.55	37.15	12.53	0.57	1297.34	17.95
	302.18	82.51	0.27	0.30	0.08	0.88	11.14	0.39	2063.27	32.26	13.40	0.55	1296.76	17.60
Mean	398.61	105.97	0.26	0.40	0.11	1.16	10.22	0.36	2065.60	29.78	11.74	0.48	1293.10	15.34
SD	197.15	56.51	0.01	0.20	0.06	0.58	1.50	0.07	22.12	5.56	1.52	0.09	6.64	2.45
COV%	49.46	53.33	5.32	49.46	53.33	49.46	14.70	19.60	1.07	18.68	12.92	17.76	0.51	16.00
Femoral Condyle Lateral Superior	1483.40	684.44	0.46	1.48	0.68	4.33	10.76	0.44	2205.13	40.55	13.14	0.52	1279.65	16.43
	1890.80	886.28	0.47	1.89	0.89	5.52	10.43	0.37	2229.38	35.54	12.64	0.60	1268.42	17.90
	2075.34	964.48	0.47	2.08	0.96	6.06	11.19	0.41	2212.42	39.23	13.05	0.52	1281.81	16.51
	1878.01	896.70	0.48	1.88	0.90	5.48	11.73	0.50	2206.91	45.60	12.18	0.50	1278.73	15.57
	2290.78	1340.69	0.59	2.29	1.34	6.69	8.48	0.33	2205.25	30.54	14.21	0.54	1284.24	17.25
	1700.44	864.25	0.51	1.70	0.86	4.97	7.82	0.32	2213.40	29.89	8.38	0.44	1280.82	13.14

	1323.00	636.83	0.48	1.32	0.64	3.86	8.19	0.29	2246.50	28.85	13.88	0.50	1287.75	16.24
	1165.56	621.62	0.53	1.17	0.62	3.40	11.66	0.40	2199.64	38.07	14.85	0.57	1289.46	18.33
	1650.90	996.93	0.60	1.65	1.00	4.82	8.79	0.28	2236.28	27.99	11.68	0.45	1291.78	14.53
	1547.33	1024.08	0.66	1.55	1.02	4.52	7.95	0.27	2248.33	26.60	9.71	0.39	1306.88	12.73
Mean	1700.56	891.63	0.52	1.70	0.89	4.97	9.70	0.36	2220.32	34.28	12.37	0.50	1284.95	15.86
SD	342.92	215.29	0.07	0.34	0.22	1.00	1.60	0.08	18.20	6.40	2.01	0.06	10.13	1.89
COV%	20.17	24.15	13.34	20.17	24.15	20.17	16.48	21.04	0.82	18.68	16.27	12.52	0.79	11.91
Tibial Plateau Medial Anterior	20.40	8.15	0.40	0.02	0.01	0.06	9.97	0.31	2205.47	30.01	5.24	0.57	1302.09	13.38
	17.22	6.43	0.37	0.02	0.01	0.05	10.26	0.32	2197.88	30.67	10.68	0.44	1322.41	14.59
	18.45	6.67	0.36	0.02	0.01	0.05	12.17	0.49	2219.76	45.78	11.77	0.48	1302.72	15.54
	17.17	6.50	0.38	0.02	0.01	0.05	9.94	0.36	2230.12	34.88	10.85	0.42	1312.74	13.90
	19.86	6.68	0.34	0.02	0.01	0.06	12.16	0.49	2223.50	45.77	7.55	0.52	1307.10	14.79
	32.30	10.01	0.31	0.03	0.01	0.09	9.06	0.32	2242.31	31.02	5.00	0.41	1307.29	10.89
	25.78	8.74	0.34	0.03	0.01	0.08	8.06	0.21	2232.10	21.78	5.52	0.47	1302.76	12.23
	21.90	7.76	0.35	0.02	0.01	0.06	8.54	0.23	2202.14	23.08	4.25	0.25	1282.01	7.20
	18.55	7.14	0.39	0.02	0.01	0.05	11.49	0.46	2250.13	44.36	3.87	0.33	1297.65	8.51
	14.11	5.70	0.40	0.01	0.01	0.04	11.99	0.44	2212.75	41.93	5.33	0.38	1307.91	10.73
Mean	20.57	7.38	0.36	0.02	0.01	0.06	10.36	0.36	2221.62	34.93	7.01	0.42	1304.47	12.18
SD	5.17	1.29	0.03	0.01	0.00	0.02	1.53	0.10	17.36	9.10	3.00	0.09	10.43	2.80
COV%	25.11	17.52	8.19	25.11	17.52	25.11	14.77	28.15	0.78	26.04	42.80	21.78	0.80	22.97
Tibial Plateau Medial Posterior	227.09	56.39	0.25	0.23	0.06	0.66	10.92	0.36	2182.96	33.85	11.69	0.49	1310.05	15.99
	253.65	65.03	0.26	0.25	0.07	0.74	10.70	0.33	2184.38	31.16	11.10	0.30	1280.87	10.14
	341.97	83.86	0.25	0.34	0.08	1.00	9.18	0.28	2180.08	27.00	11.65	0.31	1281.81	10.67
	366.38	85.62	0.23	0.37	0.09	1.07	10.29	0.36	2168.89	33.04	10.59	0.37	1284.57	12.10
	201.29	49.97	0.25	0.20	0.05	0.59	15.77	0.47	2179.50	44.86	11.31	0.35	1279.07	11.48
	244.26	63.51	0.26	0.24	0.06	0.71	10.90	0.33	2178.12	31.11	13.65	0.52	1289.04	16.91

	305.36	85.31	0.28	0.31	0.09	0.89	15.95	0.51	2161.00	47.50	8.27	0.34	1296.67	10.85
	362.59	92.02	0.25	0.36	0.09	1.06	13.74	0.47	2174.30	43.54	10.93	0.51	1304.18	16.22
	137.35	39.80	0.29	0.14	0.04	0.40	13.54	0.40	2169.68	37.63	7.97	0.54	1304.67	15.39
	166.06	43.54	0.26	0.17	0.04	0.48	14.93	0.40	2152.10	38.03	10.25	0.49	1314.80	15.76
Mean	260.60	66.51	0.26	0.26	0.07	0.76	12.59	0.39	2173.10	36.77	10.74	0.42	1294.57	13.55
SD	81.17	19.14	0.02	0.08	0.02	0.24	2.48	0.07	10.31	6.75	1.66	0.10	13.20	2.71
COV%	31.15	28.78	6.40	31.15	28.78	31.15	19.68	18.96	0.47	18.36	15.42	22.94	1.02	20.02
Tibial Plateau Lateral Anterior	94.60	19.27	0.20	0.09	0.02	0.28	14.15	0.62	2204.98	56.02	10.87	0.49	1301.06	15.61
	94.93	19.88	0.21	0.09	0.02	0.28	15.89	0.62	2202.93	57.20	9.03	0.42	1301.66	13.36
	79.38	17.52	0.22	0.08	0.02	0.23	11.19	0.34	2174.75	31.91	6.38	0.35	1281.70	10.17
	92.75	19.57	0.21	0.09	0.02	0.27	12.71	0.48	2174.53	43.50	6.37	0.50	1304.73	13.51
	111.57	24.50	0.22	0.11	0.02	0.33	12.85	0.54	2181.08	48.64	7.21	0.48	1314.64	13.92
	103.22	23.84	0.23	0.10	0.02	0.30	8.96	0.26	2174.16	24.59	5.72	0.41	1295.28	11.27
	174.50	39.77	0.23	0.17	0.04	0.51	12.88	0.47	2194.89	44.19	4.44	0.40	1308.57	10.35
	233.05	60.29	0.26	0.23	0.06	0.68	13.91	0.44	2166.64	40.72	5.37	0.36	1303.54	10.31
	309.03	74.08	0.24	0.31	0.07	0.90	12.24	0.37	2186.56	35.21	7.47	0.37	1308.54	11.54
	269.88	69.46	0.26	0.27	0.07	0.79	14.75	0.53	2185.33	49.00	11.71	0.41	1294.15	13.65
Mean	156.29	36.82	0.23	0.16	0.04	0.46	12.95	0.47	2184.58	43.10	7.45	0.42	1301.39	12.37
SD	84.85	22.60	0.02	0.08	0.02	0.25	1.94	0.12	12.93	10.37	2.38	0.05	9.26	1.88
COV%	54.29	61.39	8.39	54.29	61.39	54.29	14.98	25.51	0.59	24.07	31.97	13.07	0.71	15.21
Tibial Plateau Lateral Posterior	37.48	9.11	0.24	0.04	0.01	0.11	10.25	0.34	2160.06	31.30	9.76	0.20	1270.01	6.96
	32.33	7.98	0.25	0.03	0.01	0.09	10.49	0.35	2189.47	32.81	14.69	0.56	1290.52	18.12
	28.29	7.52	0.27	0.03	0.01	0.08	12.88	0.48	2182.56	44.40	11.91	0.56	1288.25	17.34
	41.34	11.34	0.27	0.04	0.01	0.12	10.19	0.30	2194.89	29.33	15.07	0.67	1308.44	21.50
	36.31	8.81	0.24	0.04	0.01	0.11	8.29	0.35	2203.18	32.17	11.67	0.61	1280.29	18.13
	38.42	10.28	0.27	0.04	0.01	0.11	9.66	0.33	2165.98	30.04	10.92	0.38	1279.12	12.19

	32.05	8.34	0.26	0.03	0.01	0.09	9.94	0.34	2179.90	31.65	11.94	0.41	1276.21	13.39
	38.52	9.44	0.25	0.04	0.01	0.11	10.91	0.36	2169.60	33.52	8.12	0.38	1289.26	11.76
	36.12	9.63	0.27	0.04	0.01	0.11	11.54	0.33	2180.85	31.90	9.09	0.39	1290.89	12.23
	25.38	6.87	0.27	0.03	0.01	0.07	10.55	0.34	2225.34	33.15	10.39	0.37	1284.09	11.93
Mean	34.62	8.93	0.26	0.03	0.01	0.10	10.47	0.35	2185.18	33.03	11.35	0.45	1285.71	14.36
SD	5.01	1.33	0.01	0.01	0.00	0.01	1.20	0.05	19.28	4.20	2.23	0.14	10.53	4.29
COV%	14.46	14.88	4.82	14.46	14.88	14.46	11.46	13.84	0.88	12.73	19.68	31.54	0.82	29.89
Mean	409.14	171.35	0.32	0.41	0.17	1.19	11.12	0.38	2184.39	35.84	10.75	0.46	1299.49	14.66
SD	537.41	291.48	0.10	0.54	0.29	1.57	2.18	0.09	51.04	8.01	2.90	0.09	15.62	3.17
COV%	131.35	170.11	30.61	131.35	170.11	131.35	19.65	22.78	2.34	22.36	26.97	20.44	1.20	21.63

Table 7. Cartilage, subchondral bone and trabecular bone raw data for cadaver 7, 72 years.

	72, Male													
	Cartilage						Subchondral Bone				Trabecular Bone			
	G' kPa	G'' kPa	Tan Delta	G' MPa	G'' MPa	E MPa	E GPa	H GPa	D nm	Load mN	E GPa	H GPa	D nm	Load mN
Femoral Condyle Medial Inferior	37.82	10.65	0.28	0.04	0.01	0.11	16.76	0.60	2189.84	55.74	20.51	0.62	1300.31	21.29
	34.12	9.69	0.28	0.03	0.01	0.10	16.47	0.55	2205.47	52.31	19.28	0.68	1286.51	22.27
	25.82	7.74	0.30	0.03	0.01	0.08	15.63	0.47	2201.88	45.73	10.16	0.51	1303.11	15.73
	49.25	15.96	0.32	0.05	0.02	0.14	17.00	0.58	2208.38	55.49	10.88	0.43	1305.83	14.24
	25.83	7.79	0.30	0.03	0.01	0.08	15.61	0.53	2210.37	50.70	11.56	0.47	1298.59	15.18
	21.25	6.37	0.30	0.02	0.01	0.06	17.63	0.64	2212.47	60.69	10.28	0.31	1332.60	11.11
	22.24	6.68	0.30	0.02	0.01	0.06	16.40	0.57	2216.62	55.11	7.87	0.24	1335.80	8.59
	21.98	6.68	0.30	0.02	0.01	0.06	15.43	0.50	2196.80	48.14	8.77	0.33	1329.40	11.24
	22.37	6.79	0.30	0.02	0.01	0.07	15.07	0.46	2209.15	44.74	11.65	0.47	1327.49	15.92
	26.87	7.95	0.30	0.03	0.01	0.08	16.36	0.56	2204.46	53.58	15.46	0.52	1332.90	18.42
Mean	28.75	8.63	0.30	0.03	0.01	0.08	16.24	0.55	2205.54	52.22	12.64	0.46	1315.25	15.40
SD	9.05	2.93	0.01	0.01	0.00	0.03	0.79	0.06	7.84	4.97	4.33	0.14	18.10	4.41
COV%	31.47	33.89	3.92	31.47	33.89	31.47	4.88	10.42	0.36	9.52	34.24	30.33	1.38	28.62
Femoral Condyle Medial Superior	24.11	7.55	0.31	0.02	0.01	0.07	12.91	0.47	2213.43	44.32	14.95	0.62	1303.93	20.15
	28.77	8.30	0.29	0.03	0.01	0.08	13.39	0.55	2206.47	50.59	14.29	0.54	1310.63	18.09
	30.10	8.90	0.30	0.03	0.01	0.09	13.28	0.46	2222.40	44.64	13.66	0.59	1307.96	19.02
	28.41	9.51	0.34	0.03	0.01	0.08	12.73	0.42	2208.66	40.83	10.63	0.49	1316.65	15.84
	14.42	6.12	0.42	0.01	0.01	0.04	14.49	0.53	2210.09	50.09	14.50	0.67	1311.05	21.36
	23.05	7.97	0.35	0.02	0.01	0.07	12.02	0.32	2164.39	30.23	13.79	0.56	1312.65	18.55

	25.98	7.85	0.30	0.03	0.01	0.08	13.84	0.53	2224.61	50.22	14.96	0.61	1314.05	20.14
	21.93	7.35	0.34	0.02	0.01	0.06	8.10	0.47	2272.36	42.37	16.54	0.60	1305.73	20.16
	18.29	6.42	0.35	0.02	0.01	0.05	12.43	0.43	2202.10	40.94	17.17	0.65	1310.38	21.71
	16.03	6.12	0.38	0.02	0.01	0.05	13.69	0.58	2213.74	53.35	18.68	0.64	1298.80	21.43
Mean	23.11	7.61	0.34	0.02	0.01	0.07	12.69	0.48	2213.82	44.76	14.92	0.60	1309.18	19.64
SD	5.46	1.15	0.04	0.01	0.00	0.02	1.76	0.08	26.44	6.77	2.20	0.05	5.24	1.81
COV%	23.63	15.10	12.37	23.63	15.10	23.63	13.91	16.04	1.19	15.13	14.77	9.05	0.40	9.24
Femoral Condyle Lateral Inferior	36.17	8.80	0.24	0.04	0.01	0.11	12.58	0.40	2203.97	38.61	12.54	0.57	1298.65	17.88
	43.52	9.98	0.23	0.04	0.01	0.13	12.47	0.41	2201.69	39.53	15.34	0.66	1305.81	21.36
	37.59	8.79	0.23	0.04	0.01	0.11	13.79	0.46	2228.97	45.12	15.15	0.69	1297.63	21.78
	45.50	10.42	0.23	0.05	0.01	0.13	15.33	0.50	2192.91	47.19	14.27	0.60	1301.77	19.36
	32.51	8.14	0.25	0.03	0.01	0.09	15.74	0.63	2218.19	58.85	14.23	0.58	1299.69	18.81
	30.33	7.95	0.26	0.03	0.01	0.09	13.88	0.46	2199.96	44.17	14.82	0.69	1294.28	21.40
	18.46	5.48	0.30	0.02	0.01	0.05	13.41	0.44	2181.60	41.37	13.21	0.53	1300.60	17.29
	21.72	6.24	0.29	0.02	0.01	0.06	10.13	0.30	2204.29	29.59	9.12	0.48	1294.70	14.48
	22.82	6.76	0.30	0.02	0.01	0.07	16.62	0.61	2270.01	61.10	12.71	0.55	1300.19	17.58
	22.43	5.92	0.26	0.02	0.01	0.07	16.92	0.66	2196.20	61.02	9.13	0.48	1296.60	14.62
Mean	31.10	7.85	0.26	0.03	0.01	0.09	14.09	0.49	2209.78	46.65	13.05	0.58	1298.99	18.46
SD	9.57	1.70	0.03	0.01	0.00	0.03	2.10	0.11	24.85	10.58	2.28	0.08	3.45	2.63
COV%	30.75	21.71	10.29	30.75	21.71	30.75	14.93	23.41	1.12	22.67	17.50	13.31	0.27	14.23
Femoral Condyle Lateral Superior	852.59	205.66	0.24	0.85	0.21	2.49	10.10	0.22	2160.98	21.69	14.90	0.56	1298.71	18.40
	889.56	234.06	0.26	0.89	0.23	2.60	15.57	0.52	2204.31	49.58	17.48	0.77	1297.59	24.49
	927.07	272.18	0.29	0.93	0.27	2.71	16.82	0.56	2206.08	53.49	14.79	0.58	1288.57	18.69
	1008.96	381.40	0.38	1.01	0.38	2.95	17.12	0.57	2218.75	55.19	13.94	0.56	1284.46	17.82
	986.73	366.88	0.37	0.99	0.37	2.88	16.62	0.58	2218.75	55.53	15.23	0.63	1297.71	20.17
	1160.54	506.65	0.44	1.16	0.51	3.39	15.50	0.50	2211.62	48.49	16.52	0.62	1294.18	20.37

	991.46	353.02	0.36	0.99	0.35	2.90	15.06	0.47	2203.45	45.61	16.28	0.70	1293.15	22.06
	898.41	272.99	0.30	0.90	0.27	2.62	17.75	0.62	2188.90	57.72	17.14	0.60	1295.55	19.95
	963.45	270.41	0.28	0.96	0.27	2.81	16.09	0.55	2184.88	51.71	19.55	0.67	1293.20	22.12
	982.53	256.20	0.26	0.98	0.26	2.87	13.93	0.43	2215.48	42.13	14.81	0.61	1295.88	19.64
Mean	966.13	311.95	0.32	0.97	0.31	2.82	15.45	0.50	2201.32	48.11	16.06	0.63	1293.90	20.37
SD	85.53	89.90	0.06	0.09	0.09	0.25	2.18	0.11	18.27	10.44	1.68	0.07	4.43	2.02
COV%	8.85	28.82	19.97	8.85	28.82	8.85	14.13	22.47	0.83	21.71	10.45	10.45	0.34	9.93
Tibial Plateau Medial Anterior	16.36	5.26	0.32	0.02	0.01	0.05	13.16	0.54	2195.04	48.86	12.70	0.54	1324.50	17.94
	19.56	6.03	0.31	0.02	0.01	0.06	9.23	0.52	2154.50	42.42	12.64	0.51	1306.13	16.74
	21.84	6.28	0.29	0.02	0.01	0.06	14.84	0.63	2175.35	56.27	8.56	0.48	1296.17	14.40
	18.32	5.54	0.30	0.02	0.01	0.05	14.12	0.56	2173.44	50.27	10.20	0.34	1284.63	11.09
	31.18	10.96	0.35	0.03	0.01	0.09	12.53	0.48	2177.65	43.36	13.56	0.67	1311.97	21.19
	29.47	9.56	0.32	0.03	0.01	0.09	12.91	0.47	2185.45	43.51	11.84	0.46	1291.27	14.87
	18.92	5.93	0.31	0.02	0.01	0.06	13.04	0.51	2184.23	46.72	15.24	0.66	1314.56	21.47
	24.56	6.61	0.27	0.02	0.01	0.07	11.24	0.40	2185.45	37.51	9.01	0.57	1319.68	17.00
	27.95	8.10	0.29	0.03	0.01	0.08	14.39	0.53	2165.28	48.28	11.61	0.49	1311.28	16.12
	22.24	6.28	0.28	0.02	0.01	0.06	12.33	0.54	2182.64	47.83	12.58	0.54	1309.53	17.54
Mean	23.04	7.05	0.31	0.02	0.01	0.07	12.78	0.52	2177.90	46.50	11.79	0.53	1306.97	16.84
SD	5.08	1.88	0.02	0.01	0.00	0.01	1.64	0.06	11.57	5.13	2.05	0.10	12.65	3.08
COV%	22.04	26.66	7.84	22.04	26.66	22.04	12.80	11.73	0.53	11.02	17.39	18.42	0.97	18.31
Tibial Plateau Medial Posterior	27.94	7.19	0.26	0.03	0.01	0.08	14.07	0.54	2214.18	50.80	7.15	0.58	1322.63	15.87
	32.05	7.85	0.25	0.03	0.01	0.09	13.02	0.46	2249.44	45.27	5.84	0.45	1302.59	12.26
	31.03	7.82	0.25	0.03	0.01	0.09	14.37	0.53	2242.36	51.50	3.62	0.38	1295.40	9.03
	43.81	10.59	0.24	0.04	0.01	0.13	14.84	0.53	2206.85	50.44	7.28	0.48	1315.85	14.12
	29.98	7.37	0.25	0.03	0.01	0.09	15.11	0.65	2250.13	61.86	6.16	0.44	1304.52	12.37
	25.56	6.68	0.26	0.03	0.01	0.07	13.62	0.52	2214.52	48.58	10.45	0.59	1316.80	18.13

	31.34	7.83	0.25	0.03	0.01	0.09	14.92	0.58	2228.59	54.81	10.69	0.50	1308.03	15.93
	38.39	9.48	0.25	0.04	0.01	0.11	13.35	0.52	2223.97	49.40	6.43	0.64	1326.63	16.19
	28.30	7.21	0.26	0.03	0.01	0.08	17.81	0.71	2207.40	65.96	4.78	0.49	1319.93	12.14
	28.58	7.55	0.26	0.03	0.01	0.08	15.58	0.63	2224.21	59.28	4.74	0.51	1278.65	11.60
Mean	31.70	7.96	0.25	0.03	0.01	0.09	14.67	0.57	2226.17	53.79	6.71	0.51	1309.10	13.76
SD	5.46	1.18	0.01	0.01	0.00	0.02	1.37	0.08	16.32	6.57	2.32	0.08	14.50	2.75
COV%	17.22	14.87	2.88	17.22	14.87	17.22	9.36	13.46	0.73	12.22	34.62	14.97	1.11	19.99
Tibial Plateau Lateral Anterior	39.19	11.84	0.30	0.04	0.01	0.11	13.35	0.49	2222.54	47.18	11.06	0.64	1313.14	19.47
	27.74	7.67	0.28	0.03	0.01	0.08	15.20	0.61	2239.80	57.85	14.69	0.62	1303.23	19.97
	24.26	6.85	0.28	0.02	0.01	0.07	11.96	0.53	2252.66	50.12	13.79	0.56	1307.42	18.41
	23.31	6.69	0.29	0.02	0.01	0.07	14.32	0.57	2209.94	53.04	13.71	0.68	1306.02	21.17
	24.27	7.26	0.30	0.02	0.01	0.07	13.18	0.54	2256.26	51.90	13.00	0.60	1303.79	19.05
	23.64	7.30	0.31	0.02	0.01	0.07	15.21	0.58	2193.56	53.70	7.91	0.39	1285.85	11.77
	26.67	7.31	0.27	0.03	0.01	0.08	18.24	0.81	2254.92	76.57	4.37	0.50	1289.77	11.19
	45.01	13.36	0.30	0.05	0.01	0.13	13.59	0.47	2181.38	43.73	7.60	0.47	1297.19	13.54
	37.78	9.98	0.26	0.04	0.01	0.11	10.90	0.36	2182.02	33.98	7.74	0.47	1300.65	13.69
	40.83	11.26	0.28	0.04	0.01	0.12	13.50	0.50	2187.72	46.35	4.97	0.46	1289.98	11.46
Mean	31.27	8.95	0.29	0.03	0.01	0.09	13.95	0.55	2218.08	51.44	9.88	0.54	1299.70	15.97
SD	8.43	2.44	0.01	0.01	0.00	0.02	2.01	0.12	31.16	11.01	3.84	0.10	8.83	3.98
COV%	26.94	27.28	5.06	26.94	27.28	26.94	14.38	21.25	1.40	21.40	38.80	17.76	0.68	24.93
Tibial Plateau Lateral Posterior	16.01	5.37	0.34	0.02	0.01	0.05	14.49	0.58	2199.58	53.18	9.18	0.56	1311.00	16.64
	16.17	5.46	0.34	0.02	0.01	0.05	10.55	0.43	2237.57	40.89	12.72	0.52	1311.50	17.22
	19.39	6.43	0.33	0.02	0.01	0.06	14.67	0.62	2252.30	59.04	8.95	0.48	1315.34	14.99
	17.04	5.60	0.33	0.02	0.01	0.05	14.30	0.55	2246.20	53.10	9.70	0.58	1311.30	17.39
	24.01	7.82	0.33	0.02	0.01	0.07	13.77	0.46	2217.72	44.33	13.18	0.56	1320.72	18.43
	30.53	10.54	0.35	0.03	0.01	0.09	13.29	0.59	2230.37	54.40	14.21	0.65	1307.26	20.80

	15.84	5.23	0.33	0.02	0.01	0.05	14.26	0.56	2222.66	52.70	13.52	0.59	1313.08	19.29
	14.36	5.43	0.38	0.01	0.01	0.04	12.98	0.50	2239.85	48.05	11.59	0.47	1318.93	15.81
	14.21	5.26	0.37	0.01	0.01	0.04	13.57	0.58	2218.79	53.79	14.48	0.61	1318.03	20.23
	19.68	6.82	0.35	0.02	0.01	0.06	14.06	0.64	2233.41	58.68	11.87	0.52	1317.92	17.02
Mean	18.72	6.40	0.34	0.02	0.01	0.05	13.59	0.55	2229.84	51.82	11.94	0.55	1314.51	17.78
SD	5.09	1.68	0.02	0.01	0.00	0.01	1.20	0.07	15.57	5.81	2.05	0.06	4.33	1.88
COV%	27.19	26.34	5.23	27.19	26.34	27.19	8.79	12.26	0.70	11.21	17.21	10.18	0.33	10.58
Mean	144.23	45.80	0.30	0.14	0.05	0.42	14.18	0.52	2210.31	49.41	12.13	0.55	1305.95	17.28
SD	314.04	105.70	0.04	0.31	0.11	0.92	1.99	0.09	24.78	8.27	3.78	0.10	12.23	3.52
COV%	217.74	230.78	14.42	217.74	230.78	217.74	14.04	17.15	1.12	16.74	31.19	17.72	0.94	20.36

Table 8. Cartilage, subchondral bone and trabecular bone raw data for cadaver 8, 72 years.

COV%	72, Male													
	Cartilage						Subchondral Bone				Trabecular Bone			
	G' kPa	G'' kPa	Tan Delta	G' MPa	G'' MPa	E MPa	E GPa	H GPa	D nm	Load mN	E GPa	H GPa	D nm	Load mN
Femoral Condyle Medial Inferior	112.17	50.65	0.45	0.11	0.05	0.33	14.98	0.60	2208.32	55.79	10.13	0.51	1298.62	15.77
	120.38	41.89	0.35	0.12	0.04	0.35	13.22	0.49	2197.54	45.66	14.13	0.61	1311.92	19.80
	102.22	30.66	0.30	0.10	0.03	0.30	13.12	0.51	2206.94	47.50	10.23	0.49	1293.90	15.13
	92.09	28.81	0.31	0.09	0.03	0.27	12.92	0.51	2236.33	48.29	10.31	0.51	1307.18	15.93
	107.12	37.70	0.35	0.11	0.04	0.31	12.33	0.45	2236.64	43.85	15.38	0.72	1308.36	22.79
	73.53	31.62	0.43	0.07	0.03	0.21	13.36	0.51	2231.54	48.89	7.65	0.55	1303.99	15.35
	55.88	28.67	0.51	0.06	0.03	0.16	12.88	0.48	2224.56	46.17	8.57	0.50	1315.01	15.16
	51.41	27.95	0.54	0.05	0.03	0.15	12.66	0.46	2223.55	43.79	14.21	0.72	1313.87	22.54
	52.54	26.04	0.50	0.05	0.03	0.15	13.07	0.46	2222.89	44.45	12.06	0.46	1303.25	15.09
	135.42	47.24	0.35	0.14	0.05	0.40	11.96	0.42	2227.03	40.30	13.24	0.54	1303.33	17.68
Mean	90.28	35.12	0.41	0.09	0.04	0.26	13.05	0.49	2221.53	46.47	11.59	0.56	1305.94	17.52
SD	30.28	8.74	0.09	0.03	0.01	0.09	0.80	0.05	13.15	4.14	2.60	0.09	6.71	3.09
COV%	33.54	24.90	21.61	33.54	24.90	33.54	6.13	10.25	0.59	8.90	22.45	16.43	0.51	17.62
Femoral Condyle Medial Superior	599.01	339.49	0.57	0.60	0.34	1.75	10.55	0.50	2215.22	44.57	4.18	0.53	1286.94	11.19
	594.61	418.54	0.70	0.59	0.42	1.74	10.39	0.46	2174.64	40.50	5.75	0.48	1297.87	12.48
	613.85	404.31	0.66	0.61	0.40	1.79	11.21	0.52	2213.55	46.94	10.00	0.49	1308.92	15.52
	620.28	422.31	0.68	0.62	0.42	1.81	11.92	0.61	2199.69	53.05	12.91	0.61	1308.96	19.49
	558.58	366.77	0.66	0.56	0.37	1.63	10.38	0.53	2207.10	46.53	17.51	0.71	1301.37	23.09
	636.19	349.35	0.55	0.64	0.35	1.86	9.97	0.43	2207.69	39.37	15.65	0.54	1299.08	17.99

	548.62	255.14	0.47	0.55	0.26	1.60	10.82	0.54	2191.57	46.74	13.66	0.57	1308.38	18.54
	631.11	292.67	0.46	0.63	0.29	1.84	10.94	0.55	2216.58	48.50	14.73	0.54	1314.87	18.38
	620.15	270.00	0.44	0.62	0.27	1.81	11.62	0.51	2194.75	45.53	14.49	0.63	1305.88	20.36
	602.29	237.83	0.40	0.60	0.24	1.76	10.56	0.53	2211.54	46.63	8.76	0.67	1311.05	18.41
Mean	602.47	335.64	0.56	0.60	0.34	1.76	10.84	0.52	2203.23	45.83	11.76	0.58	1304.33	17.54
SD	29.09	68.70	0.11	0.03	0.07	0.08	0.60	0.05	13.21	3.86	4.41	0.08	8.15	3.58
COV%	4.83	20.47	20.34	4.83	20.47	4.83	5.55	9.47	0.60	8.43	37.49	13.31	0.62	20.40
Femoral Condyle Lateral Inferior	498.97	164.93	0.33	0.50	0.16	1.46	12.40	0.40	2243.43	40.12	12.81	0.48	1302.71	15.80
	812.05	276.88	0.34	0.81	0.28	2.37	14.38	0.51	2207.01	48.10	13.13	0.47	1303.48	15.85
	1036.46	359.28	0.35	1.04	0.36	3.03	14.16	0.48	2185.72	44.86	15.93	0.61	1301.54	20.03
	1487.41	568.45	0.38	1.49	0.57	4.34	12.98	0.41	2192.48	39.42	16.65	0.58	1299.90	19.28
	856.06	305.55	0.36	0.86	0.31	2.50	15.15	0.52	2182.17	48.84	15.47	0.58	1312.57	19.57
	741.26	259.98	0.35	0.74	0.26	2.16	14.11	0.47	2192.86	44.18	17.11	0.57	1297.73	19.09
	784.01	301.66	0.39	0.78	0.30	2.29	18.16	0.59	2166.42	55.06	16.32	0.56	1289.01	18.53
	823.70	319.28	0.39	0.82	0.32	2.41	14.87	0.48	2175.55	44.89	19.78	0.76	1298.62	24.75
	700.13	255.43	0.37	0.70	0.26	2.04	15.08	0.52	2201.02	49.26	13.68	0.54	1311.37	18.00
	1298.42	533.72	0.41	1.30	0.53	3.79	14.48	0.49	2213.61	47.38	19.24	0.75	1304.22	24.65
Mean	903.85	334.52	0.37	0.90	0.33	2.64	14.58	0.49	2196.03	46.21	16.01	0.59	1302.12	19.55
SD	293.86	125.20	0.03	0.29	0.13	0.86	1.54	0.06	21.91	4.60	2.37	0.10	6.75	3.07
COV%	32.51	37.43	6.85	32.51	37.43	32.51	10.53	11.36	1.00	9.95	14.81	16.32	0.52	15.70
Femoral Condyle Lateral Superior	1445.94	331.11	0.23	1.45	0.33	4.22	15.90	0.53	2174.53	49.39	11.48	0.44	1307.83	14.56
	1441.98	344.72	0.24	1.44	0.34	4.21	15.49	0.47	2175.58	44.58	15.45	0.80	1328.08	25.48
	1035.99	217.31	0.21	1.04	0.22	3.03	12.75	0.36	2198.95	34.98	11.10	0.42	1334.12	14.66
	1232.00	262.98	0.21	1.23	0.26	3.60	14.52	0.44	2205.49	43.17	16.37	0.51	1289.36	17.08
	1435.53	310.78	0.22	1.44	0.31	4.19	16.14	0.54	2181.93	50.66	17.02	0.73	1298.28	23.36
	1252.54	254.88	0.20	1.25	0.25	3.66	17.01	0.57	2190.42	54.12	10.85	0.80	1330.12	22.97

	1352.74	309.36	0.23	1.35	0.31	3.95	15.92	0.50	2205.34	48.28	14.56	0.57	1295.91	18.49
	1400.97	360.95	0.26	1.40	0.36	4.09	15.07	0.48	2193.77	45.52	13.44	0.48	1291.73	15.72
	1456.03	438.27	0.30	1.46	0.44	4.25	12.43	0.36	2202.49	34.87	13.27	0.57	1294.62	18.20
	1319.28	416.22	0.32	1.32	0.42	3.85	14.72	0.56	2215.58	52.70	13.76	0.65	1300.60	20.34
Mean	1337.30	324.66	0.24	1.34	0.32	3.90	14.99	0.48	2194.41	45.83	13.73	0.60	1307.07	19.08
SD	133.41	69.66	0.04	0.13	0.07	0.39	1.46	0.08	13.74	6.70	2.16	0.14	17.17	3.84
COV%	9.98	21.46	16.03	9.98	21.46	9.98	9.74	16.10	0.63	14.63	15.74	23.79	1.31	20.10
Tibial Plateau Medial Anterior	49.23	15.11	0.31	0.05	0.02	0.14	16.21	0.56	2209.10	53.28	12.55	0.49	1307.96	16.10
	57.42	17.50	0.31	0.06	0.02	0.17	14.49	0.48	2200.75	45.63	12.46	0.48	1308.46	15.91
	55.51	17.49	0.32	0.06	0.02	0.16	13.46	0.50	2220.41	47.93	10.97	0.44	1306.24	14.39
	66.03	20.64	0.31	0.07	0.02	0.19	13.56	0.43	2204.87	41.84	12.91	0.57	1323.52	18.92
	88.09	28.69	0.33	0.09	0.03	0.26	13.88	0.55	2209.23	51.39	11.24	0.42	1300.99	14.01
	84.14	27.00	0.32	0.08	0.03	0.25	14.02	0.48	2224.94	46.58	12.84	0.50	1308.92	16.68
	53.11	15.29	0.29	0.05	0.02	0.16	13.26	0.36	2191.70	35.34	13.75	0.52	1307.35	17.31
	56.49	16.64	0.30	0.06	0.02	0.16	16.88	0.57	2186.63	53.75	11.58	0.48	1315.50	15.99
	63.19	18.89	0.30	0.06	0.02	0.18	17.35	0.61	2210.53	58.22	12.93	0.53	1325.99	17.82
	47.26	14.48	0.31	0.05	0.01	0.14	16.48	0.51	2195.70	49.44	14.48	0.54	1303.69	17.99
Mean	62.05	19.17	0.31	0.06	0.02	0.18	14.96	0.51	2205.39	48.34	12.57	0.50	1310.86	16.51
SD	13.91	4.94	0.01	0.01	0.00	0.04	1.59	0.07	12.10	6.53	1.09	0.05	8.24	1.56
COV%	22.42	25.77	3.80	22.42	25.77	22.42	10.61	14.45	0.55	13.51	8.67	9.27	0.63	9.46
Tibial Plateau Medial Posterior	25.45	7.56	0.30	0.03	0.01	0.07	15.87	0.54	2194.42	50.97	13.15	0.59	1315.45	19.25
	37.25	12.12	0.33	0.04	0.01	0.11	14.97	0.46	2206.72	44.82	14.94	0.60	1311.83	19.76
	46.90	13.96	0.30	0.05	0.01	0.14	15.96	0.53	2202.86	50.78	15.18	0.59	1305.37	19.60
	41.00	12.52	0.31	0.04	0.01	0.12	16.34	0.61	2217.00	57.96	15.63	0.59	1312.21	19.75
	95.03	29.31	0.31	0.10	0.03	0.28	14.86	0.48	2197.83	46.12	13.25	0.58	1318.93	19.06
	35.34	10.33	0.29	0.04	0.01	0.10	14.91	0.48	2211.41	46.76	10.41	0.57	1318.95	17.61

	46.18	13.38	0.29	0.05	0.01	0.13	20.20	0.73	2179.19	67.23	11.13	0.51	1313.59	16.39
	40.15	11.02	0.27	0.04	0.01	0.12	17.57	0.65	2200.61	60.94	16.77	0.69	1311.25	22.81
	50.28	13.92	0.28	0.05	0.01	0.15	17.72	0.59	2203.53	56.06	16.82	0.66	1307.13	21.85
	48.34	13.22	0.27	0.05	0.01	0.14	18.47	0.58	2189.57	55.26	6.13	0.47	1307.64	12.81
Mean	46.59	13.73	0.29	0.05	0.01	0.14	16.69	0.57	2200.31	53.69	13.34	0.58	1312.23	18.89
SD	18.55	5.81	0.02	0.02	0.01	0.05	1.77	0.08	10.86	7.17	3.34	0.07	4.68	2.81
COV%	39.81	42.34	5.62	39.81	42.34	39.81	10.60	14.93	0.49	13.35	25.05	11.23	0.36	14.89
Tibial Plateau Lateral Anterior	548.09	97.11	0.18	0.55	0.10	1.60	14.22	0.49	2222.69	47.38	16.12	0.45	1293.05	15.50
	599.73	104.42	0.17	0.60	0.10	1.75	12.19	0.48	2208.83	44.33	15.43	0.58	1318.08	19.58
	492.90	99.48	0.20	0.49	0.10	1.44	15.52	0.62	2212.66	57.41	15.44	0.44	1301.29	15.25
	678.09	120.42	0.18	0.68	0.12	1.98	15.16	0.52	2210.37	49.68	7.40	0.46	1287.20	13.13
	689.20	124.15	0.18	0.69	0.12	2.01	14.70	0.49	2201.12	47.12	17.43	0.86	1297.25	26.53
	638.84	116.79	0.18	0.64	0.12	1.87	14.13	0.47	2217.73	45.57	17.44	0.70	1297.33	22.71
	698.48	122.74	0.18	0.70	0.12	2.04	16.38	0.67	2219.07	62.31	14.85	0.62	1313.01	20.50
	622.01	113.55	0.18	0.62	0.11	1.82	15.32	0.54	2206.15	51.29	18.17	0.67	1295.79	21.97
	817.66	141.58	0.17	0.82	0.14	2.39	14.83	0.54	2196.52	50.67	13.57	0.58	1311.01	18.83
	823.99	144.47	0.18	0.82	0.14	2.41	14.26	0.59	2217.52	54.48	13.28	0.57	1301.46	18.41
Mean	660.90	118.47	0.18	0.66	0.12	1.93	14.67	0.54	2211.27	51.02	14.91	0.59	1301.55	19.24
SD	105.61	16.01	0.01	0.11	0.02	0.31	1.11	0.07	8.35	5.63	3.10	0.13	9.67	3.98
COV%	15.98	13.51	4.69	15.98	13.51	15.98	7.58	12.13	0.38	11.03	20.76	21.93	0.74	20.68
Tibial Plateau Lateral Posterior	720.37	453.47	0.63	0.72	0.45	2.10	15.48	0.56	2208.08	53.31	16.28	0.65	1298.01	21.13
	732.89	452.83	0.62	0.73	0.45	2.14	16.46	0.59	2199.11	55.06	19.28	0.72	1300.14	23.79
	650.72	367.69	0.57	0.65	0.37	1.90	14.10	0.55	2226.46	52.30	14.89	0.59	1303.21	19.28
	707.32	447.09	0.63	0.71	0.45	2.07	15.67	0.60	2229.34	57.30	17.15	0.69	1316.90	22.92
	672.42	417.98	0.62	0.67	0.42	1.96	15.55	0.54	2217.31	51.55	16.20	0.68	1307.31	22.24
	659.34	422.69	0.64	0.66	0.42	1.93	14.57	0.40	2181.13	38.70	13.82	0.56	1297.63	18.21

	679.25	435.90	0.64	0.68	0.44	1.98	15.03	0.51	2235.46	50.01	15.51	0.67	1308.19	21.73
	629.81	370.59	0.59	0.63	0.37	1.84	13.65	0.46	2227.89	45.15	12.10	0.54	1317.32	17.50
	692.09	401.69	0.58	0.69	0.40	2.02	14.50	0.54	2211.11	50.80	17.60	0.67	1318.23	22.64
	757.24	461.22	0.61	0.76	0.46	2.21	14.19	0.52	2224.78	49.88	10.93	0.59	1304.17	17.88
Mean	690.14	423.12	0.61	0.69	0.42	2.02	14.92	0.53	2216.07	50.41	15.38	0.64	1307.11	20.73
SD	39.61	33.85	0.03	0.04	0.03	0.12	0.87	0.06	16.58	5.25	2.54	0.06	7.96	2.31
COV%	5.74	8.00	4.35	5.74	8.00	5.74	5.82	11.25	0.75	10.41	16.51	9.84	0.61	11.16
Mean	549.20	200.55	0.37	0.55	0.20	1.60	14.34	0.51	2206.03	48.47	13.66	0.58	1306.40	18.63
SD	448.61	169.56	0.15	0.45	0.17	1.31	2.03	0.07	16.33	6.02	3.13	0.10	9.61	3.24
COV%	81.68	84.55	40.63	81.68	84.55	81.68	14.16	13.29	0.74	12.43	22.94	16.79	0.74	17.40

Table 9. Cartilage, subchondral bone and trabecular bone raw data for cadaver 9, 79 years.

	79, Male													
	Cartilage						Subchondral Bone				Trabecular Bone			
	G' kPa	G" kPa	Tan Delta	G' MPa	G" MPa	E MPa	E GPa	H GPa	D nm	Load mN	E GPa	H GPa	D nm	Load mN
Femoral Condyle Medial Inferior	388.57	162.88	0.42	0.39	0.16	1.13	14.67	0.52	2212.59	49.90	17.24	0.63	1308.46	21.13
	312.85	116.21	0.37	0.31	0.12	0.91	16.24	0.62	2208.33	57.78	16.13	0.59	1311.40	19.79
	212.68	70.60	0.33	0.21	0.07	0.62	16.05	0.57	2218.76	54.29	17.64	0.66	1297.22	21.75
	291.23	110.87	0.38	0.29	0.11	0.85	14.11	0.41	2178.35	39.55	15.51	0.53	1306.06	18.05
	193.10	65.64	0.34	0.19	0.07	0.56	13.85	0.43	2195.80	41.16	12.37	0.38	1310.42	13.17
	242.93	88.57	0.37	0.24	0.09	0.71	15.38	0.49	2183.31	46.23	9.70	0.57	1310.20	17.12
	323.06	122.98	0.38	0.32	0.12	0.94	15.25	0.50	2183.66	46.95	8.48	0.45	1303.70	13.77
	238.39	80.04	0.34	0.24	0.08	0.70	15.54	0.59	2207.14	55.36	18.43	0.64	1292.48	21.14
	200.82	66.88	0.33	0.20	0.07	0.59	14.92	0.47	2210.71	45.89	21.23	0.75	1303.94	25.14
	270.19	100.16	0.37	0.27	0.10	0.79	13.75	0.38	2207.06	37.94	13.21	0.37	1284.68	12.61
Mean	267.38	98.48	0.36	0.27	0.10	0.78	14.98	0.50	2200.57	47.50	14.99	0.56	1302.85	18.37
SD	62.19	30.75	0.03	0.06	0.03	0.18	0.88	0.08	14.24	6.82	4.01	0.12	8.80	4.19
COV%	23.26	31.23	7.70	23.26	31.23	23.26	5.86	15.50	0.65	14.36	26.76	22.36	0.68	22.79
Femoral Condyle Medial Superior	182.51	47.15	0.26	0.18	0.05	0.53	14.67	0.49	2208.90	46.70	15.17	0.53	1293.12	17.42
	244.04	62.79	0.26	0.24	0.06	0.71	14.05	0.43	2193.56	41.01	15.28	0.50	1294.60	16.81
	260.65	60.02	0.23	0.26	0.06	0.76	14.12	0.46	2210.42	44.52	15.94	0.55	1294.63	18.40
	151.67	36.57	0.24	0.15	0.04	0.44	12.20	0.39	2213.96	37.99	15.34	0.56	1290.51	18.26
	265.30	72.41	0.27	0.27	0.07	0.77	14.16	0.51	2225.29	48.76	13.74	0.45	1294.42	15.18
	183.39	45.24	0.25	0.18	0.05	0.54	13.25	0.44	2206.53	42.27	16.83	0.56	1292.05	18.58

	243.65	67.92	0.28	0.24	0.07	0.71	14.58	0.51	2173.57	47.31	15.04	0.56	1290.39	18.32
	166.36	40.13	0.24	0.17	0.04	0.49	14.39	0.54	2176.75	49.65	14.16	0.53	1295.32	17.28
	203.92	53.50	0.26	0.20	0.05	0.60	14.01	0.46	2175.22	43.05	15.73	0.59	1292.29	19.12
	317.07	85.03	0.27	0.32	0.09	0.93	13.94	0.46	2191.02	43.73	13.89	0.54	1283.50	17.12
Mean	221.86	57.08	0.26	0.22	0.06	0.65	13.94	0.47	2197.52	44.50	15.11	0.54	1292.08	17.65
SD	52.47	15.40	0.02	0.05	0.02	0.15	0.73	0.05	18.19	3.65	0.97	0.04	3.48	1.14
COV%	23.65	26.98	6.13	23.65	26.98	23.65	5.21	9.66	0.83	8.19	6.40	7.04	0.27	6.45
Femoral Condyle Lateral Inferior	198.26	38.07	0.19	0.20	0.04	0.58	14.52	0.54	2176.03	49.43	14.50	0.60	1287.03	19.11
	219.45	43.62	0.20	0.22	0.04	0.64	14.42	0.50	2175.21	46.24	12.64	0.53	1281.20	16.49
	216.35	44.23	0.20	0.22	0.04	0.63	13.46	0.47	2202.23	44.35	15.12	0.63	1289.58	19.99
	280.58	57.68	0.21	0.28	0.06	0.82	17.81	0.80	2216.49	72.60	11.96	0.48	1287.47	15.44
	261.48	56.51	0.22	0.26	0.06	0.76	10.54	0.28	2185.27	27.41	14.20	0.63	1277.88	19.47
	250.66	52.17	0.21	0.25	0.05	0.73	11.53	0.38	2202.72	36.26	11.50	0.48	1278.45	15.03
	196.13	44.29	0.23	0.20	0.04	0.57	10.79	0.33	2213.69	32.55	14.72	0.54	1300.96	17.93
	235.84	51.87	0.22	0.24	0.05	0.69	12.70	0.44	2218.38	42.61	15.00	0.83	1295.61	24.67
	257.80	56.91	0.22	0.26	0.06	0.75	14.18	0.51	2192.09	47.29	14.06	0.52	1296.39	17.04
	377.81	78.54	0.21	0.38	0.08	1.10	13.57	0.45	2180.38	42.54	12.19	0.59	1286.51	17.91
Mean	249.44	52.39	0.21	0.25	0.05	0.73	13.35	0.47	2196.25	44.13	13.59	0.58	1288.11	18.31
SD	53.03	11.37	0.01	0.05	0.01	0.15	2.14	0.14	16.74	12.17	1.37	0.10	7.76	2.78
COV%	21.26	21.71	5.06	21.26	21.71	21.26	16.04	30.00	0.76	27.59	10.08	17.50	0.60	15.18
Femoral Condyle Lateral Superior	245.70	48.66	0.20	0.25	0.05	0.72	17.68	0.71	2171.90	63.62	7.77	0.38	1279.59	11.41
	138.83	28.94	0.21	0.14	0.03	0.41	15.10	0.47	2202.33	45.33	16.70	0.66	1276.66	20.77
	138.61	29.66	0.21	0.14	0.03	0.40	17.89	0.63	2202.03	59.39	14.87	0.65	1286.04	20.20
	162.71	35.62	0.22	0.16	0.04	0.48	13.50	0.41	2206.18	40.14	9.05	0.31	1266.52	9.84
	171.07	39.29	0.23	0.17	0.04	0.50	14.52	0.46	2226.46	45.31	12.73	0.48	1289.73	15.59
	150.10	36.74	0.25	0.15	0.04	0.44	13.12	0.39	2209.31	38.62	10.56	0.36	1259.60	11.37

	182.14	44.72	0.25	0.18	0.04	0.53	13.22	0.36	2192.97	35.49	13.85	0.58	1299.45	18.60
	224.56	57.25	0.26	0.22	0.06	0.66	13.64	0.40	2221.73	39.95	8.58	0.47	1302.12	14.24
	257.38	67.75	0.26	0.26	0.07	0.75	15.05	0.48	2219.38	47.24	5.53	0.43	1308.48	11.71
	227.48	65.71	0.29	0.23	0.07	0.66	15.05	0.51	2207.86	48.42	10.60	0.39	1298.35	12.96
Mean	189.86	45.44	0.24	0.19	0.05	0.55	14.88	0.48	2206.01	46.35	11.02	0.47	1286.66	14.67
SD	45.04	14.10	0.03	0.05	0.01	0.13	1.71	0.11	15.71	9.02	3.48	0.12	16.03	3.96
COV%	23.72	31.04	11.88	23.72	31.04	23.72	11.51	22.70	0.71	19.47	31.55	25.86	1.25	26.96
Tibial Plateau Medial Anterior	49.89	15.14	0.30	0.05	0.02	0.15	13.56	0.48	2204.56	45.57	11.79	0.48	1302.14	15.64
	53.64	15.23	0.28	0.05	0.02	0.16	16.09	0.59	2181.27	54.41	14.69	0.54	1291.57	17.60
	55.03	16.44	0.30	0.06	0.02	0.16	14.92	0.58	2189.29	52.83	16.07	0.61	1299.97	20.16
	47.44	13.43	0.28	0.05	0.01	0.14	14.43	0.50	2188.93	47.06	14.98	0.61	1301.02	19.86
	48.62	13.05	0.27	0.05	0.01	0.14	13.36	0.45	2203.09	42.69	16.51	0.63	1290.15	20.46
	31.87	9.29	0.29	0.03	0.01	0.09	14.43	0.52	2225.42	49.92	5.62	0.44	1297.85	11.76
	80.55	22.04	0.27	0.08	0.02	0.24	18.27	0.65	2180.27	60.03	7.83	0.48	1306.98	14.20
	52.54	14.16	0.27	0.05	0.01	0.15	14.38	0.49	2203.51	46.38	14.97	0.57	1315.43	19.24
	35.90	10.17	0.28	0.04	0.01	0.10	13.78	0.46	2201.36	44.08	19.26	0.72	1308.74	24.15
	44.72	12.38	0.28	0.04	0.01	0.13	13.86	0.55	2174.42	49.71	13.89	0.59	1302.24	19.05
Mean	50.02	14.13	0.28	0.05	0.01	0.15	14.71	0.53	2195.21	49.27	13.56	0.57	1301.61	18.21
SD	13.09	3.56	0.01	0.01	0.00	0.04	1.48	0.06	15.25	5.30	4.11	0.09	7.61	3.55
COV%	26.17	25.16	4.16	26.17	25.16	26.17	10.04	12.17	0.69	10.75	30.28	15.08	0.58	19.49
Tibial Plateau Medial Posterior	48.89	15.90	0.33	0.05	0.02	0.14	13.96	0.54	2210.92	50.82	13.23	0.55	1303.00	17.81
	81.99	28.28	0.35	0.08	0.03	0.24	12.76	0.47	2165.71	42.30	15.94	0.52	1315.90	18.06
	63.98	20.00	0.31	0.06	0.02	0.19	15.07	0.47	2183.58	44.78	14.63	0.40	1287.17	13.78
	73.58	22.79	0.31	0.07	0.02	0.21	13.41	0.45	2195.28	42.65	16.04	0.50	1286.31	16.62
	40.06	12.46	0.31	0.04	0.01	0.12	14.50	0.51	2209.46	48.89	14.34	0.54	1319.19	18.23
	51.34	15.57	0.30	0.05	0.02	0.15	18.44	0.59	2204.75	57.11	14.80	0.52	1300.18	17.23

	29.31	8.72	0.30	0.03	0.01	0.09	12.61	0.36	2209.07	35.25	13.11	0.54	1307.05	17.64
	51.42	15.46	0.30	0.05	0.02	0.15	14.61	0.49	2208.27	46.77	14.55	0.54	1313.66	18.33
	36.01	10.11	0.28	0.04	0.01	0.11	12.86	0.48	2260.53	47.34	15.05	0.57	1312.06	19.19
	44.60	12.06	0.27	0.04	0.01	0.13	15.98	0.55	2212.80	52.52	17.13	0.66	1308.26	21.80
Mean	52.12	16.13	0.31	0.05	0.02	0.15	14.42	0.49	2206.04	46.84	14.88	0.53	1305.28	17.87
SD	16.62	6.05	0.02	0.02	0.01	0.05	1.79	0.06	24.30	6.10	1.24	0.06	11.32	2.01
COV%	31.89	37.48	6.90	31.89	37.48	31.89	12.40	13.25	1.10	13.02	8.35	11.74	0.87	11.24
Tibial Plateau Lateral Anterior	96.14	15.50	0.16	0.10	0.02	0.28	14.02	0.49	2224.78	47.06	6.80	0.52	1297.22	13.98
	126.66	20.30	0.16	0.13	0.02	0.37	15.36	0.60	2239.27	57.21	7.85	0.57	1313.94	16.02
	118.21	19.84	0.17	0.12	0.02	0.35	9.02	0.44	2235.96	39.81	8.83	0.66	1301.24	18.12
	102.11	16.96	0.17	0.10	0.02	0.30	15.29	0.53	2220.79	50.81	8.20	0.48	1298.64	14.14
	111.67	19.65	0.18	0.11	0.02	0.33	13.31	0.45	2219.54	43.93	8.57	0.52	1312.51	15.53
	154.42	24.78	0.16	0.15	0.02	0.45	14.51	0.52	2218.89	49.37	8.17	0.53	1313.38	15.60
	129.15	19.73	0.15	0.13	0.02	0.38	13.63	0.48	2244.07	46.91	9.09	0.59	1306.05	17.15
	110.28	18.85	0.17	0.11	0.02	0.32	16.11	0.56	2206.72	53.16	8.77	0.57	1301.92	16.32
	163.68	27.29	0.17	0.16	0.03	0.48	15.11	0.56	2238.13	54.03	7.81	0.57	1305.42	15.92
	212.00	34.57	0.16	0.21	0.03	0.62	15.63	0.51	2205.84	48.82	3.89	0.38	1302.62	9.43
Mean	132.43	21.75	0.16	0.13	0.02	0.39	14.20	0.51	2225.40	49.11	7.80	0.54	1305.29	15.22
SD	35.27	5.66	0.01	0.04	0.01	0.10	2.03	0.05	13.52	5.07	1.52	0.07	6.12	2.38
COV%	26.63	26.05	3.96	26.63	26.05	26.63	14.30	9.76	0.61	10.33	19.51	13.79	0.47	15.64
Tibial Plateau Lateral Posterior	60.70	14.21	0.23	0.06	0.01	0.18	12.63	0.50	2201.82	46.04	6.49	0.50	1280.22	13.13
	84.02	20.46	0.24	0.08	0.02	0.25	14.91	0.51	2197.88	47.92	8.82	0.60	1289.36	16.62
	99.77	25.80	0.26	0.10	0.03	0.29	14.00	0.46	2189.47	43.78	9.13	0.55	1292.95	15.92
	73.65	18.14	0.25	0.07	0.02	0.22	13.77	0.56	2217.52	52.39	7.65	0.48	1301.89	14.03
	83.40	20.09	0.24	0.08	0.02	0.24	13.60	0.52	2211.72	48.80	6.37	0.40	1296.83	11.48
	60.80	13.85	0.23	0.06	0.01	0.18	14.21	0.45	2171.86	42.33	5.40	0.45	1289.25	11.58

	71.53	15.43	0.22	0.07	0.02	0.21	14.03	0.44	2189.13	42.23	7.45	0.42	1305.89	12.62
	66.47	16.82	0.25	0.07	0.02	0.19	12.71	0.43	2215.48	41.33	6.84	0.53	1309.54	14.52
	41.18	9.44	0.23	0.04	0.01	0.12	14.61	0.59	2210.47	54.99	7.44	0.43	1301.00	12.70
	30.48	7.36	0.24	0.03	0.01	0.09	15.83	0.61	2205.09	57.12	7.71	0.51	1306.66	14.67
Mean	67.20	16.16	0.24	0.07	0.02	0.20	14.03	0.51	2201.04	47.69	7.33	0.48	1297.36	13.72
SD	20.48	5.41	0.01	0.02	0.01	0.06	0.96	0.06	14.29	5.60	1.12	0.06	9.34	1.74
COV%	30.48	33.49	5.30	30.48	33.49	30.48	6.86	12.78	0.65	11.75	15.29	13.18	0.72	12.65
Mean	153.79	40.19	0.26	0.15	0.04	0.45	14.31	0.49	2203.51	46.92	12.29	0.53	1297.40	16.75
SD	93.63	30.80	0.06	0.09	0.03	0.27	1.57	0.08	18.51	7.08	3.89	0.09	11.52	3.30
COV%	60.88	76.63	23.24	60.88	76.63	60.88	10.95	16.47	0.84	15.09	31.64	17.29	0.89	19.67

Table 10. Cartilage, subchondral bone and trabecular bone raw data for cadaver 10, 80 years.

	80, Male													
	Cartilage						Subchondral Bone				Trabecular Bone			
	G' kPa	G'' kPa	Tan Delta	G' MPa	G'' MPa	E MPa	E GPa	H GPa	D nm	Load mN	E GPa	H GPa	D nm	Load mN
Femoral Condyle Medial Inferior	44.07	14.04	0.32	0.04	0.01	0.13	15.25	0.54	2195.51	50.43	7.14	0.41	1299.42	12.20
	58.84	19.95	0.34	0.06	0.02	0.17	16.08	0.58	2214.01	55.36	10.90	0.55	1320.34	17.44
	41.41	12.84	0.31	0.04	0.01	0.12	15.50	0.53	2204.44	50.40	11.51	0.54	1311.24	17.22
	42.80	13.70	0.32	0.04	0.01	0.12	13.81	0.43	2194.33	41.07	12.58	0.60	1312.82	19.06
	34.27	10.88	0.32	0.03	0.01	0.10	14.42	0.51	2211.22	48.52	13.81	0.56	1307.65	18.36
	27.79	8.17	0.29	0.03	0.01	0.08	16.06	0.56	2179.41	52.12	13.14	0.50	1317.30	16.77
	71.47	27.51	0.39	0.07	0.03	0.21	15.81	0.52	2222.25	50.76	9.51	0.50	1323.53	15.69
	38.80	11.29	0.29	0.04	0.01	0.11	15.08	0.50	2205.29	48.17	10.90	0.48	1317.67	15.79
	41.87	12.93	0.31	0.04	0.01	0.12	14.80	0.49	2199.27	46.96	9.85	0.36	1302.18	12.01
	56.84	19.32	0.34	0.06	0.02	0.17	14.54	0.49	2191.98	46.18	11.35	0.46	1309.59	15.24
Mean	45.82	15.06	0.32	0.05	0.02	0.13	15.13	0.51	2201.77	49.00	11.07	0.49	1312.17	15.98
SD	12.92	5.66	0.03	0.01	0.01	0.04	0.75	0.04	12.36	3.85	1.94	0.07	7.77	2.36
COV%	28.21	37.59	8.45	28.21	37.59	28.21	4.96	8.32	0.56	7.85	17.50	14.40	0.59	14.77
Femoral Condyle Medial Superior	323.21	114.85	0.36	0.32	0.11	0.94	16.21	0.57	2185.08	52.88	13.58	0.54	1297.24	17.64
	151.69	40.99	0.27	0.15	0.04	0.44	14.26	0.45	2168.88	42.35	10.59	0.45	1293.27	14.25
	101.71	24.34	0.24	0.10	0.02	0.30	9.44	0.48	2230.66	42.88	14.08	0.57	1296.70	18.29
	142.98	49.63	0.35	0.14	0.05	0.42	15.08	0.48	2188.48	45.89	13.45	0.55	1297.75	17.83
	157.04	44.19	0.28	0.16	0.04	0.46	15.28	0.48	2188.76	46.07	9.98	0.52	1301.65	16.04
	151.21	51.06	0.34	0.15	0.05	0.44	17.11	0.58	2189.74	54.88	8.67	0.43	1306.80	13.52

	222.89	69.88	0.31	0.22	0.07	0.65	15.33	0.56	2200.69	52.85	11.54	0.45	1300.83	14.73
	103.24	25.31	0.25	0.10	0.03	0.30	16.05	0.50	2178.43	47.57	13.76	0.59	1307.32	19.09
	145.50	55.63	0.38	0.15	0.06	0.42	15.89	0.56	2209.11	53.38	12.28	0.46	1312.00	15.36
	84.11	19.02	0.23	0.08	0.02	0.25	17.36	0.62	2216.71	59.27	12.73	0.54	1308.79	17.55
Mean	158.36	49.49	0.30	0.16	0.05	0.46	15.20	0.53	2195.65	49.80	12.07	0.51	1302.23	16.43
SD	69.60	27.84	0.05	0.07	0.03	0.20	2.23	0.06	18.66	5.63	1.83	0.06	6.18	1.90
COV%	43.95	56.25	18.30	43.95	56.25	43.95	14.66	10.55	0.85	11.30	15.13	11.29	0.47	11.59
Femoral Condyle Lateral Inferior	178.38	56.15	0.32	0.18	0.06	0.52	14.18	0.61	2188.86	54.95	12.14	0.57	1291.74	17.61
	184.97	56.93	0.31	0.18	0.06	0.54	15.12	0.62	2190.24	56.19	12.15	0.47	1304.06	15.53
	524.83	142.11	0.27	0.52	0.14	1.53	13.60	0.56	2218.16	52.40	13.45	0.57	1309.94	18.65
	457.26	109.42	0.24	0.46	0.11	1.34	13.88	0.52	2197.76	48.51	13.00	0.60	1304.94	19.09
	361.27	82.51	0.23	0.36	0.08	1.05	13.17	0.55	2219.15	51.04	11.28	0.40	1295.64	13.24
	457.26	101.86	0.22	0.46	0.10	1.34	13.77	0.57	2193.52	51.47	15.60	0.70	1313.37	22.63
	772.97	184.03	0.24	0.77	0.18	2.26	13.74	0.63	2227.22	57.68	13.72	0.42	1280.74	13.95
	809.62	189.53	0.23	0.81	0.19	2.36	12.33	0.42	2174.61	39.12	15.90	0.61	1292.46	19.82
	777.13	175.05	0.23	0.78	0.18	2.27	14.63	0.56	2195.35	51.59	14.22	0.59	1299.59	19.10
	731.48	177.25	0.24	0.73	0.18	2.14	15.69	0.68	2216.63	62.24	15.57	0.92	1318.23	27.94
Mean	525.52	127.48	0.25	0.53	0.13	1.53	14.01	0.57	2202.15	52.52	13.70	0.59	1301.07	18.75
SD	240.47	52.78	0.03	0.24	0.05	0.70	0.96	0.07	17.00	6.15	1.61	0.15	11.33	4.30
COV%	45.76	41.40	13.47	45.76	41.40	45.76	6.85	12.30	0.77	11.71	11.77	25.71	0.87	22.91
Femoral Condyle Lateral Superior	1328.78	579.88	0.44	1.33	0.58	3.88	13.30	0.46	2153.77	41.66	10.05	0.61	1280.27	17.33
	1714.78	617.35	0.36	1.71	0.62	5.01	11.77	0.36	2156.70	33.20	10.17	0.58	1284.84	16.86
	977.68	388.69	0.40	0.98	0.39	2.85	12.80	0.41	2153.15	38.09	10.23	0.54	1283.61	15.96
	873.13	310.09	0.36	0.87	0.31	2.55	15.27	0.53	2202.28	50.28	10.81	0.42	1287.59	13.38
	1470.00	445.58	0.30	1.47	0.45	4.29	15.32	0.47	2160.31	43.56	10.31	0.46	1285.05	14.34
	1295.78	452.84	0.35	1.30	0.45	3.78	13.60	0.45	2202.43	43.00	6.77	0.47	1289.09	13.02

	1678.22	678.64	0.40	1.68	0.68	4.90	17.35	0.72	2249.71	68.53	7.68	0.43	1288.08	12.76
	1706.61	653.02	0.38	1.71	0.65	4.98	14.20	0.47	2176.26	44.03	6.54	0.47	1285.14	12.70
	1881.50	632.43	0.34	1.88	0.63	5.49	16.63	0.56	2205.07	53.16	5.98	0.42	1294.23	11.70
	1487.74	359.28	0.24	1.49	0.36	4.34	14.79	0.52	2189.05	48.34	8.14	0.54	1285.36	15.10
Mean	1441.42	511.78	0.36	1.44	0.51	4.21	14.50	0.49	2184.87	46.39	8.67	0.49	1286.33	14.31
SD	328.24	135.43	0.06	0.33	0.14	0.96	1.72	0.10	31.07	9.69	1.84	0.07	3.73	1.92
COV%	22.77	26.46	15.56	22.77	26.46	22.77	11.88	19.79	1.42	20.89	21.25	13.75	0.29	13.44
Tibial Plateau Medial Anterior	29.73	9.08	0.31	0.03	0.01	0.09	15.97	0.59	2212.77	55.43	12.29	0.55	1316.27	17.95
	25.71	7.92	0.31	0.03	0.01	0.08	19.45	0.71	2188.08	65.44	12.42	0.49	1309.61	16.34
	31.22	11.07	0.36	0.03	0.01	0.09	17.70	0.61	2179.72	56.73	9.44	0.49	1308.89	15.20
	20.65	7.03	0.34	0.02	0.01	0.06	16.75	0.53	2182.00	50.33	12.15	0.47	1309.53	15.68
	26.74	7.96	0.30	0.03	0.01	0.08	16.53	0.56	2190.31	52.57	14.41	0.55	1299.48	18.14
	23.79	7.14	0.30	0.02	0.01	0.07	17.67	0.53	2144.09	48.83	17.47	0.66	1308.38	21.99
	31.21	9.82	0.32	0.03	0.01	0.09	14.38	0.50	2181.53	46.59	17.95	0.74	1300.86	24.07
	19.16	6.25	0.33	0.02	0.01	0.06	14.28	0.47	2200.44	44.86	13.49	0.80	1299.12	23.47
	23.21	7.67	0.33	0.02	0.01	0.07	13.04	0.49	2201.12	45.76	9.01	0.64	1309.65	18.11
	32.55	9.77	0.30	0.03	0.01	0.10	14.04	0.46	2196.58	43.93	11.93	0.48	1310.52	15.78
Mean	26.40	8.37	0.32	0.03	0.01	0.08	15.98	0.54	2187.66	51.05	13.06	0.59	1307.23	18.67
SD	4.69	1.51	0.02	0.00	0.00	0.01	2.02	0.07	18.54	6.69	2.94	0.12	5.58	3.32
COV%	17.78	18.03	6.18	17.78	18.03	17.78	12.62	13.69	0.85	13.11	22.55	19.86	0.43	17.77
Tibial Plateau Medial Posterior	212.46	51.69	0.24	0.21	0.05	0.62	14.98	0.47	2200.79	44.99	13.17	0.48	1313.71	16.26
	78.36	17.30	0.22	0.08	0.02	0.23	17.79	0.62	2207.26	58.70	13.02	0.51	1306.09	16.89
	67.66	15.65	0.23	0.07	0.02	0.20	17.01	0.64	2216.14	60.36	16.36	0.73	1315.57	23.70
	48.43	11.44	0.24	0.05	0.01	0.14	15.32	0.53	2224.37	51.48	14.32	0.55	1307.16	18.37
	45.95	11.20	0.24	0.05	0.01	0.13	17.64	0.63	2243.41	61.27	15.24	0.54	1304.94	18.05
	50.12	11.49	0.23	0.05	0.01	0.15	16.96	0.61	2218.75	58.21	16.37	0.62	1298.99	20.37

	54.23	11.11	0.21	0.05	0.01	0.16	16.79	0.56	2192.13	53.13	17.47	0.70	1298.26	22.77
	84.08	17.30	0.21	0.08	0.02	0.25	15.86	0.53	2212.28	51.19	14.81	0.41	1266.23	13.49
	144.88	33.18	0.23	0.14	0.03	0.42	18.44	0.60	2195.39	56.91	13.50	0.39	1263.40	12.71
	422.97	122.65	0.29	0.42	0.12	1.24	16.96	0.58	2209.59	55.80	13.47	0.40	1271.19	13.19
Mean	120.91	30.30	0.23	0.12	0.03	0.35	16.78	0.58	2212.01	55.20	14.77	0.53	1294.55	17.58
SD	118.57	34.94	0.02	0.12	0.03	0.35	1.10	0.05	15.01	5.02	1.56	0.12	19.89	3.87
COV%	98.06	115.33	10.27	98.06	115.33	98.06	6.56	9.27	0.68	9.09	10.53	22.72	1.54	22.04
Tibial Plateau Lateral Anterior	61.25	13.91	0.23	0.06	0.01	0.18	15.15	0.63	2197.84	57.33	11.45	0.53	1301.48	16.63
	47.08	10.46	0.22	0.05	0.01	0.14	12.04	0.51	2224.99	47.45	12.29	0.51	1300.33	16.37
	40.30	8.71	0.22	0.04	0.01	0.12	16.26	0.65	2193.45	59.79	13.31	0.61	1303.72	19.48
	29.79	7.14	0.24	0.03	0.01	0.09	13.82	0.48	2180.73	44.91	10.54	0.47	1301.13	14.98
	43.29	9.99	0.23	0.04	0.01	0.13	15.49	0.64	2200.44	58.23	13.38	0.64	1302.16	19.95
	38.38	8.81	0.23	0.04	0.01	0.11	14.94	0.59	2199.49	54.37	10.93	0.44	1288.58	14.16
	46.07	10.37	0.23	0.05	0.01	0.13	13.74	0.53	2197.33	49.20	7.92	0.42	1279.81	12.40
	56.60	12.58	0.22	0.06	0.01	0.17	13.44	0.47	2186.68	43.73	8.12	0.57	1287.91	15.60
	46.96	11.18	0.24	0.05	0.01	0.14	15.41	0.56	2187.16	51.84	13.28	0.67	1299.21	20.65
	56.69	12.30	0.22	0.06	0.01	0.17	14.95	0.62	2200.57	56.37	12.77	0.51	1271.01	15.76
Mean	46.64	10.55	0.23	0.05	0.01	0.14	14.52	0.57	2196.87	52.32	11.40	0.54	1293.53	16.60
SD	9.53	2.04	0.01	0.01	0.00	0.03	1.24	0.07	12.00	5.76	2.04	0.08	11.20	2.66
COV%	20.44	19.31	3.55	20.44	19.31	20.44	8.57	11.85	0.55	11.01	17.94	15.67	0.87	16.05
Tibial Plateau Lateral Posterior	105.88	23.20	0.22	0.11	0.02	0.31	17.15	0.60	2207.85	57.31	7.18	0.48	1302.02	13.70
	84.00	19.33	0.23	0.08	0.02	0.25	17.24	0.59	2193.32	55.63	8.07	0.56	1299.37	15.70
	52.91	11.91	0.23	0.05	0.01	0.15	16.87	0.57	2218.02	55.43	12.33	0.56	1308.00	17.88
	51.16	11.08	0.22	0.05	0.01	0.15	14.28	0.48	2208.88	46.20	13.50	0.49	1305.59	16.44
	58.19	14.89	0.26	0.06	0.01	0.17	16.78	0.56	2210.96	53.74	16.36	0.64	1303.97	20.97
	44.60	13.00	0.29	0.04	0.01	0.13	17.53	0.72	2212.24	66.93	10.52	0.47	1307.78	15.11

	59.22	13.38	0.23	0.06	0.01	0.17	14.42	0.45	2240.37	44.94	13.45	0.59	1305.10	18.84
	125.93	33.78	0.27	0.13	0.03	0.37	16.73	0.54	2204.96	52.18	13.50	0.62	1313.40	19.92
	138.10	37.00	0.27	0.14	0.04	0.40	17.63	0.66	2215.43	62.38	10.52	0.44	1305.26	14.20
	82.56	17.50	0.21	0.08	0.02	0.24	16.09	0.51	2196.34	49.27	13.84	0.55	1305.06	18.06
Mean	80.25	19.51	0.24	0.08	0.02	0.23	16.47	0.57	2210.84	54.40	11.93	0.54	1305.55	17.08
SD	33.17	9.17	0.03	0.03	0.01	0.10	1.20	0.08	12.96	6.83	2.83	0.07	3.75	2.44
COV%	41.33	47.02	11.38	41.33	47.02	41.33	7.30	14.33	0.59	12.56	23.73	12.43	0.29	14.31
Mean	305.66	96.57	0.28	0.31	0.10	0.89	15.33	0.55	2198.98	51.33	12.08	0.53	1300.33	16.93
SD	480.61	170.13	0.06	0.48	0.17	1.40	1.70	0.07	19.63	6.70	2.68	0.10	12.43	3.15
COV%	157.23	176.17	20.20	157.23	176.17	157.23	11.10	13.31	0.89	13.05	22.18	18.49	0.96	18.60

Table 11. Cartilage, subchondral bone and trabecular bone raw data for cadaver 11, 86 years.

	86, Female													
	Cartilage						Subchondral Bone				Trabecular Bone			
	G' kPa	G'' kPa	Tan Delta	G' MPa	G'' MPa	E MPa	E GPa	H GPa	D nm	Load mN	E GPa	H GPa	D nm	Load mN
Femoral Condyle Medial Inferior	273.28	77.10	0.28	0.27	0.08	0.80	14.31	0.52	2182.31	48.06	13.99	0.54	1304.43	17.92
	56.89	13.44	0.24	0.06	0.01	0.17	17.91	0.59	2167.21	54.72	16.52	0.69	1287.43	21.89
	82.59	23.97	0.29	0.08	0.02	0.24	15.90	0.59	2182.20	53.94	12.26	0.55	1302.64	17.60
	87.35	23.73	0.27	0.09	0.02	0.26	15.51	0.54	2177.55	50.12	12.25	0.47	1287.94	15.07
	69.61	21.91	0.32	0.07	0.02	0.20	13.10	0.49	2216.94	46.56	12.67	0.46	1277.90	14.73
	70.44	20.08	0.29	0.07	0.02	0.21	12.97	0.47	2240.03	45.77	6.68	0.36	1272.89	10.50
	162.67	38.28	0.24	0.16	0.04	0.47	11.37	0.35	2212.20	34.02	16.54	0.81	1299.56	25.07
	374.21	110.84	0.30	0.37	0.11	1.09	11.97	0.46	2242.17	44.02	16.77	0.65	1272.21	20.30
	423.73	128.33	0.30	0.42	0.13	1.24	12.62	0.42	2210.42	40.11	13.67	0.57	1304.61	18.46
	376.67	119.85	0.32	0.38	0.12	1.10	14.03	0.53	2214.62	49.62	11.84	0.53	1292.59	16.58
Mean	197.74	57.75	0.28	0.20	0.06	0.58	13.97	0.49	2204.56	46.70	13.32	0.56	1290.22	17.81
SD	148.73	46.40	0.03	0.15	0.05	0.43	2.00	0.08	26.12	6.25	3.02	0.13	12.67	4.05
COV%	75.21	80.34	10.20	75.21	80.34	75.21	14.32	15.30	1.18	13.38	22.65	22.68	0.98	22.76
Femoral Condyle Medial Superior	288.63	62.11	0.22	0.29	0.06	0.84	16.53	0.53	2184.70	50.12	14.57	0.58	1281.27	18.45
	233.18	51.94	0.22	0.23	0.05	0.68	13.33	0.47	2175.15	43.35	12.09	0.54	1286.75	16.77
	116.05	28.14	0.24	0.12	0.03	0.34	14.80	0.50	2184.32	47.10	13.19	0.59	1290.49	18.39
	114.84	27.80	0.24	0.11	0.03	0.34	13.92	0.43	2185.98	40.87	12.35	0.56	1286.37	17.39
	195.80	46.51	0.24	0.20	0.05	0.57	15.06	0.47	2182.79	44.67	13.62	0.61	1295.04	19.20
	289.15	70.05	0.24	0.29	0.07	0.84	17.40	0.55	2139.62	49.97	14.62	0.65	1295.44	20.54

	190.85	45.20	0.24	0.19	0.05	0.56	14.78	0.51	2206.56	48.88	13.44	0.54	1282.48	17.20
	532.24	132.47	0.25	0.53	0.13	1.55	16.70	0.54	2177.74	50.76	13.39	0.50	1290.77	16.27
	745.91	192.91	0.26	0.75	0.19	2.18	14.62	0.50	2201.65	47.56	11.15	0.46	1301.43	14.88
	827.27	233.67	0.28	0.83	0.23	2.42	14.01	0.51	2189.66	47.26	11.92	0.60	1293.23	18.23
Mean	353.39	89.08	0.24	0.35	0.09	1.03	15.12	0.50	2182.82	47.05	13.03	0.56	1290.33	17.73
SD	257.74	72.45	0.02	0.26	0.07	0.75	1.34	0.04	18.05	3.21	1.14	0.06	6.26	1.59
COV%	72.93	81.33	7.59	72.93	81.33	72.93	8.84	7.30	0.83	6.83	8.75	9.88	0.48	8.98
Femoral Condyle Lateral Inferior	758.77	466.12	0.61	0.76	0.47	2.22	14.42	0.46	2199.25	44.05	7.50	0.41	1286.91	12.24
	766.18	413.80	0.54	0.77	0.41	2.24	11.49	0.34	2168.91	31.83	10.75	0.68	1281.95	19.16
	695.87	384.99	0.55	0.70	0.38	2.03	12.89	0.44	2183.86	41.44	5.81	0.34	1293.39	9.87
	707.97	368.18	0.52	0.71	0.37	2.07	12.37	0.40	2166.63	37.56	11.27	0.57	1301.73	17.62
	693.88	346.56	0.50	0.69	0.35	2.03	13.40	0.44	2199.38	42.09	9.62	0.70	1283.45	18.88
	701.00	328.06	0.47	0.70	0.33	2.05	13.46	0.46	2213.95	44.21	8.16	0.65	1293.93	17.26
	708.46	318.55	0.45	0.71	0.32	2.07	15.31	0.72	2207.58	64.60	9.10	0.52	1292.89	15.28
	708.22	302.76	0.43	0.71	0.30	2.07	12.32	0.41	2209.07	39.50	14.64	0.55	1302.44	18.15
	684.83	300.25	0.44	0.68	0.30	2.00	13.23	0.49	2195.34	45.82	8.42	0.44	1312.94	13.66
	645.80	288.29	0.45	0.65	0.29	1.89	13.09	0.52	2184.07	47.49	5.45	0.35	1289.46	9.84
Mean	707.10	351.75	0.50	0.71	0.35	2.06	13.20	0.47	2192.80	43.86	9.07	0.52	1293.91	15.20
SD	34.57	56.84	0.06	0.03	0.06	0.10	1.08	0.10	16.44	8.56	2.72	0.13	9.54	3.59
COV%	4.89	16.16	12.26	4.89	16.16	4.89	8.19	22.01	0.75	19.52	29.96	25.89	0.74	23.65
Femoral Condyle Lateral Superior	451.74	879.62	1.95	0.45	0.88	1.32	10.50	0.42	2203.44	38.73	13.35	0.57	1282.71	17.87
	504.32	825.99	1.64	0.50	0.83	1.47	11.46	0.39	2192.62	36.64	14.17	0.61	1277.55	18.87
	563.68	811.40	1.44	0.56	0.81	1.65	11.51	0.49	2201.24	44.61	12.57	0.58	1300.47	18.38
	611.04	762.65	1.25	0.61	0.76	1.78	14.03	0.54	2212.50	50.30	12.37	0.92	1302.99	25.25
	563.25	760.02	1.35	0.56	0.76	1.64	14.19	0.51	2201.32	48.36	10.09	0.57	1271.82	16.32
	526.52	781.86	1.49	0.53	0.78	1.54	12.23	0.43	2251.51	42.19	8.49	0.55	1277.97	15.33

	498.39	784.81	1.58	0.50	0.78	1.46	13.05	0.55	2229.93	51.57	9.25	0.53	1291.79	15.63
	464.78	777.26	1.67	0.46	0.78	1.36	12.50	0.46	2206.59	43.35	18.45	0.72	1285.08	23.13
	473.19	763.96	1.61	0.47	0.76	1.38	11.02	0.58	2244.87	51.89	15.28	0.67	1289.94	20.93
	525.58	822.48	1.57	0.53	0.82	1.53	10.38	0.40	2213.57	37.65	13.65	0.55	1289.49	17.55
Mean	518.25	797.00	1.55	0.52	0.80	1.51	12.09	0.48	2215.76	44.53	12.77	0.63	1286.98	18.93
SD	50.25	37.90	0.19	0.05	0.04	0.15	1.36	0.07	19.81	5.79	2.97	0.12	9.99	3.26
COV%	9.70	4.76	12.39	9.70	4.76	9.70	11.24	14.14	0.89	13.00	23.30	18.80	0.78	17.23
Tibial Plateau Medial Anterior	85.99	25.47	0.30	0.09	0.03	0.25	15.31	0.60	2214.41	56.05	11.33	0.68	1295.73	19.92
	100.82	32.47	0.32	0.10	0.03	0.29	15.00	0.53	2178.94	48.82	11.16	0.53	1300.84	16.59
	248.05	83.97	0.34	0.25	0.08	0.72	13.36	0.42	2173.45	39.26	9.83	0.47	1302.99	14.66
	542.13	426.56	0.79	0.54	0.43	1.58	12.56	0.40	2167.95	37.57	9.10	0.62	1299.67	17.44
	444.99	277.71	0.62	0.44	0.28	1.30	15.60	0.57	2182.51	52.26	4.88	0.50	1299.79	12.01
	118.40	39.41	0.33	0.12	0.04	0.35	14.75	0.51	2192.82	47.84	14.80	0.64	1286.90	20.15
	123.12	40.59	0.33	0.12	0.04	0.36	11.95	0.36	2154.77	33.44	15.14	0.74	1293.15	22.71
	268.60	128.25	0.48	0.27	0.13	0.78	15.25	0.53	2174.47	49.36	12.39	0.60	1299.75	18.75
	276.31	134.51	0.49	0.28	0.13	0.81	10.50	0.41	2173.97	37.12	16.15	0.69	1297.93	22.09
	251.10	103.60	0.41	0.25	0.10	0.73	10.74	0.58	2168.33	48.30	5.70	0.45	1304.87	12.15
Mean	245.95	129.25	0.44	0.25	0.13	0.72	13.50	0.49	2178.16	45.00	11.05	0.59	1298.16	17.64
SD	151.59	128.77	0.16	0.15	0.13	0.44	1.96	0.09	16.16	7.54	3.81	0.10	5.17	3.80
COV%	61.63	99.63	36.03	61.63	99.63	61.63	14.50	17.43	0.74	16.75	34.49	17.12	0.40	21.55
Tibial Plateau Medial Posterior	979.96	1580.38	1.61	0.98	1.58	2.86	13.70	0.67	2189.88	58.34	9.63	0.61	1299.44	17.67
	919.91	1507.86	1.64	0.92	1.51	2.69	16.22	0.66	2178.39	59.00	8.77	0.64	1304.55	17.71
	982.20	1590.07	1.62	0.98	1.59	2.87	11.36	0.43	2200.01	39.71	5.35	0.44	1288.54	11.40
	1166.52	1994.89	1.71	1.17	1.99	3.41	14.18	0.47	2185.27	44.54	4.35	0.44	1282.95	10.39
	1140.50	2165.75	1.90	1.14	2.17	3.33	14.06	0.50	2178.83	45.94	5.48	0.43	1285.52	11.38
	1168.63	1361.23	1.17	1.17	1.36	3.41	13.65	0.56	2195.29	51.16	11.09	0.59	1299.89	18.04

	1175.95	1659.03	1.41	1.18	1.66	3.43	12.48	0.42	2181.95	39.27	10.22	0.74	1297.47	20.34
	1118.85	1413.78	1.26	1.12	1.41	3.27	17.00	0.85	2189.79	73.57	17.23	0.68	1295.12	21.95
	983.17	1128.75	1.15	0.98	1.13	2.87	15.28	0.66	2176.63	58.70	13.29	0.56	1308.05	18.23
	812.52	880.83	1.08	0.81	0.88	2.37	14.62	0.55	2174.43	50.36	8.35	0.54	1312.36	15.78
Mean	1044.82	1528.26	1.46	1.04	1.53	3.05	14.26	0.58	2185.05	52.06	9.37	0.57	1297.39	16.29
SD	126.26	375.35	0.28	0.13	0.38	0.37	1.66	0.13	8.50	10.59	3.93	0.11	9.62	3.97
COV%	12.08	24.56	19.20	12.08	24.56	12.08	11.65	23.34	0.39	20.33	41.92	18.55	0.74	24.40
Tibial Plateau Lateral Anterior	89.73	18.71	0.21	0.09	0.02	0.26	12.70	0.53	2249.71	50.47	12.16	0.63	1283.56	18.75
	53.00	11.51	0.22	0.05	0.01	0.15	14.24	0.53	2187.44	49.15	7.81	0.42	1281.63	12.33
	56.34	12.90	0.23	0.06	0.01	0.16	14.24	0.50	2189.96	46.45	7.60	0.57	1273.33	15.03
	66.69	15.50	0.23	0.07	0.02	0.19	13.62	0.45	2189.07	42.66	13.36	0.52	1298.82	16.95
	102.80	22.49	0.22	0.10	0.02	0.30	12.18	0.49	2206.32	45.00	14.30	0.66	1299.78	20.77
	56.02	12.08	0.22	0.06	0.01	0.16	12.56	0.51	2222.72	47.69	11.69	0.70	1278.31	19.86
	68.49	13.34	0.20	0.07	0.01	0.20	14.35	0.54	2191.66	50.26	14.21	0.82	1287.55	23.88
	80.79	16.57	0.21	0.08	0.02	0.24	11.28	0.31	2146.16	28.85	11.00	0.55	1309.80	17.16
	55.52	11.25	0.20	0.06	0.01	0.16	10.96	0.28	2177.16	27.35	14.98	0.75	1295.48	23.00
	56.32	11.77	0.21	0.06	0.01	0.16	12.19	0.41	2251.63	40.60	12.71	0.63	1317.32	20.11
Mean	68.57	14.61	0.21	0.07	0.01	0.20	12.83	0.45	2201.18	42.85	11.98	0.62	1292.56	18.78
SD	17.13	3.71	0.01	0.02	0.00	0.05	1.24	0.09	32.57	8.40	2.57	0.12	14.18	3.53
COV%	24.99	25.36	5.40	24.99	25.36	24.99	9.64	20.73	1.48	19.60	21.45	18.76	1.10	18.81
Tibial Plateau Lateral Posterior	96.86	21.94	0.23	0.10	0.02	0.28	15.07	0.54	2190.14	50.41	16.54	0.64	1288.21	20.70
	70.39	15.79	0.22	0.07	0.02	0.21	15.08	0.47	2166.75	43.66	13.35	0.59	1293.60	18.58
	47.63	11.27	0.24	0.05	0.01	0.14	16.46	0.61	2200.81	56.75	11.07	0.46	1295.18	14.71
	65.43	14.54	0.22	0.07	0.01	0.19	14.90	0.51	2184.68	47.38	16.14	0.59	1289.49	19.21
	98.05	23.14	0.24	0.10	0.02	0.29	14.95	0.50	2198.54	47.25	9.96	0.50	1300.12	15.47
	49.25	10.49	0.21	0.05	0.01	0.14	16.74	0.57	2182.65	53.55	9.75	0.42	1292.37	13.37

	56.60	12.28	0.22	0.06	0.01	0.17	7.98	0.33	2189.25	29.84	10.64	0.58	1293.71	17.35
	73.65	16.07	0.22	0.07	0.02	0.22	16.47	0.60	2182.41	54.99	11.47	0.62	1293.27	18.53
	59.11	12.95	0.22	0.06	0.01	0.17	15.85	0.52	2186.76	49.15	13.81	0.63	1310.34	20.12
	56.46	13.66	0.24	0.06	0.01	0.16	17.46	0.58	2169.04	53.53	12.89	0.55	1311.97	17.95
Mean	67.34	15.21	0.23	0.07	0.02	0.20	15.10	0.52	2185.10	48.65	12.56	0.56	1296.83	17.60
SD	17.90	4.26	0.01	0.02	0.00	0.05	2.65	0.08	10.96	7.74	2.42	0.07	8.21	2.39
COV%	26.58	28.02	4.33	26.58	28.02	26.58	17.56	15.65	0.50	15.91	19.25	13.31	0.63	13.57
Mean	400.40	372.87	0.61	0.40	0.37	1.17	13.76	0.50	2193.18	46.34	11.64	0.58	1293.30	17.50
SD	343.11	523.29	0.54	0.34	0.52	1.00	1.93	0.09	22.60	7.73	3.21	0.11	10.14	3.42
COV%	85.69	140.34	88.36	85.69	140.34	85.69	14.05	18.49	1.03	16.68	27.54	18.70	0.78	19.56

Table 12. Cartilage, subchondral bone and trabecular bone raw data for cadaver 12, 88 years.

	88, Male													
	Cartilage						Subchondral Bone				Trabecular Bone			
	G' kPa	G'' kPa	Tan Delta	G' MPa	G'' MPa	E MPa	E GPa	H GPa	D nm	Load mN	E GPa	H GPa	D nm	Load mN
Femoral Condyle Medial Inferior	624.34	139.22	0.22	0.62	0.14	1.82	17.41	0.51	2175.05	48.96	13.75	0.46	1310.24	15.67
	515.84	106.93	0.21	0.52	0.11	1.51	11.89	0.29	2161.23	28.24	14.34	0.47	1306.81	16.13
	696.90	163.17	0.23	0.70	0.16	2.03	12.88	0.40	2196.36	38.37	13.34	0.35	1280.90	11.96
	1642.25	294.68	0.18	1.64	0.29	4.80	16.39	0.52	2173.55	48.76	14.34	0.49	1305.33	16.72
	1310.88	244.72	0.19	1.31	0.24	3.83	14.28	0.42	2195.99	41.06	10.12	0.49	1302.93	15.40
	1312.87	271.41	0.21	1.31	0.27	3.83	15.51	0.50	2188.10	47.37	16.32	0.48	1301.30	16.44
	1654.03	411.34	0.25	1.65	0.41	4.83	17.02	0.55	2181.82	51.87	16.43	0.54	1319.38	18.75
	124.76	36.62	0.29	0.12	0.04	0.36	15.79	0.52	2184.49	49.01	13.24	0.37	1308.10	12.96
	287.88	78.80	0.27	0.29	0.08	0.84	12.35	0.37	2204.91	35.74	14.02	0.44	1323.38	15.50
	121.06	36.01	0.30	0.12	0.04	0.35	13.93	0.40	2209.70	39.81	20.11	0.59	1317.44	20.73
Mean	829.08	178.29	0.24	0.83	0.18	2.42	14.75	0.45	2187.12	42.92	14.60	0.47	1307.58	16.03
SD	601.46	123.83	0.04	0.60	0.12	1.76	1.97	0.08	15.01	7.52	2.61	0.07	11.89	2.51
COV%	72.55	69.45	18.04	72.55	69.45	72.55	13.36	18.79	0.69	17.52	17.89	15.06	0.91	15.69
Femoral Condyle Medial Superior	49.50	11.27	0.23	0.05	0.01	0.14	13.51	0.41	2174.66	38.69	13.11	0.44	1307.99	14.97
	68.96	14.81	0.22	0.07	0.01	0.20	14.52	0.47	2171.73	44.03	10.93	0.40	1303.30	13.27
	149.52	29.77	0.20	0.15	0.03	0.44	13.36	0.39	2176.22	36.91	14.21	0.56	1312.06	18.51
	137.76	26.19	0.19	0.14	0.03	0.40	14.52	0.53	2171.81	48.45	14.80	0.54	1308.87	18.03
	118.74	24.59	0.21	0.12	0.02	0.35	14.09	0.46	2164.21	42.75	13.01	0.47	1310.22	15.93
	89.63	20.43	0.23	0.09	0.02	0.26	11.65	0.37	2203.84	35.63	13.15	0.58	1324.00	19.08

	44.59	10.68	0.24	0.04	0.01	0.13	14.86	0.46	2189.03	44.15	13.64	0.64	1314.95	20.44
	35.10	8.87	0.25	0.04	0.01	0.10	14.93	0.53	2193.27	49.67	17.43	0.64	1307.98	21.56
	41.28	9.79	0.24	0.04	0.01	0.12	14.41	0.52	2194.37	48.37	16.65	0.63	1311.57	21.13
	54.74	12.40	0.23	0.05	0.01	0.16	16.26	0.57	2182.74	53.26	13.51	0.48	1318.95	16.44
Mean	78.98	16.88	0.22	0.08	0.02	0.23	14.21	0.47	2182.19	44.19	14.04	0.54	1311.99	17.94
SD	42.44	7.70	0.02	0.04	0.01	0.12	1.21	0.07	12.56	5.84	1.88	0.09	5.98	2.75
COV%	53.73	45.62	8.78	53.73	45.62	53.73	8.51	14.37	0.58	13.21	13.38	16.28	0.46	15.33
Femoral Condyle Lateral Inferior	57.71	16.72	0.29	0.06	0.02	0.17	15.20	0.48	2182.20	45.15	13.86	0.49	1288.07	16.03
	26.17	7.33	0.28	0.03	0.01	0.08	14.51	0.41	2174.69	38.98	14.43	0.48	1286.03	15.91
	33.85	8.55	0.25	0.03	0.01	0.10	14.20	0.46	2168.68	43.21	17.72	0.61	1296.42	20.36
	42.53	10.84	0.26	0.04	0.01	0.12	15.37	0.51	2174.47	47.22	12.33	0.48	1296.36	15.73
	40.34	10.46	0.26	0.04	0.01	0.12	15.59	0.51	2192.27	48.68	11.59	0.48	1287.16	15.18
	35.76	9.22	0.26	0.04	0.01	0.10	14.52	0.49	2195.81	46.32	14.37	0.45	1287.71	15.18
	40.20	9.41	0.23	0.04	0.01	0.12	15.25	0.53	2192.24	50.12	12.42	0.52	1298.48	16.78
	48.30	11.12	0.23	0.05	0.01	0.14	15.02	0.49	2195.24	46.30	12.34	0.45	1295.98	14.81
	26.62	6.44	0.24	0.03	0.01	0.08	15.29	0.45	2204.33	43.84	13.64	0.53	1299.97	17.39
	23.39	6.50	0.28	0.02	0.01	0.07	14.85	0.45	2194.49	43.11	10.12	0.48	1309.56	15.30
Mean	37.49	9.66	0.26	0.04	0.01	0.11	14.98	0.48	2187.44	45.29	13.28	0.50	1294.57	16.27
SD	10.69	3.01	0.02	0.01	0.00	0.03	0.45	0.04	11.65	3.19	2.06	0.05	7.42	1.64
COV%	28.51	31.13	7.71	28.51	31.13	28.51	2.99	7.83	0.53	7.05	15.49	9.46	0.57	10.07
Femoral Condyle Lateral Superior	68.05	22.83	0.34	0.07	0.02	0.20	12.21	0.38	2240.40	38.36	11.89	0.52	1297.93	16.54
	125.15	49.65	0.40	0.13	0.05	0.37	11.60	0.36	2231.42	35.44	13.38	0.43	1297.97	14.49
	98.75	30.35	0.31	0.10	0.03	0.29	14.86	0.58	2239.59	55.72	11.91	0.47	1297.21	15.19
	52.85	16.43	0.31	0.05	0.02	0.15	12.46	0.39	2218.15	38.31	11.56	0.55	1283.27	16.81
	65.71	22.83	0.35	0.07	0.02	0.19	12.78	0.34	2209.08	34.03	16.69	0.60	1289.16	19.68
	92.29	35.96	0.39	0.09	0.04	0.27	17.80	0.71	2231.42	67.17	15.55	0.60	1278.87	19.06

	77.62	29.52	0.38	0.08	0.03	0.23	16.36	0.66	2216.69	61.37	14.49	0.55	1300.52	18.09
	40.42	12.35	0.31	0.04	0.01	0.12	12.84	0.38	2211.21	37.26	13.19	0.46	1281.34	14.95
	45.66	14.32	0.31	0.05	0.01	0.13	12.84	0.40	2223.80	39.23	15.29	0.56	1280.80	17.92
	54.62	17.60	0.32	0.05	0.02	0.16	12.44	0.42	2206.40	40.33	13.30	0.51	1282.29	16.38
Mean	72.11	25.18	0.34	0.07	0.03	0.21	13.62	0.46	2222.82	44.72	13.73	0.52	1288.94	16.91
SD	26.66	11.49	0.04	0.03	0.01	0.08	2.03	0.13	12.44	11.97	1.74	0.06	8.61	1.76
COV%	36.97	45.62	10.48	36.97	45.62	36.97	14.94	29.20	0.56	26.76	12.64	11.24	0.67	10.40
Tibial Plateau Medial Anterior	55.66	22.24	0.40	0.06	0.02	0.16	12.98	0.44	2186.41	41.19	13.05	0.65	1330.22	21.05
	44.25	16.51	0.37	0.04	0.02	0.13	13.85	0.51	2213.40	48.02	10.38	0.40	1300.14	13.04
	31.55	12.06	0.38	0.03	0.01	0.09	11.56	0.35	2179.46	33.35	9.00	0.48	1300.06	14.54
	57.61	22.65	0.39	0.06	0.02	0.17	13.62	0.47	2222.36	45.51	15.56	0.61	1304.07	20.00
	66.47	27.81	0.42	0.07	0.03	0.19	15.25	0.55	2186.58	51.03	14.75	0.67	1315.23	21.78
	71.80	30.48	0.43	0.07	0.03	0.21	13.96	0.47	2198.42	44.33	13.12	0.63	1305.91	19.85
	171.53	106.99	0.62	0.17	0.11	0.50	15.50	0.62	2189.25	56.59	9.03	0.35	1309.33	11.52
	132.23	65.69	0.50	0.13	0.07	0.39	13.53	0.48	2179.59	44.42	10.02	0.48	1303.15	15.18
	69.82	29.68	0.43	0.07	0.03	0.20	14.50	0.49	2173.52	45.11	8.58	0.46	1286.84	13.67
	67.20	27.28	0.41	0.07	0.03	0.20	15.12	0.48	2183.95	45.57	9.89	0.74	1295.93	20.06
Mean	76.81	36.14	0.43	0.08	0.04	0.22	13.99	0.48	2191.29	45.51	11.34	0.55	1305.09	17.07
SD	42.48	28.78	0.07	0.04	0.03	0.12	1.19	0.07	15.64	6.04	2.56	0.13	11.66	3.83
COV%	55.30	79.64	17.25	55.30	79.64	55.30	8.49	14.45	0.71	13.28	22.54	23.94	0.89	22.42
Tibial Plateau Medial Posterior	79.90	32.63	0.41	0.08	0.03	0.23	13.26	0.46	2231.85	44.87	12.29	0.49	1308.81	16.29
	97.93	42.64	0.44	0.10	0.04	0.29	13.04	0.47	2233.75	45.14	8.95	0.39	1285.24	12.19
	99.16	42.41	0.43	0.10	0.04	0.29	12.31	0.42	2259.30	42.34	14.07	0.53	1308.42	17.74
	63.87	23.02	0.36	0.06	0.02	0.19	12.39	0.39	2223.02	38.68	10.90	0.46	1313.85	15.10
	98.96	43.40	0.44	0.10	0.04	0.29	13.65	0.48	2225.98	46.09	11.26	0.58	1294.92	17.60
	55.81	19.65	0.35	0.06	0.02	0.16	11.65	0.39	2177.20	36.21	10.07	0.44	1299.73	14.00

	92.85	37.83	0.41	0.09	0.04	0.27	10.97	0.35	2193.33	33.56	11.15	0.49	1305.58	15.69
	44.56	15.64	0.35	0.04	0.02	0.13	13.96	0.49	2199.30	45.95	10.16	0.55	1298.57	16.61
	42.34	14.46	0.34	0.04	0.01	0.12	11.96	0.39	2219.28	37.78	6.32	0.38	1286.29	10.85
	41.94	15.57	0.37	0.04	0.02	0.12	12.74	0.42	2230.60	41.32	14.70	0.51	1307.17	17.15
Mean	71.73	28.72	0.39	0.07	0.03	0.21	12.59	0.43	2219.36	41.19	10.99	0.48	1300.86	15.32
SD	24.72	12.28	0.04	0.02	0.01	0.07	0.93	0.05	23.57	4.45	2.42	0.07	9.71	2.33
COV%	34.45	42.75	9.77	34.45	42.75	34.45	7.35	10.67	1.06	10.80	21.99	13.74	0.75	15.19
Tibial Plateau Lateral Anterior	621.80	530.68	0.85	0.62	0.53	1.82	13.49	0.45	2188.43	42.79	9.10	0.49	1303.09	14.84
	622.60	439.39	0.71	0.62	0.44	1.82	13.39	0.43	2200.93	41.43	13.48	0.62	1310.67	19.85
	586.60	366.60	0.63	0.59	0.37	1.71	15.75	0.53	2195.80	49.95	9.96	0.76	1306.91	20.86
	576.60	422.62	0.73	0.58	0.42	1.68	14.80	0.60	2189.46	54.47	13.43	0.60	1314.34	19.36
	607.82	449.51	0.74	0.61	0.45	1.77	13.06	0.45	2176.57	41.46	10.14	0.62	1306.04	18.30
	652.77	464.94	0.71	0.65	0.46	1.91	14.73	0.57	2198.58	52.74	13.55	0.55	1301.83	17.88
	702.09	480.61	0.69	0.70	0.48	2.05	15.64	0.57	2187.36	52.51	9.91	0.62	1303.51	18.17
	676.35	495.78	0.73	0.68	0.50	1.97	16.69	0.58	2180.44	53.62	11.80	0.62	1256.58	17.75
	454.66	292.26	0.64	0.45	0.29	1.33	14.44	0.52	2200.94	49.04	10.36	0.57	1280.92	16.69
	440.56	260.48	0.59	0.44	0.26	1.29	12.99	0.53	2214.40	48.86	10.47	0.64	1282.08	18.23
Mean	594.19	420.29	0.70	0.59	0.42	1.74	14.50	0.52	2193.29	48.69	11.22	0.61	1296.60	18.19
SD	86.29	87.91	0.07	0.09	0.09	0.25	1.27	0.06	11.13	5.06	1.70	0.07	17.90	1.67
COV%	14.52	20.92	10.43	14.52	20.92	14.52	8.73	11.37	0.51	10.39	15.15	11.65	1.38	9.16
Tibial Plateau Lateral Posterior	294.01	58.21	0.20	0.29	0.06	0.86	15.31	0.52	2157.27	47.80	9.81	0.65	1309.22	18.73
	300.80	59.85	0.20	0.30	0.06	0.88	15.79	0.60	2180.01	54.91	11.88	0.55	1299.75	17.20
	641.79	150.41	0.23	0.64	0.15	1.87	17.00	0.56	2158.12	51.68	12.07	0.50	1304.89	16.22
	788.13	173.37	0.22	0.79	0.17	2.30	13.66	0.41	2176.45	38.86	14.80	0.77	1302.26	23.70
	716.63	158.56	0.22	0.72	0.16	2.09	17.35	0.63	2201.22	59.32	6.41	0.29	1305.04	9.28
	277.60	51.77	0.19	0.28	0.05	0.81	15.57	0.55	2177.13	50.78	11.33	0.47	1305.87	15.21

	321.71	56.69	0.18	0.32	0.06	0.94	13.95	0.41	2152.82	38.38	8.34	0.54	1305.24	15.63
	155.12	34.61	0.22	0.16	0.03	0.45	12.25	0.32	2128.16	29.92	6.99	0.47	1290.43	13.08
	93.53	19.48	0.21	0.09	0.02	0.27	18.24	0.63	2198.12	59.40	9.62	0.50	1294.26	15.07
	93.15	19.91	0.21	0.09	0.02	0.27	18.43	0.60	2163.51	55.74	10.92	0.57	1292.82	17.27
Mean	368.25	78.29	0.21	0.37	0.08	1.08	15.75	0.52	2169.28	48.68	10.22	0.53	1300.98	16.14
SD	255.93	59.04	0.02	0.26	0.06	0.75	2.04	0.11	21.97	9.92	2.54	0.13	6.39	3.73
COV%	69.50	75.42	8.69	69.50	75.42	69.50	12.97	20.48	1.01	20.38	24.83	23.81	0.49	23.09
Mean	266.08	99.18	0.35	0.27	0.10	0.78	14.30	0.48	2194.10	45.15	12.43	0.52	1300.82	16.73
SD	360.96	144.06	0.16	0.36	0.14	1.05	1.68	0.08	23.04	7.37	2.63	0.09	12.30	2.70
COV%	135.66	145.25	46.28	135.66	145.25	135.66	11.74	17.65	1.05	16.32	21.18	17.74	0.95	16.13

Table 13. Anterior cruciate ligament, posterior cruciate ligament, medial collateral ligament and lateral collateral ligament raw data for all cadavers.

Age Years	Gender	OA ICRS Grade	Ligament	Length mm	Cross Section Average mm^2	Linear Force N	Linear Stress Mpa	Linear Strain mm	Linear Strain %	Young's (Secant) Modulus Mpa	Tangent Modulus Mpa	Failure Load N	Failure Stress Mpa	Failure Strain mm	Failure Strain %	Stiffness N/mm	Failure Site: Mid Substance (MS), Insertion (I), Bony Avulsion (BA)
31	Female	0	ACL	40	63.80	574.78	9.01	4.96	12.40	29.06	171.04	629.94	9.87	5.79	14.48	46.36	I
31	Female	0	LCL	62	17.10	477.63	27.93	10.98	17.71	97.79	95.80	545.90	31.92	11.81	19.05	26.98	MS
31	Female	0	MCL	103	24.51	332.35	13.56	6.74	6.54	213.56	85.96	438.48	17.89	8.40	8.16	50.82	MS
31	Female	0	PCL	36	86.53	624.66	7.22	4.34	12.05	21.57	238.72	930.27	10.75	8.50	23.62	51.84	MS
37	Female	0	ACL	30	48.46	1345.42	27.76	6.75	22.50	37.03	239.08	1554.16	32.07	8.42	28.05	59.81	BA
37	Female	0	PCL	30	48.82	1107.59	22.69	9.72	32.41	21.00	293.42	1336.49	27.37	10.56	35.19	34.17	BA
37	Female	0	LCL	55	71.75	280.88	3.91	7.89	14.34	15.02	70.23	479.73	6.69	11.22	20.40	19.59	I
37	Female	0	MCL	40	18.19	33.21	1.83	4.06	10.15	7.19	14.32	47.93	2.63	4.90	12.24	3.27	MS
43	Female	0	ACL	32	71.27	467.52	6.56	5.78	18.08	11.61	126.42	576.94	8.09	9.95	31.10	25.86	MS
43	Female	0	PCL	30	76.53	369.20	4.82	6.83	22.78	6.35	73.99	1220.92	15.95	15.17	50.56	16.21	MS
43	Female	0	MCL	108	28.29	343.16	12.13	11.16	10.34	126.76	75.41	727.51	25.72	19.50	18.05	33.20	MS
43	Female	0	LCL	61	12.83	81.49	6.35	4.39	7.19	53.89	34.31	426.52	33.25	11.05	18.12	11.33	MS
49	Male	1	ACL	40	34.68	229.22	6.61	6.87	17.17	15.40	120.79	340.82	9.83	9.37	23.42	13.35	MS
49	Male	1	PCL	44	84.79	777.84	9.17	5.96	13.55	29.79	229.97	963.21	11.36	9.29	21.12	57.41	MS

49	Male	1	MCL	101	22.37	137.53	6.15	10.92	10.81	57.44	35.88	552.09	24.68	17.59	17.41	12.72	MS
49	Male	1	LCL	52	39.91	279.40	7.00	15.88	30.55	11.92	67.32	438.52	10.99	21.72	41.76	9.15	MS
51	Male	1	PCL	34	59.24	378.24	6.38	4.89	14.38	15.10	120.23	1052.61	17.77	15.72	46.24	26.31	I
51	Male	1	LCL	47	45.15	341.77	7.57	7.04	14.97	23.77	81.27	419.25	9.29	15.37	32.70	22.83	I
51	Male	1	ACL	28	53.64	249.76	4.66	4.89	17.48	7.46	53.79	504.97	9.41	12.39	44.27	14.29	MS
51	Male	1	MCL	114	41.18	279.31	6.78	7.32	6.42	120.38	61.30	354.33	8.61	13.99	12.27	43.48	MS
58	Male	2	PCL	46	98.67	980.12	9.93	6.89	14.99	30.49	220.75	1380.78	13.99	10.23	22.23	65.41	I
58	Male	2	ACL	41	95.79	169.90	1.77	6.97	17.00	4.28	55.47	664.31	6.93	14.47	35.29	10.00	MS
58	Male	2	MCL	127	28.80	150.06	5.21	7.85	6.18	107.01	30.76	514.05	17.85	14.52	11.43	24.27	MS
58	Male	2	LCL	58	36.03	388.10	10.77	5.88	10.14	61.60	103.30	629.39	17.47	9.22	15.89	38.27	MS
72 (1)	Male	3	MCL	121	33.41	235.88	7.06	8.33	6.88	124.16	71.24	458.47	13.72	12.49	10.32	34.28	I
72 (1)	Male	3	PCL	41	62.51	344.93	5.52	7.67	18.71	12.09	79.10	524.83	8.40	11.84	28.88	18.43	BA
72 (1)	Male	3	ACL	34	49.75	569.38	11.44	3.96	11.66	33.39	197.08	808.34	16.25	5.63	16.56	48.85	MS
72 (1)	Male	3	LCL	60	66.07	251.52	3.81	9.87	16.46	13.88	51.08	379.68	5.75	15.71	26.18	15.28	MS
72 (2)	Male	3	ACL	29	101.84	265.33	2.61	2.35	8.10	9.33	189.12	613.77	6.03	4.85	16.72	32.76	I
72 (2)	Male	3	PCL	31	91.34	1059.28	11.60	5.03	16.23	22.15	321.15	1432.70	15.69	6.70	21.60	65.28	MS
72 (2)	Male	3	MCL	110	58.68	120.41	2.05	3.64	3.31	68.15	62.58	227.10	3.87	13.64	12.40	36.35	MS
72 (2)	Male	3	LCL	68	44.46	282.10	6.35	7.18	10.55	40.89	66.36	352.48	7.93	11.34	16.68	26.73	MS
79	Male	2	ACL	32	37.78	145.15	3.84	7.43	23.21	5.30	46.39	187.78	4.97	10.76	33.63	6.25	I
79	Male	2	MCL	120	39.57	264.96	6.70	17.86	14.89	53.98	51.74	326.72	8.26	19.53	16.27	17.80	I
79	Male	2	LCL	62	18.98	532.16	28.03	8.81	14.21	122.29	87.79	628.01	33.08	12.15	19.59	37.44	I
79	Male	2	PCL	32	70.34	356.25	5.06	5.61	17.54	9.24	100.22	642.60	9.14	12.28	38.37	20.31	MS
80	Male	4	LCL	74	50.01	250.44	5.01	11.65	15.74	23.54	59.90	445.35	8.91	21.65	29.26	15.91	BA
80	Male	4	PCL	35	154.25	65.96	0.43	4.89	13.98	1.07	29.79	261.57	1.70	15.73	44.94	4.72	I
80	Male	4	ACL	38	74.89	139.35	1.86	5.67	14.91	4.74	77.25	373.94	4.99	9.00	23.68	9.35	MS
80	Male	4	MCL	116	27.62	399.01	14.45	7.68	6.62	253.25	73.99	492.60	17.84	12.68	10.93	60.29	MS

86	Female	1	ACL	30	24.98	84.17	3.37	2.57	8.58	11.78	58.95	134.33	5.38	5.91	19.69	9.81	I
86	Female	1	PCL	43	66.54	67.81	1.02	4.68	10.89	4.02	40.68	281.04	4.22	13.85	32.21	6.23	I
86	Female	1	LCL	60	14.17	89.69	6.33	6.91	11.52	32.98	33.56	263.26	18.58	13.58	22.63	7.79	MS
88	Male	3	ACL	33	64.32	144.40	2.25	5.18	15.68	4.72	58.76	277.47	4.31	9.34	28.31	9.21	I
88	Male	3	PCL	34	95.25	212.68	2.23	6.33	18.60	4.08	91.30	414.07	4.35	9.66	28.41	11.43	I
88	Male	3	LCL	58	24.78	101.97	4.12	6.44	11.10	21.50	31.79	337.54	13.62	13.94	24.03	9.19	I
88	Male	3	MCL	120	35.55	232.72	6.55	9.55	7.96	98.69	41.48	444.18	12.49	17.05	14.21	29.24	MS

Chapter Ten: Publications

Tissue material properties and computational modelling of the human tibiofemoral joint: a critical review

Abby E. Peters[1,2], Riaz Akhtar[2], Eithne J. Comerford[1,2,3] and Karl T. Bates[1]

[1] Department of Musculoskeletal Biology, Institute of Ageing and Chronic Disease, University of Liverpool, Liverpool, UK
[2] Department of Mechanical, Materials and Aerospace Engineering, School of Engineering, University of Liverpool, Liverpool, UK
[3] Institute of Veterinary Science, University of Liverpool, Liverpool, UK

ABSTRACT

Understanding how structural and functional alterations of individual tissues impact on whole-joint function is challenging, particularly in humans where direct invasive experimentation is difficult. Finite element (FE) computational models produce quantitative predictions of the mechanical and physiological behaviour of multiple tissues simultaneously, thereby providing a means to study changes that occur through healthy ageing and disease such as osteoarthritis (OA). As a result, significant research investment has been placed in developing such models of the human knee. Previous work has highlighted that model predictions are highly sensitive to the various inputs used to build them, particularly the mathematical definition of material properties of biological tissues. The goal of this systematic review is two-fold. First, we provide a comprehensive summation and evaluation of existing linear elastic material property data for human tibiofemoral joint tissues, tabulating numerical values as a reference resource for future studies. Second, we review efforts to model tibiofemoral joint mechanical behaviour through FE modelling with particular focus on how studies have sourced tissue material properties. The last decade has seen a renaissance in material testing fuelled by development of a variety of new engineering techniques that allow the mechanical behaviour of both soft and hard tissues to be characterised at a spectrum of scales from nano- to bulk tissue level. As a result, there now exists an extremely broad range of published values for human tibiofemoral joint tissues. However, our systematic review highlights gaps and ambiguities that mean quantitative understanding of how tissue material properties alter with age and OA is limited. It is therefore currently challenging to construct FE models of the knee that are truly representative of a specific age or disease-state. Consequently, recent tibiofemoral joint FE models have been highly generic in terms of material properties even relying on non-human data from multiple species. We highlight this by critically evaluating current ability to quantitatively compare and model (1) young and old and (2) healthy and OA human tibiofemoral joints. We suggest that future research into both healthy and diseased knee function will benefit greatly from a subject- or cohort-specific approach in which FE models are constructed using material properties, medical imagery and loading data from cohorts with consistent demographics and/or disease states.

Submitted 22 June 2017
Accepted 8 January 2018
Published 25 January 2018

Corresponding author
Abby E. Peters, abby.peters@liv.ac.uk

Academic editor
Jun Pang

Additional Information and Declarations can be found on page 37

DOI **10.7717/peerj.4298**

How to cite this article Peters et al. (2018), Tissue material properties and computational modelling of the human tibiofemoral joint: a critical review. **PeerJ 6:e4298; DOI 10.7717/peerj.4298**

Subjects Bioengineering, Biotechnology, Computational Biology
Keywords Ligaments, Bone, Finite element, Cartilage, Human knee, Material properties

INTRODUCTION

The knee joint is a primary component of the musculoskeletal system that aids the absorption and transition of weight bearing forces. As an integral part of biomechanical movement the knee joint is often subjected to injury or disease such as ligament rupture (*Mullaji et al., 2008*; *Hill et al., 2005*), meniscal tears (*Lange et al., 2007*) and osteoarthritis (OA) (*Zhang & Jordan, 2008*). OA is one of the most common musculoskeletal conditions in the elderly population causing structural degeneration of tissues and ultimately leading to a decline in function (*Rousseau & Garnero, 2012*). The most common type of OA exists in the knee joint which is the leading cause of locomotor disability (*Zhang & Jordan, 2008*). The disease is encouraged by heredity influence, ageing, gender, obesity and trauma or injury to the affected joint (*Manninen et al., 1996*), known as secondary OA, and can often lead to joint replacement (*Nigg & Herzog, 2006*). Where the cause of the disease is unknown this is referred to as primary OA (*Buckwalter & Martin, 2006*). It is approximated that 40% of adults over the age of 70 will be affected by OA of the knee in the United States of America (*Punzi, Oliviero & Ramonda, 2010*), with direct lifetime medical costs of $12,400 per person (*Losina et al., 2015*). OA does not just present with direct joint degeneration but is intrinsically linked to other diseases and neuromuscular complications which can further exacerbate age-related issues such as sarcopenia and a loss of movement control. Individuals with OA have increased variability of gait spatial–temporal parameters (*Kiss, 2011*) which in turn can decrease locomotor stability and increase the risk of falls (*Lord, Lloyd & Li, 1996*; *Hausdorff, Rios & Edelberg, 2001*; *Owings & Grabiner, 2004*; *Brach et al., 2005*; *Hollman et al., 2007*).

Typically, research surrounding OA focuses on the deterioration of articular cartilage; however recent studies have highlighted the need to consider structural changes of subchondral bone in the progression of OA (*Nigg & Herzog, 2006*). Significant relationships have been identified between changes occurring in different tissues specifically observing molecular crosstalk (*Lories & Luyten, 2011*; *Mahjoub, Berenbaum & Houard, 2012*). OA is therefore more recently seen as a disease of the entire joint with biochemical and biomechanical factors influencing the progression and status of the disease. Each tissue has a specific role and functionality within the knee joint in order to aid movement and stability. Individual tissues have a distinct structure and material properties that define its adaptive and responsive behaviour in accordance with the biomechanics of movement (*Punzi, Oliviero & Ramonda, 2010*). Biochemical and mechanical changes naturally occur during ageing even in the absence of clinically defined injury or disease and these changes have been shown to modify form–function relationships at the knee joint (*Hansen, Masouros & Amis, 2006*); however, data is limited.

In order to fully understand the onset and progression of OA it is essential to characterise the basic relationships between structure and function within a healthy human knee and how tissues age in the absence of disease. Understanding biomechanics of anatomically complex structures like the knee joint is challenging particularly in

humans where experimental approaches must largely be non-invasive. The difficulty of achieving direct quantitative measures of tissue behaviour together with more widespread availability of imaging technology (i.e. magnetic resonance imaging (MRI), X-ray computed tomography (CT)) has led to an increasing use of computational approaches, notably finite element (FE) analysis, to study knee joint form and function (*Peña et al., 2005*, *2006*; *Wang, Fan & Zhang, 2014*). Once suitably validated such FE models may potentially circumvent the issues surrounding direct invasive measurement of tissue mechanics by producing quantitative predictions of the mechanical and physiological behaviour of multiple tissues simultaneously, thereby inherently calculating tissue interaction. This could be particularly useful in identifying tissue interaction that may occur during ageing and in the presence of disease.

Through use of parameterisation, models can also be used in a predictive capacity to address questions that cannot ethically or even practically be asked by experimentation on humans or animals. Specifically, iterations of the same model can be generated where aspects of structure including gross anatomy and material properties, and loading behaviour are non-invasively manipulated to quantify the impact on function. In this way parameterisation enables cause–effect relationships between anatomy and mechanics to be identified, whilst allowing the impact of individual and combinations of morphological characteristics to be isolated (*Li, Lopez & Rubash, 2001*). Model manipulations can also be used for testing surgical interventions, treatment strategies and prosthetics (*Baldwin et al., 2012*; *Tuncer et al., 2013*).

Models are by definition abstractions of reality and their constituent parts or input parameters are typically tailored to address a specific research question or hypothesis. Consequently models of the same anatomical structure, such as the knee joint, may vary considerably between studies according to the research objective. In the context of the human knee, for example it is common for researchers to use models to answer questions on one specific tissue (e.g. ligament injuries under specific stress and strain) and as such effort and complexity is invested in these specific tissues while it is deemed sufficient to invest less towards input values for other tissues (i.e. therefore simplifying cartilage representation to a linear elastic material, or bone treated as a rigid body). However, tissues within a joint inherently interact and behaviour of one is influenced by others, although to what extent to which tissues interact has not extensively been studied.

Subject specific FE modelling is useful in the application of OA as it can investigate the true interaction between multiple tissues and how changes in one can lead to implications in an adjacent tissue, which may lead to disease initiation or progression. For example, ligament ruptures are histologically known to occur in the presence of OA (*Mullaji et al., 2008*), yet the impact or causative link to cartilage degeneration is unknown. Whilst efforts have been made to investigate this disease through computational approaches, it is indeed clear that there is a lack of baseline healthy measurements providing a foundation for comparative analyses. Research into the material properties of young healthy tissues surrounding the human knee is needed to compare to other cohort-specific groups. In the context of joint biomechanics this is crucial to understanding how, for example component parts of the joint function so that corrective therapeutics can restore joint

function to the normal baseline as per the healthy sample measurements. Baseline healthy measurements are also crucial for basic science contexts such as sports biomechanics, where increasing biomechanical function is directly linked to performance. The accuracy of computational modelling approaches in general has been shown repeatedly to rely on good input data (*Guo, Maher & Spilker, 2013*; *Kazemi, Dabiri & Li, 2013*; *Freutel et al., 2014*). Direction of future research towards understanding the influence of donor age and 'healthy' versus pathological conditions on material properties with these new techniques has been cited as a key goal (*Lewis & Nyman, 2008*), but it is presently unclear of extent to which this has been achieved in the context of the human knee joint.

Evidently the human knee joint is crucial in biomechanical movement and function and has therefore the relevant literature has been reviewed extensively in recent years. Specifically, several reviews have discussed computational modelling of individual tissues of the knee joint. For example, *Wilson et al. (2005)* reviewed articular cartilage representations of behavioural and injury mechanisms, whilst *Taylor & Miller (2006)* reviewed both micro- and macro-level representation of cartilage tissue. Computational modelling of ligaments has also been reviewed by *Woo, Johnson & Smith (1993)* and *Weiss & Gardiner (2001)* focusing on viscoelasticity and one-dimensional to three-dimensional (3D) representations respectively. Whole knee joint modelling has also been reviewed in recent years by *Peña et al. (2007a)*, *Elias & Cosgarea (2007)* and *Kazemi, Dabiri & Li (2013)*. Whilst these reviews focused on advances in modelling, to date no review paper has critically evaluated the nature of material property available for human knee joint tissues and subsequently how this data has been transferred to FE models, with particular reference to ageing and OA.

The aim of this review paper is two-fold. Firstly, to conduct a review of scientific literature to understand what material property data currently exists for cartilage, bone and ligament samples from the human knee joint in an attempt to understand alterations during healthy ageing and disease status. Secondly, this paper aims to determine how this data has been subsequently applied within biomedical engineering in the form of existing FE models of the whole human knee joint. In doing so we collate a comprehensive database of material properties of human knee joint cartilage, bone and ligaments to substantiate our critical review of recent advances and current limitations, whilst also serving as a resource for future research in this important area. The critical aspect of our review focuses on the question 'how systematic or holistic is the material property data that exists for the human knee in terms of its ability to represent a specific human cohort or demographic?' To evaluate this question we focus on young healthy representation of material properties to understand the current baseline for accurate comparison to old OA representation.

SURVEY METHODOLOGY

Firstly, published scientific papers were sourced for review that contained material property data of soft and hard tissue from the human knee joint only. The selection criteria are outlined below. Literature search engines were used, including ScienceDirect, PubMed (NCBI), MedLine, SpringerLink and Wiley Online Library. Terminology

including *cartilage, bone, ligament, human, knee, joint, femoral, femur, tibia, tibial, anterior, posterior, cruciate, medial, lateral, collateral, material properties, elastic modulus, Young's modulus, compression, tensile, indentation, FE, model, modelling, three dimensional,* and *computational* were used. All relevant studies meeting search criteria were included in this review.

For cartilage and bone material properties the research must have been on distal femoral and proximal tibia only (excluding patella samples). Studies must have also incorporated the use of compression or indentation techniques for ease of comparison of testing techniques and data obtained (as opposed to tensile elongation, three-point bending, four-point bending or buckling techniques) to collate the elastic modulus, shear modulus or comparable parameters. For ligament material properties studies must have incorporated at least one of the following: anterior cruciate ligament (ACL), posterior cruciate ligament (PCL), medial collateral ligament (MCL) and lateral collateral ligament (LCL) from the human knee tested using tensile techniques. Compression and tensile testing techniques were specifically chosen to mimic primary biological in vivo mechanics. Combined experimental-modelling is sometimes utilised to predict material properties (inverse calculation of material properties from known geometries, loads and deformations) (*Robinson et al., 2016*); however, this review focuses on more direct measurements of material properties.

Secondly, published scientific papers were sourced for review if they incorporated a 3D FE model of a whole human knee joint. This included any study modelling the femoral and tibial bone and cartilage structures and the four main ligaments of the knee joint—ACL, PCL, MCL and LCL. Studies did not need to include the patella or menisci, as these are less commonly modelled and represented, although were not specifically excluded. Studies not including all these structures were excluded. Studies of meniscectomies, insoles or footwear, joint replacement or arthroplasty mechanics, and ligament reconstructions were also excluded. In addition, we included models representing OA.

Structure, composition and material property data obtained from human tibiofemoral joints were to initially be reviewed separately for cartilage, bone and ligament tissue (Section A—Material Properties), followed by a review of use of data within currently published human tibiofemoral joint FE models (Section B: FE Modelling).

SECTION A—MATERIAL PROPERTIES

Articular cartilage

Articular cartilage is a type of fibrous connective tissue composed of cells forming between 2% and 15% of the total weight and an extracellular matrix (ECM) forming the remaining 85–98%, of which 65–80% is water (*Martini, 1998*). Its primary function is to maintain a smooth surface allowing lubricated, near-frictionless movement and to help transmit articular forces, thereby minimising stress concentrations across the joint. It is most commonly found within synovial and diarthrodial joints forming a 1–6 mm thickness and covering the epiphysis of bone. The knee joint is composed of both hyaline and fibrocartilage in the form of articular cartilage covering the end of bones articulating within the joint and fibrocartilage forming the menisci (*Martini, 1998*).

Material properties of articular cartilage have been widely reported giving compressive, tensile and shear forces at the macro- (*Armstrong & Mow, 1982*; *Setton, Elliott & Mow, 1999*; *Kleemann et al., 2005*), micro- (*Stolz et al., 2009*; *Desrochers, Amrein & Matyas, 2010*) and nano-scale (*Stolz et al., 2009*) within the ECM of multiple species. Various techniques have been utilised including confined and unconfined compression (*Kleemann et al., 2005*; *Hori & Mockros, 1976*; *Franz et al., 2001*) and more recently atomic force microscopy (AFM) (*Wen et al., 2012*; *Wilusz, Zauscher & Guilak, 2013*; *Wang et al., 2013*) and nanoindentation (*Taffetani et al., 2014*). Custom made indentation instruments have also previously been used to measure articular cartilage stiffness during compression (*Hori & Mockros, 1976*; *Kempson, Freeman & Swanson, 1971*; *Lyyra et al., 1995*; *Kiviranta et al., 2008*) as well as being used to calculate dynamic modulus (*Kiviranta et al., 2008*), creep modulus (*Kempson, Freeman & Swanson, 1971*), shear, bulk and elastic modulus and Poisson's ratio (*Hori & Mockros, 1976*).

One of the first studies to explore human knee joint cartilage material properties utilised uniaxial confined compression on 20 proximal tibia samples. Age and gender of donors were not specified; however each sample was classified with a grade of OA using the Bollet system (*Bollet, Handy & Sturgill, 1963* cited in *Hori & Mockros (1976)*). Progressive compression loads were manually applied giving an elastic modulus between 1.3 and 10.2 MPa. When categorising elastic modulus to grade of OA averages were 6.82, 6.74, 4.76 and 2.99 MPa for grades 0, 1, 2 and 3 respectively, although this correlation was not significant (*Hori & Mockros, 1976*). Testing specifications and resultant data can be seen in Table 1 alongside information from all reviewed human knee joint cartilage material property research.

In more recent decades there has been considerable focus on microscale unconfined compression testing. In consecutive studies by *Shepherd & Seedhom (1997*, *1999a)*, human femoral condyle and tibial plateau cartilage were tested. Earlier research utilised a total of five donors although no age or gender was specified. Results indicated an elastic modulus of between 2.6 and 18.6 MPa depending on physiological loading rate (*Shepherd & Seedhom, 1997*). In the latter study 11 humans cadavers (three males and eight females, aged 33–80 years old) were tested giving an elastic modulus of 6.0–11.8 MPa (Table 1) across all cadavers with no correlation to age (*Shepherd & Seedhom, 1999a*).

Thambyah, Nather & Goh (2006) tested cartilage from seven fresh frozen healthy human male tibias (62–70 years old) using uniaxial tensile testing at a rate of 300 kPa/s to compare articular cartilage from beneath the menisci to that independent from the menisci. Results showed an individual mean elastic modulus from all seven cadavers between 2.13 and 5.13 MPa (Table 1) across varying testing locations. Hydration maintenance was not specified within the methodology.

Kleemann et al. (2005) explored the macroscopic composition of articular cartilage within 15 females and 6 males OA tibial plateau samples (70 ± 13 years old). Research obtained architectural data from histology using haematoxylin and eosin staining and elastic modulus of cartilage was determined by unconfined uniaxial compression. An inverse correlation was observed between the elastic modulus of the articular cartilage against the International Cartilage Repair Society (ICRS) grade (*Brittberg & Peterson, 1998*)

Table 1 Summary of cartilage material properties.

Author	Quantity and locality	Age, gender and health status	Testing technique	Results per Cohort: elastic modulus (MPa)	
Hori & Mockros (1976)	20 × Donors Proximal tibia	Age: NS Gender: NS Health: healthy and OA grade 1	Uniaxial confined compression 10–30.4 mm indenter	*Healthy and OA grade 1*	1.3–10.2
Shepherd & Seedhom (1997)	5 × Donors Femoral condyle and tibial plateau	Age: NS Gender: NS Health: healthy	Spring-loaded indentation 1.59 mm indenter	*Healthy*	2.6–18.6
Shepherd & Seedhom (1999a)	11 × Donors Femoral condyle and tibial plateau	Age: 33–80 Gender: 8F/3M; Health: healthy	Spring-loaded indentation 1.59 indenter	*Healthy*	6.0–11.8
Franz et al. (2001)	24 × Femoral Condyle	Age: 32–89 Gender: NS Health: healthy and OA grade 1	Handheld indentation 1.0 mm indenter	*Healthy and OA grade 1*	4.3–4.9
Kleemann et al. (2005)	21 × Donors Tibial plateau	Age: 70 ± 13 Gender: 15 F/6 M; Health: OA grades 1–3	Uniaxial unconfined compression	*OA grade 1* *OA grade 2* *OA grade 3*	0.5 0.4 0.3
Thambyah, Nather & Goh (2006)	7 × Donors Tibia	Age: 62–70 Gender: M Health: healthy	Uniaxial unconfined compression 1.0 mm indenter	*Healthy*	2.1–5.1
Wen et al. (2012)	3 × Donors Knee samples	Age: 35–59 Gender: F Health: healthy and OA grade 1	AFM 10 nm indenter	*Healthy OA grade 1*	2650.0–3700.0* 2370.0–5640.0*
Wilusz, Zauscher & Guilak (2013)	8 × Donors Femoral condyle	Age: 53–83 Gender: NS Health: healthy and OA grades 2–3	AFM 5 μm indenter	*Healthy* *PCM and ECM* *OA grade 2–3 PCM and ECM*	0.1 and 0.3 0.1 and 0.5
Wang et al. (2013)	5 × Donors Femoral condyle	Age: NS Gender: NS Health: healthy and OA grade 1–3	AFM 40 nm indenter	*Healthy* *OA grade 1* *OA grade 2–3*	0.2 0.6 0.2

Notes:
Summary of current literature for human knee cartilage material property compression or indentation testing including age, gender, health status of specimens, number and location of samples tested and technique used to obtain elastic modulus values.
NS, not specified; F, female; M, male; OA, osteoarthritis; AFM, atomic force microscopy; ECM, extra cellular matrix; PCM, peri-cellular matrix.
* Samples were dehydrated prior to testing.

seen in Fig. 1 (Grade 1 0.50 MPa, Grade 2 0.37 MPa, and Grade 3 0.28 MPa (Table 1)). The research also suggested a relationship between changes in histology, structure and mechanics of the articular cartilage during all stages of OA degeneration although this was not compared with age of donor. Moreover *Bae et al. (2003)* found decreased indentation stiffness and an increased ICRS score was associated with degeneration of cartilage rather than with age or cartilage thickness. This suggests that it is possible

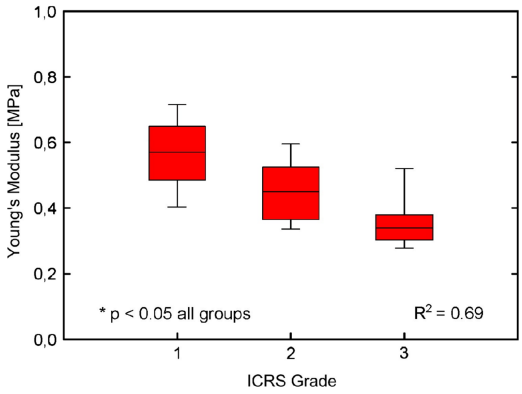

Figure 1 Cartilage stiffness during degeneration. Stiffness reduction of degenerated cartilage with increasing International Cartilage Repair Society (ICRS) Grade related to boxplots displaying median values and interquartile range. (Adapted from *Kleemann et al. (2005)*: Elsevier License Permission: 4226450501899). Full-size DOI: 10.7717/peerj.4298/fig-1

to reliably distinguish degeneration of cartilage by microscopic histological analysis and macroscopic observations.

Franz et al. (2001) used a handheld indenter with a constant load of 300 μm to collate the shear modulus of 24 human cartilage samples (32–89 years old) obtained from the medial and lateral femoral condyles. Shear modulus was converted to elastic modulus (using the Poisson's ratio expressed in the original research) for the purpose of this paper, which were 4.32 MPa and 4.88 MPa (Table 1) in the lateral and medial femoral condyles respectively; however this was not correlated to the age of cadaver. Cartilage samples were graded for OA using the Mankin system (*Mankin et al., 1971*) and results indicated a positive correlation between a slightly roughened cartilage surface and stiffness at the medial femoral condyle. However, it should be noted that no samples presented with gross fibrillation or surface irregularities. Sample shear modulus was, however, presented in age categories with corresponding proteoglycan and collagen content which are known to adapt during ageing and disease.

The development of increasingly sophisticated testing techniques has further advanced our understanding of cartilage material properties by allowing measurements to be made at the nanoscale. With the use of nanoscale indentation stiffening of cartilage due to age-related influences alongside stiffness differences in healthy and OA cartilage can be detected more accurately in comparison to microindentation (*Stolz et al., 2009*). It has been shown that microindentation is either unable to detect such changes or produces a lower stiffness measurement when compared to nanoindentation leading some to question its accuracy (*Stolz et al., 2004*, *2009*). Additionally, stiffness is higher in articular cartilage collagen fibrils than in proteoglycans; however when measured at microscale, this differentiation may not be detected (*Loparic et al., 2010*). A change in the structure and content of proteoglycans often accompanies the process of OA along with reduced

stiffness through loosening of the collagen network causing alteration to the material properties, further enhancing the need for testing at the nanoscale (*Wang et al., 2013*).

Incorporating nanotechnology, *Wen et al. (2012)* utilised AFM at a loading rate of 2.11 nm/s to test elastic modulus of tibial plateau articular cartilage fragments obtained from three female patients undergoing arthroplasty surgery. Samples from the surface, superficial middle, deep middle and bone–cartilage interface regions were graded for OA with the Outerbridge scoring system (*Outerbridge, 1961*). Collagen fibres were obtained from the overlap zone from each layer which can be mechanically stiffer than collagen fibres in the gap region (*Minary-Jolandan & Yu, 2009*). Results show there is a significant mechanical stiffening of individual human collagen fibrils between healthy (aged 35 years old) and mild OA (aged 52 and 59 years old), at the surface of articular cartilage (2,650–3,110 MPa respectively) through to the bone–cartilage interface (3,700–5,640 MPa respectively) (Table 1). It must be noted that tissue samples were dehydrated with ethanol prior to testing which will alter the true mechanical properties of cartilage; however the aim of this research was to identify the differences in elastic modulus of healthy and OA tissues where mechanical alterations would change simultaneously in both healthy and OA samples.

Wilusz, Zauscher & Guilak (2013) also used AFM at a rate of 15 μm/s on eight human femoral condyles (six females and two males) aged 53–83 years old. Cadavers were graded for OA using the Collins System (*Collins, 1939*, *1949* cited in *Wilusz, Zauscher & Guilak (2013)*) giving four healthy and four OA samples grades 2–3. Results indicate that elastic modulus of the pericellular matrix (PCM) decreased in OA samples (0.096 ± 0.016 MPa) when compared to healthy controls (0.137 ± 0.022 MPa). Also the ECM elastic modulus was decreased in OA samples (0.270 ± 0.076 MPa) when compared to healthy controls (0.491 ± 0.112 MPa) (Table 1); although this was only significant on the medial femoral condyle. In agreement, *Wang & Peng (2015)* used AFM to quantify elastic modulus of 12 knee articular cartilage samples (age and gender not specified) in various grades of OA and found an increase in elastic modulus in the presence of mild and moderate OA but a decrease with severe OA, although actual values are not stated.

Atomic force microscopy has also been used to identify nanoscale adaptations at varying indentation depths in five human (age and gender not specified) femoral condyles obtained from healthy, mild and severe OA cartilage (*Wang et al., 2013*). Cartilage samples were graded using the Outerbridge scoring system (*Outerbridge, 1961*) and exposed to PBS during testing to maintain hydration. Stiffness was higher at a lower indentation depth for all cohorts; however, stiffness was highest with mild OA (0.61 MPa) and lowest with healthy controls (0.16 MPa) when comparing to severe OA (0.19 MPa) (Table 1) (*Wang & Peng, 2015*).

Bone

There are two different types of bone including cortical and trabecular material. The cortical material is found on the outside of bone and is highly dense in nature and the trabecular material is located inside of the bone and has a greater porosity. The low and high densities work in coordination to absorb stresses through the rigid outer surface

and strains through the spongy inner material in order to resist breaking or deformation (*Nigg & Herzog, 2006*; *Martini, 1998*).

Recent research has started to direct focus onto the relationship between cartilage and bone in the progression of OA. Research has observed abnormal remodelling of subchondral bone in OA showing the trabecular structure alters in density, quantity and separation, with the greatest proliferation in volume evident at the bone–cartilage interface (*Kamibayashi et al., 1995*; *Bobinac et al., 2003*). This suggests a synergistic relationship between bone and cartilage during the progression of OA. The role of subchondral bone in OA appears to be an essential component in the initiation and advancement of the disease (*Burr, 1998*; *Lajeunesse & Reboul, 2003*; *Madry, van Dijk & Mueller-Gerbl, 2010*). However research is unclear as to whether disruption of subchondral bone remodelling occurs pre- or post-initiation of OA (*Intema et al., 2010*; *Kuroki, Cook & Cook, 2011*). *Kuroki, Cook & Cook (2011)* suggested that a more comprehensive understanding of the disease mechanisms of OA including material properties of all tissues involved could yield considerable progression in clinical practice and treatment methods.

In previous decades uniaxial compression testing of human femoral and tibial trabecular bone was carried out by several researchers in order to obtain macroscale material properties. *Behrens, Walker & Shoji (1974)* tested both femoral condyle and tibial plateau trabecular bone samples from six females and four males (40–92 years old) resulting in an elastic modulus of 158.9–277.5 MPa for femoral bone and 139.3–231.4 MPa for tibial samples (Table 2). Testing only femoral condyle trabecular bone, *Ducheyne et al. (1977)* found a slightly lower elastic modulus of 1.9–166.1 MPa (Table 2) based on donors aged 43–77 years old (four males, two females).

Carter & Hayes (1977) tested 100 human trabecular bone samples (age and gender unspecified) from tibial plateaus by uniaxial compression and found an elastic modulus between 56.6 and 83.7 MPa (Table 2). Also using uniaxial compression, *Lindahl (1976)* tested four females and four males human cadavers (14–89 years old) showing a higher elastic modulus in males (average 34.6 MPa) compared to females (average 23.1 MPa) (Table 2).

Interestingly, as well as differences between male and female cadavers, material properties also vary according to anatomical location. *Goldstein et al. (1983)* utilised uniaxial compression testing to determine the elastic modulus of trabecular bone from the tibial plateau from five cadavers (50–70 years old) across varying depths of the joint. Results showed high variation across cadavers and testing location (4.2–430 MPa (Table 2)) with the highest values at load bearing sites. Utilising an alternative method, *Hvid & Hansen (1985)*, used an osteopenetrometer on the tibial plateau of 12 healthy human donors aged 26–83 years old (three females and nine males). Medial tibial plateau samples had an elastic modulus of 13.8–116.4 MPa and lateral tibial plateau samples had a lower elastic modulus of 9.1–47.5 MPa (Table 2) further evidencing high variability in material properties across the joint.

Burgers et al. (2008) obtained four male and four female human cadavers (totalling 10 femurs aged 45–92 years old). Cylindrical trabecular specimens ($n = 28$) were tested

Table 2 Summary of bone material properties.

Author	Quantity and locality	Age, gender and health status	Testing technique	Results per Cohort: elastic modulus (MPa)	
Behrens, Walker & Shoji (1974)	10 × Donors Femoral condyle and tibial plateau trabecular bone	Age: 40–92 Gender: 6F/4M Health: healthy	Uniaxial compression	*Femoral condyle* *Tibial plateau*	158.9–277.5 139.3–231.4
Lindahl (1976)	8 × Donors Tibial plateau trabecular bone	Age: 14–89 Gender: 4F/4M Health: healthy	Uniaxial compression	*Males* *Females*	34.6 23.1
Carter & Hayes (1977)	100 × Samples Tibial plateau trabecular bone	Age: NS Gender: NS Health: Healthy	Uniaxial compression		56.6–83.7
Ducheyne et al. (1977)	6 × Donors Femoral condyle trabecular bone	Age: 43–77 Gender: 2F/2M Health: healthy	Uniaxial compression		1.9–166.1
Goldstein et al. (1983)	5 × Donors Tibial plateau trabecular bone	Age: 50–70 Gender: 2F/3M Health: healthy	Uniaxial compression		4.2–430
Hvid & Hansen (1985)	12 × Donors Tibial plateau trabecular bone	Age: 26–83 Gender: 3F/9M Health: healthy	Uniaxial compression 2.5 mm indenter	*Medial* *Lateral*	13.8–116.4 9.1–47.5
Zysset, Sonny & Hayes (1994)	6 × Donors Tibial trabecular bone	Age: 61–91 Gender: NS Health: OA grades 1–3	Uniaxial compression	*Subchondral epiphyseal/ metaphyseal*	31.0–1116.0* 8.0–1726.0*
Rho, Tsui & Pharr (1997)	2 × Donors Tibial cortical bone	Age: 57 and 61 Gender: M Health: healthy	Nanoindentation 20 nm indenter		22500.0–25800.0
Burgers et al. (2008)	10 × Donors Femoral condyle trabecular bone	Age: 45–92 Gender: NS Health: healthy	Uniaxial compression		131.0–664.0

Notes:
Summary of current literature for human knee bone material property compression or indentation testing including age, gender, health status of specimens, number and location of samples tested and technique used to obtain elastic modulus values.
GNS, gender not specified; F, female; M, male; OA, osteoarthritis.
* Elastic modulus value for individual OA grade not specified—value taken as approximation from graph.

using unconfined compression. Results were separated into superior or inferior and medial or lateral samples giving a pooled elastic modulus of 376 ± 347 MPa (Table 2) with the greatest variation apparent between superior and inferior femoral condyle samples.

Previous studies researching human knee bone material properties, specifically in OA, are abundantly missing; however one study by *Zysset, Sonny & Hayes (1994)* explored human tibial material properties from six cadavers (61–91 years old) with grades 1–3 OA, scored using the Ahlback system (*Ahlback, 1968*). Compression tests were conducted on cuboidal specimens giving an axial elastic modulus of the subchondral trabecular bone between 31 and 1,116 MPa which decreased with increasing grades of OA. Although

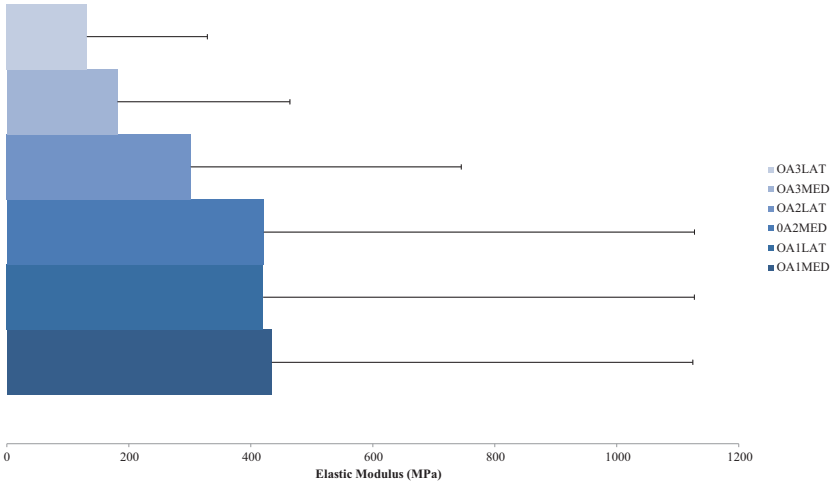

Figure 2 Compressive elastic modulus of subchondral bone in osteoarthritis. Compressive axial elastic modulus of subchondral bone for a range of osteoarthritis (OA) grades (1–3). Average elastic modulus decreases with degenerative grade in the medial (MED) and especially lateral (LAT) compartments. (Redrawn from *Zysset, Sonny & Hayes (1994)*: Elsevier License Permission: 4226540285665).
Full-size DOI: 10.7717/peerj.4298/fig-2

epiphyseal and metaphyseal trabecular bone samples showed that elastic modulus increased with OA grade in the axial (102–1,726 MPa) and coronal (8–287 MPa) planes (Table 2). Corresponding OA grade and elastic modulus values can be seen in Fig. 2.

In more recent years, testing bone at the tissue level has proven to be more accurate (*Nigg & Herzog, 2006*) particularly for the inclusion of FE models; however this has rarely been applied to femoral or tibial human bone. Using nanoindentation *Rho, Tsui & Pharr (1997)* explored the tissue level material properties of a single osteon and interstitial lamellae of two longitudinal human (57 and 61 years old) tibial cortical bone. Results presented an elastic modulus of 22,500 MPa and 25,800 MPa for osteon and interstitial lamellae samples respectively (Table 2).

Ligaments

Ligaments are soft tissues that are fibrous in nature and composed primarily of collagen. They have a hierarchal structure of fibres, fibrils, subfibrils, microfibrils and tropocollagen but also contain water, proteoglycans and several glycoproteins. They function to guide and resist motion at a joint by connecting bone to bone. It has also been suggested that they act as a strain sensor to restrict degrees of freedom in order to stabilise the joint and prevent excessive movement (*Harner et al., 1995*; *Woo et al., 2006*). Ligaments have direct and indirect insertions into the bone and periosteum respectively allowing variation in fibre bundles to respond to different movements and resist loading during ranges of rotation at the joint. The entheses portion of the ligament is stiffer compared to the medial

Figure 3 Example bone–ligament–bone sample. Photograph of a medial collateral bone–ligament–bone sample. Image from the authors' own work. (Ethics granted by NRES (15/NS/0053)).
Full-size DOI: 10.7717/peerj.4298/fig-3

portion allowing decreased concentrations of stress and therefore reducing the opportunity for damage or tears at the bone–ligament interface (*Woo et al., 2006*).

When measuring material properties of knee ligaments (ACL, PCL, MCL and LCL) typical analyses includes tensile stress and strain at ultimate failure, tangent modulus and strain energy density, primarily obtained using a tensile testing machine. These parameters are tested in vitro by taking either a cross-section of the involved ligament (*Quapp & Weiss, 1998*) or more commonly a bone–ligament–bone sample (e.g. Fig. 3). During this process bone blocks are ordinarily embedded within polymethyl-methacrylate (PMMA) and the ligaments are wrapped in saline soaked gauze for protection (*Harner et al., 1995*; *Butler et al., 1992*; *Momersteeg et al., 1995*; *Hewitt et al., 2001*; *Robinson, Bull & Amis, 2005*; *Bonner et al., 2015*). Additionally samples may be tested as a whole structure or divided into anatomical fibre bundles. *Woo et al. (2006)* suggests that the ACL has an anteromedial and posterolateral bundle and the PCL has an anterolateral and posteromedial bundle which are loaded differently. Ligaments therefore may need to be separated during tensile testing, in order to gain a true understanding of their unique material properties. A summary of the reviewed ligament material property research papers is provided in Table 3.

Harvesting a cross-sectional area of a ligament, *Quapp & Weiss (1998)* explored the longitudinal and transverse mechanical behaviour of the MCL from 10 human cadavers (62 ± 18 years old). Specimens were preconditioned and loaded to failure. Results included average tensile strength (38.6 and 1.7 MPa), average ultimate strain (17.1% and

Table 3 Summary of ligament material properties.

Author	Quantity and locality	Age, gender and health status	Testing technique	Results					
				Tissue type	Stiffness (N/mm)	Failure load (N)	Elastic modulus (MPa)	Max stress (MPa)	Max strain (%)
Trent, Walker & Wolf (1976)	7 × ACL, PCL, MCL and LCL	Age: 29–55	Bone–ligament–bone	*ACL*	138.3	620.8			
		Gender: NS		*PCL*	179.5	658.0			
		Health: healthy		*MCL*	70.6	515.8			
				LCL	59.8	376.6			
Noyes & Grood (1976)	26 × ACL	Age: 16–86	Bone–ligament–bone	*Young*	182.0	1730.0	*111.0*	*37.8*	*44.3*
		Gender: NS		*Old*	129.0	734.0	*65.3*	*13.3*	*30.0*
		Health: healthy							
Butler, Kay & Stouffer (1986)	3 × ACL, PCL and LCL	Age: 21–30	Bone–ligament–bone	*ACL*			*278.0–310.0*[*]	*30.0–40.0*[*]	*14.0–16.0*[*]
		Gender: 2F/1M		*PCL*			*280.0–447.0*[*]	*34.0–44.0*[*]	*14.0–19.0*[*]
		Health: healthy		*LCL*			*375.0–25.0*[*]	*31.0–43.0*[*]	*11.0–17.0*[*]
Woo et al. (1991)	27 × ACL bilateral	Age: 22–97	Bone–ligament–bone	*Young 22–35*	218.0–242.0	1602.0–2160.0			
		Gender: NS		*Middle 40–50*	192.0–220.0	1160.0–1503.0			
		Health: healthy		*Old 60–97*	124.0–180.0	495.0–658.0			
Butler et al. (1992)	7 × ACL	Age: 26 ± 4	Bone–ligament–bone	*Anteromedial fibers*			238.1	54.7	19.1
		Gender: NS		*Anterolateral fibers*			285.9	30.6	16.1
		Health: healthy		*Posterior fibers*			154.9	15.4	15.2
Race & Amis (1994)	10 × PCL	Age: 53–98	Bone–ligament–bone	*Anterolateral fibers*	*347.0*	1620.0	248.0	35.9	18.0
		Gender: NS		*Posteromedial fibers*	*77.0*	258.0	145.0	24.4	19.5
		Health: healthy							
Harner et al. (1995)	5 × PCL	Age: 48–77	Bone–ligament–bone	*Anterolateral fibers*	120.0	1120.0			
		Gender: NS		*Posteromedial fibers*	57.0	419.0			
		Health: healthy							

Table 3 (continued).

Author	Quantity and locality	Age, gender and health status	Testing technique	Results					
				Tissue type	Stiffness (N/mm)	Failure load (N)	Elastic modulus (MPa)	Max stress (MPa)	Max strain (%)
Quapp & Weiss (1998)	10 × MCL	Age: 62 ± 18	Ligament sample only	*Longitudinal*			38.6		17.1
		Gender: NS		*Transverse*			1.7		1.7
		Health: healthy							
Robinson, Bull & Amis (2005)	8 × MCL	Age: 77 ± 5.3	Bone–ligament–bone	*Superficial MCL*		534.0			
		Gender: NS		*Deep MCL*		194.0			
		Health: healthy		*Posteromedial capsule*		425.0			
Chandrashekar et al. (2006)	17 × ACL	Age: 17–50	Bone–ligament–bone	*ACL total*	250.0	1526.0	113.0	24.4	
		Gender: 9F/8M		*Male*	308.0	1818.0	128.0	26.4	
		Health: healthy		*Female*	199.0	1266.0	99.0	22.8	

Notes:
Summary of current literature for human knee ligament material properties including location and number of samples, age, gender, health status of donors, testing technique and resultant data. N.B. for comparison purposes only those papers testing ligaments to failure will be included in this table.
GNS, gender not specified; F, female; M, male; ACL, anterior cruciate ligament; PCL, posterior cruciate ligament; MCL, medial collateral ligament; LCL, lateral collateral ligament.
* Values are approximated from graph data.

1.7%) and average tangent modulus (332.2 and 11.0 MPa) for longitudinal and transverse specimens respectively (Table 3).

Further research on the tensile properties of ligaments utilised the bone–ligament–bone method. One of the first studies to explore ligament material properties harvested the ACL, PCL, MCL and LCL from seven healthy human cadavers aged 29–55 years old (gender not specified). Ligaments were preconditioned over five cycles and loaded to failure at 100% strain rate, which is a change in strain equivalent to the initial length of the ligament. Stiffness was measured at 138.3, 179.5, 70.3 and 59.8 N/mm for the ACL, PCL, MCL and LCL respectively, whilst failure load resided at 620.8, 658.0, 515.8 and 376.6 N (Table 3) (*Trent, Walker & Wolf, 1976*).

Noyes & Grood (1976) tested young (16–26 years old) and old (48–86 years old) anterior cruciate bone–ligament–bone material properties, also at a 100% strain rate, although excluded any preconditioning. The research found a reduction in stiffness (129 and 182 N/mm), failure load (734.0 and 1730.0 N), elastic modulus (65.3 and 111.0 MPa), maximum stress (13.3 and 37.8 MPa) and strain (30.0% and 44.3%) when comparing older samples to younger samples respectively (Table 3).

Butler, Kay & Stouffer (1986) also tested young (21–30 years old) ACL, PCL and LCL elastic modulus (278–447 MPa), maximum stress (30–44 MPa) and maximum strain (11–19%) where ranges were inclusive of all ligaments. Approximate values are given in Table 3 estimated from presented graphs (*Butler, Kay & Stouffer, 1986*). The ligaments were divided into their fibre bundles and tested to failure at a 100%/s strain rate (Table 3). Further research by *Butler et al. (1992)* looked at the differences in seven human ACL (26 ± 4 years old) divided into anteromedial, anterolateral and posterior fibre bundles. Specimens were not exposed to preconditioning but were loaded to failure at a 100%/s strain rate. This resulted in anterior fibres having a higher maximum modulus (284 MPa), stress (38 MPa) and strain rate (17.6%) when compared to posterior fibres (155 MPa, 15 MPa, 15.2%) at failure (Table 3).

Race & Amis (1994) and *Harner et al. (1995)* loaded to failure the anterolateral and posteromedial fibres bundles of the human PCL. *Race & Amis (1994)* obtained 10 samples from donors aged 53–98 years old which resulted in higher stiffness (347.0 and 770 N/mm), failure load (1620.0 and 258.0 N), elastic modulus (248.0 and 145.0 MPa) and maximum stress (35.9 and 24.4 MPa) for the anterolateral fibres in comparison to the posteromedial fibres respectively (Table 3). Interestingly maximum strain was lower for the anterolateral fibres (18.0%) when compared to the posteromedial fibres (19.0%). *Harner et al. (1995)* tested five samples (48–77 years old) and also found a higher failure load in the anterolateral fibres (1120.0 N) in comparison to the posteromedial fibres (419.0 N) (Table 3) showing in both studies wide variation depending on the location of the tissue.

A more recent study by *Robinson, Bull & Amis (2005)* harvested three sections of the femur–MCL–tibia complex from eight humans (77 ± 5.3 years old), namely the superficial MCL (SMCL), deep MCL (DMCL) and posteromedial capsule (PMC) based on fibre orientation and tested samples using the bone–ligament–bone approach. The SMCL is often used to define the overall MCL length; however, it is thought that each

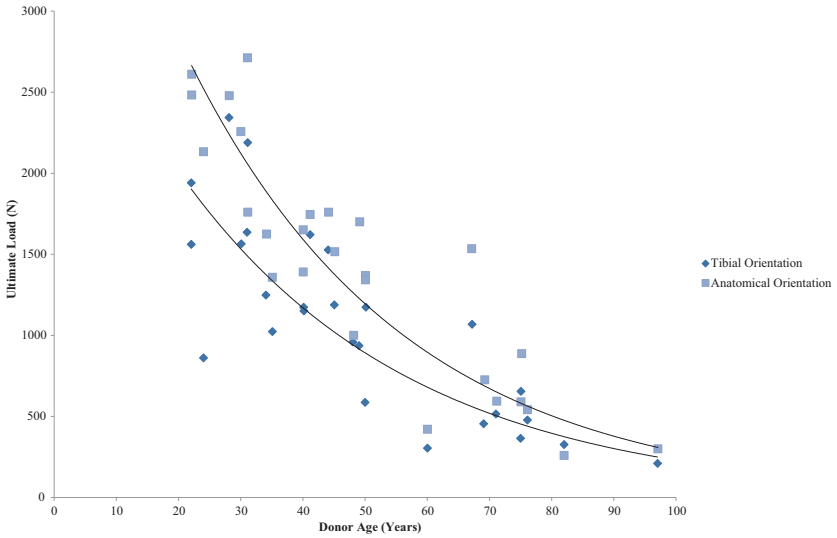

Figure 4 Effect of specimen age on anterior cruciate ligament ultimate load. Effect of specimen age on anterior cruciate ligament (ACL) ultimate load. Data on ultimate load as a function of specimen age and orientation demonstrated that the strength of the ACL decreases in an exponential manner. (Redrawn from *Woo et al. (1991)*: Sage License Permission: 4226541340810).

Full-size DOI: 10.7717/peerj.4298/fig-4

section tenses and fully elongates under different loading axis or directions and functions to stabilise the knee joint in various ways. Samples were preconditioned and loaded to failure resulting in failure loads of 534, 194 and 425 N for the SMCL, DMCL and PMC respectively (Table 3). The results indicated a bony avulsion in 75% of tested samples after which the bone was removed and the end of the ligament was attached directly in the clamps and re-loaded to failure. Additionally mid-substance failure of the ligament as opposed to bony avulsion equated to 74% higher maximum load.

Further variations in tensile properties can exist due to the angle of the femur in correlation to the tibia and the loading axis in correlation to ligament fibre loading direction. *Woo et al. (1991)* preconditioned and tested the ACL to failure along both the tibial and ligament axis and found higher stiffness values on the ligament axis with increasing extension angle when testing young and old cadavers. Significant variations in anatomical orientation failure load were apparent between age groups: 2,160 N for 22–35 years old ($N = 9$), 1,503 N for 40–50 years old ($N = 9$) and 658 N for 60–97 years old ($N = 9$) (Table 3) as seen in Fig. 4. However, there was no correlation between age and orientation.

Interestingly, *Chandrashekar et al. (2006)* found gender-based differences in tensile properties showing human female ACL ($N = 9$) (17–50 years old) had 22.49% lower elastic modulus and 8.3% and 14.3% lower maximum strain and stress respectively when compared to human male ACL ($N = 8$) (26–50 years old) (Table 3). These differences can

be partially accounted for due to the physically smaller size of the female ACL (*Anderson et al., 2001*; *Chandrashekar, Slauterbeck & Hashemi, 2005*); however, when adjusted for covariates the tensile properties of the ACL are still lower. This may in turn explain the higher rates of ACL injuries in female athletes (*Chandrashekar et al., 2006*).

Finally an analysis by *Momersteeg et al. (1995)* chose not to separate the fibre bundles but instead tilted the orientation of the loading axis at 5° increments (up to 25°) to recruit different fibres at varying angles to explore the changes in tensile properties during sub-ultimate testing. Bone–ligament–bone samples were harvested for the ACL, PCL, MCL and LCL of five human cadavers (63–81 years old) and subjected to preconditioning before applying up to 7% and 10% strain rates for the collateral and cruciate ligaments respectively. Results indicate that strain levels were higher for cruciate ligaments than collateral ligaments and for every 5° of tilt there was a decrease in tensile stiffness (averages: -11.6 Nmm^{-1} ACL, -20.96 Nmm^{-1} PCL, -2.66 Nmm^{-1} MCL, -3.76 Nmm^{-1} LCL) (Table 3). The research suggests there is a greater decrease in stiffness for the cruciate ligaments as they have a shorter and wider morphology when compared to the long thin nature of collateral ligaments. These authors go on to conclude that ligaments are highly sensitive to a small change in orientation and therefore unidirectional tensile testing is not effective at defining ligament stiffness properties (*Momersteeg et al., 1995*).

SECTION B: FE MODELLING

Freutel et al. (2014) presented a non-systematic review on the current research on FE modelling within soft tissues with a specific focus on the human knee joint and intervertebral disc. They reviewed strategies for modelling various material properties, considering the interaction between soft tissues during contact and their sensitivity to changes in properties and environment (i.e. loading and boundary conditions). Their review concluded that inaccuracy or abstraction in each of these areas could manifest into important limitations in structurally complex models such as those of the human knee joint. Material property definition was cited by *Freutel et al. (2014)* and indeed by others (*Gardiner & Weiss, 2003*), as a research area with potential for significant improvement either through improved modelling approaches or in vivo inclusion of material properties particularly given the advances in techniques for characterising biological tissue behaviour in recent decades.

Following on from this review of available material property data for human knee joint tissues in 'Section A—Material Properties' (above) we focus subsequently on the material property data that has actually been utilised in published whole-joint FE models of the human knee. It is our hope that clarifying the FE models that currently exist in the literature and their accuracy according to how they have obtained their material property data (i.e. primary data collection or from various data sets and donors) will help identify gaps within the knowledge and aid future directions for research.

Advances in FE modelling have allowed researchers to present cartilage as a non-linear anisotropic material with varying material properties as opposed to the traditional representation of a linear elastic isotropic material. This advance means cartilage can now be represented with greater biofidelity and therefore computational predictions of behaviours are likely to be more accurate. Several authors have adopted this advanced

approach in recent years (*Tanska, Mononen & Korhonen, 2015*; *Halonen et al., 2013*); however, due to the complexity and computation expense of such models, individual tissues are often modelled in isolation, meaning other structures not relevant to the research hypothesis are excluded. Although useful in particular applications, if representing OA of the knee joint, modelling tissues in isolation has its limitations. It is now well established that this is a disease of the entire joint with molecular crosstalk and changes in subchondral bone structure (*Lories & Luyten, 2011*; *Mahjoub, Berenbaum & Houard, 2012*), and histological evidence of ligament structural changes (*Mullaji et al., 2008*). Therefore if investigating such diseases it is now inherently clear that whole-joint representation is needed to fully understand the implications of tissue interaction and disease progression on the knee joint.

When cartilage is modelled with linear elasticity it assumes an instantaneous response to stress and strain; however, nonlinear representation allows for viscoelastic or time dependent factors such as those represented in *Mononen et al. (2011, 2012)*. It is now well established that cartilage and ligaments are nonlinear and viscoelastic and material property testing is starting to incorporate time-dependent testing by including a hold period. This review is intended to analyse whole-joint representations only. Studies presenting only singular tissues of the human knee joint with more detailed material behaviours are outside the scope of this review, although the recent efforts in modelling hyperelastic formulations of cartilage and efforts towards representing tissue anisotropy and viscoelasticity are summarised below.

Modelling cartilage as a fibril reinforced poroviscoelastic tissue with multiple material properties, *Tanska, Mononen & Korhonen (2015)* explored chondrocyte compression during walking, whilst research by *Halonen et al. (2013)* explored cartilage deformation under large compression. Further, work by *Dabiri & Li (2013)* also modelled cartilage with depth-dependent properties, making it possible to use a fibril-reinforced model to explore inhomogeneity and fluid pressurisation within the tissue. *Meng et al. (2014)* considered cartilage as a fibril reinforced biphasic material to explore knee joint contact behaviour under body weight. Other examples of research representing cartilage as a poroelastic or poroviscoelastic material include the work of *Kazemi et al. (2011)* and *Mononen et al. (2011, 2012)*. These studies represented whole-joints and are therefore discussed in more detail below.

For the purpose of this review, research papers that have presented a FE model of a healthy human knee joint incorporating the femur, tibia, cartilage and four major ligaments each within a 3D form will be presented, addressing how and where these models have sourced material property data for their models. Following this, models that have included all these structures but most commonly represented them in a simplified form of one, two and 3D forms will also be reviewed. Finally the existing attempts to simulate the effects of OA within the knee joint using FE models will be discussed.

3D FE models of healthy human knee joints

This review reveals that FE models most commonly use previously published data for material properties; however, there is usually a lengthy referencing chain when tracing

these material properties to their original and primary data research article. Material properties are likely to vary with age, gender and disease status (*Kleemann et al., 2005*; *Lindahl, 1976*; *Woo et al., 1991*; *Chandrashekar et al., 2006*) and therefore donor demographics in previously published material property studies will undoubtedly impact upon the quantitative results obtained in FE analyses. Our review highlights a wide spectrum of matches in this respect to the extent that the absence of appropriate data has in some cases led to the use of non-human material properties in FE models of the knee. Material property sources from reviewed FE models are summarised in Table 4.

Wang, Fan & Zhang (2014) attempted to estimate cartilage stress under forces incurred during kneeling in a young healthy male (26-year-old), using primary MRI data to create their FE model, which it should be noted included the patella (Fig. 5). The referencing chain starting from *Wang, Fan & Zhang (2014)* follows up to five secondary references until the original research article is cited. Original demographics include human tibial plateau and femoral neck samples for bone (*Rho, Ashman & Turner, 1993*; *Zysset et al., 1999*), human femoral condyle and tibial plateau samples for cartilage (*Shepherd & Seedhom, 1999a*), human (*Tissakht & Ahmed, 1995*) and bovine menisci (*Skaggs, Warden & Mow, 1994*) and human ACL, PCL, LCL, quadriceps tendon and patella ligament samples for ligament material properties (*Race & Amis, 1994*; *Woo et al., 1991*; *Staubli et al., 1999*; *Blankevoort, Huiskes & De Lange, 1988*; *Brantigan & Voshell, 1941*). Where human samples were used for bone material properties the original research articles either do not state donor age (*Rho, Ashman & Turner, 1993*) or donor age was 53–93 years old (*Zysset et al., 1999*). Human cartilage ranged from 33 to 80 years old (*Shepherd & Seedhom, 1999a*) whilst menisci was either 29–45 years old (*Skaggs, Warden & Mow, 1994*) or information was not available. Human ligament samples had an average age of 24.9 years old (*Staubli et al., 1999*), an age range of 53–98 years old (*Race & Amis, 1994*), 43–74 years old (*Blankevoort, Huiskes & De Lange, 1988*), or it stated that donors were 'young' (*Butler, Kay & Stouffer, 1986*) or it was unspecified (*Brantigan & Voshell, 1941*) (Table 4). The specific material properties used within *Wang, Fan & Zhang (2014)*, can be found in the Table 5 alongside the material properties from other FE modelling studies reviewed.

Consecutive studies by *Peña et al. (2005, 2006)* carried out FE modelling of a healthy knee joint using CT and MRI data of a healthy male volunteer (age not specified) to generate a model that included bone, ligaments, tendons and articular and meniscal cartilages using previously published material property data. The aims of these studies were to compare stress and strain in a healthy human knee to those experienced after meniscal tears and meniscectomies (*Peña et al., 2005*) and to analyse the non-uniform stress–strain fields that the menisci and ligaments encounter during the loading of the human knee joint (*Peña et al., 2006*). The referencing chain starting from *Peña et al. (2006)* also follows up to four secondary references until the original research article is cited. As bones were modelled as rigid this requires no material property input; cartilage material properties could not be traced; menisci material properties were based on canine meniscal material properties (*LeRoux & Setton, 2002*) and ligaments on human ACL, PCL, MCL and LCL material properties with ages specified as 38 years old (*Butler et al., 1990*), 37–61 years old (91), 43–74 years old (*Blankevoort, Huiskes & De Lange, 1988*) or simply

Table 4 Summary of human knee finite element models.

	Purpose	Bone	Cartilage	Menisci	Ligaments
Blankevoort et al. (1991)	Rigid and deformable articular contact during axial and varus/valgus rotations	N/a	Information untraceable**	N/a	Human (ACL, PCL, LCL) 43–74 years Some information untraceable (*Butler, Kay & Stouffer, 1986*; *Blankevoort, Huiskes & De Lange, 1988****)
Blankevoort & Huiskes (1991)	Ligament–bone interaction during axial and varus/ valgus rotations	N/a	Information untraceable**	N/a	Human (ACL, PCL, LCL) 43–74 years Some information untraceable (*Butler, Kay & Stouffer, 1986*; *Blankevoort, Huiskes & De Lange, 1988****)
Bendjaballah, Shirazi-Adl & Zukor (1995)	Articular cartilage deformation under compression up to 1,000 N	N/a	Human (tibial plateau) 48–70 years (*Hayes & Mockros, 1971*)	Human (menisci) 29–45 years Some information untraceable (*Tissakht & Ahmed, 1995*)	Human (ACL, PCL, LCL) 53–98 year* (*Butler, Kay & Stouffer, 1986*; *Race & Amis, 1994*)
Bendjaballah, Shirazi-Adl & Zukor (1997)	Role of collateral ligaments in varus–valgus motion	N/a	Human (tibial plateau) 48–70 years (*Hayes & Mockros, 1971*)	Human (menisci) 29–45 years Some information untraceable (*Tissakht & Ahmed, 1995*)	Human (ACL, PCL, LCL) 53–98 year* (*Butler, Kay & Stouffer, 1986*; *Race & Amis, 1994*)
Jilani, Shirazi-Adl & Bendjaballah (1997)	Non-linear elastostatic response of ligaments during axial rotation with 10 N torque	N/a	Human (tibial plateau) 48–70 years (*Hayes & Mockros, 1971*)	Human (menisci) 29–45 years Some information untraceable (*Tissakht & Ahmed, 1995*)	Human (ACL, PCL, LCL) 53–98 year* (*Butler, Kay & Stouffer, 1986*; *Race & Amis, 1994*)
Bendjaballah, Shirazi-Adl & Zukor (1998)	Anterior–posterior drawer forces on cartilage under compression up to 400 N loads	N/a	Human (tibial plateau) 48–70 years (*Hayes & Mockros, 1971*)	Human (menisci) 29–45 years Some information untraceable (*Tissakht & Ahmed, 1995*)	Human (ACL, PCL, LCL) 53–98 year* (*Butler, Kay & Stouffer, 1986*; *Race & Amis, 1994*)
Li et al. (1999)	Ligament forces in response to internal–external moments up to 10 Nm	N/a	Information untraceable**	N/a	Human (ACL, PCL, LCL) 43–74 years Some information untraceable (*Butler, Kay & Stouffer, 1986*; *Blankevoort, Huiskes & De Lange, 1988****)
Li, Lopez & Rubash (2001)	Cartilage contact stress sensitivity analysis with compression up to 1,400 N	N/a	Information untraceable	N/a	Human (ACL, PCL, LCL) 43–74 years Some information untraceable (*Butler, Kay & Stouffer, 1986*; *Blankevoort, Huiskes & De Lange, 1988****)

(Continued)

Table 4 (continued).

	Purpose	Bone	Cartilage	Menisci	Ligaments
Moglo & Shirazi-Adl (2003)	Cruciate ligament behaviour under 100 N femoral load in flexion	N/a	Human (tibial plateau) 48–70 years (*Hayes & Mockros, 1971*)	Human (menisci) 29–45 years Some information untraceable (*Tissakht & Ahmed, 1995*)	Human (ACL, PCL, LCL) 53–98 year* (*Butler, Kay & Stouffer, 1986*; *Race & Amis, 1994*)
Beillas et al. (2004)	In vivo kinematics and ground reaction forces during one leg hop with compression up to 1,790 N	Human (proximal femur and mid femur) 28–91 years* Bovine (distal femur and patella) Some information untraceable (*Lotz, Gerhart & Hayes, 1991*; *Reilly & Burstein, 1975*; *Mente & Lewis, 1994*)	Human (tibial plateau) age not specified* Some information untraceable (*Repo & Finlay, 1977*)	Human (menisci) age not specified* (*Fithian, Kelly & Mow, 1990*)	Human (ACL, PCL, MCL, LCL) 16–97 years* Some information untraceable (*Trent, Walker & Wolf, 1976*; *Noyes & Grood, 1976*; *Woo et al., 1991*)
Peña et al. (2005)	Compare stresses on menisci and cartilage healthy joints to meniscal tears and meniscectomies under compression up to 1,150 N	N/a	Information untraceable	Canine (menisci) (*LeRoux & Setton, 2002*)	Theoretical data (*Weiss & Gardiner, 2001*)
Peña et al. (2006)	Ligament and Menisci behaviour in healthy during compressive load transmission up to 1,150 N	N/a	Information untraceable	Canine (menisci) (*LeRoux & Setton, 2002*)	Human (ACL, PCL, MCL, LCL) 37–74 years* (*Butler, Kay & Stouffer, 1986*; *Gardiner & Weiss, 2003*; *Blankevoort, Huiskes & De Lange, 1988****; *Brantigan & Voshell, 1941****; *Butler et al., 1990*)
Donlagic et al. (2008)	Simulated knee joint kinematics during flexion	Human (proximal femur and mid femur) years* Bovine (distal femur and patella) Some information untraceable (*Lotz, Gerhart & Hayes, 1991*; *Reilly & Burstein, 1975*; *Mente & Lewis, 1994*)	Human (tibial plateau) age not specified* Bovine (femoral condyle and tibial plateau) Porcine (femoral condyle and tibial plateau) Some information untraceable (*Repo & Finlay, 1977*; *Laasanen, 2003*)	Human (menisci) age not specified* (*Fithian, Kelly & Mow, 1990*)	Human (ACL, PCL, MCL, LCL) 16–97 years* Some information untraceable (*Trent, Walker & Wolf, 1976*; *Noyes & Grood, 1976*; *Woo et al., 1991*)
Shirazi, Shirazi-Adl & Hurtig (2008)	Role of collagen fibrils under compression up to 2,000 N	N/a	Human (tibial plateau) 48–70 years (*Hayes & Mockros, 1971*)	Human (menisci) 29–45 years Some information untraceable (*Tissakht & Ahmed, 1995*)	Human (ACL, PCL, LCL) 53–98 year* (*Butler, Kay & Stouffer, 1986*; *Race & Amis, 1994*)

Table 4 (continued).

	Purpose	Bone	Cartilage	Menisci	Ligaments
Guo, Zhang & Chen (2009)	Cartilage contact pressures during the gait cycle	Information untraceable	Information untraceable	Canine (menisci) (*LeRoux & Setton, 2002*)	Information untraceable
Yang et al. (2010)	Tibiofemoral angle effect on cartilage pressure during stance phase of gait	N/a	Information untraceable**	Information untraceable	Human (ACL, PCL, LCL) 43–74 years Some information untraceable (*Butler, Kay & Stouffer, 1986*; *Blankevoort, Huiskes & De Lange, 1988****)
Kazemi et al. (2011)	Creep behaviour of cartilage and menisci under 300 N compression in healthy	N/a	Bovine (humeral head) (*Langelier & Buschmann, 1999*; *Woo, Akeson & Jemmott, 1976*)	Human (menisci) 29–45 years (*Tissakht & Ahmed, 1995*)	Human (patella tendon, Achilles tendon) 29–93 years; Rat (tail tendon) (*Hansen et al., 2006*; *Johnson et al., 1994*; *Louis-Ugbo, Leeson & Hutton, 2004*; *Ault & Hoffman, 1992a*)
Wang, Fan & Zhang (2014)	Cartilage stress during kneeling and standing with up to 1,000 N compression	Human (tibial plateau and femoral neck) 53–93 years* (*Rho, Ashman & Turner, 1993*; *Zysset et al., 1999*)	Human (femoral condyle and tibial plateau) 33–80 years (*Shepherd & Seedhom, 1999a*)	Human (menisci) 29–45 years* Bovine (menisci) Some information untraceable (*Tissakht & Ahmed, 1995*; *Skaggs, Warden & Mow, 1994*)	Human (ACL, PCL, LCL, quadriceps tendon, patella ligament) 24–98 years* Some information untraceable (*Butler, Kay & Stouffer, 1986*; *Race & Amis, 1994*; *Staubli et al., 1999*; *Blankevoort, Huiskes & De Lange, 1988****; *Brantigan & Voshell, 1941****)
Mootanah et al. (2014)	Joint forces/pressures due to malalignment with axial loads of 374 N	Human (femoral condyle and tibial plateau) 45–68 years (*Hobatho et al., 1991*)	Human (femoral condyle and tibial plateau) 33–80 years (*Shepherd & Seedhom, 1997*; *Blankevoort, Huiskes & De Lange, 1988****)	Information untraceable	Human (ACL, PCL, MCL, LCL) 50 years primary data
Kazemi & Li (2014)	Viscoelastic poromechanical response of cartilage and menisci with compression up to 700 N	N/a	Human (tibial plateau) 48–70 years Bovine (humeral head) (*Langelier & Buschmann, 1999*; *Woo, Akeson & Jemmott, 1976*; *Hayes & Mockros, 1971*)	Human (menisci) 29–45 years (*Tissakht & Ahmed, 1995*)	Human (ACL, PCL, LCL, patella tendon, Achilles tendon) 29–98 years* Rat (tail tendon) (*Butler, Kay & Stouffer, 1986*; *Race & Amis, 1994*; *Blankevoort, Huiskes & De Lange, 1988****; *Brantigan & Voshell, 1941****; *Hansen et al., 2006*; *Johnson et al., 1994*; *Louis-Ugbo, Leeson & Hutton, 2004*; *Ault & Hoffman, 1992a*)

Notes:

Summary of recent FE models of whole human knee joints and the type of sample each original primary data collection was based on including location of sample, and age if human samples were used.

ACL, anterior cruciate ligament; PCL, posterior cruciate ligament; MCL, medial collateral ligament; LCL, lateral collateral ligament.

* Age not specified in original research article.

** Multiple references are available in cited reference—unclear as to which study the FE model is using.

*** Material properties are not represented—papers are referenced with use of geometry and orientation of structure.

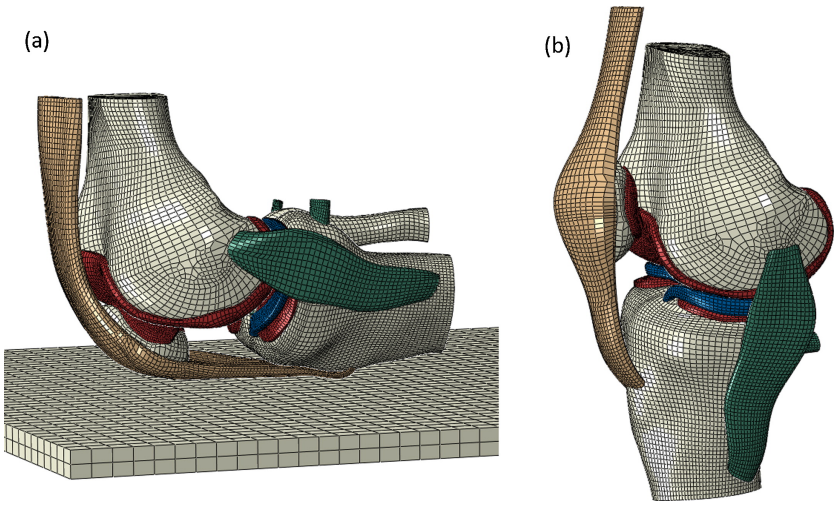

Figure 5 A finite element model of the knee joint. A FE model of the knee joint in (A) Kneeling position and (B) standing position. All structures are modelled in three dimension including the distal femur, proximal tibia and patella bones, femoral and tibial cartilage, medial and lateral menisci, ACL (anterior cruciate ligament), PCL (posterior cruciate ligament), MCL (medial collateral ligament), LCL (lateral collateral ligament) and patella tendon. (Reused from *Wang, Fan & Zhang (2014)*: Elsevier License Permission: 4226550209690). Full-size DOI: 10.7717/peerj.4298/fig-5

denoted as 'young' (*Butler, Kay & Stouffer, 1986*) or unspecified (*Brantigan & Voshell, 1941*). *Peña et al. (2005)* used the same original sources for cartilage and menisci material properties and adopted ligament material property data from a review article (*Weiss & Gardiner, 2001*) for the representation of a healthy knee joint, summarised in Table 4.

Guo, Zhang & Chen (2009) created a 3D human knee joint model from a CT scan on a 45-year-old healthy female to understand the contact pressures on the femoral and tibial cartilages during different phases of the gait cycle. Material properties were referenced from previous FE modelling papers; however, the referencing chain provides information that menisci data was originally presented by *LeRoux & Setton (2002)* based on canine meniscal properties. Unfortunately, bone, cartilage and ligament material property sources cannot be traced back to a primary data collection reference (Table 4).

A recent FE study explored misalignment differentiation of the knee joint to understand how this influences contact pressure (*Mootanah et al., 2014*). An MRI of a 50-year-old cadaveric male was used for geometry and validation of the model through mounting the knee joint and matching loading and boundary conditions. *Mootanah et al. (2014)* obtained material properties from the literature with a referencing chain going back through three other research papers to the original primary research article. Bone material properties were based on human femoral condyle and tibial plateau samples aged 45–68 years old (*Hobatho et al., 1991*) whilst cartilage was based on ages stated as 33–80 years old (*Shepherd & Seedhom, 1997*, *1999b*). It is unclear how the meniscal material properties were obtained. Ligament material property data was obtained through primary

Table 5 Summary of material properties included in finite element models.

	Bone		Cartilage		Menisci		ACL		PCL		MCL		LCL	
	E (MPa)	*v*	*E* (MPa)	*v*	*E* (MPa)	*v*	*E* (MPa) or stiffness (N)	Initial strain (%/mm)	*E* (MPa) or stiffness (N)	Initial strain (%/mm)	*E* (MPa) or stiffness (N)	Initial strain (%/mm)	*E* (MPa) or stiffness (N)	Initial strain (%/mm)
Wang, Fan & Zhang (2014)	20,000	0.3	10	0.05–0.45	20–140	0.2	NS	0.0–0.1%	NS	0.0–0.1%	NS	0.0–0.1%	NS	0.0–0.1%
Peña et al. (2006)	Rigid	Rigid	5	0.46	59	0.49	1.95 MPa	0.0–0.1%	3.25 MPa	0.0–0.1%	1.44 MPa	0.0–0.1%	1.44 MPa	0.0–0.1%
Peña et al. (2005)	Rigid	Rigid	5	0.46	59	0.49	5.83 MPa	NS	6.06 MPa	NS	6.43 MPa	NS	6.06 MPa	NS
Guo, Zhang & Chen (2009)	11,000	0.3	5	0.45	59	0.46	NS	NS	NS	NS	NS	NS	NS	NS
Mootanah et al. (2014)	1,000	0.3	25	0.45	20–120	0.2–0.3	154 MPa	NS	40 MPa	NS	43 MPa	NS	56 MPa	NS
Kazemi et al. (2011)	Rigid	Rigid	0.26–1,600	0.36	0.5–28	0.36	10–14,000 MPa	NS	10–14,000 MPa	NS	10–14,000 MPa	NS	10–14,000 MPa	NS
Kazemi & Li (2014)	Rigid	Rigid	0.41–367.14	NS	0.0–12.84	NS	46.47–1,118.6 MPa	2.5%	46.47–1,118.6 MPa	0%	46.47–1,118.6 MPa	2%	46.5–1,118.6 MPa	2%
Donlagic et al. (2008)	1,000	0.3	67.6	0.3	130	0.3	200–260 MPa	NS	200–260 MPa	NS	114–134 MPa	NS	114–134 MPa	NS
Li, Lopez & Rubash (2001)	Rigid	Rigid	3.5–10	0.45	NM	NM	5,000 N	0.3–0.8 mm	9,000 N	2.3–3 mm	2,750 N	0.2–0.4 mm	2,000 N	−0.4 mm
Li et al. (1999)	Rigid	Rigid	5	0.45	NM	NM	5,000 N	0.3–0.8 mm	9,000 N	2.3–3 mm	2,750 N	0.2–0.4 mm	2,000 N	−0.4 mm
Blankevoort et al. (1991)	Rigid	Rigid	5	0.45	NM	NM	5,000 N	0.06–0.1%	9,000 N	−0.03 to −0.24%	2,750 N	0.03–0.04%	2,000 N	−0.05 to −0.25%
Blankevoort & Huiskes (1991)	Rigid	Rigid	5	0.45	NM	NM	5,000 N	0.06–0.1%	9,000 N	−0.03 to −0.24%	2,750 N	0.03–0.04%	2,000 N	−0.05 to −0.25%
Bendjaballah, Shirazi-Adl & Zukor (1995)	Rigid	Rigid	12	0.45	8–15	0.45	NS	1.2–4%	NS	−1 to −16.9%	NS	1.8–3.4%	NS	2.6–5%
Bendjaballah, Shirazi-Adl & Zukor (1997)	Rigid	Rigid	12	0.45	8–15	0.45	NS	1.2–4%	NS	−1 to −16.9%	NS	1.8–3.4%	NS	2.6–5%
Bendjaballah, Shirazi-Adl & Zukor (1998)	Rigid	Rigid	12	0.45	8–15	0.45	NS	1.2–4%	NS	−1 to −16.9%	NS	1.8–3.4%	NS	2.6–5%
Jilani, Shirazi-Adl & Bendjaballah (1997)	Rigid	Rigid	12	0.45	8–15	0.45	NS	1.2–4%	NS	−1 to −16.9%	NS	1.8–3.4%	NS	2.6–5%

(Continued)

Table 5 (continued).

	Bone		Cartilage		Menisci		ACL		PCL		MCL		LCL	
	E (MPa)	*v*	*E* (MPa)	*v*	*E* (MPa)	*v*	*E* (MPa) or stiffness (N)	Initial strain (%/mm)	*E* (MPa) or stiffness (N)	Initial strain (%/mm)	*E* (MPa) or stiffness (N)	Initial strain (%/mm)	*E* (MPa) or stiffness (N)	Initial strain (%/mm)
Moglo & Shirazi-Adl (2003)	Rigid	Rigid	12	0.45	8–15	0.45	NS	1.2–4%	NS	−1 to −16.9%	NS	1.8–3.4%	NS	2.6–5%
Shirazi, Shirazi-Adl & Hurtig (2008)	Rigid	Rigid	12	0.45	8–15	0.45	NS	1.2–4%	NS	−1 to −16.9%	NS	1.8–3.4%	NS	2.6–5%
Yang et al. (2010)	Rigid	Rigid	15	0.45	20–140	0.2–0.3	5,000 N	0.06–0.1%	9,000 N	−0.03 to −0.24%	2,750 N	0.03–0.04%	2,000 N	−0.05 to −0.25%
Beillas et al. (2004)	75–17,500	0.3	20	0.45	250	0.45	150 MPa	NS	150 MPa	NS	60 MPa	NS	60 MPa	NS

Notes:
Material property values included in each of the finite element modelling studies.
E, elastic modulus; *v*, Poisson's ratio; NM, not modelled; NS, not specified; ACL, anterior cruciate ligament; PCL, posterior cruciate ligament; MCL, medial collateral ligament; LCL, lateral collateral ligament.

data collection of the ACL, PCL, MCL and LCL giving validated values for the geometry of the FE model (Table 4).

Kazemi et al. (2011) used a MRI scan of a healthy 26-year-old male to construct an FE model to understand the differences in creep behaviour of intact knee joints that have undergone meniscectomies. Subsequent research by *Kazemi & Li (2014)* similarly used an MRI of a healthy 27-year-old male, and modelled structures with the same modelling theories as *Kazemi et al. (2011)*, although marginally adapted these material property inputs in order to understand the poroelastic response of soft tissues in the knee joint under large compression forces. Original data collection for material properties used within both studies was derived from bovine humeral head cartilage (*Langelier & Buschmann, 1999*; *Woo, Akeson & Jemmott, 1976*) and human tibial plateau (29–45 years old) along with human menisci (*Tissakht & Ahmed, 1995*). However ligament material properties, specifically toe region fibril data, were based on previous studies of the human patella tendon aged 29–93 years old (*Hansen et al., 2006*; *Johnson et al., 1994*) and human calcaneal (Achilles) tendon aged 57–93 years old (*Louis-Ugbo, Leeson & Hutton, 2004*). The non-fibril ligament material properties can be traced back to a theoretical modelling paper (*Ault & Hoffman, 1992a*), whose results are represented in a companion paper with experimental work carried out on a rat tail tendon (*Ault & Hoffman, 1992b*). Ligament initial strains used within *Kazemi & Li (2014)* can be traced back to *Peña et al. (2006)* which as discussed previously are originally sourced from human specimens aged 43–74 years old (*Blankevoort, Huiskes & De Lange, 1988*), 53–98 years old (*Race & Amis, 1994*), or ages are described as 'young' (*Butler, Kay & Stouffer, 1986*) or unspecified (*Brantigan & Voshell, 1941*) (Table 4).

Simplified FE models of the healthy human knee joint

For computational simplicity FE models of a human knee joint often make adjustments to their model including representing ligaments as non-linear one dimensional springs (*Li, Lopez & Rubash, 2001*; *Blankevoort & Huiskes, 1991*; *Blankevoort et al., 1991*; *Li et al., 1999*; *Donlagic et al., 2008*), bones as rigid bodies lacking material properties (*Li, Lopez & Rubash, 2001*; *Li et al., 1999*; *Bendjaballah, Shirazi-Adl & Zukor, 1995*; *Jilani, Shirazi-Adl & Bendjaballah, 1997*; *Shirazi, Shirazi-Adl & Hurtig, 2008*) or exclusion of particular structures such as the menisci (*Blankevoort & Huiskes, 1991*; *Blankevoort et al., 1991*) or ligaments (*Guess et al., 2010*; *Donahue et al., 2002*, *2003*).

Models that have been highly simplified but still integrate all the main structures of the knee joint include studies by *Blankevoort et al. (1991)* and *Blankevoort & Huiskes (1991)* who created mathematical models of the knee joint, developed originally by *Wismans et al. (1980)*, specifically focusing on the articular contact and interaction between ligaments and bones. Utilising the previously developed modelling theories (*Blankevoort & Huiskes, 1991*; *Blankevoort et al., 1991*). *Li et al. (1999)* and *Li, Lopez & Rubash (2001)* used a MRI of a 65-year-old male cadaver to create a 3D model of the knee joint and conducted a sensitivity analysis varying input parameters to assess the effect on joint contact stresses. In continuation, *Yang et al. (2010)* also utilised the work proposed by *Blankevoort et al. (1991)* and *Blankevoort & Huiskes (1991)* to define MRI scans from three young volunteers

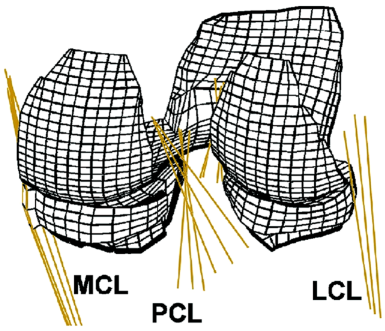

Figure 6 Human knee finite element mesh. Posterior view of a finite element mesh showing soft tissues (menisci and articular cartilage layers). Ligaments are modelled as one dimensional line elements. Rigid bodies representing the femur and the tibia are not shown. (Adapted from *Shirazi, Shirazi-Adl & Hurtig (2008)*: Elsevier License Number: 4226550481987). Full-size DOI: 10.7717/peerj.4298/fig-6

(21–23 years old) to determine cartilage contact stress during gait; however, noticeable differences between studies include the representation of the menisci within *Yang et al. (2010)*.

Within these corresponding studies ligaments were modelled as 'bars,' which are one-dimension (1D) non-linear tension-only elements with just two nodes, although material properties are still assigned. It should also be noted that *Li, Lopez & Rubash (2001)* stated that ligament stiffness was optimised for the model to ensure numerical stability and model convergence rather than utilising a value measured experimentally. *Blankevoort et al. (1991)*, *Blankevoort & Huiskes (1991)*, *Yang et al. (2010)*, *Li et al. (1999)* and *Li, Lopez & Rubash (2001)* sourced ligament material properties from human ACL, PCL and LCL samples aged 'young' (*Butler, Kay & Stouffer, 1986*) or aged 43–74 years old (*Blankevoort, Huiskes & De Lange, 1988*). Unfortunately, cartilage material properties were ambiguous due to multiple references available in the cited sources (*Kempson, 1980*; *Mow, Lai & Holmes, 1982*) making the origin of the input data unclear. Additionally, the menisci were modelled within *Yang et al. (2010)*; however, the original data collection reference could not be traced. Referencing information from these FE studies are summarised in Table 4.

In addition to simplifying anatomical geometry it is also common for investigators to reuse medical image data sets to create different models. In sequential studies CT data of a 27-year-old female was used to construct a FE model of the human knee joint to explore contact pressures (*Bendjaballah, Shirazi-Adl & Zukor, 1995*), varus and valgus alignment (*Bendjaballah, Shirazi-Adl & Zukor, 1997*), axial rotation (*Jilani, Shirazi-Adl & Bendjaballah, 1997*), anterior–posterior forces (*Bendjaballah, Shirazi-Adl & Zukor, 1998*), ACL and PCL coupling (*Moglo & Shirazi-Adl, 2003*) and cartilage collagen fibril response to compression (*Shirazi, Shirazi-Adl & Hurtig, 2008*). Figure 6 illustrates the model created within these studies and highlights the differences in comparison to Fig. 5 in mesh generation and inclusion of all structures in 3D form. When tracing the material properties assigned to structures within these corresponding FE models cartilage primary data was ascertained from human tibial plateau samples aged 48–70 years old (*Hayes &*

Mockros, 1971), ligaments from human ACL, PCL and LCL samples, referenced with ages of 53–98 years old (*Race & Amis, 1994*), or from samples described as 'young' (*Butler, Kay & Stouffer, 1986*). Menisci material properties were based on human meniscal samples aged 29–45 years old (*Tissakht & Ahmed, 1995*) alongside additional data which could not be traced (Table 4).

Another simplified FE model was developed by *Beillas et al. (2004)* who modelled the whole lower limb of a 30-year-old male and coordinated this with in vivo kinematics of a one-leg hop. However, this model was simplified with a 1D representation of the ligaments. Bone material properties were originally obtained from proximal femur and mid femur human samples aged either 28–91 years old (*Lotz, Gerhart & Hayes, 1991*), or age was unspecified (*Reilly & Burstein, 1975*), or bovine samples were used (*Mente & Lewis, 1994*). Cartilage material properties can be traced to human tibial plateau samples although age was not specified (*Repo & Finlay, 1977*) and some further cartilage information was untraceable. Menisci data also came from human samples although again age was not specified (*Fithian, Kelly & Mow, 1990*). Finally, ligament material properties were based on human ACL, PCL, MCL and LCL data obtained from donors aged 16–86 years old (*Noyes & Grood, 1976*), 29–55 years old (*Trent, Walker & Wolf, 1976*), and 22–97 years old (*Woo et al., 1991*) (Table 4).

Incorporating some of the material properties presented by *Beillas et al. (2004)*, *Donlagic et al. (2008)* utilised a patient specific approach to derive geometry and loads for their FE model using an MRI of a 22- and 52-year-old male alongside primary kinematic data of flexion and extension locomotion. However, additional material property sources were also used for the representation of the cartilage including bovine and porcine femoral condyle and tibial plateau samples (*Laasanen, 2003*) (Table 4).

FE models of OA human knee joints

It was discussed previously (Section A—Material Properties, above) that changes in tissues structure during OA progression can result in changes in material properties. This in turn would correlate with a change in the response to loads and biomechanics of the whole knee joint. With this in mind, FE modelling has the potential to analyse such alterations in the presence of OA, assuming that tissue material properties representative of diseased tissues are incorporated into models. Although some FE studies have attempted to investigate contact stresses to understand how OA can initiate and progress (*Peña et al., 2007b*; *Dong et al., 2011*; *Mononen et al., 2011*, *2012*, *2016*; *Venäläinen et al., 2016*) or how arthroplasty procedures can affect the knee joint (*Baldwin et al., 2012*; *Tuncer et al., 2013*) there is only a handful of research papers that utilise a whole knee joint FE model based specifically on healthy versus OA material properties.

One of the first studies to attempt this examined how osteochondral defects influence the ongoing degeneration and stress concentrations of cartilage in the knee joint during compression based on the geometry and anatomical location of the defect (*Peña et al., 2007b*). Healthy material properties were identical to *Peña et al. (2006)* described in detail above and therefore included human and canine tissue. However, when modelling cartilage with defects the elastic modulus of the cartilage was adjusted to 1.5 MPa with data originally

sourced from *Athanasiou et al. (1995)* who explored the elastic modulus of rabbit cartilage with artificially induced OA. A similar study by *Dong et al. (2011)* also explored the cartilage defects but kept the elastic modulus consistent for both healthy and OA simulations.

Although not modelling a whole knee, consecutive studies by *Mononen et al. (2011, 2012)* segmented the femoral and tibial cartilage from 29- and 61-year-old healthy males for FE analysis modelling the cartilage with fibril-reinforced poroviscoelastic properties. *Mononen et al. (2011)* compared normal, OA and repaired cartilage giving a strain dependent fibril network modulus of 673, 168 and 7–505 MPa respectively; an initial fibril network modulus of 0.47, 0.47 and 0.005–0.35 MPa respectively; an elastic modulus of 0.31, 0.08 and 0.31 MPa respectively; and finally a Poisson's ratio of 0.42 for all samples. *Mononen et al. (2012)* compared only normal and OA samples with the same material properties. When following the referencing chain and tracing cartilage material properties back to their original research they used input data from bovine articular cartilage (*DiSilvestro & Suh, 2001*; *Korhonen et al., 2003*) where OA was artificially induced (*Korhonen et al., 2003*).

DISCUSSION

Material properties

There is considerable variation in the elastic modulus of articular cartilage obtained from the human knee joint within the literature. This can be at least attributed to differences in testing parameters and structure and quality of the tissue sample, in addition to known and ambiguous variation in donor characteristics. To summarise, samples within the literature include hydrated (*Wilusz, Zauscher & Guilak, 2013*; *Kleemann et al., 2005*; *Hori & Mockros, 1976*; *Franz et al., 2001*; *Wang et al., 2013*; *Shepherd & Seedhom, 1997*, *1999a*) and dehydrated (*Wen et al., 2012*) femoral and tibial localities and ages between 32 and 89 years old. Furthermore OA samples have been graded using the Collins (*Collins, 1939*, *1949* cited in *Wilusz, Zauscher & Guilak (2013)*), Bollet (*Bollet, Handy & Sturgill, 1963* cited in *Hori & Mockros (1976)*) and Outerbridge (*Outerbridge, 1961*) scoring systems, creating inconsistencies in categorisation. Both confined and unconfined compression testing has been employed (*Kleemann et al., 2005*; *Hori & Mockros, 1976*; *Thambyah, Nather & Goh, 2006*) alongside indentation techniques (*Franz et al., 2001*; *Shepherd & Seedhom, 1997*, *1999a*) and AFM (*Wen et al., 2012*; *Wilusz, Zauscher & Guilak, 2013*; *Wang et al., 2013*). Research also incorporates extensive ranges in testing specifications including indentation tip radius (10–30.4 mm) (*Hori & Mockros, 1976*; *Wen et al., 2012*; *Franz et al., 2001*; *Shepherd & Seedhom, 1997*, *1999a*; *Thambyah, Nather & Goh, 2006*; *Wilusz, Zauscher & Guilak, 2013*; *Wang et al., 2013*), loading force (0.019–11.8 N) (*Kleemann et al., 2005*; *Hori & Mockros, 1976*) and recovery phases if included (5 min) (*Thambyah, Nather & Goh, 2006*).

As discussed in 'Section A—Material Properties,' length scale dependency can affect the values derived from testing. For example, heterogeneity can be more easily identified in cartilage using nanoindentation when compared to microindentation (*Stolz et al., 2009*, *2004*), which is particularly important when changes due to OA can be subtle. When reviewing current efforts at measuring elastic modulus of human knee joint cartilage,

variation will indeed exist due to differing length scales between 10 nm (*Wen et al., 2012*) and 30.4 mm (*Hori & Mockros, 1976*) which may have an effect on obtained modulus. Moreover, studies also present varying elastic modulus, namely instantaneous (*Franz et al., 2001*; *Hori & Mockros, 1976*; *Shepherd & Seedhom, 1997*; *Shepherd & Seedhom, 1999a*; *Thambyah, Nather & Goh, 2006*; *Wilusz, Zauscher & Guilak, 2013*) and equilibrium modulus with some citing a 30 s (*Wen et al., 2012*) to 10 min (*Kleemann et al., 2005*) hold period. The circumstances under which tissues are measured will influence the results, and therefore the ability to compare across studies and accurately apply such data in FE models. It has previously been shown that there are considerable differences in instantaneous and equilibrium modulus, where instantaneous produces a much higher value (*Julkunen et al., 2009*), highlighting the need for a more standardised method of testing to determine any subtle change in material properties during healthy ageing and OA that may not be comparable across multiple data sources.

With these variations in mind elastic modulus for hydrated healthy cartilage samples varies between 0.1and 18.6 MPa (*Wilusz, Zauscher & Guilak, 2013*; *Thambyah, Nather & Goh, 2006*; *Brittberg & Peterson, 1998*; *Bae et al., 2003*; *Shepherd & Seedhom, 1997*, *1999a*), hydrated OA grade 1 samples range between 0.5 and 10.2 MPa (*Kleemann et al., 2005*; *Hori & Mockros, 1976*; *Franz et al., 2001*; *Wang et al., 2013*) and hydrated OA grade 2 and 3 between 0.1 and 0.5 MPa (*Wilusz, Zauscher & Guilak, 2013*; *Kleemann et al., 2005*; *Wang et al., 2013*), noting that different OA grading systems are used across these studies. Furthermore, age ranges stated within the literature have a wide variation, the broadest being 33–80 years old within one study (*Shepherd & Seedhom, 1999a*). Some values cannot be explicitly linked to age ranges. Future work is required to more definitely define changes in cartilage material properties associated to explicitly with age and therefore help understand how alterations through disease can be separated from alterations during healthy ageing.

In comparison to the available data on human knee joint cartilage, there is significantly less data for femoral or tibial bone samples. Indeed, this research found only one study that quantitatively measured material properties of cortical bone from the human knee joint (*Rho, Tsui & Pharr, 1997*). Data on trabecular properties is present but it is difficult compare data from different anatomical locations collected with different techniques, specifically traditional compression approaches (*Lindahl, 1976*; *Goldstein et al., 1983*; *Burgers et al., 2008*) and more recent nanoindentation methods (*Rho, Tsui & Pharr, 1997*), which is yet to be applied to the human femoral condyle. Similar ambiguity in the relationship between age and material properties also exists. Age ranges vary between 14 and 92 years old across studies with the smallest age cohort (with the exception of individual donors) spanning 20 years in one study (*Goldstein et al., 1983*). Some studies also used donors under the age of 30 where donors may not have reached skeletal maturity and material properties may not reflect peak bone mass (*Matkovic et al., 1994*). Overall, trabecular bone elastic modulus ranges from 1.9 MPa to 664.0 MPa across reviewed studies (*Behrens, Walker & Shoji, 1974*; *Ducheyne et al., 1977*; *Carter & Hayes, 1977*; *Lindahl, 1976*; *Goldstein et al., 1983*; *Hvid & Hansen, 1985*; *Burgers et al., 2008*; *Zysset, Sonny & Hayes, 1994*) and cortical bone from 22,500 MPa to 25,800 MPa (*Rho, Tsui & Pharr, 1997*).

Studies reviewed in 'Section A—Material Properties' mostly involve experimental work on trabecular bone which is less commonly used within FE models. Compression techniques utilised to obtain macroscale measurements of trabecular bone as a whole structure as opposed to measuring individual trabeculae, will inevitably produce lower elastic modulus values due to the nature of testing; however, more sophisticated techniques incorporating tissue level material properties can more accurately represent a structure such as trabecular bone at the level in which it is typically modelled in FE research (*Nigg & Herzog, 2006*). This variability in techniques inevitably makes a comparison between studies challenging as well as the lack of distinct age cohorts to ultimately define young and old parameters in order to definitively link this to a change in properties due to injury or disease, such as OA. Despite some research incorporating material properties of varying OA grades there are no healthy controls included to explicitly link significant findings to OA status (*Zysset, Sonny & Hayes, 1994*). Evidently there is also no material property data for human trabecular bone obtained from the distal femur or proximal tibia at the tissue level, comparing healthy and OA samples.

It should be noted that the studies cited herein utilised varying indenter sizes ranging from 20 nm (*Rho, Tsui & Pharr, 1997*) to 2.5 mm (*Hvid & Hansen, 1985*). A length scale under 200 nm is able to determine more heterogeneity in bone structure than those applied above 200 nm (*Yao et al., 2011*). When comparing studies discussed herein it should be considered that comparisons are challenging, and indeed reiterates the importance of site and subject-specific material properties, preferably obtained at the nanoscale to accurately present the human knee joint using FE modelling (*Yao et al., 2011*).

Likewise, there is also significant variation in ligament tensile properties reported in the literature and this could be attributed to a number of factors including the variation in cadaver cohorts, equipment and testing protocol and technique. Experimental procedures for ligament material properties vary between cross-sectional samples (*Momersteeg et al., 1995*) or bone–ligament–bone samples spanning a variety of age ranges with current data in the literature ranging from 16 to 97 years old (*Harner et al., 1995*; *Quapp & Weiss, 1998*; *Butler et al., 1992*; *Robinson, Bull & Amis, 2005*; *Trent, Walker & Wolf, 1976*; *Noyes & Grood, 1976*; *Butler, Kay & Stouffer, 1986*; *Race & Amis, 1994*; *Woo et al., 1991*; *Chandrashekar et al., 2006*). Preconditioning, which is often included as a 'warm up' for the ligament to achieve load-displacement parameters that are repeatable (*Momersteeg et al., 1995*) is absent from some research studies (*Momersteeg et al., 1995*; *Noyes & Grood, 1976*). Furthermore data varies across individual studies where elastic modulus of the knee ligaments ranges between 1.7 and 447.0 MPa (*Quapp & Weiss, 1998*; *Butler et al., 1992*; *Noyes & Grood, 1976*; *Butler, Kay & Stouffer, 1986*; *Race & Amis, 1994*; *Chandrashekar et al., 2006*) and failure load between 194.0 and 2160.0 N (*Harner et al., 1995*; *Robinson, Bull & Amis, 2005*; *Trent, Walker & Wolf, 1976*; *Noyes & Grood, 1976*; *Race & Amis, 1994*; *Woo et al., 1991*; *Chandrashekar et al., 2006*). Comparisons between young and old have been correlated for the ACL in two studies (*Noyes & Grood, 1976*; *Woo et al., 1991*) both concluding that young donors have a higher stiffness and failure load. However, this is yet to be explored in the PCL, MCL and LCL along with

research into how ligament tensile properties are correlated to pathological existence in the form of OA.

FE modelling

Finite elements models have been used for various applications involving the whole knee joint including healthy representation (*Peña et al., 2006*; *Wang, Fan & Zhang, 2014*), joint replacement mechanics (*Baldwin et al., 2012*; *Tuncer et al., 2013*), meniscectomy research (*Tanska, Mononen & Korhonen, 2015*), cartilage contact stresses (*Li, Lopez & Rubash, 2001*; *Guo, Zhang & Chen, 2009*) and ligament–bone interaction (*Blankevoort et al., 1991*) to name a few. Material properties used within the reviewed FE models are often sourced from the literature including previous modelling studies or primary experimental research. This typically results in highly variable data sets based on multiple structures and species. The material properties of human tissue vary according to its mineral and protein composition and the orientation of its micro-architecture (*Wilusz, Zauscher & Guilak, 2013*; *Marticke et al., 2010*; *Temple-Wong et al., 2009*). These factors in turn vary with anatomical location (e.g. femur vs humerus; knee vs ankle), age and health of the tissue. Therefore, donor characteristics will significantly impact results. It is clear that current whole joint FE models use material properties with highly variable, or non-specific material properties, with variation in the age, species, location and disease state of the tissue from which material properties were obtained.

When the values used for material properties within published FE models are traced to their original research citation it becomes clear that there is considerable variation in terms of age range. FE models produced by *Beillas et al. (2004)* and *Donlagic et al. (2008)* have a total age range across all structures of 16–97 years old. The smallest age range used for material properties within a single study is 43–74 years old (*Li, Lopez & Rubash, 2001*; *Blankevoort & Huiskes, 1991*; *Blankevoort et al., 1991*; *Li et al., 1999*; *Yang et al., 2010*), with other ages ranging between 37 and 74 years old (*Peña et al., 2005*), 33–80 years old (*Mootanah et al., 2014*), 29–93 years old (*Kazemi & Li, 2014*), 29–98 years old (*Kazemi & Li, 2014*; *Bendjaballah, Shirazi-Adl & Zukor, 1995*; *Jilani, Shirazi-Adl & Bendjaballah, 1997*; *Shirazi, Shirazi-Adl & Hurtig, 2008*; *Bendjaballah, Shirazi-Adl & Zukor, 1997*, *1998*; *Moglo & Shirazi-Adl, 2003*) and 25–98 years old (*Wang, Fan & Zhang, 2014*). In many FE modelling studies, some information including age of donors from the original sources of material properties could not be traced (*Peña et al., 2005*, *2006*; *Wang, Fan & Zhang, 2014*; *Li, Lopez & Rubash, 2001*; *Guo, Zhang & Chen, 2009*; *Mootanah et al., 2014*; *Kazemi & Li, 2014*; *Blankevoort & Huiskes, 1991*; *Blankevoort et al., 1991*; *Li et al., 1999*; *Donlagic et al., 2008*; *Bendjaballah, Shirazi-Adl & Zukor, 1995*, *1997*, *1998*; *Jilani, Shirazi-Adl & Bendjaballah, 1997*; *Shirazi, Shirazi-Adl & Hurtig, 2008*; *Yang et al., 2010*; *Moglo & Shirazi-Adl, 2003*; *Beillas et al., 2004*). Where material properties are categorised by age there are considerable differences between cohorts, most noticeably in ligament data (*Noyes & Grood, 1976*; *Woo et al., 1991*). In particular *Woo et al. (1991)* recorded the site of failure in ligaments when loaded in the anatomical location and concluded that in younger donors the ACL will predominantly fail by avulsion and in older donors the ACL will predominantly fail at the mid-substance, due to a change in material properties.

This is especially important to factor into FE models if safety factors in the joint are being researched. The effect of using material properties from broad, and in some cases unknown age ranges, impacts on the conclusions of FE modelling is currently unclear because at present no study has compared these models to one constructed using anatomical geometry and material properties for all tissues from the same individual, or a homogeneous age and gender cohort of individuals. Such a model would clearly represent the 'gold-standard' with respect to geometry and material property definition in a FE knee model.

As well as wide variation in age, some FE models use material property data based just on tibial plateau cartilage (*Kazemi & Li, 2014*; *Donlagic et al., 2008*; *Bendjaballah, Shirazi-Adl & Zukor, 1995*, *1997*, *1998*; *Jilani, Shirazi-Adl & Bendjaballah, 1997*; *Shirazi, Shirazi-Adl & Hurtig, 2008*; *Moglo & Shirazi-Adl, 2003*; *Beillas et al., 2004*) or bone samples lacking any femoral condyle measurements (*Wang, Fan & Zhang, 2014*). Furthermore, they may be based on non-knee joint anatomical locations including femoral neck and mid femur bone material properties (*Donlagic et al., 2008*; *Beillas et al., 2004*) and humeral head for cartilage material properties (*Kazemi et al., 2011*; *Kazemi & Li, 2014*). As an example of the magnitude of disparity in material properties between different anatomical locations, *Shepherd & Seedhom (1999a)* tested the elastic modulus of ankle, knee and hip joint cartilage finding differences of up to 6.8 MPa (36.6%) between ankle and knee cartilage samples from the same donor and 3.6 MPa (30.54%) between knee and hip cartilage samples from the same donor. Indeed, it has been shown that variations in material properties from the same tissue exists within and across the knee joint suggesting that a location dependent modulus for various tissues would be most appropriate for FE models (*Behrens, Walker & Shoji, 1974*; *Deneweth, Arruda & McLean, 2015*; *Akizuki et al., 1986*). Thus, while better than using values from outside the knee joint itself, representing structures with homogeneous (i.e. only one value) properties, or for example, assuming tibial and femoral material properties are identical, may be sub-optimal and functionally important. Ligament material properties are also often replicated where original data is only based on selective ligaments of the knee joint (*Wang, Fan & Zhang, 2014*; *Li, Lopez & Rubash, 2001*; *Kazemi & Li, 2014*; *Blankevoort & Huiskes, 1991*; *Blankevoort et al., 1991*; *Li et al., 1999*; *Bendjaballah, Shirazi-Adl & Zukor, 1995*, *1997*, *1998*; *Jilani, Shirazi-Adl & Bendjaballah, 1997*; *Shirazi, Shirazi-Adl & Hurtig, 2008*; *Yang et al., 2010*; *Moglo & Shirazi-Adl, 2003*). In some instances tendon data is used for the representation of ligament material properties including the quadriceps tendon (*Wang, Fan & Zhang, 2014*), patella tendon (*Wang, Fan & Zhang, 2014*; *Kazemi et al., 2011*; *Kazemi & Li, 2014*), Achilles tendon (*Kazemi et al., 2011*; *Kazemi & Li, 2014*) and rodent tail tendon (*Kazemi et al., 2011*; *Kazemi & Li, 2014*).

Animal material property data is also commonly used in the representation of human knee FE models including bovine (*Wang, Fan & Zhang, 2014*; *Mootanah et al., 2014*; *Shepherd & Seedhom, 1999b*; *Kazemi & Li, 2014*; *Donlagic et al., 2008*; *Beillas et al., 2004*; *Mononen et al., 2011*, *2012*), canine (*Peña et al., 2005*, *2006*; *Guo, Zhang & Chen, 2009*), porcine (*Donlagic et al., 2008*), rat (*Kazemi et al., 2011*; *Kazemi & Li, 2014*) and rabbit (*Peña et al., 2007b*) data. A number of recent studies have highlighted the structural,

mechanical and physiological differences between bovine and human soft tissue and questioned the suitability of bovine material property data for functional studies of humans (*Demarteau et al., 2006*; *Jeffrey & Aspden, 2006*; *Nissi et al., 2007*; *Pedersen et al., 2013*; *Plumb & Aspden, 2005*). *Athanasiou et al. (1991)* explored the differences between material properties of cartilage from the femoral condyle of different species and found variation between the Poisson's ratio of human (0.074–0.098), canine (0.3–0.372), bovine (0.383–0.396) and rabbit (0.197–0.337) along with aggregate modulus of human (0.588–0.701 MPa), canine (0.603–0.904 MPa), bovine (0.894–0.899 MPa) and rabbit (0.537–0.741 MPa). Although differences were not statistically significant, potentially due to low samples numbers ($n = 4$–10) there was evidently a difference between species all of which have been used in some of the reviewed FE models. Further, it has also been shown that not only do material properties vary by species but they vary spatially within the same joint. For example, *Peters et al. (2017)* found differences of up to 10.5 MPa in elastic modulus of cartilage samples taken from different locations within a single canine knee joint. This can indeed have an effect on subsequent FE model behaviour predictions and should be taken into consideration where possible in future studies.

As discussed earlier, it is very common for FE modelling studies to source and reference their material property data from previous modelling studies rather than the original experimental studies in which practical measurements were obtained. However, when the referencing chain is followed through sequentially cited modelling papers it is often the case that the primary experimental source of material property data is untraceable (*Yang et al., 2010*; *Peña et al., 2006*). In other instances it eventually becomes clear that material property values are not source for direct experimental measures, but have been derived directly or indirectly from theoretical research in which mathematical solutions for modelling a specific structure have been derived (*Mak, Lai & Mow, 1987* cited in *Peña et al. (2005*, *2006)*, *Li, Lopez & Rubash (2001)*, *Guo, Zhang & Chen (2009)*).

Use of varying ages, species and anatomical locations for material property information undoubtedly represent important limitations in current FE models, but the magnitude of error is presently difficult to quantify and probably varies widely across studies due to the highly 'mixed' nature of input data used. At present, the best indication of error comes from studies that have conducted sensitivity analyses on material properties. *Li, Lopez & Rubash (2001)* conducted a sensitivity analysis varying cartilage elastic modulus from 3.5 MPa to 10 MPa and showed that peak contact stresses linearly increased by up to 10%, whilst an increase in Poisson's ratio significantly varied peak von Mises stress by 100% in the knee joint cartilage. Additionally, a more sophisticated sensitivity analysis was carried out by *Dhaher, Kwon & Barry (2010)* who adjusted the intrinsic material properties of knee joint ligaments to aid understanding of the functional consequences of different activity levels, age, gender and even species. The research measured simulation outcomes by incorporating a multi-factorial global assessment, which indicated a change in tibial–femoral internal and external rotation, patella tilt and patella peak contact stresses, associated with modified ligament material properties (*Dhaher, Kwon & Barry, 2010*).

This review of published material property (Section A—Material Properties) and FE modelling (Section B: FE Modelling, above) studies of the human knee raises the question

of how well specific cohorts or even human demographics can currently be accurately represented in a FE model. For example, does sufficient material property data exist to construct a whole-knee joint FE model representative of a young, healthy human or to represent a knee of any age with a specific category of OA? Attempting to build an FE model of a healthy knee joint from the literature data tabulated in 'Section A—Material Properties' (Tables 1–3) yields data for healthy femoral and tibial cartilage, although without the breakdown of age specific material properties; healthy tibial cortical bone from older donors; healthy ACL, PCL, MCL and LCL from young donors, and ACL, PCL and MCL from healthy older donors. Thus, 'healthy' material properties can be pieced together from different studies for most tissues but mixing gender and a considerable age range (16–97 years old) is necessary. In terms of a model for studying OA, data exists for cartilage material properties based on OA grades 1–3 although this is not broken down into age categories, whilst trabecular bone material properties do exist for OA grades 1–3 for older donors although challenges occur as no healthy control was used within this particular study as a baseline measurement. Further no study has yet explored the effect of OA on cortical bone material properties in the human knee. There is currently no data incorporating the effect of OA on ligament material properties despite it being well known that there is a relationship between OA and ligament injury (*Mullaji et al., 2008*; *Cushner et al., 2003*). However, there are currently no research papers to the authors' knowledge that have collected primary data on bone and cartilage material properties and used these measurements to build a subject specific FE model. Hence, material properties are still collated from various sources within the literature. A key goal for future research should be adoption of a more subject specific approach in which material properties from all tissues are derived from homogenous donor cohorts to improve accuracy and precision of knee FE models.

CONCLUSIONS AND FUTURE DIRECTIONS

Integrating tissues-specific material property data into FE models has the potential to provide considerable insight into both healthy and diseased knee joint mechanics, circumventing the difficulty of direct invasive measures of human functionality. Herein, we have provided a comprehensive summation and evaluation of existing material property data for human knee joint tissues with all numerical values tabulated as a reference resource for future studies. A renaissance in material testing and engineering approaches in the last decade has yielded an abundance of data on the mechanical properties of both hard and soft tissues from the human knee joint. However, comparison of material properties between studies can be challenging due to the differences in cadaver age, data collection techniques, including orientation of the tissue and loading specifics (*Chandrashekar et al., 2006*). It is well documented that material properties alter during ageing (*Hansen, Masouros & Amis, 2006*), therefore the demographics of cadavers will highly influence material property data. Our review highlights that material properties from multiple (>1) tissue types have rarely been collected from cadavers with homogeneous age, gender and health status characteristics. More consistent data collection with particular emphasis on extracting data on multiple tissues from the same

donors will enable a much more robust examination of the structural and mechanical changes occurring during ageing, injury and disease, notably during OA progression which currently represents a significant socio-economic burden that is likely to increase further within ageing populations.

The benefits of a more exhaustive subject- or cohort-specific approach to materials testing will inherently feed directly into improved FE models of whole-knee function. Efforts have been made to produce an openly available FE model for clinical and basic science research (*Erdemir, 2016*). With more accurate material property data from cohort specific sources data could be applied into this freely available model without the need to obtain medical imagery to create a new FE model which is costly in time and resources. More demographically homogenous material property data sets will eliminate the current widespread use of material properties sourced from distinctively diverse human cadavers and/or animal specimens. Embracing this more systematic subject- or cohort-specific approach to FE modelling can only improve comparisons between injured and diseased tissue within the knee joint, and enhance understanding of behavioural response to mechanical loads observed during ageing or disease progression. It is notable at present that no FE modelling study has compared healthy and OA whole-knee joints. Increasing ageing populations within western societies provide particular incentive for this research with a clear need to direct research efforts into better integration of mechanical engineering approaches and biomechanical simulation, particularly in the presence of disease status.

ADDITIONAL INFORMATION AND DECLARATIONS

Funding

The research is funded by BBSRC, grant number BB/J014516/1, and the School of Engineering, University of Liverpool. The funders had no role in study design, data collection and analysis, decision to publish, or preparation of the manuscript.

Grant Disclosures

The following grant information was disclosed by the authors:
BBSRC: BB/J014516/1.
School of Engineering, University of Liverpool.

Competing Interests

The authors declare that they have no competing interests.

Author Contributions

- Abby E. Peters conceived and designed the experiments, performed the experiments, analysed the data, contributed reagents/materials/analysis tools, wrote the paper, prepared figures and/or tables, reviewed drafts of the paper.
- Riaz Akhtar conceived and designed the experiments, reviewed drafts of the paper.
- Eithne J. Comerford conceived and designed the experiments, reviewed drafts of the paper.
- Karl T. Bates conceived and designed the experiments, reviewed drafts of the paper.

Data Availability

The following information was supplied regarding data availability:

The research in this article did not generate data or code as this is a literature review.

REFERENCES

Ahlback S. 1968. Osteoarthrosis of the knee. A radiographic investigation. *Acta Radiologica: Diagnosis* **277**:7–72.

Akizuki S, Mow VC, Müller F, Pita JC, Howell DS, Manicourt DH. 1986. Tensile properties of human knee joint cartilage: I. Influence of ionic conditions, weight bearing, and fibrillation on the tensile modulus. *Journal of Orthopaedic Research* **4(4)**:379–392 DOI 10.1002/jor.1100040401.

Anderson AF, Dome DC, Gautam S, Awh MH, Rennirt GW. 2001. Correlation of anthropometric measurements, strength, anterior cruciate ligament size, and intercondylar notch characteristics to sex differences in anterior cruciate ligament tear rates. *American Journal of Sports Medicine* **29(1)**:58–66 DOI 10.1177/03635465010290011501.

Armstrong CG, Mow VC. 1982. Variations in the intrinsic mechanical properties of human articular cartilage with age, degeneration, and water content. *Journal of Bone and Joint Surgery* **64(1)**:88–94 DOI 10.2106/00004623-198264010-00013.

Athanasiou K, Fischer R, Niederauer G, Puhl W. 1995. Effects of excimer laser on healing of articular cartilage in rabbits. *Journal of Orthopaedic Research* **13(4)**:483–494 DOI 10.1002/jor.1100130403.

Athanasiou K, Rosenwasser M, Buckwalter J, Malinin T, Mow V. 1991. Interspecies comparisons of in situ intrinsic mechanical properties of distal femoral cartilage. *Journal of Orthopaedic Research* **9(3)**:330–340 DOI 10.1002/jor.1100090304.

Ault H, Hoffman A. 1992a. A composite micromechanical model for connective tissues: part II—application to rat tail tendon and joint capsule. *Journal of Biomechanical Engineering* **114(1)**:142–146 DOI 10.1115/1.2895438.

Ault H, Hoffman A. 1992b. A composite micromechanical model for connective tissues: part I—theory. *Journal of Biomechanical Engineering* **114(1)**:137–141 DOI 10.1115/1.2895437.

Bae WC, Temple MM, Amiel D, Coutts RD, Niederauer GG, Sah RL. 2003. Indentation testing of human cartilage: sensitivity to articular surface degeneration. *Arthritis & Rheumatism* **48(12)**:3382–3394 DOI 10.1002/art.11347.

Baldwin MA, Clary CW, Fitzpatrick CK, Deacy JS, Maletsky LP, Rullkoetter PJ. 2012. Dynamic finite element knee simulation for evaluation of knee replacement mechanics. *Journal of Biomechanics* **45(3)**:474–483 DOI 10.1016/j.jbiomech.2011.11.052.

Behrens J, Walker P, Shoji H. 1974. Variations in strength and structure of cancellous bone at the knee. *Journal of Biomechanics* **7(3)**:201–207 DOI 10.1016/0021-9290(74)90010-4.

Beillas P, Papaioannou G, Tashman S, Yang K. 2004. A new method to investigate in vivo knee behavior using a finite element model of the lower limb. *Journal of Biomechanics* **37(7)**:1019–1030 DOI 10.1016/s0021-9290(03)00435-4.

Bendjaballah MZ, Shirazi-Adl A, Zukor D. 1995. Biomechanics of the human knee joint in compression: reconstruction, mesh generation and finite element analysis. *Knee* **2(2)**:69–79 DOI 10.1016/0968-0160(95)00018-k.

Bendjaballah M, Shirazi-Adl A, Zukor D. 1997. Finite element analysis of human knee joint in varus-valgus. *Clinical Biomechanics* **12(3)**:139–148 DOI 10.1016/s0268-0033(97)00072-7.

Bendjaballah M, Shirazi-Adl A, Zukor D. 1998. Biomechanical response of the passive human knee joint under anterior–posterior forces. *Clinical Biomechanics* **13(8)**:625–633 DOI 10.1016/s0268-0033(98)00035-7.

Blankevoort L, Huiskes R. 1991. Ligament-bone interaction in a three-dimensional model of the knee. *Journal of Biomechanical Engineering* **113(3)**:263–269 DOI 10.1115/1.2894883.

Blankevoort L, Kuiper J, Huiskes R, Grootenboer H. 1991. Articular contact in a three-dimensional model of the knee. *Journal of Biomechanics* **24(11)**:1019–1031 DOI 10.1016/0021-9290(91)90019-j.

Blankevoort L, Huiskes R, De Lange A. 1988. The envelope of passive knee joint motion. *Journal of Biomechanics* **21(9)**:705–709, 711–720 DOI 10.1016/0021-9290(88)90280-1.

Bobinac D, Spanjol J, Zoricic S, Maric I. 2003. Changes in articular cartilage and subchondral bone histomorphometry in osteoarthritic knee joints in humans. *Bone* **32(3)**:284–290 DOI 10.1016/s8756-3282(02)00982-1.

Bollet AJ, Handy JR, Sturgill BC. 1963. Chondroitin sulfate concentration and protein-polysaccharide composition of articular cartilage in osteoarthritis. *Journal of Clinical Investigation* **42(6)**:853–859 DOI 10.1172/jci104777.

Bonner TJ, Newell N, Karunaratne A, Pullen AD, Amis AA, Bull AM, Masouros SD. 2015. Strain-rate sensitivity of the lateral collateral ligament of the knee. *Journal of the Mechanical Behavior of Biomedical Materials* **41**:261–270.

Brach JS, Berlin JE, VanSwearingen JM, Newman AB, Studenski SA. 2005. Too much or too little step width variability is associated with a fall history in older persons who walk at or near normal gait speed. *Journal of Neuroengineering and Rehabilitation* **2(1)**:1.

Brantigan OC, Voshell AF. 1941. The mechanics of the ligaments and menisci of the knee joint. *Journal of Bone and Joint Surgery* **23(1)**:44–66.

Brittberg M, Peterson L. 1998. Introduction of an articular cartilage classification. *ICRS Newsletter* **1(1)**:5–8.

Buckwalter JA, Martin AM. 2006. Osteoarthritis. *Advanced Drug Delivery Reviews* **58**:150–167.

Burgers TA, Mason J, Niebur G, Ploeg HL. 2008. Compressive properties of trabecular bone in the distal femur. *Journal of Biomechanics* **41(5)**:1077–1085 DOI 10.1016/j.jbiomech.2007.11.018.

Burr DB. 1998. The importance of subchondral bone in osteoarthrosis. *Current Opinion in Rheumatology* **10(3)**:256–262 DOI 10.1097/00002281-199805000-00017.

Butler DL, Guan Y, Kay MD, Cummings JF, Feder SM, Levy MS. 1992. Location-dependent variations in the material properties of the anterior cruciate ligament. *Journal of Biomechanics* **25(5)**:511–518 DOI 10.1016/0021-9290(92)90091-e.

Butler DL, Kay MD, Stouffer DC. 1986. Comparison of material properties in fascicle-bone units from human patellar tendon and knee ligaments. *Journal of Biomechanics* **19(6)**:425–432 DOI 10.1016/0021-9290(86)90019-9.

Butler D, Sheh M, Stouffer D, Samaranayake V, Levy MS. 1990. Surface strain variation in human patellar tendon and knee cruciate ligaments. *Journal of Biomechanical Engineering* **112(1)**:38–45 DOI 10.1115/1.2891124.

Carter DR, Hayes WC. 1977. The compressive behavior of bone as a two-phase porous structure. *Journal of Bone and Joint Surgery* **59(7)**:954–962 DOI 10.2106/00004623-197759070-00021.

Chandrashekar N, Mansouri H, Slauterbeck J, Hashemi J. 2006. Sex-based differences in the tensile properties of the human anterior cruciate ligament. *Journal of Biomechanics* **39(16)**:2943–2950 DOI 10.1016/j.jbiomech.2005.10.031.

Chandrashekar N, Slauterbeck J, Hashemi J. 2005. Sex-based differences in the anthropometric characteristics of the anterior cruciate ligament and its relation to intercondylar notch geometry: a cadaveric study. *American Journal of Sports Medicine* **33(10)**:1492–1498 DOI 10.1177/0363546504274149.

Collins DH. 1939. The pathology of osteoarthritis. *British Journal of Rheumatology* **1(248)**:e62.

Collins DH. 1949. *The Pathology of Articular and Spinal Diseases.* London: Edward Arnold.

Cushner FD, La Rosa DF, Vigorita VJ, Scuderi GR, Scott WN, Insall JN. 2003. A quantitative histologic comparison: ACL degeneration in the osteoarthritic knee. *Journal of Arthroplasty* **18(6)**:687–692 DOI 10.1016/s0883-5403(03)00256-0.

Dabiri Y, Li L. 2013. Influences of the depth-dependent material inhomogeneity of articular cartilage on the fluid pressurization in the human knee. *Medical Engineering & Physics* **35(11)**:1591–1598 DOI 10.1016/j.medengphy.2013.05.005.

Demarteau O, Pillet L, Inaebnit A, Borens O, Quinn T. 2006. Biomechanical characterization and in vitro mechanical injury of elderly human femoral head cartilage: comparison to adult bovine humeral head cartilage. *Osteoarthritis and Cartilage* **14(6)**:589–596 DOI 10.1016/j.joca.2005.12.011.

Deneweth JM, Arruda EM, McLean SG. 2015. Hyperelastic modeling of location-dependent human distal femoral cartilage mechanics. *International Journal of Non-Linear Mechanics* **68**:146–156 DOI 10.1016/j.ijnonlinmec.2014.06.013.

Desrochers J, Amrein MA, Matyas JR. 2010. Structural and functional changes of the articular surface in a post-traumatic model of early osteoarthritis measured by atomic force microscopy. *Journal of Biomechanics* **43(16)**:3091–3098 DOI 10.1016/j.jbiomech.2010.08.009.

Dhaher YY, Kwon T, Barry M. 2010. The effect of connective tissue material uncertainties on knee joint mechanics under isolated loading conditions. *Journal of Biomechanics* **43(16)**:3118–3125 DOI 10.1016/j.jbiomech.2010.08.005.

DiSilvestro MR, Suh JF. 2001. A cross-validation of the biphasic poroviscoelastic model of articular cartilage in unconfined compression, indentation, and confined compression. *Journal of Biomechanics* **34(4)**:519–525 DOI 10.1016/s0021-9290(00)00224-4.

Donahue TLH, Hull M, Rashid MM, Jacobs CR. 2002. A finite element model of the human knee joint for the study of tibio-femoral contact. *Journal of Biomechanical Engineering* **124(3)**:273–280 DOI 10.1115/1.1470171.

Donahue TLH, Hull M, Rashid MM, Jacobs CR. 2003. How the stiffness of meniscal attachments and meniscal material properties affect tibio-femoral contact pressure computed using a validated finite element model of the human knee joint. *Journal of Biomechanics* **36(1)**:19–34 DOI 10.1016/s0021-9290(02)00305-6.

Dong Y, Hu G, Zhang L, Hu Y, Dong Y, Xu Q. 2011. Accurate 3D reconstruction of subject-specific knee finite element model to simulate the articular cartilage defects. *Journal of Shanghai Jiaotong University (Science)* **16(5)**:620–627 DOI 10.1007/s12204-011-1199-z.

Donlagic D, Cigale B, Heric D, Cibula E, Zazula D, Potocnik B. 2008. A patient-specific knee joint computer model using MRI data and 'in vivo' compressive load from the optical force measuring system. *Journal of Computing and Information Technology* **16(3)**:209–222 DOI 10.2498/cit.1001126.

Ducheyne P, Heymans L, Martens M, Aernoudt E, de Meester P, Mulier JC. 1977. The mechanical behaviour of intracondylar cancellous bone of the femur at different loading rates. *Journal of Biomechanics* **10(11–12)**:747–762 DOI 10.1016/0021-9290(77)90089-6.

Elias JJ, Cosgarea AJ. 2007. Computational modeling: an alternative approach for investigating patellofemoral mechanics. *Sports Medicine and Arthroscopy Review* **15(2)**:89–94 DOI 10.1097/jsa.0b013e31804bbe4d.

Erdemir A. 2016. Open knee: open source modeling and simulation in knee biomechanics. *Journal of Knee Surgery* **29(2)**:107–116 DOI 10.1055/s-0035-1564600.

Fithian DC, Kelly MA, Mow VC. 1990. Material properties and structure–function relationships in the menisci. *Clinical Orthopaedics and Related Research* **252**:19–31 DOI 10.1097/00003086-199003000-00004.

Franz T, Hasler E, Hagg R, Weiler C, Jakob R, Mainil-Varlet P. 2001. In situ compressive stiffness, biochemical composition, and structural integrity of articular cartilage of the human knee joint. *Osteoarthritis and Cartilage* **9(6)**:582–592 DOI 10.1053/joca.2001.0418.

Freutel M, Schmidt H, Dürselen L, Ignatius A, Galbusera F. 2014. Finite element modeling of soft tissues: material models, tissue interaction and challenges. *Clinical Biomechanics* **29(4)**:363–372 DOI 10.1016/j.clinbiomech.2014.01.006.

Gardiner JC, Weiss JA. 2003. Subject-specific finite element analysis of the human medial collateral ligament during valgus knee loading. *Journal of Orthopaedic Research* **21(6)**:1098–1106 DOI 10.1016/s0736-0266(03)00113-x.

Goldstein SA, Wilson DL, Sonstegard DA, Matthews LS. 1983. The mechanical properties of human tibial trabecular bone as a function of metaphyseal location. *Journal of Biomechanics* **16(12)**:965–969 DOI 10.1016/0021-9290(83)90097-0.

Guess TM, Thiagarajan G, Kia M, Mishra M. 2010. A subject specific multibody model of the knee with menisci. *Medical Engineering & Physics* **32(5)**:505–515 DOI 10.1016/j.medengphy.2010.02.020.

Guo H, Maher SA, Spilker RL. 2013. Biphasic finite element contact analysis of the knee joint using an augmented Lagrangian method. *Medical Engineering & Physics* **35(9)**:1313–1320 DOI 10.1016/j.medengphy.2013.02.003.

Guo Y, Zhang X, Chen W. 2009. Three-dimensional finite element simulation of total knee joint in gait cycle. *Acta Mechanica Solida Sinica* **22(4)**:347–351 DOI 10.1016/s0894-9166(09)60283-4.

Halonen KS, Mononen ME, Jurvelin JS, Töyräs J, Korhonen RK. 2013. Importance of depth-wise distribution of collagen and proteoglycans in articular cartilage—a 3D finite element study of stresses and strains in human knee joint. *Journal of Biomechanics* **46(6)**:1184–1192 DOI 10.1016/j.jbiomech.2012.12.025.

Hansen U, Masouros S, Amis AA. 2006. (iii) Material properties of biological tissues related to joint surgery. *Current Orthopaedics* **20(1)**:16–22 DOI 10.1016/j.cuor.2005.12.001.

Hansen P, Bojsen-Moller J, Aagaard P, Kjaer M, Magnusson SP. 2006. Mechanical properties of the human patellar tendon, in vivo. *Clinical Biomechanics* **21(1)**:54–58 DOI 10.1016/j.clinbiomech.2005.07.008.

Harner CD, Xerogeanes JW, Livesay GA, Carlin GJ, Smith BA, Kusayama T, Kashiwaguchi S, Woo SL. 1995. The human posterior cruciate ligament complex: an interdisciplinary study. Ligament morphology and biomechanical evaluation. *American Journal of Sports Medicine* **23(6)**:736–745 DOI 10.1177/036354659502300617.

Hausdorff JM, Rios DA, Edelberg HK. 2001. Gait variability and fall risk in community-living older adults: a 1-year prospective study. *Archives of Physical Medicine and Rehabilitation* **82(8)**:1050–1056 DOI 10.1053/apmr.2001.24893.

Hayes WC, Mockros LF. 1971. Viscoelastic properties of human articular cartilage. *Journal of Applied Physiology* **31(4)**:562–568 DOI 10.1152/jappl.1971.31.4.562.

Hewitt J, Guilak F, Glisson R, Vail TP. 2001. Regional material properties of the human hip joint capsule ligaments. *Journal of Orthopaedic Research* **19(3)**:359–364 DOI 10.1016/s0736-0266(00)00035-8.

Hill CL, Seo GS, Gale D, Totterman S, Gale ME, Felson DT. 2005. Cruciate ligament integrity in osteoarthritis of the knee. *Arthritis & Rheumatism* **52(3)**:794–799 DOI 10.1002/art.20943.

Hobatho M, Rho J, Ashman R, Van Der Perre G, Lowet G, Borgwardt A. 1991. *In Vivo Assessment of Bone Quality by Vibration and Wave Propagation Techniques. Part II.* Leuven: ACCO Publishing, 7–32.

Hollman JH, Kovash FM, Kubik JJ, Linbo RA. 2007. Age-related differences in spatiotemporal markers of gait stability during dual task walking. *Gait & Posture* **26(1)**:113–119 DOI 10.1016/j.gaitpost.2006.08.005.

Hori RY, Mockros L. 1976. Indentation tests of human articular cartilage. *Journal of Biomechanics* **9(4)**:259–268 DOI 10.1016/0021-9290(76)90012-9.

Hvid I, Hansen SL. 1985. Trabecular bone strength patterns at the proximal tibial epiphysis. *Journal of Orthopaedic Research* **3(4)**:464–472 DOI 10.1002/jor.1100030409.

Intema F, Hazewinkel H, Gouwens D, Bijlsma J, Weinans H, Lafeber F, Mastbergen S. 2010. In early OA, thinning of the subchondral plate is directly related to cartilage damage: results from a canine ACLT-meniscectomy model. *Osteoarthritis and Cartilage* **18(5)**:691–698 DOI 10.1016/j.joca.2010.01.004.

Jeffrey JE, Aspden RM. 2006. The biophysical effects of a single impact load on human and bovine articular cartilage. *Proceedings of the Institution of Mechanical Engineers, Part H: Journal of Engineering in Medicine* **220(6)**:677–686 DOI 10.1243/09544119jeim31.

Jilani A, Shirazi-Adl A, Bendjaballah M. 1997. Biomechanics of human tibio-femoral joint in axial rotation. *Knee* **4(4)**:203–213 DOI 10.1016/s0968-0160(97)00266-4.

Johnson GA, Tramaglini DM, Levine RE, Ohno K, Choi N, Woo SL-Y. 1994. Tensile and viscoelastic properties of human patellar tendon. *Journal of Orthopaedic Research* **12(6)**:796–803 DOI 10.1002/jor.1100120607.

Julkunen P, Harjula T, Iivarinen J, Marjanen J, Seppänen K, Närhi T, Arokoski J, Lammi MJ, Brama PA, Jurvelin JS, Helminen HJ. 2009. Biomechanical, biochemical and structural correlations in immature and mature rabbit articular cartilage. *Osteoarthritis and Cartilage* **17(12)**:1628–1638 DOI 10.1016/j.joca.2009.07.002.

Kamibayashi L, Wyss U, Cooke T, Zee B. 1995. Trabecular microstructure in the medial condyle of the proximal tibia of patients with knee osteoarthritis. *Bone* **17(1)**:27–35 DOI 10.1016/8756-3282(95)00137-3.

Kazemi M, Li L. 2014. A viscoelastic poromechanical model of the knee joint in large compression. *Medical Engineering & Physics* **36(8)**:998–1006 DOI 10.1016/j.medengphy.2014.04.004.

Kazemi M, Li L, Savard P, Buschmann M. 2011. Creep behavior of the intact and meniscectomy knee joints. *Journal of the Mechanical Behavior of Biomedical Materials* **4(7)**:1351–1358 DOI 10.1016/j.jmbbm.2011.05.004.

Kazemi M, Dabiri Y, Li LP. 2013. Recent advances in computational mechanics of the human knee joint. *Computational and Mathematical Methods in Medicine* **2013**:1–27 DOI 10.1155/2013/718423.

Kempson G, Freeman M, Swanson S. 1971. The determination of a creep modulus for articular cartilage from indentation tests on the human femoral head. *Journal of Biomechanics* **4(4)**:239–250 DOI 10.1016/0021-9290(71)90030-3.

Kempson GE. 1980. The mechanical properties of articular cartilage. *Joints and Synovial Fluid* **2**:177–238 DOI 10.1016/b978-0-12-655102-0.50011-4.

Kiss RM. 2011. Effect of severity of knee osteoarthritis on the variability of gait parameters. *Journal of Electromyography and Kinesiology* **21(5)**:695–703 DOI 10.1016/j.jelekin.2011.07.011.

Kiviranta P, Lammentausta E, Töyräs J, Kiviranta I, Jurvelin J. 2008. Indentation diagnostics of cartilage degeneration. *Osteoarthritis and Cartilage* **16(7)**:796–804 DOI 10.1016/j.joca.2007.10.016.

Kleemann R, Krocker D, Cedraro A, Tuischer J, Duda G. 2005. Altered cartilage mechanics and histology in knee osteoarthritis: relation to clinical assessment (ICRS Grade). *Osteoarthritis and Cartilage* **13(11)**:958–963 DOI 10.1016/j.joca.2005.06.008.

Korhonen RK, Laasanen MS, Töyräs J, Lappalainen R, Helminen HJ, Jurvelin JS. 2003. Fibril reinforced poroelastic model predicts specifically mechanical behavior of normal, proteoglycan depleted and collagen degraded articular cartilage. *Journal of Biomechanics* **36(9)**:1373–1379 DOI 10.1016/s0021-9290(03)00069-1.

Kuroki K, Cook C, Cook J. 2011. Subchondral bone changes in three different canine models of osteoarthritis. *Osteoarthritis and Cartilage* **19(9)**:1142–1149 DOI 10.1016/j.joca.2011.06.007.

Laasanen M. 2003. *Development and Validation of Mechano-Acoustic Techniques and Instrument for Evaluation of Articular Cartilage*. Kuopion yliopisto.

Lajeunesse D, Reboul P. 2003. Subchondral bone in osteoarthritis: a biologic link with articular cartilage leading to abnormal remodelling. *Current Opinion in Rheumatology* **15(5)**:628–633 DOI 10.1097/00002281-200309000-00018.

Lange A, Singh MF, Smith R, Foroughi N, Baker M, Shnier R, Vanwanseele B. 2007. Degenerative meniscus tears and mobility impairment in women with knee osteoarthritis. *Osteoarthritis and Cartilage* **15(6)**:701–708 DOI 10.1016/j.joca.2006.11.004.

Langelier E, Buschmann M. 1999. Amplitude dependent mechanical alteration and nonlinearity of articular cartilage material behavior in unconfined compression. *ORS Transactions* **24**:647.

LeRoux MA, Setton LA. 2002. Experimental and biphasic FEM determinations of the material properties and hydraulic permeability of the meniscus in tension. *Journal of Biomechanical Engineering* **124(3)**:315–321 DOI 10.1115/1.1468868.

Lewis G, Nyman JS. 2008. The use of nanoindentation for characterizing the properties of mineralized hard tissues: state-of-the art review. *Journal of Biomedical Materials Research Part B: Applied Biomaterials* **87(1)**:286–301 DOI 10.1002/jbm.b.31092.

Li G, Gil J, Kanamori A, Woo S. 1999. A validated three-dimensional computational model of a human knee joint. *Journal of Biomechanical Engineering* **121(6)**:657–662 DOI 10.1115/1.2800871.

Li G, Lopez O, Rubash H. 2001. Variability of a three-dimensional finite element model constructed using magnetic resonance images of a knee for joint contact stress analysis. *Journal of Biomechanical Engineering* **123(4)**:341–346 DOI 10.1115/1.1385841.

Lindahl O. 1976. Mechanical properties of dried defatted spongy bone. *Acta Orthopaedica Scandinavica* **47(1)**:11–19 DOI 10.3109/17453677608998966.

Loparic M, Wirz D, Daniels A, Raiteri R, VanLandingham MR, Guex G, Martin I, Aebi U, Stolz M. 2010. Micro-and nanomechanical analysis of articular cartilage by indentation-type atomic force microscopy: validation with a gel-microfiber composite. *Biophysical Journal* **98(11)**:2731–2740 DOI 10.1016/j.bpj.2010.02.013.

Lord SR, Lloyd DG, Li SK. 1996. Sensori-motor function, gait patterns and falls in community-dwelling women. *Age and Ageing* **25(4)**:292–299 DOI 10.1093/ageing/25.4.292.

Lories RJ, Luyten FP. 2011. The bone–cartilage unit in osteoarthritis. *Nature Reviews Rheumatology* **7(1)**:43–49.

Losina E, Paltiel AD, Weinstein AM, Yelin E, Hunter DJ, Chen SP, Klara K, Suter LG, Solomon DH, Burbine SA. 2015. Lifetime medical costs of knee osteoarthritis management in the United States: impact of extending indications for total knee arthroplasty. *Arthritis Care & Research* **67(2)**:203–215 DOI 10.1002/acr.22412.

Lotz JC, Gerhart TN, Hayes WC. 1991. Mechanical properties of metaphyseal bone in the proximal femur. *Journal of Biomechanics* **24(5)**:317327–325329 DOI 10.1016/0021-9290(91)90350-v.

Louis-Ugbo J, Leeson B, Hutton WC. 2004. Tensile properties of fresh human calcaneal (Achilles) tendons. *Clinical Anatomy* **17(1)**:30–35 DOI 10.1002/ca.10126.

Lyyra T, Jurvelin J, Pitkänen P, Väätäinen U, Kiviranta I. 1995. Indentation instrument for the measurement of cartilage stiffness under arthroscopic control. *Medical Engineering & Physics* **17(5)**:395–399 DOI 10.1016/1350-4533(95)97322-g.

Madry H, van Dijk CN, Mueller-Gerbl M. 2010. The basic science of the subchondral bone. *Knee Surgery, Sports Traumatology, Arthroscopy* **18(4)**:419–433 DOI 10.1007/s00167-010-1054-z.

Mahjoub M, Berenbaum F, Houard X. 2012. Why subchondral bone in osteoarthritis? The importance of the cartilage bone interface in osteoarthritis. *Osteoporosis International* **23(S8)**:841–846 DOI 10.1007/s00198-012-2161-0.

Mak A, Lai W, Mow V. 1987. Biphasic indentation of articular cartilage—I. *Theoretical analysis, Journal of Biomechanics* **20(7)**:703–714 DOI 10.1016/0021-9290(87)90036-4.

Mankin HJ, Dorfman H, Lippiello L, Zarins A. 1971. Biochemical and metabolic abnormalities in articular cartilage from osteo-arthritic human hips. II. Correlation of morphology with biochemical and metabolic data. *Journal of Bone and Joint Surgery* **53(3)**:523–537 DOI 10.2106/00004623-197153030-00009.

Manninen P, Riihimaki H, Heliovaara M, Makela P. 1996. Overweight, gender and knee osteoarthritis. *International Journal of Obesity and Related Metabolic Disorders: Journal of the International Association for the Study of Obesity* **20(6)**:595–597.

Marticke JK, Hösselbarth A, Hoffmeier KL, Marintschev I, Otto S, Lange M, Plettenberg HK, Spahn G, Hofmann GO. 2010. How do visual, spectroscopic and biomechanical changes of cartilage correlate in osteoarthritic knee joints? *Clinical Biomechanics* **25(4)**:332–340 DOI 10.1016/j.clinbiomech.2009.12.008.

Martini F. 1998. *Anatomy and Physiology' 2007 Ed.* San Francisco: Benjamin Cummings.

Matkovic V, Jelic T, Wardlaw GM, Ilich JZ, Goel PK, Wright JK, Andon MB, Smith KT, Heaney RP. 1994. Timing of peak bone mass in Caucasian females and its implication for the prevention of osteoporosis. Inference from a cross-sectional model. *Journal of Clinical Investigation* **93(2)**:799–808 DOI 10.1172/jci117034.

Meng Q, Jin Z, Wilcox R, Fisher J. 2014. Computational investigation of the time-dependent contact behaviour of the human tibiofemoral joint under body weight. *Proceedings of the Institution of Mechanical Engineers, Part H: Journal of Engineering in Medicine* **228(11)**:1193–1207 DOI 10.1177/0954411914559737.

Mente P, Lewis J. 1994. Elastic modulus of calcified cartilage is an order of magnitude less than that of subchondral bone. *Journal of Orthopaedic Research* **12(5)**:637–647 DOI 10.1002/jor.1100120506.

Minary-Jolandan M, Yu M. 2009. Nanomechanical heterogeneity in the gap and overlap regions of type I collagen fibrils with implications for bone heterogeneity. *Biomacromolecules* **10(9)**:2565–2570 DOI 10.1021/bm900519v.

Moglo K, Shirazi-Adl A. 2003. On the coupling between anterior and posterior cruciate ligaments, and knee joint response under anterior femoral drawer in flexion: a finite element study. *Clinical Biomechanics* **18(8)**:751–759 DOI 10.1016/s0268-0033(03)00140-2.

Momersteeg T, Blankevoort L, Huiskes R, Kooloos J, Kauer J, Hendriks J. 1995. The effect of variable relative insertion orientation of human knee bone–ligament–bone complexes on the tensile stiffness. *Journal of Biomechanics* **28(6)**:745–752 DOI 10.1016/0021-9290(94)00121-j.

Mononen M, Julkunen P, Töyräs J, Jurvelin J, Kiviranta I, Korhonen R. 2011. Alterations in structure and properties of collagen network of osteoarthritic and repaired cartilage modify knee joint stresses. *Biomechanics and Modeling in Mechanobiology* **10(3)**:357–369 DOI 10.1007/s10237-010-0239-1.

Mononen ME, Mikkola MT, Julkunen P, Ojala R, Nieminen MT, Jurvelin JS, Korhonen RK. 2012. Effect of superficial collagen patterns and fibrillation of femoral articular cartilage on knee joint mechanics—a 3D finite element analysis. *Journal of Biomechanics* **45(3)**:579–587 DOI 10.1016/j.jbiomech.2011.11.003.

Mononen ME, Tanska P, Isaksson H, Korhonen RK. 2016. A novel method to simulate the progression of collagen degeneration of cartilage in the knee: data from the osteoarthritis initiative. *Scientific Reports* **6(1)**:21415 DOI 10.1038/srep21415.

Mootanah R, Imhauser CW, Reisse F, Carpanen D, Walker RW, Koff MF, Lenhoff MW, Rozbruch SR, Fragomen AT, Dewan Z, Kirane YM, Cheah K, Dowell JK, Hillstrom HJ. 2014. Development and validation of a computational model of the knee joint for the evaluation of surgical treatments for osteoarthritis. *Computer Methods in Biomechanics and Biomedical Engineering* **17(13)**:1502–1517 DOI 10.1080/10255842.2014.899588.

Mow V, Lai W, Holmes M. 1982. Advanced theoretical and experimental techniques in cartilage research. In: Huiskes R, van Campen DH, de Wijn JR, eds. *Biomechanics: Principles and Applications*. The Hague: Martinus Nijhoff, 47–74.

Mullaji AB, Marawar SV, Simha M, Jindal G. 2008. Cruciate ligaments in arthritic knees: a histologic study with radiologic correlation. *Journal of Arthroplasty* **23(4)**:567–572 DOI 10.1016/j.arth.2007.05.024.

Nigg B, Herzog W. 2006. *Biomechanics of the Musculoskeletal System*. Third Edition. West Sussex: Wiley.

Nissi M, Rieppo J, Töyräs J, Laasanen M, Kiviranta I, Nieminen M, Jurvelin J. 2007. Estimation of mechanical properties of articular cartilage with MRI–dGEMRIC, T 2 and T 1 imaging in different species with variable stages of maturation. *Osteoarthritis and Cartilage* **15(10)**:1141–1148 DOI 10.1016/j.joca.2007.03.018.

Noyes FR, Grood ES. 1976. The strength of the anterior cruciate ligament in humans and Rhesus monkeys. *Journal of Bone and Joint Surgery* **58(8)**:1074–1082 DOI 10.2106/00004623-197658080-00006.

Outerbridge R. 1961. The etiology of chondromalacia patellae. *Journal of Bone & Joint Surgery* **43**:752–757.

Owings TM, Grabiner MD. 2004. Step width variability, but not step length variability or step time variability, discriminates gait of healthy young and older adults during treadmill locomotion. *Journal of Biomechanics* **37(6)**:935–938 DOI 10.1016/j.jbiomech.2003.11.012.

Pedersen DR, Goetz JE, Kurriger GL, Martin JA. 2013. Comparative digital cartilage histology for human and common osteoarthritis models. *Orthopedic Research and Reviews* **2013(5)**:13–20 DOI 10.2147/orr.s38400.

Peña E, Calvo B, Martinez M, Doblare M. 2006. A three-dimensional finite element analysis of the combined behavior of ligaments and menisci in the healthy human knee joint. *Journal of Biomechanics* **39(9)**:1686–1701 DOI 10.1016/j.jbiomech.2005.04.030.

Peña E, Calvo B, Martinez M, Palanca D, Doblaré M. 2005. Finite element analysis of the effect of meniscal tears and meniscectomies on human knee biomechanics. *Clinical Biomechanics* **20(5)**:498–507 DOI 10.1016/j.clinbiomech.2005.01.009.

Peña E, Del Palomar AP, Calvo B, Martínez M, Doblaré M. 2007a. Computational modelling of diarthrodial joints. Physiological, pathological and pos-surgery simulations. *Archives of Computational Methods in Engineering* **14(1)**:47–91 DOI 10.1007/s11831-006-9001-3.

Peña E, Calvo B, Martínez MA, Doblaré M. 2007b. Effect of the size and location of osteochondral defects in degenerative arthritis. A finite element simulation. *Computers in Biology and Medicine* **37(3)**:376–387 DOI 10.1016/j.compbiomed.2006.04.004.

Peters AE, Comerford EJ, Macaulay S, Bates KT, Akhtar R. 2017. Micromechanical properties of canine femoral articular cartilage following multiple freeze-thaw cycles. *Journal of the Mechanical Behavior of Biomedical Materials* **71**:114–121 DOI 10.1016/j.jmbbm.2017.03.006.

Plumb M, Aspden R. 2005. The response of elderly human articular cartilage to mechanical stimuli in vitro. *Osteoarthritis and Cartilage* **13(12)**:1084–1091 DOI 10.1016/j.joca.2005.07.002.

Punzi L, Oliviero F, Ramonda R. 2010. New horizons in osteoarthritis. *Swiss Medical Weekly* **140**:16 DOI 10.4414/smw.2010.13098.

Quapp K, Weiss JA. 1998. Material characterization of human medial collateral ligament. *Journal of Biomechanical Engineering* **120(6)**:757–763 DOI 10.1115/1.2834890.

Race A, Amis AA. 1994. The mechanical properties of the two bundles of the human posterior cruciate ligament. *Journal of Biomechanics* **27(1)**:13–24 DOI 10.1016/0021-9290(94)90028-0.

Reilly DT, Burstein AH. 1975. The elastic and ultimate properties of compact bone tissue. *Journal of Biomechanics* **8(6)**:393IN9397–396IN11405 DOI 10.1016/0021-9290(75)90075-5.

Repo RU, Finlay JB. 1977. Survival of articular cartilage after controlled impact. *Journal of Bone and Joint Surgery* **59(8)**:1068–1076 DOI 10.2106/00004623-197759080-00012.

Rho JY, Ashman RB, Turner CH. 1993. Young's modulus of trabecular and cortical bone material: ultrasonic and microtensile measurements. *Journal of Biomechanics* **26(2)**:111–119 DOI 10.1016/0021-9290(93)90042-d.

Rho J, Tsui TY, Pharr GM. 1997. Elastic properties of human cortical and trabecular lamellar bone measured by nanoindentation. *Biomaterials* **18(20)**:1325–1330 DOI 10.1016/s0142-9612(97)00073-2.

Robinson JR, Bull AM, Amis AA. 2005. Structural properties of the medial collateral ligament complex of the human knee. *Journal of Biomechanics* **38(5)**:1067–1074 DOI 10.1016/j.jbiomech.2004.05.034.

Robinson DL, Kersh ME, Walsh NC, Ackland DC, de Steiger RN, Pandy MG. 2016. Mechanical properties of normal and osteoarthritic human articular cartilage. *Journal of the Mechanical Behavior of Biomedical Materials* **61**:96–109 DOI 10.1016/j.jmbbm.2016.01.015.

Rousseau JC, Garnero P. 2012. Biological markers in osteoarthritis. *Bone* **51(2)**:265–277 DOI 10.1016/j.bone.2012.04.001.

Setton LA, Elliott DM, Mow VC. 1999. Altered mechanics of cartilage with osteoarthritis: human osteoarthritis and an experimental model of joint degeneration. *Osteoarthritis and Cartilage* **7(1)**:2–14 DOI 10.1053/joca.1998.0170.

Shepherd DE, Seedhom BB. 1997. A technique for measuring the compressive modulus of articular cartilage under physiological loading rates with preliminary results. *Proceedings of the Institution of Mechanical Engineers. Part H, Journal of Engineering in Medicine* **211(2)**:155–165 DOI 10.1243/0954411971534278.

Shepherd DE, Seedhom BB. 1999a. The 'instantaneous' compressive modulus of human articular cartilage in joints of the lower limb. *Rheumatology* **38(2)**:124–132 DOI 10.1093/rheumatology/38.2.124.

Shepherd DE, Seedhom BB. 1999b. Thickness of human articular cartilage in joints of the lower limb. *Annals of the Rheumatic Diseases* **58(1)**:27–34 DOI 10.1136/ard.58.1.27.

Shirazi R, Shirazi-Adl A, Hurtig M. 2008. Role of cartilage collagen fibrils networks in knee joint biomechanics under compression. *Journal of Biomechanics* **41(16)**:3340–3348 DOI 10.1016/j.jbiomech.2008.09.033.

Skaggs D, Warden W, Mow V. 1994. Radial tie fibers influence the tensile properties of the bovine medial meniscus. *Journal of Orthopaedic Research* **12(2)**:176–185 DOI 10.1002/jor.1100120205.

Staubli HU, Schatzmann L, Brunner P, Rincon L, Nolte LP. 1999. Mechanical tensile properties of the quadriceps tendon and patellar ligament in young adults. *American Journal of Sports Medicine* **27(1)**:27–34 DOI 10.1177/03635465990270011301.

Stolz M, Gottardi R, Raiteri R, Miot S, Martin I, Imer R, Staufer U, Raducanu A, Düggelin M, Baschong W. 2009. Early detection of aging cartilage and osteoarthritis in mice and patient samples using atomic force microscopy. *Nature Nanotechnology* **4(3)**:186–192 DOI 10.1038/nnano.2008.410.

Stolz M, Raiteri R, Daniels A, VanLandingham MR, Baschong W, Aebi U. 2004. Dynamic elastic modulus of porcine articular cartilage determined at two different levels of tissue organization by indentation-type atomic force microscopy. *Biophysical Journal* **86(5)**:3269–3283 DOI 10.1016/s0006-3495(04)74375-1.

Taffetani M, Gottardi R, Gastaldi D, Raiteri R, Vena P. 2014. Poroelastic response of articular cartilage by nanoindentation creep tests at different characteristic lengths. *Medical Engineering & Physics* **36(7)**:850–858 DOI 10.1016/j.medengphy.2014.03.008.

Tanska P, Mononen ME, Korhonen RK. 2015. A multi-scale finite element model for investigation of chondrocyte mechanics in normal and medial meniscectomy human knee joint during walking. *Journal of Biomechanics* **48(8)**:1397–1406 DOI 10.1016/j.jbiomech.2015.02.043.

Taylor ZA, Miller K. 2006. Constitutive modeling of cartilaginous tissues: a review. *Journal of Applied Biomechanics* **22(3)**:212–229 DOI 10.1123/jab.22.3.212.

Temple-Wong MM, Bae WC, Chen MQ, Bugbee WD, Amiel D, Coutts RD, Lotz M, Sah RL. 2009. Biomechanical, structural, and biochemical indices of degenerative and osteoarthritic deterioration of adult human articular cartilage of the femoral condyle. *Osteoarthritis and Cartilage* **17(11)**:1469–1476 DOI 10.1016/j.joca.2009.04.017.

Thambyah A, Nather A, Goh J. 2006. Mechanical properties of articular cartilage covered by the meniscus. *Osteoarthritis and Cartilage* **14(6)**:580–588 DOI 10.1016/j.joca.2006.01.015.

Tissakht M, Ahmed A. 1995. Tensile stress–strain characteristics of the human meniscal material. *Journal of Biomechanics* **28(4)**:411–422 DOI 10.1016/0021-9290(94)00081-e.

Trent PS, Walker PS, Wolf B. 1976. Ligament length patterns, strength, and rotational axes of the knee joint. *Clinical Orthopaedics and Related Research* **117**:263–270 DOI 10.1097/00003086-197606000-00034.

Tuncer M, Cobb JP, Hansen UN, Amis AA. 2013. Validation of multiple subject-specific finite element models of unicompartmental knee replacement. *Medical Engineering & Physics* **35(10)**:1457–1464 DOI 10.1016/j.medengphy.2013.03.020.

Venäläinen MS, Mononen ME, Salo J, Räsänen LP, Jurvelin JS, Töyräs J, Virén T, Korhonen RK. 2016. Quantitative evaluation of the mechanical risks caused by focal cartilage defects in the knee. *Scientific Reports* **6(1)**:37538 DOI 10.1038/srep37538.

Wang Y, Fan Y, Zhang M. 2014. Comparison of stress on knee cartilage during kneeling and standing using finite element models. *Medical Engineering & Physics* **36(4)**:439–447 DOI 10.1016/j.medengphy.2014.01.004.

Wang M, Peng Z, Price J, Ketheesan N. 2013. Study of the nano-mechanical properties of human knee cartilage in different wear conditions. *Wear* **301(1–2)**:188–191 DOI 10.1016/j.wear.2012.12.015.

Wang M, Peng Z. 2015. Investigation of the nano-mechanical properties and surface topographies of wear particles and human knee cartilages. *Wear* **324–325**:74–79 DOI 10.1016/j.wear.2014.11.033.

Weiss JA, Gardiner JC. 2001. Computational modeling of ligament mechanics. *Critical Reviews™ in Biomedical Engineering* **29(3)**:303–371 DOI 10.1615/critrevbiomedeng.v29.i3.20.

Wen C, Wu C, Tang B, Wang T, Yan C, Lu W, Pan H, Hu Y, Chiu K. 2012. Collagen fibril stiffening in osteoarthritic cartilage of human beings revealed by atomic force microscopy. *Osteoarthritis and Cartilage* **20(8)**:916–922 DOI 10.1016/j.joca.2012.04.018.

Wilson W, Van Donkelaar C, Van Rietbergen R, Huiskes R. 2005. The role of computational models in the search for the mechanical behavior and damage mechanisms of articular cartilage. *Medical Engineering & Physics* **27(10)**:810–826 DOI 10.1016/j.medengphy.2005.03.004.

Wilusz RE, Zauscher S, Guilak F. 2013. Micromechanical mapping of early osteoarthritic changes in the pericellular matrix of human articular cartilage. *Osteoarthritis and Cartilage* **21(12)**:1895–1903 DOI 10.1016/j.joca.2013.08.026.

Wismans J, Veldpaus F, Janssen J, Huson A, Struben P. 1980. A three-dimensional mathematical model of the knee-joint. *Journal of Biomechanics* **13(8)**:677–685 DOI 10.1016/0021-9290(80)90354-1.

Woo SL, Abramowitch SD, Kilger R, Liang R. 2006. Biomechanics of knee ligaments: injury, healing, and repair. *Journal of Biomechanics* **39(1)**:1–20 DOI 10.1016/j.jbiomech.2004.10.025.

Woo S, Akeson W, Jemmott G. 1976. Measurements of nonhomogeneous, directional mechanical properties of articular cartilage in tension. *Journal of Biomechanics* **9(12)**:785–791 DOI 10.1016/0021-9290(76)90186-x.

Woo S, Johnson G, Smith B. 1993. Mathematical modeling of ligaments and tendons. *Journal of Biomechanical Engineering* **115(4B)**:468 DOI 10.1115/1.2895526.

Woo SL, Hollis JM, Adams DJ, Lyon RM, Takai S. 1991. Tensile properties of the human femur-anterior cruciate ligament-tibia complex. The effects of specimen age and orientation. *American Journal of Sports Medicine* **19(3)**:217–225 DOI 10.1177/036354659101900303.

Yang NH, Nayeb-Hashemi H, Canavan PK, Vaziri A. 2010. Effect of frontal plane tibiofemoral angle on the stress and strain at the knee cartilage during the stance phase of gait. *Journal of Orthopaedic Research* **28(12)**:1539–1547 DOI 10.1002/jor.21174.

Yao H, Dao M, Carnelli D, Tai K, Ortiz C. 2011. Size-dependent heterogeneity benefits the mechanical performance of bone. *Journal of the Mechanics and Physics of Solids* **59(1)**:64–74 DOI 10.1016/j.jmps.2010.09.012.

Zhang Y, Jordan JM. 2008. Epidemiology of osteoarthritis. *Rheumatic Disease Clinics of North America* **34(3)**:515–529.

Zysset PK, Guo XE, Hoffler CE, Moore KE, Goldstein SA. 1999. Elastic modulus and hardness of cortical and trabecular bone lamellae measured by nanoindentation in the human femur. *Journal of Biomechanics* **32(10)**:1005–1012 DOI 10.1016/s0021-9290(99)00111-6.

Zysset P, Sonny M, Hayes W. 1994. Morphology-mechanical property relations in trabecular bone of the osteoarthritic proximal tibia. *Journal of Arthroplasty* **9(2)**:203–216 DOI 10.1016/0883-5403(94)90070-1.

Journal of the mechanical behavior of biomedical materials 71 (2017) 114–121

Contents lists available at ScienceDirect

Journal of the Mechanical Behavior of Biomedical Materials

journal homepage: www.elsevier.com/locate/jmbbm

Micromechanical properties of canine femoral articular cartilage following multiple freeze-thaw cycles

Abby E. Peters[a,b,*], Eithne J. Comerford[a,b,c], Sophie Macaulay[a], Karl T. Bates[a], Riaz Akhtar[b]

[a] Department of Musculoskeletal Biology, Institute of Ageing and Chronic Disease, University of Liverpool, The William Henry Duncan Building, 6 West Derby Street, Liverpool L7 8TX, UK
[b] Department of Mechanical, Materials and Aerospace Engineering, School of Engineering, University of Liverpool, The Quadrangle, Brownlow Hill, Liverpool L69 3GH, UK
[c] Institute of Veterinary Science, Leahurst Campus, University of Liverpool, Chester High Road, Neston, Wirral CH64 7TE, UK

ARTICLE INFO

Keywords:
Canine
Femoral
Cartilage
Freezing
Nanoindentation

ABSTRACT

Tissue material properties are crucial to understanding their mechanical function, both in healthy and diseased states. However, in certain circumstances logistical limitations can prevent testing on fresh samples necessitating one or more freeze-thaw cycles. To date, the nature and extent to which the material properties of articular cartilage are altered by repetitive freezing have not been explored. Therefore, the aim of this study is to quantify how articular cartilage mechanical properties, measured by nanoindentation, are affected by multiple freeze-thaw cycles. Canine cartilage plugs (n = 11) from medial and lateral femoral condyles were submerged in phosphate buffered saline, stored at 3–5 °C and tested using nanoindentation within 12 h. Samples were then frozen at −20 °C and later thawed at 3–5 °C for 3 h before material properties were re-tested and samples re-frozen under the same conditions. This process was repeated for all 11 samples over three freeze-thaw cycles. Overall mean and standard deviation of shear storage modulus decreased from 1.76 ± 0.78 to 1.21 ± 0.77 MPa (p = 0.91), shear loss modulus from 0.42 ± 0.19 to 0.39 ± 0.17 MPa (p=0.70) and elastic modulus from 5.13 ± 2.28 to 3.52 ± 2.24 MPa (p = 0.20) between fresh and three freeze-thaw cycles respectively. The loss factor increased from 0.31 ± 0.38 to 0.71 ± 1.40 (p = 0.18) between fresh and three freeze-thaw cycles. Inter-sample variability spanned as much as 10.47 MPa across freezing cycles and this high-level of biological variability across samples likely explains why overall mean "whole-joint" trends do not reach statistical significance across the storage conditions tested. As a result multiple freeze-thaw cycles cannot be explicitly or statistically linked to mechanical changes within the cartilage. However, the changes in material properties observed herein may be sufficient in magnitude to impact on a variety of clinical and scientific studies of cartilage, and should be considered when planning experimental protocols.

1. Introduction

Articular cartilage is a viscoelastic heterogeneous material divided into layered zones with varying material properties and functionalities (Silver et al., 2002). The extracellular matrix (ECM) is heterogeneous in nature, where variations exist in composition, structure and vascularity at a micro-level. It is composed of proteoglycans, collagens and glycoproteins, which are all macromolecular components (Silver et al., 2002). Cartilage also contains chondrocytes that become embedded within the matrix, maturing and dividing to deposit new cartilage. Its primary function is to maintain a smooth surface allowing lubricated frictionless movement and to help transmit articular forces, therefore minimising stress concentrations across the joint (Nigg and Herzog, 2006).

Knowledge of material properties of cartilage is crucial to understanding its mechanical function and morpho-functional alterations that occur during ageing, disease and injury (Wen et al., 2012, Kleemann et al., 2005). Whilst valuable data in isolation, material property information is also crucial to other mechanical analyses, including computational models that attempt to predict *in vivo* joint

Abbreviations: AFM, Atomic Force Microscopy; CSM, Continued Stiffness Measurement; E, Elastic Modulus; ECM, Extra Cellular Matrix; G',, Shear Modulus; G", Storage Modulus; PBS, Phosphate Buffered Solution; SD, Standard Deviation, Standard Error Mean (SEM)

* Corresponding author at: Department of Musculoskeletal Biology, Institute of Ageing and Chronic Disease, University of Liverpool, The William Henry Duncan Building, 6 West Derby Street, Liverpool L7 8TX, UK.
E-mail addresses: abby.peters@liverpool.ac.uk (A.E. Peters), ejc@liverpool.ac.uk (E.J. Comerford), s.a.macaulay@liverpool.ac.uk (S. Macaulay), k.t.bates@liverpool.ac.uk (K.T. Bates), r.akhtar@liverpool.ac.uk (R. Akhtar).

http://dx.doi.org/10.1016/j.jmbbm.2017.03.006
Received 18 October 2016; Received in revised form 23 February 2017; Accepted 5 March 2017
Available online 07 March 2017

behaviour (e.g. Wang et al., 2014, Guo et al., 2009, Pena et al., 2006). Material properties of articular cartilage ECM have been widely reported utilising varying testing, storage and preservation techniques (e.g. Shepherd and Seedhom, 1997, Kleemann et al., 2005, Wen et al., 2012). Specific testing techniques have changed over time and varied according to investigator preference and overall experimental goals. In general, however, all studies seeking to quantify the mechanical behaviour of biological tissues strive to maintain biological fidelity of the testing conditions in the experiment; for example testing fresh tissue samples under hydrated conditions that are representative of the internal environment of the studied organism (Brandt et al., 2010). However, accomplishing this may be challenging for numerous reasons including the need for transportation between dissection and testing locations, availability or failure of testing equipment and the desire to test large sample numbers from individual specimens thereby minimising tissue waste. In such circumstances it is standard practice to store and preserve samples, often requiring tissue to undergo one or more freeze-thaw cycles before mechanical tests can be carried out (e.g. Wilusz et al., 2013, Lau et al., 2008; Li et al., 2006).

Therefore in situations where logistical limitations prevent testing of fresh samples, it is beneficial to explore if preservation of tissues samples through freezing can be utilised without compromising mechanical properties. In recent years there have been a number of systematic investigations into the effects of multiple freeze-thaw cycles on the mechanical properties of ligaments and tendon (Huang et al., 2011, Moon et al., 2006, Woo et al., 1986). Although some variation between individual studies exists, these analyses suggest that ligament and tendon tissue can undergo a minimum of two freeze-thaw cycles before significant changes to their material properties occur, thereby providing important constraints on experimental designs involving these tissues. However, despite its fundamental importance to joint biomechanics, to the best of our knowledge, no such data exists exploring the effect of more than one freeze-thaw cycle on material properties of articular cartilage. The aim of this paper is therefore to quantify how articular cartilage mechanical properties are affected by multiple freeze-thaw cycles directly addressing this important gap in knowledge. Dynamic nanoindentation is used to determine the shear storage modulus (G'), shear loss modulus (G''), elastic modulus (E) and the loss factor ($tan\ \delta$) of canine femoral condyle articular cartilage across three freeze-thaw cycles.

2. Materials and methods

2.1. Specimen preparation

One disease free canine cadaveric knee joint from a skeletally mature Staffordshire Bull cross mix was dissected 36 h after being euthanized. Ethical permission for use of this cadaveric material was granted by the Veterinary Research Ethics Committee, University of Liverpool (VREC327). Healthy articular cartilage samples (n = 11) measuring < 1 cm^2, were harvested from the medial and lateral bilateral femoral condyles (Fig. 1) using a low speed band saw (deSoutter Medical, Bucks, UK). Gross examination of the samples showed no sign of fibrillation or wear.

Following dissection, each of the 11 samples were submerged in phosphate buffered saline (PBS) and stored in cooled temperatures (3–5 °C) for up to 12 h until they were tested when still fresh using nanoindentation techniques, as detailed below. Following testing, all 11 samples were then frozen at −20 °C for up to 48 hours. Samples were then individually thawed for three hours at 3–5 °C and re-tested using the same nanoindentation protocol after having undergone one freeze-thaw cycle. This was completed within one hour and hydration of cartilage was maintained through constant exposure to PBS prior to and during testing (Brandt et al., 2010). This freeze-thaw procedure was repeated for three cycles and material properties of all 11 samples were measured after each freeze-thaw cycle. Samples were specifically thawed in cooled conditions (3–5 °C), as room temperatures have been shown to thaw cartilage samples too quickly and cause damage to the ECM (Szarko et al., 2010).

Fig. 1. Photograph of the medial and lateral femoral condyle of the canine specimen to scale (cm), from which samples were harvested.

2.2. Nanoindentation testing

Cartilage samples underwent dynamic nanoindentation (G200 Nanoindenter, Keysight Technologies, Chandler, AZ, USA) equipped with an ultra-low load DCM-II actuator utilising a Continuous Stiffness Measurement (CSM) module to determine the micromechanical complex shear modulus.

Samples were mounted into a custom made liquid cell holder, with a 1 cm radius and 2 mm deep well, which could allow partial submersion of the samples in PBS during testing (Fig. 2). Samples were then examined under the built-in optical microscope to randomly select ten indent locations per sample (> 100 μm spacing between each indentation to avoid immediate overlap) totalling 110 measurements per cycle of freezing. Given that it was not possible to differentiate between microstructural features in the cartilage with the optical microscope, indentation sites were based on topographical homogeneity for accu-

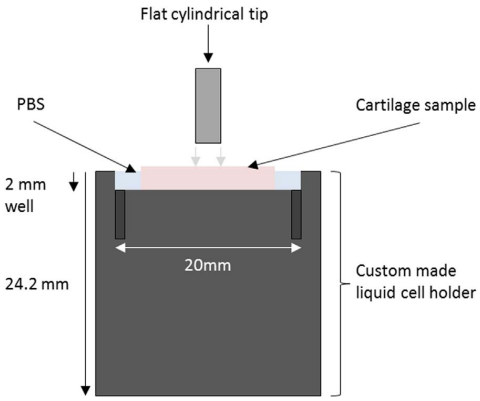

Fig. 2. A schematic of the custom made liquid cell holder holding the cartilage sample and phosphate buffered saline (PBS).

rate surface detection. Repetition or overlapping indentations in subsequent cycles of freezing was possible although it has previously been reported that there is no visible deformation of cartilage following low loads such as those experienced during nanoindentation when a recovery time is incorporated (Franke et al., 2011). Similarly to previous research investigating viscoelastic materials (e.g. Cheng et al., 2000, Jurvelin et al., 2000), a flat-ended cylindrical 100 μm punch tip (Synton-MDP Ltd, Nidau, Switzerland) was utilised as opposed to a sharp Berkovich tip which has been used in other studies testing cartilage (Hargrave-Thomas et al., 2015, Campbell et al., 2012, Franke et al., 2007, Gupta et al., 2005).

A Poisson's ratio of 0.46 (Jin and Lewis, 2004) was assumed for cartilage allowing the calculation of G', G'' and the loss factor (i.e. ratio of G'' / G') after each indentation. The theoretical basis is outlined in brief below and has been described in more detail previously (Herbert et al., 2008 and Herbert et al., 2009). Complex shear modulus (G*) is calculated by adding the shear storage modulus G' (real intrinsic elastic component) to the shear loss modulus G'' (imaginary viscous component):

$$G^* = G' + iG'' \quad (1)$$

Sneddon's analysis (Sneddon, 1965) is used to calculate the shear storage modulus using the Poisson's ratio (v), contact stiffness (S) and tip diameter (D), based on using a flat cylindrical punch:

$$G' = \frac{S(1 - v)}{(2D)} \quad (2)$$

The above components along with contact damping (Cw) can be used to calculate the shear loss modulus: modulus:

$$G'' = \frac{Cw(1 - v)}{(2D)} \quad (3)$$

Contact stiffness (S) is calculated by subtracting the instrument stiffness (Ki) from the total measured stiffness (Ks):

$$S = Ks - Ki \quad (4)$$

Contact damping (Cw) is calculated by subtracting the instrument damping (Ciw) from the total measured damping (Csw):

$$Cw = Csw - Ciw \quad (5)$$

The elastic modulus (E) was then calculated using the shear storage modulus (G') and Poisson's Ratio (v) (Landau and Lifshitz, 1986):

$$E = 2G' (1 + v) \quad (6)$$

After the indenter head detected the surface of the sample, a pre-compression of 8 μm was applied until the indenter was fully in contact with the sample. The surface detection was determined by a phase shift of the displacement measurement. In order to accurately detect the surface, the phase shift was monitored over a number of data points which has previously been shown to be effective (Akhtar et al., 2016). Once the surface detection requirement was fulfilled over the pre-defined number of data points, the initial contact was determined from the first data point in the sequence. Once the indenter was fully in contact with the sample surface it vibrated at a fixed frequency of 110 Hz (the resonant frequency of the indenter) with 500 nm oscillation amplitude. Contact stiffness and damping were obtained through electromagnetic oscillation sequences. The initial oscillation measured instrument stiffness and damping and these were subtracted from the total measurement to obtain the contact response. Material properties were then obtained during the second oscillation.

After each indentation, the tip was cleaned to prevent any transfer of biological material to the subsequent indentation site which may affect measurements. This was achieved by indenting an adjacent sample holder which was mounted with 3 M double-sided Scotch tape. This method was found to be effective at cleaning the tip without picking up any residue from the Scotch tape. Following testing of each sample, further indents were made on fused silica with the test sites remaining free of any residue, hence confirming that the tip was clean before further cartilage testing.

2.3. 2.3 Statistical analysis

An a-priori power analysis was performed using G*Power software (Faul et al., 2007) which specified a total of eight samples would be required to distinguish an effect size of 0.8 with α error probability of 0.05 and power of 0.95 across four groups of testing parameters. Statistical analysis of G', G'' and E, as well as the loss factor, were conducted using a repeated measures ANOVA in SPSS (SPSS software, Version 22.0, SPSS, Inc., Chicago, IL), specifically Mauchly's Test of Sphericity, after which a Bonferroni post-hoc test was performed if results were significant, producing pairwise comparisons. Individual sample means were analysed after each cycle of freezing, as well as the means of all samples combined, to give a whole specimen analysis.

3. Results

3.1. Overall Trends

The overall mean G', G'', E and loss factor for all 11 samples combined for the different cycles are presented in Fig. 3. Shear modulus (G') decreased from 1.76 ± 0.78, 1.41 ± 0.77, 1.25 ± 0.54 to 1.21 ± 0.77 MPa (mean ± standard deviation (SD)) between fresh samples and samples tested after one, two and three freeze-thaw cycles respectively (Fig. 3a). Shear loss modulus (G'') increased from 0.42 ± 0.19 to 0.46 ± 0.18 MPa (mean ± SD) between fresh and one freeze-thaw cycle, but then decreased to 0.43 ± 0.15 and 0.39 ± 0.17 MPa following two and three freeze-thaw cycles respectively (Fig. 3b). Elastic Modulus (E) were 5.13 ± 2.28, 4.11 ± 2.25, 3.64 ± 1.57 and 3.52 ± 2.24 MPa (mean ± SD) during fresh, one, two and three freeze-thaw cycles respectively (Fig. 3c). The mean and SD of the loss factor changed throughout each cycle from 0.31 ± 0.38, 0.58 ± 1.66, 0.41 ± 0.26 and 0.71 ± 1.40 when using a mean of all 11 samples during fresh, one, two and three freeze-thaw cycles respectively (Fig. 3d). Changes in the values for G', G'', E and the loss factor, across freeze-thaw cycles were not found to be statistically significant (Mauchley's Test of Sphericity, $p = 0.91$, $p = 0.70$, $p = 0.20$, $p = 0.18$ respectively).

3.2. Inter-Sample Variability

Numerical results for individual samples are tabulated in Tables 1–4. Repeated freeze-thaw cycles led to some significant differences in G' ($p = 0.016$) and E ($p = 0.019$) across individual samples but no differences in G'' ($p = 0.122$) or the loss factor ($p = 0.178$). Bonferroni post-hoc pairwise comparisons showed between freeze-thaw cycle effects on the individual sample mean G' and E were not statistically significant between fresh and one freeze-thaw cycle ($p = 0.45$), one freeze-thaw and two freeze-thaw cycles ($p = 1.00$), and two freeze-thaw and three freeze-thaw cycles ($p = 1.00$). Further post-hoc pairwise comparison was not necessary for G'' or the loss factor, as these were not statistically significant.

A high degree of variability in each mechanical property was observed both within and between the 11 discrete samples analysed at each freeze-thaw cycle, as indicated by high standard deviations about the overall mean values (as listed above) and the substantial absolute ranges of individual sample means and coefficient of variation (CoV) (Tables 1–4). For example, the E value in an individual sample in the same cycle of fresh testing varied by as much as 10.47 MPa equivalent to a change of up to 96.29% of the overall mean value on one occasion (Table 3). Across the 11 samples tested, E varied by as much as 14.73 MPa or equivalent to a 188.89% change to the overall mean within the same cycle of freezing (mean / SD) seen in Table 3. Inter-sample variation was such that in some instances individual samples

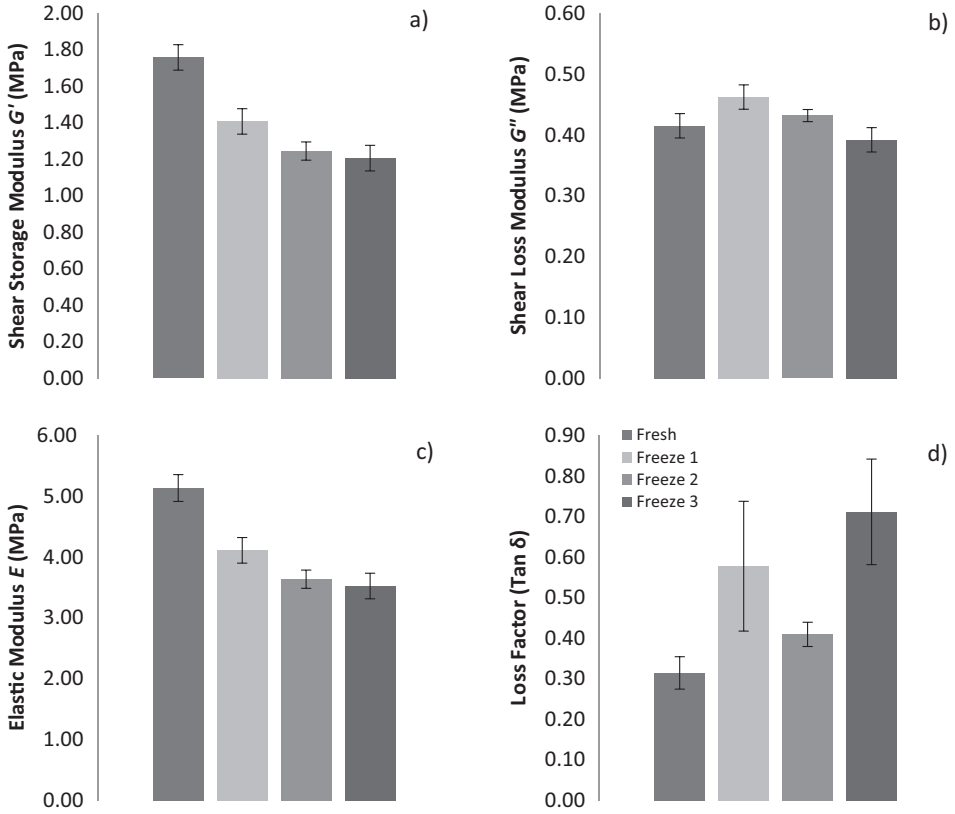

Fig. 3. a) Mean shear storage modulus (*G'*), b) Shear loss modulus (*G''*), c) Elastic modulus (*E*) and the d) Loss factor for all samples combined during different storage and freezing conditions. Error bars represent the standard error of mean (SEM).

exhibited changes in mechanical properties across freeze-thaw cycles that differed qualitatively from the overall mean trends (Fig. S1).

4. Discussion

This study provides the first systematic investigation of the effects of multiple freeze-thaw cycles on the mechanical properties of articular cartilage. Szarko et al., (2010) compared the mechanical properties of canine femoral articular cartilage stored at −20 °C, −80 °C and snap frozen in liquid nitrogen using indentation techniques. They found that with rapid thawing (37.5 °C) and exposure to PBS, both −20 °C and −80 °C can be used as reliable preservation methods for one freeze-thaw cycle as this produced results consistent with those from fresh samples. However, snap freezing tissue can cause ice crystallisation to form on the sample and therefore compromises the integrity of the tissue. Further research (Moore and Burris, 2015) also considered the

Table 1
Mean ± standard deviation (SD), standard error mean (SEM) and coefficient of variation (CoV) for Shear storage modulus (MPa) for each tested sample during each cycle of freezing.

Shear Storage Modulus *G'* (MPa)												
	Fresh			Freeze 1			Freeze 2			Freeze 3		
Sample	Mean ± SD	SEM	CoV%	Mean ± SD	SEM	CoV%	Mean ± SD	SEM	CoV%	Mean ± SD	SEM	CoV%
1	2.57 ± 0.39	0.12	15.17	2.61 ± 0.28	0.09	10.73	1.24 ± 0.42	0.13	33.87	1.65 ± 0.45	0.14	27.27
2	1.11 ± 0.13	0.04	11.71	1.16 ± 0.12	0.04	10.34	1.04 ± 0.43	0.14	41.35	1.29 ± 0.13	0.04	10.08
3	2.58 ± 1.05	0.33	40.70	0.77 ± 0.58	0.18	75.32	0.76 ± 0.50	0.16	65.79	0.54 ± 0.52	0.16	96.30
4	2.22 ± 0.26	0.08	11.71	2.20 ± 0.35	0.11	15.91	1.64 ± 0.24	0.08	14.63	2.32 ± 0.65	0.21	28.02
5	1.05 ± 0.47	0.15	44.76	1.04 ± 0.53	0.17	50.96	1.06 ± 0.22	0.07	20.75	0.19 ± 0.15	0.05	78.95
6	1.72 ± 0.37	0.12	21.51	0.70 ± 0.21	0.07	30.00	1.36 ± 0.22	0.07	16.18	1.38 ± 0.19	0.06	13.77
7	2.07 ± 0.21	0.07	10.14	2.12 ± 0.12	0.04	5.66	1.25 ± 0.12	0.04	9.60	1.84 ± 0.10	0.03	5.43
8	2.41 ± 0.28	0.09	11.62	1.85 ± 0.24	0.08	12.97	1.85 ± 0.22	0.07	11.89	1.40 ± 0.79	0.25	56.43
9	1.31 ± 0.17	0.05	12.98	1.12 ± 0.12	0.04	10.71	0.79 ± 0.15	0.05	18.99	0.22 ± 0.02	0.01	9.09
10	1.70 ± 0.55	0.17	32.35	1.63 ± 0.58	0.18	35.58	2.10 ± 0.45	0.14	21.43	1.64 ± 0.50	0.16	30.49
11	0.60 ± 0.39	0.12	65.00	0.29 ± 0.17	0.05	58.62	0.61 ± 0.07	0.02	11.48	0.79 ± 0.12	0.04	15.19

Table 2
Mean ± standard deviation (SD), standard error mean (SEM) and coefficient of variation (CoV) for Shear loss modulus (MPa) for each tested sample during each cycle of freezing.

Shear Loss Modulus *G"*(MPa)												
	Fresh			Freeze 1			Freeze 2			Freeze 3		
Sample	Mean ± SD	SEM	CoV%	Mean ± SD	SEM	CoV%	Mean ± SD	SEM	CoV%	Mean ± SD	SEM	CoV%
1	0.54 ± 0.06	0.02	11.11	0.62 ± 0.08	0.03	12.90	0.44 ± 0.13	0.04	29.55	0.53 ± 0.08	0.02	15.09
2	0.24 ± 0.02	0.01	8.33	0.31 ± 0.02	0.01	6.45	0.25 ± 0.09	0.03	36.00	0.28 ± 0.02	0.01	7.14
3	0.42 ± 0.48	0.15	114.29	0.48 ± 0.18	0.06	37.50	0.49 ± 0.12	0.04	24.49	0.49 ± 0.17	0.05	34.69
4	0.60 ± 0.07	0.02	11.67	0.74 ± 0.09	0.03	12.16	0.53 ± 0.05	0.02	9.43	0.60 ± 0.10	0.03	16.67
5	0.37 ± 0.14	0.04	37.84	0.42 ± 0.14	0.04	33.33	0.45 ± 0.07	0.02	15.56	0.06 ± 0.05	0.01	83.33
6	0.40 ± 0.07	0.02	17.50	0.38 ± 0.03	0.01	7.89	0.37 ± 0.03	0.01	8.11	0.33 ± 0.03	0.01	9.09
7	0.49 ± 0.02	0.01	4.08	0.58 ± 0.01	0.00	1.72	0.37 ± 0.03	0.01	8.11	0.43 ± 0.02	0.01	4.65
8	0.45 ± 0.03	0.01	6.67	0.38 ± 0.04	0.01	10.53	0.39 ± 0.03	0.01	7.69	0.50 ± 0.18	0.06	36.00
9	0.40 ± 0.03	0.01	7.50	0.57 ± 0.06	0.02	10.53	0.68 ± 0.03	0.01	4.41	0.39 ± 0.02	0.01	5.13
10	0.46 ± 0.11	0.03	23.91	0.47 ± 0.11	0.04	23.40	0.58 ± 0.07	0.02	12.07	0.48 ± 0.10	0.03	20.83
11	0.19 ± 0.06	0.02	31.58	0.13 ± 0.03	0.01	23.08	0.21 ± 0.02	0.01	9.52	0.22 ± 0.01	0.00	4.55

effects of one freeze-thaw cycle at −80 °C on the mechanical properties of bovine femoral and tibial articular cartilage in comparison to fresh samples. Using a custom made indenter samples were exposed to PBS to maintain hydration and thawed at room temperature. No significant change in material properties was found with a tensile modulus of 4.1 ± 2.2 MPa for fresh samples and 4.5 ± 2.4 MPa for frozen samples (Moore and Burris, 2015). However, individual samples were randomly assigned to a fresh or frozen cohort and testing was not repeated on the same sample. Therefore results did not account for biological variability that may exist spatially within one specimen or cadaver. Wilusz et al. (2013) used two freeze thaw cycles at −20 °C of human femoral articular cartilage prior to atomic force microscopy (AFM)-based indentation. Justification for using two freeze-thaw cycles was recommended by Athanasiou et al. (1991) who established this aspect of the protocol on anecdotal unpublished data. Samples were exposed to PBS to maintain hydration and results from healthy cartilage ECM presented an *E* of 491 kPa. However in this study, a comparison to fresh samples was not made therefore what effect two freeze-cycles had on the material properties is unknown (Wilusz et al., 2013).

Our research study demonstrated that mean cartilage *G'* and *E* for the joint overall showed a sharp decreasing trend after one cycle of freezing, although this reduction appeared to lessen following two and three freeze-thaw cycles, despite not reaching statistical significance (Fig. 3). Interestingly *G"* and the loss factor showed no such trends and both increased and decreased during various cycles of freezing (Fig. 3). The loss factor in particular showed high standard error mean (SEM) (Fig. 3) in comparison to other parameters. When analysing the SD it appears that there is no consistent trend or change in *G'* and *E* where values both increase and decrease in various cycles of freezing (Tables 1 and 3). With the exception of two outliers *G"* and the loss factor SD remains unchanged during all cycles of freezing (Tables 2 and 4).

Systematic testing of articular cartilage across multiple freeze-thaw cycles in our study shows that samples can undergo three freezing cycles without statistically significant changes to material properties when handled and stored correctly (Fig. 3). These results therefore provide some support for the use of freezing as a method of preservation of cartilage where material properties are required to remain unchanged for mechanical testing. However the authors note that a number of changes in individual mean material properties for the joint were observed here (Fig. S1), and although these fell below thresholds of statistical significance in this study they may represent meaningful magnitudes in the context of other studies. For example, the overall mean *E* showed relatively large decreases with increasing number of freeze thaw cycles such that the values decreased by 1.02 MPa (one freeze-thaw), 0.47 MPa (two freeze-thaw) and 0.12 MPa (three freeze-thaw) of the mean value compared to fresh samples. Such relative changes in magnitude may well be extremely important in the context of comparative studies such as comparison of material properties between cohorts of different age and/or disease status (Wen et al., 2012, Kleemann et al., 2005, Franz et al., 2001) and computational modelling studies of joint biomechanics (Mononen et al., 2012, Pena et al., 2007, Blankevoort et al., 1991). Kleemann et al., (2005) researched the differences in cartilage material properties obtained from human tibial plateau samples and found that changes of as little as 0.1 MPa or 20% can be found between grade one and grade two osteoarthritic samples (graded by the International Cartilage Repair Society). Furthermore, in a human knee finite element model sensitivity analysis by Li et al. (2001) the material properties of cartilage were

Table 3
Mean ± standard deviation (SD), standard error mean (SEM) and coefficient of variation (CoV) for Elastic modulus (MPa) for each tested sample during each cycle of freezing.

Elastic Modulus *E* (MPa)												
	Fresh			Freeze 1			Freeze 2			Freeze 3		
Sample	Mean ± SD	SEM	CoV%	Mean ± SD	SEM	CoV%	Mean ± SD	SEM	CoV%	Mean ± SD	SEM	CoV%
1	7.52 ± 1.14	0.36	15.16	7.62 ± 0.83	0.26	10.89	3.61 ± 1.22	0.38	33.80	4.83 ± 1.32	0.42	27.33
2	3.24 ± 0.39	0.12	12.04	3.39 ± 0.35	0.11	10.32	3.04 ± 1.27	0.40	41.78	3.76 ± 0.39	0.12	10.37
3	7.55 ± 3.07	0.97	40.66	2.24 ± 1.68	0.53	75.00	2.22 ± 1.46	0.46	65.77	1.57 ± 1.51	0.48	96.18
4	6.48 ± 0.75	0.24	11.57	6.42 ± 1.02	0.32	15.89	4.80 ± 0.71	0.22	14.79	3.79 ± 1.89	0.60	49.87
5	3.08 ± 1.38	0.44	44.81	3.04 ± 1.55	0.49	50.99	3.10 ± 0.65	0.21	20.97	0.56 ± 0.44	0.14	78.57
6	5.01 ± 1.09	0.34	21.76	2.05 ± 0.63	0.20	30.73	3.97 ± 0.65	0.21	16.37	4.04 ± 0.56	0.18	13.86
7	6.04 ± 0.61	0.19	10.10	6.19 ± 0.36	0.11	5.82	3.65 ± 0.35	0.11	9.59	5.37 ± 0.31	0.10	5.77
8	7.03 ± 0.80	0.25	11.38	5.39 ± 0.70	0.22	12.99	5.39 ± 0.63	0.20	11.69	4.09 ± 2.31	0.73	56.48
9	3.83 ± 0.49	0.15	12.79	3.28 ± 0.34	0.11	10.37	2.31 ± 0.43	0.14	18.61	0.66 ± 0.07	0.02	10.61
10	4.97 ± 1.60	0.51	32.19	4.75 ± 1.70	0.54	35.79	6.13 ± 1.30	0.41	21.21	4.79 ± 1.46	0.46	30.48
11	1.75 ± 1.15	0.36	65.71	0.84 ± 0.49	0.16	58.33	1.77 ± 0.21	0.07	11.86	2.29 ± 0.34	0.11	14.85

Table 4
Mean ± standard deviation (SD), standard error mean (SEM) and coefficient of variation (CoV) for Loss factor for each tested sample during each cycle of freezing.

Loss Factor												
	Fresh			Freeze 1			Freeze 2			Freeze 3		
Sample	Mean ± SD	SEM	CoV%	Mean ± SD	SEM	CoV%	Mean ± SD	SEM	CoV%	Mean ± SD	SEM	CoV%
1	0.21 ± 0.03	0.01	14.29	0.24 ± 0.01	0.00	4.17	0.36 ± 0.04	0.01	11.11	0.34 ± 0.11	0.04	32.35
2	0.22 ± 0.01	0.00	4.55	0.27 ± 0.01	0.00	3.70	0.25 ± 0.03	0.01	12.00	0.22 ± 0.01	0.00	4.55
3	0.21 ± 0.14	0.04	66.67	2.46 ± 5.33	1.69	216.67	0.85 ± 0.46	0.14	54.12	2.02 ± 2.41	0.76	119.31
4	0.27 ± 0.01	0.00	3.70	0.34 ± 0.03	0.01	8.82	0.33 ± 0.03	0.01	9.09	0.27 ± 0.04	0.01	14.81
5	0.36 ± 0.05	0.02	13.89	0.45 ± 0.13	0.04	28.89	0.43 ± 0.06	0.02	13.95	0.31 ± 0.01	0.00	3.23
6	0.24 ± 0.02	0.01	8.33	0.61 ± 0.24	0.07	39.34	0.28 ± 0.04	0.01	14.29	0.24 ± 0.02	0.00	8.33
7	0.24 ± 0.02	0.01	8.33	0.27 ± 0.01	0.00	3.70	0.30 ± 0.01	0.00	3.33	0.24 ± 0.00	0.00	0.00
8	0.19 ± 0.01	0.00	5.26	0.21 ± 0.01	0.00	4.76	0.21 ± 0.01	0.00	4.76	1.83 ± 3.42	1.08	186.89
9	0.31 ± 0.04	0.01	12.90	0.51 ± 0.07	0.02	13.73	0.88 ± 0.12	0.04	13.64	1.76 ± 0.11	0.04	6.25
10	0.28 ± 0.05	0.02	17.86	0.31 ± 0.06	0.02	19.35	0.29 ± 0.04	0.01	13.79	0.30 ± 0.04	0.01	13.33
11	0.93 ± 1.12	0.35	120.43	0.68 ± 0.62	0.20	91.18	0.34 ± 0.02	0.01	5.88	0.29 ± 0.04	0.01	13.79

varied between 3.5 and 10 MPa, to understand the effect on joint contact stresses. Results showed that magnitude changes had substantial effects on the functional predictions of the model, specifically that *E* linearly increased with peak contact stresses and a Poisson's ratio increase significantly increased peak von Mises stress and hydrostatic pressure in the knee joint cartilage.

Given the absolute and relative changes in overall material properties measured across freeze-thaw cycles (Fig. 3), it may be preferable for experiments seeking to test multiple tissue types from the same cadaver to prioritise cartilage for fresh testing (or minimal freeze-thaw cycles), particularly given that previous research has suggested that other joint tissues are relatively insensitive to freezing (Jung et al., 2011, Huang et al., 2011, Moon et al., 2006, Woo et al., 1986). For example, Jung et al., (2011) concluded that the human patella-tendon can be exposed to eight freeze-thaw cycles, without compromising mechanical properties; provided testing conditions and tissue handling are approached with great care. This protocol involved allowing samples to re-freeze for a minimum of 6 h and thaw at room temperature for 6 h with exposure to saline. Furthermore, a study has shown the human flexor digitorum superficialis and flexor pollicis longus can undergo three freeze-thaw cycles before the integrity of their material properties is compromised. In addition freeze-thawing over five times also results in decreased mechanical and structural behaviour (Huang et al., 2011). Other studies focusing on ligaments include Woo et al. (1986) who explored the mechanical properties of the rabbit medial collateral ligament (MCL) following one prolonged freezing cycle and concluded that this has no effect when compared to fresh samples. Moon et al. (2006) also used the rabbit MCL to determine the effect when two freeze-thaw cycles and likewise concluded that no apparent changes to material properties occurred when compared to fresh samples. Therefore most published studies are in agreement that at least two freeze-cycles, under the correct handling and storage conditions, allow ligament and tendon samples to remain mechanically unchanged (Jung et al., 2011, Huang et al., 2011, Moon et al., 2006, Woo et al., 1986).

The modulus values obtained within this study fall within the range of those reported in the literature for other mammalian femoral condylar articular cartilage. Shepherd and Seedhom (1999) and Wilusz et al. (2013) reported a range of *E* from 0.1 to 18.6 MPa for human femoral condyle articular cartilage, although Moore and Burris (2015) reported lower values of 0.62 ± 0.10 MPa for bovine stifle cartilage. In our study mean values for *E* lie between 0.56 and 7.62 MPa, falling within this range already reported; however in both the literature and the current study there is a high variability of modulus. More specifically, previous canine research has found an *E* of 0.12 ± 0.10 MPa (Leroux et al., 2001), and 0.385–0.964 MPa (Jurvelin et al., 2000) when samples have undergone indentation testing following one freeze cycle. These values are generally lower than those reported in our study and have smaller absolute variability. Previous canine cartilage studies have reported CoV's of up to 23.61% (Jurvelin et al., 2000), which although being quite considerable are much lower than the CofV's reported here up to 96.3% for *G'* and 114.29% for *G"* (Tables 1–4). Although the current data is more variable than previous canine research, it should be noted that it is less variable than the human studies discussed above.

Cartilage is a highly heterogeneous material and therefore some variability of modulus is widely expected and accepted (e.g. Jurvelin et al., 2000); however differences seen in the current study as compared to other studies in the literature may be as a result of the frequency-dependent properties of cartilage. Higher frequencies have been shown to increase *G'* (Pearson and Espino, 2013) and *E* (Taffetani et al., 2015); however *G"* remains unaffected (Pearson and Espino, 2013). In our study, 110 Hz was selected for the testing because it is the resonant frequency of the indenter and thus most sensitive frequency for the surface detection. In other studies in the literature, a range of frequencies have been used including 0.5 Hz (Taffetani et al., 2015), 10 Hz (Franke et al., 2011) and much higher frequencies up to 200 Hz (Taffetani et al., 2015) and 250 Hz (Franke et al., 2011) where dynamic nanoindentation (Franke et al., 2011) and mechanical analysis methods were also utilised (Taffetani et al., 2015). Although high frequencies may account for increases in *G'* when compared to other canine studies (Leroux et al., 2001; Jurvelin eta l., 2000), the most important comparison is that seen between each freeze cycle, where frequency used remained standardised throughout testing cycles.

Additional limitations to the current study which may also affect variability include indenting sites affected by preceding measurements; however it has been suggested that low load indentation has been shown to cause no visible deformation of samples (Franke et al., 2011). Although some variability may be expected from the nanoindentation technique used in the current study, we have found that it yields highly repeatable data on other compliant materials which have a more homogenous structure than cartilage e.g. on a type of ballistic gelatine (Perma-Gel) the CoV for the elastic modulus was 3.3% following ten indentation tests (Moronkeji et al., 2016).

As the nanoindenter was unable to differentiate between cellular and non-cellular substance, the current study is subject to high variability in results depending on the exact material tested, limiting interpretation of changes to modulus. Other studies have attempted to differentiate the material properties of cartilage sub-components using AFM and found variation between *E* of the peri- (0.1 MPa) and extra cellular matrix (0.3 MPa) (Wilusz et al., 2013). However soft tissues are often dehydrated during AFM testing and maintaining hydration can be challenging (Wen et al., 2012).

With these considerations in mind, future research could aim to

accurately assess the effect of freezing on articular cartilage by first repeatedly indenting the same site of a fresh sample to fully understand the effect and variability of material properties seen in an identical position. Then secondly, indenting an identical position following multiple freeze-thaw cycles, aided by marking an area of the cartilage and noting at which exact position the sample was tested to understand the effect of freezing.

5. Conclusion

In summary, the results of this study suggest that three freeze-thaw cycles do not have a statistically significant effect on the overall 'whole-joint' material properties of canine femoral condyle cartilage samples provided the correct handling, storage and hydration of the tissue are maintained throughout preparation and testing. However, relative changes in mean material properties are observed and the failure to reach thresholds for statistical significance is likely the product of high biological variability across the joint. Therefore the changes in material properties observed over multiple freeze-thaw cycles may be sufficient to significantly impact on certain comparative or functional studies, such as finite element modelling, where subtle changes in material properties can indeed modify the true behaviour of articular cartilage under mechanical stress. Changes in material properties reported here should be considered when planning experimental protocols, as they may be sufficient in magnitude to impact on clinical or scientific cartilage studies.

Conflict of interest

There are no conflicts of interest to declare.

Acknowledgments

The authors would like to thank Mr. Lee Moore and the staff at the Veterinary Training Suite, Institute of Veterinary Science, for their assistance with cadaveric acquisition and dissection. RA is grateful to the Royal Society for funding (Research Grant. RG130629).

Funding: This project was funded by BBSRC and the School of Engineering, University of Liverpool.

Appendix A. Supporting information

Supplementary data associated with this article can be found in the online version at doi:10.1016/j.jmbbm.2017.03.006.

References

Akhtar, R., Draper, E.R., Adams, D.J. & Pfaff, H. 2016, "Complex shear modulus of hydrogels using dynamic nanoindentation method", *Mechanics of Biological Systems and Materials*, Proceedings of the 2015 Annual Conference on Experimental and Applied Mechanics, vol. 6, pp. 141–145.

Athanasiou, K., Rosenwasser, M., Buckwalter, J., Malinin, T., Mow, V., 1991. Interspecies comparisons of in situ intrinsic mechanical properties of distal femoral cartilage. J. Orthop. Res. 9 (3), 330–340.

Blankevoort, L., Kuiper, J., Huiskes, R., Grootenboer, H., 1991. Articular contact in a three-dimensional model of the knee. J. Biomech. 24 (11), 1019–1031.

Brandt, J., Briere, L., Marr, J., MacDonald, S., Bourne, R., Medley, J., 2010. Biochemical comparisons of osteoarthritic human synovial fluid with calf sera used in knee simulator wear testing. J. Biomed. Mater. Res. A 94 (3), 961–971.

Campbell, S.E., Ferguson, V.L., Hurley, D.C., 2012. Nanomechanical mapping of the osteochondral interface with contact resonance force microscopy and nanoindentation. Acta Biomater. 8 (12), 4389–4396.

Cheng, L., Xia, X., Yu, W., Scriven, L., Gerberich, W., 2000. Flat-punch indentation of viscoelastic material. J. Polym. Sci. B: Polym. Phys. 38 (1), 10–22.

Faul, F., Erdfelder, E., Lang, A., Buchner, A., 2007. G* Power 3: a flexible statistical power analysis program for the social, behavioral, and biomedical sciences. Behav. Res. Methods 39 (2), 175–191.

Franke, O., Durst, K., Maier, V., Göken, M., Birkholz, T., Schneider, H., Hennig, F., Gelse, K., 2007. Mechanical properties of hyaline and repair cartilage studied by nanoindentation. Acta Biomater. 3 (6), 873–881.

Franke, O., Göken, M., Meyers, M., Durst, K., Hodge, A., 2011. Dynamic nanoindentation of articular porcine cartilage. Mater. Sci. Eng.: C 31 (4), 789–795.

Franz, T., Hasler, E., Hagg, R., Weiler, C., Jakob, R., Mainil-Varlet, P., 2001. In situ compressive stiffness, biochemical composition, and structural integrity of articular cartilage of the human knee joint. Osteoarthr. Cartil. 9 (6), 582–592.

Guo, Y., Zhang, X., Chen, W., 2009. Three-dimensional finite element simulation of total knee joint in gait cycle. Acta Mech. Solid Sin. 22 (4), 347–351.

Gupta, H., Schratter, S., Tesch, W., Roschger, P., Berzlanovich, A., Schoeberl, T., Klaushofer, K., Fratzl, P., 2005. Two different correlations between nanoindentation modulus and mineral content in the bone–cartilage interface. J. Struct. Biol. 149 (2), 138–148.

Hargrave-Thomas, E., van Sloun, F., Dickinson, M., Broom, N., Thambyah, A., 2015. Multi-scalar mechanical testing of the calcified cartilage and subchondral bone comparing healthy vs early degenerative states. Osteoarthr. Cartil. 23 (10), 1755–1762.

Herbert, E., Oliver, W., Lumsdaine, A., Pharr, G.M., 2009. Measuring the constitutive behavior of viscoelastic solids in the time and frequency domain using flat punch nanoindentation. J. Mater. Res. 24 (03), 626–637.

Herbert, E., Oliver, W., Pharr, G., 2008. Nanoindentation and the dynamic characterization of viscoelastic solids. J. Phys. D: Appl. Phys. 41 (7), 074021.

Huang, H., Zhang, J., Sun, K., Zhang, X., Tian, S., 2011. Effects of repetitive multiple freeze–thaw cycles on the biomechanical properties of human flexor digitorum superficialis and flexor pollicis longus tendons. Clin. Biomech. 26 (4), 419–423.

Jin, H., Lewis, J.L., 2004. Determination of Poisson's ratio of articular cartilage by indentation using different-sized indenters. J. Biomech. Eng. 126 (2), 138–145.

Jung, H., Vangipuram, G., Fisher, M.B., Yang, G., Hsu, S., Bianchi, J., Ronholdt, C., Woo, S.L., 2011. The effects of multiple freeze–thaw cycles on the biomechanical properties of the human bone-patellar tendon-bone allograft. J. Orthop. Res. 29 (8), 1193–1198.

Jurvelin, J.S., Arokoski, J.P., Hunziker, E.B., Helminen, H.J., 2000. Topographical variation of the elastic properties of articular cartilage in the canine knee. J. Biomech. 33 (6), 669–675.

Kleemann, R., Krocker, D., Cedraro, A., Tuischer, J., Duda, G., 2005. Altered cartilage mechanics and histology in knee osteoarthritis: relation to clinical assessment (ICRS Grade). Osteoarthr. Cartil. 13 (11), 958–963.

Landau, L.D., Lifshitz, E., 1986. Theory of elasticity, vol. 7. Course Theor. Phys. 3, 109.

Lau, A., Oyen, M.L., Kent, R.W., Murakami, D., Torigaki, T., 2008. Indentation stiffness of aging human costal cartilage. Acta Biomater. 4 (1), 97–103.

Leroux, M., Cheung, H.S., Bau, J., Wang, J., Howell, D., Setton, L., 2001. Altered mechanics and histomorphometry of canine tibial cartilage following joint immobilization. Osteoarthr. Cartil. 9 (7), 633–640.

Li, C., Pruitt, L.A., King, K.B., 2006. Nanoindentation differentiates tissue-scale functional properties of native articular cartilage. J. Biomed. Mater. Res. Part A 78 (4), 729–738.

Li, G., Lopez, O., Rubash, H., 2001. Variability of a three-dimensional finite element model constructed using magnetic resonance images of a knee for joint contact stress analysis. J. Biomech. Eng. 123 (4), 341–346.

Mononen, M., Mikkola, M., Julkunen, P., Ojala, R., Nieminen, M., Jurvelin, J., Korhonen, R., 2012. Effect of superficial collagen patterns and fibrillation of femoral articular cartilage on knee joint mechanics—A 3D finite element analysis. J. Biomech. 45 (3), 579–587.

Moon, D.K., Woo, S.L., Takakura, Y., Gabriel, M.T., Abramowitch, S.D., 2006. The effects of refreezing on the viscoelastic and tensile properties of ligaments. J. Biomech. 39 (6), 1153–1157.

Moore, A., Burris, D., 2015. Tribological and material properties for cartilage of and throughout the bovine stifle: support for the altered joint kinematics hypothesis of osteoarthritis. Osteoarthr. Cartil. 23 (1), 161–169.

Moronkeji, K., Todd, S., Dawidowska, I., Barrett, S., Akhtar, R., 2016. The role of subcutaneous tissue stiffness on microneedle performance in a representative in vitro model of skin. J. Control Release.

Nigg, B., Herzog, W., 2006. Biomechanics of the Musculoskeletal System 3rd edn. Wiley, West Sussex.

Pearson, B., Espino, D.M., 2013. Effect of hydration on the frequency-dependent viscoelastic properties of articular cartilage. Proc. Inst. Mech. Eng. H: J. Eng. Med. 227 (11), 1246–1252.

Pena, E., Calvo, B., Martinez, M., Doblare, M., 2006. A three-dimensional finite element analysis of the combined behavior of ligaments and menisci in the healthy human knee joint. J. Biomech. 39 (9), 1686–1701.

Pena, E., Calbo, B., Martinez, M., Doblare, M., 2007. Effect of the size and location of osteochondral defects in degenerative arthritis. A finite element simulation. Comput. Biol. Med. 37 (3), 376–387.

Shepherd, D.E., Seedhom, B.B., 1999. The 'instantaneous' compressive modulus of human articular cartilage in joints of the lower limb. Rheumatol. (Oxf. Engl.) 38 (2), 124–132.

Shepherd, D.E., Seedhom, B.B., 1997. A technique for measuring the compressive modulus of articular cartilage under physiological loading rates with preliminary results. Proc. Inst. Mech. Eng. H: J. Eng. Med. 211 (2), 155–165.

Silver, F.H., Bradica, G., Tria, A., 2002. Elastic energy storage in human articular cartilage: estimation of the elastic modulus for type II collagen and changes

associated with osteoarthritis. Matrix Biol. 21 (2), 129–137.
Sneddon, I.N., 1965. The relation between load and penetration in the axisymmetric Boussinesq problem for a punch of arbitrary profile. Int. J. Eng. Sci. 3 (1), 47–57.
Szarko, M., Muldrew, K., Bertram, J.E., 2010. Freeze-thaw treatment effects on the dynamic mechanical properties of articular cartilage. BMC Musculoskelet. Disord. 11 (1), 231.
Taffetani, M., Raiteri, R., Gottardi, R., Gastaldi, D., Vena, P., 2015. A quantitative interpretation of the response of articular cartilage to atomic force microscopy-based dynamic nanoindentation tests. J. Biomech. Eng. 137 (7), 071005.
Wang, Y., Fan, Y., Zhang, M., 2014. Comparison of stress on knee cartilage during kneeling and standing using finite element models. Med. Eng. Phys. 36 (4), 439–447.
Wen, C., Wu, C., Tang, B., Wang, T., Yan, C., Lu, W., Pan, H., Hu, Y., Chiu, K., 2012. Collagen fibril stiffening in osteoarthritic cartilage of human beings revealed by atomic force microscopy. Osteoarthr. Cartil. 20 (8), 916–922.
Wilusz, R.E., Zauscher, S., Guilak, F., 2013. Micromechanical mapping of early osteoarthritic changes in the pericellular matrix of human articular cartilage. Osteoarthr. Cartil. 21 (12), 1895–1903.
Woo, S.L., Orlando, C.A., Camp, J.F., Akeson, W.H., 1986. Effects of postmortem storage by freezing on ligament tensile behavior. J. Biomech. 19 (5), 399–404.

SCIENTIFIC REPORTS

OPEN

The effect of ageing and osteoarthritis on the mechanical properties of cartilage and bone in the human knee joint

Received: 30 June 2017
Accepted: 27 February 2018
Published online: 12 April 2018

Abby E. Peters[1,2], Riaz Akhtar[2], Eithne J. Comerford[1,2,3] & Karl T. Bates[1]

Osteoarthritis is traditionally associated with cartilage degeneration although is now widely accepted as a whole-joint disease affecting the entire osteochondral unit; however site-specific cartilage and bone material properties during healthy ageing and disease are absent limiting our understanding. Cadaveric specimens (n = 12; 31–88 years) with grades 0–4 osteoarthritis, were dissected and spatially correlated cartilage, subchondral and trabecular bone samples (n = 8 per cadaver) were harvested from femoral and tibial localities. Nanoindentation was utilised to obtain cartilage shear modulus (*G′*) and bone elastic modulus (*E*). Cartilage *G′* is strongly correlated to age ($p = 0.003$) and osteoarthritis grade ($p = 0.007$). Subchondral bone *E* is moderately correlated to age ($p = 0.072$) and strongly correlated to osteoarthritis grade ($p = 0.013$). Trabecular bone *E* showed no correlation to age ($p = 0.372$) or osteoarthritis grade ($p = 0.778$). Changes to cartilage *G′* was significantly correlated to changes in subchondral bone *E* ($p = 0.007$). Results showed preferential medial osteoarthritis development and moderate correlations between cartilage *G′* and sample location ($p = 0.083$). Also demonstrated for the first time was significant correlations between site-matched cartilage and subchondral bone material property changes during progressive ageing and osteoarthritis, supporting the role of bone in disease initiation and progression. This clinically relevant data indicates a causative link with osteoarthritis and medial habitual loading.

Osteoarthritis (OA) is one of the most prevalent musculoskeletal conditions amongst the adult population with the most common diagnosis at the knee joint[1]. Individuals with OA have increased variability in gait spatial-temporal parameters[2], which in turn can lead to a decline in locomotor stability and increase the risk of falls through reduced functionality[3]. Ageing is a high risk factor for the development and progression of knee OA and is known to influence mechanical and biochemical changes within tissue structure, even in the absence of OA and other disease or injury status[4,5].

OA is traditionally associated with degeneration of the articular cartilage; however it is now more widely accepted that OA is a whole-joint disease that alters the integrity of multiple tissues of the osteochondral unit[6]. A recent review suggests tissue-level adaptations of the subchondral bone are thought to occur in OA prior to degeneration of the overlying articular cartilage;[7] however this has been rarely explored in the human knee joint. Abnormal remodeling of the subchondral bone has been identified, including high proliferation of volume at the bone-cartilage interface, with observations of changes to density, separation and quantity of the trabecular bone[8,9]. These structural modifications of bone and cartilage occur in synergy further suggesting subchondral bone plays an important but mostly unexplored role in the initiation and progression of the disease[10].

These structural adaptations may logically influence the mechanical strength of such tissues. Research shows that cartilage elastic modulus (*E*) declines with progressive grades of OA[11,12]. However, there is minimal research on the effect of OA on subchondral bone material properties. Indeed there has been no comparison

[1]Department of Musculoskeletal Biology, Institute of Ageing and Chronic Disease, University of Liverpool, The William Henry Duncan Building, 6 West Derby Street, Liverpool, L7 8TX, UK. [2]Department of Mechanical, Materials and Aerospace Engineering, School of Engineering, University of Liverpool, The Quadrangle, Brownlow Hill, Liverpool, L69 3GH, UK. [3]Institute of Veterinary Science, Leahurst Campus, University of Liverpool, Chester High Road, Neston, Wirral, CH64 7TE, UK. Correspondence and requests for materials should be addressed to A.E.P. (email: abby.peters@liverpool.ac.uk)

	Age (Years)	Gender	Limb	OA ICRS Grade*	Cartilage G' (MPa)	Subchondral Bone E (GPa)	Trabecular Bone E (GPa)
					Mean ± SD	Mean ± SD	Mean ± SD
Cadaver 1	31	Female	Left	Grade 0	1.30 ± 0.65	—	13.13 ± 3.34
Cadaver 2	37	Female	Left	Grade 0	1.0 ± 0.74	11.96 ± 1.90	12.29 ± 2.87
Cadaver 3	43	Female	Right	Grade 0	0.90 ± 0.55	11.89 ± 1.64	11.67 ± 2.88
Cadaver 4	49	Male	Left	Grade 0–1	0.65 ± 0.51	—	13.37 ± 2.16
Cadaver 5	51	Male	Right	Grade 0–1	0.96 ± 0.50	12.83 ± 1.64	13.09 ± 2.75
Cadaver 6	58	Male	Right	Grade 1–2	0.41 ± 0.54	11.12 ± 2.18	10.75 ± 2.90
Cadaver 7	72	Male	Right	Grade 2–3	0.14 ± 0.31	14.18 ± 1.99	12.13 ± 3.78
Cadaver 8	72	Male	Left	Grade 1–3	0.55 ± 0.45	14.34 ± 2.03	13.66 ± 3.13
Cadaver 9	79	Male	Left	Grade 1–2	0.15 ± 0.09	14.31 ± 1.57	12.29 ± 3.89
Cadaver 10	80	Male	Left	Grade 1–4	0.31 ± 0.48	15.33 ± 1.70	12.08 ± 2.68
Cadaver 11	86	Female	Right	Grade 0–1	0.40 ± 0.34	13.76 ± 1.93	11.64 ± 3.21
Cadaver 12	88	Male	Right	Grade 1–3	0.27 ± 0.36	14.30 ± 1.68	12.43 ± 2.63

Table 1. Mean and standard deviation (SD) of cartilage shear storage modulus (G') (MPa), subchondral bone elastic modulus (E) (GPa) and trabecular bone elastic modulus (E) (GPa) for samples across the whole joint. Age, osteoarthritis (OA) International Cartilage Repair Society (ICRS) grade (0–4) and limb side is also shown. *Note. OA grade is based on all 8 samples extracted, hence multiple grades per cadaver due to regional spatial variation in OA across the joint.

of the material properties of site matched cartilage and bone from the same donor in the presence of OA when compared to healthy controls. Knowledge of material properties of all tissues involved would enhance the development of treatment and clinical outcomes by advancing our understanding of disease mechanisms[13].

Subsequently the aim of this research is to systematically quantify age and OA related trends in the material properties of multiple tissues from the human knee joint. Articular cartilage, subchondral bone and trabecular bone samples from a cohort of donors spanning a large age range are tested using nanoindentation techniques. This study includes samples with varying grades of OA in order to understand how ageing and disease status affects multiple tissues of the knee joint simultaneously. Extraction of multiple, spatially distributed samples of all tissues from the same donors allows us to explicitly test for localised changes within tissues and furthermore for correlated changes between tissues during ageing and OA progression for the first time.

Results

Overall cartilage shear storage modulus (G') (0.14–1.30 MPa), subchondral bone E (11.12–15.33 GPa) and trabecular bone E (10.75–13.66 GPa) varied considerably across cadavers. The average mean and standard deviation (SD) across samples from the whole joint for all tissues can be seen in Table 1, along with age and grade of OA of the cadaver. Note that results herein present cartilage G' and subchondral and trabecular bone E. Values of all parameters including the addition of bone hardness (H), cartilage shear loss modulus (G'') and cartilage loss factor can be found in Supplementary Material 1.

Effect of Ageing. Increasing age is strongly correlated to a decrease in cartilage G' ($\tau b = -0.657$, $p = 0.003$) and moderately correlated to an increase in subchondral bone E ($\tau b = 0.449$, $p = 0.072$) using overall joint means. However there is no significant correlation between increasing age and trabecular E ($\tau b = -0.198$; $p = 0.372$). These trends are shown in Figure 1 by combined sample mean and SD plotted against age, along with the mean of each of the eight individual spatially correlated samples.

Increasing age was also strongly correlated to cartilage G'' ($\tau b = -0.565$; $p = 0.011$) and cartilage E ($\tau b = -0.657$; $p = 0.003$), and moderately correlated to cartilage loss factor ($\tau b = -0.462$; $p = 0.039$), subchondral bone H ($\tau b = 0.276$; $p = 0.277$) and trabecular bone H ($\tau b = 0.394$; $p = 0.083$) (calculated using Kendall's Tau-b for overall joint means) (see values in Supplementary Material 1).

Effect of Osteoarthritis. Increasing grade of OA is correlated to a decrease in cartilage G' ($\tau b = -0.625$; $p = 0.007$) and an increase in subchondral bone E ($\tau b = 0.645$; $p = 0.013$) using overall joint grading (Fig. 2). Trabecular bone E showed no significant correlation between overall joint OA grade ($\tau b = -0.066$; $p = 0.778$) (Fig. 2).

Overall joint grade of OA was strongly correlated to cartilage G'' ($p = 0.002$), cartilage loss factor ($p = 0.006$), cartilage E ($p = 0.007$) and subchondral bone H ($p = 0.033$), and moderately correlated to trabecular bone E ($p = 0.087$) (calculated using Kendall's Tau-b). (see values in Supplementary Material 1).

There is also a significant positive correlation between age and overall joint grade of OA ($\tau b = 0.663$; $p = 0.005$) (Fig. 3).

Cartilage and Bone Tissue Interaction. Correlations between the multiple tested tissues can be seen in Figure 4. There is a significant negative correlation between site-matched cartilage G' and subchondral bone E ($\rho = -0.299$; $p = 0.007$). However there is no significant correlation between site-matched cartilage G' and trabecular bone E ($\rho = 0.105$; $p = 0.309$), or site-matched subchondral versus trabecular bone E ($\rho = 0.210$; $p = 0.061$).

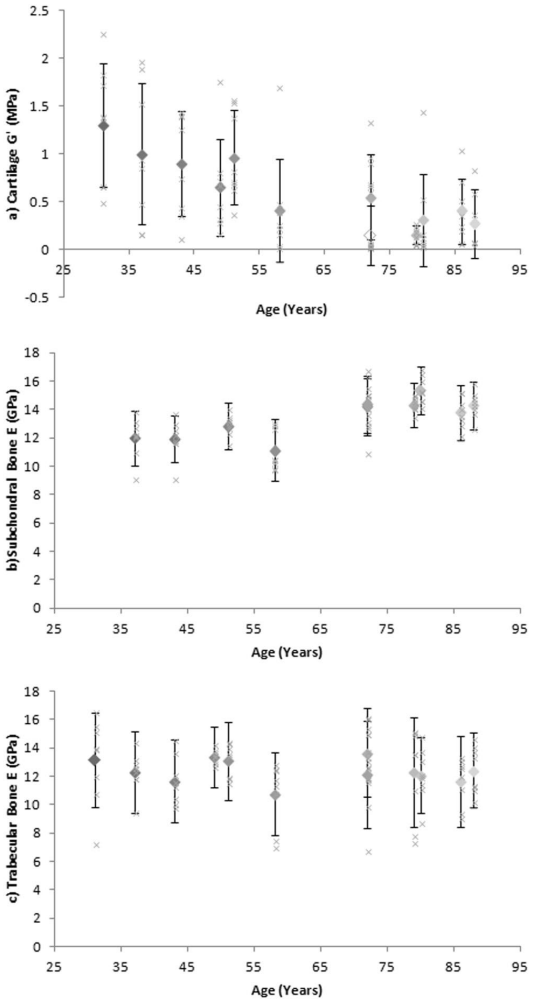

Figure 1. Mean of combined sample (**a**) Cartilage shear storage modulus (G') (MPa), (**b**) Subchondral bone elastic modulus (E) (GPa) and (**c**) Trabecular bone elastic modulus (E) (GPa) correlated to age (diamonds). Error bars represent standard deviation (SD). The mean of each eight individual spatially correlated samples from cadavers correlated against age (crosses).

Spatial Distribution of Cartilage and Bone. Across the 12 cadavers, combined site mean cartilage G' showed a moderate correlation to spatial locations ($\tau b = -0.500$; $p = 0.083$) (Fig. 5). Differences were most common between the mean of femoral and tibial sites, with the lowest G' found at the TPMA and highest at the FCLS. Lower values of G' were more marked at medial sites. Mean and SD femoral and tibial cartilage G' was 0.77 ± 0.62 and 0.40 ± 0.47 MPa respectively, whilst medial versus lateral G' were 0.53 ± 0.63 MPa and 0.64 ± 0.53 respectively.

Subchondral bone and trabecular bone E also varied across site-specific locations but no consistent patterns or differences were seen at any one particular site. Mean and SD femoral and tibial subchondral bone E was 13.34 ± 1.69 and 13.46 ± 1.78 GPa respectively and medial versus lateral samples were 13.46 ± 1.77 and 13.34 ± 1.70 GPa respectively. Mean and SD femoral and tibial trabecular bone E was 12.65 ± 1.79 and 12.10 ± 2.36 GPa respectively and medial versus lateral E was 12.48 ± 2.02 and 12.27 ± 2.19 GPa respectively.

Combined Effect of Variables. To consider individual sample material properties both within and between subjects, while adjusting for both age and OA grade as variables, a compound symmetry mixed linear model was used, showing the random effects on individual sample cartilage G' were significantly different

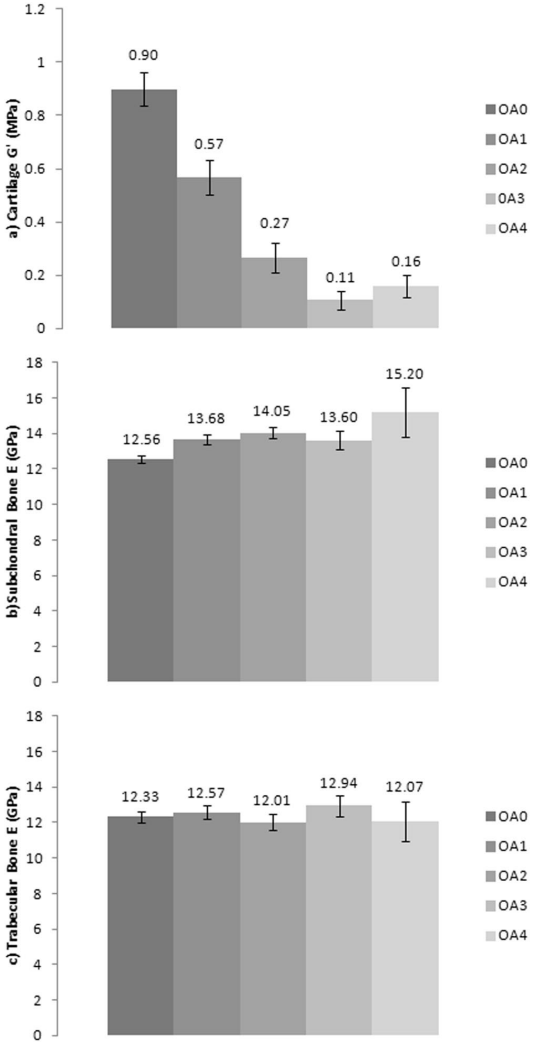

Figure 2. The relationship between (**a**) Cartilage shear storage modulus (G') (MPa), (**b**) Subchondral bone elastic modulus (E) (GPa), and (**c**) Trabecular bone elastic modulus (E) (GPa) to osteoarthritis International Cartilage Repair Society (ICRS) grade (0–4). Error bars represent 95% confidence interval and figures represent standard deviation (SD).

between subjects ($p = <0.001$), but not within subjects ($p = 0.429$). This suggests there was no significant difference of within-subject cartilage G'. Using these model assumptions, cartilage G' was significantly correlated to age ($p = 0.003$) but not OA grade ($p = 0.052$), when adjusted for one another and within-subject effects. The random effects of subchondral and trabecular bone E were also significantly different between subjects (both $p = <0.001$), but not within subjects ($p = 0.132$ and $p = 0.547$ respectively). Subchondral bone E was significantly correlated to age ($p = 0.010$), but not OA grade ($p = 0.892$) when adjusted for one another and within-subject effects. Trabecular bone E was not correlated to either age ($p = 0.432$) or OA grade ($p = 0.809$).

Discussion

This study presents the first systematic quantification of changes in the material properties of multiple human knee tissues by applying a single method to a cohort of cadaveric specimens spanning a wide range in age (31–88 years) and disease state (OA ICRS grade 0–4). These results allow us to determine how properties of all tissues change in the absence of confounding factors of variation of donor demographics and testing methods between

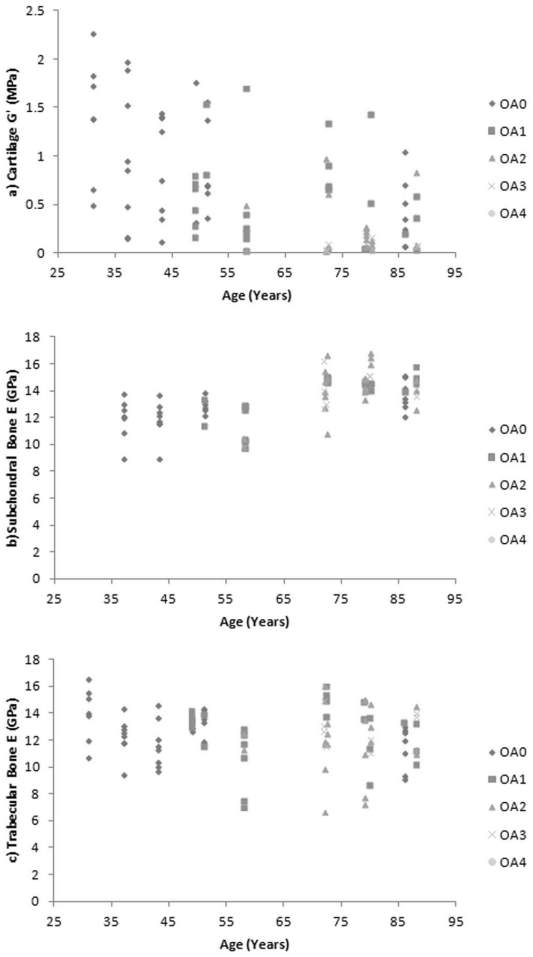

Figure 3. (**a**) Cartilage shear storage modulus (G') (MPa), (**b**) Subchondral bone elastic modulus (E) (GPa) and (**c**) Trabecular bone elastic modulus (E) (GPa) correlated to age (years) representing n = 8 samples from each cadaver, grouped according to osteoarthritis (OA) International Cartilage Repair Society (ICRS) grade (0–4).

studies for the first time (Figs. 1–5). Spatial sampling of multiple tissues also allows us to assess these correlations at the sub-joint level, which is crucial given suggestions of preferential regional development and progression of OA[14] as well as local changes to tissue morphology and structure thought to be associated with medial compartment mechanical loading of the human knee during habitual locomotion[15].

A number of previous studies have reported the material properties of healthy human knee joint articular cartilage [e.g.[16,17]] and compared data from healthy samples to those with OA [e.g.[11,12,18–20]]. These studies consistently report a decline in modulus in the presence of disease as an independent variable, which correlates with the statistically significant and highly correlated[21] negative relationship found here (Fig. 2). Healthy and OA grade 1 human knee joint cartilage G' has been reported between 0.07–6.7 MPa assuming a Poisson's ratio of 0.46[22], whilst OA grades 2–3 samples fall between 0.07–0.17 MPa [e.g.[11,12,16–20]]. Most recently Robinson *et al.*[23], found that cartilage G' at tibial and femoral sites in old (69.7 ± 9.3 years) healthy controls was 6.0 ± 1.6 MPa compared to OA samples (4.6 ± 1.8 MPa). However these earlier studies have not categorised samples according to age, or tested a wide span of age and therefore our ability to understand age-related trends and their influence on OA was limited.

The new data generated herein demonstrates clear changes in the material properties of knee joint tissues with ageing as well as in the presence of disease (Figs. 1–3). The absolute G' values reported for healthy and grade 1 OA samples tend to fall towards the lower end of previously reported results (Fig. 2a) whilst values of OA grades 2–4 tend to fall towards the higher end of previously reported results (Fig. 2a). Variation across previous studies may be due to different testing techniques, donor demographics and preservation and storage methods, which

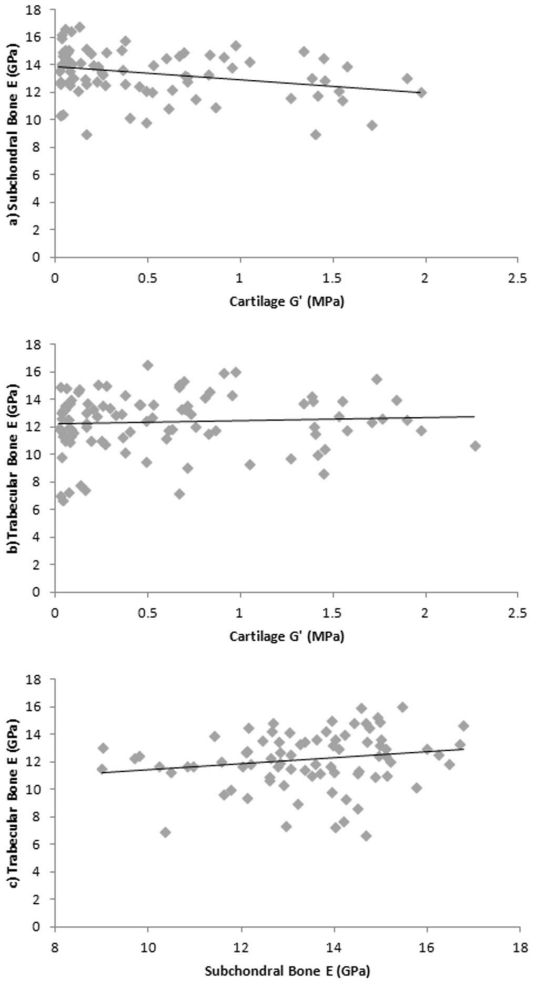

Figure 4. (**a**) Cartilage shear storage modulus (G') (MPa) and subchondral bone elastic modulus (E) (GPa) correlation, (**b**) Cartilage shear storage modulus (G') (MPa) and trabecular bone elastic modulus (E) correlation (GPa), (**c**) Subchondral bone elastic modulus (E) (GPa) and trabecular bone elastic modulus (E) (GPa) correlation.

make it challenging to accurately compare data. Importantly, some previous studies and the data generated herein focus primarily on the intrinsic viscoelastic response of cartilage which has been shown to functionally identify surface changes in the presence of early OA[24]. Whilst there is a body of literature also exploring the poroelastic response of cartilage considering the fluid-flow mechanics [e.g.[25,26]], such measurements are outside the scope of the current research. Interestingly, when determining the changes in cartilage G' in a multi-variable analysis, this was correlated to age but not OA grade ($p = 0.052$) when adjusted for one another and the dependence effect of multiple samples per donor. This suggests that ageing has a more prominent effect on cartilage G' than OA grade.

Our study also found evidence for a linear increase in subchondral bone E with increasing age (Fig. 1) and OA (Fig. 2). Therefore this data demonstrates, for the first time, a significantly correlated relationship between a change in site-matched cartilage and subchondral bone material properties (Fig. 4). These findings provide direct support for conceptual representations of cartilage and subchondral bone as a single functional unit[6]. Values between 22.0–25.8 GPa have previously been reported for healthy cortical bone E from the human knee joint[27], which are relatively higher than the average samples means across the whole joint with values reported in this study of 11.12–15.33 GPa. However more recently Zuo *et al.*[28], characterised tissue level mechanical strength of the subchondral bone in OA samples and found higher stiffness values in lamellae of grade 4 samples (17.33 ± 3.13 GPa) when compared to grade 1 samples (13.90 ± 2.75 GPa); however there were no healthy

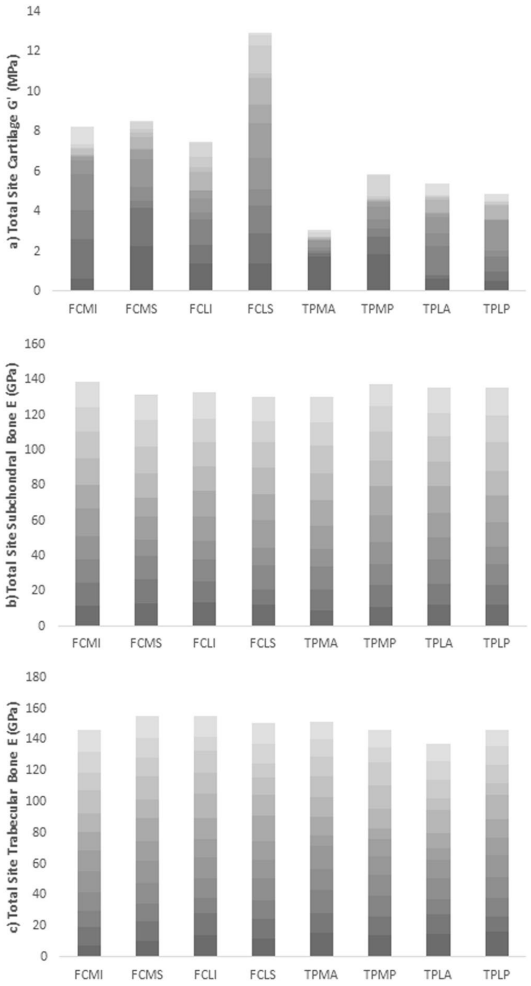

Figure 5. Collated values for (**a**) Cartilage shear storage modulus (G') (MPa), (**b**) Subchondral bone elastic modulus (E) (GPa) and (**c**) Trabecular bone elastic modulus (E) (GPa) from all cadavers at site specific locations. Femoral condyle medial inferior (FCMI), femoral condyle medial superior (FCMS), femoral condyle lateral inferior (FCLI), femoral condyle lateral superior (FCLS), tibial plateau medial anterior (TPMA), tibial plateau medial posterior (TPMP), tibial plateau lateral anterior (TPLA), tibial plateau lateral posterior (TPLP). Age of cadaver is represented in increasing transparency of colour.

controls included in this study. Thus prior to this research (Figs 2b, 3b) it has not been possible to systematically assess OA material property trends in subchondral bone. Specifically, in the current study older cadavers with OA had higher subchondral bone E when compared to healthy aged-matched controls (Fig. 3), further supporting the involvement of subchondral bone in the presence of disease. Endochondral ossification is observed with advancing OA and may cause mechanical stiffening of the subchondral bone[29], which could account for the increase in E with increasing grade of OA (Fig. 2). Our multi-variable analysis also correlated a change in subchondral bone E to age, but not OA grade when adjusting for one another, indicating, as with cartilage G', that age has a more prominent effect on subchondral bone E than increasing OA grade, but it is difficult to isolate these variables as they usually happen concurrently.

Previous research has also suggested that a change in the density and separation of trabecular bone occurs in the presence of OA[8,9]; however due to inconsistencies in cadaver demographics and variation in testing methods it was previously impossible to gauge how trabecular E changes with age or disease. Human knee joint trabecular bone E has previously been reported with values between 0.002–1.15 GPa [e.g.[30–33]] spanning three orders of magnitude. It should be noted that these studies represent varying testing methods and tip geometries which can

account for some variation in results; however this concurrently makes inter-study comparison between cohorts challenging. Data generated herein shows no systematic change in material properties (ICRS 0: 12.33 ± 3.04 GPa; ICRS 4: 12.07 ± 1.83 GPa) (Figs 1,2), suggesting that changes seen in the presence of OA[8,9] may be limited to structural adaptations. Further supporting this, our multi-variable analysis showed no correlation of trabecular bone *E* to age or OA when adjusted for one another.

An additional notable finding here which may contribute to varying results from within and between subject analysis, is the relative high level of variability in material properties in all three tissue types, and in particular cartilage, within cadavers of all genders, ages and disease status (Figs 1,2). No obvious or systematic trends in the magnitude of variability with increasing age or OA were identified in the data. The heterogeneous nature of the extracellular matrix of articular cartilage is influenced by variations in composition, structure and vascularity at the micro-level where cartilage material property variability within one specimen at different localities has previously been identified[34]. This strengthens the need to represent such structures locally with interchangeable material properties.

Furthermore the geometry, density and spatial locality plays a role in the variability of bone material properties[35]. The functional importance of spatial heterogeneity in material properties has been conceptually demonstrated in computer simulations of joint mechanics. For example, Mononen *et al.*[36], represented cartilage as a heterogeneous tissue, varying *E* accordingly to healthy and OA spatial material properties. Regions with OA, and therefore a reduced cartilage *E*, had increased tissue deformation and strain and significantly altered contact and pore pressures, where stresses increased at the interface between healthy and OA tissue[36]. Herein site specific cartilage material property differences exist in individual cadavers (Fig. 5) with absolute differences of up to 1.77 MPa equivalent to a relative difference of 461.2%. Therefore with the current data in mind this suggests a more local approach should be considered in attempts to understand the mechanical function of knee joint tissues, particularly in the presence of OA (Fig. 2).

The data presented in this study demonstrates that OA affects medially located samples more than laterally located ones. The individual ICRS grading of cartilage samples along with G' also suggests preferential development of OA medially, which is consistent with current diagnostic literature[14]. Additionally, motion analysis of healthy individuals also shows increased loading during gait on the medial femoral-tibial joint compared to lateral[15] as well as increased cartilage strains[37]. This is highly suggestive of a causative link between habitual joint loading and the suggested increase in medial OA seen within the current study. Medial femoral condyle cartilage G' declines with ageing; however such differences are not seen between medial and lateral samples in young healthy cadavers (Fig. 5a & Supplementary Material 1). Interestingly, regional development of OA has previously been applied in finite element (FE) models showing medial femoral condyle OA may create potential failure regions in the lateral condyle[36]. With the current data in consideration this would suggest that a decline in material properties seen in this study in ageing and with the presence of OA may be related to regional joint loading. Of note, cadaver BMI, which may affect magnitude of joint loading, was analysed in the current study against cartilage G', subchondral bone *E* and trabecular bone *E*, although no correlations were found, likely due to low sample numbers.

Spatially correlated material properties (Fig. 5) are practically important for the assessment of OA and resultant interventions. Developing targeted OA therapies relies on understanding alterations of multiple tissues involved in whole-joint function[38]. As suggested by Wen *et al.*[39], alterations in OA therapies will come from a more in-depth knowledge of the role subchondral bone plays in disease progression, which may include physical therapy, pharmaceuticals, or the development of biomimetic materials. Bisphosphonates such as alendronate inhibit bone remodeling and as a consequence reduce cartilage degeneration in animal experimental models[40]. With the current study supporting the role of an increase in bone to a decrease in cartilage mechanical stiffness (Fig. 4), such therapeutic interventions may be introduced in the presence of OA in an attempt to inhibit disease progression. Applications that rely on material property data such as polymer hydrogels are also increasingly being used to mimic viscoelastic properties of articular cartilage due to their structural similarities[41,42]. Tissue engineering including repair, replacement and regeneration of cellular scaffolding using these biomimetic materials should be based on accurate material properties sourced from healthy spatially distributed cartilage.

Our study has, for the first time, provided novel material property data across a wide span of age and OA grade for site matched cartilage and bone from varying localities in the human knee joint. This data demonstrates that cartilage and bone material properties alter in a synergistic relationship during ageing and disease, where a decrease in cartilage G' is accompanied by an increase in subchondral bone *E*. However this relationship appears to be isolated to the subchondral bone and not the trabecular structure despite morphological changes known to occur during disease[8,9]. Furthermore cartilage and subchondral bone material properties are also strongly correlated to age and OA grade independantly, whilst changes in cartilage are also site dependent. Medial preferential development of OA was also noted where cartilage *G* was strongly correlated to site dependency. This may suggest higher mechanical loading previously observed is a causative link to disease progression. This clinically relevant data can now be applied therapeutically via physical therapy, pharmaceuticals or the development of biomimetic materials where a subject- or cohort-specific approach would be more biologically representative.

Methods

Specimens. Fresh-frozen human knee joints (n = 12) were sourced aged 31–88 years (4 female, 8 male). Specific cadaver demographics can be seen in Table S1 (Supplementary Material 2), including height, weight, body mass index (BMI) and cause of death. All cadaveric specimens underwent one freeze-thaw cycle prior to dissection, which has been shown to cause no significant change to integrity of tissues [e.g.[43,44]].

Individual samples dissected from each cadaver (n = 8 samples per tissue type from each cadaver) were graded for OA using the International Repair Cartilage Society (ICRS) grading system, which is defined in Table S2 (Supplementary Material 2). The cadaveric knee joints were photographed and blind graded by two individuals

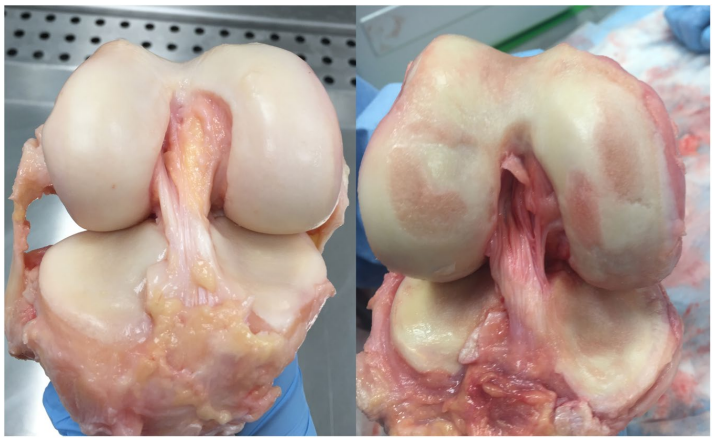

Figure 6. Photographs of young (43 years) healthy (left) and old (88 years) osteoarthritic (right) knee joint specimens.

at a later date three times, one week apart, with the mean score used. Example photographs from one young healthy and one old OA cadaver knee joint can be seen in Figure 6. Photographs from each cadaver can be seen in Figures S1–S12 (Supplementary Material 2).

Eight articular cartilage, eight subchondral bone and eight trabecular bone samples from each of the 12 cadavers were extracted using a low speed oscillating saw (deSoutter Medical, Bucks, UK). Samples were extracted from the following localities: femoral condyle medial inferior (FCMI), femoral condyle medial superior (FCMS), femoral condyle lateral inferior (FCLI), femoral condyle lateral superior (FCLS), tibial plateau medial anterior (TPMA), tibial plateau medial posterior (TPMP), tibial plateau lateral anterior (TPLA) and tibial plateau lateral posterior (TPLP).

Cartilage. The overlying cartilage (n = 96 samples (n = 8 per cadaver)) was separated from the subchondral bone using a scalpel blade. Cartilage samples were fully submerged in phosphate buffered saline (PBS), transferred on ice and stored at 3–5 °C until testing. All cartilage samples were tested within 72 hours post dissection to avoid any change to material properties[45].

Dynamic Nanoindentation Testing. Dynamic nanoindentation (G200 Nanoindenter, Keysight Technologies, Chandler, AZ, USA) was used to obtain the complex shear modulus (G^*) of articular cartilage at the micro level. The indenter was equipped with an ultra-low load DCM-II actuator utilising a Continuous Stiffness Measurement (CSM) module and a flat-ended cylindrical 100 µm punch tip (Synton-MDP Ltd, Nidau, Switzerland). Samples were partially submerged in PBS during testing through mounting in a custom-made liquid cell holder measuring a 1 cm radius and 2 mm deep well. Spatially correlated indentation locations (>100 µm spacing between each indentation) were randomly chosen under the optical microscope to achieve 10 measurements per individual sample.

The calculation of shear storage modulus (G'), shear loss modulus (G'') and the loss factor (tan delta (δ)) (i.e. ratio of G''/G') were applied following each indentation by assuming a Poisson's ratio of 0.46[22]. The theoretical basis is detailed elsewhere[46–49] and has been applied using this method previously[43], and is briefly outlined here.

Complex shear modulus (G^*) is calculated by adding G' (real intrinsic elastic component) to G'' (imaginary viscous component):

$$G^* = G' + iG'' \tag{1}$$

Sneddon's analysis is used to calculate the shear storage modulus using the Poisson's ratio (v), contact stiffness (S) and tip diameter (D), based on using a flat cylindrical punch:

$$G' = \frac{S(1 - v)}{(2D)} \tag{2}$$

The above components along with contact damping (Cw) can be used to calculate the shear loss modulus:

$$G'' = \frac{Cw\ (1 - v)}{(2D)} \tag{3}$$

Contact stiffness (S) is calculated by subtracting the instrument stiffness (Ki) from the total measured stiffness (Ks):

$$S = Ks - Ki \tag{4}$$

Contact damping (Cw) is calculated by subtracting the instrument damping (Ciw) from the total measured damping (Csw):

$$Cw = Csw - Ciw \tag{5}$$

The elastic modulus (E) was then calculated using the shear storage modulus (G') and Poisson's Ratio (v):

$$E = 2G'(1 + v) \tag{6}$$

After the indenter head detected the surface of the sample, a pre-compression of 8 μm was applied until the indenter was fully in contact with the sample. The surface detection was determined by a phase shift of the displacement measurement. In order to accurately detect the surface, the phase shift was monitored over a number of data points. Once the surface detection requirement was fulfilled over the predefined number of data points, the initial contact was determined from the first data point in the sequence. Once the indenter was fully in contact with the sample surface it vibrated at a fixed frequency of 110 Hz (the resonant frequency of the indenter) with 500 nm oscillation amplitude. Contact stiffness and damping were obtained through electromagnetic oscillation sequences. The initial oscillation measured instrument stiffness and damping and these were subtracted from the total measurement to obtain the contact response. Material properties were then obtained during the second oscillation.

After each indentation an adjacent sample holder mounted with 3 M double-sided Scotch tape was indented, in order to clean the tip and prevent the transfer of biological material to subsequent test sites, as this may affect measurements. Following testing of each sample fused silica was indented to ensure the tip remained free from residue. Accuracy of the technique and measurements has previously been evidenced on other compliant homogenous structures[50].

Bone. Bone samples (n = 80 subchondral bone, n = 96 trabecular bone (n = 8 per cadaver)) were temporarily stored in 70% ethanol to preserve their physiological state[51]. Note: Subchondral bone samples were unable to be tested for cadaver 1 and 4 due to difficulties in polishing preparation. Samples were then washed in a piezoelectric ultrasonic bath using distilled water and pure ethanol to remove any debris, before being embedded in a low viscosity epoxy resin at a transverse angle as to expose both subchondral and trabecular surfaces. Samples were then grinded with progressive silicon carbide paper (300, 600, 1200, 2400, 4000 grit) whilst under constant water irrigation to remove any debris, and polished with alumni paste to a surface finish on 1 μm and colloidal silica to 40 nm.

Quasi-Static Nanoindentation Testing. Bone samples underwent quasi-static nanoindentation (G200 Nanoindenter, Keysight Technologies, Chandler, AZ, USA) to determine the nano-mechanical hardness (H) and E. Samples were examined under the optical microscope to randomly choose ten spatially correlated indents per sample (>100 μm spacing between each indentation). A Berkovich sharp pyramidal tip was utilised (20 nm radius) and a Poisson's ratio of 0.3[52] was assumed for bone. A penetration depth of 2000 nm was used for subchondral bone and 1200 nm for trabecular bone with a peak hold time of 30 seconds to factor in any viscoelastic response of tissues[53]. Due to the porous nature of trabecular bone the surface approach distance was set at 2000 nm to address any topographic variation in sample height. For subchondral bone this was set to 1000 nm. Surface stiffness detection was limited to 125 Nm^{-1} and samples were unloaded to 90% and held before final unloading to establish thermal drift, which was set to an acceptance level of 0.15 Nm/s[54]. The nanoindenter was calibrated using fused silica prior and after testing, which has known material property values[55].

This protocol thus achieves continuous loading and partial unloading of samples with an indenter of known geometry and material properties, with loading and penetration depth precisely measured. This approach allows the calculation of H and E using an established theory[55], which is briefly outlined here.

Hardness (H) is calculated by dividing the maximum load (P) reached at peak penetration depth, by the contact area (A):

$$H = \frac{P\,\max}{A} \tag{7}$$

The initial unloading stiffness is calculated as below where P is the load and h is the depth and dP/dh is the slope of the line in tangent to the initial unloading curve in the load-displacement plot.

$$S = \frac{dP}{dh} = \frac{2}{\sqrt{\pi}} E_r \sqrt{A} \tag{8}$$

The reduced indentation modulus (E_r) is then calculated as below where v and v_i represent the sample and indenter Poisson's ratio respectively, and E and E_i are the sample and the indenter modulus respectively.

$$\frac{1}{E_r} = \frac{(1 - v^2)}{E} + \frac{(1 - v_i^2)}{E_i} \tag{9}$$

Statistical Analysis. An a-priori power analysis was performed using G*Power software[56]. A total of 42 samples per tissue type was required to distinguish either an effect size of 0.8 with α error probability of 0.05 and power of 0.95 when determining the relationship between multiple tissue means; or an effect size of 0.5 with α error probability of 0.05 and power of 0.95 for correlations to age, OA grade, spatial distribution and BMI. Normal distribution of all measured individual sample material properties was analysed using a Kolmogorov-Smirnov test accounting for skewness and kurtosis of results. Where data was not significant and therefore normally distributed, homogeneity of variance was analysed using the Levene's test. Homoscedastic data was then tested for linearity using a two-tailed Pearson's correlation. Data violating the assumptions of Pearson's correlation testing were analysed using a two-tailed Spearman's Rank (SPSS software, Version 22.0, SPSS, Inc., Chicago, IL). Specifically bivariate correlation coefficients with significance to age, OA, spatial distribution and BMI of samples was determined. Individual sample and combined sample mean and standard deviation (SD), and 95% confidence interval (CI) were analysed for each tissue from each cadaver. The overall joint mean material properties were also correlated to age and overall joint OA grade ($n = 12$), and to sample site ($n = 8$ locations) using a Kendall's Tau-b test. Joint means were used to account for within-subject dependence of samples. The effect of within and between-subject variables were analysed using a mixed linear model, combing the effects of both age and OA.

The results primarily focus on the intrinsic viscoelastic G' of cartilage and E of subchondral and trabecular bone, as these are the most commonly reported and therefore comparable results. Shear and elastic properties are also most closely linked to tissue function *in vivo*. However to aid a full interpretation of data collected, additional data is also reported within Supplementary Material 1.

All data generated or analysed during this study are included in this published article (and its Supplementary Information files).

Ethical permission for use of this human cadaveric material was sponsored by the University of Liverpool and granted by the NRES (15/NS/0053) who approved all protocols. All experiments were performed in accordance with relevant guidelines and regulations.

References

1. Zhang, Y. & Jordan, J. M. Epidemiology of Osteoarthritis. *Rheumatic Disease Clinics of North America.* **34**, 515–529 (2008).
2. Kiss, R. M. Effect of severity of knee osteoarthritis on the variability of gait parameters. *Journal of Electromyography and Kinesiology.* **21**, 695–703 (2011).
3. Hollman, J. H., Kovash, F. M., Kubik, J. J. & Linbo, R. A. Age-related differences in spatiotemporal markers of gait stability during dual task walking. *Gait & Posture.* **26**, 113–119 (2007).
4. Hansen, U., Masouros, S. & Amis, A. A. (iii) Material properties of biological tissues related to joint surgery. *Current Orthopaedics.* **20**, 16–22 (2006).
5. Manninen, P., Riihimaki, H., Heliovaara, M. & Makela, P. Overweight, gender and knee osteoarthritis. *International Journal of Obesity and Related Metabolic Disorders: Journal of the International Association for the Study of Obesity.* **20**, 595–597 (1996).
6. Mahjoub, M., Berenbaum, F. & Houard, X. Why subchondral bone in osteoarthritis? The importance of the cartilage bone interface in osteoarthritis. *Osteoporosis International.* **23**, 841–846 (2012).
7. Burr, D. B. & Gallant, M. A. Bone remodelling in osteoarthritis. *Nature Reviews Rheumatology.* **8**, 665–673 (2012).
8. Kamibayashi, L., Wyss, U., Cooke, T. & Zee, B. Trabecular microstructure in the medial condyle of the proximal tibia of patients with knee osteoarthritis. *Bone.* **17**, 27–35 (1995).
9. Bobinac, D., Spanjol, J., Zoricic, S. & Maric, I. Changes in articular cartilage and subchondral bone histomorphometry in osteoarthritic knee joints in humans. *Bone.* **32**, 284–290 (2003).
10. Madry, H., van Dijk, C. N. & Mueller-Gerbl, M. The basic science of the subchondral bone. *Knee Surgery, Sports Traumatology, Arthroscopy.* **18**, 419–433 (2010).
11. Kleemann, R., Krocker, D., Cedraro, A., Tuischer, J. & Duda, G. Altered cartilage mechanics and histology in knee osteoarthritis: relation to clinical assessment (ICRS Grade). *Osteoarthritis and Cartilage.* **13**, 958–963 (2005).
12. Wilusz, R. E., Zauscher, S. & Guilak, F. Micromechanical mapping of early osteoarthritic changes in the pericellular matrix of human articular cartilage. *Osteoarthritis and Cartilage.* **21**, 1895–1903 (2013).
13. Kuroki, K., Cook, C. & Cook, J. Subchondral bone changes in three different canine models of osteoarthritis. *Osteoarthritis and Cartilage.* **19**, 1142–1149 (2011).
14. Pelletier, J. *et al*. Risk factors associated with the loss of cartilage volume on weight-bearing areas in knee osteoarthritis patients assessed by quantitative magnetic resonance imaging: a longitudinal study. *Arthritis Research & Therapy.* **9**, R74 (2007).
15. Kumar, D., Manal, K. T. & Rudolph, K. S. Knee joint loading during gait in healthy controls and individuals with knee osteoarthritis. *Osteoarthritis and Cartilage.* **21**, 298–305 (2013).
16. Shepherd, D. E. & Seedhom, B. B. The 'instantaneous' compressive modulus of human articular cartilage in joints of the lower limb. *Rheumatology (Oxford, England).* **38**, 124–132 (1999).
17. Thambyah, A., Nather, A. & Goh, J. Mechanical properties of articular cartilage covered by the meniscus. *Osteoarthritis and Cartilage.* **14**, 580–588 (2006).
18. Hori, R. Y. & Mockros, L. Indentation tests of human articular cartilage. *Journal of Biomechanics.* **9**, 259–268 (1976).
19. Franz, T. *et al*. *In situ* compressive stiffness, biochemical composition, and structural integrity of articular cartilage of the human knee joint. *Osteoarthritis and Cartilage.* **9**, 582–592 (2001).
20. Wang, M., Peng, Z., Price, J. & Ketheesan, N. Study of the nano-mechanical properties of human knee cartilage in different wear conditions. *Wear.* **301**, 188–191 (2013).
21. Cohen, J. Statistical power analysis for the behavioural sciences. (Lawrence Earlbaum Associates, 1988).
22. Jin, H. & Lewis, J. L. Determination of Poisson's ratio of articular cartilage by indentation using different-sized indenters. *Journal of Biomechanical Engineering.* **126**, 138–145 (2004).
23. Robinson, D. L. *et al*. Mechanical properties of normal and osteoarthritic human articular cartilage. *Journal of the Mechanical Behavior of Biomedical Materials.* **61**, 96–109 (2016).
24. Desrochers, J., Amrein, M. & Matyas, J. Viscoelasticity of the articular cartilage surface in early osteoarthritis. *Osteoarthritis and Cartilage.* **20**, 413–421 (2012).
25. Taffetani, M., Gottardi, R., Gastaldi, D., Raiteri, R. & Vena, P. Poroelastic response of articular cartilage by nanoindentation creep tests at different characteristic lengths. *Medical Engineering & Physics.* **36**, 850–858 (2014).
26. Nia, H. T., Han, L., Li, Y., Ortiz, C. & Grodzinsky, A. Poroelasticity of cartilage at the nanoscale. *Biophysical Journal.* **101**, 2304–2313 (2011).

27. Rho, J., Tsui, T. Y. & Pharr, G. M. Elastic properties of human cortical and trabecular lamellar bone measured by nanoindentation. *Biomaterials.* **18**, 1325–1330 (1997).
28. Zuo, Q. *et al*. Characterization of nano-structural and nano-mechanical properties of osteoarthritic subchondral bone. *BMC Musculoskeletal Disorders.* **17**, 367 (2016).
29. Cox, L., van Donkelaar, C., van Rietbergen, B., Emans, P. & Ito, K. Alterations to the subchondral bone architecture during osteoarthritis: bone adaptation vs endochondral bone formation. *Osteoarthritis and Cartilage.* **21**, 331–338 (2013).
30. Behrens, J., Walker, P. & Shoji, H. Variations in strength and structure of cancellous bone at the knee. *Journal of Biomechanics.* **7**, 201–207 (1974).
31. Ducheyne, P. *et al*. The mechanical behaviour of intracondylar cancellous bone of the femur at different loading rates. *Journal of Biomechanics.* **10**, 747–762 (1977).
32. Burgers, T. A., Mason, J., Niebur, G. & Ploeg, H. L. Compressive properties of trabecular bone in the distal femur. *Journal of Biomechanics.* **41**, 1077–1085 (2008).
33. Zysset, P., Sonny, M. & Hayes, W. Morphology-mechanical property relations in trabecular bone of the osteoarthritic proximal tibia. *The Journal of Arthroplasty.* **9**, 203–216 (1994).
34. Moore, A. & Burris, D. Tribological and material properties for cartilage of and throughout the bovine stifle: support for the altered joint kinematics hypothesis of osteoarthritis. *Osteoarthritis and Cartilage.* **23**, 161–169 (2015).
35. Zysset, P. K., Guo, X. E., Hoffler, C. E., Moore, K. E. & Goldstein, S. A. Elastic modulus and hardness of cortical and trabecular bone lamellae measured by nanoindentation in the human femur. *Journal of Biomechanics.* **32**, 1005–1012 (1999).
36. Mononen, M. *et al*. Effect of superficial collagen patterns and fibrillation of femoral articular cartilage on knee joint mechanics—A 3D finite element analysis. *Journal of Biomechanics.* **45**, 579–587 (2012).
37. Adouni, M., Shirazi-Adl, A. & Shirazi, R. Computational biodynamics of human knee joint in gait: from muscle forces to cartilage stresses. *Journal of Biomechanics.* **45**, 2149–2156 (2012).
38. Goldring, S. R. & Goldring, M. B. Changes in the osteochondral unit during osteoarthritis: structure, function and cartilage-bone crosstalk. *Nature Reviews Rheumatology.* **12**, 632–644 (2016).
39. Wen, C., Lu, W. W. & Chiu, K. Y. Importance of subchondral bone in the pathogenesis and management of osteoarthritis from bench to bed. *Journal of Orthopaedic Translation.* **2**, 16–25 (2014).
40. Hayami, T. *et al*. The role of subchondral bone remodeling in osteoarthritis: reduction of cartilage degeneration and prevention of osteophyte formation by alendronate in the rat anterior cruciate ligament transection model. *Arthritis & Rheumatism.* **50**, 1193–1206 (2004).
41. Li, W., Wang, D., Yang, W. & Song, Y. Compressive mechanical properties and microstructure of PVA–HA hydrogels for cartilage repair. *RSC Advances.* **6**, 20166–20172 (2016).
42. Wang, Q., Hou, R., Cheng, Y. & Fu, J. Super-tough double-network hydrogels reinforced by covalently compositing with silica-nanoparticles. *Soft Matter.* **8**, 6048–6056 (2012).
43. Peters, A. E., Comerford, E. J., Macaulay, S., Bates, K. T. & Akhtar, R. "Micromechanical properties of canine femoral articular cartilage following multiple freeze-thaw cycles. *Journal of the Mechanical Behavior of Biomedical Materials.* **71**, 114–121 (2017).
44. Moon, D. K., Woo, S. L., Takakura, Y., Gabriel, M. T. & Abramowitch, S. D. The effects of refreezing on the viscoelastic and tensile properties of ligaments. *Journal of Biomechanics.* **39**, 1153–1157 (2006).
45. Changoor, A., Fereydoonzad, L., Yaroshinsky, A. & Buschmann, M. D. Effects of refrigeration and freezing on the electromechanical and biomechanical properties of articular cartilage. *Journal of Biomechanical Engineering.* **132**, 064502 (2010).
46. Herbert, E., Oliver, W., Lumsdaine, A. & Pharr, G. M. Measuring the constitutive behavior of viscoelastic solids in the time and frequency domain using flat punch nanoindentation. *Journal of Materials Research.* **24**, 626–637 (2009).
47. Herbert, E., Oliver, W. & Pharr, G. Nanoindentation and the dynamic characterization of viscoelastic solids. *Journal of Physics D: Applied Physics.* **41**, 074021 (2008).
48. Sneddon, I. N. The relation between load and penetration in the axisymmetric Boussinesq problem for a punch of arbitrary profile. *International Journal of Engineering Science.* **3**, 47–57 (1965).
49. Landau, L. D. & Lifshitz, E. Theory of Elasticity, vol. 7. *Course of Theoretical Physics.* **3**, 109 (1986).
50. Moronkeji, K., Todd, S., Dawidowska, I., Barrett, S. & Akhtar, R. The role of subcutaneous tissue stiffness on microneedle performance in a representative *in vitro* model of skin. *Journal of Controlled Release.* (2016).
51. Linde, F. & Sørensen, H. C. F. The effect of different storage methods on the mechanical properties of trabecular bone. *Journal of Biomechanics.* **26**, 1249–1252 (1993).
52. Reilly, D. T. & Burstein, A. H. The elastic and ultimate properties of compact bone tissue. *Journal of Biomechanics.* **8**, 393IN9397–396IN11405 (1975).
53. Chudoba, T. & Richter, F. Investigation of creep behaviour under load during indentation experiments and its influence on hardness and modulus results. *Surface and Coatings Technology.* **148**, 191–198 (2001).
54. Oyen, M. Nanoindentation of biological and biomimetic materials. *Experimental Techniques.* **37**, 73–87 (2013).
55. Oliver, W. C. & Pharr, G. M. An improved technique for determining hardness and elastic modulus using load and displacement sensing indentation experiments. *Journal of Materials Research.* **7**, 1564–1583 (1992).
56. Faul, F., Erdfelder, E., Lang, A. & Buchner, A. G* Power 3: A flexible statistical power analysis program for the social, behavioral, and biomedical sciences. *Behavior Research Methods.* **39**, 175–191 (2007).

Acknowledgements

This project was funded by BBSRC (Research Grant: BB/J014516/1) and the School of Engineering, University of Liverpool. RA is grateful to the Royal Society for equipment funding (Research Grant: RG130629). The authors would like to thank Mr Phil Jackson and the staff at the Newcastle Surgical Training Centre, who supported obtainment of cadaveric specimens; Mr Dave Atkinson of the School of Engineering, University of Liverpool, who supported bone sample preparation; Ms Val Adams and the staff at MARIARC, Technology Directorate, University Of Liverpool who supported MRI imaging; Science Care who supported CT imaging; Mr Lee Moore and the staff at the Veterinary Training Suite, Institute of Veterinary Science, University of Liverpool, for the use of surgical tools.

Author Contributions

Study conception and design: A.E.P., R.A., E.J.C., K.T.B.; Acquisition of data: A.E.P., E.J.C., K.T.B.; Analysis and interpretation of data: A.E.P.; Wrote the paper: A.E.P.; Contributed to the paper: R.A., E.J.C., K.T.B.

Additional Information

Supplementary information accompanies this paper at https://doi.org/10.1038/s41598-018-24258-6.

Competing Interests: The authors declare no competing interests.